Coastal Erosion and Sedimentation of Pukehina Beach and Waihi Estuary

A thesis
submitted in partial fulfilment
of the requirements for the
Degree of Master of Science
in Earth Science
at the
University of Waikato.

Hayden Russell Easton

The University of Waikato
Te Whare Wānanga o Waikato

April 2002

Frontispiece: Oblique view of the Waihi Estuary and Pukehina shoreline. Photograph taken by author (12/8/2001)

Abstract

The Pukehina coastal sector is subject to severe frontal dune erosion. This has led to concern from local residents who reside in frontal houses. Accordingly, this investigation was initiated to assess the sedimentary and physical processes within the Pukehina coastal sector, with the aim of identifying causes of enhanced frontal dune erosion.

To investigate this problem the following processes were investigated: wave focusing from offshore bathymetric lenses, sediment lost due to the Waihi Estuary acting as a sediment sink, and/or a change in sediment volume or sediment transport processes within the Pukehina coastal sector. Methods to investigate these processes included: collection and analysis of surficial sediment samples from Pukehina Beach and Waihi Estuary, construction of a digital terrain model, side scan sonar surveying, calculation of offshore suspended sediment concentrations, numerical modelling of wave refraction and sediment transport processes, and collection and analysis of wave and estuarine current, depth, and direction data.

Wave data were collected at eastern and western ends of the study location, during two separate deployments during July 2000 and March 2001. Outcomes depict differing incoming wave directions at each site, due to offshore undulations in bathymetry. Wave energy focusing was observed along the Pukehina coastal sector (specifically at benchmarks 30, 29, 27 and 26a) during average wave conditions recorded, and enhanced as wave period and wave height increased (approximately 0.2–2.0 m in each simulation, respectively). Wave focusing is significantly influenced by the ebb tidal delta offshore from Waihi Estuary, leading to larger wave heights present in eroding regions of Pukehina Beach.

Potential sediment transport rates were investigated, utilising collected wave data. Outcomes illustrate a potential sediment transport to the east. A negative littoral drift gradient, was observed between a) Okurei Point and Waihi Estuary inlet, and a positive littoral drift gradient between b) benchmark 29 and 26. This implies a potential accumulation of sediments near Waihi Estuary inlet (some of which, would be lost to infilling of Waihi Estuary). However, a long-term deficit (~12 m^3/m per year) of sediment is lost along Pukehina Beach, due to the apparent positive littoral drift gradient. This outcome is identified as a major component of the long-term 'erosion' problem at Pukehina Beach.

Tidal and current gauges were deployed within Waihi Estuary. Data revealed strong evidence that the estuary is acting as a sediment sink. Tidal asymmetry, attenuation of the tidal signal and a dominance of sediment transport into the estuary, depict that Waihi Estuary is an influential component of the erosion occurring at Pukehina Beach. The Waihi Estuary is calculated by geomorphic and hydraulic analysis to be tending towards deposition in the inlet, leading to a general instability of the Waihi Estuary inlet.

Nearshore sediment transport rates within the region are significantly influenced by localised wind patterns within the Pukehina coastal sector. The Pukehina coastal sector was identified as having a net deficit of sediment, approximately 4,500 m^3/year or -0.5 m^3/m per year. However, due to errors involved in estimate calculations, this value may be larger.

Sediment textural distributions have altered since previous surveys conducted in 1993 by PHIZACKLEA. Particularly, an influx of sediment to the Okurei Point region, reducing the area of exposed bedrock, suggests a change of sediment transport patterns within this region. Texturally, offshore sediments vary from fine sand sized sediments to very coarse sand, while beach sediments are predominantly medium sand sized particles, with a decrease in sediment size towards Okurei Point (fine sand sized particles), indicating a sediment transport direction to the west.

Causes of significant long-term erosion to the Pukehina coastal sector, have been identified as: a) beach-nearshore sediment being lost or 'sucked out' of the coastal sector, due to the combination of a positive littoral drift gradient along Pukehina Beach, and wave energy focusing; and b) infilling of the Waihi Estuary. Other processes, such as aeolian transport etc., do reduce the volume of available sediment to Pukehina Beach, but are not implicated to the long-term 'erosion' problem occurring.

Possible remedial solutions, influenced by data observations, are suggested to reduce current frontal dune erosion. However, further research is recommended to identify what coastal management options are required for the Pukehina Beach shoreline.

Acknowledgments

There have been many people who have helped and guided me through my thesis, which I am indebted to. Firstly I would like to thank my supervisor Professor Terry Healy for initiating the project and giving me both intellectual and moral support throughout my thesis, your constructive criticism and knowledge was valued.

Thank you to Environment Bay of Plenty for financial support, enthusiasm and data provided for this thesis. Particular thanks goes to Dougall Gordon, John McIntre, Mark Stringfellow and Shane Iremonger.

I would also like to thank Dr Willem de Lange and Gareth Vaughan for his input and suggestions whilst Terry was on sabbatical leave, and Professor Kerry Black for the use of his software and help with questions.

A very big thankyou must go to Dirk Immenga for his experience and technical knowledge in fieldwork, your interest and support for my project was greatly appreciated. To the many people who helped me with my fieldwork, thankyou, in particular Ian Blair, Paul 'sleeps with his eyes open' King, Heeni, Kyle, Brad, Paul Klinac and Brett. A big thanks goes to 'hard as nails' Cush for her help with my estuary coring.

Big thanks goes to Rob and Lynn Phillips for the use of the charter vessel *Black Shag*, and for the meals and accommodation provided whilst undertaking fieldwork.

To the flatties, Antonio Dolphin cheers for the good times and help with my questions, and all the others cheers for putting up with the endless piles of paper.

Much appreciation goes to Rodger Briggs and Brendan Mischewski for understanding and helping me through my times of ill health, and the doctors and surgeons who made this the longest MSc thesis of all time.

To my family, Mum, Dad, Kylie and Grant cheers for the support you have given me through my University years.

All my friends, cheers for the good times and great laughs, especially proto Dr Maartje, Terrence, Tashy, Matt, Wuz for the endless emails!!

And finally Teresa, thanks for the good times, support and showing me there is more to life than just a book, luv ya!!

Catch ya later Haydz ☺

Table of Contents

Chapter Seven: Summaries, Conclusions and Potential Remedial Solutions for Pukehina Beach

List of Figures

Chapter One

Chapter Two

Chapter Three

Chapter Four

Chapter Five

Chapter Six

Chapter Seven

List of Tables

Chapter Three

Chapter Four

Chapter Five

Chapter Six

Chapter One
Introduction

1.0 Introduction

The Pukehina coastline of Bay of Plenty, North Island, currently undergoes cyclic erosion and accretion patterns. Greatest changes are evident along the Pukehina Spit (BOPRC, 1991). Previous studies of the Bay of Plenty coastline have indicated that erosion occurring at Pukehina has been an ongoing problem over the past century, with Pukehina Beach and Spit undergoing 10-30 m of retreat since 1912 (HODGES AND DEELY, 1997).

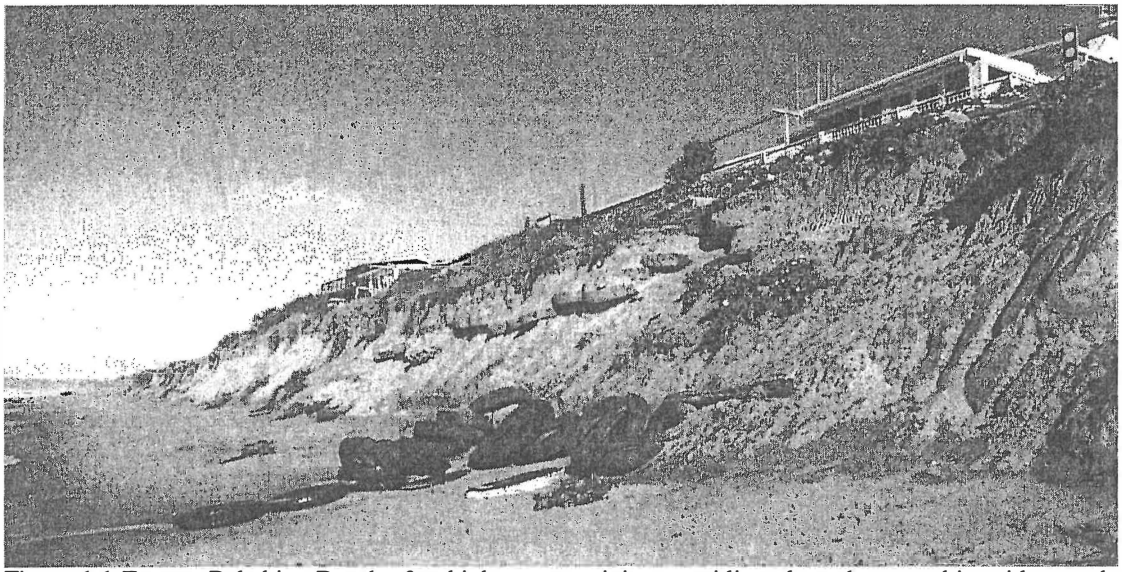

Figure 1.1 Eastern Pukehina Beach after high storm activity, providing clear photographic evidence why research of coastal processes is needed. Photograph taken by B. Harding 11/7/2000.

Pukehina shoreline comprises a Holocene barrier spit that encloses the Waihi Estuary, and to the northwest is a small headland called Okurei Point, also known as Town Point (BOPRC, 1991), as illustrated in figure 1.2.

Pukehina Spit has undergone substantial residential development in the past two decades (BOPRC, 1991). Concern by residents of ongoing frontal dune retreat has prompted an investigation into reasons for the shoreline erosion. What is the rate at which erosion is occurring? And what may be done to restrict further ongoing shoreline retreat?

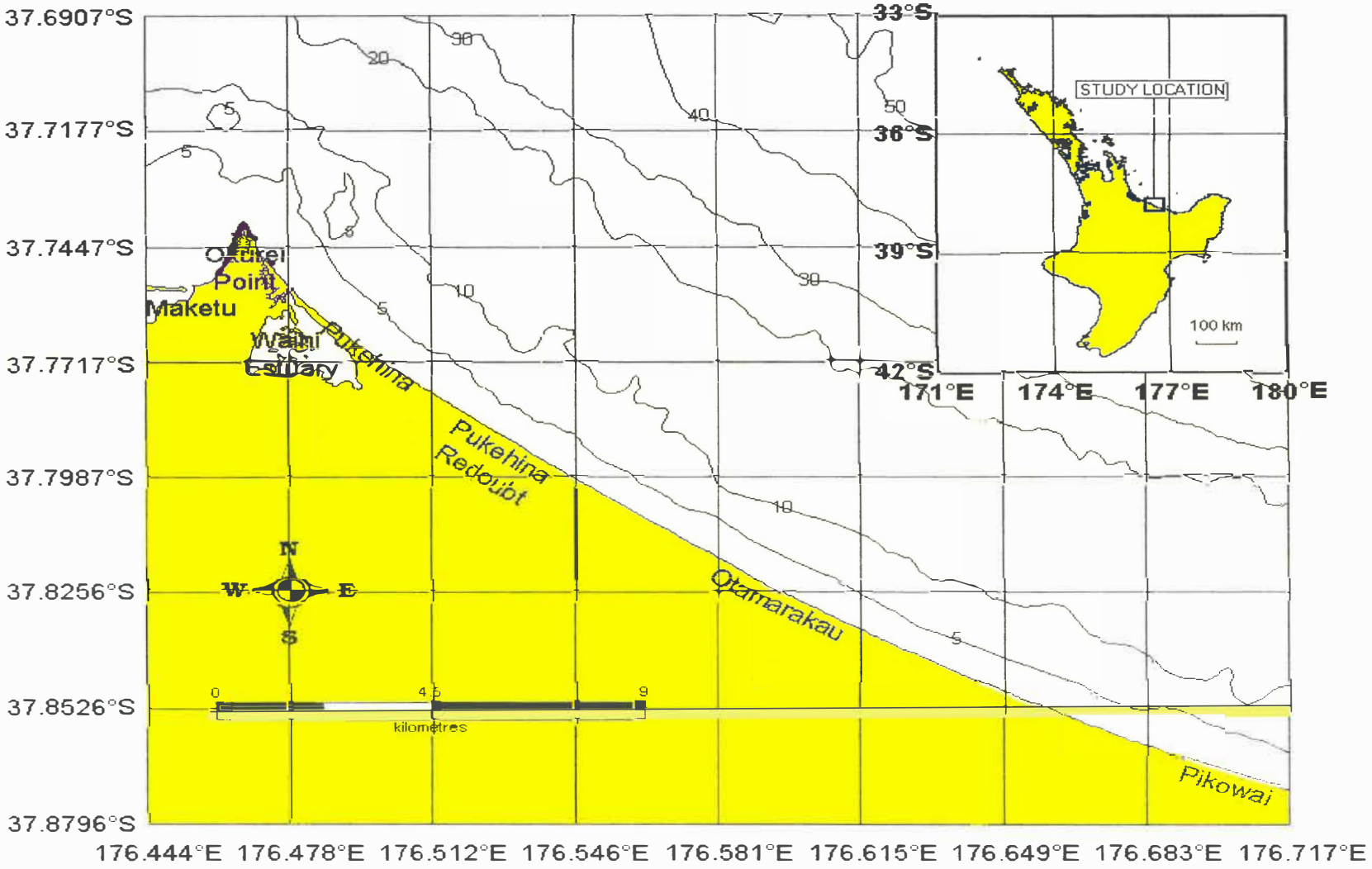

Figure 1.2 Location of Pukehina Beach and Waihi Estuary, in relation to adjacent coastal geomorphology and offshore bathymetry (m).

1.1 The Problem Background of Pukehina Beach

Investigations by HEALY *et al.* (1977), HEALY (1978), PHIZACKLEA (1993), PICKETT *et al.* (1997) and others, have indicated that Pukehina is in an erosive state. However, limited research has been carried out specifically identifying the processes that are causing erosion at Pukehina Beach.

Local inhabitants of Pukehina are concerned about the retreat of the frontal dune along Pukehina beach. HODGES AND DEELY (1997, pp. 33-34) state there is a 'net average shoreline retreat of approximately 10 m^3/m along all benchmark locations along Pukehina Beach'. Residents along beachfront sections are particularly concerned, due to the possibility of erosion claiming their properties, as figure 1.1 identifies.

Housing subdivision in the Pukehina region is poorly planned. Houses backing the frontal dune may experience dune scarping and/or dune blowouts either side of dwellings (HEALY *et al.*, 1977). HEALY *et al.* (1977) stated in relation to coastal subdivisions in the Bay of Plenty coastal zone that "Pukehina showed the greatest potential for disaster".

In an attempt to reduce or prevent further frontal dune retreat, some protection measures have already been constructed. Currently sections along the frontal dune ridge have a meshed sand fence and the ridge is colonised by dune vegetation (primarily *Spinifex*). The implementation of coastal protection began in 1997, in order to increase the frontal dune dimensions. However, since the use of these protection measures, comparisons with historical beach profiles suggest that areas with protection are not reducing the rate of dune retreat.

1.2 Sand Mining Issues

In the minds of some local inhabitants of Pukehina Beach, ongoing sand extraction from Otamarakau (approximately 10 km east of Pukehina Beach) is reducing the volume of sediment transported into the region by littoral drift. This has therefore been cited by

Pukehina Beach inhabitants, as a reason for why the frontal dune at Pukehina Beach is eroding.

The sustainability of sand extraction from Otamarakau has been a controversial issue among coastal scientists, ever since J.W. Paterson and Sons Limited began mining high quality aggregate sediment in 1985 (SMITH, 1986; PHIZACKLEA, 1993; HODGES AND DEELY, 1997; TONKIN & TAYLOR LIMITED, 1999).

To reduce observed localised beach erosion, mining has been concentrated in three different locations (figure 1.3). Each area is mined once on a yearly basis, to separate mining activity from users of the beach and to avoid nesting by New Zealand dotterals, which may nest in the designated mining sites (SMITH *et al.*, 1997).

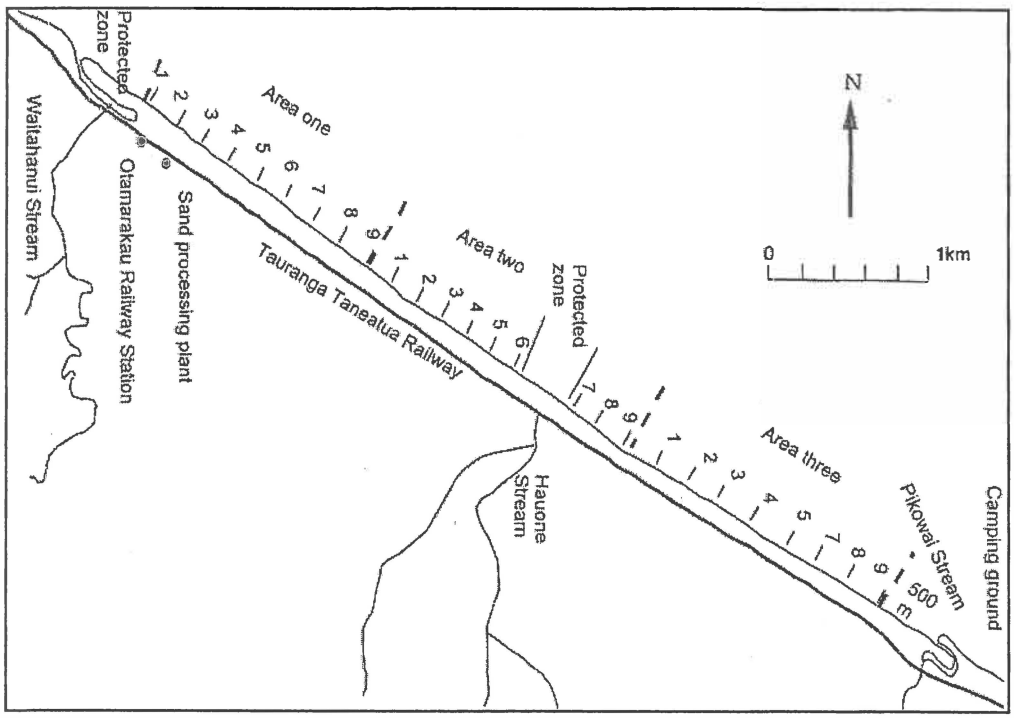

Figure 1.3 Location of designated mining sites at Otamarakau (Source: SMITH *et al.*, 1997).

Sediment from each mined region is derived from erosion of the local catchment material, which is transported by local streams, erosion of submarine outcrops in the Okurei Point – Otamarakau region, littoral drift into the sector and possible reworking of

pre-Holocene sediments (TONKIN & TAYLOR LIMITED, 1999). From 1985 to 1995, 20,000 m^3/year was extracted from Otamarakau under licences issued by the Department of Conservation. This volume was increased to 27,000 m^3/year in 1995 following authorisation from the Minister of Conservation (TONKIN & TAYLOR LIMITED, 1999).

To assess erosion and sustainability of mining operations, monitoring is carried out by the National Institute of Water and Atmospheric Research (NIWA) on behalf of J.W. Paterson & Sons Limited. The current coastal permit states that "Beach profiles must be every 200 m along the 5.4 km mining region and compared with unmined zones either side of the mined site. Extraction must not commence if there is less than a minimum volume of 110 m^3/m (above MSL) of beach foreshore and a minimum foreshore volume following extraction of 62 m^3/m (above MSL) based on assessments of the 100 year storm demand of the beach" (TONKIN & TAYLOR LIMITED, 1999).

Figure 1.4. Mining machinery and sand stock pile at Otamarakau, 9/1/2001.

Currently, comparison of historic beach profiling with present beach profiles is used to assess the effects of sand extraction upon the Pukehina shoreline. If extraction was to cause significant erosion to the Pukehina coastline, the excursion distance (distance from benchmark to mean sea level) would be expected to decrease, as extraction would cause a down-drift erosional effect in the direction of littoral drift.

PICKETT *et al.* (1997) analysed 48 beach profile sites within the Bay of Plenty region and identified whether their equilibrium status was erosive or accretional. For sites within the Pukehina coastal sector, results indicated that all profiles were erosional.

1.3 Thesis Objectives

The aim of this thesis is to investigate the factors facilitating erosion at Pukehina Beach. Assessment of these factors may be made, by investigating the following objectives:

To construct a digital terrain model of the nearshore/shoreface and identify zones of sediment scour or accumulation.

Using data collected by PHIZACKLEA (1993), Environment Bay of Plenty (EBOP) and the Royal New Zealand Navy, a digital terrain model may be created to assess offshore bathymetry and the sedimentary morphology of the coastal sector. A digital terrain model may identify possible volumes of sediment scoured or deposited within the Pukehina coastal sector. In turn this may be used to identify changes to offshore sedimentation patterns since data were obtained PHIZACKLEA (1993).

Assessment of the Waihi Estuary as a sediment sink of sediments from the adjacent coastline, and of Okurei Point for inhibiting sediment transport in the littoral drift system by providing a sheltering effect.

The influence of Waihi Estuary on the sedimentary morphodynamics of the Bay of Plenty littoral system has not been previously investigated. PHIZACKLEA (1993) suggested that Waihi Estuary acted as a sediment sink. By analysing the estuarine hydrodynamics and sediment characteristics of Waihi Estuary, assessment of whether sediment in the littoral drift system is being deposited within the Waihi Estuary may be made.

Ascertain the importance of wave energy focussing leading to localised enhanced dune retreat at the eroded sectors of the Pukehina coastline.

The effects of wave energy focussing due to wave refraction, which have been outlined by HEALY (1987) along the Bay of Plenty coastline and have been examined briefly by HAY (1991)have not been investigated for the Pukehina region.
PHIZACKLEA (1993) identified from side scan sonagraphs, the presence of rock outcrops in the vicinity of Okurei Point and Pukehina Redoubt. The possibility of wave refraction induced by these outcrops may be identified, thereby inducing wave energy focusing upon the Pukehina shoreline.

Estimation of the net littoral drift direction and sediment transport rates within the Pukehina coastal sector by construction of an integrated sediment budget, from which, significant processes inducing sediment loss within the sector may be identified.

Studies of the littoral drift system within the Pukehina coastal sector have often been conflicting. WILLIAMS (1985) and PHIZACKLEA (1993) suggest that the direction of littoral drift is bi-directional in the region, while studies by HEALY *et al.* (1977) and HODGES AND DEELY (1997) indicated a net littoral drift direction towards the southeast. In comparison, SMITH *et al.* (1997) and SMITH (1999) perceived the net littoral drift direction to be towards the northwest. The main reasons for these different conclusions probably revolve around the absence or presence of geomorphic indicators.
Utilising the numerical model WBEND (BLACK AND ROSENBERG, 1992), sediment transport directions and approximations of suspended sediment concentrations may be obtained. These can be assessed against previously collected information (PHIZACKLEA, 1993). From obtained and existing data, an integrated sediment budget may be collated to identify net sediment transfer rates for the Pukehina coastal sector. Processes inducing significant sediment loss may be identified from the integrated sediment budget.

Review cyclic ocean-atmosphere interactions, and identify whether climatic processes influence the available sediment supply to Pukehina Beach.

With the use of both historical beach profile data collected by PHIZACKLEA (1993), Environment Bay of Plenty and current beach profile data, erosive and depositional sedimentary cycles may be assessed. From available climate data, climatic influences such as El Niño Southern Oscillation (ENSO) cycles and Inter-decadal Pacific Oscillation (IPO) may be identified to see if they influence erosional cycles upon the Pukehina shoreline.

Suggest possible remedial solutions for the eroded sector of Pukehina Beach.

After investigating possible explanations as to why Pukehina Beach may be undergoing cyclic patterns of erosion and accretion, possible remedial solutions may be suggested to reduce the likelihood of further dune retreat.

1.4 Thesis Structure

Chapter 2 describes the geological setting in which the Pukehina region lies, and also provides an introduction to the environmental setting. Historical wind and wave climate data are also discussed.

Chapter 3 consists of an investigation of the nearshore/shoreface morphology of the Pukehina coastal sector. With the use of relevant side scan sonar data and the creation of a digital terrain model, analysis of areas where sediment accumulation or scour are occurring is assessed.

Chapter 4 focuses on the relevance of the Waihi Estuary to the coastal sediment budget. By analysing the hydrodynamics and sedimentology of the estuary, with the use of

directional current meters, pressure sensors and estuarine cores, conclusions may be made as to whether Waihi Estuary is acting as a sediment sink.

Wave energy focussing due to the refraction of waves by the submarine topography is investigated in chapter 5. This is analysed by the use of a wave refraction model, WBEND. The model is introduced and results gathered using a variety of scenarios. From wave direction results, an attempt to assess the possibility of Okurei Point inhibiting longshore sediment transport may be made.

Sediment budgets for the Pukehina region and the possibility that climatic influences cause the cyclic erosion, are examined in chapter 6. By the calculation of sediment inputs, outputs and transfers data, as well as analysing obtained and existing current beach profile data, a conceptual model of the sediment transport dynamics is proposed for the Pukehina region.

Main summaries and conclusions from this thesis are discussed in chapter 7, followed by ideas of potential remedial solutions to reduce or restrict ongoing long-term frontal dune retreat at Pukehina Beach.

1.5 Previous Work Relevant to Beach Erosion at Pukehina Beach

Research of the Bay of Plenty beaches has focussed mainly on sedimentary processes, while studies of sediment morphodynamics in the Pukehina region have been limited. PHIZACKLEA (1993) investigated littoral sediment budgets and beach morphodynamics from Pukehina through to Matata as part of an MSc thesis. He suggested that the littoral drift pattern for the region is bi-directional, with a north-westerly net littoral drift occurring at Pukehina Spit and a south-easterly net littoral drift occurring between Otamarakau and Matata.

HEALY *et al.* (1977) assessed beach erosion within the Bay of Plenty coastal region. Included was an analysis of the Pukehina coastal sector, which was described as being in

an erosive state. Further, HEALY (1978a) analysed changes to beach profiles within the Bay of Plenty. In regard to Pukehina, HEALY (1978a) measured beach profiles quasi-monthly, during the year 1977 at Benchmark 27, located at Pukehina East. Results indicated that a accretionary berm developed seasonally, and accretion also occurred above the scarp in the toe of the frontal dune, but otherwise little change was measured over the year (HEALY, 1978a).

HEALY (1978b) investigated nearshore bar formations within the Bay of Plenty. In regard to Pukehina, he noted the presence of multiple offshore bars at Pukehina East (benchmark 27). At Pukehina East, a well-developed swash bar and a poorly developed offshore bar was illustrated, while elsewhere within the Pukehina coastal sector, very poor bar development was present, if any.

Reports by SMITH *et al.* (1997) and SMITH (1999) investigate the sustainability of sand mining at Otamarakau. A compilation of local geology, offshore sediment and coastal stability data collected by SMITH *et al.* (1997) and SMITH (1999) are included in each report. TONKIN AND TAYLOR LIMITED (1999) respond to a resource consent application by J.W. Paterson and Son, in regard to mining of beach sand from Otamarakau Beach. The report includes a constructed sediment budget for Otamarakau Beach, littoral drift analysis, and effects of mining within the coastal sector. Similar to this appraisal, PHIZACKLEA (1999) details an overall synopsis of mining issues related to the coastal sector. Influences that mining generate to affect the Pukehina coastline are also discussed.

Environment Bay of Plenty currently survey beach profiles at 44 sites, four times a year along the Bay of Plenty coast, extending from Waihi Beach to the Tarawera River mouth. Particularly, intense beach profiling is conducted at Otamarakau due to the strict restrictions on sand mining in this area.

Investigations of the neighbouring Maketu Estuary by BURTON (1987) and DOMIJAN *et al.* (1997), and DOMIJAN (2000) may be used to compare with results obtained from Waihi Estuary, due to similar physical characteristics (both are 'perched' estuaries and have

similar tidal amplitudes). DOMIJAN (2000) analysed the hydrodynamic and estuarine physics of Maketu Estuary, while BURTON (1987) studied the tidal hydraulics and stability of the Maketu Estuary.

Chapter Two
Environmental Processes Influencing Sediment Budget

2.0 Introduction

Major physical factors that influence the sediment budget and beach erosion of Pukehina Beach, may potentially be linked from geological and atmospheric effects. In this chapter, a review of the literature is discussed, focusing on local geology, river catchment geology, wind and wave climates, tropical cyclones and storm surges, as these affect the coastal erosion processes as summarised.

Figure 2.1 illustrates locations referred to in this chapter, which may influence the sediment budget of Pukehina Beach, or are locations of previous nearby research, which have similar characteristics to Pukehina Beach.

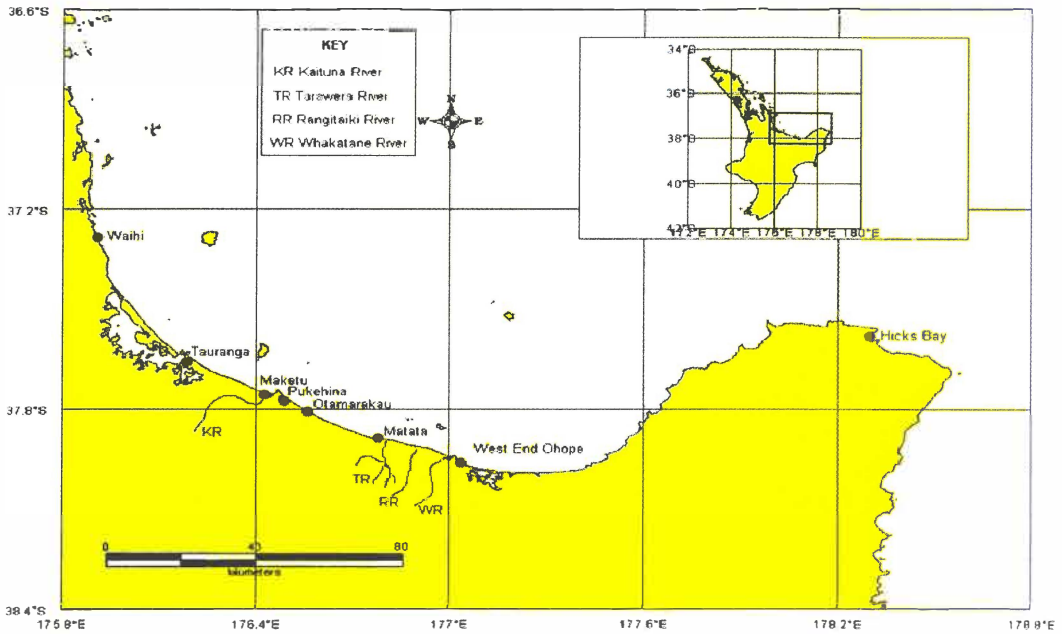

Figure 2.1 Locations referred to in this chapter that may influence the sediment budget of Pukehina Beach or where nearby investigations are of similar characteristics to Pukehina Beach.

2.1 Geology of Bay of Plenty

Eroded catchment material may provide a substantial quantity of sediment to the beach system by means of littoral transport, stream and river networks (KOMAR, 1998). Investigating textural characteristics of sediments from the surrounding catchments may indicate whether or not these areas are the provenance of sediments delivered to Pukehina Beach.

2.1.1 Local Geology

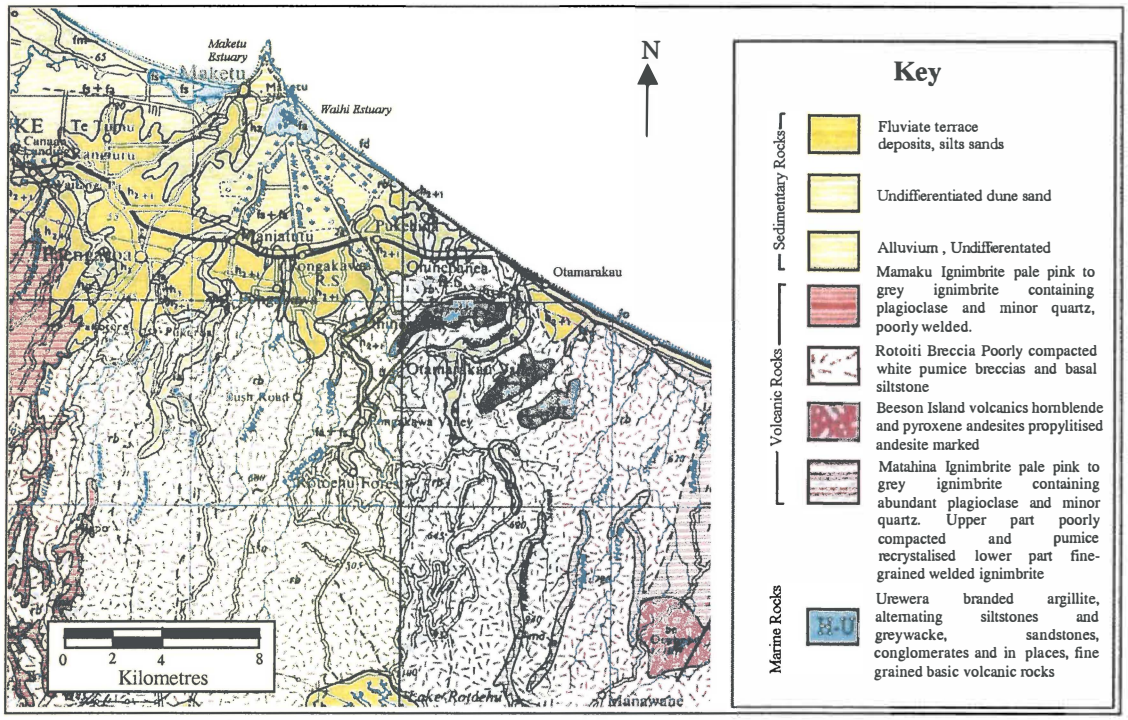

Figure 2.2 Geology of the Pukehina-Otamarakau region. Common geology is Rotoiti Breccia, alluvium, and varieties of Ignimbrite. Most rock types have been identified as provenance of sediment along Pukehina Beach via river and stream networks (NAIRN, 1975; PHIZACKLEA (1993)). Figure adapted from HEALY *et al.*, 1964

WEHRMANN (2000) studied the geology of the Okurei Point as part of an MSc project.

She described Okurei Point as comprised of mid Pleistocene fluvial and volcaniclastic silts, sands, gravels and conglomerates covered by late Quarternary tephras and

palaeosols. Surrounding lowland areas consist of Holocene peats, swamps and ancient dune sands.

Two main components of Okurei Point that are visually seen to be actively eroding are: the Little Waihi Formation and the Newdicks Member. These may be potential sources of sediment to the Pukehina coastal sector sediment budget.

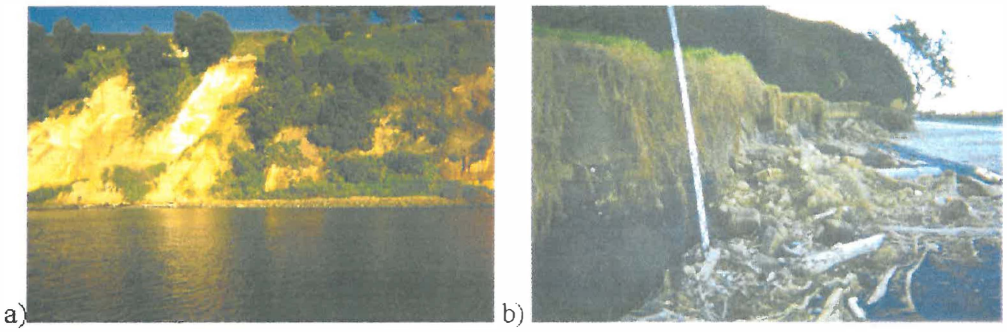

Figure 2.3. Existing active erosion of the local catchment a) Eastern side of Okurei Point b) Holocene dune at Newdicks Beach.

The Little Waihi Formation consists of pale yellow pumiceous fluvial sands and gravels, with grain size diameters ranging from 10 mm to a maximum of 30 mm. Rare angular clasts of ignimbrite and rhyolite are also present with grain size up to 10 mm diameter (WEHRMANN, 2000). Undifferentiated white siltstone forms the lowermost unit of the Little Waihi formation, which at Okurei Point is exposed at mean sea level. The formation also occurs horizontally at 10 m elevation east and west of and at Newdicks Beach (WEHRMANN, 2000).

The Newdicks Member occurs extensively around the Okurei Point, however, it is not seen at Pukehina or inland. The main unit is composed of a multilithologic conglomerate set in a matrix of coarse sands and gravels. Sorting is very poor, with boulders up to 5m in diameter set in a pumiceous sandy-gravel matrix. The matrix is depleted of fine sediments and consists of angular particles (WEHRMANN, 2000).

PHIZACKLEA (1993) estimated that cliffs of Okurei Point are eroding at an annual rate of 5.47 mm per year, or approximately 30 m^3 per year over the entire coastal cliffs at Okurei Point, is available to the Pukehina sediment budget. However, this estimate is conflicting, as PHIZACKLEA's (1993) estimate was based on research undertaken by GORDON (1993) of the Waitemata formation, which he regarded as similar structural lithology (PHIZACKLEA, 1993). However, from investigations by MOON AND HEALY (1994) of the Waitemata formation, structural lithology is not comparable between the two formations, therefore PHIZACKLEA's (1993) estimate is incorrect.

The rate of erosion of the Okurei Point cliffs was estimated using available historical aerial photographs taken in 1943, 1981, and 1993. Ground truthing was used to geo-reference (using MapInfo Professional Version 6.0 *) the aerial photographs against existing beach survey benchmarks and fixed points of known locations, such as the Pukehina Spit slipway. The location of fixed point were important when geo-referencing the 1943 survey, as there were no benchmarks.

By measuring the distance of cliff erosion between aerial photographs taken in 1943, 1981, and 1993, and subsequently divided by period of time between each aerial survey. The rate of cliff retreat was found to be relatively constant between years 1993 and 1943 and was estimated as 9.33 mm/year or 59 m^3/year from the entire coastal cliff length.

Since similar geology is apparent at Pukehina Redoubt (figure 2.2), the same estimate of cliff retreat can also be applied (9.33 mm/year), from which an estimate of 8 m^3/year was obtained.

* MapInfo Professional Version 6.0 by MapInfo Corporation, 1985

2.1.2 Geology of Local Rivers and their Catchments

Fluvial sediments discharged from river mouths within the study region are primarily sourced from the Taupo Volcanic Zone (TVZ), in particular the Okataina Volcanic centre. PHIZACKLEA (1993) and SMITH (1997) also report Urewera greywacke outcrops in the vicinity of Otamarakau, which are observed as beach sediment and occasionally deposited in the headwaters of the Hauone and Waitahanui streams.

Mineralogy of sediment load from rivers, reflect the regions from which they were derived. Common minerals discharged from local rivers are: quartz, feldspar and volcanic glass. Heavy minerals such as hypersthene, augite, hornblende, cummingtonite and titanomagnetite are also present as fluvial discharge sediments as noted by MURRAY (1978) and PHIZACKLEA (1993).

HEALY (1978c) analysed the textural and mineralogical characteristics of sediments from the foreshore of the Rangitaiki Plains and the Tarawera, Rangitaiki and Whakatane Rivers. Results indicated that sediments from each of these rivers contribute to the littoral system of the Bay of Plenty. The Kaituna River likewise, provides sediment to the Bay of Plenty littoral system but not, however, to the same quantities as the preceding three, as illustrated by figure 2.4 (source: NIWA, 2001).

This chapter will only discuss the Kaituna and Tarawera rivers. HEALY *et al.* (1977) and WILLIAMS (1985) suggest that even though the Whakatane and Rangitaiki rivers provide substantial sediment to the Bay of Plenty littoral system, they are unlikely to contribute significantly to the Pukehina coastal sector sediment budget due to the net eastwards littoral drift in that sector.

2.1.2.1 Potential Littoral Sediment Input from the Kaituna River / Maketu Estuary

The Kaituna River catchment covers 1284 km^2. Active erosion within the catchment, has been implicated to changes in land use, high intensity rainstorms and the erodible nature of the volcanic soils and some of the underlying rock types, particularly volcanic breccias (NAIRN, 1975). Terrace and fan deposits composed of silts, sands, gravels, redeposited Rotoiti breccia, rhyolite and ignimbrite form the majority of the lower Kaituna catchment. The terrace deposits are classified as unstable sediments due to weak compaction (NAIRN, 1975). Consequently a high percentage of the Kaituna River sediment load may be obtained from these sediments.

MURRAY (1978) analysed estuarine sediment from Maketu Estuary. His mineral analysis indicated that collected sediment samples comprised of volcanic glass, quartz, plagioclase, and of a lesser amount, hornblende, augite and hypersthene. MURRAY (1978) attributes glass, pumice rich sediments to cliff erosion from Okurei Point. BURTON (1987) reported that offshore from Maketu Estuary, sediments comprise quartz, other terrigenous rock fragments, pumice, and shell hash, which have some similarity (excluding shell hash) to Kaituna River sediments, as previously suggested by NAIRN (1975).

2.1.2.2 Potential Littoral Sediment Input from the Tarawera River

The Tarawera River catchment covers 984 km^2 and is bounded by a mountainous region. The upper catchment contains Lake Tarawera and associated lakes that feed into Tarawera River. HEALY (1978c) identified that the Tarawera River is a major supplier to the littoral sedimentary system. Glass, alkaline feldspar, rock fragments and pumice are the predominant sediments discharged.

Figure 2.4 illustrates annual mean suspended sediment discharged (tonnes/year) from the Tarawera and Kaituna rivers during the period 1954-1991. Measurements were obtained from the National Institute of Water and Atmospheric Research (NIWA). The Tarawera

and Kaituna rivers were measured at Awakaponga and Te Matai respectively. Awakaponga is approximately 1 km south from the mouth of the Tarawera River, while Te Matai is approximately 4~5 km southwest from Maketu Estuary inlet. Sediment abrasion, particularly applicable to pumiceous sediment, may induce higher sediment loads, therefore, the quantity of sediment actually discharged from each river is unknown. Sediment abrasion causes the formation of smaller grainsizes, which can be held in suspension for a longer period of time due to their lighter density and possible planar shape (BRUUN, 1978). Therefore sediment discharged from both the Tarawera and Kaituna rivers may be higher than figure 2.4 suggests.

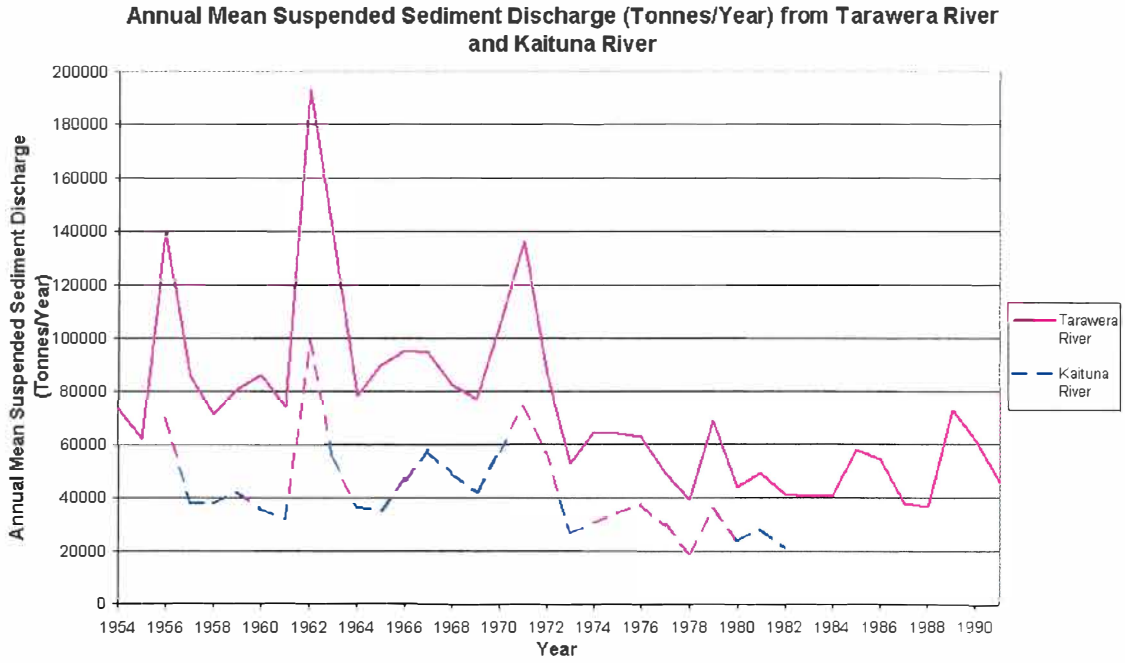

Figure 2.4 Annual mean suspended sediment discharge (tonnes/year) from Tarawera River and Kaituna River from 1954-1991, measurements taken at Awakaponga and Te Matai respectively (Data provided by NIWA, 2001).

Significantly larger suspended sediment discharges were recorded in years 1956, 1962 and 1971. A possible explanation could be afforestation, as Tasman Forestry began large-scale afforestation of *Pinus radiata* in 1962, but heaviest planting occurred between 1969 and 1975 (PANG, 1993). These dates of afforestation coincide with largest suspended sediment discharges from Tarawera River. The use of heavy machinery to enable plantation of vegetation, therefore, may have produced increased suspended

sedimentation discharge from Tarawera River. Tasman Forestry also includes part of the Kaituna catchment, therefore, afforestation may likely be implicated to increased sediment discharged from the Kaituna River as well.

2.1.2.3 Potential Littoral Sediment Input from the Streams within Pukehina-Matata Coastal Sector

Four streams, which may provide sediment to the Pukehina coastal sector, are the Pikowai, Hauone, Waitahanui and Herepuru streams (figure 2.5 and figure 2.6).

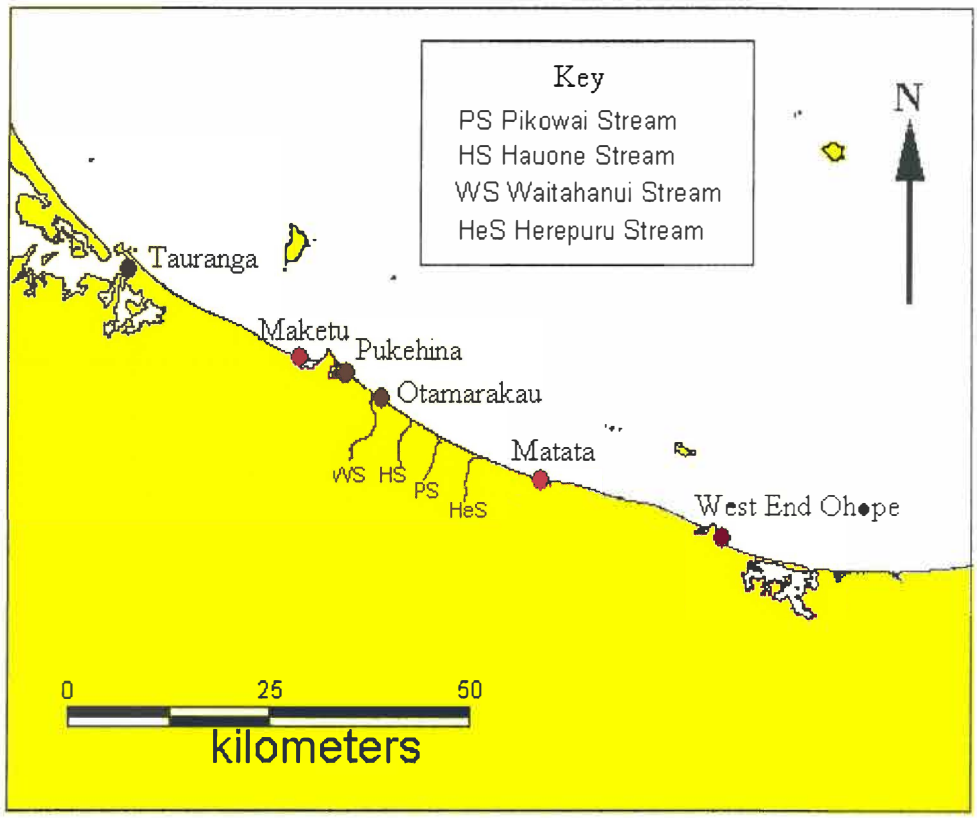

Figure 2.5 Location map of Pikowai, Hauone, Waitahanui and Herepuru streams.

All streams are classified as 'beach impounded' systems, meaning that the inlets are subject to blocking by beach berm formation, allowing streams to migrate up and down the beach (BOPRC, 1991). Stream offset has been suggested by KOMAR (1998) to be

controlled by: wave angle approach, driving littoral drift, high littoral drift volumes, and a well developed berm with an accreting beach system.

Waitahanui Stream has the greatest discharge, whilst Hauone Stream has the least. Hauone Stream has been completely beach impounded or cut off from the coast on at least two occasions (September 1943 and April 1993) (SMITH, 1997).

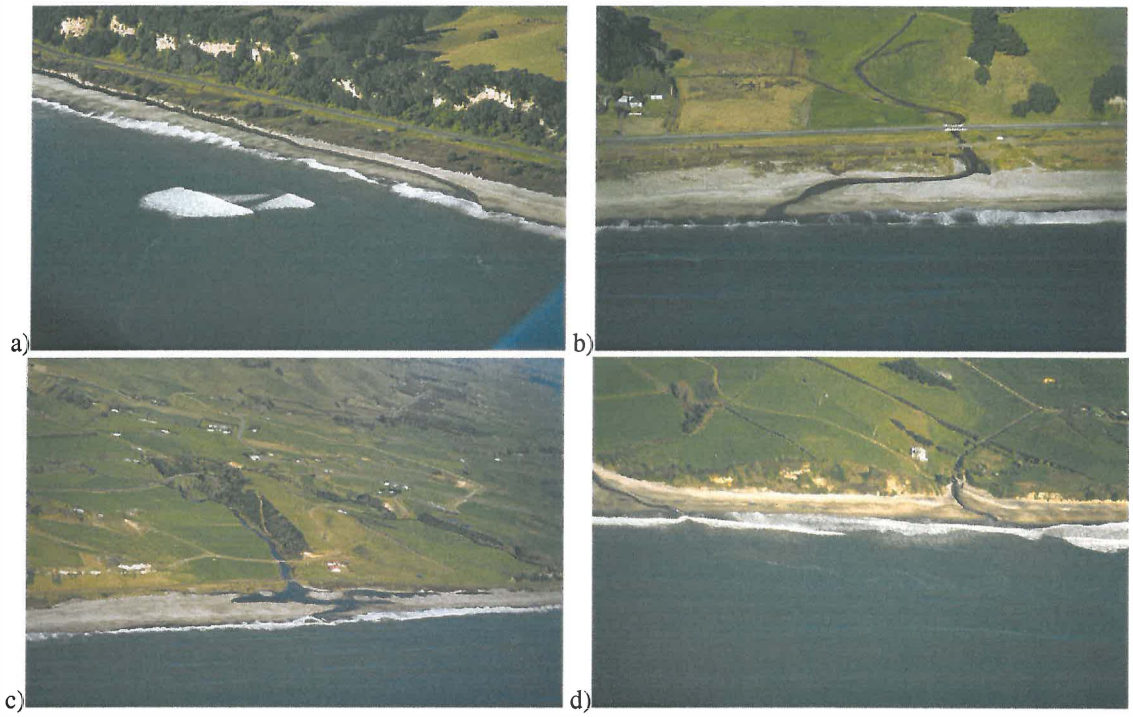

Figure 2.6. Streams that may supply sediment to the Pukehina coastal sector a) Pikowai Stream b) Hauone Stream c) Waitahanui Stream d) Herepuru/Mimihia Streams, (Herepuru Stream on the right). Note differing stream orientations, possibly due to differing parameters influencing orientation, as discussed. East is to the left of each photograph. (Photographs taken by author 12/8/2001).

Sediment composition of the lower reaches of the streams are typical of low gradient streams with a pasture-dominated catchment, with discharged sediments commonly sand and silt sized particles (SMITH *et al.*, 1997). Mineralogy of sediments discharged from each stream is dependent on its associated catchment geology. Common minerals discharged are: quartz, alkaline feldspar, pumice, volcanic glass, rock fragments and of

less abundance plagioclase, hornblende, hypersthene, augite, cummingtonite and other opaque minerals (PHIZACKLEA, 1993).

Investigations by SMITH *et al.* (1997), of the Pikowai, Hauone and Waitahanui Streams in an application for resource consent for sand extraction at Otamarakau, described the three streams with the following morphology.

> 'The Hauone, like the Pikowai, had a very shallow oxygenated layer and a deep deposit of fine sediments, including a lot of pumice sand. Between two surveys the particle size in the Hauone Stream increased. The coarser substrate in the Hauone Stream appeared to coincide with a widening in its exit channel through the beach to the sea, as seen in the Pikowai. The larger, faster flowing Waitahanui Stream had the coarsest sediment distribution within the main channel, consisting mostly of sand. No major changes in channel morphology or substrate composition were noted at this stream' (SMITH *et al.*, 1997, pp 48-49).

2.1.2.4 Waihi Estuary

The Waihi Estuary catchment is located between the Rotorua lakes and the adjacent Bay of Plenty coast. Four fluvial systems drain the catchment, these being the Kaikokopu, Wharere and Pongakawa streams, and the Pukehina Canal. The Kaikokopu, Wharere and Pongakawa streams drain the majority of the catchment, while the Pukehina Canal drains the existing coastal dunes and remanent coastal terraces.

Basement geology of the catchment is comprised of Rotoiti Breccia, which is a pumiceous pyroclastic flow. The mineralogy of this deposit is glass, feldspar and other rock fragments (HALL *et al.*, 1993). PHIZACKLEA (1993) identified minerals from samples taken from all streams. Common minerals discharged from the streams include: pyroxene material (feldspar), glass, quartz, pumice, rock fragments, hypersthene and lesser amounts of augite, green hornblende, cummingtonite and opaque minerals.

Currently no data are available on sediment load discharges from these streams into the Waihi Estuary. HALL *et al.* (1993), however, investigated the sediment transport capabilities of Kaikokopu and Pongakawa streams. The Kaikokopu, Wharere and Pongakawa streams currently require excavation of sands and silts on a three-yearly cycle due to sedimentation in the lower reaches of the streams. Extraction of the streams is an on going controversial issue among local Pukehina inhabitants (D.Gordon, EBOP, *pers comm.*), as they believe extraction is reducing the potential for sediment to alleviate erosion currently occurring at Pukehina Beach.

Samples taken from Kaikokopu and Pongakawa streams indicated that the material was generally well-sorted, rounded material with particle sizes ranging from fine sand (0.1 mm diameter) to fine gravel (8 mm diameter). HALL *et al.* (1993) calculated from water discharge and sediment characteristic results, that stress exerted on the sediment to induce entrainment, was well below the critical tractive stress. Therefore, sediment transport is limited at the lower reaches of the streams. In flood events, water flows would be expected to increase, therefore, there would be potential for the critical stress level being exceeded, subsequently enabling sediment transport into the estuary.

2.2 Wind Climate of the Bay of Plenty and Implications it has Towards Coastal Erosion at Pukehina Beach

HEALY (1980, p. 13) states that erosion and accretion patterns occur naturally within the Bay of Plenty, and are dependent on seasonal and meteorological (including wind) conditions. HAY *et al.* (1991) also suggest that wind climate within the Bay of Plenty region is a critical parameter of coastal erosion rates within the region.

DE LISLE and KERR (1963) and QUAYLE (1984) have investigated weather and climate of the Bay of Plenty region. They both suggest that mountain ranges surrounding the Bay of Plenty provide a sheltering effect from the predominant westerly winds. However, the region is exposed in the northerly and north-easterly direction.

Airstreams from the north and northeast derive from the warm Pacific Ocean typically have long trajectories. This airflow once reaching the Bay of Plenty coastline causes humid conditions and often produces heavy rain (QUAYLE, 1984). Other airstreams that influence the climate of the Bay of Plenty are from the south to southeast. South to southeast airstreams normally produce rain on Bay of Plenty's surrounding ranges but bring dry weather over the low lying regions (QUAYLE, 1984).

Wind data relevant to the coastal processes in the Bay of Plenty are obtainable from shipping reports. BRENSTRUM (1994) investigated spatial and temporal variations of coastal winds around New Zealand from automatic weather stations onboard research vessels. Results indicate that offshore sea winds are generally stronger than winds recorded from adjacent land stations. Friction, damming, position of the lee trough of frontal systems and topographic channelling are commonly the causes for these differences. An example of this difference was recorded at Hicks Bay on the East Cape of the North Island. Recordings from the research vessel were 30 – 45 knots while simultaneous recordings from Whakatane Airport and Mahia Peninsula (closest land based stations) indicated a wind speed of only 10 – 15 knots (BRENSTRUM, 1994). Therefore relating land based coastal wind records to wave generating processes may not be representative.

HAY (1991) and HAY *et al.* (1991) created an extensive storm database for the western Bay of Plenty, by analysing historical newspaper records from 1873 to 1990. From such a database, it is possible to assess historical wave events and interpret if such events were

implicated by of the El Niño Southern Oscillation (ENSO), and/or other ocean-atmospheric cyclic patterns, such as the Inter-decadal Pacific Oscillation (IPO).

Mean annual frequency of wind speed and direction for the Bay of Plenty over a 41 year period, is illustrated in figure 2.7. From figure 2.7, northwest airstreams are dominant at Whakatane Airport, while west to southwesterly airstreams are illustrated to be predominant at Tauranga Airport. Since wind climate within the Bay of Plenty region was suggested to be a critical parameter of coastal erosion rates within the region (HEALY, 1980; HAY, 1991), data from QUAYLE (1984) may suggest that Tauranga is more inclined to erosion than Whakatane. Tauranga's predominant winds are onshore, therefore, larger waves would be expected, while Whakatane's predominant winds are offshore, therefore small waves would be observed.

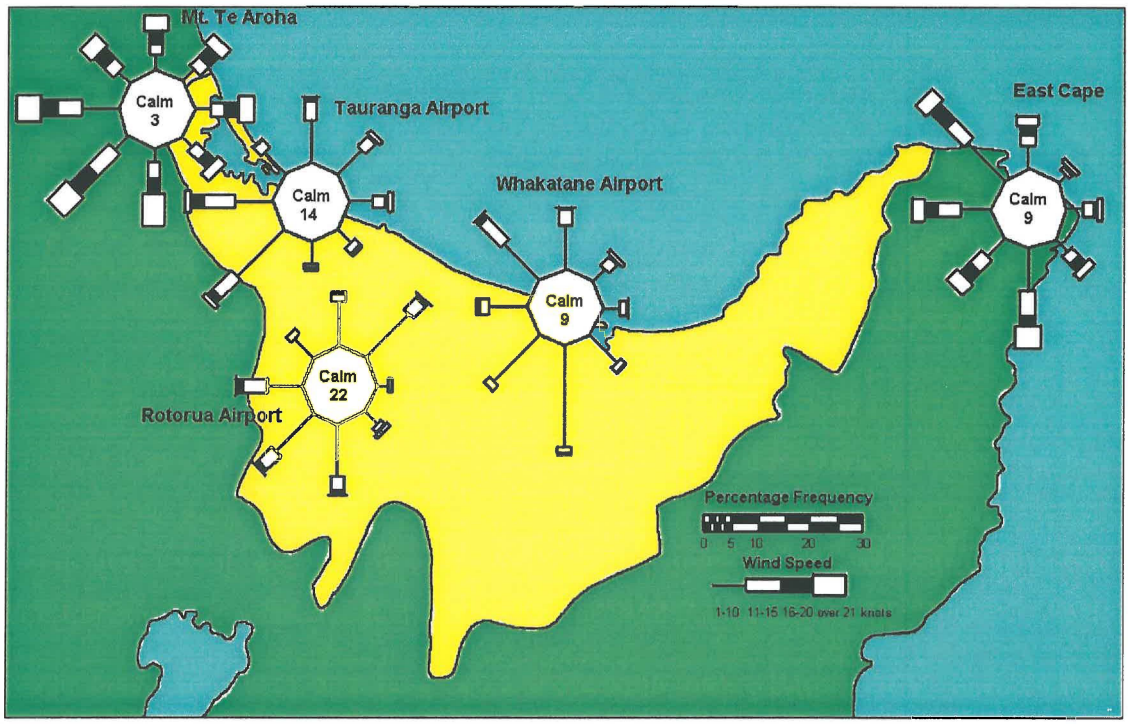

Figure 2.7 Mean annual frequency of wind speed and direction, calculated from data collected 1942 to 1983: Source (QUAYLE, 1984).

The El Niño Southern Oscillation (ENSO) is a fluctuation of intertropical pressure, wind, sea surface temperature, rainfall and an exchange of air between the south-east Pacific subtropical high and the Indonesian equatorial low (STURMAN AND TAPPER, 1996).

The El Niño phase affects New Zealand wind climate by creating more persistent westerly and south-westerly winds. This is associated with widespread rainfall over much of the equatorial east Pacific. In regard to New Zealand, increased precipitation over western ranges is a common occurrence. Tropical cyclone activity tends to generate to the north-east of their average locations, in the south-western Pacific (ALLAN *et al.*, 1996). La Niña phases are associated with a strengthening of the tropical Pacific easterlies and a weakening of circumpolar westerlies (HAY, 1991). Impacts of La Niña are the opposite of the El Niño phase. During the La Niña phase, wet conditions are experienced in northeast Australia, while central to eastern equatorial Pacific experiences low rainfall, and during the El Niño phase vice versa is observed (ALLAN *et al.*, 1996).

El Niño and La Niña may impact beach processes at Pukehina Beach. DE LANGE (1996) states that north eastern New Zealand is expected to experience higher sea levels and more erosion during the La Niña phase than the El Niño phase, because of predominant onshore winds. These are investigated in chapter 6.

2.3 Wave Climate of the Bay of Plenty

HEALY *et al.* (1977), described the Bay of Plenty wave climate as " A mild meso-energy swell environment with an offshore significant wave height of approximately 1.5 m and a nearshore significant wave height of 0.6 m. Refraction over the twenty kilometre continental shelf tends to modify the wave angle approach so that the waves become aligned near normal to the shoreline, with some refraction also occurring around offshore islands".

Sea and swell waves are greatly influenced by wind in the Bay of Plenty. Large swell waves are less frequent due to the Bay of Plenty embayment, sheltering large waves from

the north to southeast quadrants. The Bay of Plenty is also protected from cold ocean currents induced by the prevailing westerly wind, but it is influenced by the warm East Auckland Current, which travels around the north of the North Island and down the east coast (QUAYLE, 1984).

SAUNDERS (1999) measured offshore and nearshore wave data at West End Ohope beach at water depths 30 m and 10 m respectively. S4ADW (nearshore) and S4DW (offshore) electromagnetic current and wave meters, were used in multiple deployments to obtain data for approximately 200 days at different seasons throughout a year (6/12/97-20/2/98, 20/7/98- 20/8/98, and 9/9/98-9/11/98). Results obtained indicated that offshore significant wave heights were larger during winter (H_s = 0.81 m ± 0.24 m), and larger wave events were more variable in frequency and duration than over the summer (H_s = 1.09 m ± 0.63 m). Mean significant wave height at the nearshore was very similar for both seasons, but during summer wave conditions were more variable.

Significant wave period offshore of West End Ohope was typically 8 s during both seasons, but maximum significant wave period over summer was 16 s compared to the maximum winter significant wave period of 11 s. SAUNDERS (1999) attributes this to the influence of local winds on wave generation during the winter period.

Nearshore wave period varied between the seasons. During the summer deployment (December 1997-Febuary 1998), SAUNDERS (1999) recorded a significant wave period of 9 s, while during spring a 7 s significant wave period was recorded. A smaller variability in maximum wave period compared with offshore data was also observed, 15 s and 12 s for summer and spring respectively, suggesting that the local winds generate the largest waves off the beach (SAUNDERS, 1999).

PHIZACKLEA's (1993) study of beach morphodynamics of the coastal sector between Pukehina and Matata included deployment of a S4DW current meter from 16 July to 25

August 1993, at the southeastern end of Pukehina Spit. PHIZACKLEA (1993, pp. 226-227) states an mean average wave height was 0.64 m and average wave period was 6.36 s, was recorded during the deployment period. Maximum conditions were H_s= 2.79 m and T_s= 11.13 s. Average wave direction over this period of time was 12° True. Conclusions from this deployment suggested that wind-driven circulation predominated on the Pukehina nearshore and inner shelf regions over this time.

DE LANGE (1991) reviewed wave data collected over the period 1989-1991 at Tauranga. Data were collected from A Beacon at the entrance to Tauranga Harbour from a pressure transducer situated in 13 m water depth. Results showed a persistent oceanic swell with a mean height of 0.3 m and a period of 12-16 s.

QUAYLE's 1984 dataset of 41 years of wind records is used for relating coastal processes along Pukehina Beach. Indications of coastal processes such as: direction of stream offset and the cause of opposing direction alignment of Pukehina Spit and Maketu Spit either side of Okurei Point. Long-term wave power may provide explanations to these open questions. KOMAR, (1976, p. 86) states that the 'total energy in a fully developed sea is being proportional to the fifth power of the wind speed'. Since regional Bay of Plenty data may not generate a fully developed sea, the long-term wave power is therefore only an indication of wave power.

Using wind direction vectors at Tauranga and Whakatane Airports, from figure 2.7, resultant vectors are calculated from onshore winds at each location (offshore winds are disregarded as these will not implicate wave generation, thereby influencing spit and stream orientation). The resultant vector provides an indication of the direction of application of the long-term wave power. Resultant vectors for both Tauranga and Whakatane Airports are used, in order to predict long-term wave power within the Pukehina coastal sector.

Long-term wave power calculated from wind data at both Tauranga and Whakatane Airports, indicate resultant vectors in a north northeasterly direction (24° Tauranga Airport and 22° Whakatane Airport). Directions of resultant vectors of long-term wave power, in terms of shoreline orientation, suggest that net littoral drift at Tauranga is slightly to the east, while at Whakatane, littoral drift is difficult to distinguish, as the resultant vector is perpendicular to the shoreline. However, by applying the same resultant vector directions from Tauranga and Whakatane Airports to Pukehina Beach, a possible net littoral drift direction to the east is identified.

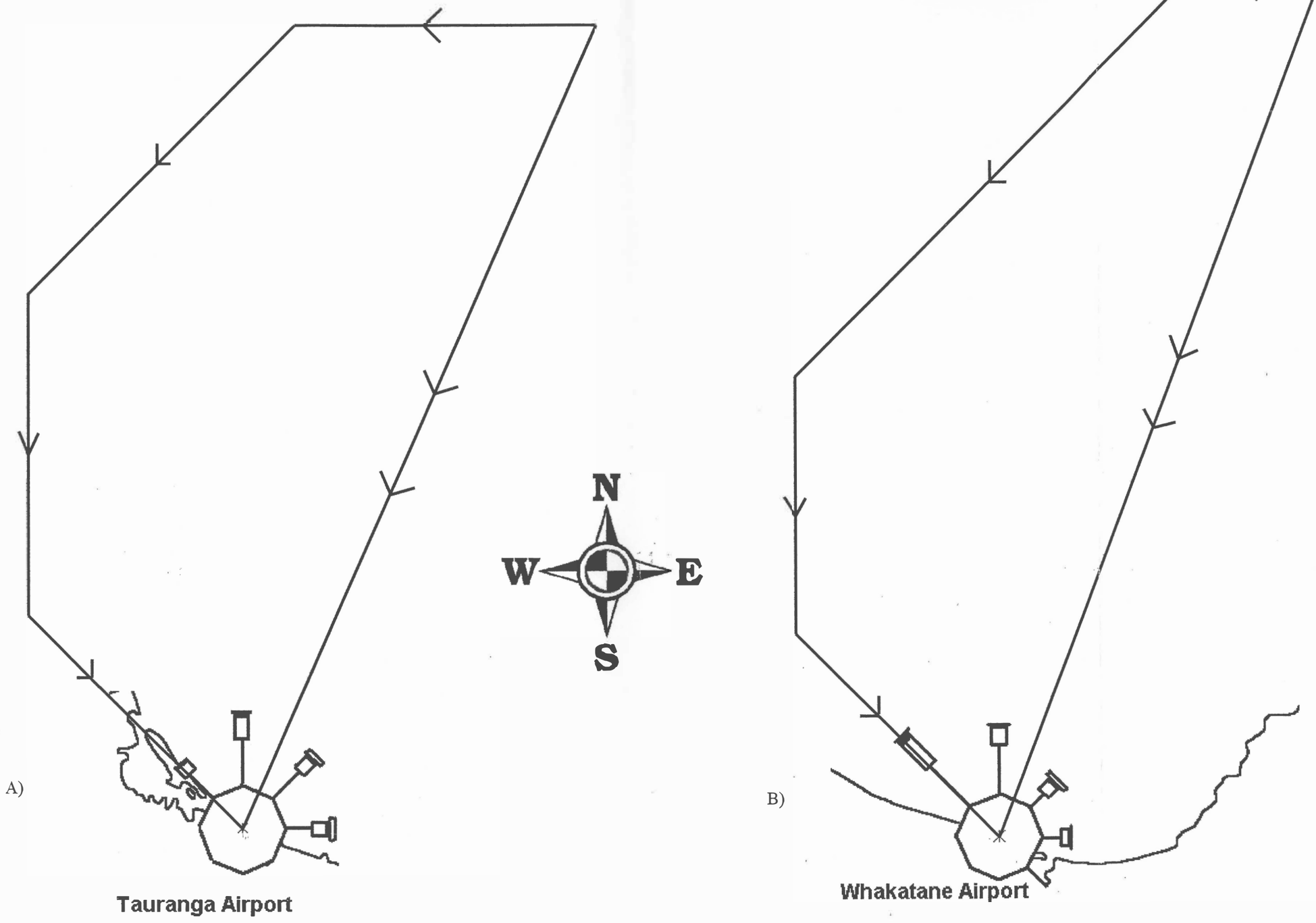

Figure 2.8 Resultant vectors of long-term wave power at A) Tauranga Airport and B) Whakatane Airport, as calculated by long-term wind data from QUAYLE (1984).

2.4 Tropical Cyclones and Storms

HAY (1991) examined historic storm events within the Bay of Plenty wave climate. A total of 153 storms were recorded from 1873 to 1990, comprising 53 Tasman depressions, 13 tropical cyclones, 11 occluded fronts and 94 unclassified storms. Using assumptions from recorded wind speeds, he concluded that the Bay of Plenty may experience a grade 9 (strong gale, 75-88 $kmhr^{-1}$) storm can be expected every 30 years, a grade 8 (gale, 62-74 $kmhr^{-1}$) every 14 years and a grade 7 (near gale, 50-61 $kmhr^{-1}$) every 0.71 years. Since erosion of the frontal dune at Pukehina Beach does occur during storm and cyclonic activity (figure 1.1 and PHIZACKLEA (1993)), knowledge of storm and tropical cyclone impacts on the beach is critical if potential remedial solutions are to be designed adequately to prevent frontal dune erosion. This will be further investigated in chapter 7.

2.4.1 Tropical Cyclones

A tropical cyclone is defined as a non-frontal, synoptic-scale, cyclonic rotational low-pressure system of tropical origin, in which 10 minute mean winds of at least $17.5ms^{-1}$ occur, and the belt of maximum winds are in the vicinity of the systems centre (STURMAN AND TAPPER, 1996). Tropical cyclonic activity is predominant throughout the months of November to April in the Bay of Plenty, but cyclonic events may occur at other times. New Zealand commonly experiences tropical cyclones at a rate of 2-3 per year (HARRIS, 1985). Trajectories of these cyclones commonly move northwest to southeast, passing the Bay of Plenty approximately 300 km offshore (HARRIS, 1985).

South Pacific tropical cyclones that affect the Bay of Plenty, typically originate north-east of the median position of 14°S and 170°E for a negative Southern Oscillation Index (SOI), and south-west of this position for a positive SOI (HAY, 1991). For a tropical cyclone to develop, sea surface temperature must be at least 26.5°C and remain greater than 20°C to maintain intensity. Therefore, a greater quantity of cyclonic events may be

experienced in the eastern Pacific regions during periods of El Niño, due to a band of anomalously warm water that develops across the central to eastern equatorial Pacific (ALLAN *et al.*, 1996).

2.4.2 Storm Surges

Enhanced aeolian transport of beach sediments and the formation of storm surges are the predominant ways in which the Bay of Plenty coastline recedes during cyclonic activity.

A positive storm surge is defined as a rise in mean water level, in addition to normal tidal variations (KOMAR, 1998). A storm surge is induced meteorologically by either a low atmospheric pressure system creating an inverse barometric effect, and/or by strong winds piling water up on the coast.

A low barometric pressure causes a higher sea level than a high barometric pressure system. In an ideal ocean, an adjustment of about ±0.01 m of mean sea waterlevel occurs for ±1 hPa change in pressure, with respect to the average barometric pressure over the New Zealand region of 1014 hPa (BELL AND GORING, 1996).

The influence of wind stress is harder to predict than that of pressure, as sea level at the coast will rise because of onshore wind stress until sufficient pressure is created to drive a return flow along the seabed. Friction from the seabed may reduce the bottom return current speed, resulting in a higher water level at the coast (Figure 2.9) (DE LANGE, 1996).

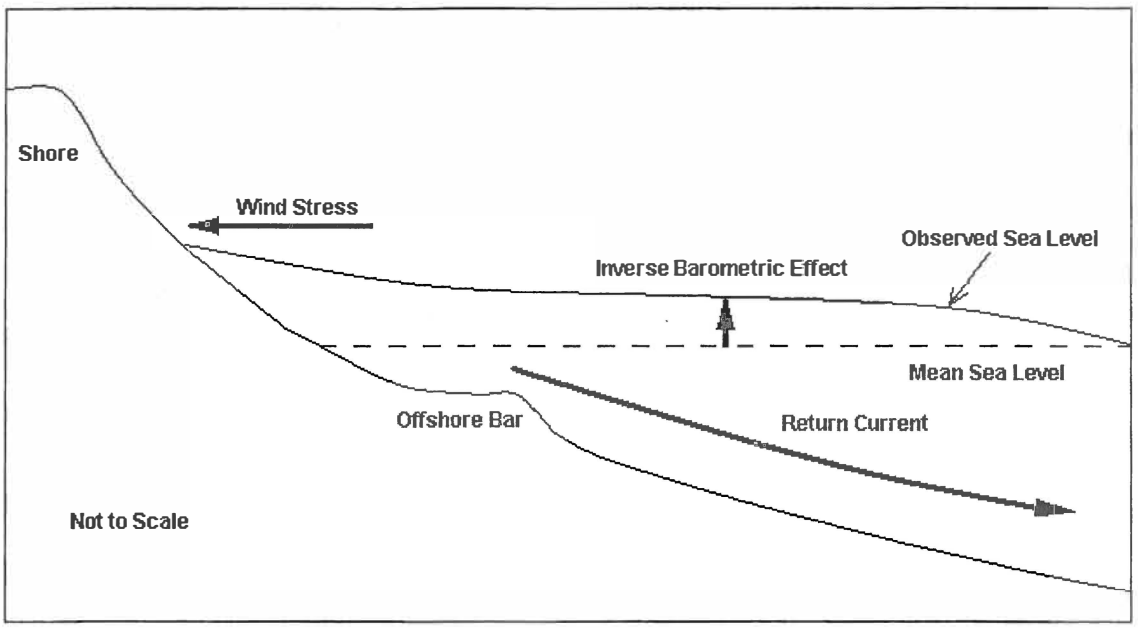

Figure 2.9 Components contributing to a storm surge. The wind stress component varies with water depth across the inner shelf, increasing with decreasing depth. The increased water level at the shore drives a return current near the seabed.

Erosion of the shoreline, particularly the frontal dune, may be severe during a storm surge event (DE LANGE, 1996). An increase of sea level will also increase wave run-up, thereby inducing a greater probability of the frontal dune being eroded.

Extra-tropical cyclones are associated with the largest storm surges, as recorded in Tauranga by DE LANGE AND GIBB (2000). Such events are characterised by central barometric pressures down to 960-980 hPa and sustained winds of 50-80 knots (DE LANGE AND GIBB, 2000). Wind direction also appears to have a major influence on the magnitude of storm surge at Bay of Plenty, as easterly winds were associated with the largest surge (546 mm recorded at Moturiki Island). While winds from the north, northeast, southeast and south produced small surges (in some cases negative value surges were recorded at Moturiki Island) (HAY, 1991).

Storm events within the Bay of Plenty region are usually 'duration limited' due to the constant movement of the storms (HARRIS, 1985). Thus, a storm of excessive wave

energy may not develop, as the duration required to generate large storm waves is insufficient. Durations recorded varied from 6 to 39 hours, with 63.6% of the storms having durations less than 12 hours, and 78.8% have durations less than 24 hours (HAY, 1991). From HAY (1991), cyclonic events in the Bay of Plenty cause rough to extremely rough seas and these have been associated with extensive erosion to dune faces, sand movement inland via wind erosion, and confinement of ships to ports.

2.5 Summary

The objective of this chapter was to identify and review the physical parameters that may influence the sediment budget of the Pukehina coastal sector. Parameters identified were:

- *Local geology*. Sediments of the surrounding region of the Pukehina coastal sector (particularly cliffs of Okurei Point and Pukehina Redoubt) are comprised of mid Pleistocene and volcaniclastic silts, sands, gravels and conglomerates covered by Quarternary tephras and paleosoles (WEHRMANN, 2000). Mineralogy of these sediments has not been identified. The rate of cliff retreat at Okurei Point, was found to be relatively constant between years 1993 and 1943 and was estimated as 9.33 mm/year or 59 m^3/year from the entire coastal cliff length. Utilising the same rate of cliff retreat at Pukehina Redoubt, an estimate of 8 m^3/year was provided.
- *River/Stream sediment discharges* of the Pukehina coastal sector commonly comprise quartz, alkaline feldspar, pumice, volcanic glass and rock fragments. Of less abundance are plagioclase, hornblende, hypersthene, augite, cummingtonite, titanomagnetite and other opaque minerals (PHIZACKLEA, 1993). The sediment budget of Pukehina Beach varies, due to volumes of sediment discharged by rivers, which is dependent on the vegetation present within the catchment, and also whether recent deforestation or afforestation has occurred. Sediment load discharged from streams entering the Waihi Estuary is suggested to be limited (HALL *et al.* 1993). Assessment of this statement will be examined in chapter 4.
- Localised *wind climate* is a critical parameter in alteration of erosion and accretion patterns within the Bay of Plenty. Wind direction and velocities vary

within the Bay of Plenty region, due to the surrounding topography at each weather station.

- *Wave climate* within the Bay of Plenty is greatly influenced by the wind direction. It is suggested by HEALY *et al.* (1977) that waves in the Bay of Plenty, are influenced by wave refraction from offshore islands and bottom topography. The significance of wave refraction causing increased wave energy at the shoreline in Pukehina is investigated in chapter 5.

  Long-term wind records were assessed and utilised to calculated long-term wave power. Outcomes of longterm wave power illustrated that net littoral drift at Tauranga is slightly to the east, while at Whakatane, littoral drift is difficult to distinguish, as the resultant vector is perpendicular to the shoreline. Subsequently, in regard to Pukehina Beach, by applying the same resultant vector directions from Tauranga and Whakatane Airports, a net littoral drift direction to the east was also identified at Pukehina Beach. It is highly possible that the direction of littoral drift varies short-term, however, as a result of local wind patterns altering wave parameters, within the coastal sector.

- *Storm/Cyclonic influences* were discussed to assess, how a storm and cyclonic event may cause more erosion than under 'normal' conditions. The inverse barometric effect and wind stresses exerted will increase sea level, thereby increasing the likelihood of frontal dune erosion, via an increased wave run-up. Most storms of the Bay of Plenty are identified as duration limited, with storms commonly having durations between 6 and 39 hours. However, extra tropical cyclones, which cause largest storm surge elevations, are still able to induces sustained winds of 50-80 knots and have low barometric pressures of 960-980 hPa.

Chapter Three
Beach Morphodynamics and Sediment Characteristics of the Pukehina Coastal Sector

3.0 Introduction

Sediments in the nearshore zone, defined as the area seaward from the shoreline to just beyond the region in which waves break (KOMAR, 1998), are subjected to continual reworking and abrasion from nearshore currents and waves. In the short term, accretion and erosion of the beach profile is dependent on the wave period, wave steepness, and nearshore currents, including wind stress-induced currents, such that an equilibrium profile is formed.

The backshore zone, defined as the area of beach profile extending landward from the sloping foreshore, to the point of development of vegetation or change in physiography (sea cliff, dune field, etc.) (KOMAR, 1998), is also a morphodynamically active zone.
In order to understand sedimentation processes at Pukehina Beach, such as the potential for erosion, this chapter investigates sediment characteristics from both onshore and offshore. From this, possible sources of sediment samples collected from the Pukehina coastal sector, may be ascertained.

Hydrographic surveying of nearshore profiles, may be used to assess trends or relationships in erosion and accretion patterns, while side scan sonar images can identify wave-induced bedforms and sediment distributions. Bedforms are significant in that they are indicators of sediment transport by currents, which are induced by wave motion (TRENHAILE, 1997).

Nearshore sediment transport varies in response to spatial and temporal influences of wave and current processes on variable nearshore sediments (NIEDORODA *et al.* 1984). In order to identify the potential of nearshore sediment transport, suspended sediment concentrations in the nearshore zone are investigated. Sediment is suspended in the water column when current velocities exceed the sediment entrainment threshold for that specific sediment particle. By measuring the concentration of sediment suspension in the water column, this will assist with estimates of the magnitude of sediment exchange, via diabathic transport, which is required for the sediment budget, investigated in chapter 6.

3.1 Literature Review of Previous Sedimentary Investigations Within the Bay of Plenty

PHIZACKLEA (1993) investigated sediment textures of the coastal sector between Pukehina and Matata. His comprehensive analysis involved investigation of sediment composition for both onshore and offshore sediments.

Table 3.1 illustrates the sediment compositions found by PHIZACKLEA (1993) in the Pukehina-Matata coastal sector.

Mineral	Greywacke	Rhyolite	Rhyolitic Ash	Andesite	Andesitic Ash	Basalt Scoria
Quartz	35	30	VL	L	VL	-
Acid Feldspar	40	30	30	5	-	-
Andesite	10	-	-	40	40	20
Acid-intermediate glass	1	30	60	5	30	-
Basic glass	-	-	-	-	-	20
Chlorites	5	-	-	-	-	-
Muscovite	5	-	-	-	-	-
Biotite	5	1	-	5	5	5
Hornblende A	1	1	-	10	10	-
Hornblende B	1	-	1	-	-	-
Hypersthene	-	1	1-3	5	5	-
Enstatite	-	-	-	-	-	5
Augite-Diopside	1	-	1	5	5	10
Epidote	1	-	-	-	-	-
Pumpellyite	P	-	-	-	-	-
Olivine	-	-	-	1	-	5
Calcite	1	-	-	-	-	-
Apatite	1	-	P	P	-	-
Garnet	1	-	-	-	-	-
Tourmaline	1	-	-	-	-	-
Sphene	P	-	-	-	-	-
Rulite	-	-	P	P	-	-
Zircon	1	-	-	P	-	-
Ilmenite	-	-	P	1-5	1-5	1-5
Magnetite	-	1	1	1-5	1-5	1-5

VL = very low, L = low, P = present, hornblende A = green & brown hornblende, hornblende B= cummingtonite

Table 3.1 Typical general assemblages of minerals weathered from selected parent rocks within the Pukehina-Matata coastal sector. Values indicate approximate percentages of mineral grains in each sample, as determined by PHIZACKLEA (1993).

PHIZACKLEA (1993) estimated that light minerals (including terrigenous components) constitute between 92.1 to 98.5% of the beach sediments (terrigenous components (rock fragments and pumice) comprise approximately 2 to 20% of the light mineral component), while 0.2 to 5.6% were heavy minerals, and the remainder originated from biogenic production. The high percentage of light minerals is consistent with the evident quartzo-felspathic origin of sediments from the Okataina volcanic centre, ejected from the surrounding rivers and streams or as tephras directly into the ocean. PHIZACKLEA (1993) identified from his data that there was an increasing abundance of heavy minerals from Waihi Estuary towards Otamarakau, ceasing in a peak at Hauone Stream (figure 3.1).

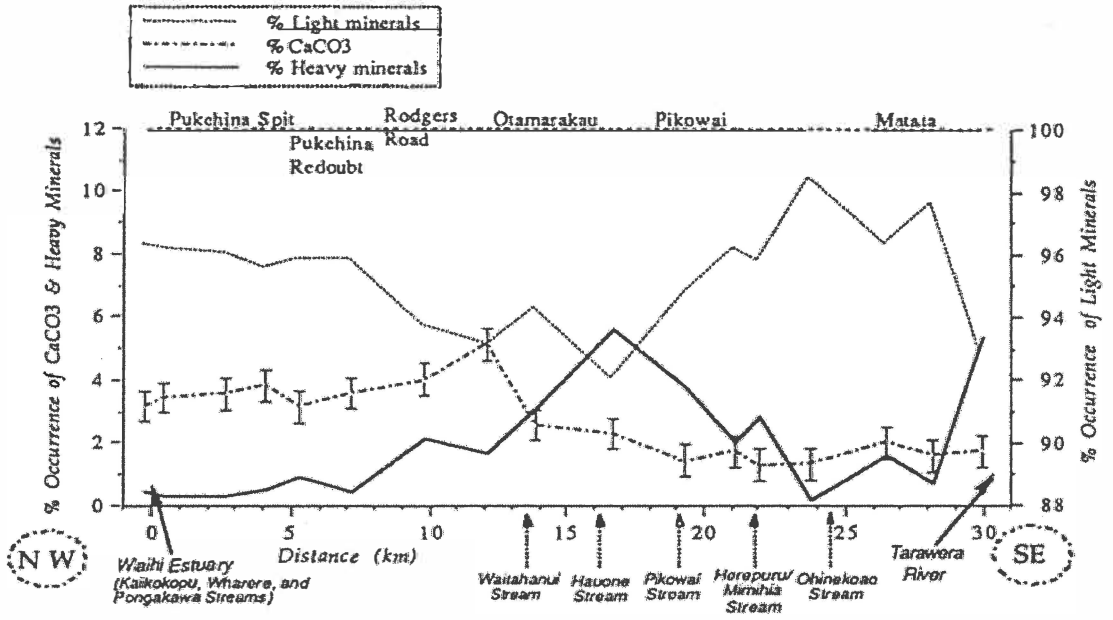

Figure 3.1 Composition by weight of the light minerals, heavy minerals, and carbonate ($CaCO_3$) in beachface surficial sediments within the Pukehina-Matata coastal sector, as determined by PHIZACKLEA (1993).

In terms of identifying littoral drift direction inferred from sediment mineral species abundance, PHIZACKLEA (1993) states (p. 194) that minerals show varying degrees of certainty for indicating littoral drift direction. PHIZACKLEA (1993) identified that mineral species: K-feldspar, volcanic glass and pumice all depict a north westerly littoral drift direction with a high degree of confidence, while rock fragments and heavy minerals also depict a north westerly littoral drift direction, but with less confidence.

Offshore sediments have also been investigated by PHIZACKLEA (1993). Utilising side scan sonagraphs, zones of differing sediment textures were identified. Bedforms illustrated by side scan sonagraphs, were subsequently ground truthed by SCUBA divers, which supported side scan sonagraph outcomes. Megaripple bedforms were found to be shore parallel, induced from previous wave action. Surrounding bottom sediments, in areas with bedrock present (Okurei Point, basal end of Pukehina Spit), however, were observed as having undergone intense scouring. PHIZACKLEA (1993) suggests possible downwelling currents were the cause.

PICKETT *et al.* (1997) investigated coastal hazard identification of 48 beach profiles along the Bay of Plenty coastline by application of the Dean Equilibrium Beach Profile (EBP). The implication of the EBP is that it can identify whether a profile is out of equilibrium, and by what volume. If the existing profile were out of equilibrium then erosion or accretion would likely occur, in the need for the profile to return to equilibrium.
PICKETT *et al.* (1997) fitted an equation of the form,

$$y = Ax^b \qquad \text{(Eqn. 3.1)}$$

to beach-nearshore profiles, by the least squares method, where y is the water depth, x is distance offshore from the still water shoreline (often taken as mean sea level), A is the scale factor governing steepness of the profile, and b is the shape factor.

Outcomes indicated that most beaches in the Bay of Plenty region, including Pukehina Beach, are out of equilibrium. The clear implication is that erosion of the profile would occur, in order for the profile to regain equilibrium. PICKETT *et al.* (1997, p. 358) stated however, that 'the scale of erosion predicted seems to be unreasonable', because of the scale factor, associated in terms of parameter *x* (distance offshore to closure depth, which was calculated by the Hallermeier outer limit). The scale factor was illustrated by PICKETT *et al.* (1997) as too small, thereby resulting in an enhanced erosional outcome. PICKETT *et al.* (1997) concluded that the Hallermeier inner limit should be used for parameter *x*, thereby resulting in a more realistic outcome.

HEALY (1978a), analysed beach surveys from 51 sites within the Bay of Plenty region including Pukehina Beach. Assessment of erosion to beach profiles during storms, were estimated from profiles taken in 1977. HEALY (1978a) concluded that on average 65-80 m^3/m of beach material, is likely to be removed in a storm event or series of storm events within the Bay of Plenty. HEALY (1978a) did remark, however, that 1977 was a 'storm-free' year and the likelihood that these values are underestimated, is high. However, SMITH *et al.*(1997) estimated from beach profile observations at Otamarakau, that ~49m^3/m of beach would erode during a storm event.

HEALY (1978b) investigated the nearshore zone by conducting a hydrographic survey. Particular interest was focused on beach bar formation present in the Bay of Plenty. With regard to Pukehina, HEALY (1978b) noted a very poor bar development, if any, instead the presence of a horizontal sub-tidal platform was indicated. Since no offshore bar was present during the time of HEALY's (1978b) observation, the amount of wave energy expected at the shoreline should be greater than a beach with an offshore bar. An offshore bar can decrease the amount of wave energy at the shoreline, as the incoming wave will break on the bar (because of the decreased water depth) and subsequently wave energy will be lost. However, since HEALY (1978b) observed no offshore bar present at Pukehina Beach, one may expect increased wave run-up and subsequent frontal dune erosion, than at other locations with an offshore bar.

3.2 Topographic and Hydrographic Survey of the Pukehina Coastal Sector

3.2.1. Aims and Objectives

Hydrographic surveying enables measurement of topographical features of the seafloor in a similar way to that in which maps are made of land areas. The primary use of these surveys, commonly conducted by the Royal New Zealand Navy (RNZN), is for hydrographic charts.

In this analysis, data collected from the RNZN, in the form of fair sheets of soundings, and onshore surveying of the Pukehina frontal dune, are used to create a digital terrain model. A digital terrain model constructed by PHIZACKLEA (1993) is then used for comparative analysis with the current digital terrain model, in an attempt identify zones of sediment accumulation or scour.

3.2.2 Dune and Sub-aerial Beach Surveying

Dune and sub-aerial beach surveying was undertaken on 23rd August 2001, using the rapid survey method, or also known as the Emery method.

The rapid survey method is a technique that is reliable, simple, and takes little time. This common technique is used nationally and internationally for obtaining open ocean beach profiles (HSU AND WANG, 1997; SMITH *et al.*, 1997; SAUNDERS, 1999).

Using a Dumpy level, a horizontal line of sight is used to estimate elevation from a graduated staff held vertically over points of interest. Over a profile, the Dumpy may have to be repositioned in order to continue surveying, this is known as a backsight. Observations made from the Dumpy at different positions are linked by making repetitive measurements of the same survey point, from adjacent level stations (refer to figure 3.2). A tape measure is used to ensure that the Dumpy and graduated staff were maintained perpendicular to the shoreline during each survey.

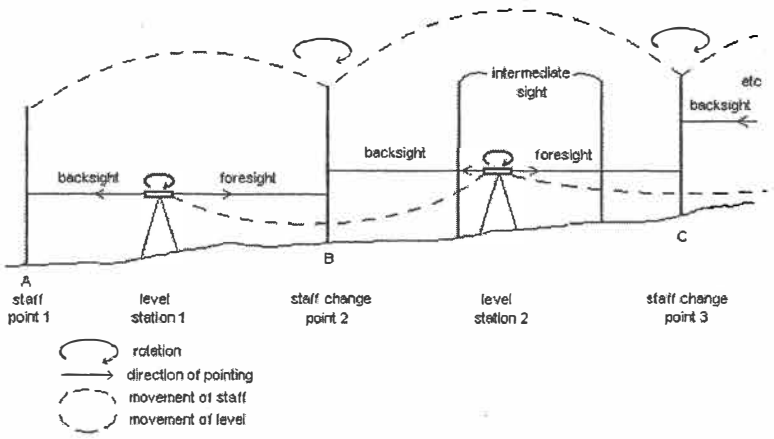

Figure 3.2 Rapid beach profile surveying technique used during this investigation. Note that beach profiles are usually surveyed down-slope, rather than up-slope as depicted in this schematic. (Adopted from SAUNDERS, 1999).

Surveys were undertaken at low tide to maximise survey excursion distance and an attempt was made to include as much nearshore bathymetry as possible, by wading into the water, until uncertainty of measurements became large (± 0.1 m in vertical measurements and ± 0.3 m in the horizontal measurements).

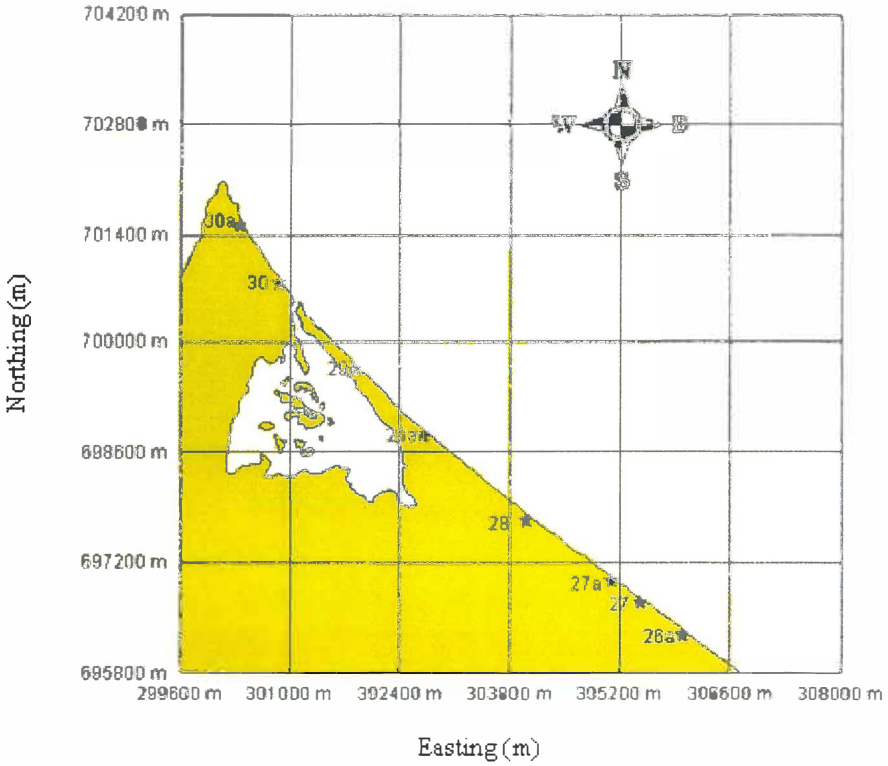

Figure 3.3 Benchmark locations used for rapid surveying of Pukehina frontal dune. GPS co-ordinates of benchmarks are presented in Appendix I.

Figure 3.3 illustrates the locations where dune and beach profile survey was undertaken, using the rapid survey technique. GPS co-ordinates of benchmarks are presented in Appendix I.

3.2.3 Nearshore Bathymetry Surveying

Using the latest fair sheet of soundings made by the RNZN (soundings were made from the 23rd May to the 24th June 1994), offshore bathymetry can be integrated with onshore survey data, in order to generate a digital terrain model. Soundings taken by the RNZN are as point locations, therefore, resolution varies throughout the survey.

Conversion of fair sheet of soundings into a digital format is achieved by the use of a digitiser. Referencing the fair sheet of soundings to a projection involves identifying specific locations, which have a known reference in the used projection. Here, Maketu

trig, Okurei Point and Pukehina Redoubt were used as reference locations. Once data from the fair sheet of sounding is digitised, onshore data can be assimilated, as benchmark locations and elevations above Moturiki datum are known (Tidal gauge benchmark located on the seaward end of Moturiki Island (37° 38' S, 176° 11' E).

3.2.4 Survey Uncertainties

Whilst undertaking surveys using the rapid survey method, uncertainty of measurement parameters, were endeavoured to be minimised. The uncertainty in vertical elevation was estimated to be ± 0.05 m. This was calculated by the increment distance detailed on the 5 m graduated staff. The uncertainty in horizontal distance is expected to be larger due to the undulating topography along the profile. The use of a 30 m tape restricted the horizontal uncertainty to ± 0.15 m.

Uncertainties during the offshore hydrographic survey are expected to be minimal. The use of heave and tilt compensators reduce the amount of uncertainty, due to the sway or up and down motion of the vessel. Uncertainty of using differing datums in each of the surveys is minimal (±4-5 mm), as the benchmarks used were of 1st and 2nd order (rating system of the accuracy of datum position. A 0 order datum is regarded as the most accurate (±0.003 m), while a 10th order is the least (± 40 m)). The offshore hydrographic survey uses datum's BM BC84 (positioned at Port of Tauranga Ltd) and BM Whale Island 2 (Whale Island), while the onshore rapid survey uses Moturiki Datum.

3.2.5. Rapid Survey (Beach Profile) and Digital Terrain Model (DTM) Outcomes

Beach and dune profiles obtained from surveying are available in Appendix II.
Figure 3.4 illustrates the digital terrain model created by PHIZACKLEA (1993) using the software WINGZ. Figure 3.5 illustrates a digital terrain model created, using current hydrographic and topographic data.

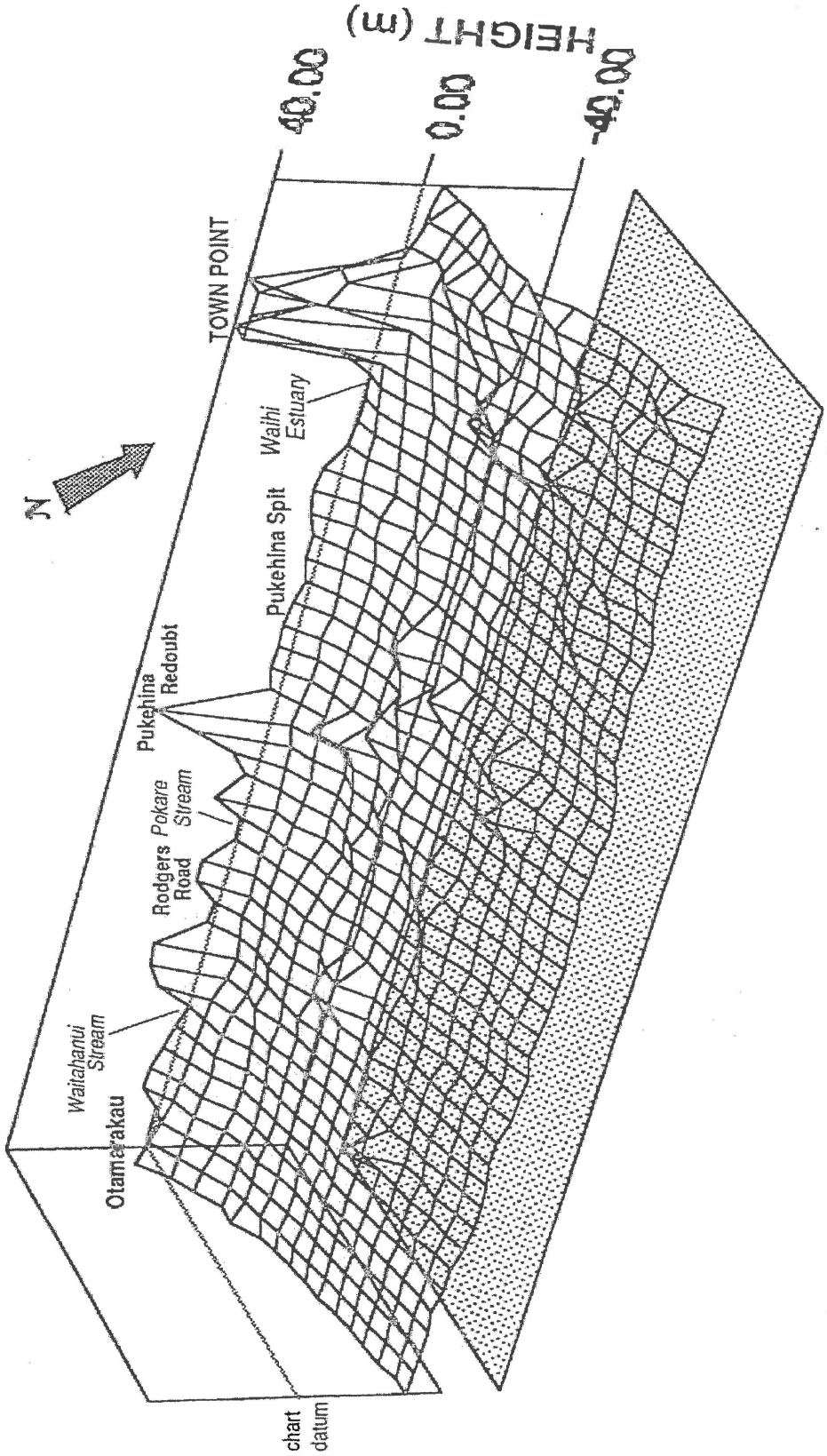

Figure 3.4 WINGZ™ plot of nearshore Bathymetry between Okurei Point and Otamarakau. (Source: PHIZACKLEA, 1993)

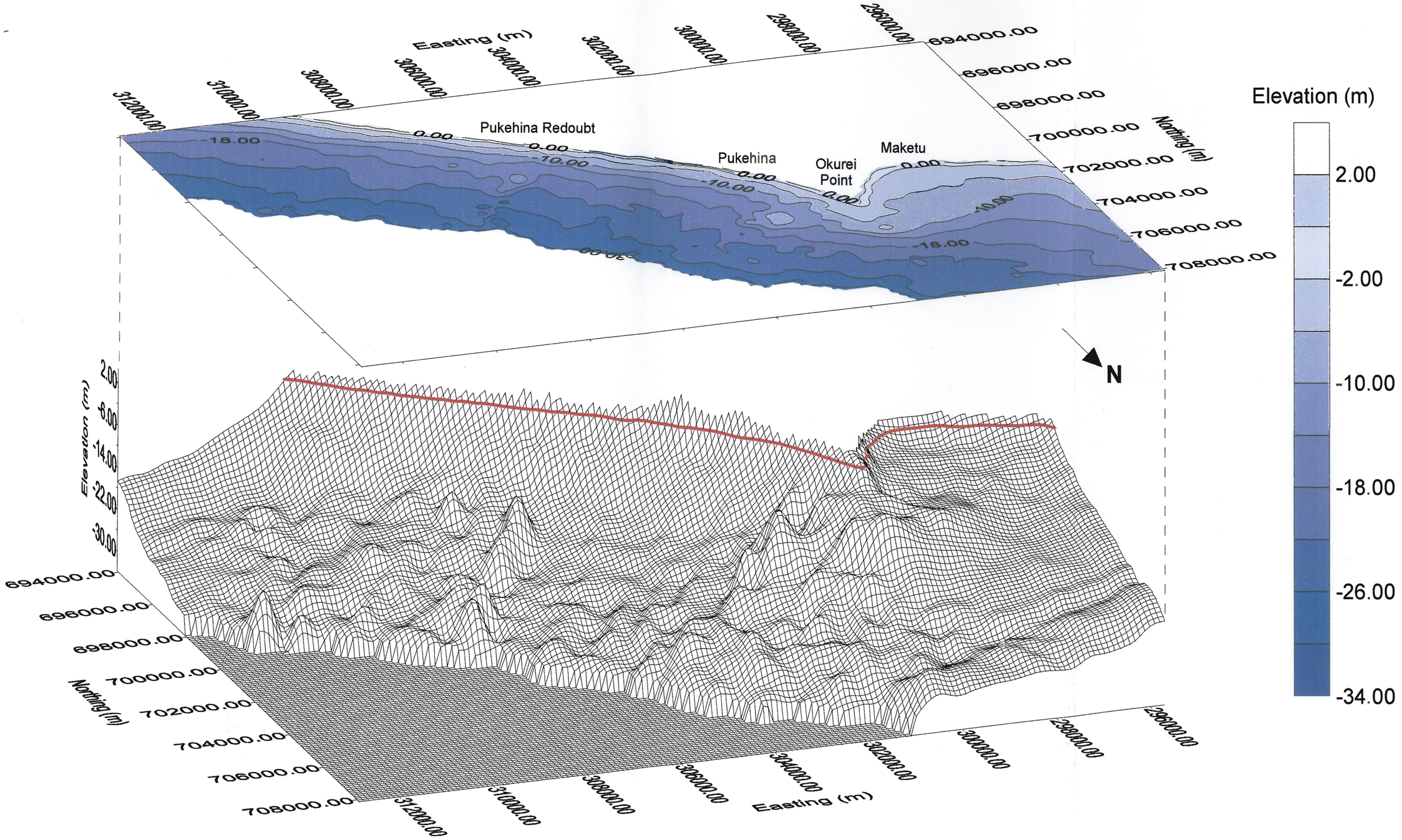

Figure 3.5 Digital Terrain Model (DTM) created from RNZN fair sheet of soundings collected 1994 and dune, sub-aerial beach surveying undertaken 23/8/2001. Note: Red line indicates mean sea level. Plots created by SURFER32.

3.2.6. Discussion

The low resolution of figure 3.4, in comparison to figure 3.5, means assessing exact changes in topography and bathymetry is difficult. Comparison of figure 3.5 DTM to PHIZACKLEA's (1993) DTM, figure 3.4, allows one to identify zones of bathymetric change, which may indicate an alteration in nearshore or offshore processes, such as wave orbital motion and/or currents.

Preferably the two DTM's (figures 3.4 and 3.5) would be overlayed, with elevations from each DTM, at the same location, subtracted from one another. The resultant figure would subsequently illustrate an outcome of change in bathymetry and topography. Unfortunately, survey data used to generate PHIZACKLEA's (1993) DTM (figure 3.4) is not available, eliminating the possibility of such analysis. Therefore, comparative analysis is restricted to visual assessment between the two DTM's.

Major undulations offshore from Okurei Point, Pukehina Redoubt and east of Pukehina Redoubt are of similar locations. This indicates that changes to the offshore bathymetry within the Pukehina coastal sector have been limited, and so offshore sediment transport processes may have not significantly altered since PHIZACKLEA's 1993 survey.

From figure 3.5, one may consider that the average offshore depth in the vicinity of Okurei Point is much less than depths at the Pukehina Redoubt vicinity. PHIZACKLEA (1993) states that nearshore sediment transport offshore from Okurei Point is limited, due to the rocky nature of the coast around the apex of Okurei Point. The possibility of Motiti Island acting as a sheltering effect from wave activity from the east-northeast quadrant, and also that the Okurei Point region is proximate to sources of sediment (predominantly the Okurei Point cliffs and the Kaituna River), can also be suggested as possible reasons why depths in the Okurei Point vicinity are smaller than in the Pukehina Redoubt vicinity.

Increases in bathymetry northeast offshore from Pukehina Redoubt, can be attributed to large boulders, approximately 1-1.5 m high, as observed by PHIZACKLEA (1993).

Significant differences of onshore topography are illustrated between the two DTM's. However, this can be attributed to differing excursion distances that were used to generate each model. PHIZACKLEA's 1993 DTM, figure 3.4, illustrates coastal cliffs in the Okurei Point and Pukehina Redoubt vicinity. In creation of figure 3.5 beach profiles did not exceed elevations 14 m above MSL.

SURFER32[†] used to create figure 3.5, calculated the grid using the Kriging method. Kriging is a geo-statistical griding method that has proven useful and popular in many fields (GOLDEN SOFTWARE INC., 1997). This method produces visually appealing contour and surface plots from irregularly spaced data. Kriging attempts to express trends that are suggested in data, so that, for example, high points might be connected along a ridge, rather than isolated by 'bull's-eye' type contours. However, when data is too irregularly spaced, the Kriging method cannot interpolate trends with precision. Only eight onshore profiles were used here, so the Kriging method will not portray the onshore topography accurately and comparative analysis of onshore topography, is therefore, unreasonable.

3.3 Side Scan Sonar Imagery

3.3.1 Side Scan Sonar Aims and Field Program

With side scan sonar imagery, surficial sediment patterns present on the seafloor, may be illustrated. Alterations in sediment texture within the surveyed region, may identify possible sediment sources and zones where wave orbital currents are initiating sediment transport in the Pukehina coastal sector.

[†] SURFER32 (version 6.04), software by Golden Software Inc, 1997.

A survey of the coastal sector, between Pikowai and Okurei Point, from water depths of to 6 m to 30 m was conducted. The reason for this field program was to enable comparisons with previous data collected by PHIZACKLEA (1993). Side scan surveying was extended to Pikowai, to identify whether the offshore bar observed by PHIZACKLEA (1993) was still present and whether sediment dredging was having an adverse affect on the offshore bar at Otamarakau.

Surveying was undertaken over two field excursions, each consisting of two days in April and July 2001, due to vessel availability and storm activity. Surveying was undertaken using a local Whakatane charter vessel, *Black Shag*. Excursion one covered depths 30 m to 22 m. Excursion two surveyed the remaining area inshore to 6 m.

In water depths 30-14 m, survey run-lines were 300 m apart, but decreased to 150 m in the shallow water (<14 m). With this survey scheme, and having slightly overlapping swath widths, full coverage of the nearshore seafloor was realised.

A Klein 595 side scan sonar system was used for the survey. Data collected were in analog form as a hardcopy printout from the Klein unit, and as a digital copy using *Isis* (section 3.3.2), which may be used to process and compile runlines into an integrated side scan sonar map.

3.3.2. Side Scan Sonar Data Acquisition Methods and Data Processing

Isis is a shipboard data acquisition and image processing system (TRITON ELICS INTERNATIONAL, INC. 1988). *Isis* simultaneously collects acoustic data and navigational data, from the Klein system and a DGPS (Differential Global Positioning System) respectively, allowing for real-time positioning of any pixel of imagery (geo-coding). Data collected by *Isis* is then rendered as playback to correct the data for bottom tracking, slant, boat speed and heave.

Sonar data is then compiled into an empty mosaic with a specified resolution.

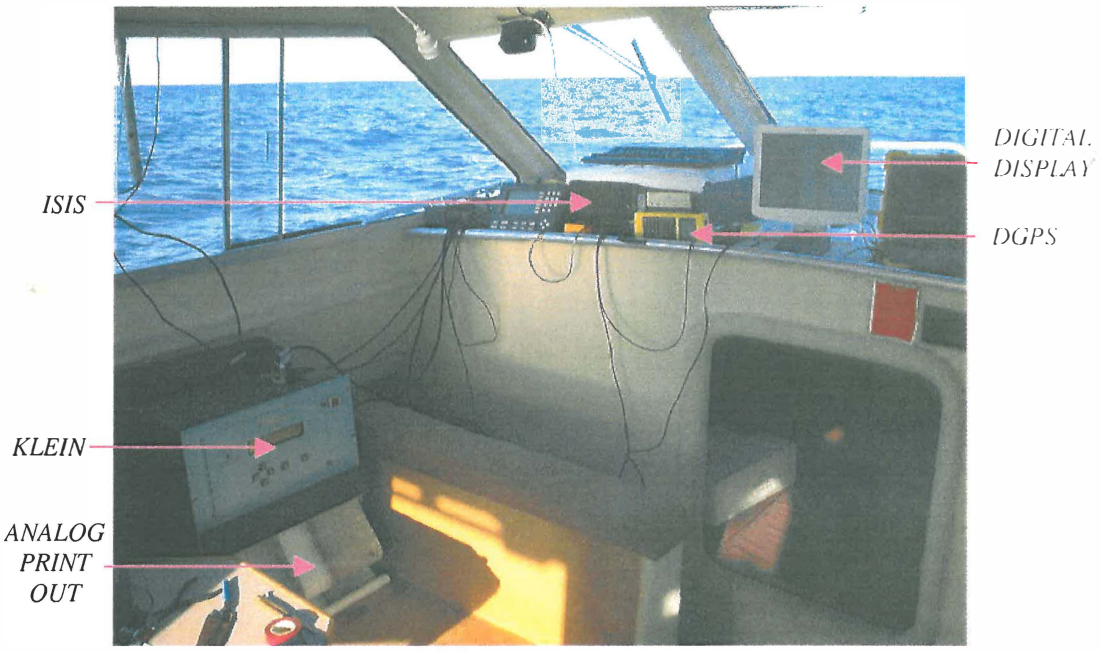

Figure 3.6 Equipment and set up for side scan sonar surveying on board the charter vessel *Black Shag*.

Delphmap is used to compile multiple layers of mosaics. Once compiled, the image can then be saved as a 'GeoTiff' image, which is a 'Tiff' file (tagged image file format) with navigational information included.

GeoTiff images are opened in *Map Info* and are layered with a shoreline map created by RNZN hydrographic maps. Presentable maps of side scan imagery can be created with associated griding, scale bar and image information.

Analysis of bedforms and sediment morphology may be identified from the created sonar image. The analog print out may also be used to define obscure textural patterns, as the analog print out is of higher resolution than the digitally created sonar image.

3.3.3. Interpretation of Sonagraphs

RIDDLE (2000) investigated the surficial sediments of the outer Hauraki Gulf. Using side scan sonagraphs, detection of bedforms and sediment characteristics within the surveyed

area was attempted. Following interpretation methods of RIDDLE (2000), sonagraph outputs were assessed for bedforms.

From sonagraphs, figure 3.7a and figure 3.7b depict the major sonagraph outputs obtained within the Pukehina-Pikowai coastal sector.

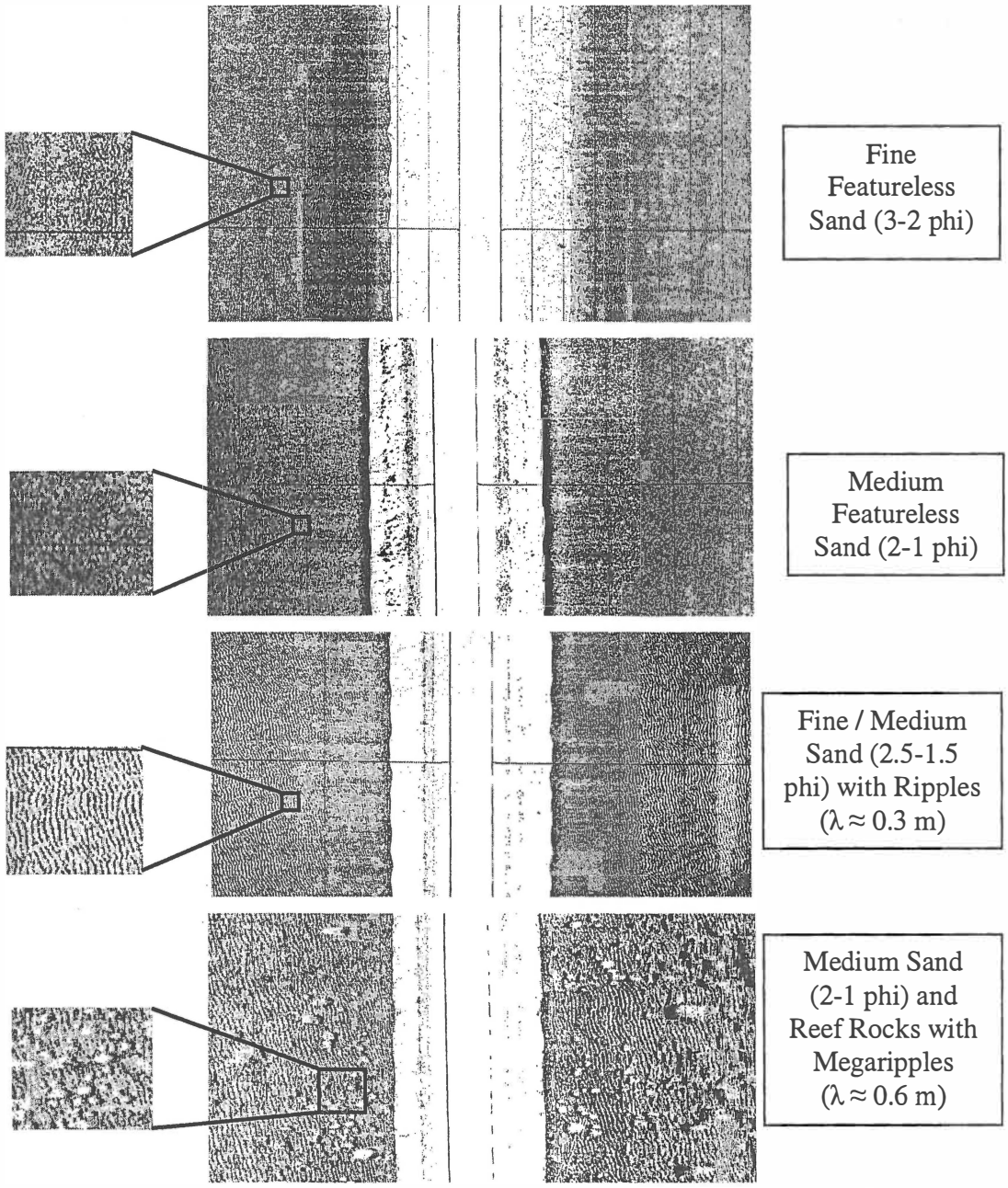

Figure 3.7 Varying side scan sonagraph outputs within study region.

3.3.4. Outcome of Side Scan Sonar Survey

Side scan sonar coverage of the field area did not achieve the desired 100% coverage, due to instrument malfunctions. Figure 3.8 illustrates the runlines that the vessel, *Black Shag* underwent. Unfortunately, due to instrument malfunctions, digital data could not be collected on the second excursion. This required conversion of analog data into a digital format using manual techniques.

Runline data (position and time) are stored using HYDROPRO[‡]. Analog data, therefore, can be manually compiled into a digital format (figure 3.9) using the HYDROPRO data, as analog sonagraphs include a time stamp also. Accuracy of the included analog data, however, is not as accurate as the digital data, as when combining the analog data to the digital data, it is a matter of interpretation where sediment morphology boundaries are.

[‡] HYDROPRO by Trimble.

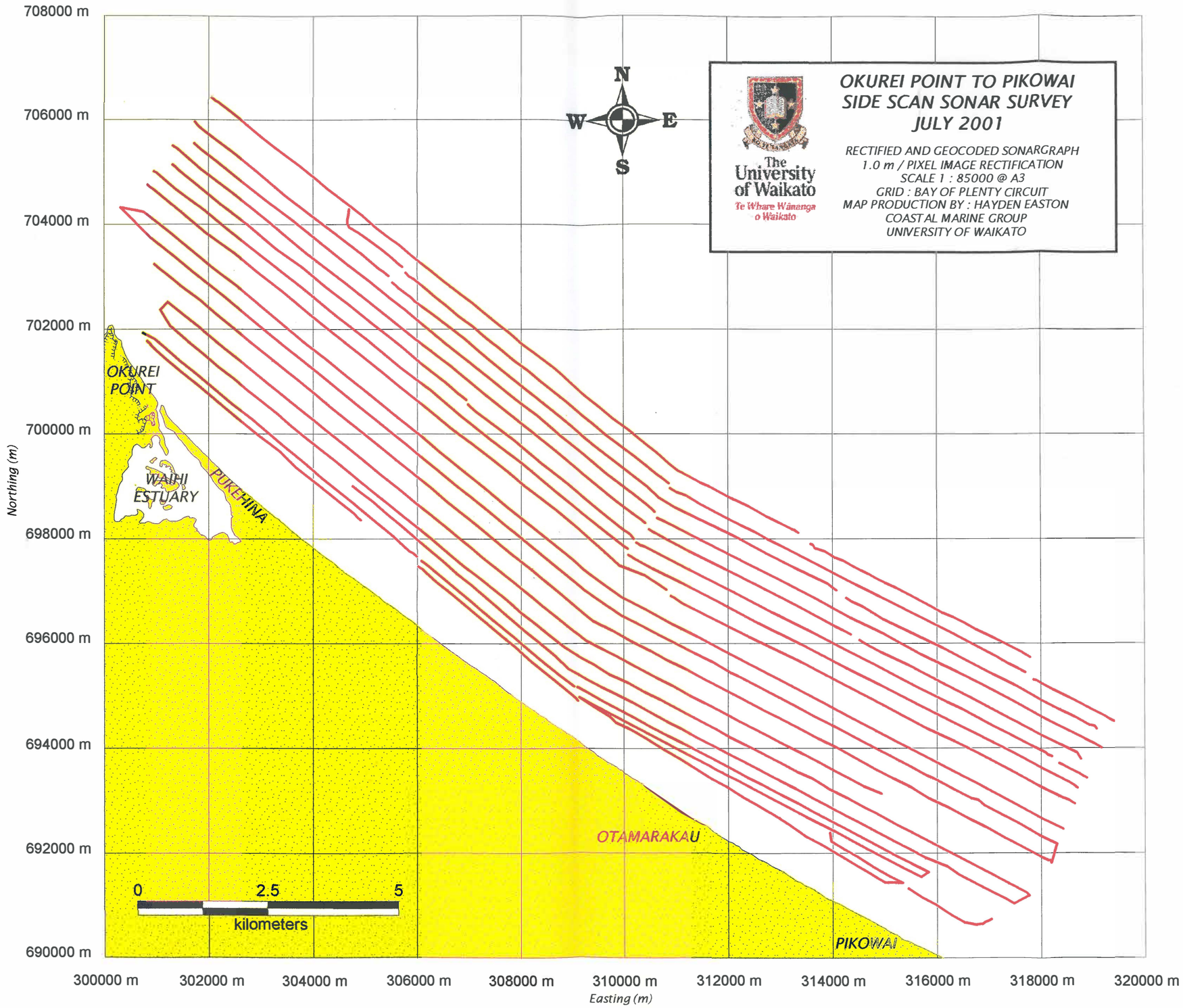

Figure 3.3 Survey runlines taken for side scan sonar survey, at depths 6 - 30 m between Okurei Point and Pikowai.

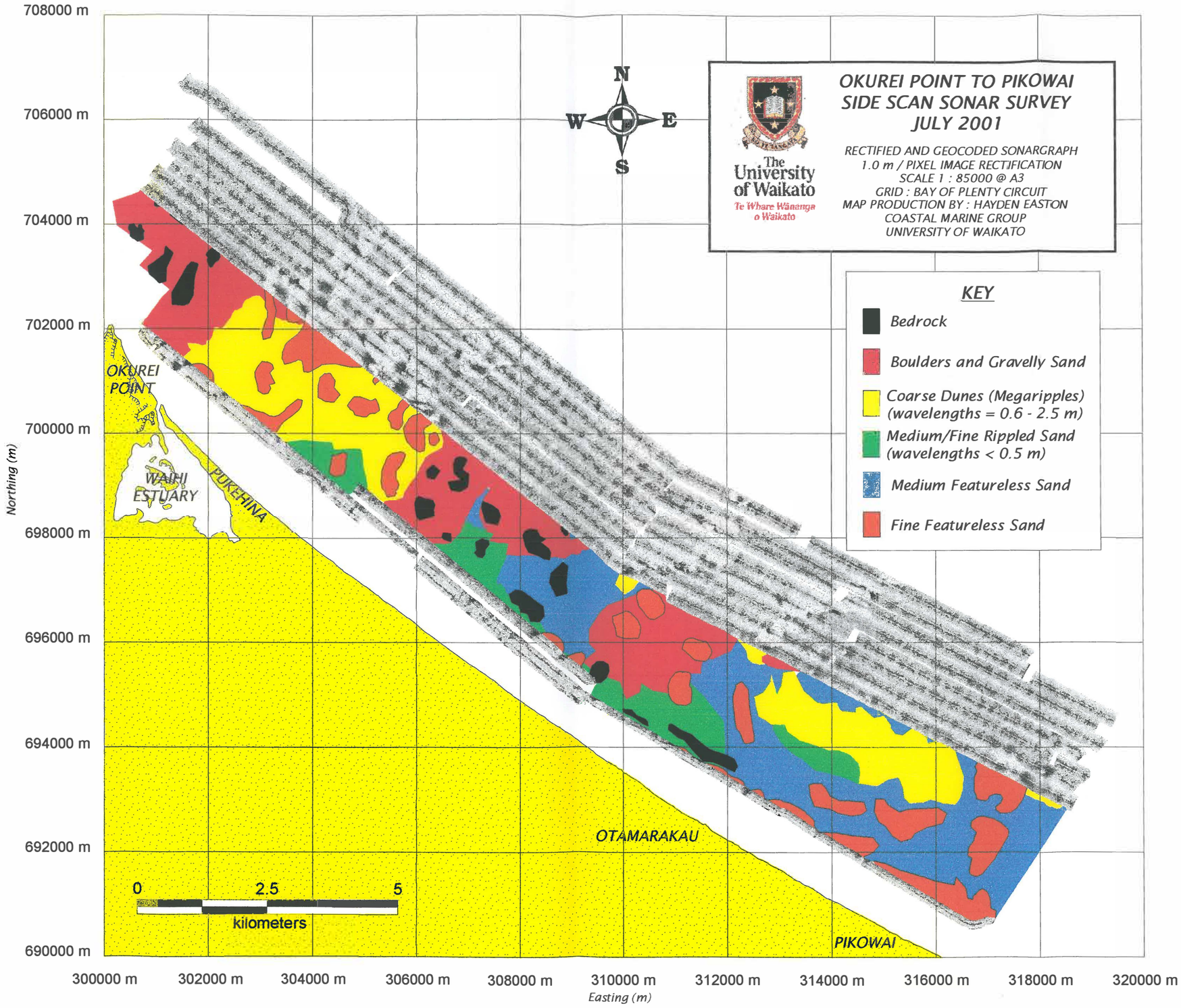

Figure 3.9 Rectified and geocoded side scan output, at depths 6 - 30 m between Okurei Point and Pikowai. Analog data from depths 7 - 22 m is intergrated with digital data, due to an instrument malfunction.

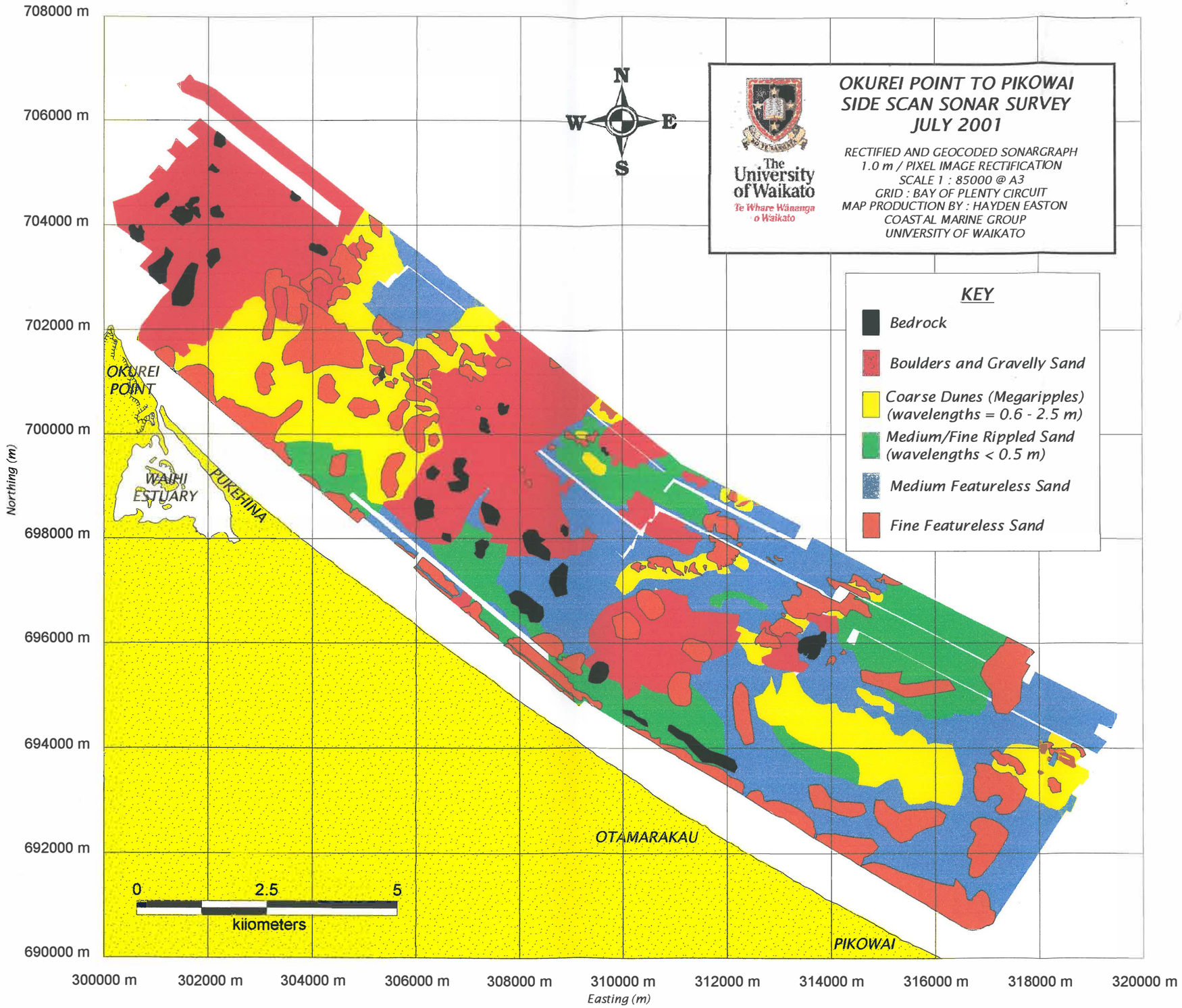

Figure 3.10 Sediment morphologies and distributions identified from side scan sonagraph output, at depths 6 - 30 m between Okurei Point and Pikowai.

3.3.5. *Discussion and Interpretation of the Sedimentary Features Identified from Side Scan Sonar*

Side scan sonar images of the Pukehina-Pikowai region, as illustrated by figure 3.10, may be divided alongshore into four distinct areas of differing sediment texture.

- Okurei Point to Waihi Estuary - mainly bedrock, boulders and gravelly sand.
- Waihi Estuary to Pukehina Redoubt - coarse megaripples, medium/fine rippled sand and fine featureless sand.
- Pukehina Redoubt to Otamarakau - coarse megaripples, bedrock, boulders and gravelly sand, medium/fine rippled sand and fine featureless sand.
- Otamarakau to Pikowai - coarse megaripples, medium/fine rippled sand and fine featureless sand.

A difference of sediment textural distributions between nearshore (6 m water depth) and offshore (15-30 m water depth) can be observed from figure 3.10. Nearshore sediment textures (particularly fine featureless sand), illustrate larger areas of sediment textural distributions, while in the offshore region, sediment textural distributions are smaller and more randomly scattered. Possible reasons as to why fine featureless sediments are distributed differently between the nearshore and offshore regions, may be because fine sediments offshore are transported or winnowed away, due to bottom currents acting on the sediments. Nearshore turbulence and agitation of sediments is dominated, therefore, fine sediments could remain. Another reason may be that fine sediments are being transported onshore from the deeper regions, resulting in an increased concentration of finer sediments at the shoreline.

Comparing the side scan sonar outcome (figure 3.10) with a side scan sonar survey obtained by PHIZACKLEA (1993) (figure 3.11), side scan sonar outcomes illustrate some similar properties. PHIZACKLEA (1993) also identifies four areas of predominant sediment textural distributions. The locations of these areas are predominantly the same (PHIZACKLEA, 1993 describes a boundary at Rodgers Road, while current side scan sonar imagery suggests a boundary at Otamarakau), however, there are differences in the

location of individual sediment textures within each of the four areas. In comparing figures 3.10 and 3.11, it appears that the area of bedrock has reduced significantly since 1993, particularly at Okurei Point and Rogers Road. An increased volume of sediment to these areas may imply changes in sediment transport patterns. Such increased volumes may be induced by a change in wave direction (discussed in chapter 5), an increase of sediment supply to the region, or a cyclic oscillation (possibly El Niño Southern Oscillation or Inter-decadal Pacific Oscillation, as discussed in chapter 6). Another hypothesis is that sediment transport may be occurring in pulses, thus giving the change in sediment distribution. Sediment transport pulses may be defined as sediment transport into a region that occurs asymmetrically, or of varying rates (HUME *et al.*, 1997).

HUME *et al.* (1997), investigated sediment transport at Cape Rodney (a large coastal headland in the Hauraki Gulf, located at the north of North Island, New Zealand). They noted that sediment transport occurred asymmetrically and concluded that phase eddies were the cause. No evidence of eddies are evident in available aerial photographs of the Pukehina coastal sector. However, SAUNDERS (1999) noted an eddy formed offshore from Kohi Point near Whakatane, indicating that eddies do occasionally form in the Bay of Plenty. The possibility of an eddy causing the increase volume of sediment to the Okurei Point region is, however, unlikely, as HUME *et al.* (1997) found banding or zoning of sediments where eddies were conflicting with the seabed. From the present side scan sonagraphs there is no banding present in the Okurei Point region. PHIZACKLEA (1993) however, did note small banding of sediments in the Okurei Point vicinity, but small banding of sediments is to be expected at this location, due to variations in wave energy across the surf zone. The possibility small eddies providing the substantial increased volume of sediment to this area, as figure 3.10 illustrates, is also unlikely.

The most likely reasons why there has been alteration in sediment distributions, may be because of a cyclic oscillation as previously stated or an increase in sediment from a close source, such as the Kaituna River.

Cyclic oscillations, such as the El Niño Southern Oscillation (ENSO) and Inter-decadal Pacific Oscillation (IPO), are a combination of changes in oceanic and atmospheric

circulation over the Pacific Ocean. Oscillations such as IPO and ENSO have been recognised as causes of change to beach morphology and shoreline location (DE LANGE, 2001). The duration of ENSO fluctuates from 2 –10 years (DE LANGE AND GIBB, 2000), while the IPO operates at 25-35 years. Cyclic oscillations affect the sea level, frequency of storms and onshore winds and currents, as well as wave climate. A change in such a climate parameter, for example, wind strength, wind direction, or storm event, might conceivably have changed sediment textures within the Pukehina coastal sector. The possibility of cyclic oscillations influencing the beach morphology within the Pukehina coastal sector will be further examined in chapter 6.

An increase of sediment offshore of Okurei Point may be sourced from river/stream discharge, littoral drift into the region, diabathic transport or erosion of local geology. Since the predominant sediment covering the bedrock is gravels and boulders, the most likely source are the Kaituna River and/or erosion from Okurei Point, as sediment elsewhere in the Pukehina coastal sector are composed of finer sediments (as discussed in section 3.4 and by PHIZACKLEA, (1993)).

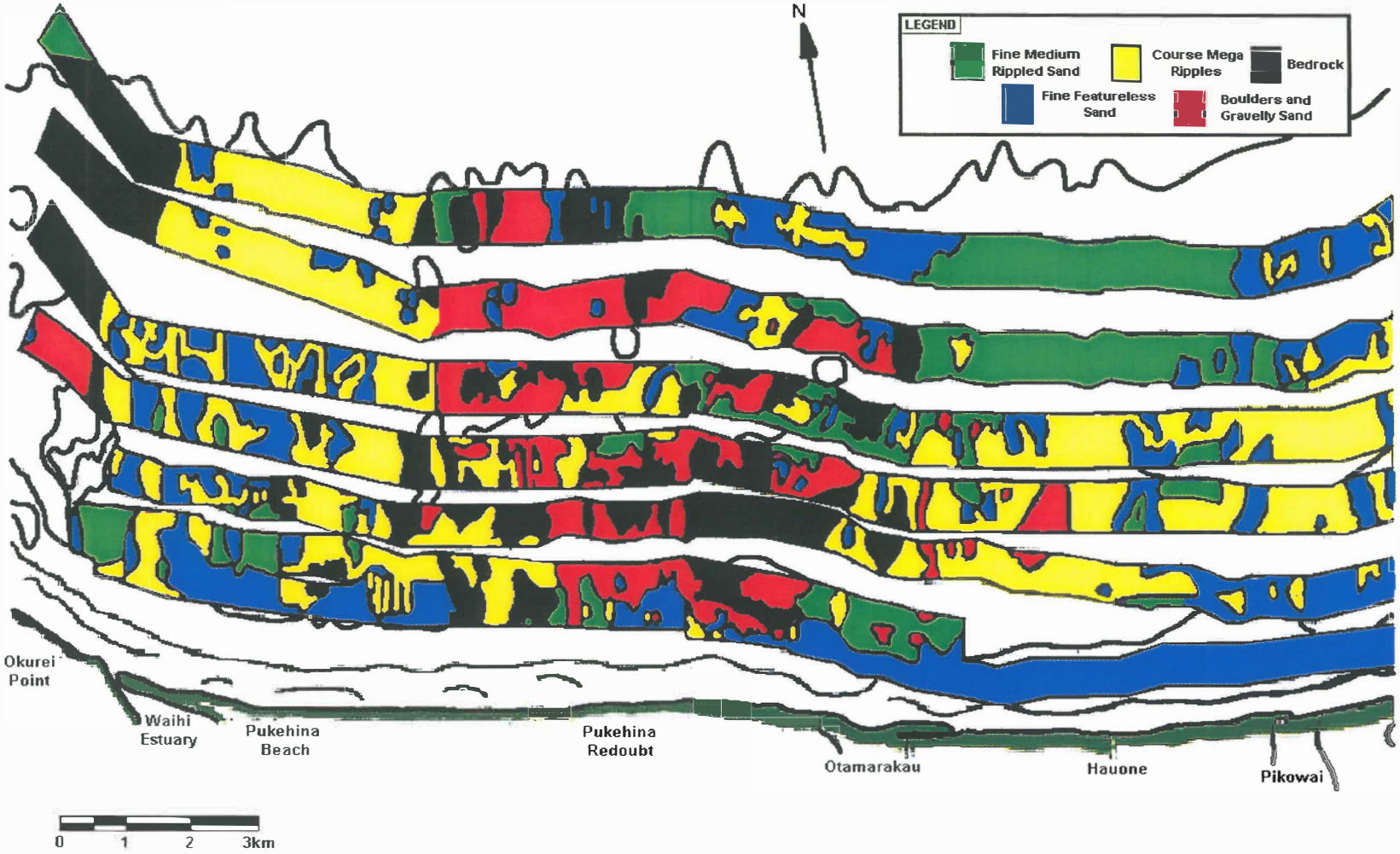

Figure 3.11 Offshore sediment distribution and morphology map between Okurei Point and Pikowai. Data obtained by and figure adapted from PHIZACKLEA (1993).

3.4 Nearshore Sediment Texture

3.4.1 Aims and Objectives for Collecting and Analysing Nearshore Sediments

Investigation of sediment textural characteristics may provide information about sediment transport patterns at Pukehina Beach. By assessing the nature and distribution of nearshore sediments in both onshore and nearshore zones of Pukehina Beach, sediment sources to Pukehina Beach may be identified.

Sediment characteristics of potential interest here, are the textural characteristics mean grain size, sorting and skewness. Mean grain size and sorting are of significant interest, as these characteristics can confirm the sedimentary environment CARRANZA-EDWARDS (2001).

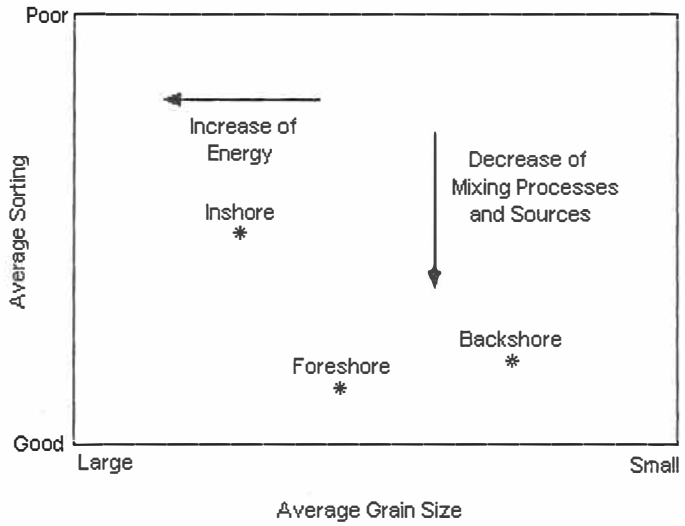

Figure 3.12 Average grain size and sorting for beach subzones. Adapted from CARRANZA-EDWARDS (2001).

Using sediment characteristics, littoral transport directions may be identified by applying littoral drift models. Three were examined here: the SUNAMURA AND HORIKAWA (1972) model, the MCLAREN (1981) model, and the Waihi model.

3.4.2. The SUNAMURA AND HORIKAWA (1972) Model

Using the sediment characteristics mean grain size and sorting, SUNAMURA AND HORIKAWA (1971; 1972) formulated a model to estimate littoral drift direction by relating the spatial variations of mean grain size and sorting to sediment sources (figure 3.13). The SUNAMURA AND HORIKAWA (1972) model, however, does have some limitations. The model assumes a uniform mineralogy, meaning that it expects a singular mineral throughout the entire region sampled. The model also assumes that there is only one sediment source. As both of these limitations are not satisfied within the Pukehina coastal sector, one must assume possible errors in determining sediment transport directions.

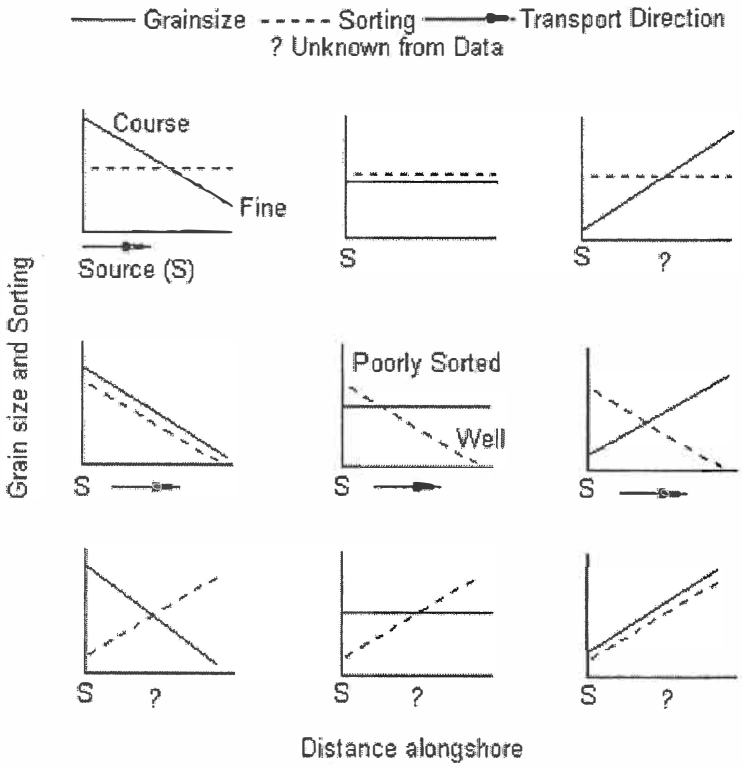

Figure 3.13 Criteria for the inference of sediment transport direction according to the model of SUNAMURA AND HORIKAWA (1972). Certain combinations of grain size and sorting may indicate littoral drift direction. Source: SUNAMURA AND HORIKAWA (1972).

The model has been utilised by DE LANGE (1988) at Pilot Bay, Mt Maunganui, and PHIZACKLEA (1993) within the Pukehina-Matata region. Both achieved reasonable success, as visual evidence at each location supported model outcomes.

Figure 3.13 illustrates nine different combinations of trends in mean grain size and sorting that potentially may occur from sediment textural data, and the inferred alongshore sediment transport directions for each. Using these combinations of mean grain size and sorting may indicate littoral drift direction SUNAMURA AND HORIKAWA (1972).

3.4.3. MCLAREN (1981) Model

Differing from the SUNAMURA AND HORIKAWA (1972) model, the MCLAREN (1981) model additionally incorporates skewness into the assessment of littoral drift direction. According to this model, grain size distributions will change in response to erosion, transport and deposition, producing three possible scenarios (MCLAREN, 1981; MCLAREN AND BOWLES, 1985):

- Case 1: Complete Deposition
  - Sediment will become finer and more negatively skewed in the direction of transport.
- Case 2: Partial Deposition
  - A sediment lag will be coarser and more positively skewed than its source.
- Case 3: Partial Deposition
  - If sediment in transport undergoes selective deposition, the resulting deposit may be either finer or coarser than its source with a more positive skew.

Likewise, the MCLAREN model (1981) has the same limitations as the SUNAMURA AND HORIKAWA (1972) model, therefore, results must also be treated as having probable errors.

3.4.4. Waihi Model

The Waihi model is similar to the MCLAREN (1981) model, except it allows for the effect of grain shape and variations in mineralogy. Sediment transported from source to deposit

will become coarser, better sorted, and be more negatively skewed (due to the addition of coarser sized grains). The resultant source sediment will become finer, better or poorly sorted and more positively skewed.

PHIZACKLEA (1993) assessed the sediment transport pathways using all three sediment transport models. However, the results obtained from the Waihi model gave sediment pathways that did not compare well with visual evidence from the region. PHIZACKLEA (1993) discusses how the Waihi model suggests Otamarakau is a site sediment deposition, but streams in this locality are known to discharge coarse grained sediments, thereby contradicting the model outcome. Likewise, Pukehina Redoubt was suggested to be a sediment sink, therefore, one would expect this region to be accreting, in reality however, this region is in an erosional state. Because of this uncertainty in the applicability of output from the Waihi model in the Pukehina-Matata coastal sector, it will not be used here.

3.4.5. Collection and Processing of Surficial Beach Sediment Samples

Surficial beach sediment samples were collected at the mean sea level mark, approximately half way between the high tide line and the low water level. Eight samples were collected, each at the benchmark locations as indicated by asterisks in figures 3.15 and 3.16. GPS co-ordinates of benchmarks are presented in Appendix I.

Sediments obtained from the nearshore varied from very fine sand sized particles through to gravel sized particles, therefore, sieves were used in the analysis, as the RSA (explained in section 3.7.2.) is incapable of measuring the gravel-sized particles with accuracy.

Sieve phi size ranged from –3 to 2.75 Ø, except for sample benchmark 30a, which was sieved from –3 to 4 Ø, due to the presence of very fine sands. 0.25 Ø intervals were used in all analyses.

3.4.6. Surficial Beach Sediment Sample Outcomes

Results of sieve analyses and sediment descriptions are compiled in appendix III.

Average mean grain size and sorting values obtained along the Pukehina coastal sector were 1.12 Ø (medium sand) and 0.89 Ø (moderately sorted) respectively. Average skewness and kurtosis values along the Pukehina coastal sector were –0.92 Ø (strongly coarse skewed) and 5.86 Ø (extremely leptokurtic) respectively. However, these average sediment characteristic values are influenced by sediment samples collected at Benchmark 30a. Benchmark 30a had a high concentration of titanomagnetite when sampled. Titanomagnetite is a fine grained sediment, which is also commonly very well sorted (as figure 3.14 illustrates). The Pukehina coastal sector as previously stated, is a quartzo-felspathic region, therefore, grain sizes would be expected to be medium to coarse sized grains, with moderate sorting. A high concentration of titanomagentite will therefore, mask true average sediment characteristic statistics of the region, as it has done here.

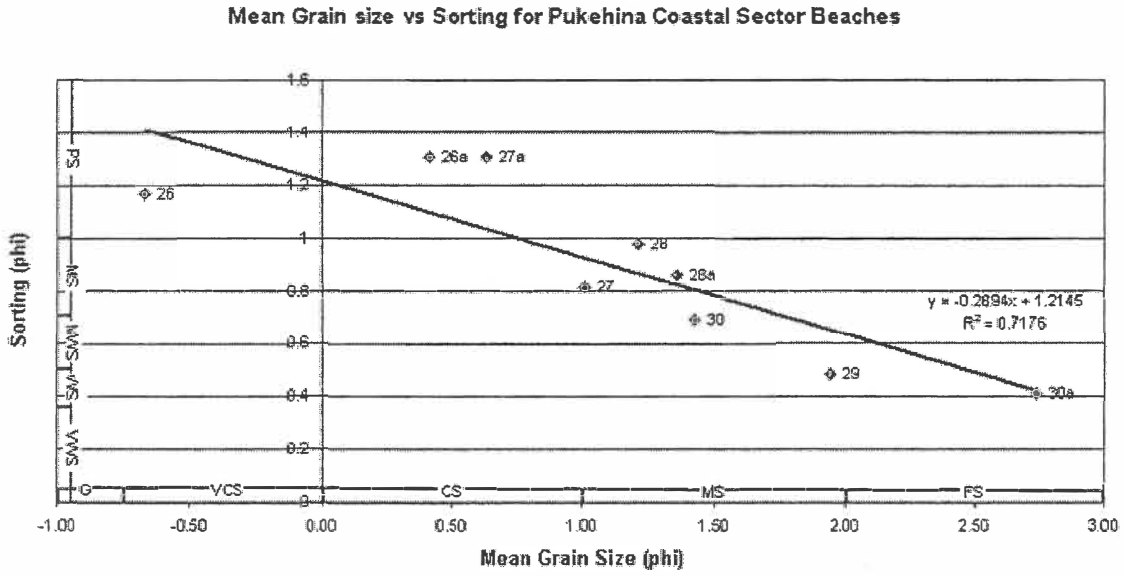

Figure 3.14 Bi-variate analysis of mean grain size and sorting for Pukehina coastal sector (benchmarks 26-30a). The linear trendline indicates that the further east in the coastal sector, energy and mixing processes increase. Different sources of sediment are identified, which are indicated by clustered data and non-clustered data. G = Granule, VCS =Very coarse sand, CS = Coarse sand, MS =Medium sand and FS =Fine sand. VWS= Very well sorted, WS =Well sorted, MWS = Moderately well sorted, MS =Moderately sorted and PS =Poorly sorted.

CARRANZA-EDWARDS (2001, p. 41) (from figure 3.11), states 'Increases in mixing processes induce a decrease in sorting values, indicating better sorting in beach sands'. Acknowledging this statement, benchmarks 26, 26a and 27a would be expected to be high energy regions, thereby being more exposed to frontal dune erosion. However, calculated average sorting obtained by CARRANZA-EDWARDS (2001) were from locations around the Gulf of Mexico and the Gulf of California, which all had values less than 0.8 Ø (average 0.76 Ø - Inshore, 0.64 Ø - Foreshore and 0.66 Ø - Backshore). Along the Pukehina coastal sector 67% of sampled analysed, are greater than 0.8 Ø. This indicates that there are obviously differing coastal processes occurring within the Pukehina coastal sector.

The cluster of results in figure 3.14 (samples 28, 27, 28a and 30), indicate that these may be from the same sediment source or sources, while data points such as benchmark 26 indicate an input from another sediment source. This is also evident from sediment mineralogy observations as clustered samples comprised of similar mineralogies, while others had inclusion of different minerals.

Observations of surficial sediment samples indicate that sediment of the Pukehina coastal sector were predominantly comprised of quartz, feldspar, glass, and other light minerals. However, sites such as benchmark 26, have a high percentage of greywacke. Offshore greywacke outcrops observed by HEALY *et al.* (1977) and adjacent streams, are likely sources of this sediment to the foreshore. This would mean that diabathic transport occurs at this location, and so movement of granule-sized particles (as per sediment mineralogy results) by onshore current and wave action would occur.

PHIZACKLEA (1993) concluded that heavy minerals in the Pukehina-Matata coastal sector were sourced from cliff erosion and fluvial inputs, in particular the Pikowai stream.
BURTON (1987) analysed the neighbouring Maketu Estuary and the Kaituna River, and found that heavy minerals are being discharged from both. PHIZACKLEA (1993) also noted that heavy minerals (particularly biotite) may be eroding from the Little Waihi formation

and overlying tephras, present within cliffs at Okurei Point. So both the Maketu Estuary and Okurei Point may be suppling heavy minerals to Newdicks Beach (Benchmark 30a).

Results of the SUNAMURA AND HORIKAWA (1972) model are illustrated in figure 3.15, comparative assessment of sediment textural parameters is presented in Appendix IV.

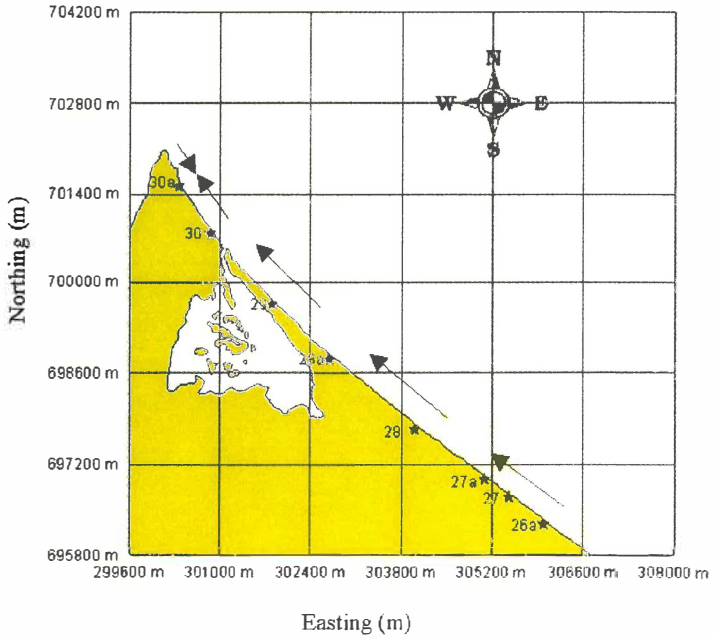

Figure 3.15 Sediment transport directions as determined using SUNAMURA AND HORIKAWA (1972) model. Asterisks indicate sediment sample location. Note arrows only give indication of sediment transport direction.

Results of the MCLAREN (1981) model are illustrated in figure 3.16, comparative assessment of sediment textural parameters is presented in Appendix IV.

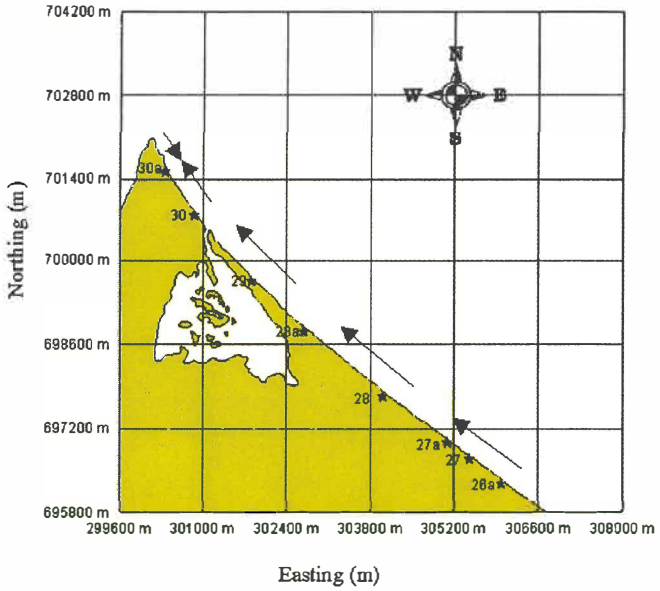

Figure 3.16 Sediment transport directions as determined using McLAREN (1981) model. Asterisks indicate sediment sample location. Note arrows only give indication of sediment transport direction.

Mean grain size, sorting textural models, based on the field data analysed in this study, indicate sediment transport is to the northwest from Pukehina Redoubt to the distal end of Pukehina Spit. Bi-directional sediment transport was indicated by both models at Newdicks Beach. However, if converging littoral drift was present at Newdicks Beach, this would be expected to induce sedimentary accumulation at this point. However, there is no obvious geomorphic manifestation of sediment accumulation evident, therefore, sediment transport implications by both the SUNAMURA AND HORIKAWA (1972) and McLAREN (1981) models may be incorrect.

The dominance of titanomagnetite, at site benchmark 30a is an indicator that sediment transport is occurring at this point. Since titanomagnetite is a heavy density mineral (4600 kg/m^3) compared to lighter density minerals such as quartz (2650 kg/m^3), and that the Pukehina Beach occurs in a region dominated by quartzo-felspathic geology, the light minerals were likely to have been transported or winnowed elsewhere. Storm activity is the likely cause of this high abundance of heavy mineral at Newdicks Beach. Storm activity increases transporting turbulence at the beach, and also increases wave run-up. Wave run-up may cause erosion of the frontal dune and berm, inducing water percolation

through the sediments and erosion of the berm as it returns to the ocean. Since titanomagnetite is a higher density mineral than quartz, titanomagnetite requires a greater stress exerted on the sediment by the water than quartz, therefore, titanomagnetite is commonly observed as a lag deposit after storm events, if the mineral is present in the beach sediments. In chapter 5 this possibility will be investigated, by analysing wave energy focussing (hence inducing increased wave run-up), which may be created from offshore undulating bathymetry, as figure 3.10 suggests.

PHIZACKLEA's (1993, p. 155) statement that 'Okurei Point is acting as a shelter to the influence of north and northeasterly generated waves, thereby creating a more complex current pattern than what occurs further east', seems to be consistent from surfical sediment textures analysed in this study and applied in both the SUNAMARA AND HORIKAWA (1972) model and MCLAREN (1981) model. This is supported by the complexity of the model predicted sediment transport at Newdicks Beach. The concentration of titanomagnetite exposed at Newdicks Beach indicates that erosion occurred at this location prior to the time of observation.

3.5 Offshore Sediment Texture

3.5.1 Aims and Objectives of Analysing Offshore Sediment Texture

Analysis of sediment characteristics may explain changes in sediment transport patterns, possible sediment sources and/or areas of strong wave/current interaction. It also provides a means of ground truthing side scan sonar interpretations.

Offshore sediment samples have earlier been collected by PHIZACKLEA (1993). New sediment samples should have been taken, in order to judge both change in coastal processes and to update existing data. Unfortunately due to instrument failure and weather constraints, only limited offshore sampling could be undertaken. However, with the aid of underwater video imagery (refer to section 3.4.6 for video locations) and side

scan sonagraphs (section 3.3), estimations of changes in sediment textures from PHIZACKLEA (1993) may be made.

3.4.7. Outcomes of Offshore Sediment Texture Analysis

From video imagery and side scan sonagraphs, alteration of PHIZACKLEA'S (1993) offshore sediment textural results, overall has been limited. However, changes in sediment textural patterns particularly offshore from Okurei Point, have been noticeable, as found with sonagraph results (section 3.3).

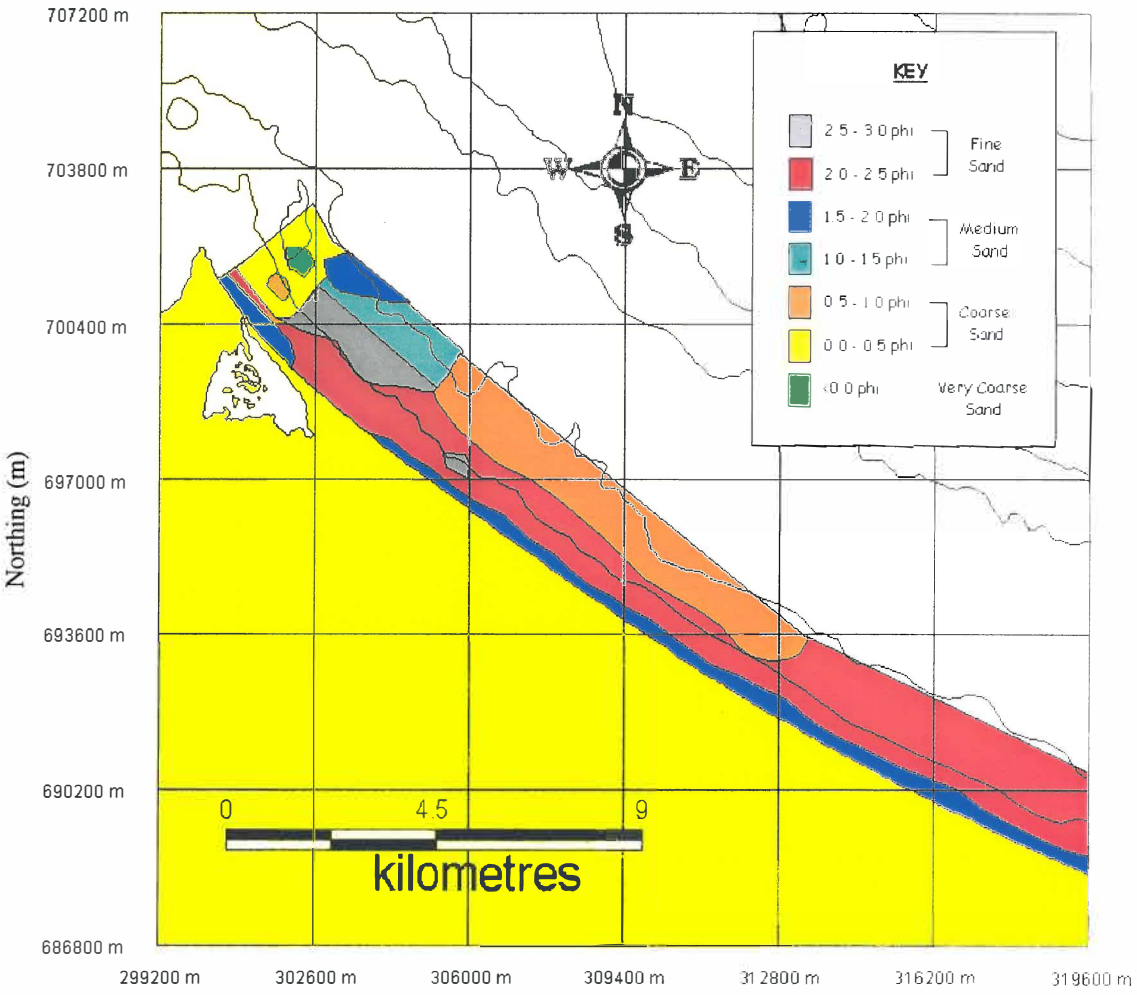

Figure 3.17 Mean grain size distributions taken from offshore sediment samples between Okurei Point and Pikowai. Adopted from PHIZACKLEA (1993).

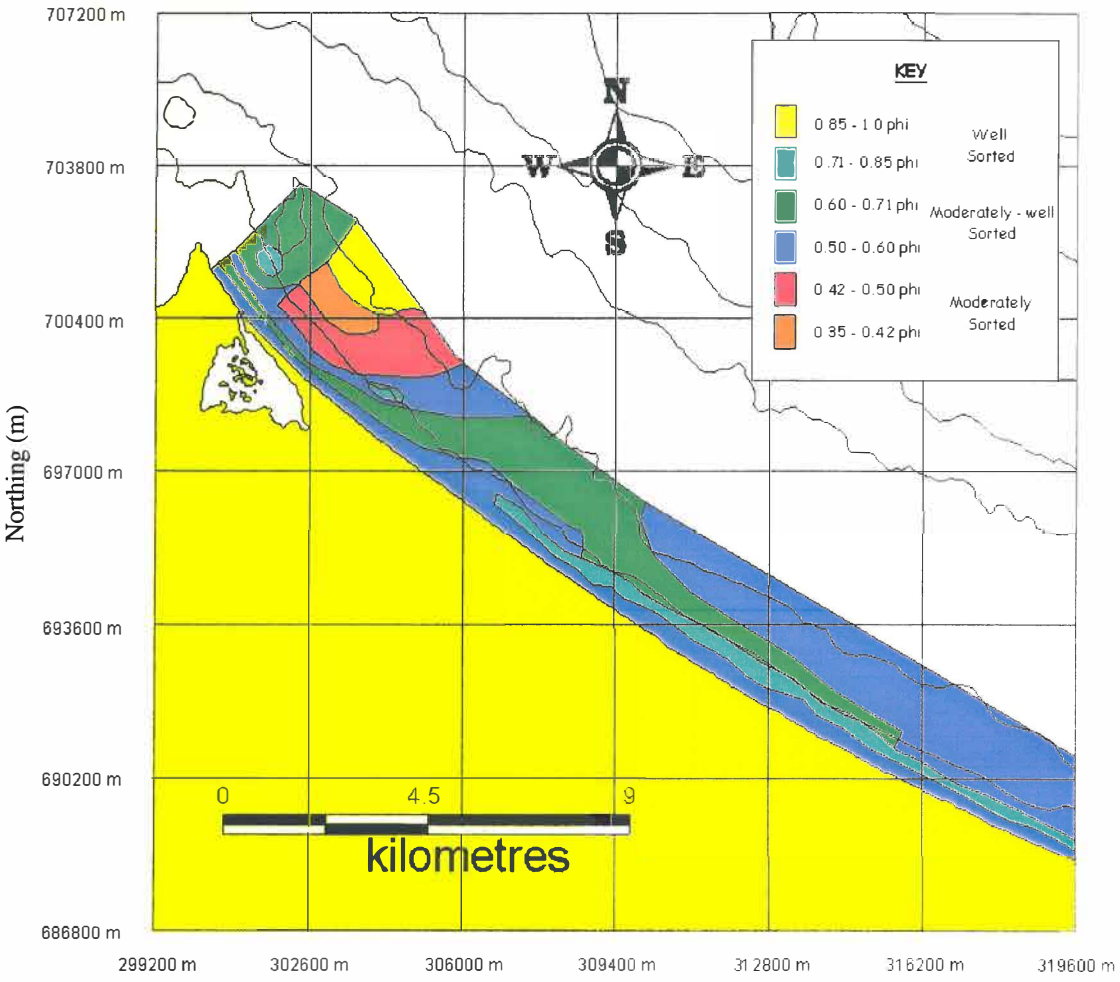

Figure 3.18 Sorting distributions taken from offshore sediment samples between Okurei Point and Pikowai. Adopted from PHIZACKLEA (1993).

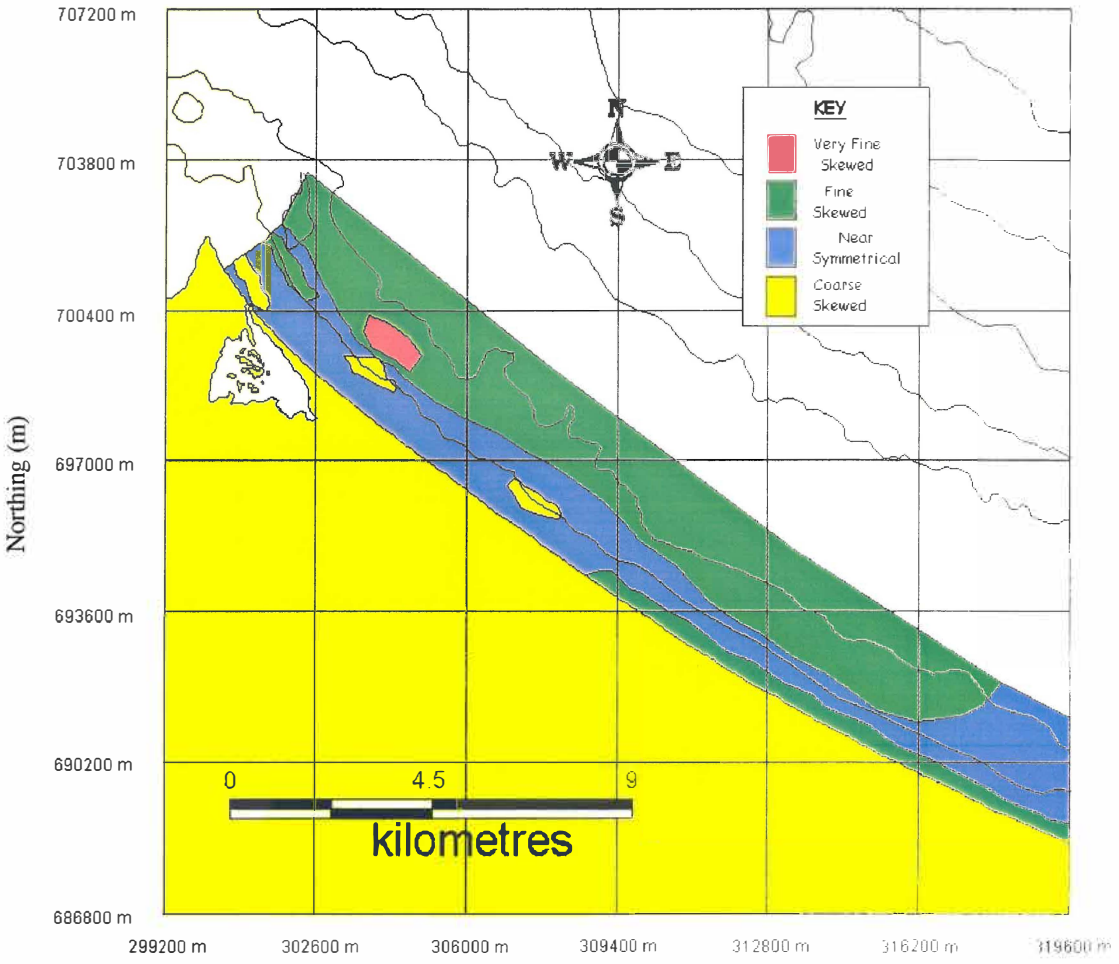

Figure 3.19 Skewness distributions taken from offshore sediment samples between Okurei Point and Pikowai. Adopted from PHIZACKLEA (1993).

3.4.8. *Discussion of Sediment Textural Patterns in Relation to Side Scan Sonar Outcomes*

FREDSØE AND DEIGAARD (1992, p. 90) state that 'megaripples are commonly formed from coarse grain sized sediment particles'. From current side scan sonar imagery (figure 3.10) and side scan sonar imagery undertaken by PHIZACKLEA (1993), regions where megaripples were observed, are not always consistent to associated regions of coarse sand. Specifically megaripples were located offshore from Pukehina Spit, a region associated with a predominance of fine sized sediment particles.

This paradox may be explained by analysing the components, which generate differing bedforms. Figure 3.20 illustrates the relationship between total bed shear stress (τ_b) and flow velocity (V) for different bedforms, as adopted from FREDSØE AND DEIGAARD (1992).

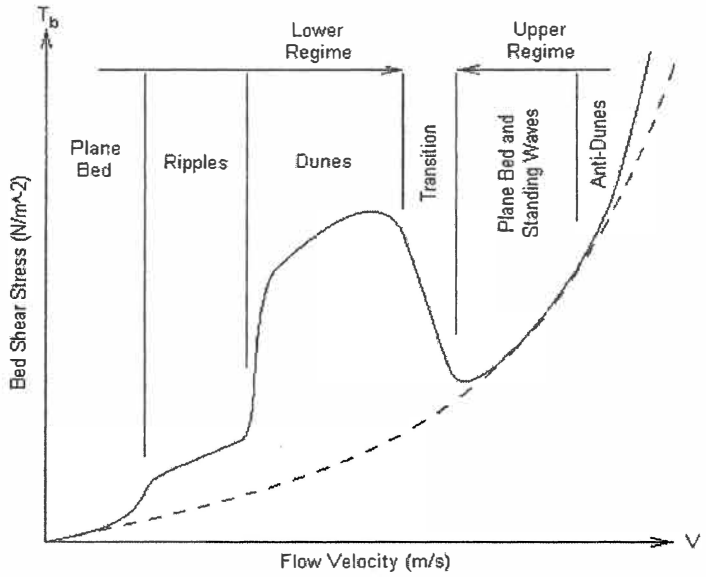

Figure 3.20 Relationship between total bed shear stress (τ_b) and flow velocity (V) for different bedforms. Adopted from FREDSØE AND DEIGAARD (1992).

The parabolic relationship, illustrated by the dashed line is defined by the equation

$$\tau_b = \tfrac{1}{2}\rho f V^2 \qquad \text{Eqn. 3.2}$$

where τ_b is the total bed shear stress, ρ is the density of seawater (1025 kgm^{-3}), f is the friction factor (or hydraulic resistance factor) and V is the flow velocity (ms^{-1}).

FREDSØE AND DEIGAARD (1992, p. 94) state that the 'formation of a particular bedform is related to the bed shear stress and the flow velocity at the bed, where a high bed shear stress value is commonly associated with a coarse grained sediment'. However, sediment with a high density will also have a large bed shear stress value, as it would require a higher flow velocity, at the bed, to entrain a heavy density mineral than a light density mineral.

From offshore sediment samples obtained by PHIZACKLEA (1993), sediment mineralogy offshore from Pukehina Spit is dominated by light minerals, but an increased concentration of heavy minerals are also present in this region in comparison to other surrounding regions. Titanomagnetite is a heavy mineral, which was obtained in surficial sediment samples at benchmark 30a (section 3.4.6.), in high concentrations. As previously stated titanomagenetite is commonly a fine to very fine grained sediment. It may therefore be possible that sediment texture offshore from Pukehina Spit are subject to high bed shear stresses, thereby allowing megaripple formation.

3.5 Offshore Bedforms

3.5.1 Aims and Objectives of Assessing Offshore Bedforms

Near bed currents are primarily induced by waves, which may initiate sediment transport by sheet flow and form rhythmic morphological features, termed bedforms (TRENHAILE, 1997). Analysing bedforms in the Pukehina coastal sector, therefore may indicate sediment transport directions, transport behaviours (i.e. relative transport volume), and delineation of sediment pathways.

To observe bedforms a drop video camera (a video camera enclosed in a waterproof casing or also known as a 'splash cam') was used. A scale bar and compass were attached to the video casing to enable the determination of bedform size and orientation.

3.5.2 Characteristics of Bedforms

Previous studies of bedforms in the Bay of Plenty have noted the presence of a range of bedforms including ripples: megaripples, sand waves and sand ridges (HARMS, 1989; BRADSHAW, 1991; FOSTER, 1991; HICKS AND HUME, 1993; PHIZACKLEA, 1993; SAUNDERS, 1999).

LARSON *et al.* (1997), group these bedforms into four categories: ripples, dunes, planar beds and antidunes.

- *Ripples* are small bedforms with a crest-to-crest distance of 0.6 m or less. Ripples are further classified into five subgroups, which are illustrated in figure 3.21.
- *Dunes* are bedforms with crest-to-crest distances of 0.6 m to 1000 m, previously named megaripples and/or sand waves in literature. Dunes are also subdivided into two groups as either two or three-dimensional. A two-dimensional bedform is created due to the flow pattern of water being relatively unchanged and perpendicular to its overall direction, while a three-dimensional bedform is developed from near-bed eddies or variable vortices (LARSON *et al.*, 1997)
- *Planar beds* are horizontal beds. They do not have elevations or depressions larger than the maximum size of the exposed sediment. Planar beds occur under two hydraulic conditions;
    - The transition zone between the region of no movement and the initiation of dunes.
    - The transition zone between ripples and antidunes, at mean flow velocities between 1-2 ms^{-1} (LARSON *et al.*, 1997).
- *Antidunes* are morphological features that are in phase with water surface gravity waves. The height and wavelength of a antidune is dependent on the fluid and the characteristics of the bed material (LARSON *et al.* 1997).

	Ripples	**Dunes**	**Plane bed**	**Antidunes**
Crest-to-crest distance	λ<0.6m	0.6m≤λ>1000m	n/a	n/a
Geometry	1. Straight 2. Sinuous 3. Catenary 4. Linguoid 5. Lunate	1. Small (0.6λ<5m) 2. Medium (5λ<10m) 3. Large (10λ<100m) 4. Very Large (λ>100m)	n/a	n/a
Typical flow velocity (m/s)	0.1-0.97	0.35-2	>.97	>1.7
Detection	Divers	Divers/sonagraphs/ echo-sounder	Divers/ sonagraphs	Divers/ sonagraphs

Table 3.2 Bedform classification scheme adopted for this study. After LARSON *et al.* (1997).

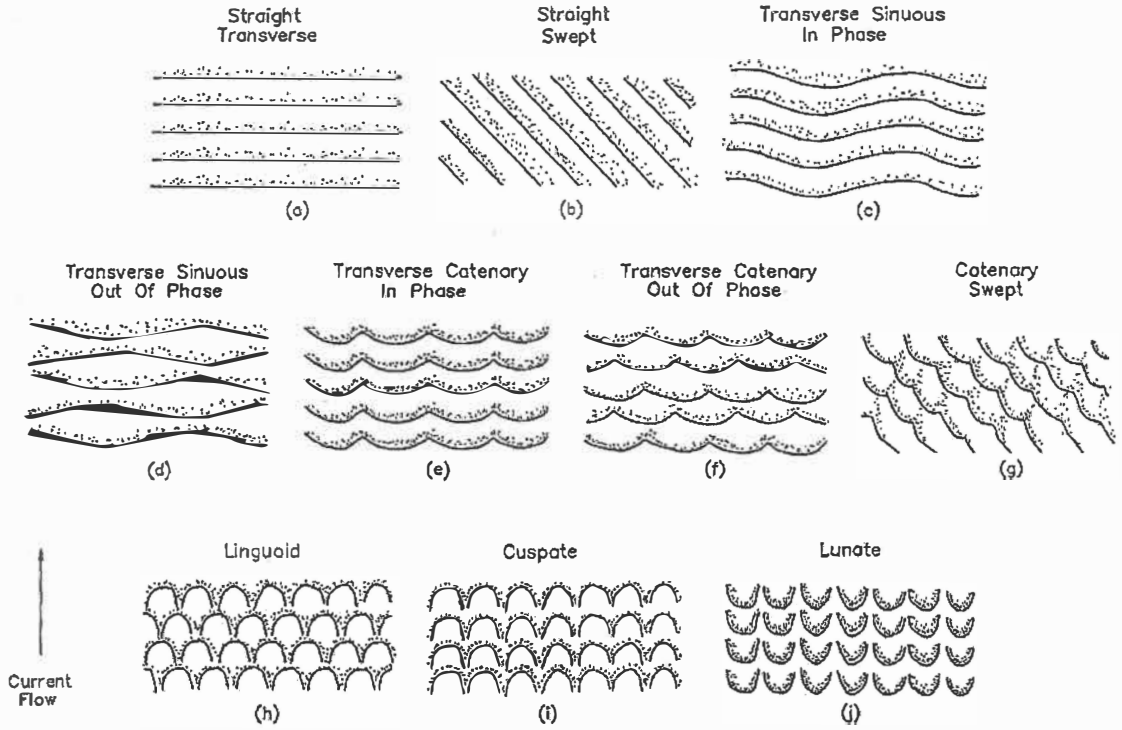

Figure 3.21 Ripple classification based on ripple crest morphology. Five types of ripple can be identified: straight (a-b); sinuous (c-d); caternary (e-g); linguoid (h) and lunate (j). Adopted from LARSON *et al.* (1997).

3.5.3 Interpretations of Offshore Bedforms

Figure 3.22 illustrates the locations where video imaging was conducted. GPS co-ordinates of video imaging sites, are presented in Appendix I. Locations were selected from specific locations of interest (sediment textural boundaries, bedforms and rock outcrops) identified from side scan sonagraphs.

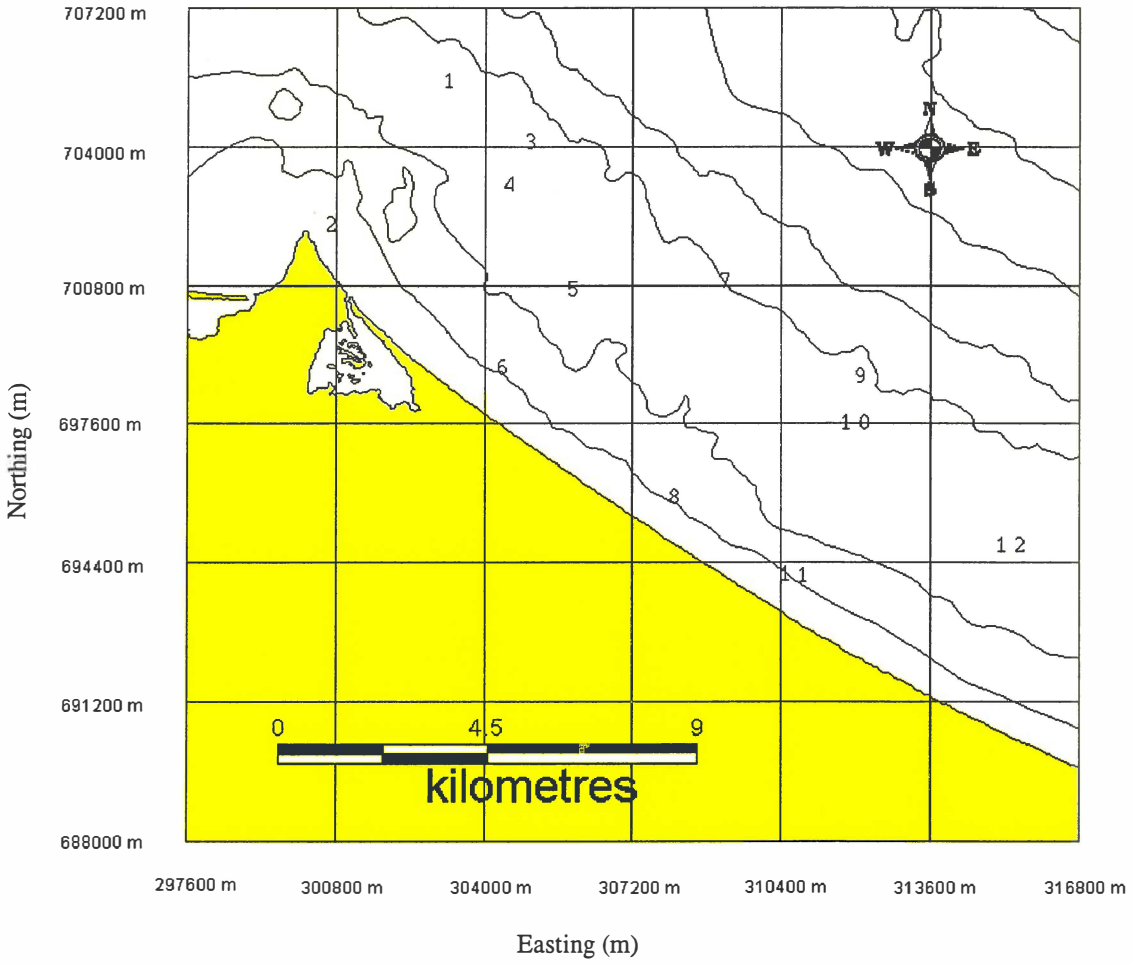

Figure 3.22 Video imaging locations taken from Okurei Point to Pikowai, to assess sediment characteristics and the presence of bedforms and their associated size and orientation. GPS co-ordinates of video locations may be obtained from appendix I.

Figure 3.23 illustrates examples of video imagery recorded and types of bedforms present within the Pukehina coastal sector. Rock outcrops present in the area are common in the Okurei Point region and were observed at video locations 1, 2, 3 and 4. This is verified by results obtained from side scan sonagraphs. Outcrops are also present in the Pukehina Redoubt area. These outcrops are more widely dispersed than in the Okurei Point area, but had similar dimensions.

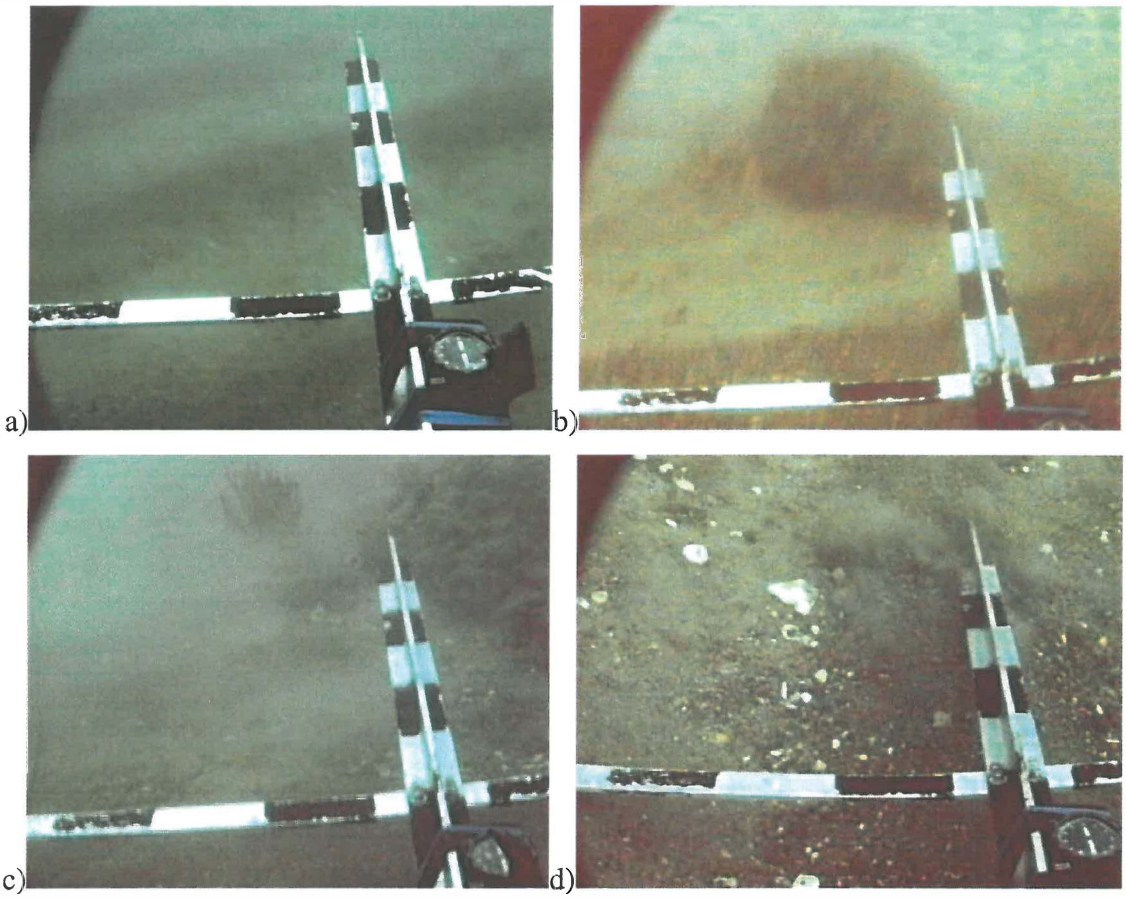

Figure 3.23 Typical bedforms present in Pukehina coastal sector. A) Dunes present at site 3 (λ= 0.9m, η=0.1m). B and C) Rock outcrops and bedforms present at Okurei Point (sites 1 and 2) in 22m water depth. D) Ripples (λ= 0.5m, η=0.05m) and coarse shell deposits at Pukehina Redoubt (site 4) in 30m water depth. (Photographs taken by author).

PHIZACKLEA (1993) analysed distributions of coarse dunes in the Pukehina-Matata sector, in attempt to assess offshore sediment transport pathways. Bedform distribution, orientation and characteristics (λ and η) were used in the analysis. PHIZACKLEA (1993, p. 257) states that there was an overall trend of bedform orientation to the northwest, in the Okurei Point-Pikowai coastal sector, indicating a directed sediment transport to the southeast at the time of observations. However, when examining results of PHIZACKLEA (1993), bedform orientation was not northwest but northeast, therefore incurring a sediment transport in the southwesterly direction at the time of observation (figure 3.24).

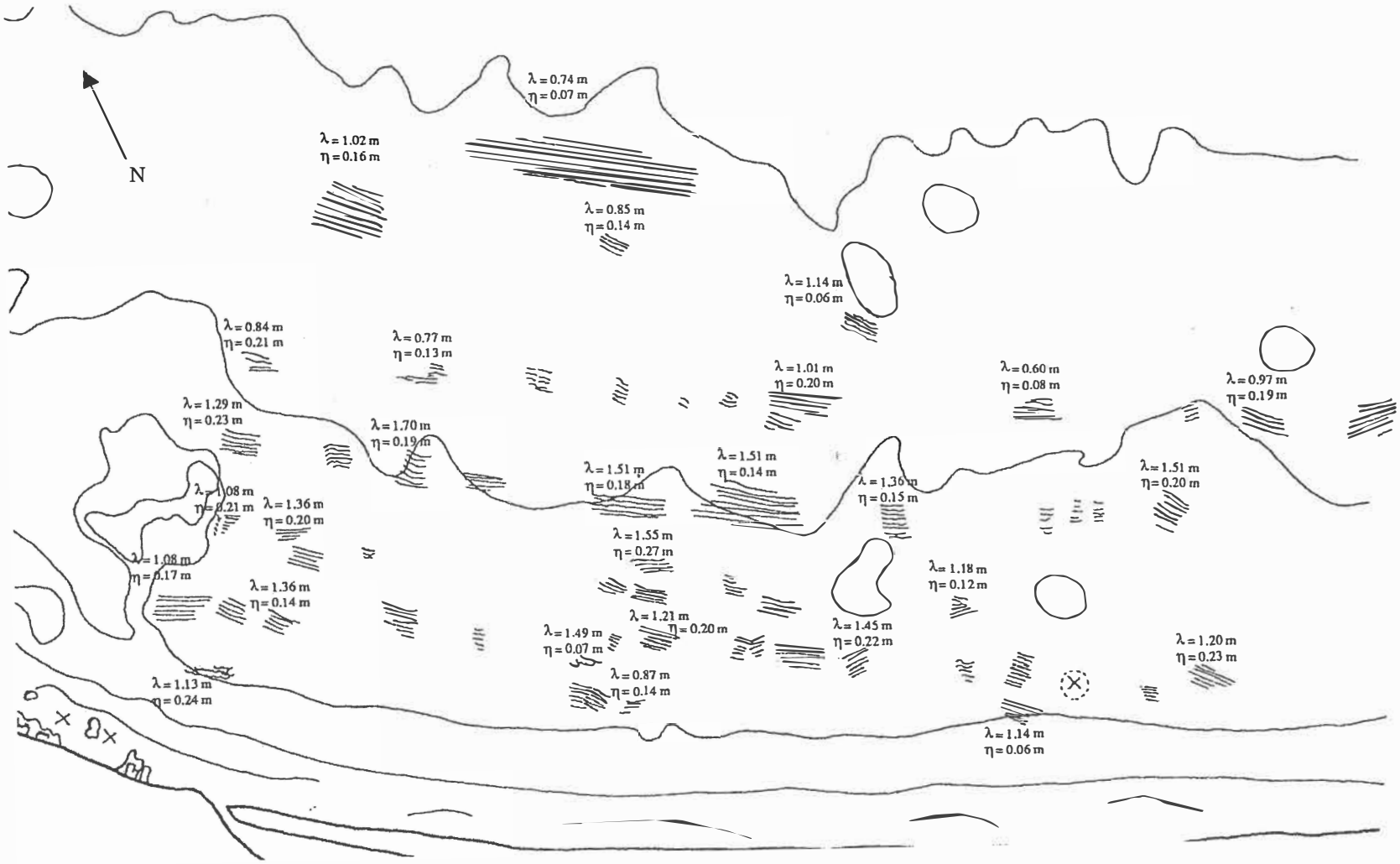

Figure 3.24 Approximated distribution, orientation, and bedform characteristics of dunes from Okurei Point to Pukehina Redoubt, based on sonograph measurements of visible bed forms, observed by PHIZACKLEA (1993).

PHIZACKLEA (1993, p. 306) also stated that' areas where bedrock is present, especially in the Okurei Point region, possible downwelling currents may cause intense scouring of bottom sediments, since current flows are restricted and intensified, forming bands and patches of coarse grained dunes'. In bedform observations obtained here, similar patches of coarse-grained dunes were present. However, bands were not present, indicating that the downwelling currents predicted by PHIZACKLEA (1993), may not be occurring at the time of observation.

Following the methods of PHIZACKLEA (1993) and SAUNDERS (1999), dune lengths were estimated from sonagraphs using:

$$H=z.s/l, \qquad \text{(Eqn. 3.3)}$$

where H is the height of object. z is the height of side scan tow fish above seabed, s is the acoustic shadow length of the object(s) and l is horizontal distance of the object from the fish (BLACK AND HEALY, 1983).

From the analysis of side scan sonagraphs, bedform characteristics (illustrated in figure 3.25) were found to be very similar to observations made by PHIZACKLEA (1993) (figure 3.24). However, dune orientation has changed overall to a more shore normal orientation (north-northeast), therefore, indicating different wave activity prior to bedform observations. In some areas (particularly offshore from Pukehina Redoubt), dunes exhibit a northeast orientation indicating a more westerly movement of sediment than sediment movement offshore from Newdicks Beach. The possibility of exposed bedrock in this region, may attribute to the alteration in wave action and currents, as found by similar results offshore from Okurei Point by PHIZACKLEA (1993).

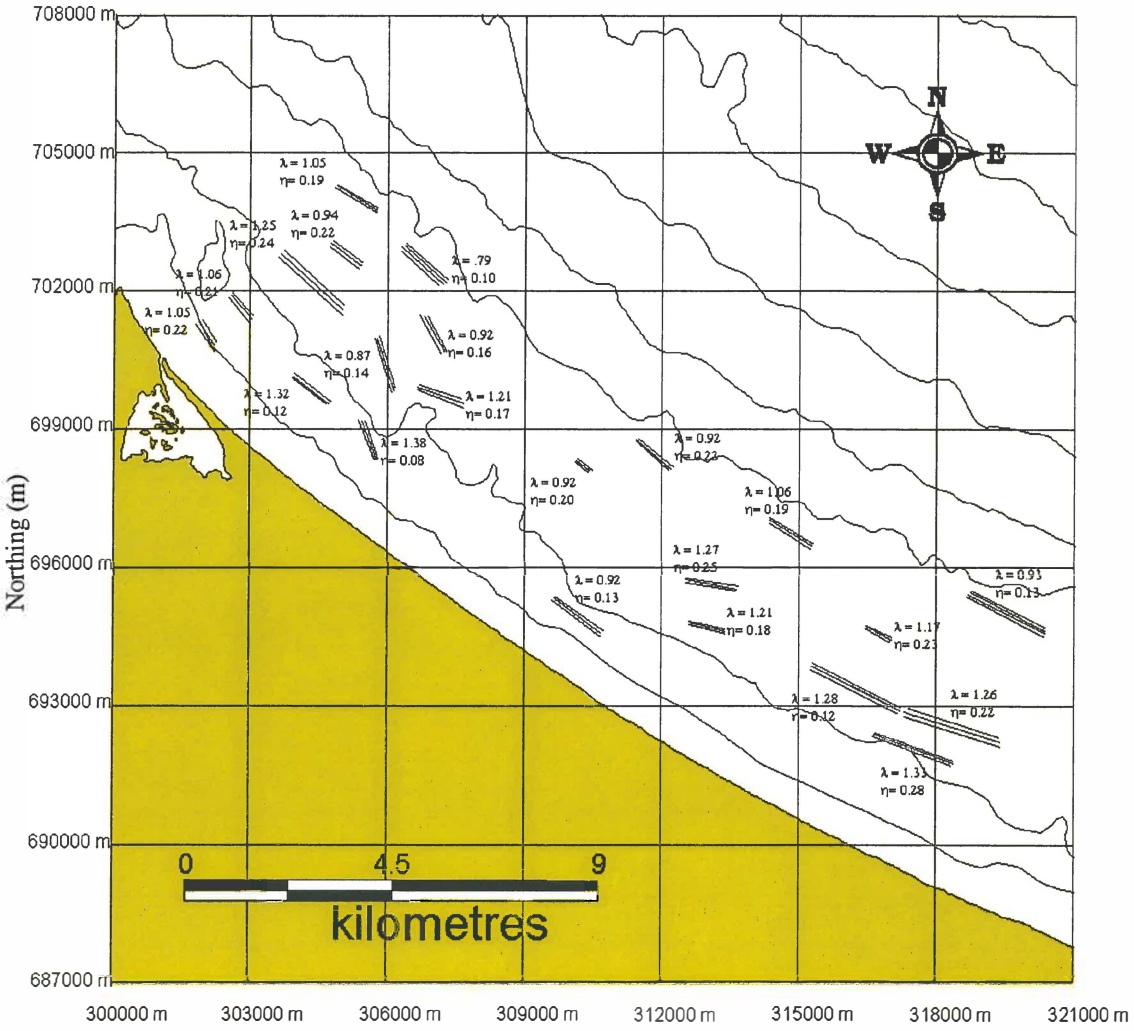

Figure 3.25. Approximated distribution, orientation, and bedform characteristics of coarse dunes from Okurei Point to Pikowai, based on sonagraph measurements of visible bedforms.

3.6 Sediment Trap Analysis

3.7.1. Aims and Objectives of Utilising Sediment Traps

Sediment traps are used to assess suspended sediment concentration within the water column. Sediment suspension is created by wave orbital motion and other currents, causing stress on the seabed. Once stress exceeds a sediment suspension threshold (defined by sediment particle shape and density), sediment will become entrained. The

elevation at which a particle becomes suspended in the water column is dependent on the wave orbital dimensions, and currents within the water column. KANA (1978) noted that principal factors controlling suspended sediment concentration are in order of importance: 1) elevation above the bed, 2) breaker type, 3) distance relative to the breakpoint, 4) beach slope and 5) wave height. BLACK AND ROSENBERG (1994) further noted that suspended sediment concentration is strongly dependent on breaker type wave properties, such as wave period and height. For example, plunging waves create larger vortices than spilling waves, and so turbulence created by plunging waves extend deeper into the water column, increasing the potential for higher suspended sediment concentration.

Settling velocity is also dependent on the density and shape of suspended particles. Determination of the settling velocity and sediment characteristics of sediment obtained in traps, were performed with the Rapid Sediment Analyser (RSA), which is discussed in section 3.7.2.

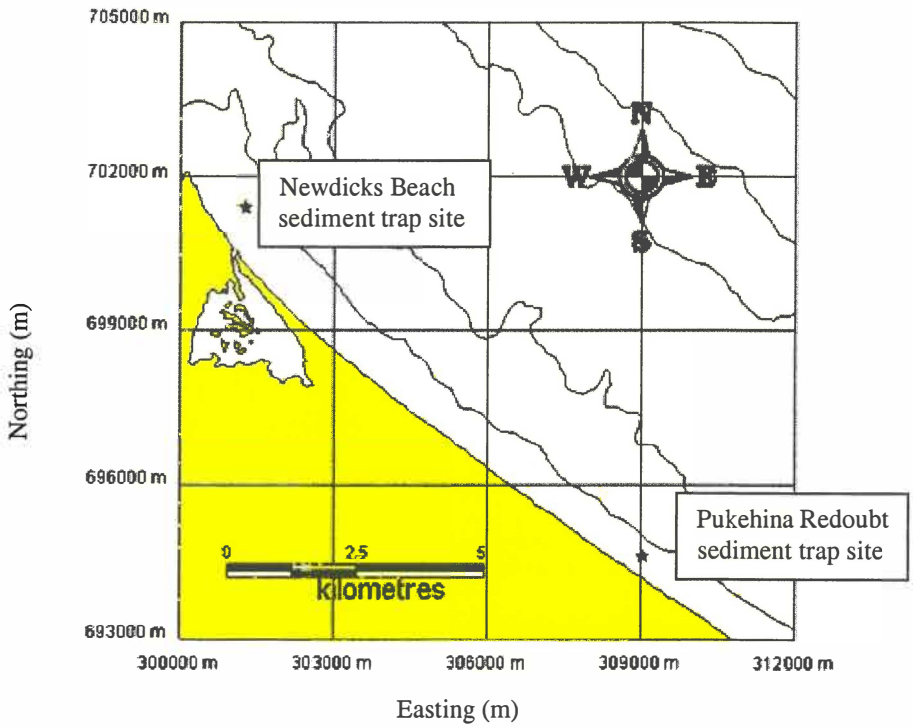

Figure 3.26. Sediment trap locations at Newdicks Beach and Pukehina Redoubt, to assess suspended sediment concentrations. GPS co-ordinates of sediment trap locations are presented in Appendix I.

Sediment traps were deployed at two stations, as shown by figure 3.26. GPS co-ordinates of sediment trap locations, are presented in Appendix I. At each station four traps were deployed at elevations of 0.35 m, 0.5 m, 0.8 m and 1.2 m above the seabed.

3.7.2. Rapid Sediment Analyser

Sediment grain size analysis was carried out using the Rapid Sediment Analyser (RSA). The RSA is a double-skinned perspex settling tube, which uses Stokes law (equation 3.4) to determine grain size and settling velocity by calculating the time it takes for a particular sediment particle to fall though a water column a known distance. Cumulative weight data is recorded and data are represented as Ø and ω values for grain size and settling velocity respectively.

$$\omega = \frac{1}{18}\frac{\left(\rho_s - \rho_f\right) g D^2}{\mu} \qquad \text{Eqn. 3.4}$$

where ω is settling velocity (ms^{-1}), ρ_s is the density of the sediment (kgm^{-3}), ρ_f is the density of the fluid inside the RSA (kgm^{-3}). g is gravitational acceleration (9.81 $m^{-1}s^{-2}$), D is the mean sediment diameter (m) and μ is the viscosity of fluid (m^2s^{-1}).

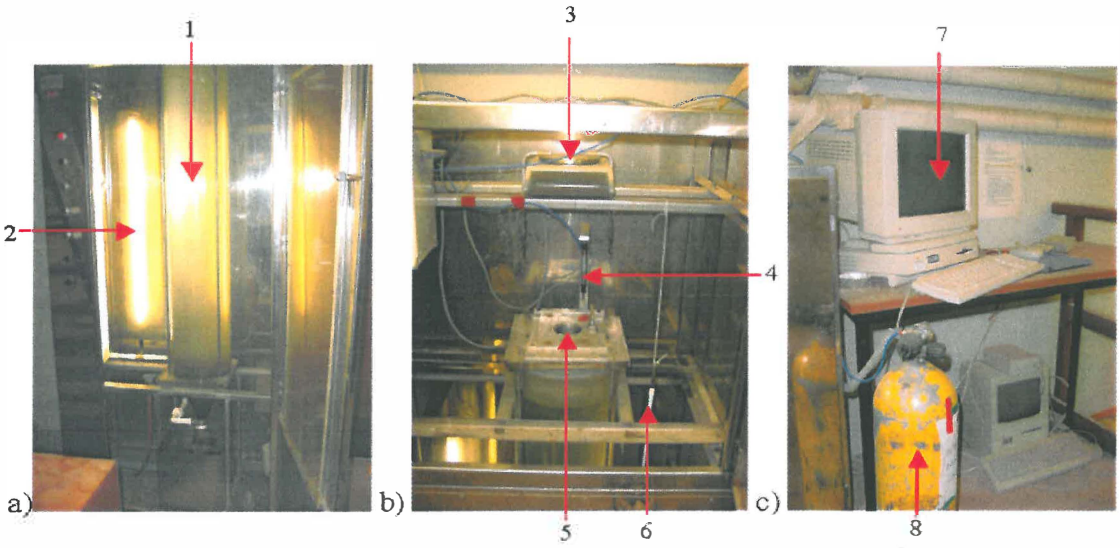

Figure 3.27 a) Values are obtained by timing the duration sediment takes to fall through the water column a known distance, results given are mean values for each sediment trap elevation. b) Sediment release cassette and scales. c) Macintosh computer linked to RSA.

Figures 3.27 a, b, and c depict the RSA, and associated apparatus. Figure a illustrates the settling tube (1), which is filled with tap water. Lights are used to maintain a constant water temperature throughout measurements (2). Scales (3) are used to measure the cumulative weight of sediment that falls on to the 'pan', which is situated at the bottom of the settling tube and is attached to the scales via two nylon strings. Water temperature must be measured before each analysis with a thermometer (6), as temperature is proportional to the density of the fluid inside the settling tube. Sediment is released into the water column, by means of a gas cylinder (8), releasing air and firing a pneumatic trigger (4), which opens the cassette (5), a 'trapdoor-like' mechanism, which is linked to the Macintosh computer (7) and begins collecting and storing data once the pneumatic trigger has been fired. Calculations of wanted variables may be obtained after each analysis or at a later date.

3.7.3. Sediment Trap Analysis Results

Outcomes of RSA analysis, including sediment characteristics and settling velocities are included in Appendix V. Table 3.3 summarises average moment sediment characteristic parameters, obtained from sediments deposited inside sediment traps, located offshore from Newdicks Beach and Pukehina Redoubt in 5 m water depth.

Deployment Location and Duration	Mean Grain Size	Sorting	Skewness	Kurtosis
Newdicks Beach Winter deployment (17/5/2000 – 8/6/2000)	2.33	0.798	-0.65	4.85
Pukehina Redoubt Winter deployment (17/5/2000 – 8/6/2000)	2.36	0.77	-0.46	4.80
Newdicks Beach Summer deployment (10/3/2001 – 9/4/2001)	2.56	1.00	-0.70	3.85
Pukehina Redoubt Summer deployment (10/3/2001 – 9/4/2001)	2.90	0.77	-0.65	4.92

Table 3.3 Average moment sediment characteristics obtained from sediments deposited inside sediment traps located offshore from Newdicks Beach and Pukehina Redoubt. Units are all phi (Ø).

Average moment statistical information obtained from sediment collected in the sediment traps, denotes that parameters are all of similar classification. From FOLK (1968), all sediments obtained can be classified as extremely leptokurtic (sediments closely distributed to the mean), strongly coarse skewed (higher concentration of coarser than finer sized sediments), and moderately sorted. Mean grain sizes of the sampled sediments were fine grained sediments.

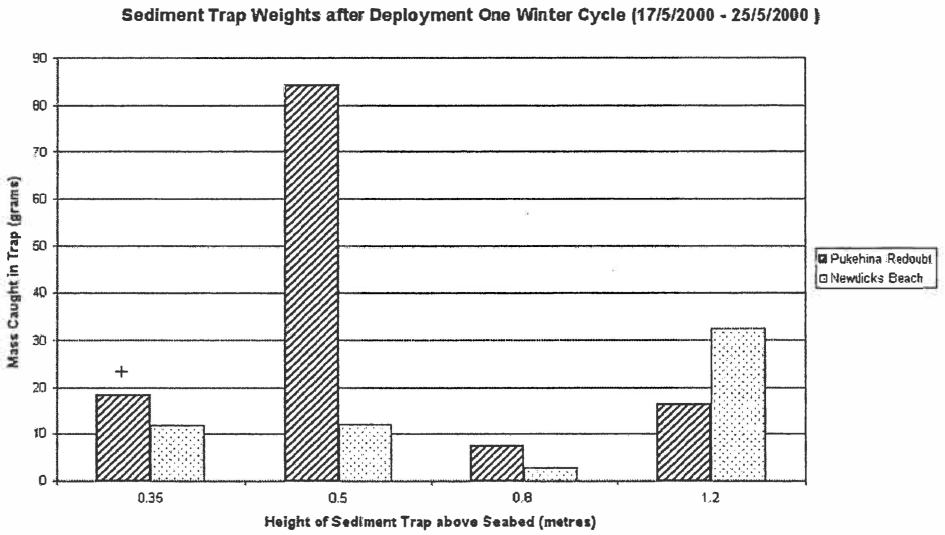

A)

Figure 3.28a Sediment trap analysis results for Pukehina Redoubt and Newdicks Beach during winter deployment one (17/5/2000 – 25/5/2000). Note, + indicates biological organism found in trap.

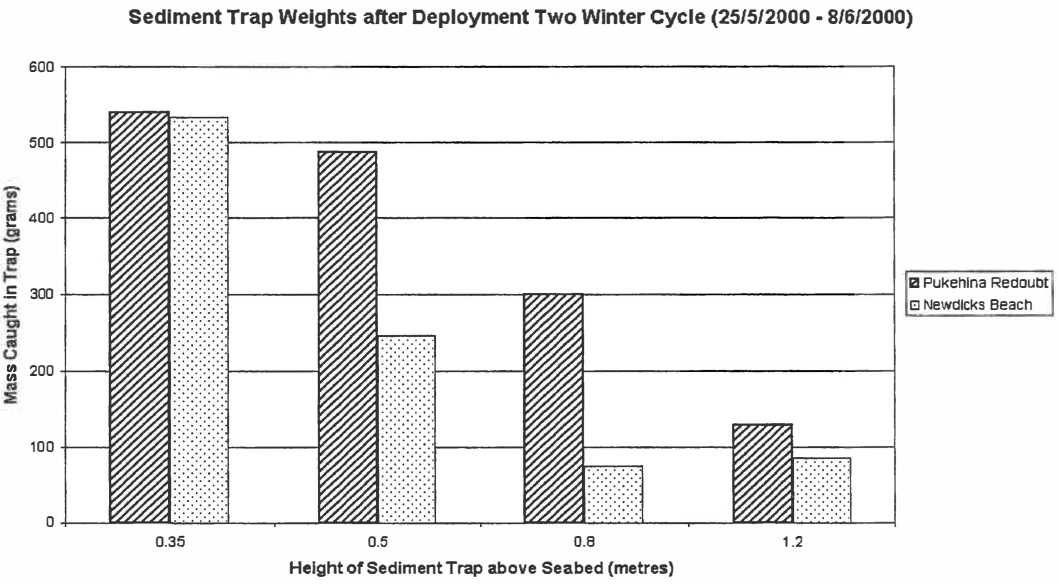

B)

Figure 3.28b Sediment trap analysis results for Pukehina Redoubt and Newdicks Beach during winter deployment two (25/5/2000 – 8/6/2000).

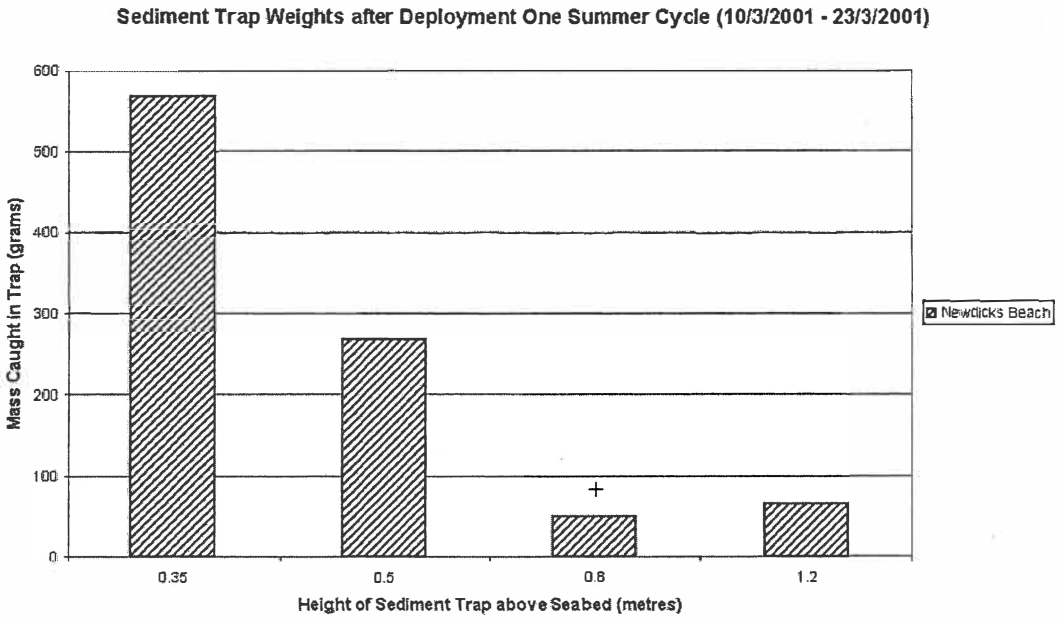

A)

Figure 3.29a Sediment trap analysis results for Newdicks Beach during summer deployment one (10/3/2001 – 23/3/2001). Note + indicates biological organism found in trap.

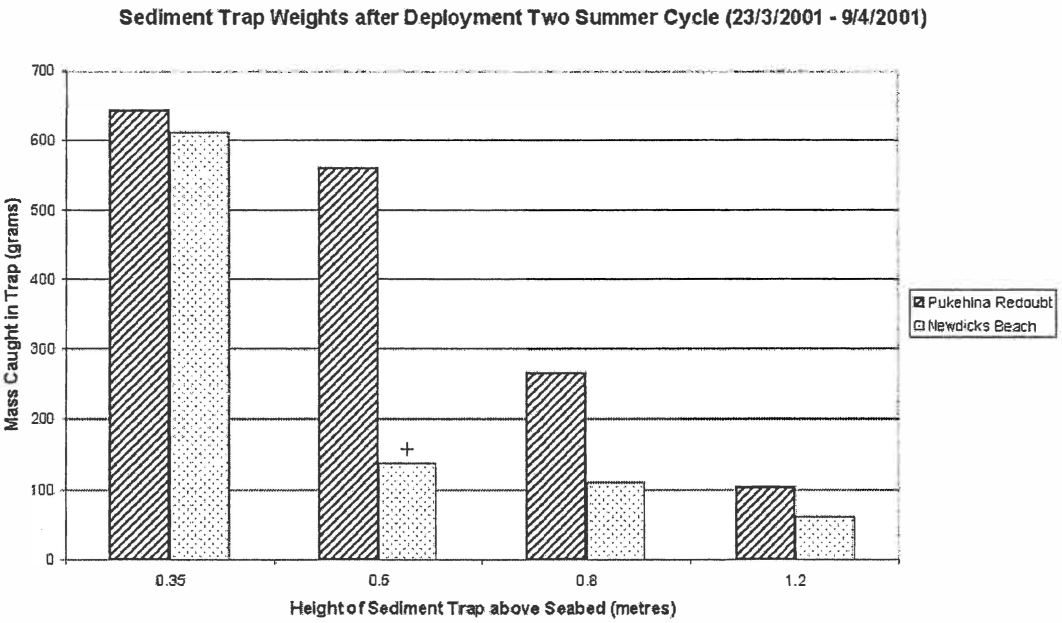

B)

Figure 3.29b Sediment trap analysis results for Pukehina Redoubt and Newdicks Beach during summer deployment two (23/3/2001 – 9/4/2001). Note Pukehina Redoubt results are over entire summer deployment (10/3/2001 – 9/4/2001), + indicates biological organism found in trap.

3.7.3.1. Discussion

The masses of sediment accumulated over the trap deployments specified, have not shown the trends that were expected. Typically, the highest mass would be expected closest to the bed (as stated by FLINT (1998, p. 23), as the water column with suspended sediment above the trap aperture is greatest at this elevation. Sediment accumulation would then be expected to decrease as elevation above the bed increases. The anomalous results shown in figures 3.28 and 3.29, may be attributed to biological activity. During summer deployments, two *Octopus Zealandia* (figure 3.30), (classified by POWELL (1979)), were found in sediment traps (Newdicks Beach deployment one 0.8 m and Newdicks Beach deployment two 0.5 m). Also during one deployment (Pukehina Redoubt deployment one winter cycle 0.35 m), an 8 cm long *Sardinops neopilchardus* (classified by THOMPSON (1981)) was found inside the sediment trap. An octopus or fish in a sediment trap will obviously inhibit the amount of sediment accumulated in the trap by its movements. Resuspension of accumulated sediment and increased currents around the aperture of the trap, are the most likely causes of sediment loss in a sediment trap due to biological activity.

Figure 3.30 *Octopus Zealandia* (POWELL, 1979) found in two sediment traps. Pen for scale (≈ 14cm).

Differences between the sediment mass collected from winter deployment one and two may be attributed to predominant wind direction during the two deployments.

Deployment one recorded predominantly offshore winds (figure 3.31a), while deployment two recorded onshore and offshore winds, as illustrated in figure 3.31b.

The increase of sediment accumulation in deployment two, may possibly be attributed to sediment being suspended from an offshore bar by wave orbital motion and undergoing diabathic transport towards the beach.

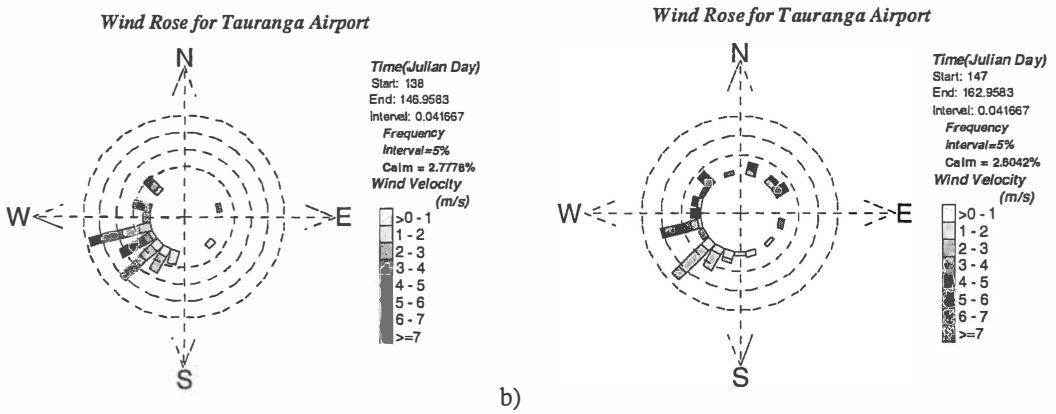

Figure 3.31 Wind roses for deployment one (a), and two (b) during winter cycle. Each frequency band denotes 5% of the total number of wind recordings, with wind velocity increasing with shade and direction in degrees true. Wind roses plots created by ROSES[♀].

Comparing wind data obtained during summer deployment (figure 3.32) with winter data (figure 3.31) indicates a more variable wind direction. In summer, however, wind velocities between each deployment are similar. Masses of sediment in traps are also similar in both summer deployments. Since results indicate the above, the influence of onshore winds increasing suspended sediment concentration in the water column, becomes a more evident statement.

[♀] ROSES by Rick Liefting, NIWA, *pers. comm.* 1998.

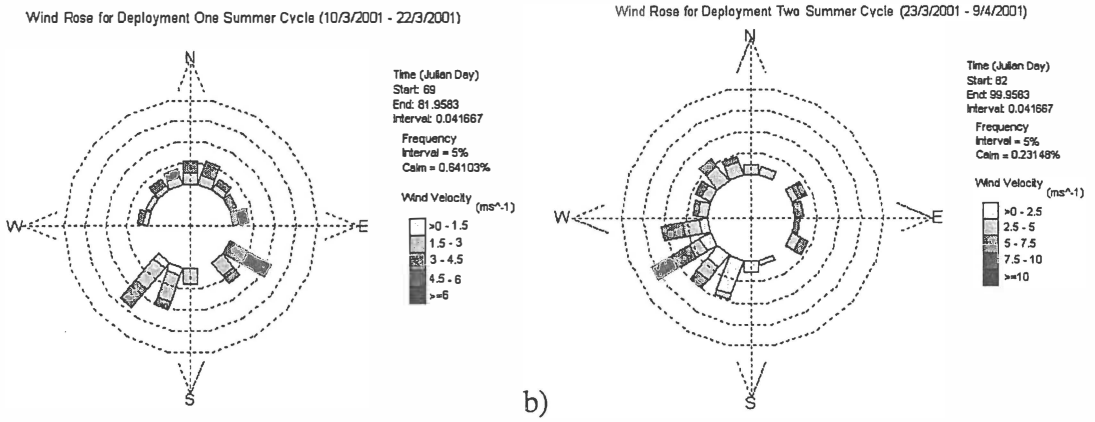

Figure 3.32 Wind roses for deployment one (a), and two (b) during summer cycle. Each frequency band denotes 5% of the total number of wind recordings, with wind velocity increasing with shade and direction in degrees true.

3.7.4. Sediment Characteristics

Analysing sediment characteristics at each location and elevation may indicate differing wave energies from one location to another. Greater orbital motion and currents created by large waves would induce coarser sediments to be entrained higher above the seabed. If this were to be valid, sorting must also be analysed to assess whether the suspended sediment is of various phi classes or just one predominant phi class.

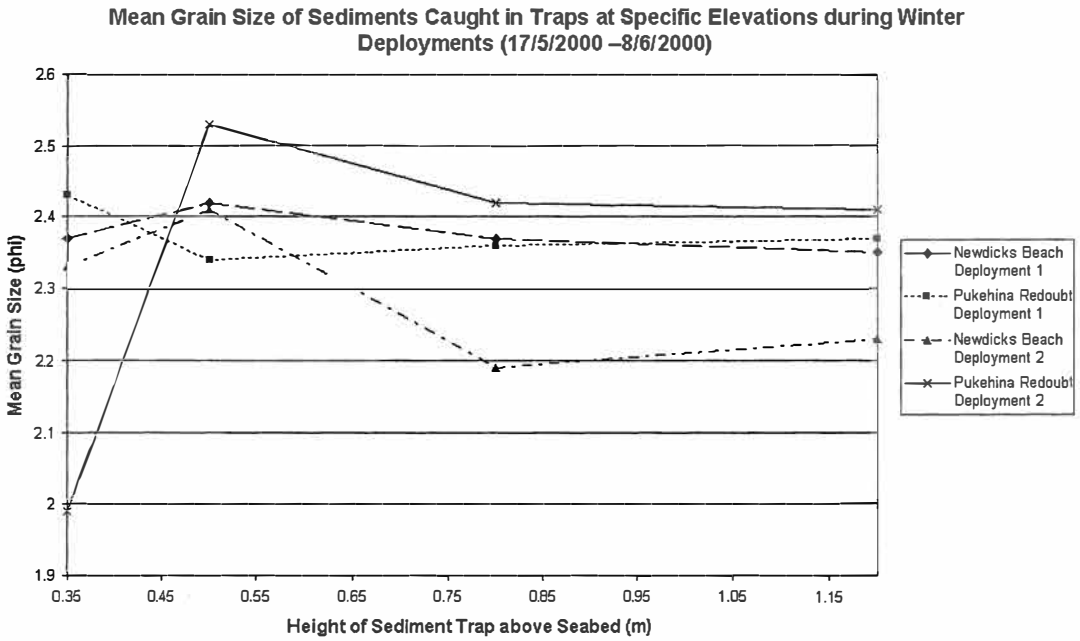

Figure 3.33 Mean grain size of sediments caught in sediment traps at specific elevations during winter deployments. Deployment one (17/5/2000 – 25/5/2000). Deployment two (25/5/2000 – 8/6/2000).

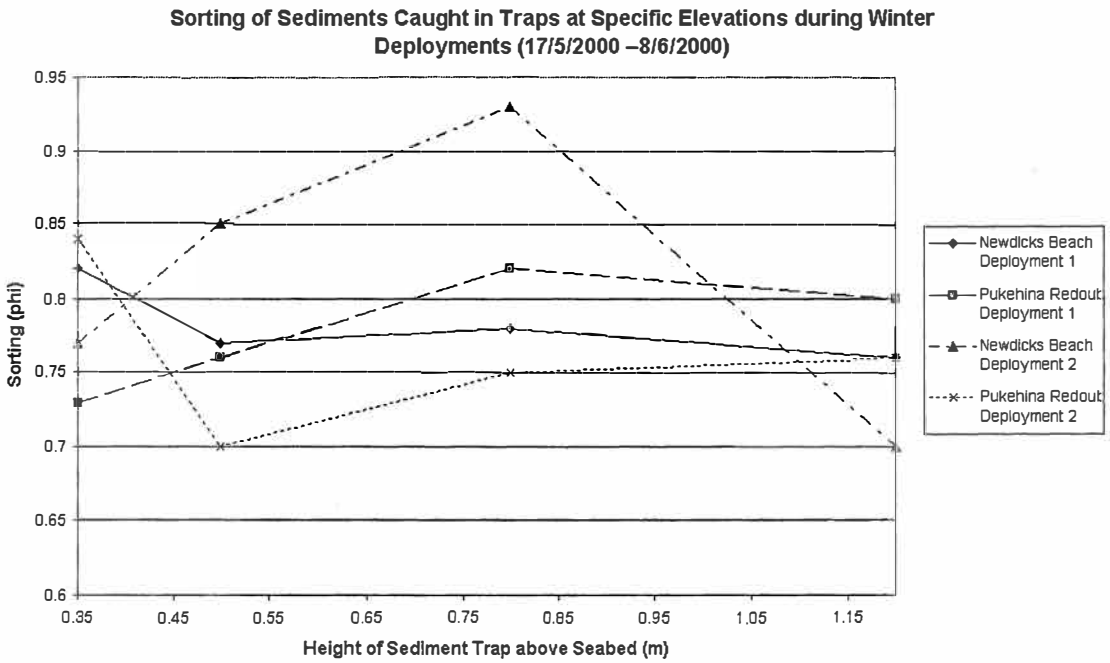

Figure 3.34 Sorting of sediments caught in sediment traps at specific elevations during winter deployments. Deployment one (17/5/2000 – 25/5/2000). Deployment two (25/5/2000 – 8/6/2000).

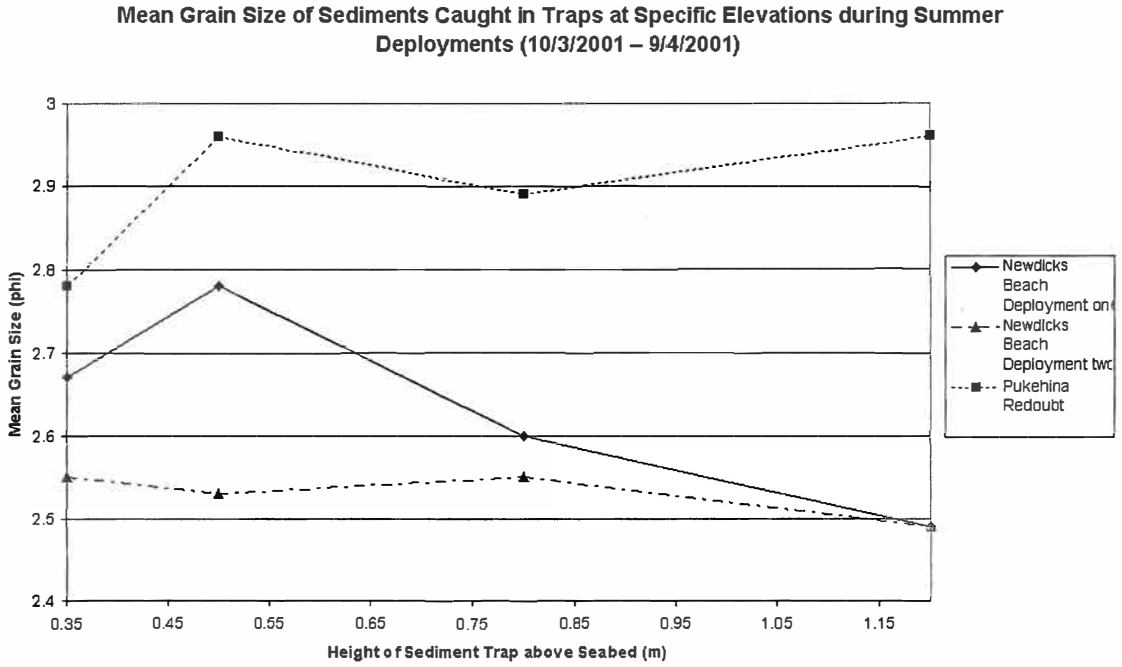

Figure 3.35 Mean grain size of sediments caught in sediment traps at specific elevations during summer deployments. Deployment one (10/3/2001 – 23/3/2001). Deployment two (23/3/2001 – 9/4/2001). Note: Pukehina Redoubt results are over entire summer deployment (10/3/2001 – 9/4/2001).

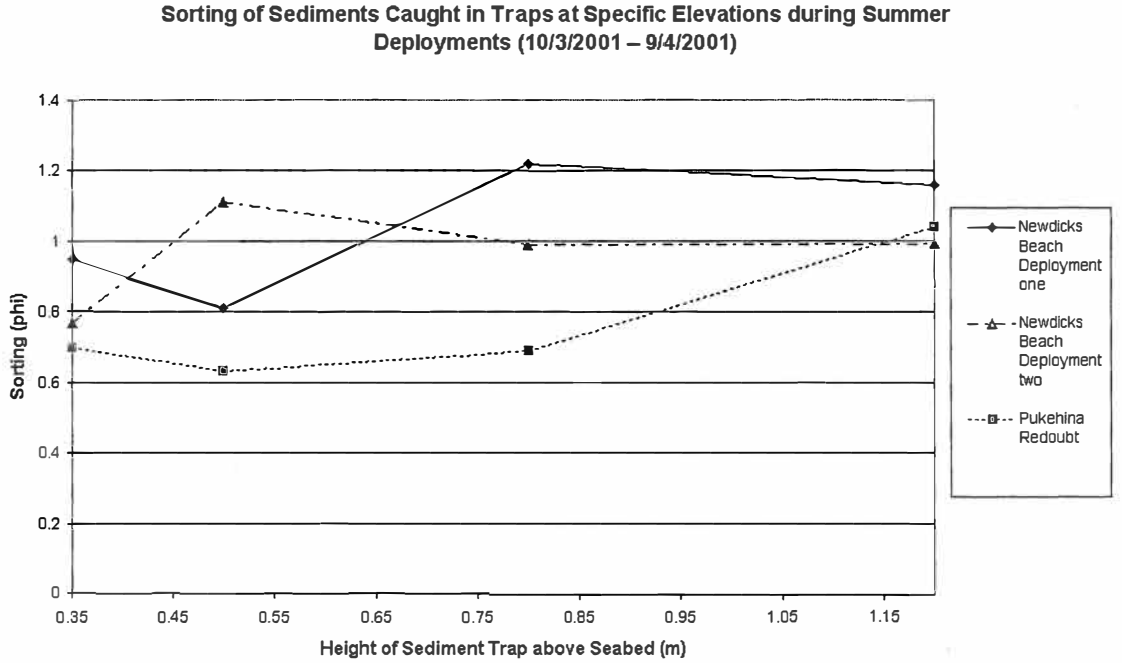

Figure 3.36 Sorting of sediments caught in sediment traps at specific elevations during summer deployments. Deployment one (10/3/2001 – 23/3/2001). Deployment two (23/3/2001 – 9/4/2001). Note: Pukehina Redoubt results are over entire summer deployment (10/3/2001 – 9/4/2001).

From results, sediments obtained from winter cycles at both locations varied from gravel bearing detrital sediment or slightly gravely sand, through to gravel free detrital sediment or sand, as classified by the WENTWORTH-UDDEN scaling system for sediments. In comparison, summer deployments, varied from gravel free detrital sediment or sand, through to gravel bearing detrital sediment or slightly gravely muddy sand.

Sediments closer to the seabed were not always found to be of largest grain size. During both winter deployment and summer deployments, the station located at Newdicks Beach had greatest mean grain size results at higher elevations (1.2 m for both summer deployments and during winter deployment one). In contrast, the station at Pukehina Redoubt had greatest mean grain size results at 0.35 m above seabed. This result, is therefore an implication of possible differing wave characteristics, as sediment characteristics and mineralogy were of little difference from either location. The justification of this statement will be investigated in chapter 5.

3.7.5. Settling Velocity

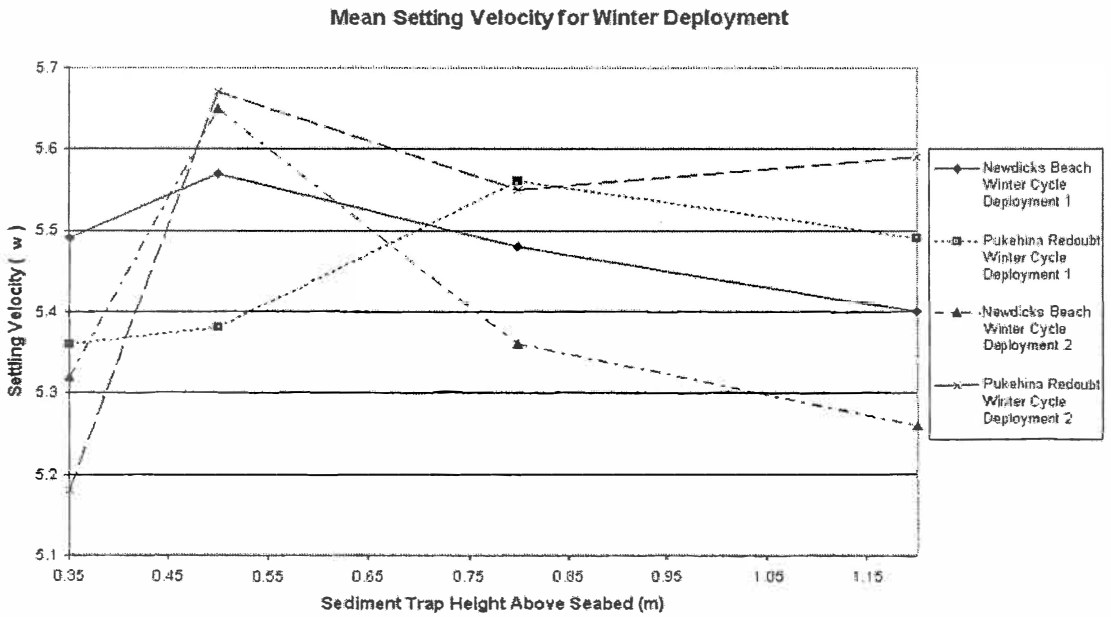

Figure 3.37 Settling velocity analysis results for Pukehina Redoubt and Newdicks Beach during winter deployment, a) Deployment one (17/5/2000 – 25/5/2000), b) Deployment two (25/5/2000 – 8/6/2000).

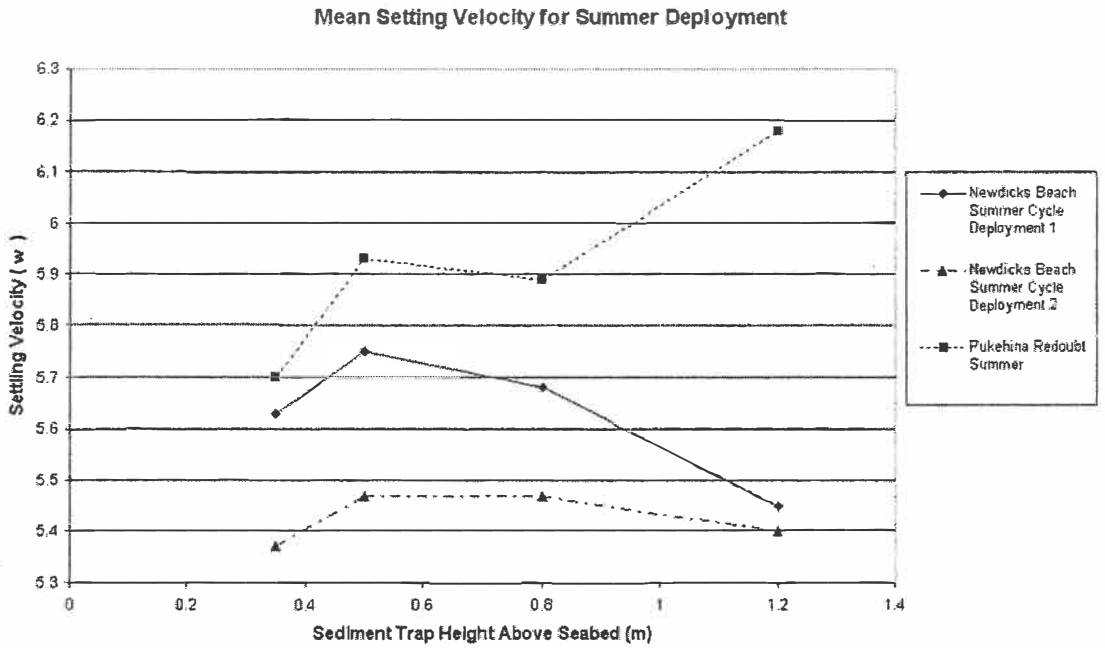

Figure 3.38 Settling velocity analysis results for Pukehina Redoubt and Newdicks Beach during summer deployment, a) Deployment one (10/3/2001 – 23/3/2001), b) Deployment two (23/3/2001 – 9/4/2001). Note: Pukehina Redoubt results are over entire summer deployment (10/3/2001 – 9/4/2001).

3.7.5.1. Discussion

Settling velocities are measured by the particle fall parameter ω, defined from equation 3.4, as the velocity at which a sediment particle falls through a fluid of a known distance. Settling velocity is dependent on the density of both the sediment and fluid, the viscosity of the fluid, and the diameter or size of the sediment particle. Larger values of ω imply that settling velocities are small, likewise a small ω value represents a greater settling velocity.

Sediment characteristics and mineralogical results of sediment collected from the traps were as expected. Pukehina Redoubt sediments at 0.35 m above the seabed had the largest mean grain size and density, and therefore, the greatest settling velocity. Likewise, at Newdicks Beach, sediment collected at 1.2 m above the seabed had the greatest mean grain size, and therefore, the greatest settling velocity.

Implications of a high settling velocity, include the fact that it would require a more turbulent, or more intensive bottom current to entrain a sediment particle, than a particle with a low settling velocity. This has large influence on the sediment volume moved by diabathic transport, and subsequently this may determine the volume of available sediment to the nearshore beach. Average settling velocities for both locations, however, did not vary significantly between each seasonal deployment at each station site, therefore, one could assume that there is not a significant difference of diabathic transport from season to season.

As previously stated in section 3.7.4, average sediment densities for each sample do not differ significantly.

To identify why coarser sediments are held in suspension higher above the seabed at Newdicks Beach than at Pukehina Redoubt, suspended sediment concentrations must be assessed to ascertain whether turbulent diffusion and gravity are acting on the sediment. Analysis of wave dynamics (chapter 5), may then further be used to verify the possibility of it's involvement of this finding.

3.7.6. Suspended Sediment Concentration

Using equations 3.5 and 3.6, FLINT (1998) used settling velocities to estimate average suspended sediment concentrations at each elevation of sediment trap above seabed.

$$F_d = \mathrm{M/A}/t \qquad \text{Eqn. 3.5}$$

Where F_d is a downward flux with units of $kg.m^{-2}s^{-1}$, M is the mass of sediment collected, A is the aperture of the trap and t is the time period of sampling. Average suspended sediment concentration at an elevation z, is then calculated by:

$$C_z = F_d / \omega \qquad \text{Eqn. 3.6}$$

Where C_z is the average suspended sediment concentration at an elevation z above the seabed, and ω is the mean settling velocity of the sediment.

FLINT (1998) describes an exponential relationship for the vertical distribution of suspended sediment. The balancing of the turbulent diffusion and the gravitational effect on the sediment results in a decrease in concentration with an increase in the elevation above the bed.

BLACK (1994) comprised an advection-diffusion equation for the time dependent vertical distribution of suspended sediment, given by:

$$\frac{\partial C}{\partial t} + \omega \frac{\partial C}{\partial z} = \frac{\partial}{\partial z}\left[\varepsilon_s \frac{\partial C}{\partial z} \right] \qquad \text{Eqn. 3.7}$$

where t is time (s), z is height above seabed, C is the volume concentration of sediment, and ε_s is the eddy diffusivity.

Much debate, however, is concerned with the eddy diffusivity and its relation to suspended sediment concentration profiles (FLINT, 1998). FLINT (1998) analysed three differing applications of eddy diffusivity, each with differing interpretations of eddy diffusivity throughout the water column. FLINT (1998), concluded that the NIELSON (1986), application is best applied to areas located within the surf zone. In the NIELSON (1986) application, a uniform eddy diffusivity is used throughout the water column.

The time-averaged solution to equation 3.7 when turbulence and mixing are assumed vertically uniform is given by:

$$C_z = C_o \exp^{(-z/\,l_s)} \qquad \text{Eqn. 3.8}$$

where C_z is the concentration of sediment at elevation z, C_o is the concentration of sediment at the bed and l_s is the mixing length (scale of turbulence, given by ε_s/w).

Applying this method, results obtained from both Newdicks Beach and Pukehina Redoubt stations are shown by figure 3.39.

3.7.6.1. Suspended Sediment Concentration Profile Outcomes and Interpretations

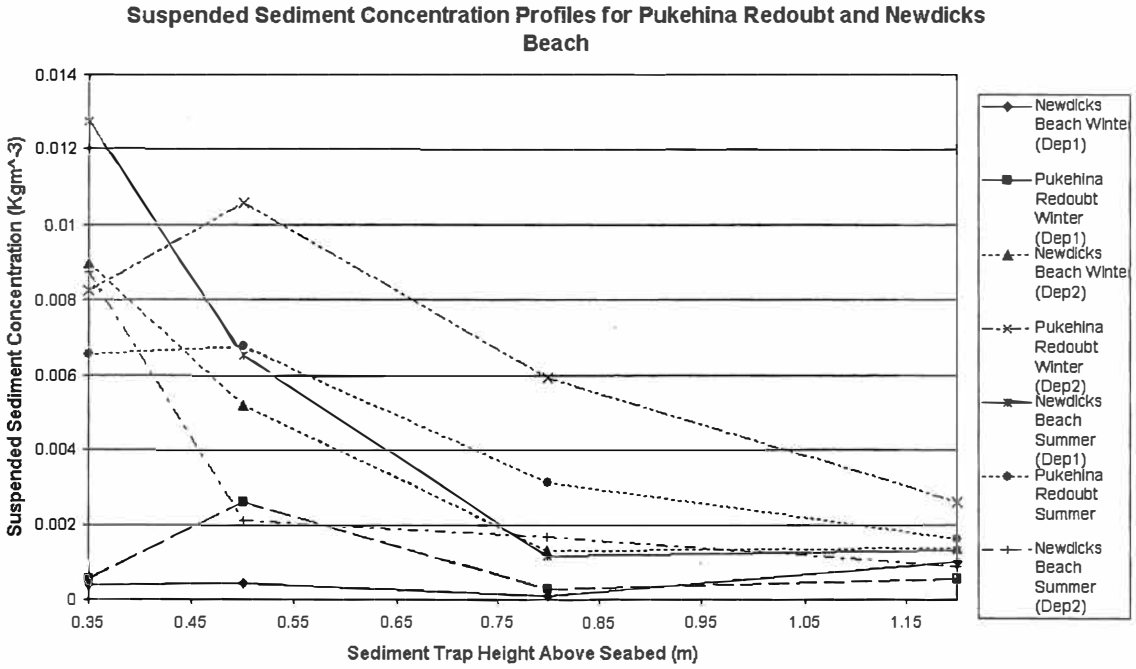

Figure 3.39 Suspended sediment concentration profiles for Pukehina Redoubt and Newdicks Beach, for all deployments. Winter deployment one: 17/5/2000 – 25/5/2000, deployment two: 25/5/2000 – 8/6/2000. Summer deployment one: 10/3/2001 – 23/3/2001, deployment two: 23/3/2001 – 9/4/2001.

The outcomes obtained were as expected. Highest suspended sediment concentrations were at near bed and concentrations decreased as height above seabed increased (apart from those which were influenced by biological activity).

From figure 3.39, one would assume that there would be a difference in the volumes of sediment exchange via diabathic transport. Particularly, a difference would have been observed during the two winter deployment periods at both Newdicks Beach and Pukehina Redoubt sites. As previously stated, volumes of sediment obtained in each

sediment trap during the winter deployments varied considerably. Differences of volumes obtained were attributed to differing wave directions during each deployment period. From suspended sediment concentrations obtained, one may assume that diabathic transport rates within the Pukehina coastal sector are also largely influenced by localised wind climate, which subsequently modifies local wave climate.

An exponential regression analysis was applied to results obtained (Table 3.4), to validate FLINT's (1998) statement that 'sediment concentration declines exponentially with elevation from seabed'. Results of the exponential regression analysis indicated that both Pukehina Redoubt and Newdicks Beach sites are following an exponential relationship.

Location, Season, Deployment no.	Exponential Regression	R-squared Value
Newdicks Beach, Winter, Dep. One.	y = 0.0002e0.7513x	0.0807
Pukehina Redoubt, Winter, Dep. One.	y = 0.0013e-0.9684x	0.142
Newdicks Beach, Winter, Dep. Two.	y = 0.0155e-2.2886x	0.7899
Pukehina Redoubt, Winter, Dep. Two.	y = 0.0179e-1.5207x	0.8778
Newdicks Beach, Summer, Dep. One.	y = 0.0245e-2.7925x	0.7773
Newdicks Beach, Summer, Dep. Two.	y = 0.0116e-2.266x	0.7786
Pukehina Redoubt, Summer.	y = 0.0138e-1.7858x	0.9649

Table 3.4 Exponential regression analysis results of suspended sediment concentrations. R-squared values are given to indicate the quality of fit.

R-squared values are used to assess the 'fit' or how related the data points are to the regression.

Most results vary from 0.7773 or 77% to 0.9649 or 96%. A surprising result was that both Newdicks Beach summer deployments (which had *Octopus Zealandia* present) illustrated reasonably good R-squared values. The influence of *Octopus Zealandia*, may therefore, not have caused significant movement of sediment inside of the trap. However, data collected in deployment one of winter cycle (17/5/2000 – 25/5/2000), indicated very poorly related data. A poor R-squared value indicates that data is not fitting the region well, this can be explained due the *Sardinops neopilchardus* found inside the sediment trap at 0.35 m elevation above the sea bed.

In reference to Newdicks Beach, a high quantity of mass (predominantly of coarse sand) was collected at 1.2 m elevation, during both summer and winter cycles. Having a high suspended sediment concentration at this elevation (figure 3.39) also implies that either sediment was entrained at an extremely high sediment concentration for a short period of time (which would be an unlikely scenario), or wave processes are continually causing coarse sediments to be suspended higher in the water column at the Newdicks Beach site, than at Pukehina Redoubt site. An investigation into whether wave energy focussing is causing this increased suspended sediment concentration, will be addressed in chapter 5.

3.8 Summary

Assessments of sediment textural patterns, utilising side scan sonar, video imagery, and a digital terrain model, all illustrate changes in distributions of sediment textures, offshore from Okurei Point since previously surveyed by PHIZACKLEA (1993). A decrease in the amount of exposed bedrock indicates a change in the sediment transport patterns within this region of coast. Evidence from sediment trap outcomes, illustrate that sediment transport within the Pukehina coastal sector is significantly influenced by local wind climate. Therefore, an alteration in average wind direction prior to current textural observations, compared to textural observations made by PHIZACKLEA (1993), may be a possible explanation for increased sediment at this region. An investigation of whether cyclic processes, inducing changes in localised wind and wave climates, thereby, increasing sediment volumes via diabathic transport and littoral drift, will be further investigated in chapter 6.

Sediment samples collected nearshore, indicate that sediments within the Pukehina coastal sector are predominantly medium sand sized particles with a decrease in sediment size towards Okurei Point (fine sand sized particles). This trend indicates an overall nearshore sediment transport to the northwest, as suggested by the SUNAMURA AND HORIKAWA (1972) model and the MCLAREN (1981) model.

Offshore bedforms observed by video imagery indicate small change to bedform orientation, than those collected by PHIZACKLEA (1993). Bedforms have orientated more shore normal indicating an onshore or south south-westerly offshore sediment transport direction at time of observation, compared to a southwest sediment transport direction depicted from PHIZACKLEA'S (1993) observations. Difference could be attributed to differing synoptic conditions between the two observation periods. This further justifies the sediment availability within the Pukehina coastal sector, is influenced by current wind and wave climates.

Suspended sediment concentrations were found to increase with the influence of onshore winds. A larger grain size may be suspended in the water column at Pukehina Redoubt than at Newdicks Beach during all seasons, possibly indicating a higher energy regime at Pukehina Redoubt that at Newdicks Beach. Similarly, assessments of sediment textural characteristics along the Pukehina shoreline do indicate a higher energy regime towards the east (Pukehina Redoubt), compared to the west (Newdicks Beach). Further examination of wave energy associated at the shoreline, will be assessed in Chapter 5, with an investigation of wave refraction modelling, within the Pukehina coastal sector.

Chapter Four
Hydrodynamics of Waihi Estuary and Estuarine Sediments

4.0 Introduction

Waihi Estuary can be described as a barrier-enclosed, low microtidal, estuarine lagoon. It covers an area of approximately 2.4 km^2, and has three streams entering the estuary (HALL *et al.* 1993; BRUERE, 1994). In this chapter, the hydrodynamics and sediment transport patterns of Waihi Estuary are investigated in order to assess whether the estuary affects the adjacent ocean coastal sediment transport processes. Investigation involves: examination of whether or not the estuary is acting as a sediment sink, and includes analysis of the tidal dynamics within the estuary, water velocities entering and leaving the inlet, tidal inlet stability, and sediment distribution throughout the estuary.

4.1 Literature Review of Waihi Estuary and Maketu Estuary

Research relating to Waihi Estuary is very limited. HALL *et al.* (1993) have investigated the catchment management strategy of the estuary, focusing on catchment assessment, drainage, flooding, ecology and water quality. They noted that sediment accumulation within the estuary is having a primary impact on the ecology and water quality of the estuary. In particular, the lower reaches of the streams are a major problem. Pages 38-39, state 'Sediment transport within the lower reaches of the streams is not occurring. The solution to promote transport would be by increasing the channel slope and altering the channel dimensions'.

BURTON (1987) investigated the tidal inlet hydraulics and stability of Maketu Estuary. From tidal investigations undertaken, BURTON (1987) concluded that the Maketu tidal

inlet is hydraulically stable during favourable conditions, but during periods of storm activity, sediment injection into the estuary may be experienced. This instability has contributed to the breaching of Maketu spit on multiple occasions. Breaching (or 'breakthroughs' as described by BRUUN, 1978) causes a large volume of sediment to be deposited in the lower estuary, which may consequently induce spit erosion by wind and flood tide transport of sediment into the estuary. From available reports, and discussions with Pukehina local inhabitants, Pukehina Spit has not been breached.

BURTON (1987) further concluded, that sediments within the Maketu Estuary range from fine to medium-coarse sand, reflecting three major sediment sources: cliff erosion of Okurei Point, the littoral environment, and sediments discharged from the Kaituna River. The finding of littoral sediments within the Maketu Estuary, suggests that the estuary is infilling. A possible reason why this may occur might be attributed to estuarine hydrodynamics. By similarly assessing the hydrodynamics of the Waihi Estuary to identify such processes as tidal damping and tidal asymmetry, possible infilling of Waihi Estuary may be identified.

DOMIJAN (2000) investigated the hydrodynamics and estuarine physics of the Maketu Estuary. Similar in characteristics to Waihi Estuary and only 3km to the east, Maketu Estuary represents an excellent location for a comparative study. Both estuaries are shallow, barrier protected 'perched' estuaries that have tidal amplitudes of approximately 1m at their associated inlets. DOMIJAN (2000) concluded that tidal damping and tidal asymmetry (explained in section 4.2) occur. Such events may implicate the sediment transport within the estuary and the adjacent ocean. Since Waihi and Maketu Estuaries have similar characteristics, it may therefore be possible, that similar events occur within Waihi Estuary.

4.2 Estuarine Hydrodynamics

Estuaries can be categorised as sources, sinks of sediment to the open coast littoral system, or as being in a state of equilibrium. Definition of whether an estuary is a sink, source or in equilibrium is dependent on the hydrodynamics of the estuary, and the sediment inputs. Hydrodynamic investigations involve tidal analysis within the estuary and analysis of currents.

4.2.1 Tidal Analysis

4.2.1.1 Aims, Objectives and Methods

Tidal damping and tidal asymmetry are common tidal observations within sheltered estuarine environments (DYER, 1973). To assess if events such as these were occurring within Waihi Estuary a Falmouth Scientific Instrument 3D Acoustic Current Meter WAVE MODEL (FSI 3DACM) and a Dobie were used during the winter deployment (16/5/2000 – 25/5/2000). The FSI 3DACM was positioned on the sub-tidal flat and the Dobie at the estuary inlet (Figure 4.1). GPS co-ordinates of instrument location, are presented in Appendix I. Preferably two FSI 3DACM's would have been deployed (as the Dobie is incapable of measuring currents), but due to non-availability of instruments this was not possible.

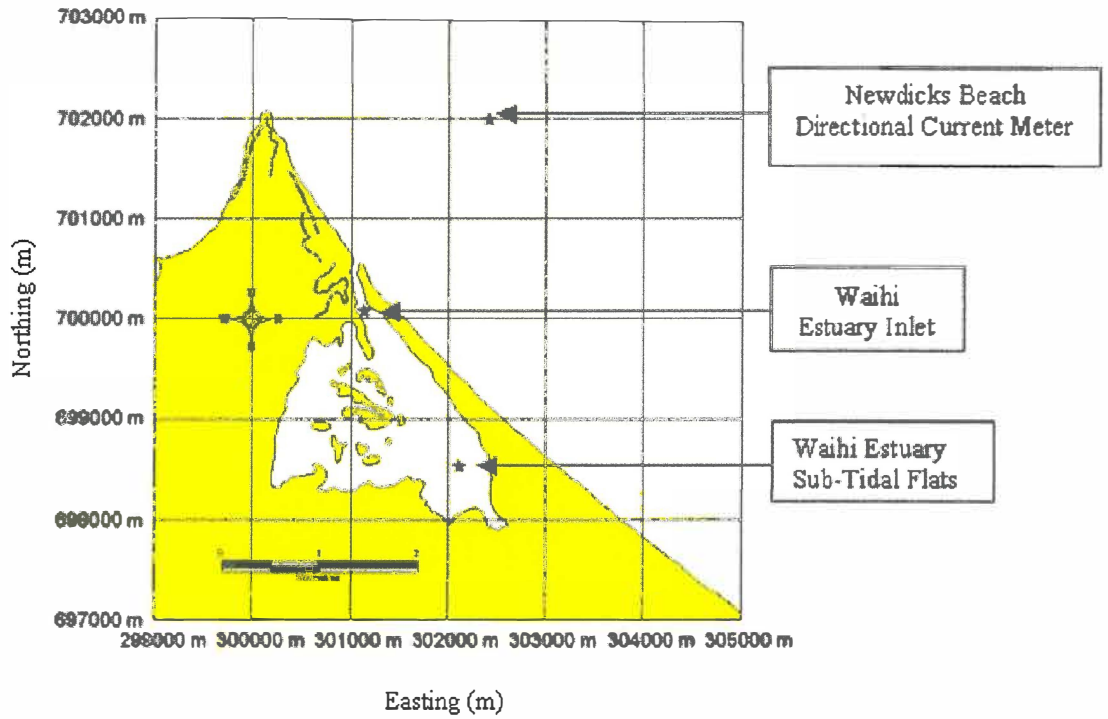

Figure 4.1 Locations of instrument deployment to determine tidal dynamics within Waihi Estuary. Deployed off Newdicks Beach was an S4 directional current meter, Waihi Estuary inlet had deployed a Dobie during the winter deployment and a FSI3DACM during summer deployment, while Waihi Estuary sub-tidal flats had FSI3DACM during both winter and summer deployments. GPS co-ordinates of instruments deployed may be obtained from appendix I.

Tidal data for the open ocean was obtained by an InterOcean S4 ADW, deployed upon a taut mooring (refer to figure 5.5) at 16 m water depth offshore from Newdicks Beach. The instrument was vertically suspended by the mooring 6 m below the water surface and was programmed to sample at 15 minutes every 60 minutes. The S4ADW samples at 2 Hz compared to 5.47 Hz, and 5 Hz by the FSI 3DACM and Dobie respectively, therefore, data points collected by the S4 ADW are not simultaneous with data inside the estuary.

During summer deployment (9/3/2001 – 21/3/2001) two FSI 3DACM's were used, enabling currents to be measured at the estuary inlet mouth. During each deployment, estuary instruments were programmed to collect simultaneous time interval data (7minutes on time every 30 minutes). The Dobie, however, samples at 5 Hz, while the FSI 3DACM samples at 5.37 Hz. To adjust the FSI 3DACM frequency to match the

frequency of the Dobie, CMCVRT5[†] is used. CMCVRT5 is a DOS run programme, which interpolates data points to a determined frequency by using cubic spline integration between two data points. FSIBURST3[‡], also a DOS run programme, is then used to return the interpolated data back into the burst interval specified and also creates a statistical document of the interpolated data.

4.2.1.2. Tidal Damping Theory

Tidal damping is a common observation in shallow estuaries (DYER, 1973). Driven primarily by loss of energy due to friction with the seabed, the tidal amplitude is reduced. This scenario may induce a reduction of water current velocity at the far reaches of the estuary and possible accretion of suspended sediments. By deploying pressure sensors at each end of the estuary, tidal damping within Waihi Estuary may be identified.

4.2.1.3. Tidal Asymmetry Theory

DYER (1973) defines tidal asymmetry as a difference in durations between the rise (flood) and fall (ebb) of water level as a tidal oscillation progresses. Induced by the tidal wave travelling at a speed, which is dependent on water depth, the crest will travel at a faster duration than the trough (DYER, 1973).

The occurrence of tidal asymmetry at Maketu Estuary was investigated by DOMIJAN (2000) in terms of the tidal duration parameter, D (equation 4.1):

$$D = [(T_{rise} - T_{fall})/(T_{rise} + T_{fall})]x100 \qquad \text{(Eqn. 4.1)}$$

where and T_{Rise} and T_{Fall} = durations of the flood and ebb tide.

[†] CMCRVT5 by Richard Gorman *pers. comm.*, NIWA. 1994
[‡] FSIBURST3 by Richard Gorman *pers. comm.*, NIWA. 1994.

Parameter D is represented as a percentage, for which the more negative the value is, the less duration of the flood, compared to the ebb tide and vice versa if the value is positive. The more negative or positive D indicates the asymmetry of the tidal curve. If D is 0, then the tidal curve is symmetrical.

4.2.1.4 Tidal Gauging Results at Newdicks Beach and Waihi Estuary Sites

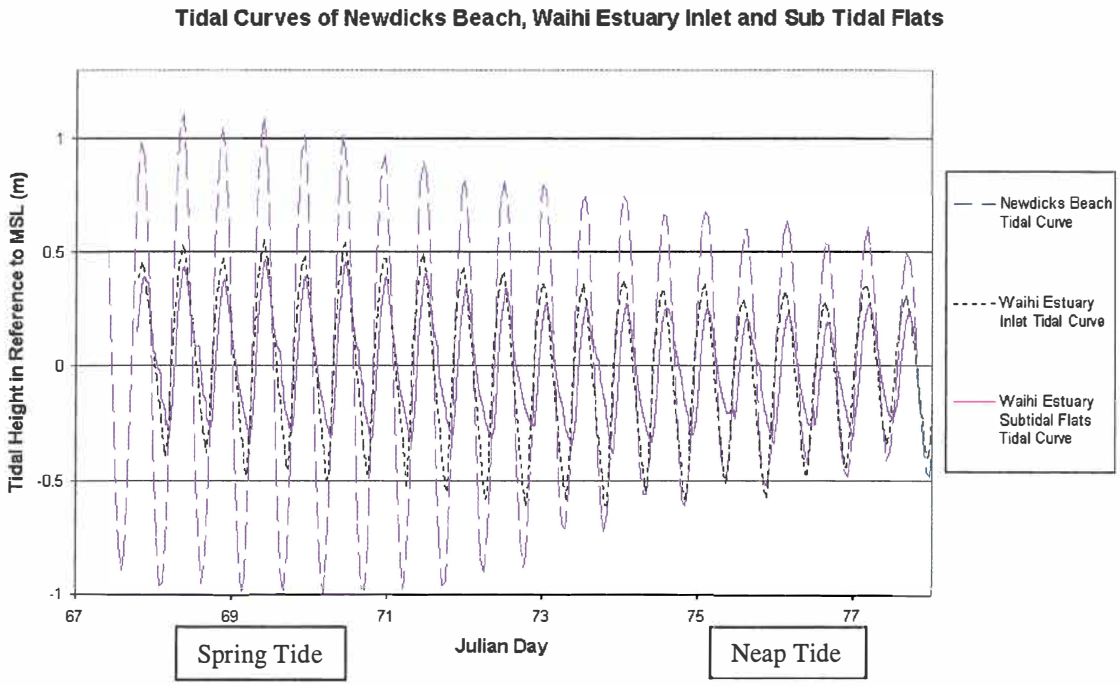

Figure 4.2 Tidal Curves within Waihi Estuary and at Newdicks Beach, as collected by instruments during summer deployment 9/3/2001 - 20/3/2001.

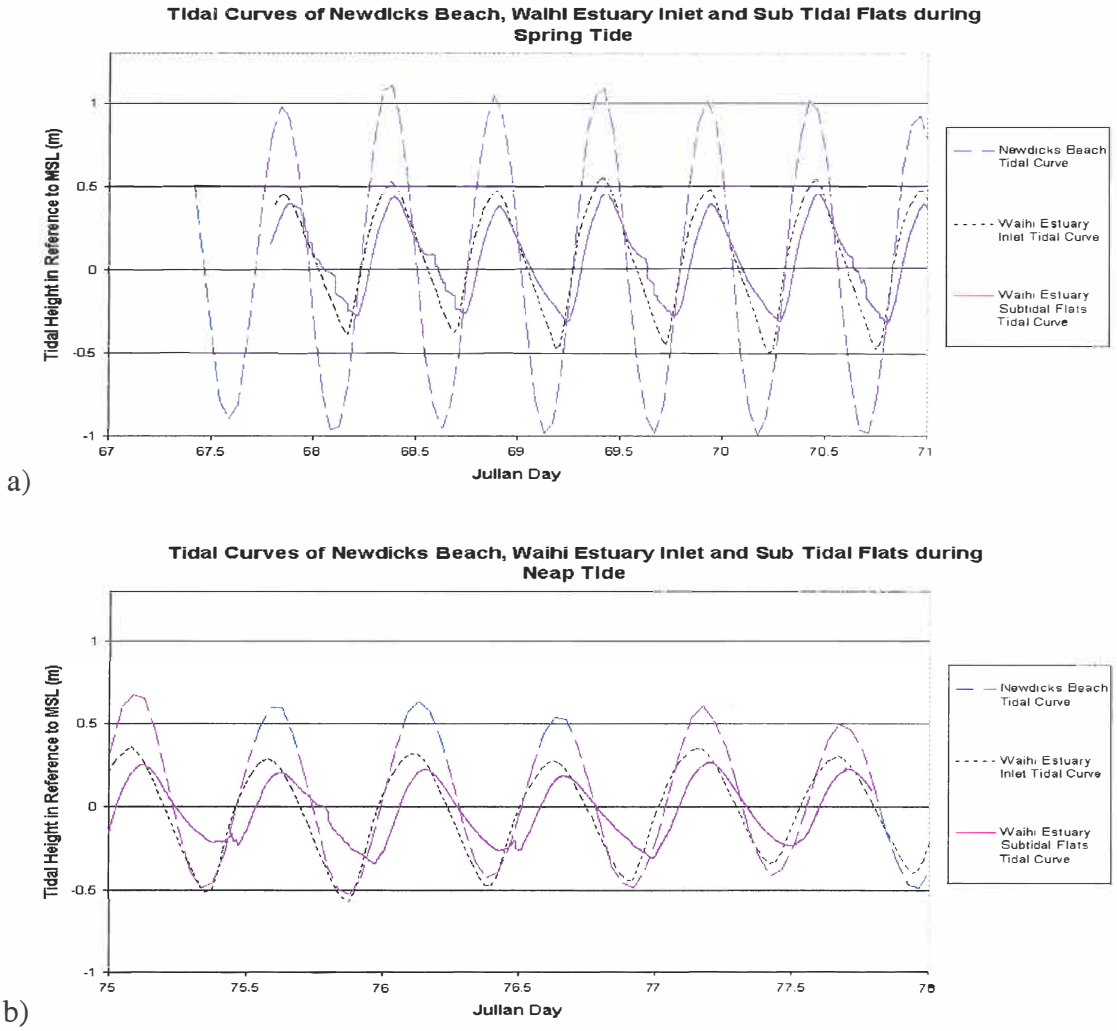

Figure 4.3a) Spring tide recordings from Newdicks Beach, Waihi Estuary inlet and sub-tidal flats. b) Neap tide recordings from Newdicks Beach, Waihi Estuary inlet and sub-tidal flats.

Tidal Range	Newdicks Beach	Waihi Estuary Inlet	Waihi Estuary Sub-tidal Flats
Spring (m)	2.07	1.01	0.78
Neap (m)	1.09	0.75	0.45

Table 4.1 Mean tidal ranges obtained from data, at instruments deployed offshore from Newdicks Beach, Waihi Estuary inlet and Waihi Estuary sub-tidal flats during summer deployment 9/3/2001 - 20/3/2001.

Figures 4.2 and 4.3, and table 4.1, illustrate and detail tidal damping results respectively, which were obtained from instruments deployed at Newdicks Beach, Waihi Estuary inlet and Waihi Estuary sub-tidal flats. As previously stated, tidal amplitude outside of the

estuary is greater than tidal amplitudes recorded within the estuary. Figures 4.3a and 4.3b illustrate more detailed plots of spring and neap tides respectively.

Table 4.1 illustrates that the mean tidal range at Newdicks Beach during a spring and neap tides is 2.07 m and 1.09 m, respectively. In comparison with the Moturiki Island tidal gauge (digital Fisher and Porter water level recorder, installed at the seaward end of Moturiki Island (37° 38' S 176° 11' E)), demonstrates mean tidal ranges for spring and neap tides of 1.65 m and 1.27 m, respectively (BELL AND GORING, 1998). The difference of tidal ranges between the two records may be attributed to the variation of the tidal wave characteristics, as it progresses around the New Zealand coast. DYER (1973) states bed friction may attribute to decreasing amplitude of the tidal wave.

Mean tidal range data collected by DOMIJAN (2000) within the neighbouring Maketu Estuary inlet was 1.2 m and 0.95 m at spring and neap tides, respectively. Values of 1.01 m (spring tide) and 0.75 m (neap tide) collected at Waihi Estuary inlet suggest differing estuary properties, however, the instrument deployed at Waihi Estuary was not in the mouth of the inlet, instead, it was deployed in the throat of the estuary. The reason for deploying the instrument in this location was because of fear of instrument damage, due to boat traffic at the mouth of Waihi Estuary. The difference, therefore, may be partially due to bed friction reducing the tidal amplitude (as DYER (1973) suggests), and partially due to the variations of the tidal wave at the open coast.

4.2.1.5 Tidal Damping Results

Figure 4.2 illustrates that tidal damping within Waihi Estuary is occurring. Tidal amplitude between the inlet and the sub-tidal flat, decreases on average by 0.3 m or 69%. DOMIJAN (2000) measured an amplitude decay of 68% at the far reaches of the Maketu Estuary. The similarity of amplitude decay in both estuaries is dependent on bed friction and the distance the instruments are from their associated inlets (DYER, 1973). Assessing the distance each instrument from their inlet, indicates that instruments were not

comparable (2570 m at Maketu Estuary, 2050 m Waihi Estuary), therefore, sediments from Waihi Estuary may be of coarser sediment texture than at Maketu Estuary, as bed friction must be greater.

4.2.1.6 Tidal Asymmetry Results

Analysis of the tidal curve at the sub-tidal flat of Waihi Estuary, illustrates tidal asymmetry. Figure 4.4 illustrates 1.5 days of spring tidal data at Waihi Estuary sub-tidal flats. Tidal asymmetry is also observed during neap tide.

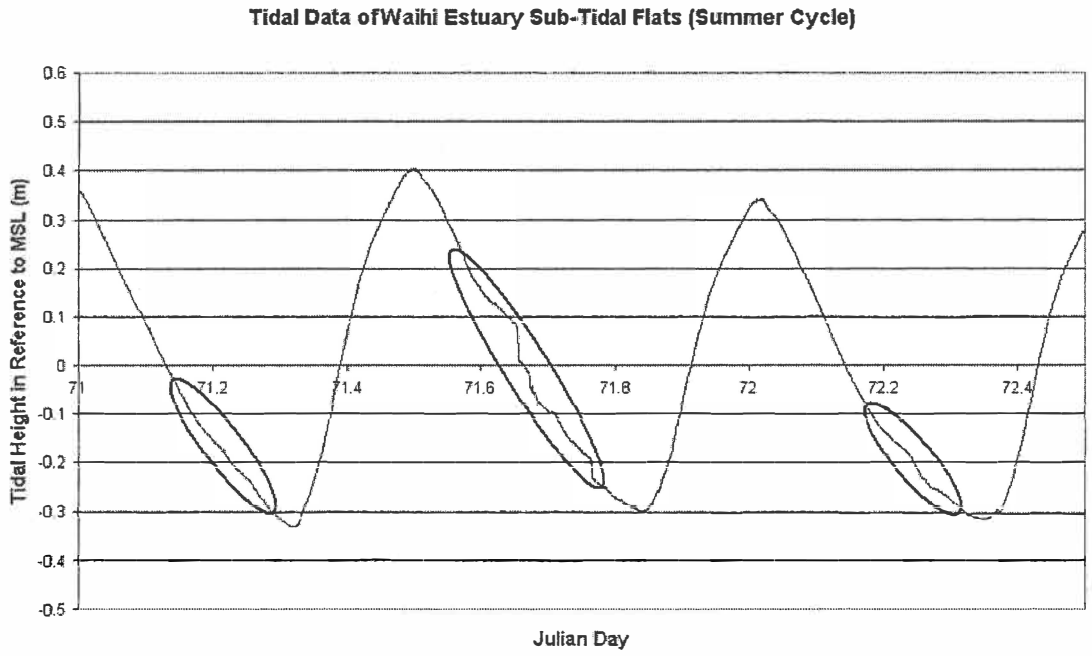

Figure 4.4 1.5 days tidal data at Waihi Estuary sub-tidal flats illustrating tidal asymmetry (tidal data is during spring tide, but is also present during neap tide). Note: variable depth fluctuations on ebb tide, as indicated by the ellipses (discussed in section 4.2.2).

Following methods of DOMIJAN (2000), as discussed in section 4.2.1.3, tidal asymmetry may be assessed using the parameter D (tidal duration asymmetry parameter). Results obtained from data collected at Waihi Estuary inlet and Waihi Estuary sub-tidal flats are presented in table 4.2.

Pressure Sensor Location	Winter 2000(Dep. 1)			Winter 2000(Dep. 2)			Summer 2001		
	Ave. ebb hh:mm	Ave. flood hh:mm	D (%)	Ave. ebb hh:mm	Ave. flood hh:mm	D (%)	Ave. ebb hh:mm	Ave. flood hh:mm	D (%)
Inlet	6:57	5:20	-13.16	7:04	5:15	-14.75	6:53	5:30	-11.17
Sub-Tidal	7:54	4:23	-28.63	7:44	4:43	-24.23	7:52	4:31	-27.05

Table 4.2 Tidal asymmetry (average ebb and average flood) at Waihi Estuary. D = Tidal duration asymmetry parameter (Eqn. 4.1).

In comparison DOMIJAN (2000) measured tidal curves from three different locations in the Maketu Estuary. He concluded that values obtained for D varied from –24.9% to –36.5%. Prior to the Kaituna River being partially re-diverted into the Maketu Estuary, DOMIJAN (2000) further concluded that D became increasingly negative in value as distance from the inlet increased, which implies that the difference in duration between ebb and flood is greater.

From DOMIJAN (2000), Waihi Estuary does not experience the magnitude of tidal asymmetry as evident at Maketu Estuary, but implications for sediment transport due to tidal asymmetry are still valid.

4.2.1.7 Implications for Sediment Processes from Tidal Curves

For tidal inlet estuaries with demonstrated tidal asymmetry, and assuming no fluvial input, water velocities during the flood tidal cycle must be greater, as the volume of water entering and exiting the estuary inlet during one tidal cycle would be approximately the same (less water exiting due to infiltration and evaporation loss). This effect also influences sediment transport, as higher current velocities promote greater sediment transport. BRUNN (1978, p. 208) discusses how sediment transport is a function of bed shear stress, and how velocity is a critical parameter in the calculation of the volume of sediment transported per unit time. Acknowledging BRUNN's (1978) discussion and applying this to Waihi Estuary, the flood tide has greater velocities than the ebb tide, so therefore, Waihi Estuary is a flood-dominated estuary. The evident implications for

Waihi Estuary, is the greater sediment transporting capability of the flood tide, which is promoting infilling of the estuary, with sediment most likely provided from the adjacent littoral system. However, Waihi Estuary is an 'open estuary', i.e. it has fluvial inputs, which may influence the tidal curve. An investigation of the water velocities at the Waihi Estuary inlet, must therefore, be undertaken.

4.2.1.8 Estuarine Currents

Figure 4.5a and figure 4.5b illustrate results obtained from the FSI 3DACM deployed at Waihi Estuary inlet during the summer deployment (9/3/2001-21/3/2001). Highest water velocities were normally evident on the ebb tide. Average ebb tide water velocity was 0.47 ms^{-1}, whilst the average flood tide water velocity recorded was 0.31 ms^{-1}.

This difference in water velocity, and the fact that Waihi Estuary is experiencing tidal asymmetry, indicates possible freshwater input from the Pongakawa, Wharere, Kaikokopu streams and Pukehina Canal is of a significant volume.

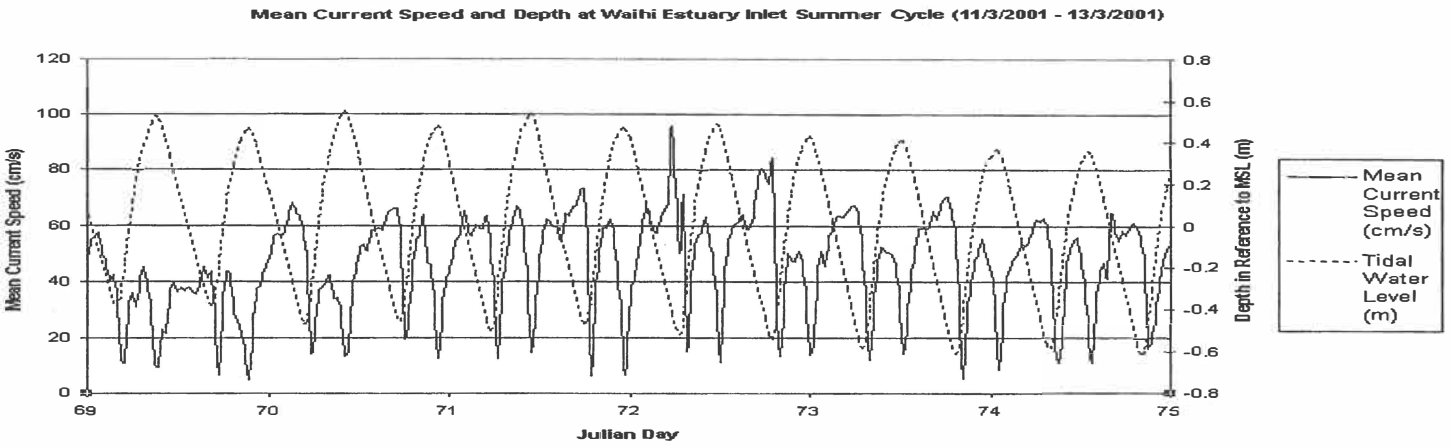

a)

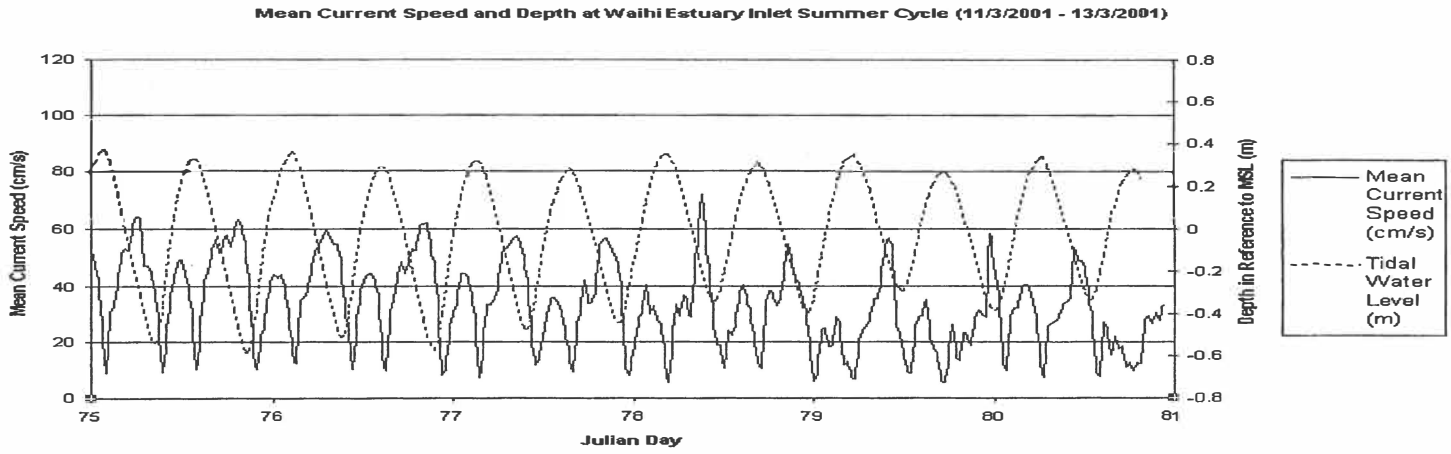

b)

Figure 4.5a Mean water velocity and depth recordings taken at Waihi Estuary Inlet during the summer deployment (9/3/2001-21/3/2001) during spring tide and b) neap tide.

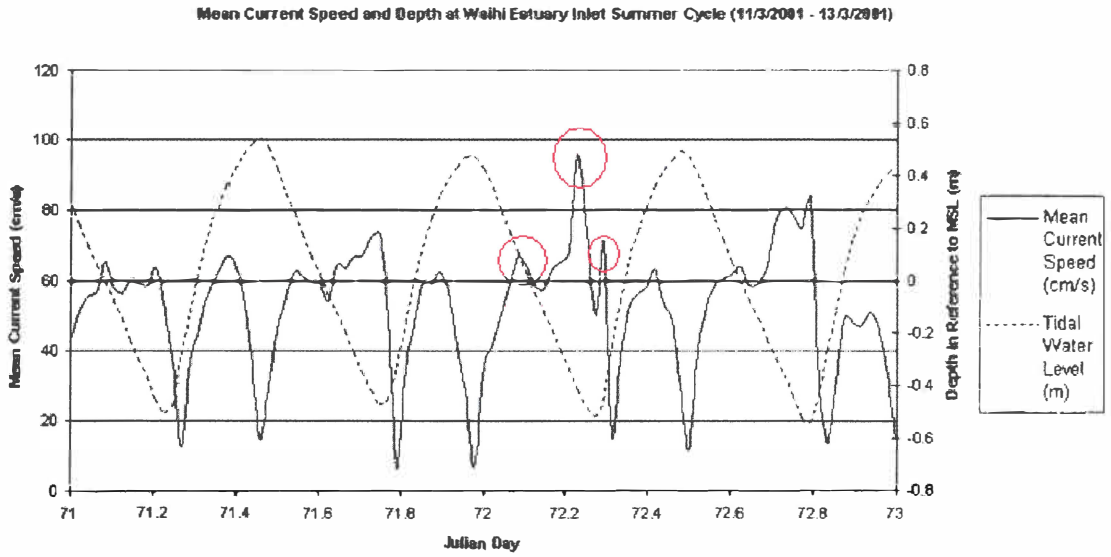

Figure 4.6 Expanded plot of mean water velocity and depth recordings taken at Waihi Estuary inlet during the summer deployment. Unfamiliar outcomes of mean current speed are illustrated by red circles, which could be related to waves entering into the estuary inlet from the adjacent coast.

Figure 4.6 illustrates an expanded plot of mean water velocity and depth recordings taken at Waihi Estuary inlet during the summer deployment. Illustrated in figure 4.6 are red circles, which are obscure mean water velocity recordings. These recordings could be due to multiple reasons. One possibility, however, could be due to waves entering the estuary inlet and generating significantly larger currents at the instrument location.

Figure 4.7 illustrates significant wave height at Newdicks Beach site measured by S4ADW between the 8th of March and the 7th of April 2001. Comparing figures 4.5a and 4.5b with significant wave height data (figure 4.7) collected over the same period, higher wave heights recorded at Newdicks Beach coincide with an increase of obscure mean water velocity recordings at Waihi Estuary inlet. The possibility of waves pushing water into the estuary, due to an increased wave set-up and wave run-up, may therefore be a reasonable explanation.

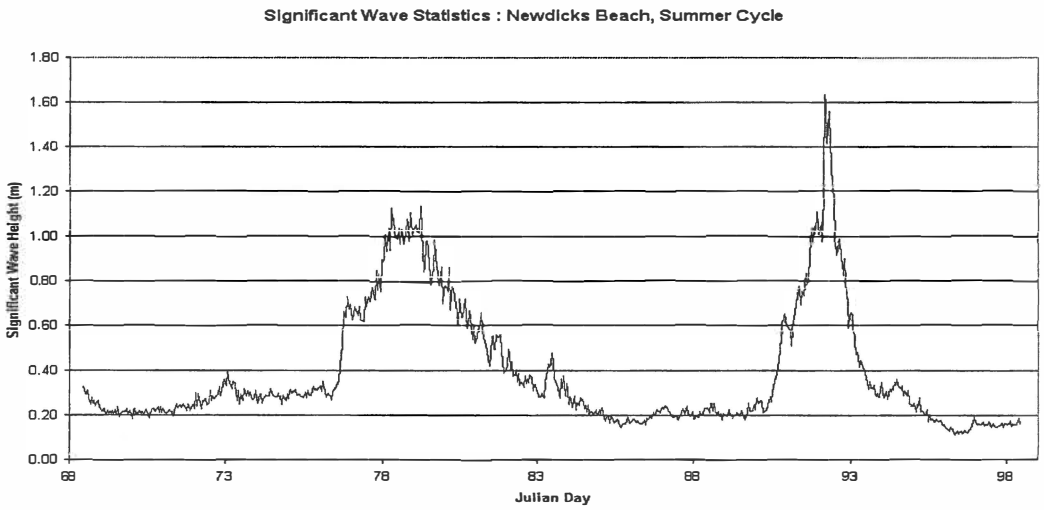

Figure 4.7 Time series of significant wave height at Newdicks Beach site measured by S4ADW between (8^{th} March 2001 – 7^{th} April 2001).

Significant decreases of mean water velocity recordings are related to the change of tide. Mean water velocity reduces as the water direction changes from ebb to flood flow and vice versa.

Environment Bay of Plenty gauge the Pongakawa and Kaikokopu streams on a regular basis, as these are regarded as the most significant contributors of freshwater to the estuary, due to their catchments being larger than the other surrounding catchments. Figures 4.8 and 4.9 illustrate the depth (m) and velocity (ms^{-1}) recordings taken from field excursions of 11/7/2001.

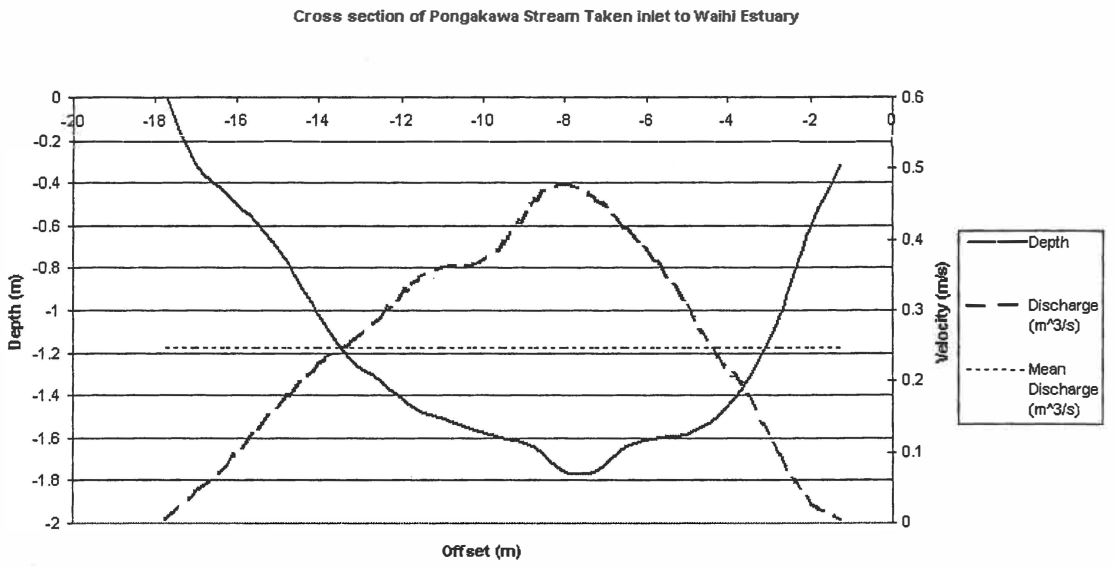

Figure 4.8 Cross section of Pongakawa Stream and associated section discharges (Data obtained from Environment Bay of Plenty (11/7/2001)).

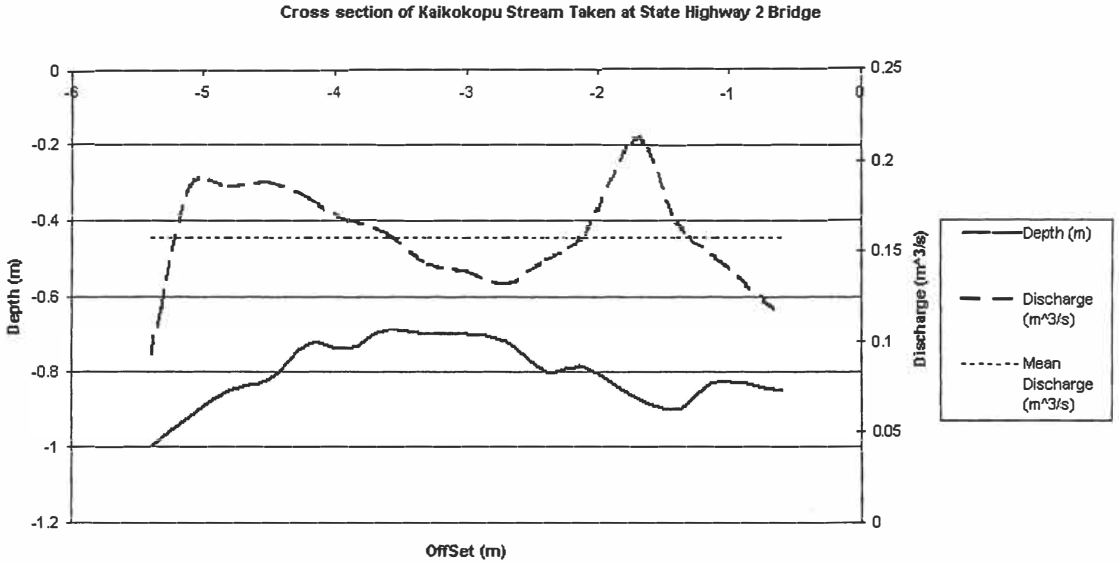

Figure 4.9 Cross section of Kaikokopu Stream and associated section discharges (Data obtained from Environment Bay of Plenty (11/7/2001))

Gauging locations are different for each stream. Pongakawa Stream is gauged 1 km from the stream inlet to the estuary, while the Kaikokopu Stream is gauged at the State Highway 2 Bridge, approximately 5 km from the mouth of the stream.

From the gauging, cross sectional discharge for each stream was estimated from between 5.396 m^3s^{-1} to 6.013 m^3s^{-1} with 95% confidence limits for Pongakawa Stream, and 2.327 m^3s^{-1} to 2.704 m^3s^{-1} with 95% confidence limits for Kaikokopu Stream. Since Kaikokopu Stream has a significantly smaller cross sectional discharge than Pongakawa Stream, it may be possible that sediment at Kaikokopu Stream (at location of measurement) is not being entrained by water velocities, therefore, a difference of bottom topography is illustrated. A similar result was also noted by HALL *et al.* (1993), in which they stated that water velocities were insufficient to exceed sediment entrainment.

Gauging of the Waihi Estuary has never been previously conducted, and therefore identifying whether or not there is another influence causing the increased ebb flow from the inlet, cannot be made.

4.2.2 Ebb Tide Fluctuations

Figure 4.4 (tidal data recorded from the sub-tidal flats at Waihi Estuary), illustrates an uncommon occurrence on the ebb tide. The ebb tide exhibits fluctuations of tidal water depth, as highlighted by the circled regions in figure 4.4. These fluctuations indicate that tidal depth decreases approximately 0.1 m over a duration of 1-2 minutes. Explanation of this phenomenon is not an objective of this research, however, several hypothesis of what may cause such an event are outlined.

One possible explanation for this phenomenon, might be aberrant instrument recording. However, the use of two different FSI 3DACM's in two separate deployments, with both instruments obtaining similar results, suggests instrument cause is unlikely. Another possible reason for such events occurring may be explained by hydraulic gradients acting within or outside the estuary. Figure 4.10 explains graphically the movement of water via hydraulic gradients.

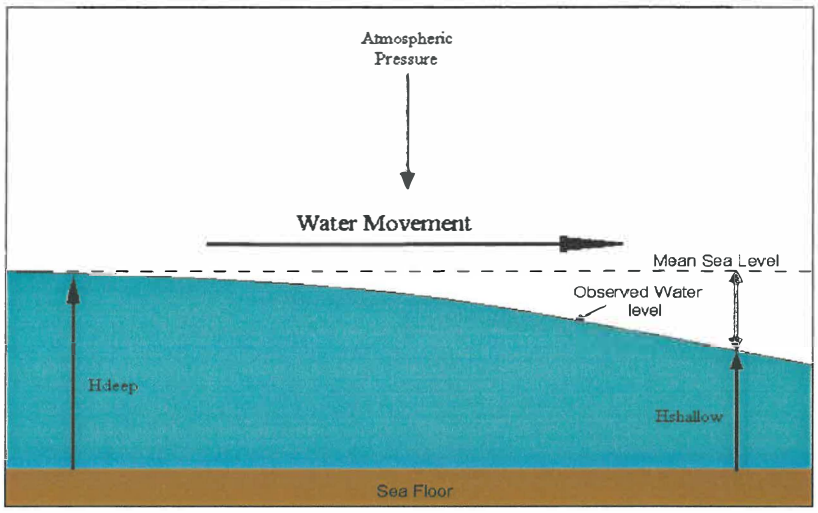

Figure 4.10 Hydraulic gradients are created by differing water elevations at two different locations. Elevations differ either by tidal lagging, infragravity wave presence, seiching and to a minimal extent atmospheric difference. Water is driven from H_{deep} to $H_{shallow}$ by pressure head gradient.

Figure 4.11 examines the duration and frequency of the ebb tide fluctuations at the sub-tidal flats of Waihi Estuary.

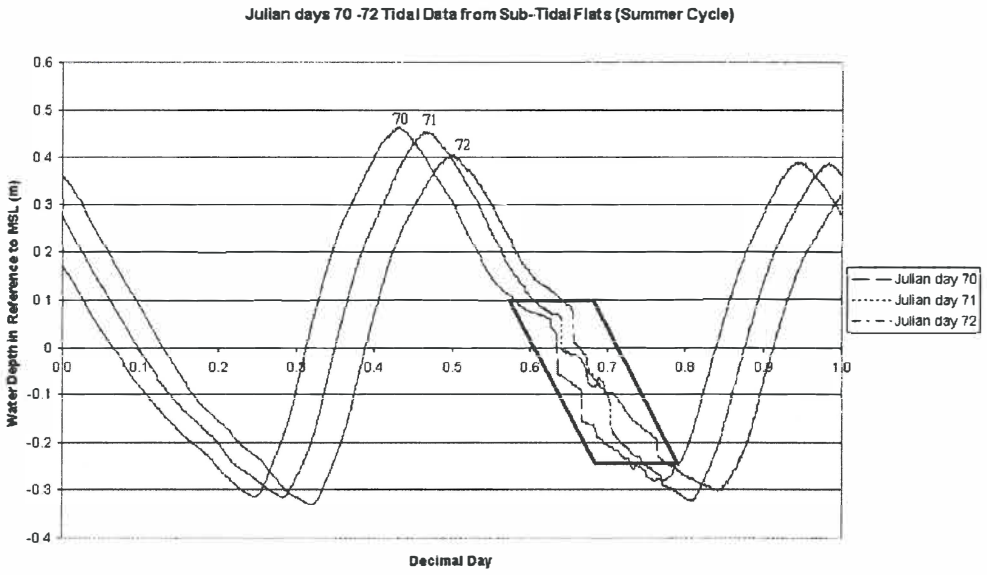

Figure 4.11 First four days of tidal data of Waihi Estuary sub-tidal flats, during summer deployment (11/3/2001-13/3/2001). Decimal day represents each Julian day as a decimal, enabling data to be overlayed. The black box indicates that ebb tide fluctuations are most common during the afternoon ebb tide. Initiation depth of fluctuations are identifiable, as occurring at similar water depth on the afternoon ebb tide.

Figure 4.11 indicates that the water movement due to possible hydraulic gradient are predominantly occurring on the afternoon ebb tide, as illustrated by the boxed data. The initiation depth of the water motion varies from 0.08-0.06 m, above Mean Sea Level (MSL).

One explanation that may alter the hydraulic gradient is seiching, which is contained within the estuary. A seiche is the free oscillation of water in a closed or semi-enclosed basin, at its natural period (MONSERRAT AND TINTORE, 1993). Since, however, the tidal curve does not illustrate a continuous occurrence of fluctuations, an external influence outside of the estuary, may therefore, be initiating the fluctuation at mid ebb tide in the afternoon. An external influence such as edge wave activity or coastal-trapped waves may induce a change of hydraulic gradient between the outside and inside of Waihi Estuary, thereby initiating a seiche to occur (HEALY, 2002 *pers comm.*).

BLACK (1983) noted the rhythmic fluctuations in a tidal curve obtained from Whangarei Harbour, New Zealand, and concluded that a seiche was being generated from influences outside of the harbour. Similarly STEPHENS (2001) investigated the possibility of coastal-trapped waves at Gisborne, New Zealand. Generated by alongshore wind stress or by a coastal flux pulsing through a coastal strait, STEPHENS (2001) found by model simulation (model 3DD*), that coastal-trapped waves were being generated. The coastal-trapped waves predicted had amplitudes of 0.1 m and wave periods of approximately 2.5 days (STEPHENS, 2001, *pers comm.)*. The presence of edge or coastal-trapped waves at the adjacent coastline of Pukehina is possible, but further investigation must be undertaken.

Another possible hypothesis that may alter the hydraulic gradient of the estuary are, channel and bed friction influences. Figure 4.12 illustrates how water depth may alter due to the channel and frictional influences within the estuary.

* 3DD by Kerry Black, Department of Earth Science, University of Waikato, 1995.

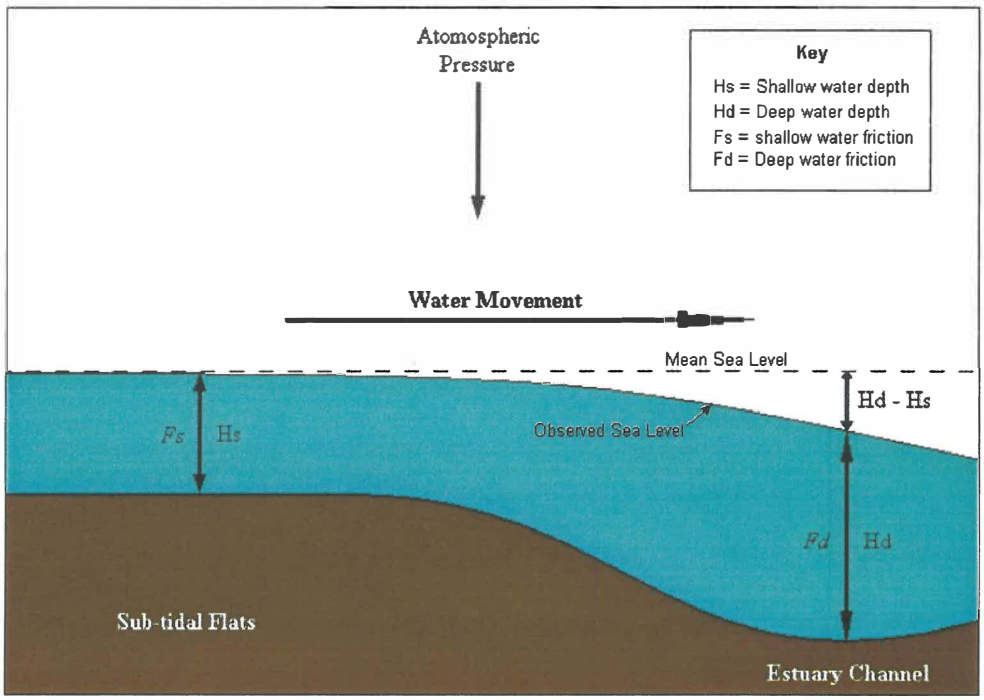

Figure 4.12 Depth alters due to the frictional differences within the estuary. More bed friction is experienced at the sub-tidal flats than at the channel, and this allows flow on the sub-tidal flats to become retarded, whilst water at the channel decreases. Once H_d-H_s exceeds the frictional attraction at the sub-tidal flats, water will then move from the sub-tidal flat to the estuary channel.

More bed friction is experienced on the sub-tidal flats than in the channel due to coarser sediment particles present (from figure 4.18). Therefore, water is held on the sub-tidal flat, whilst water depth at the channel recedes. Once H_d-H_s exceeds the frictional attraction at the sub-tidal flats, water will then rapidly move from the sub-tidal flat to the estuary channel.

Time variations of when water reduces, may be dependent on external influences, such as wind. Winds from the northeast may cause a set-up, which would increase water elevation, therefore delaying the rapid change in water depth at the sub-tidal flat.

Figure 4.13 Main channels present within Waihi Estuary. Red dots indicate instrument location.

Figure 4.13 illustrates the main channels present within Waihi Estuary, and the locations of instruments to obtain data.

4.2.3 THANAL Analysis

THANAL[††] is a tidal analysis program used to derive tidal constituents by using least squares harmonic analysis.

Astronomical variables are established by THANAL, which are then used to identify tide-generating forces. These variables are (all at time t):

- s(t) mean longitude of the moon;
- h(t) mean longitude of the sun;
- p(t) mean longitude of the lunar perigee;
- N'(t) negative of the longitude of the mean ascending node; and
- P'(t) mean longitude of the solar perihelion.

(DE LANGE *et al.* 1993)

From data analysis, THANAL produces results of astronomical phase angle (V), nodal modulation phase (u) and amplitude (f) for each of the tidal constituents.

[††] THANAL by Willem de Lange *et al. pers. comm.,* Department of Earth Science, University of Waikato. 1993

Using THANAL's associated program THPRED[‡‡], predicted tidal values for a specified time period may be obtained from tidal constituents produced by THANAL. By subtracting original data from data produced from THPRED, residual data can be presented. Residual tidal results, therefore, include non-tidal components. However, if the data set is not of sufficient duration, not all tidal components will be extracted by THANAL. Non-tidal components are dominated by water level and current fluctuations. Water levels within an estuary are affected in the same way as in the open ocean. Atmospheric pressure and wind cause depressions and elevations in the water level. The range is generally small compared to that of the tide within the estuary, and the importance of water level changes might not be recognised until an extreme event coincides with an extreme tidal event.

4.2.3.1 Summary of THANAL Outcomes and Discussion

Outcomes of THANAL analysis for Waihi Estuary are presented in Appendix VI, but are summarised and discussed here.

Results obtained from THANAL, indicate an incomplete or insufficient duration of data. This is illustrated by one set of results (Waihi Estuary inlet, summer cycle), in figure 4.14. The bold black line indicates an oscillating residual component, most likely being a fortnightly tidal component.

[‡‡] THPRED by Willem de Lange *et al. pers. comm.*, Department of Earth Science, University of Waikato. 1993

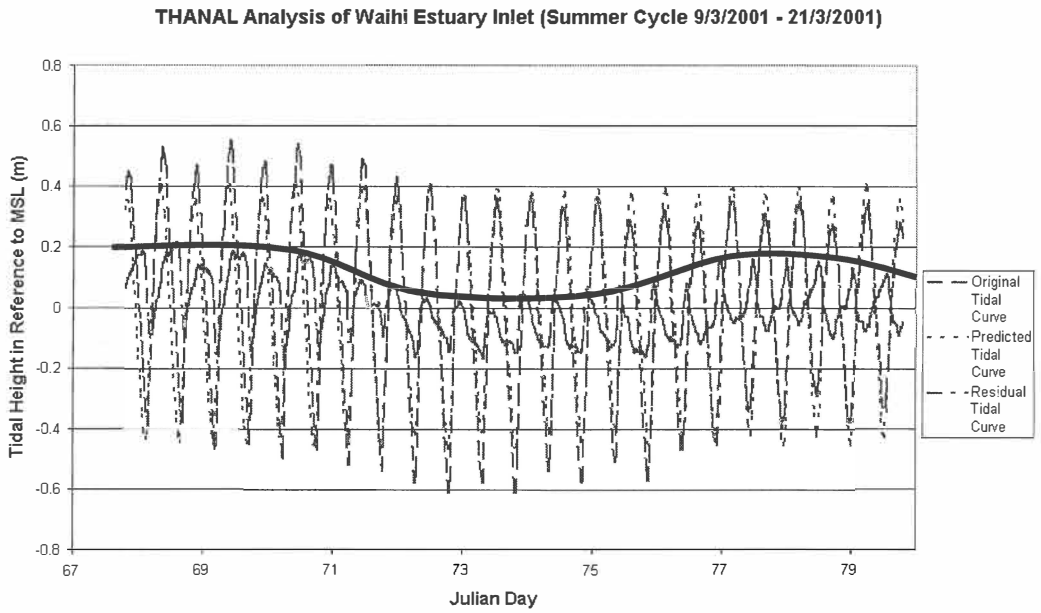

Figure 4.14 THANAL analysis result from Waihi Estuary inlet indicating an incomplete or insufficient data set. The bold black line indicates an oscillating curve, indicative of fortnightly tidal components not included in THANAL analysis.

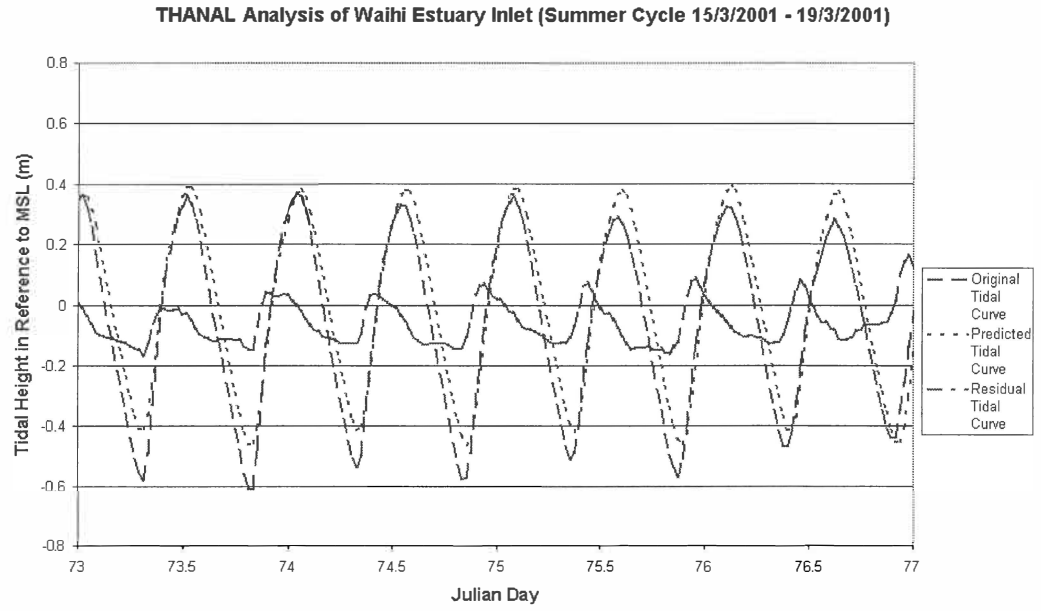

Figure 4.15 Zoomed illustration of THANAL analysis result from Waihi Estuary inlet, 9/3/2001 – 12/3/2001.

Even though all tidal components were not extracted during the THANAL analysis, the primary components or components that have the greatest amplitude were extracted, Z_o,

M_2, S_2, N_2, K_2, K_1, O_1 (DE LANGE *et al.*, 1993). Results obtained, may therefore, be used to provide assumptions, but cannot identify the extremity of some estuarine processes.

Results of tidal residuals indicate similar trends to the original tidal data, but at smaller amplitudes, as residual flood tides are of a shorter duration than residual ebb tides. This indicates that tidal asymmetry within the estuary could be associated with currents within the estuary. Comparing results from Waihi Estuary with results collected from Maketu Estuary by DOMIJAN (2000) (see figure 4.16), the amplitude of the residuals is similar to that of amplitudes calculated at Waihi Estuary. Trends, however, do not follow similar patterns, as ebb tide durations do not exceed flood tide durations.

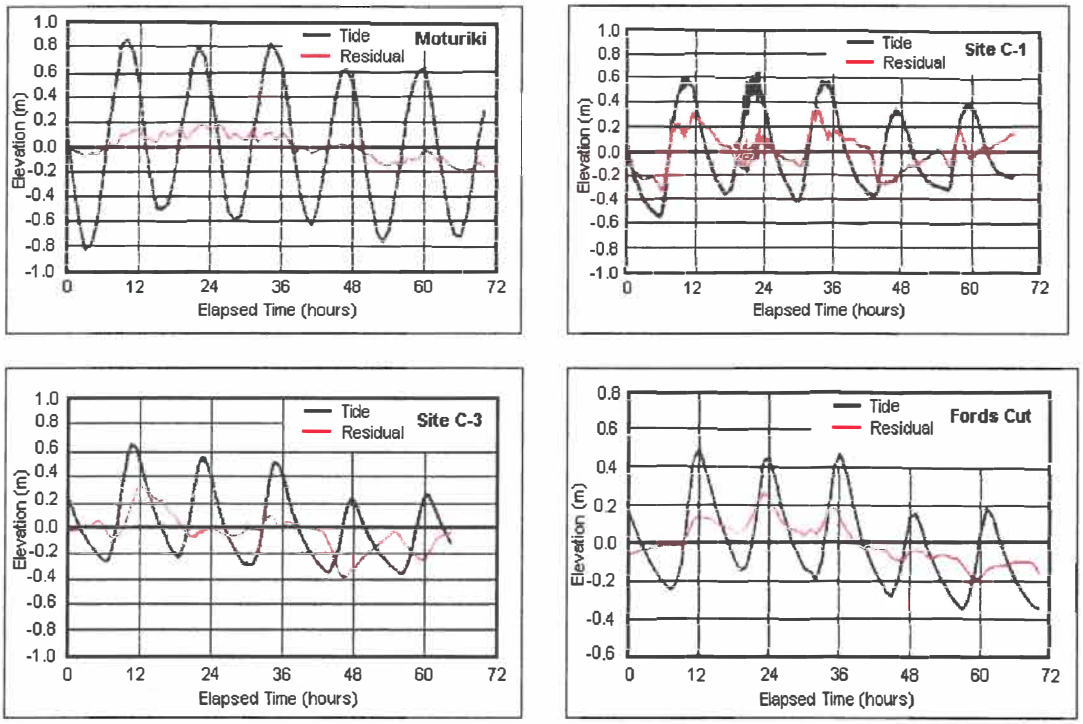

Figure 4.16 Examples of results obtained from THANAL analysis at Maketu Estuary by DOMIJAN (2000). Moturiki is an open ocean tide gauge, situated at Mount Maunganui. Site C-1 was situated at Maketu Estuary inlet, Site-3 positioned mid way in the estuary and Fords Cut was positioned near the Fords Cut channel.

4.3 Estuarine Sediments

4.3.1 Aim, Objectives and Methods

Analysing and assessing sediment characteristics within Waihi Estuary may provide a detailed explanation of the hydrodynamic patterns within the estuary. In regions where currents are of high velocity, it would be expected that the mean grain size of sediment in the associated area, would be coarser than regions where the current velocity is less, due to the winnowing effect of higher shear stresses. Likewise, if shear stress were reduced in a location, one would expect deposited sediment to be of finer grain size.

To investigate sediment characteristics of Waihi Estuary, 15 cores, 30cm in length, were taken strategically throughout the estuary in locations, where possible changes in sediment characteristics may differ. Figure 4.17 illustrates the 15 core locations. GPS co-ordinates of cores taken, are presented in Appendix I

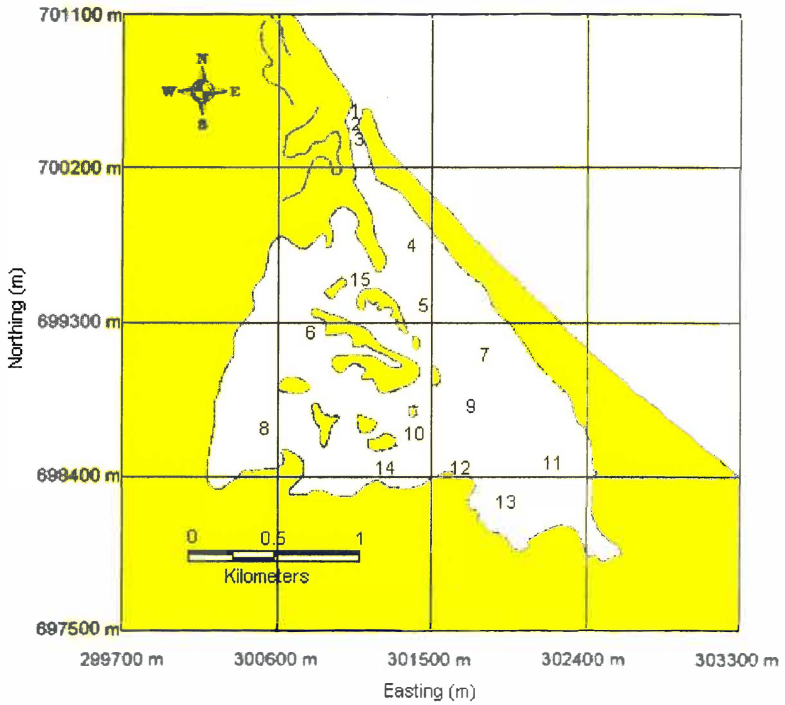

Figure 4.17 15 sediment core locations taken from Waihi Estuary, for assessment of sediment characteristics in attempt to identify hydrodynamic patterns of Waihi Estuary.

Cores were taken vertically into the estuary bed with a vertical-weighted drop corer used to drive 100mm diameter PVC pipe into the sediment. Cores were then capped until sediment characteristic analyses were performed.

Sediment analysis was carried out using the Rapid Sediment Analyser (refer to chapter 3, section 3.7.2 for a description), as the sediment morphology was predominantly sand sized particles. Analysis involved identifying differing sediment layers within the core, and RSA analysis of each layer for sediment texture. RSA results of each layer are presented in Appendix VII, while photographed cross-sections of the cores taken are presented in Appendix VIII.

Predominantly sediment samples were gravel bearing detrital sediments, or slightly gravelly sands. On the sub-tidal flats of the estuary, sediment texture remained slightly gravelly sands. The lack of fine sediments in this region, may imply that current velocities are high, consequently finer sediments are winnowed away. This possibility strengthens the hypothesis that hydraulic gradients could be present in this region.

Figures 4.18 to 4.20 illustrate the mean grain size, sorting and skewness of the surficial sediments taken from Waihi Estuary, as identified by the 15 cores.

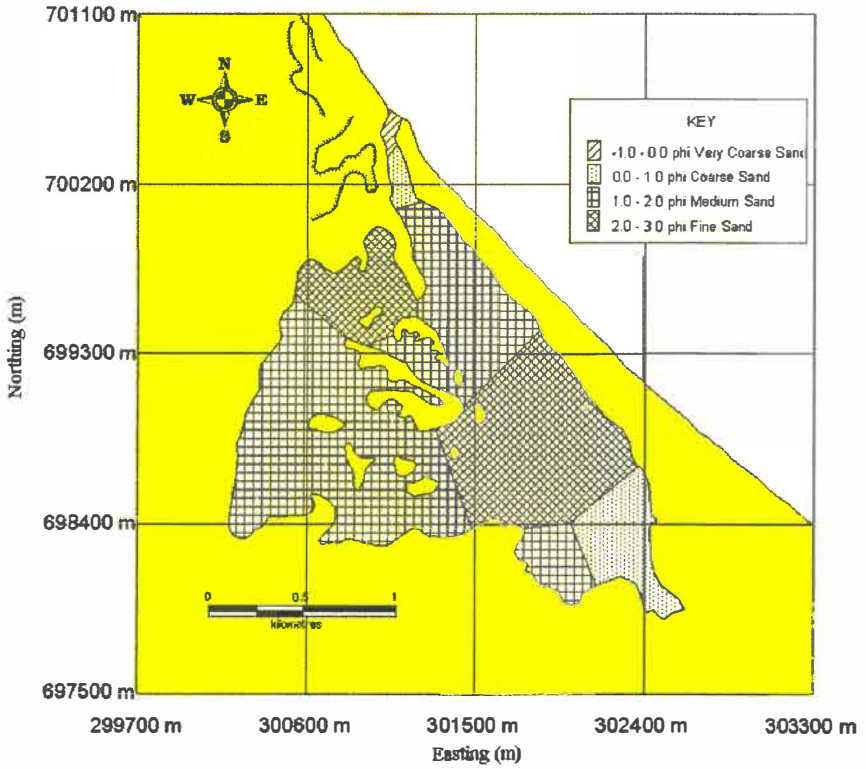

Figure 4.18 Mean grain size of surficial sediments within Waihi Estuary, based on 15 cores used for sediment characteristics analysis.

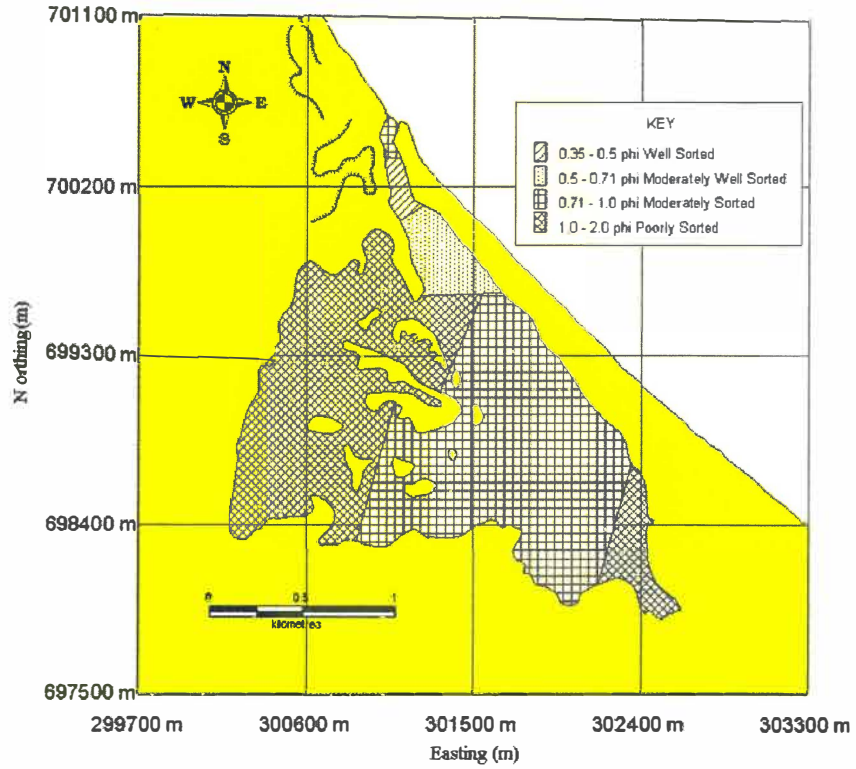

Figure 4.19 Sorting of surficial sediments within Waihi Estuary, based on 15 cores used for sediment characteristics analysis.

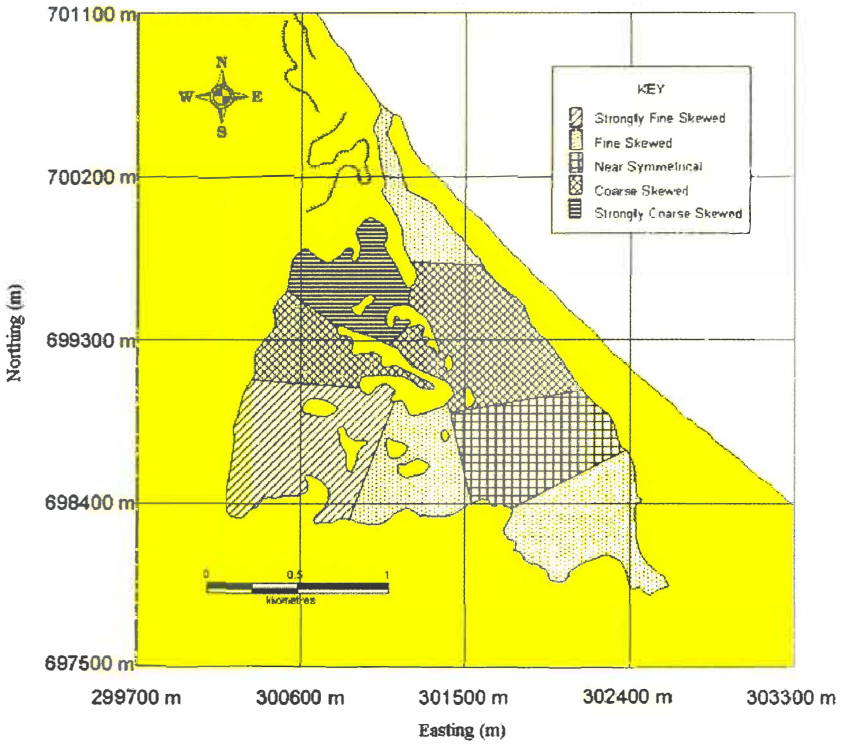

Figure 4.20 Skewness of surficial sediments within Waihi Estuary, based on 15 cores used for sediment characteristics analysis.

A sediment lag is observed in the estuary inlet, illustrated by figure 4.18. Sediments located in the estuary inlet are of larger phi size, and then gradually reduce as the distance from the estuary inlet increases. Water velocity decreases as the tidal wave progresses into the estuary, due to frictional dissipation. Subsequently suspended sediments can settle out (coarse sediment at the inlet and fining towards the throat), thereby creating the observed sediment lag.

4.3.2 Sediment Transport Pathways

Utilising outcomes of textural analysis of the estuarine sediments, obtained from the RSA, possible indications of sediment transport patterns, within the Waihi Estuary, may be identified.

MCLAREN (1981) and MCLAREN AND BOWLES (1985) have investigated the possibility of identifying sediment transport pathways (as previously discussed in chapter 3 section 3.4.3).

PAPPS AND PRIESTLEY (1997) applied the McLaren model to the main tidal channel of the Lower Waitemata Harbour and Half Moon Bay Marina. LOOMB (2001) also applied the McLaren model to Westpark Marina, to assess whether the marina was acting as a sediment sink, and where the source of sediment to the marina was coming from. Results from each investigation, imply that the model can be used in both open ocean and sheltered estuarine environments. PHIZACKLEA (1993) has also used the McLaren model to identify sediment transport patterns along the Pukehina-Matata coastal sector.

The MCLAREN (1981) model utilises textural parameters (mean grain size (mΦ), standard deviation (sorting) and skewness (SkΦ)) from the 15 cores collected (figure 4.17) and analysed by the RSA, to identify sediment transport pathways.

By assuming the following factors are valid, mapping of sediment movement may be made.

- Deposits within the investigated region are a product of a single sediment source,
- the probability for movement of finer sediment is greater than the movement of coarser sediments, and
- the probability of coarser sediments being deposited from suspension is greater than that for finer sediments.

The first assumption can be satisfied for Waihi Estuary. HALL *et al.* (1993) noted that streams entering the Waihi Estuary are limited sources of significant volumes of sediment to Waihi Estuary, during 'normal' conditions. This assumption, however, would not be correct during times of high water discharge, such as during a flood event, as it is highly

likely sediment would be discharged from the streams. Since there is no other sediment source within the estuary, one can assume that there is only one sediment source present, which is the sediment that may enter and leave the estuary inlet.

The following two assumptions may not be valid, however, for Waihi Estuary. PHIZACKLEA (1993) noted the presence of titanomagnetite in sediment samples taken within the Waihi Estuary. As stated in chapter 3, titanomagnetite is a heavy density mineral, which is commonly observed as a fine to very fine sediment sized particle. Since titanomagnetite is present within the estuary, it would require a greater current velocity to transport titanomagnetite, than a lighter density mineral, such as quartz. Therefore, outcomes obtained from the MCLAREN (1981) model, are to be treated as an indication of possible sediment transport pathways within the Waihi Estuary.

By comparative analysis of each sediment texture (refer to Appendix XI), sediment pathways are identified. A region with coarser grain sizes, poor sorting and positive skewness might be a sediment source to regions with characteristics of finer grain size, better sorting and negative skewness.

Figure 4.21 illustrates the sediment pathways, as calculated by the McLaren model.

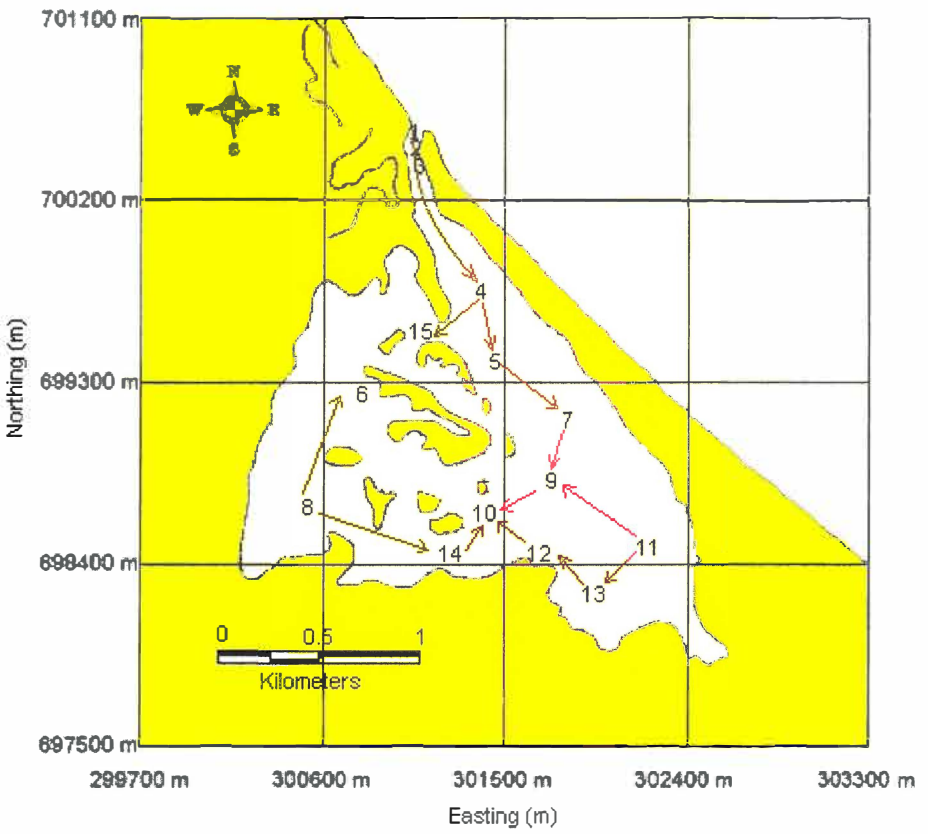

Figure 4.21 Sediment pathways of Waihi Estuary as calculated from the McLaren model using textural parameters mean grain size (mΦ), standard deviation (sorting) and skewness (SkΦ) as obtained from 15 sediment samples.

4.3.2.1. Discussion

Results obtained from the McLaren model inside the estuary are representative of both visual observations, and the textural parameter data collected. Sediment transport at Waihi Estuary is flood-dominated. This is in agreement with tidal data collected at Waihi Estuary inlet, and visual evidence of the estuary. The formation of flood tidal delta is an indicative observation, which denotes that sediment is being transported into the estuary. HALL *et al.*'s (1993) statement that the streams supplying limited sediment to the estuary is supported by sediment transport outcomes obtained. Since flood dominated transport at the mouths of the streams was obtained from the MCLAREN model outcome, this implies that sediment movement is towards the streams, and not from.

Regions of the estuary where there is convergence of sediment transport paths, most result in shallower water depths, in respect to other regions. This was observed when core samples were obtained, as transport to samples sites via boat was not possible in these areas.

Since the McLaren model illustrates that sediment transport in the Waihi Estuary is flood dominated, the stability of the estuary inlet may therefore, be uncertain and will require investigation. By analysing geomorphic and hydraulic stability of the inlet, and influences from the open ocean coastal transport system, indication of how stable Waihi Estuary is, may be made.

4.4 Inlet Stability

Figure 4.22 Waihi Estuary inlet looking northeast. NOTE: dual entrance present (Photographs taken by author, 16/6/2000).

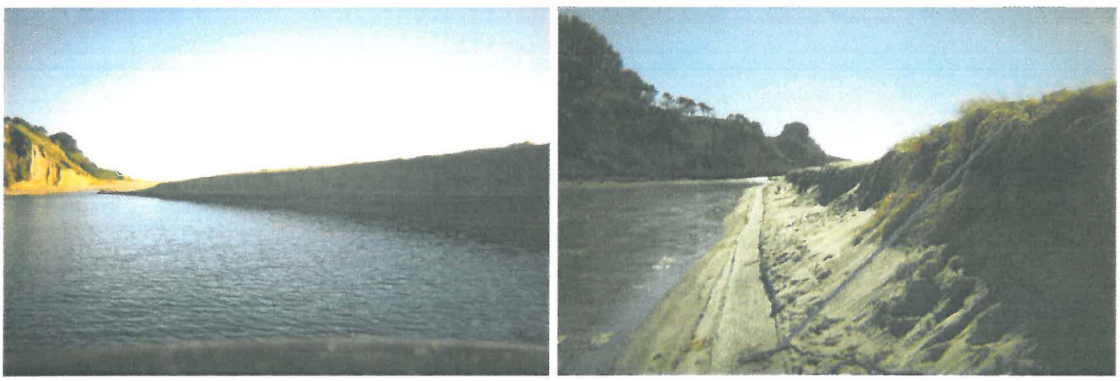

Figure 4.23 Erosion at Inner Waihi Estuary inlet (Pukehina Spit), due to SW winds generating waves, which undercut and facet the dune face (Photographs taken by author, 12/3/2001).

BRUUN (1978) postulates that there is never a stable tidal inlet on a littoral drift shore, as the inlet is always subject to continual changes in plan form, as well as its cross-sectional area and geometry.

The stability of a tidal inlet on a littoral drift shore is dependent on various processes (KOMAR, 1998). Littoral drift, flood and ebb currents, flood and ebb tidal deltas and wave action are the predominant processes that might affect the stability of a tidal inlet (BRUUN, 1978). In reference to Waihi Estuary, the predominant processes that may influence the inlet are littoral drift, flood and ebb currents, and wave action. Even though ebb and flood tidal deltas are present, the geometry of each delta is insignificant to affect the dynamics of the tidal inlet, i.e. modifications of wave approach angles. Therefore, sediment transport directions and also sediment transferring from the flood tidal delta to inlet will be minimal. This is further discussed in Chapter 5.

4.4.1 Geomorphic Stability

Geomorphic stability involves assessing the tidal inlet in plan form, usually with the use of historical aerial photographs. SMITH AND ZARILLO (1990) have assessed the use of historical aerial photography to calculate rate of shoreline retreat, and concluded that to enable accurate estimates of shoreline retreat, benchmarks or points of known location must be used in overlaying aerial photographs.

For the use of this analysis, benchmarks 30, 29 and the Pukehina slipway, were used to overlay aerial photographs taken in years 1993 and 1984. The aerial photograph taken in 1943, however, had to be overlayed using the Pukehina slipway and roof tops of houses, as benchmarks 30 and 29 were not positioned until the 1977 BOPCES (Bay of Plenty Coastal Erosion Survey) was performed. The accuracy of the overlayed 1943 aerial photograph therefore, is not as accurate as the proceeding two photographs.

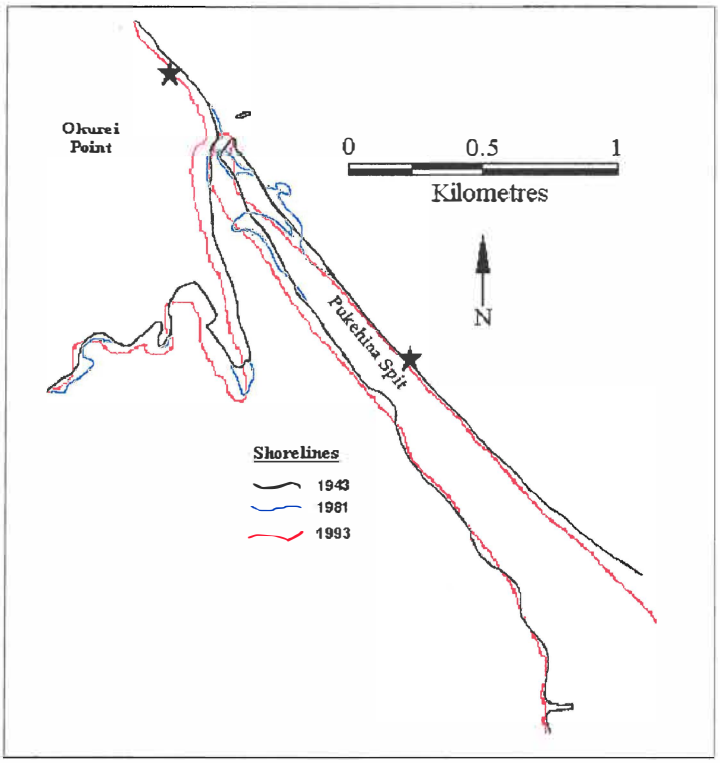

Figure 4.24 Spatial geomorphic changes to the Waihi Estuary inlet, taken from aerial photography in 1943, 1981 and 1993. Overlayed shorelines were produced by using local benchmarks (asterisks) and or fixed spot locations, for example houses, Waihi Estuary boat ramp.

Figure 4.24, illustrates that the changes to the estuary inlet are large, approximately a 150 m difference in inlet width between years 1981 and 1993. Due to these differences in the cross-sectional area of the Waihi Estuary inlet, it is clear that the inlet is in a dynamic state.

This is confirmed by the sediment textural analysis results obtained. The formation of a sedimentary lag at the estuary inlet, even though fastest currents were recorded on the ebb tide, denotes that the distal end of Pukehina Spit is continually being altered. This continual alteration is reworking sediment.

Possible processes that could be initialising this change are: the longshore or littoral drift processes and/or wave dynamics, primarily wave energy and wave direction.

4.4.2. Hydraulic Stability

Hydraulic stability of a tidal inlet can be calculated in two ways (BRUUN AND GERRITSEN, 1960). These are:

- The use of empirical formula using measured coefficients of tidal prism, inlet cross-sectional area, peak velocities, shear stresses, and discharges throughout the inlet gorge.
- An analytical approach, which involves the development of generalised formulae from understanding the specific estuarine sediment transport mechanisms of the investigated estuary.

For the purpose of this research, empirical formula will only used to indicate hydraulic stability of Waihi Estuary.

4.4.2.1 Cross-section of Waihi Estuary Inlet

A cross-section of the Waihi Estuary was taken at the deepest, shortest section of the throat on the 31/1/2002, with the use of a survey vessel. The locations of high water elevation on west and east banks (Okurei Point and Pukehina Spit sides, respectively) were obtained by differential GPS. A run-line between the two locations was then created by HYDROPRO. Depth soundings were collected at regular spaced intervals (~2 m), but locations where depth had greater fluctuations, soundings were concentrated (~0.5 m). Depths that the survey vessel could not sound, due to limited water depth, were surveyed manually using a staff with increments of 10 cm.

Current measurements at the location of the cross-section of inlet should have been obtained, but due to instrument availability at the time of measurement, this was not possible. Therefore, current measurements obtained from a representative spring tide during summer 2001 (12/3/2001) were used for calculating discharge from and into the

inlet. The results therefore, can only give an indication of the hydraulic stability of inlet, as the area cross-section most likely would have altered over time.

4.4.2.2 Ω/M_{total} Ratio

The Ω/M_{total} ratio was first introduced by BRUUN AND GERRITSEN (1960). BRUUN (1978) states (p. 260) 'The important factors determining the development of the entrance obviously are: the area of the bay and it's geometry, the width of the barrier, the length of the ocean, gorge, and bay channels, the offshore bottom slope, the tidal range, and the magnitude of wave exposure. These factors may be combined to form the "tidal prism" in m^3 (Ω) and its flushing ability, and to the flux of wave energy (E_f) towards the entrance and the adjoining shores.'

The flux of wave energy (E_f) may be defined as the longshore flux of wave energy, which causes a proportional longshore drift quantity, in units m^3year^{-1} (M_{total}) (BRUUN, 1978). Further, BRUUN (1978 pp. 261-262) classifies the Ω/M_{total} ratio into five different categories, which will be used to describe the Waihi Estuary inlet.

BRUUN's (1978) definition of a tidal prism (BRUUN, 1978 p. 260) is a complex calculation, especially in regard to Waihi Estuary. Since a hydrographic surveying has never been conducted, parameters such as the length of the gorge and bay channels, are not known. Therefore, a more achievable alternative to calculate the tidal prism is to determine the volume of water that flows into and out of the estuary over a half tidal cycle.

Using measured current velocities throughout a half a tidal cycle, and multiplying each velocity value by cross sectional bathymetry of the estuary inlet, obtains a time series (here every 30 minutes) of discharge (m^3s^{-1}) of water entering and exiting the estuary.

Then by summation of the inflow and outflow discharges and multiplying by the duration of the ebb and flood cycles (s), yields the tidal prisms for ebb and flood phases.

4.4.2.3 HUME AND HERDENDORF (1986) Area-Prism Relationship

HUME AND HERDENDORF (1986) developed an area-prism relationship for barrier enclosed estuaries, from a power function between the cross-sectional area of a stable inlet throat and the estuary tidal prism (equation 4.2).

$$A = C \cdot \Omega^n \qquad \text{Eqn. 4.2}$$

where A= inlet gorge cross-sectional area (m^2)

C, n = Constants

Ω = Tidal Prism (m^3).

The following equation (equation 4.3) represents the HUME AND HERDENDORF (1986) area-prism relationship, which was calculated from 34 different barrier enclosed estuaries, with a determination coefficient (r-squared) of 0.983.

$$A = 1.95 \times 10^{-4} \cdot \Omega^{0.94} \qquad \text{Eqn. 4.3}$$

Comparing this value with the actual cross-sectional area of the gorged inlet, may indicate whether the inlet is prone to erosion (if area-prism relationship value is greater than actual area), or deposition (if area-prism relationship is less than actual area).

4.4.2.4 Ω/M_{total} Ratio and HUME AND HERDENDORF (1986) Area-Prism Relationship Results

Figure 4.25 illustrates the cross section of Waihi Estuary, undertaken on the 31/1/2002. west bank signifies the Okurei Point side, while east bank represents Pukehina Spit.

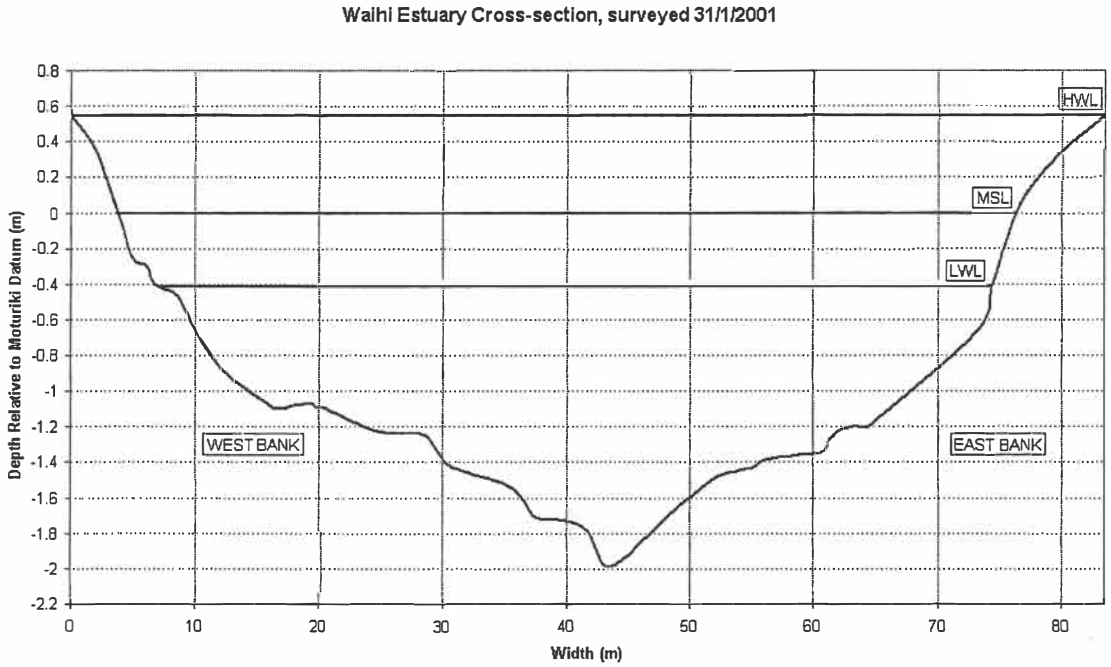

Figure 4.25 Cross-section of Waihi Estuary inlet. Survey undertaken on 31/1/2002 on a spring tide with tidal range of 0.963m. Depths are relative to Moturiki Datum, with HWL=high water level, MSL=mean sea level and LWL=low water level.

Deployment (spring /neap)	Flood Tidal Range (m)	Flood Prism (m^3)	Ebb Tidal Range (m)	Ebb Prism (m^3)	Mean Prism (m^3)	Excess Outflow (m^3)	% of Ebb Outflow
Winter Dep.2	0.76	718493	0.76	824295	771394	105802	12.8
Summer (spring)	0.96	849745	0.97	934635	892190	84890	9.1
Summer (neap)	0.75	724728	0.75	814503	769615.5	89775	11.0

Table 4.3 Flood/ebb tidal ranges calculated for each deployment during summer and winter cycles, and associated tidal prisms for each flood/ebb tide, during each winter and summer deployment. Note: Summer deployment was one singular deployment, which obtained the end and beginning of a spring and neap tide respectively. Winter deployment 1 is not included as velocity data was not collected, winter deployment 2 = 26/5/2000 – 6/6/2000 and summer deployment = 9/3/2001 – 21/3/2001.

BURTON AND HEALY (1985), estimated littoral drift to be about M_{tot} = 40,000 m^3/yr along the Maketu coastline. Assuming some sediment is not transport around Okurei Point, due to a sheltering of incident swell waves an 'uncertain' estimate of M_{tot} = 35,000 m^3/yr, shall be used here.

Deployment (spring /neap)	Ω/M_{total}
Winter Dep.2	22.0
Summer (spring)	25.5
Summer (neap)	22.0

Table 4.4 Ω/M_{total} ratios as calculated by tidal data obtained during winter and summer deployments. Winter deployment 1 is not included as velocity data was not collected, winter deployment 2 = 26/5/2000 – 6/6/2000 and summer deployment = 9/3/2001 – 21/3/2001.

From Ω/M_{total} ratios, all scenarios identify as typical 'bar-bypassers', as classified by BRUUN (1978). BRUUN's (1978) classification seems reasonable in relation to observations of Waihi Estuary inlet, as BRUUN (1978) states that navigation can be unreliable and dangerous, with the Ω/M_{total} ratio obtained. Current boat traffic entering and exiting Waihi Estuary is confined to 2 hours either side of high water level, thereby, suggesting that results obtained are reasonable.

Results using the HUME AND HERDENDORF (1986) area-prism relationship are given in table 4.5.

Deployment (Flood/Ebb)	Actual Cross-sectional area of gorged inlet (m^2)	Value calculated from HUME AND HERDENDORF (1986) area-prism relationship (m^2) (Eqn. 4.3)	Inlet Stability (erosion / deposition)
Winter Dep.2 Ebb	86.7	70.98	Deposition
Winter Dep.2 Flood	86.7	62.38	Deposition
Summer (Spring) Ebb	87.1	79.88	Deposition
Summer (Spring) Flood	87.1	73.04	Deposition
Summer (neap) Ebb	86.4	70.19	Deposition
Summer (neap) Flood	86.4	62.89	Deposition

Table 4.5 Comparison actual cross-sectional area of gorged inlet (m^2) and HUME AND HERDENDORF (1986) area-prism relationship, to identify inlet stability, during winter and summer deployments. Winter deployment 1 is not included as velocity data was not collected, winter deployment 2 = 26/5/2000 – 6/6/2000 and summer deployment = 9/3/2001 – 21/3/2001.

Results obtained indicate that the actual cross-section of the estuary inlet are above values suggested by HUME AND HERDENDORF's (1986) area-prism relationship. This implies that deposition is likely to occur at Waihi Estuary inlet.

4.4.2.5 Inlet Stability Criteria

4.4.2.5.1 Mean Maximum Velocity (V_{mm}) and Stability Shear Stress Criteria

V_{mm} is the mean maximum velocity measured in the inlet cross-section at mid spring tide.

V_{mm} is calculated using the equation

$$V_{mm} = Q_m / A \qquad \text{Eqn. 4.4}$$

Where Q_{mm} is the peak discharge in section (m^3s^{-1}), and A is the gorge cross-sectional area (m^2).

A stable inlet according to BRUUN (1978), will have value for V_{mm} 1.0 ± 0.15 ms^{-1}. This value was obtained from a variety of gorged inlets. For Waihi Estuary, values of 0.55 and (0.66) ms^{-1} were calculated for flood and ebb phase respectively. These values are below the suggested, according to BRUUN (1978). Since, Waihi Estuary is not closing, one may assume that the value calculated for V_{mm}, exceeds the value V_{crit}, where V_{crit} is the velocity at which sediment entrainment will not occur.

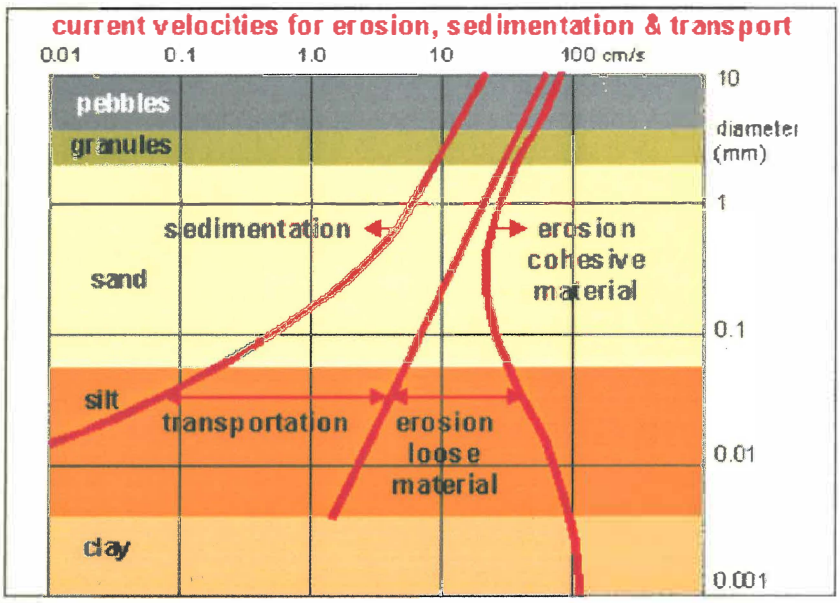

Figure 4.26 Velocity-sediment grainsize relationship, identifying velocities at which a sediment particle may be deposited, transported or eroded. (HEEZEN AND HOLLISTER, 1971).

From sediment analysis, sediment grainsize at Waihi Estuary inlet was –1.0 to 0.0 Ø, or 1 to 2 mm. Comparing current velocity and sediment grain size values obtained with figure 4.26, indicates that the Waihi Estuary may be in a scouring mode, in order to attain equilibrium.

The main parameters of a stability analysis, are the 'equilibrium bottom shear stress' and the 'actual bottom shear stress'. τ_{eq}, the equilibrium shear stress, has been defined by VAN DE KREEKE (1990), as the bottom stress induced by the tidal currents that is required to flush the sediments carried into the inlet by the longshore currents.

Equilibrium shear stress is calculated using the equation,

$$\tau_s = \frac{\rho g V^2_{mm}}{C^2}. \qquad \text{Eqn. 4.5}$$

ρ is the density of seawater (1025 kgm^{-3}), g is gravitational acceleration (9.81 ms^{-2}) and C is Chezy C resistance to flow-factor.

Chezy C may be approximated by the following:

$$C = 30+5 \log A \ (m^{1/2}s^{-1}) \qquad \text{Eqn. 4.6}$$

Where A is the surveyed mid tide cross-sectional inlet gorged area (m^2).

The actual bottom stress follows from:

$$\tau = \rho F u |u| \qquad \text{Eqn. 4.7}$$

where F is the friction factor and u is the cross-sectional averaged velocity.

The friction factor, is calculated by

$$F = g/C^2 \qquad \text{Eqn. 4.8}$$

VAN DE KREEKE (1990) states (p. 262) that 'when the actual shear stress equals the equilibrium shear stress, the inlet is in equilibrium with the hydraulic environment. When the actual shear stress is larger than the equilibrium shear stress, the inlet is in a scouring mode; when the actual shear stress is smaller then the equilibrium shear stress, the inlet is in a shoaling mode. The equilibrium is called stable if after a small change, for example resulting from a storm event, the inlet cross-sectional area unconditionally returns to its equilibrium value'.

BRUUN AND GERRITSEN (1960), from investigations, have calculated estimates of equilibrium shear stresses for tidal inlets, based on spring tide conditions (table 4.6)

Condition	τ_{eq} (N/m^{-2})
Heavier littoral drift and sediment load	5.5
Medium conditions of littoral drift and sediment load	4.5
Lighter littoral drift and sediment load	3.5

Table 4.6 Estimates of stability shear stresses for tidal inlets, based on spring tide conditions. A light littoral drift is defined as ~ 0.48 kgm^{-1}, medium ~0.88 kgm^{-1} and a high 1.33 kgm^{-1} (BRUUN AND GERRITSEN, 1960).

BRUUN AND GERRITSEN (1960) state (p. 74), however, that values indicated in table 4.6, are related to the sediment movement in the tidal inlet and not to closure of the inlet, as it depends on size of the bed material, which in this case is between 0.1 and 0.5 mm. Therefore, the value obtained for τ_{eq}, is only indicative, in terms of actual stability (VAN DE KREEKE, 1990).

4.4.2.5.2 Stability Shear Stress Criteria Results

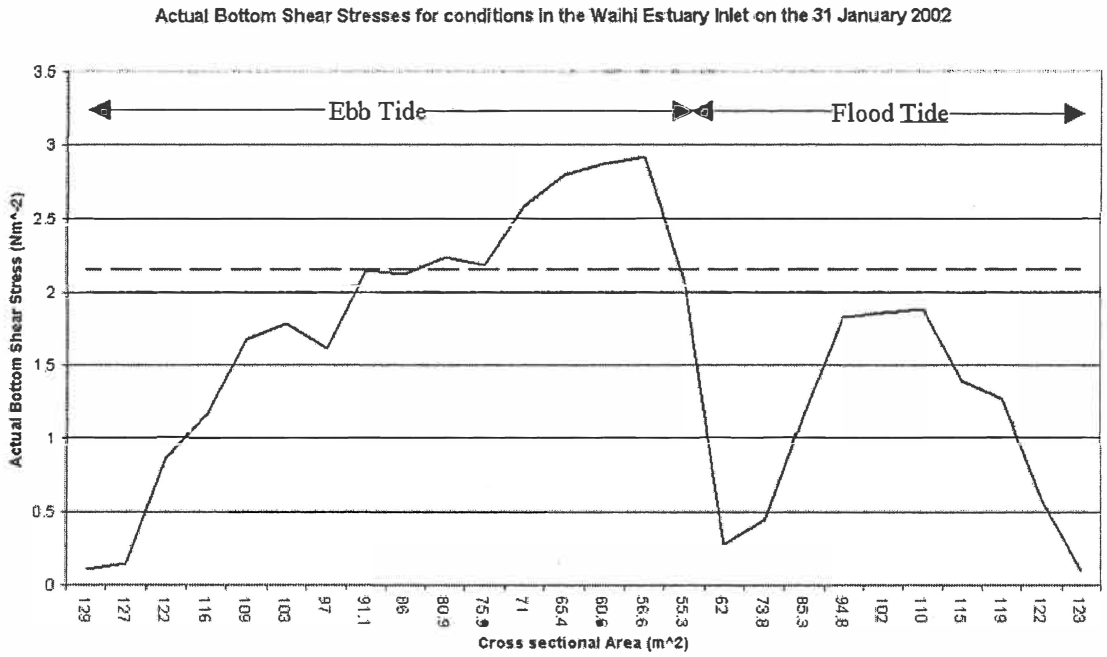

Figure 4.27 Actual bottom shear stresses for conditions in the Waihi Estuary inlet on the 31/1/2002. Dashed line indicates equilibrium shear stress for the Waihi Estuary inlet.

Figure 4.27 illustrates a plot of actual bottom shear stress (calculated by equation 4.7) over a representable tidal cycle for Waihi Estuary. Associated with the figure 4.27 plot is the equilibrium shear stress (calculated by equation 4.5) for Waihi Estuary.

From figure 4.27, the actual bottom shear stresses of Waihi Estuary ranges from 2.92 Nm^{-2} to 1.88 Nm^{-2} during ebb and flood tides respectively. Equilibrium shear stress for the Waihi Estuary inlet was 2.15 Nm^{-2}. Predominantly actual bottom shear stress is below the

equilibrium shear stress, this indicates from VAN DE KREEKE's (1990) classification, that Waihi Estuary inlet is in a shoaling state.

4.4.3. Discussion of Tidal Stability

Results obtained from geomorphic and hydraulic stability analysis, indicate that the Waihi Estuary inlet to be in a depositional or shoaling state. This is consistent with the idea that Waihi Estuary is infilling and the inlet is tending towards instability. However, since current data were not obtained during collection of cross-sectional area measurements, results can only be judged as indicative.

4.5 Summary

From research and comparisons with similar estuaries, there is a strong indication that the Waihi Estuary is acting as a sediment sink. From tidal asymmetry, tidal damping and sediment textural analysis, evidence is provided that sediment is being transported into the estuary from an open ocean sediment source. However, currents conversely suggest that sediment is being transported from the estuary. Assessment of the Bruun tidal inlet stability criteria for Waihi Estuary inlet, by geomorphic and hydraulic analysis, indicates the inlet is tending towards instability. Further investigation, therefore, is required to assess how unstable the inlet may be. Geomorphic stability assessment illustrates extensive movement of the distal end of Pukehina Spit, presumably a function of littoral drift and/or wave action could be driving the instability (this will be assessed further in chapter 5).

Ebb tide water level fluctuations were observed on the sub-tidal flats. Investigation was not carried out, but instrument failure, seiching within the estuary driven by an external process such as edge or coastal-trapped waves, and bed friction and channel influences are hypothesised as possible causes.

Sediments within Waihi Estuary vary from very coarse sand to fine sand. A sediment lag was identified in the inlet of Waihi Estuary. From sediment textural parameters, obtained from cores taken throughout the estuary, sediment transport paths were identified by utilising the McLaren sediment transport model. Outcomes indicated that sediment transport within the Waihi Estuary is flood dominated.

Chapter Five
Wave Energy Focusing upon Pukehina Beach and Nearshore Littoral Drift

5.0 Introduction

As for most Bay of Plenty beaches, the Pukehina coastal sector is subject to episodic frontal dune erosion (HEALY *et al.*, 1977). Indeed frontal dunes at Pukehina Beach have been estimated to be eroding 0-0.2 m per year over the last 60 years (PHIZACKLEA, 1999). During storm wave events, the frontal dune is likely to erode (see figure 1.1) as reported by PHIZACKLEA (1993).

Wave energy focusing may be induced by undulating offshore bathymetry refracting/diffracting waves, causing an increased concentration of wave energy along a sector of shoreline, thereby leading to enhanced frontal dune erosion (HEALY, 1987; SPERANSKI AND CALLIARI, 2001). From offshore sediment morphology investigations, as detailed in chapter 3, it can be seen that the Pukehina coastal sector comprises of a complex offshore bathymetry.

In this chapter a detailed numerical simulation of possible wave refraction/diffraction within the Pukehina coastal sector, and an investigation of wave energy focusing and deductions for enhanced frontal dune erosion, is undertaken. Investigation of potential littoral transport induced by the angle of the waves breaking on the shoreline is also included. Deduced sediment transport pathway, based upon results from chapter 3, and PHIZACKLEA's (1993) analysis of nearshore currents depict complex littoral processes acting in the vicinity of Okurei Point. From assessment of littoral transport within the Pukehina coastal sector, an assessment of the potential sheltering induced by Okurei Point is undertaken.

5.1 Literature Review of Wave Refraction using Numerical Models

Wave data collected within the Bay of Plenty has increased largely over the last decade due to an increase in coastal research (DE LANGE, 1991; DE LANGE, 1993; PHIZACKLEA, 1993; MATHEW, 1997; SAUNDERS, 1999). However, the use of wave refraction models to predict 'regions' of wave energy concentration via wave focusing has had little application among Bay of Plenty beaches.

Various wave refraction models are available (MAA *et al.* 2000). MAA *et al.* (2000) analysed six wave refraction models for their performance of assessing water wave shoaling, refraction, and diffraction. The models used in their analysis were: RCPWAVE (Regional Coastal Processes Wave, developed by EBERSOLE *et al.* 1986), Ref/Dif-1 (KIRBY AND DALRYMPLE, 1991), RDE (MAA AND HWUNG, 1997), PBCG (MAA *et al*, 1998), PMH (HSU AND WEN, 2001) and Mike 21's EMS module (MADSEN AND LARSEN, 1987). MAA *et al.* (2000) concluded that model outcomes varied due to different wave transformation theories and relationships used, and that caution is required when applying a wave refraction model to assess wave processes, such as wave focusing.

WBEND (BLACK and ROSENBERG, 1992) is a numerical model that is specifically focused on modelling wave shoaling, frictional dissipation and wave refraction processes for both monochromatic waves and wave spectra. Recent studies at Waihi Beach (STEPHENS, 1996), Raglan (HUTT, 1997), West End Ohope (SAUNDERS, 1999) and Wainui beach, Gisborne, (DUNN, 2001) have applied WBEND to investigate wave refraction patterns and obtained successful results. Therefore, WBEND will be used here for investigations of wave refraction.

The demonstration of wave focusing by numerical simulation was first illustrated by BLACK (1983) and published in BLACK AND HEALY (1988). The significance of wave focusing in coastal erosion processes was first published by HEALY (1987).

STEPHENS (1996) and STEPHENS, *et al.* (1999) used the numerical model RCPWAVE to investigate the relationship between wave focusing and arcuate duneline embayments at Waihi Beach, Bay of Plenty. Monochromatic wave statistics were used to drive the model (H_s=0.8 m, T_s=6.0 s). Results were obtained from a variety of wave directions, also a storm wave condition was applied (H_{max}=3.0 m, T_{max}=10.5 s). Marked wave energy focusing was demonstrated along Waihi Beach, consistent with the geomorphic manifestation of arcuate duneline embayments. Increased wave heights were noted extending some 8 km offshore. Wave focusing was reported as not particularly noticeable under average wave conditions (H_s=0.8 m, Ts=6.0 s), but was pronounced under storm conditions, particularly with long period waves (>10.5 s). High-energy peaks were not always found associated with historical locations of arcuate duneline embayments, but in most cases they were associated.

SAUNDERS (1999) used the model WBEND to investigate whether wave energy focusing occurs at West End Ohope, and if this could be related to accelerated frontal dune erosion. Results obtained by SAUNDERS (1999), indicated that wave energy focusing was contributing to enhanced frontal dune erosion at West End Ohope.

Similarly DUNN (2001) utilised the numerical model WBEND to identify whether wave energy focusing was apparent at Wainui Beach, Gisborne. Indications of outcomes from WBEND simulations identified that wave energy focusing was present along the Wainui Beach shoreline, which was being generated from a single offshore reef. DUNN (2001) claims that numerical model results obtained are supported by visual evidence, as surfers use the knowledge that wave heights are increased in the lee of the offshore reef, in comparison to the surrounding region.

Similar applications of wave refraction simulations, showing evidence of wave focusing and enhanced erosion of the shoreline, were later demonstrated by SPERANSKI AND CALLIARI (2001), along the Brazilian coast. They showed bathymetric lenses (or offshore bathymetric features, which induce wave focusing) were focusing incoming wave trains, which are leading to enhanced frontal dune retreat.

5.2 Wave Refraction Theory and Wave Energy Focusing

5.2.1. Wave Refraction Theory

KOMAR (1998, p. 189) defines wave refraction as 'Upon entering intermediate to shallow water, waves are subject to refraction, in which the direction of their travel changes with decreasing water depth in such a way that the crests tend to become more nearly parallel with the depth contours'.

Refraction of waves results from their wave celerity dependence on the water depth once they enter intermediate to shallow water. In linear wave theory, celerity (C) is a parameter defining the speed of the wave crest (ms^{-1}), given by:

$$C = \sqrt{gh} \qquad \text{Eqn. 5.1}$$

where g is gravitational acceleration (9.81 ms^{-2}) and h is water depth (m).

Clearly wave crest speed is a function solely of water depth, so that a wave crest in shallower water will have a smaller wave celerity, than a wave in deeper water, and therefore, the wave crest will move a greater distance in deeper water than the same wave crest in shallower water. The result is a change in wave crest approach direction, with the typical result that the wave crests tend to become more nearly parallel to the shore, except where there is wave focusing.

Figure 5.1 illustrates the wave refraction process.

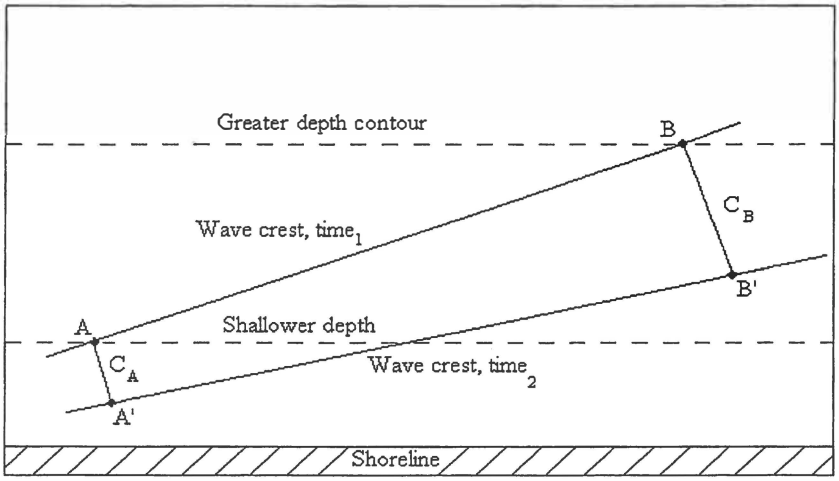

Figure 5.1 Wave refraction occurs due to larger wave celerity (C) in deep water than in shallower water. During a certain time interval, the wave crest at point B in deeper water movers further than the crest at point A in shallower water, causing the wave crest to rotate and become more nearly parallel to the shore (Source: KOMAR, 1998).

5.2.2. Wave Energy Focusing

When a wave travels over a shoal the wave will refract at that location, possibly focusing the wave train at a shoreline location and causing localised wave energy increase along a sector of shoreline (HEALY, 1987; SPERANSKI AND CALLIARI, 2001). Shape of a shoal or depression is important when observing wave focusing, because how the shoal or depression is shaped at the apex of the incoming wave (either it be concave or convex) will determine whether the wave will focus or not. Similar to the refraction of light, a convex shape will cause a focusing at a distant point, while a concave shape will cause dispersion of energy. However, in regard to waves, two areas of wave energy convergence may occur if a wave shoals over a concaved shaped apex (dispersion of energy), as the diverted wave may coincide with another incoming unrefracted wave. Figure 5.2a and 5.2b show wave divergence and wave focusing respectively.

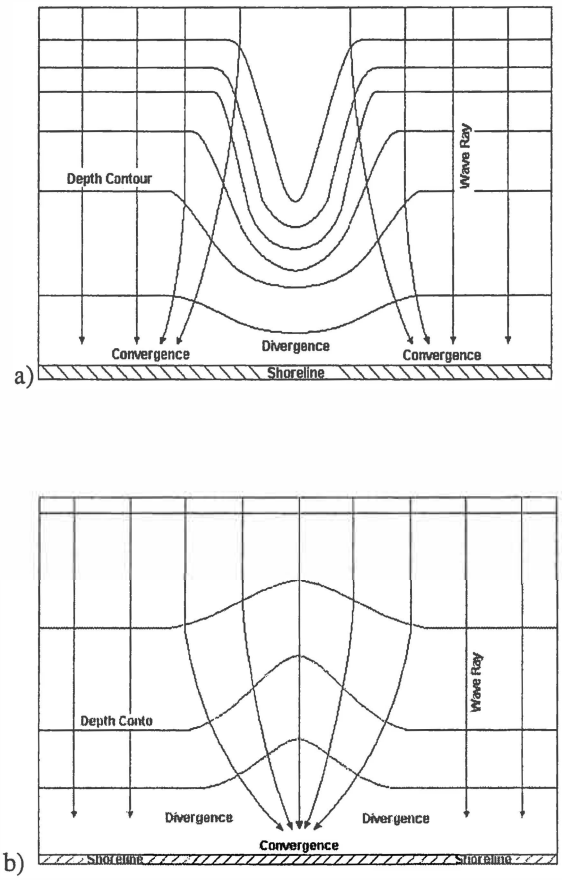

Figure 5.2.a) Wave focusing such as over a shoal. b) Wave divergence such as over a seafloor topographic depression. (Source: Komar, 1998)

A scenario, however, which does not comply with the previous paragraph, is illustrated in figure 5.3a and 5.3b. Here at Motuotau Island, Bay of Plenty, a salient can be seen forming in the lee of Motuotau Island. Even though the incoming wave train is meeting a convex shaped apex, convergence of wave energy is not occurring behind Motuotau Island.

Figures 5.3a) and b) Wave refraction patterns occurring in the lee of Motuotau Island, Mount Maunganui. (Photographs taken by author 12/8/2001).

Motuotau Island induces a shadowing effect of wave energy in the lee of the island. Waves are refracted around the island, which then break at an angle to the Mount Maunganui shoreline. This generates a localised littoral counter drift set-up, thereby inducing a salient formation in the lee of Motuotau Island. Figure 5.4 illustrates this process.

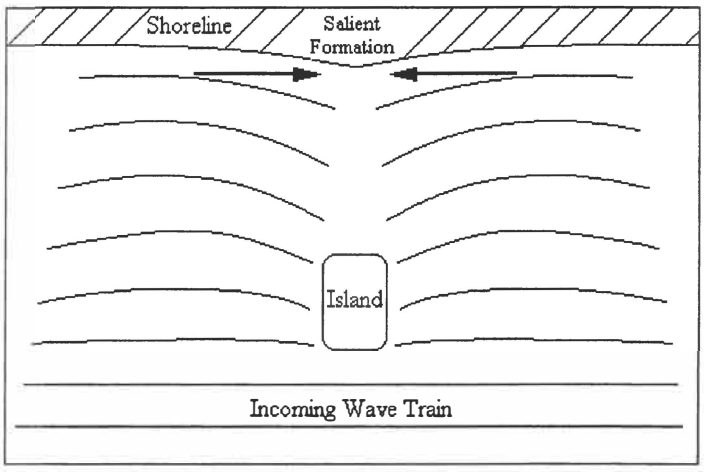

Figure 5.4 Schematic of salient formation in the lee of Motuotau Island. Arrows indicate direction of localised littoral drift due to incoming wave refracting and wave breaking at the shoreline at an angle.

The importance of wave energy focusing at beaches is that it alters wave characteristics, particularly at the shoreline. The most importance characteristic is wave height. For linear wave theory, the wave energy is a function of the wave height, which is noted in equation 5.2.

$$E = \frac{1}{8}\rho g H^2 \qquad \text{Eqn. 5.2}$$

where E is the wave energy (Jms^{-1}), g is gravitational acceleration ($9.81ms^{-2}$), ρ is the density of water (1025 kgm^{-3}) and H_b is the breaking wave height (m)

An increased wave height at the shoreline also corresponds with an increased wave set-up and wave run-up. Increased wave set-up and wave run-up are critical parameters for erosion of beaches, such as Pukehina. An increase of either of these parameters, promotes a greater chance of waves being able to erode the frontal dune of Pukehina Beach, and increases the height of the beach water table from infiltration of the beach sediments. This enhanced rise of beach water table facilitates erosion of the lower beach face, due to pore water pressure. Figure 5.5 illustrates five components of a storm surge and run-up parameters, included are wave set-up and wave run-up.

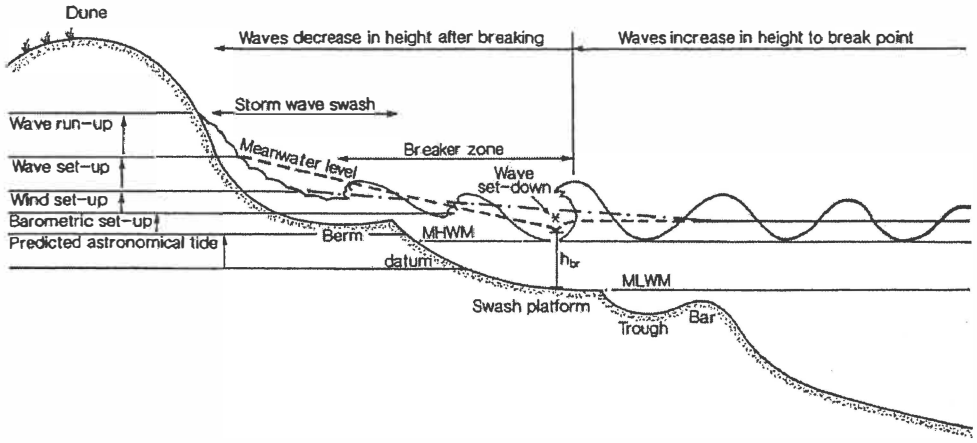

Figure 5.5 Components of a storm surge and run-up. (Source: HEALY AND DEAN, 2000)

From HEALY AND DEAN (2000), the SORENSON (1978) formula for wave set-up is outlined. The SORENSON (1978) formula assumes that wave set-up (h_s) is solely a function of breaking wave height and wave steepness

$$h_s = 0.19\left[1 - 2.82\left(H_b / \ gT^2\right)^{0.5}\right]H_b. \qquad \text{Eqn. 5.3}$$

Where g is gravitational acceleration (9.81 ms^{-2}), T is the deepwater wave period (s) and H_b (breaking wave height, m), which is calculated by

$$H_b = 0.563 H_b \Big/ \left(H_o / L_o\right)^{0.2}. \qquad \text{Eqn. 5.4}$$

H_o is deepwater wave height, usually $H_{1\%}$ (in m), and L_o is the deepwater wave length (m) calculated by

$$L_o = 1.56\ T^2 \qquad \text{Eqn. 5.5}$$

Wave run-up (h_r) is outlined in the *Shore Protection Manual* (1984), and is given by

$$h_r = \left(H_b L_o\right)^{1/2} \tan\beta \qquad \text{Eqn. 5.6}$$

Where β is the gradient of the offshore bar.

5.3 Objectives and Methods of Wave Data Collection

Offshore bathymetry was suggested by PHIZACKLEA (1993), and shown in surveys and the digital terrain model in chapter 3, to be undulating. The possibility of wave refraction being induced by offshore undulating bathymetry, thereby causing wave energy focusing and erosion of the Pukehina Beach frontal dune, must therefore, be assessed. Collecting local wave data, such as wave height, wave period and wave approach directions are essential to both understanding the local wave climate, but also to enable investigation of wave energy focusing, using the numerical model WBEND (section 5.5).

5.3.1 Instruments and Data Processing

In order to obtain local wave data, directional current meters were used to measure wave height, direction and period at Pukehina Beach (figure 5.6). GPS co-ordinates of instrument location, are presented in Appendix I. Wave data were collected in both summer and winter seasons. During the winter deployment (17/5/2000 - 6/8/2000), an S4DW and an FSI 3DACM were used offshore from Newdicks Beach and Pukehina Redoubt respectively. During the summer deployment (8/3/2001 - 7/4/2001), two

S4ADW's were used. Preferably S4ADWs would have been used at both locations and during each deployment, but due to non-availability of instruments, this was not possible.

Instruments were deployed in 16 m water depth upon taut moorings, with the instrument 6 m below MSL (Figure 5.7).

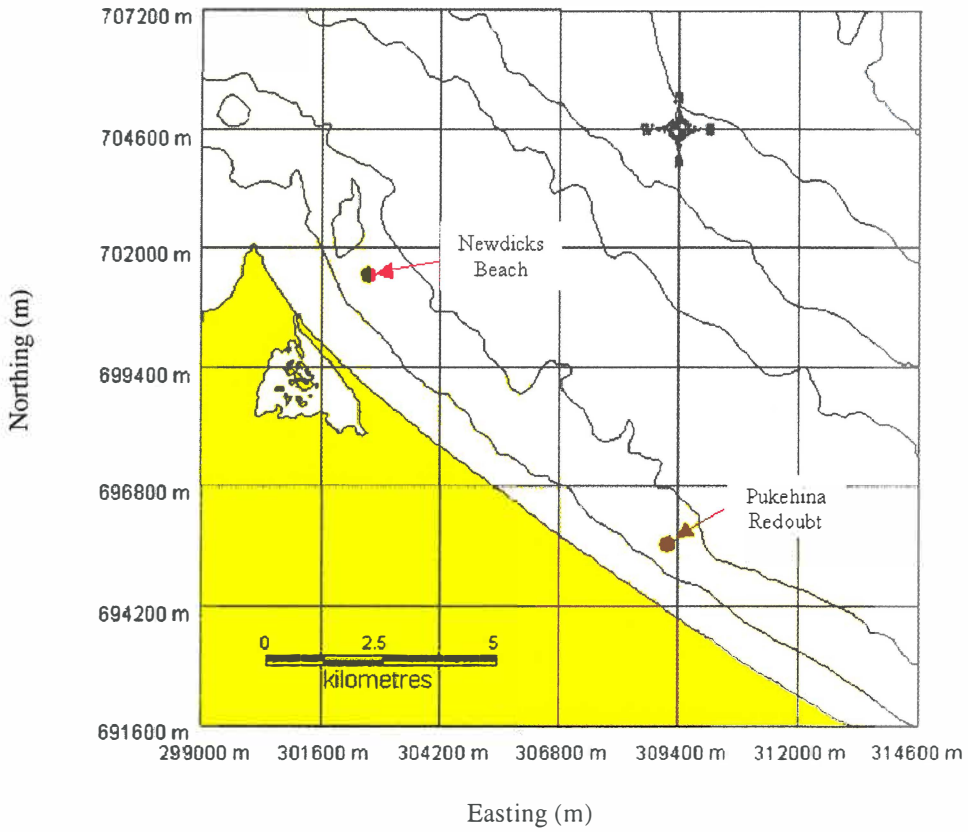

Figure 5.6 Location of directional wave instruments, deployed in 16m water depth as taut moorings with the current meters (S4ADW or FSI3DACM) 6m below MSL.

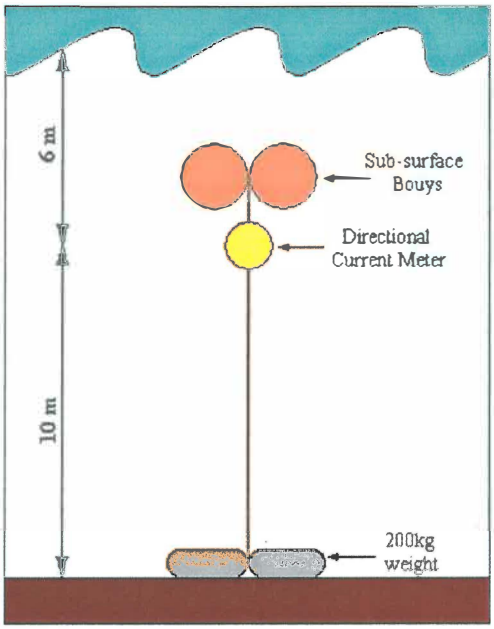

Figure 5.7 Directional current meters deployed as a taut mooring. Instrument is 6 m below MSL, at 16 m water depth.

During each seasonal deployment, instruments were programmed to measure data simultaneously. However, as outlined in chapter 4, the FSI 3DACM samples at a different frequency to the S4DW and S4ADW (5.37 Hz compared to 5.00 Hz), therefore, CMCVRT5[‡] and FSIBURST3[♀] are used to interpolate data, to a matched frequency.

Table 5.1 lists the instruments, location and sample regime used in wave data collection.

Instrument	Location	Season	Instrument sampling duration	Sampling interval time
S4DW	Newdicks Beach	(17/5/2000 - 6/6/2000)	3 minutes	60 minutes
FSI 3DACM	Pukehina Redoubt	(17/5/2000 - 6/6/2000)	3 minutes	60 minutes
S4ADW	Newdicks Beach	(8/3/2001 - 7/4/2001)	18 minutes	60 minutes
S4ADW	Pukehina Redoubt	(8/3/2001 - 7/4/2001)	18 minutes	60 minutes

Table 5.1 Directional Current Meter settings during winter and summer deployments.

[‡] CMCRVT5 by Gorman, R. NIWA. 1994
[♀] FSIBURST3 by Gorman, R. NIWA. 1994.

Data collected by the S4DW and S4ADW are initially processed by APPIBM[§]. APPIBM converts data collected by the S4DW/S4ADW current meter (S4b file format) into a S4 ASCII format (text document). The S4 ASCII file can then be used in TSERIES[¤]. TSERIES is a set of Matlab[*] routines for reading and plotting time series data. There are two major techniques commonly used to analyse wave data. These are monochromatic and spectral wave analysis. Monochromatic wave analysis usually involves performing a zero-down or zero-upcrossing analysis, where a wave is defined by the full cycle of the surface water depth through a mean datum. Significant wave statistics based on the highest 1/3 of the waves, are obtained using a monochromatic wave analysis. A spectral analysis involves calculation of a directional wave spectrum, which includes the direction of approach as well as the energy at a specific frequency band. TSERIES is able to calculate both spectral and monochromatic wave analysis. For the purpose of this investigation, monochromatic wave statistics are only analysed.

5.4 Monochromatic Wave Statistics Results

Unfortunately, due to instrument malfunction, tidal data instead of wave data were collected during the winter deployment at the Pukehina Redoubt site (obtained by the 3D ACM FSI meter). However, directional data could still be used for the WBEND calibration.

Directional current meters deployed in both winter and summer seasons, measured 'low-pressure' anomaly. A 'low-pressure' anomaly, in this context, is defined as a decrease in barometric pressure, which subsequently increases wave height due to stronger winds associated with the low-pressure system (BELL AND GORING, 1998). During the winter deployment, a low-pressure anomaly began on Julian day 143 and proceeded through to the end of the deployment. The summer deployment experienced two small low-pressure anomalies. The first began on Julian day 77 and lasted until day 83. The second began on Julian day 90 and finished on day 94.

[§] APPIBM: InterOcean systems, Inc, S4 Application Software Version 2.67
[¤] TSERIES by Gorman, R. NIWA, Hamilton, 1997
[*] Matlab by Mathworks Inc. 1997

The low-pressure anomalies, as expected, increased significant wave height by approximately 0.8-1.0 m (dependent on instrument location) and decreased wave period by approximately 2.5-3 s (dependent on instrument location).

5.4.1 Newdicks Beach

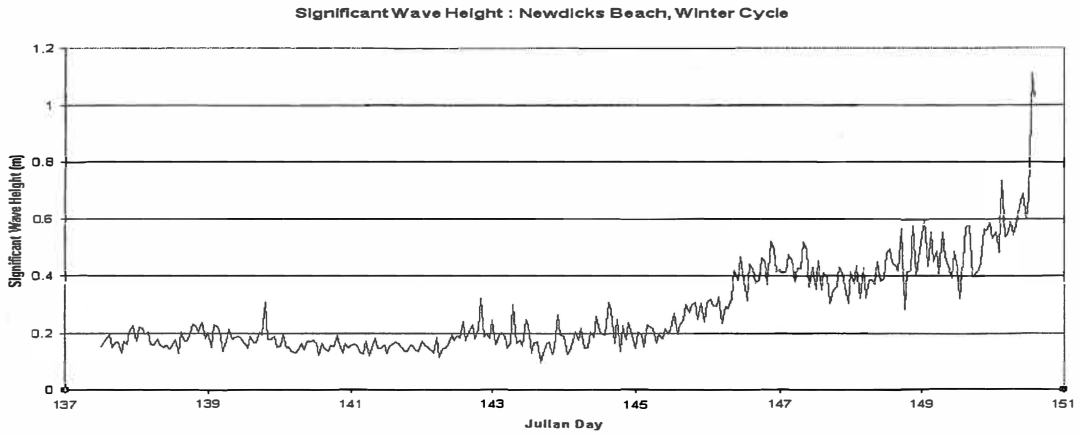

a)

Figure 5.8a) Time series of significant wave height at Newdicks Beach site measured by S4DW between (17th May 2000 – 1st June 2000).

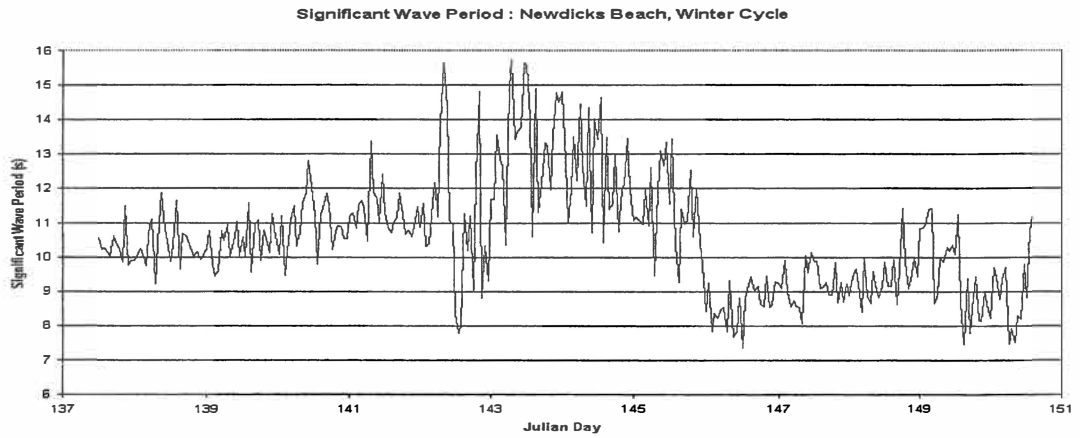

b)

Figure 5.8b) Time series of significant wave period at Newdicks Beach site measured by S4DW between (17th May 2000 – 1st June 2000).

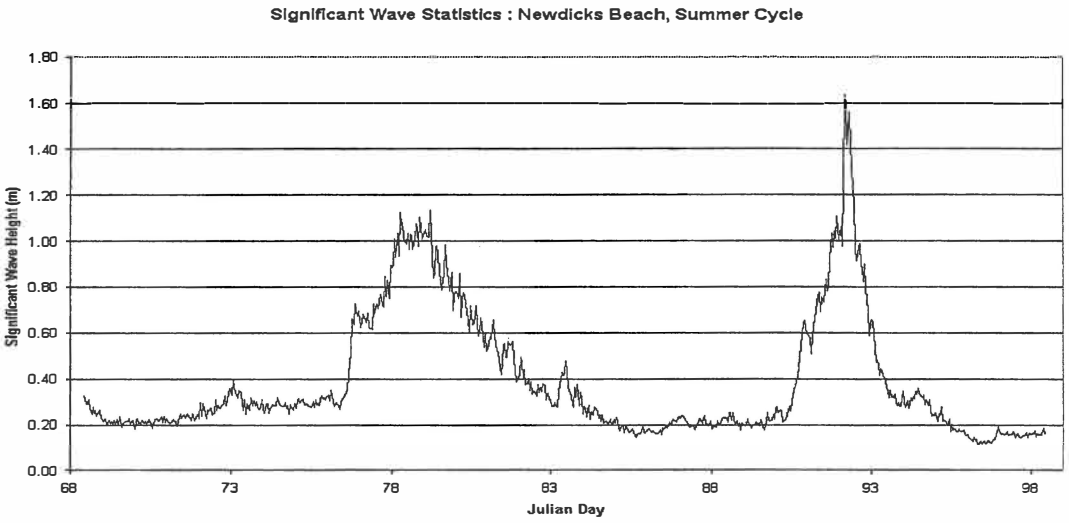

a)

Figure 5.9a) Time series of significant wave height at Newdicks Beach site measured by S4ADW between (8th March 2001 – 7th April 2001).

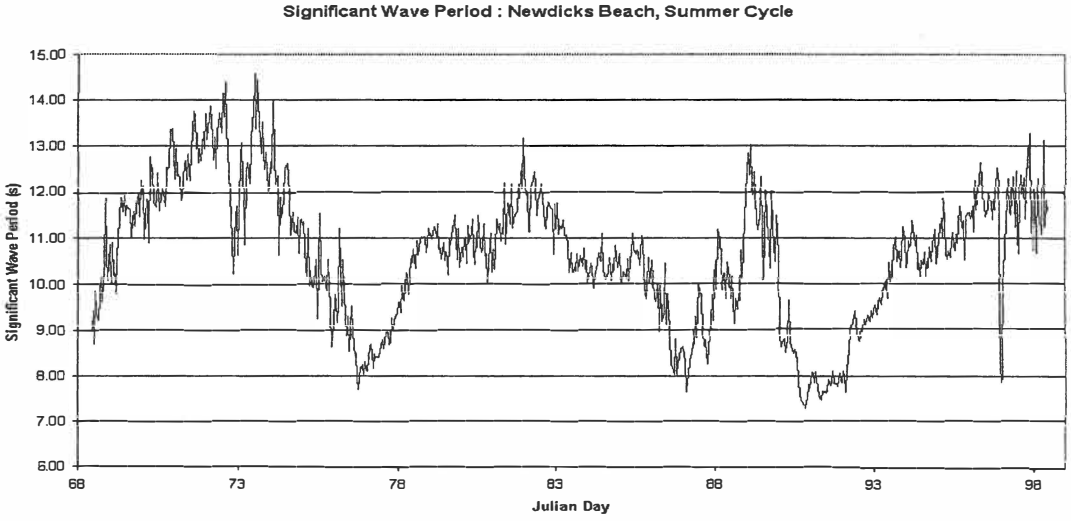

b)

Figure 5.9b) Time series of significant wave period at Newdicks Beach site measured by S4ADW between (8th March 2001 – 7th April 2001).

		Hs (m)	Ts (s)	$H_{1/10}$ (m)	$T_{1/10}$ (s)	Direction (°)
Newdicks Beach 17th May 2000 – 1st June 2000	Mean	0.27	10.59	0.33	10.54	354.5
	Std Dev	0.15	1.69	0.19	1.89	230.7
	Maximum	1.11	15.7	1.35	15.98	
	Minimum	0.1	7.37	0.11	6.87	
Newdicks Beach 8th March 2001 – 7th April 2001	Mean	0.39	10.64	0.48	10.63	356.7
	Std Dev	0.27	1.48	0.34	1.57	217.7
	Maximum	1.63	14.57	2.02	15.58	
	Minimum	0.12	7.31	0.14	7.09	

Table 5.2 Monochromatic wave statistics for Newdicks Beach during winter and summer deployments. Results obtained from a zero-down crossing analysis, as calculated by TSERIES.

From table 5.2, comparison between winter and summer deployments at Newdicks Beach, indicate that there are not notable differences in terms of mean significant wave period. However, there is a difference of 0.12 m in mean significant wave height. Further analysis of the low-pressure anomalies in the two seasons reveals that the summer low-pressure anomalies may have been larger events, as maximum significant height was 0.5 m larger in summer, compared to the largest significant wave height recorded during winter. Similarly, $H_{1/10}$ (height of highest 1/10 of waves) has a higher mean value (Table 5.2) in summer.

Wave approach directions measured by wave meters for both the winter and summer Newdicks Beach deployments are detailed in figure 5.10a and 5.10b respectively.

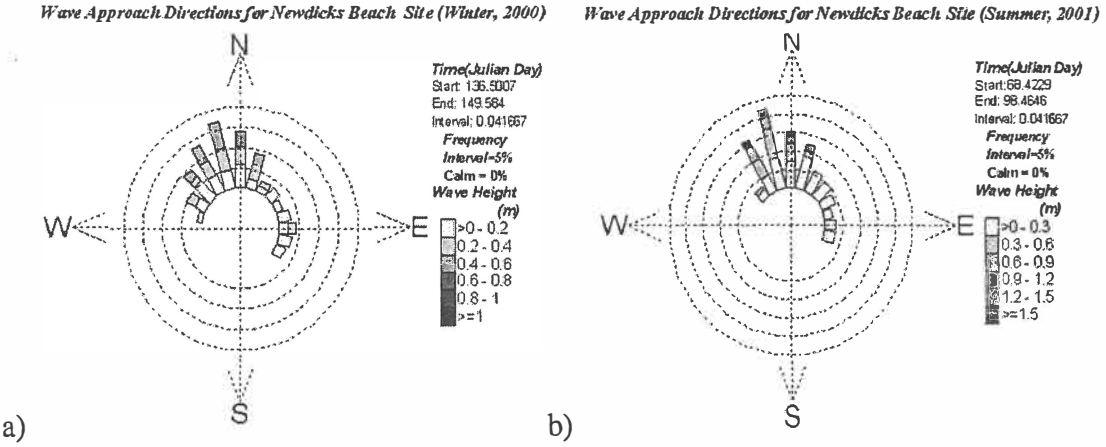

Figure 5.10 a) Wave rose (directions of wave approach) for Newdicks Beach wave gauge, winter deployment 17/5/2000 - 1/6/2000 b) Wave rose for Newdicks Beach, summer deployment 8/3/2001 - 7/4/2001. Each frequency band denotes 5% of the total number of waves, with significant wave height increasing with shade and direction in degrees true.

Wave analysis results from the Newdicks Beach site, indicate a modal wave approach direction of 355° true, throughout both winter and summer deployments. The record of wave approach, suggests sediment transport from west to east at the instrument location. This hypothesis is investigated further in section 5.7. Notably the larger waves predominantly approached from a similar orientation as the modal approach wave direction.

5.4.2 *Pukehina Redoubt*

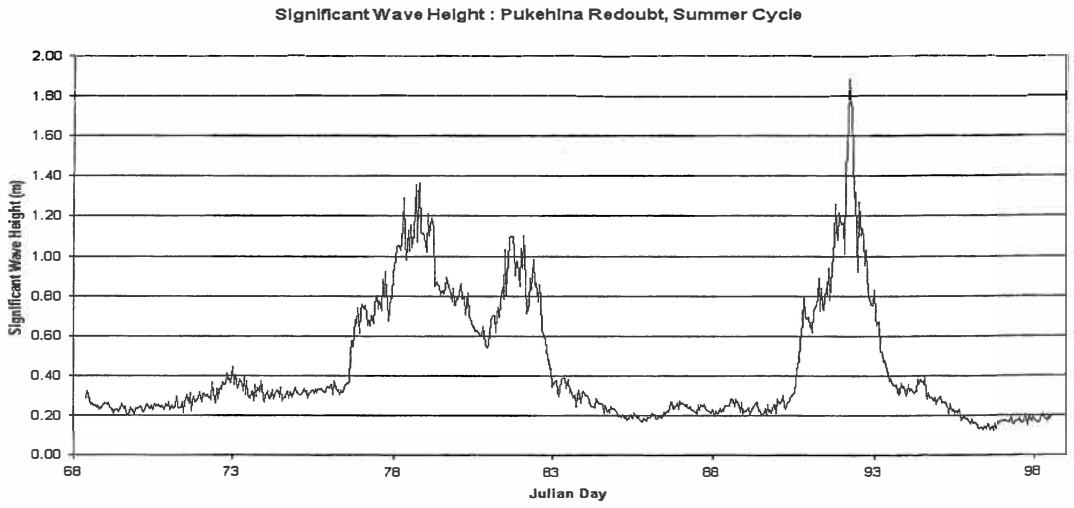

a)

Figure 5.11a Time series of significant wave height at Pukehina Redoubt site measured by S4ADW between (8th March 2001 – 7th April 2001).

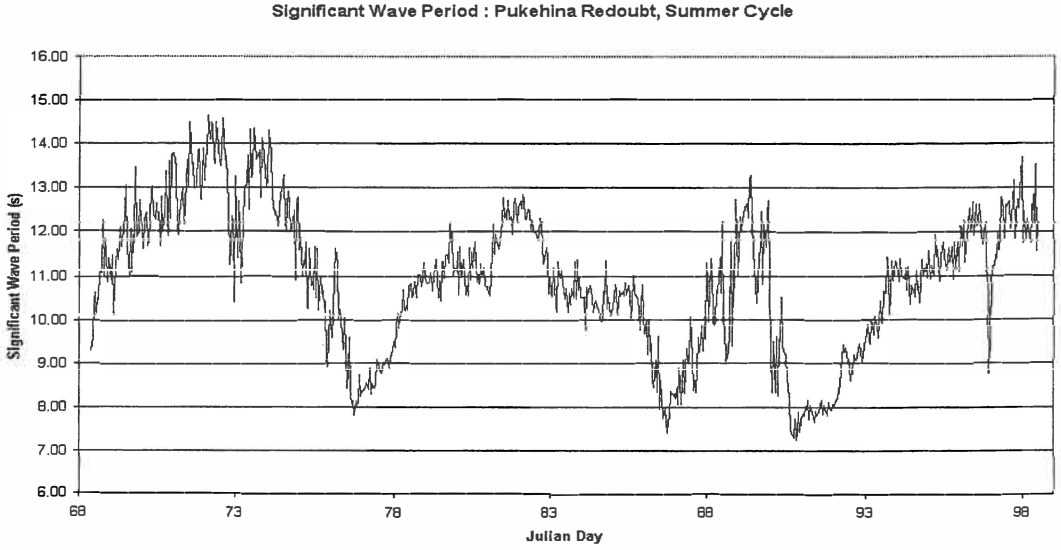

b)

Figure 5.11b Time series of significant wave period at Pukehina Redoubt site measured by S4ADW between (8th March 2001 – 7th April 2001).

		Hs (m)	Ts (s)	$H_{1/10}$ (m)	$T_{1/10}$ (s)	Direction (°)
Pukehina Redoubt (8th March 2001 – 7th April 2001)	Mean	0.44	10.91	0.55	10.93	356.1
	Std Dev	0.31	1.61	0.39	1.73	222.7
	Maximum	1.88	14.64	2.30	15.24	
	Minimum	0.12	7.25	0.15	6.91	

Table 5.3 Monochromatic wave statistics for Pukehina Redoubt during summer deployment (8th March 2001 – 7th April 2001). Results obtained from a zero-down crossing analysis, as calculated by TSERIES.

Although no comparison can be made between seasonal variations at the Pukehina Redoubt site, because of instrument failure during the winter deployment, comparison of results obtained at the Pukehina Redoubt site, may be contrasted to those collected at Newdicks Beach site.

Significant wave heights at Pukehina Redoubt were larger than at Newdicks Beach. A possible reason is due to a sheltering effect from both Okurei Point and Motiti Island, since wave approach is tending from a northerly, and north north-westerly orientation. Another possible reason may be wave focusing at the site where the Pukehina Redoubt directional current meter was deployed.

Comparison of figure 5.12 with figures 5.10a and 5.10b indicates that wave approach direction at the Pukehina Redoubt site has more variation than at the Newdicks Beach site. More waves with greater heights ($H_s \geq 0.6$ m) tended towards a shore-normal orientation (northeast quadrant) at the Pukehina Redoubt site, while at the Newdicks Beach site, waves have a more north north-westerly direction. This would imply that for the coastal sector near Pukehina Redoubt, frontal dunes have a greater chance of increased erosion than at Newdicks Beach, because of larger wave, thereby, subsequently an increased wave set-up and run-up at the shoreline. The differing wave angles may be due to refraction at Okurei Point.

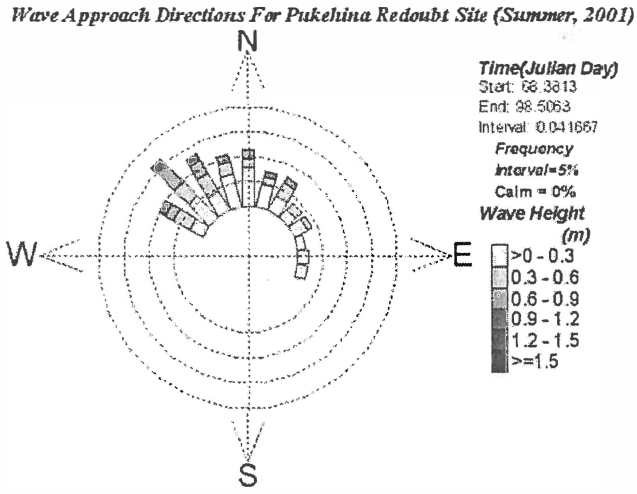

Figure 5.12 Wave rose (directions of wave approach) for Pukehina Redoubt wave gauge, summer deployment 8/3/2001 - 7/4/2001. Each frequency band denotes 5% of the total number of waves, with significant wave height increasing with shade and direction in degrees true.

Assessing wave steepness at the two directional current meter locations, can also define which area has a greater probability of enhanced dune erosion. KING (1972 p. 434) states 'Steep waves are normally destructive, lowering the level of the foreshore surface and transporting beach material seaward. The larger waves are, provided they are above the critical steepness for destructive action (dependent of sediment parameters), the greater will be removed of material from the beach, because of their greater energy'.

Wave steepness is calculated by:

$$H/L \qquad \text{Eqn 5.7}$$

where H is the wave height (m) and L is the wavelength (m) given by:

$$L = 1.56T^2 \qquad \text{Eqn 5.8}$$

where T is the wave period (s).

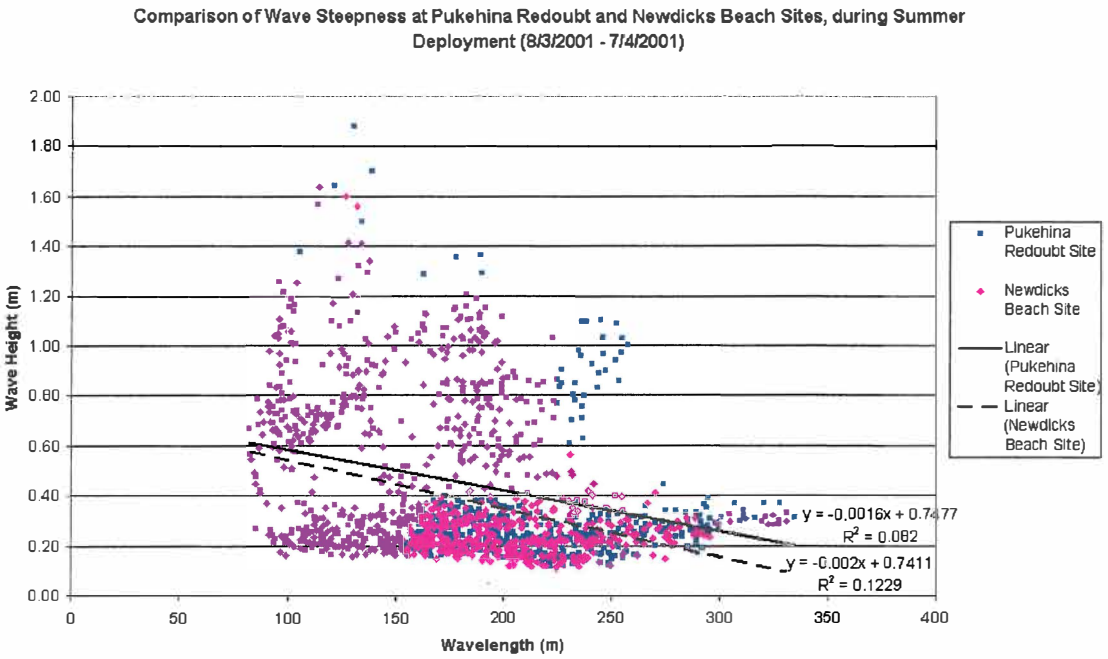

Figure 5.13 Comparison of wave steepness at Pukehina Redoubt and Newdicks Beach sites, during the summer deployment (8/3/2001 - 7/4/2001).

From figure 5.13, it can be clearly seen that the Pukehina Redoubt site had greater wave steepness over the recorded period, than the Newdicks Beach site.

Figure 5.14 illustrates a comparative plot of each average wave approach angle at Newdicks Beach and Pukehina Redoubt sites. Each data point was simultaneously collected, thereby allowing such a plot.

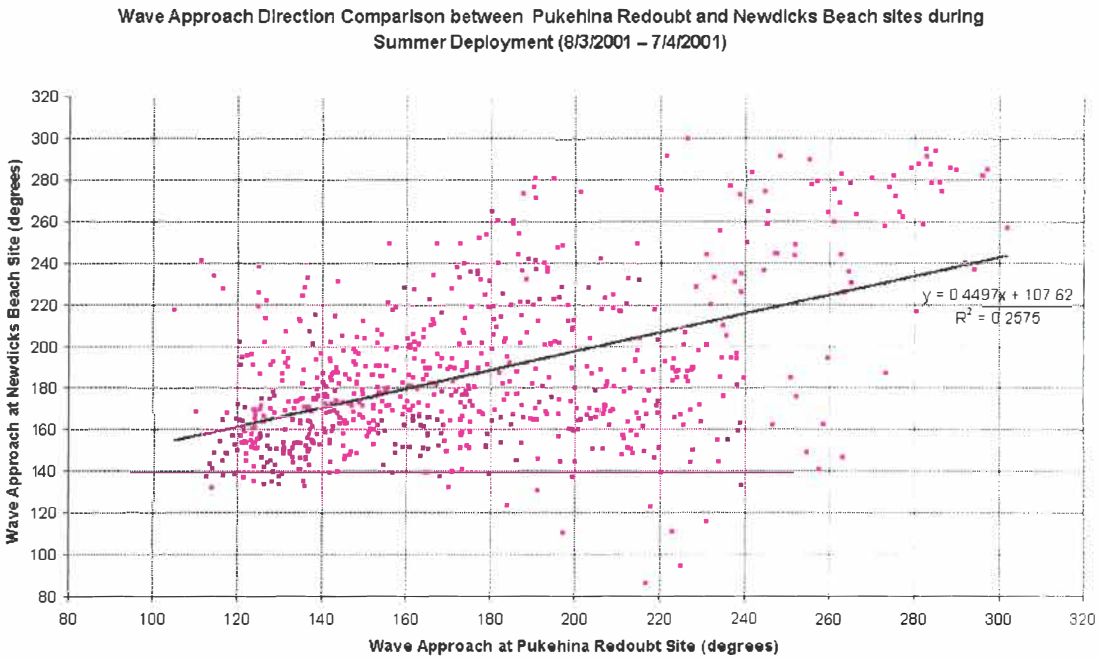

Figure 5.14 Average wave approach direction comparison between Newdicks Beach and Pukehina Redoubt sites during summer deployment (8/3/2001 – 7/4/2001).

As previously stated, figure 5.14 illustrates that wave approach directions differ at the two sites where data were collected. Data collected offshore from Newdicks Beach, tends to approach more west of simultaneous data collected offshore from Pukehina Redoubt, based on the linear regression generated. The difference may be explained by differing bathymetry surrounding each instrument location, thereby causing wave refraction and altering the wave approach direction.

5.4.3 Wave Origin

Following the same methods as SAUNDERS (1999), wave steepness may be investigated to predict origin of waves recorded, specifically if waves were generated by local storms.

Using equation 5.9, from the *Shore Protection Manual* (US ARMY CORPS OF ENGINEERS, 1984), allows one to differentiate between sea and swell waves from bi-variate data of significant wave height and significant wave period. Thus, it is possible to investigate whether the recorded waves were generated by nearshore storm systems.

$$H_s / \left(gT_s^2\right) = 0.00408 \qquad \text{Eqn. 5.9}$$

where H_s is significant wave height (m), g is gravitational acceleration ($9.81 ms^{-2}$), and T_S is significant wave period (m).

Figures 5.15 and 5.16 illustrate joint significant wave height (H_s) and significant wave period (T_s) distributions with equation 5.9 plotted to differentiate the difference between sea and swell waves for both Newdicks Beach and Pukehina Redoubt sites respectively.

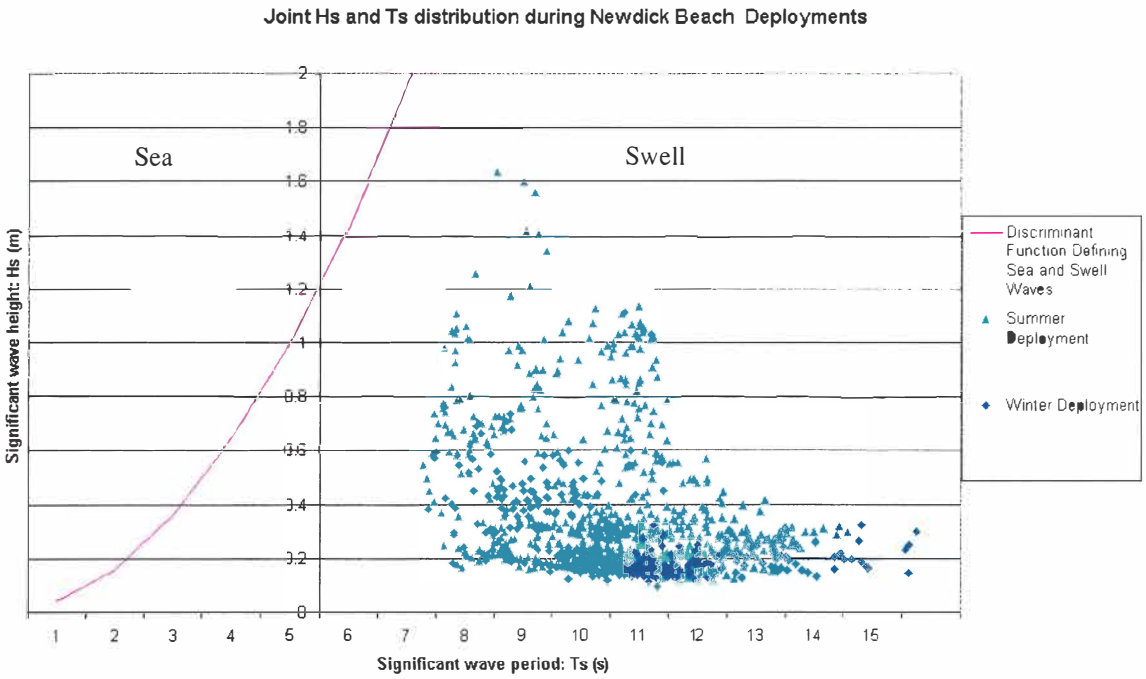

Figure 5.15 Bi-variate analysis plot of significant wave height vs. significant wave period measured off Newdicks Beach, and relation to 'sea' wave discriminant function. Winter deployment = 17/5/2000 - 6/8/2000, summer deployment = 8/3/2001 - 7/4/2001.

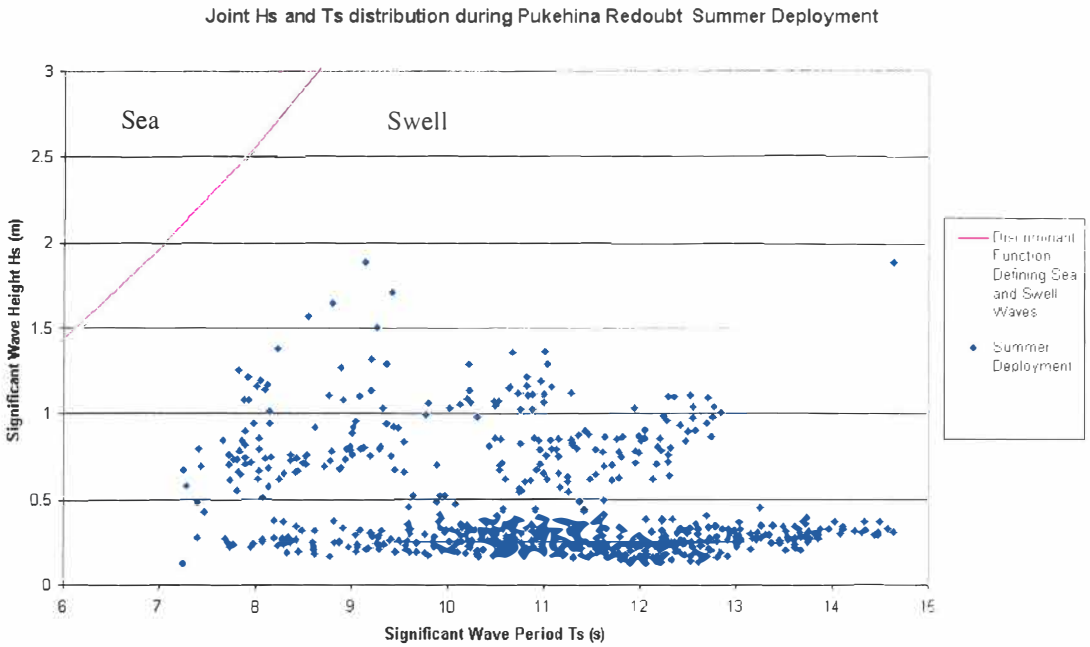

Figure 5.16 Bi-variate analysis plot of significant wave height vs. significant wave period, measured off Pukehina Redoubt, and relation to 'sea' wave discriminant function. Summer deployment = 8/3/2001 - 7/4/2001.

The bi-variate plots at both locations, indicate that critical wave steepness is not exceeded, suggesting that waves recorded by the directional current meters were not generated locally, as wave height has reduced due to wave energy dissipation.

5.5 WBEND and Methods to Generate Wave Refraction Simulations

WBEND requires an information file, a wave boundary file and a bathymetry file. The information file contains the names of the required files, output file names for the files created by the model and many other variables used by WBEND are also listed into the information file.

The wave boundary file can be defined as three different types:

1) Probability or time series files;
2) Spectrum files; or
3) Sediment transport files.

Following methods utilised by SAUNDERS (1999), monochromatic wave probability files were used, as these possess the same file format required for the sediment transport model, which will also be applied here (section 5.7).

The boundary file can include six possible variables: probability (describes the frequency of occurrence of the condition being treated), wave height, wave period, wave angle, bed friction and tidal elevation. Variables that are not known may be replaced by known data, collected from previous experiments or constants (BLACK, 2001. *pers comm.*).

Bathymetry is represented as a rectangular bathymetric grid, and WBEND requires that the shoreline is positioned on the eastern boundary, therefore, grid rotations may be necessary. Each cell is defined by an I, J co-ordinate referring to the x and y directions respectively. Positive co-ordinates are defined as co-ordinates to the east and north in x and y-axis respectively. Wave angle is defined relative to the left or east of the grid and is positive anti-clockwise (HUTT, 1997) (refer to figure 5.17)

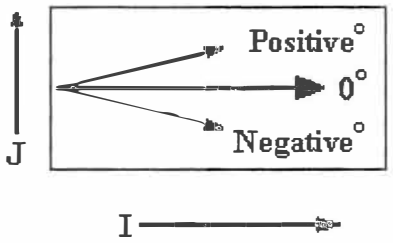

Figure 5.17 The model grid, positive I is to the east, positive J is to the north. Wave angle is defined relative to the east and is positive anticlockwise. (Source HUTT, 1997)

Bathymetry files are generated using the software package SURFER32[+], which converts the binary format file (as collected by digitised fair sheets of soundings) into a bathymetry file in ASCII format, which is subsequently converted by TOBATH[Ψ] to the required format for WBEND. The WBEND output file contains depths, heights, periods, and bottom orbital motion over the full grid, for each event in the time series.

[+] SURFER32 (version 6.04), software by Golden Software Inc, 1997
[Ψ] TOBATH by Black, K. ASR Ltd *pers comm.* 2000.

To calculate wave height in the two horizontal dimensions, WBEND uses the energy conservation equation, which is written in the form: (BLACK AND ROSENBERG (1992))

$$\frac{\partial}{\partial x}(F\cos\theta)+\frac{\partial}{\partial y}(F\sin\theta)=-F_D\,. \qquad \text{Eqn. 5.10}$$

Where x and y are orthogonal co-ordinates, θ is the wave angle, F_D is the frictional dissipation and F is the wave power for Airy waves, which is given by:

$$F=EC_g=\frac{1}{8}\rho g H^2 C_g\,. \qquad \text{Eqn. 5.11}$$

Where E is the wave energy (Jms^{-1}), C_g is the group speed (ms^{-1}), ρ is the density of water (1025 kgm^{-3}), g is gravitational acceleration ($9.81ms^{-2}$) and H is the wave height (m).

F_D, frictional dissipation is a combination of bed friction and wave breaking dissipation and is given by:

$$F_D=\frac{\rho C_f}{6\pi}\left[\frac{H\,\omega}{\sinh(kh)}\right]^3\,. \qquad \text{Eqn. 5.12}$$

Where C_f is the frictional coefficient (losses in wave height due to bed friction, dependent on the maximum wave orbital velocity BLACK AND ROSENBERG (1992)). k is the wave number, h is the water depth and ω is the radial frequency, which is given by:

$$\omega=\frac{2\pi}{T} \qquad \text{Eqn. 5.13}$$

k, the wave number is given by:

$$k=\frac{2\pi}{L}\,. \qquad \text{Eqn. 5.14}$$

Wave angles are derived from equation 5.15 for the conservation of the wave number

$$\frac{\partial}{\partial x}(|k|\sin\theta)+\frac{\partial}{\partial y}(|k|\cos\theta)=0 \qquad \text{Eqn. 5.15}$$

5.5.1 Generation of Wave Refraction Simulations

5.5.1.1 Bathymetry and Grid

Bathymetry of the Pukehina coastal sector was obtained from a digitised fair sheet of sounding, as previously discussed in chapter 3 (section 3.2.3). SURFER32 enables grid size to be determined. For wave refraction and sediment transport simulations, a grid size of 142 x 173 (i, j) was created. This grid specification was chosen, as it provided a cell of 100 m in each i and j axis co-ordinate.

Obviously some undulations are less than 100 m, therefore, the true height of the undulation is lost due to the overall averaging of heights within the cell.

5.5.1.2 Grid Rotation

WBEND requires the shoreline to be on the eastern boundary (I_{max}), therefore, the bathymetric grid is achieved this configuration, by using SURFER32 to rotate the grid. WBEND has the restriction that the wave approach angle must not exceed ± 65° from original orientation (BLACK, 2001, *pers. comm.*).

Here for model simulations for the Pukehina coastal sector, the grid was rotated 270°, similarly were wave directions rotated 270°, so realistic model runs were generated.

5.3.1.3 Calibration Procedure

Following the methods of HUTT (1997) and SAUNDERS (1999), calibration involved input of boundary information including wave height, period and direction into the model and adjusting the values of the friction co-efficient (losses in wave height due to bed friction, dependent on the maximum wave orbital velocity), breaking ratio or wave gamma (γ_b) (ratio between the breaking wave height ($H_{b)}$ and the breaking water depth (h_b), given by $\gamma_b = H_h/h_b$ (KOMAR, 1998)) and eddy viscosity (ω) (smoothing

factor, which mimics wave diffraction (BLACK AND ROSENBERG (1992)), until the model accurately predicted measured wave data.

In all model simulations, investigations were carried out using data collected from the directional current meter situated offshore from Newdicks Beach. Calibration of the model WBEND was performed so output data matched data collected simultaneously at Pukehina Redoubt.

5.6 Wave Refraction, Wave Energy Focusing analysis

5.6.1 WBEND Scenarios

Various combinations of wave height, period and direction were used in the WBEND program to investigate the patterns of breaking wave along the Pukehina shoreline. The specific aims are to identify:

i. whether wave focusing is occurring within the Pukehina coastal sector;

ii. the difference in wave height at the shoreline between an area of wave focusing and an area of wave divergence; and

iii. the probability of the frontal dune being eroded as a result of wave focusing.

In order to identify each aim, scenarios used in numerical simulations are as follows;

i. Wave angle simulations were varied by increments of 10° either side of the modal wave approach direction (355°), until model restrictions applied (proportional to grid orientation ±65°). Average mean significant wave height (0.39 m) and average mean significant wave period (10.64), as recorded by the directional current meter off Newdicks Beach, were used in all wave angle simulations.

ii. Wave height scenarios, are of maximum significant wave height recorded during instrument deployment (1.63 m), with wave angle then adjusted at 10°

increments from modal mean wave approach direction (355°), as recorded by directional current meter.

iii. To investigate the influence of wave period, T= 14.57 s (maximum mean significant wave period recorded) was used. Maximum mean significant wave period was used in simulations, as greatest wave refraction occurs with large period waves. Wave angles were then adjusted at increments of 10° from modal wave approach direction (355°).

iv. Using design storm wave characteristics, as calculated by HEALY (1983) (H_{max}= 9.9 m, T_{max}= 9.0 s), a storm scenario can be simulated. A storm scenario may identify locations within the Pukehina coastal sector, which are prone to significant frontal dune erosion. Frontal dune erosion would be expected to be significant during storm periods, as wave run-up and wave set-up would be largest during these periods, thereby the potential of frontal dune erosion would also be increased.

5.6.2 Interpretation of Model Output

Figure 5.18 illustrates a scenario of wave angle. Input values are: measured modal wave approach direction (355°), average significant wave height (0.39 m) and average significant wave period (10.63 s) during the summer deployment, as recorded from the directional current meter deployed offshore from Newdicks Beach.

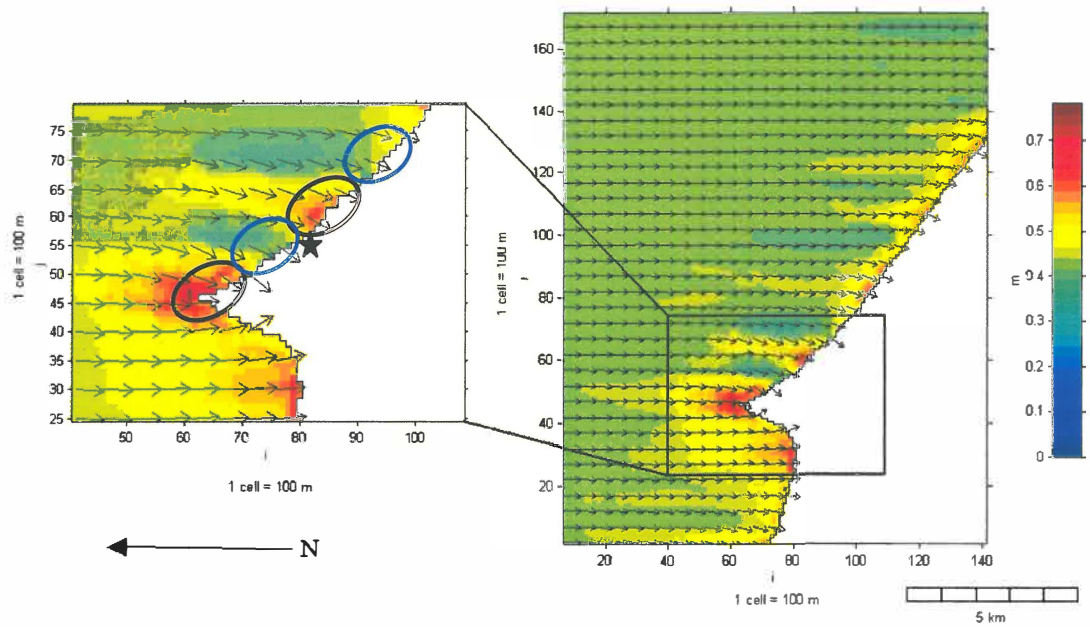

Figure 5.18 Modal wave direction and average significant wave height for Pukehina coastal sector as recorded by directional current meter during summer 2001, 8/3/2001 - 7/4/2001. Black circled areas indicate possible wave energy convergence, while areas circled blue, indicate possible wave energy divergence. The black star indicates the Waihi Estuary inlet.

As previously stated, if wave height at the shoreline were to increase, so would wave set-up and wave run-up. Observing locations with greater wave height, wave set-up and wave run-up, can be expected at the same location, therefore, one may presume that a location such as suggested may be prone to frontal dune erosion.

5.6.3 Wave Refraction, Wave Energy Focusing Results

Model simulations of wave height, wave period, wave angle and storm scenario, as stated in section 5.6.2, may be obtained from appendix X. Summaries of results from each simulation are discussed, in the following.

5.6.3.1 Discussion

5.6.3.1.1 Wave Angle Simulations (scenarios 1-12)

By varying wave approach to the northwest, indications of wave height reduce at the shoreline of Pukehina Beach, possibly due to a sheltering effect created by Okurei Point (scenario 12 (wave height 0.39 m, wave period 10.64 s, wave approach direction 56.73 °), figure 5.19). However, when waves approached more from a

northeast direction, wave heights increase (scenario 4 (wave height 0.39 m, wave period 10.64 s, wave approach direction -34.73 °), figure 5.20).

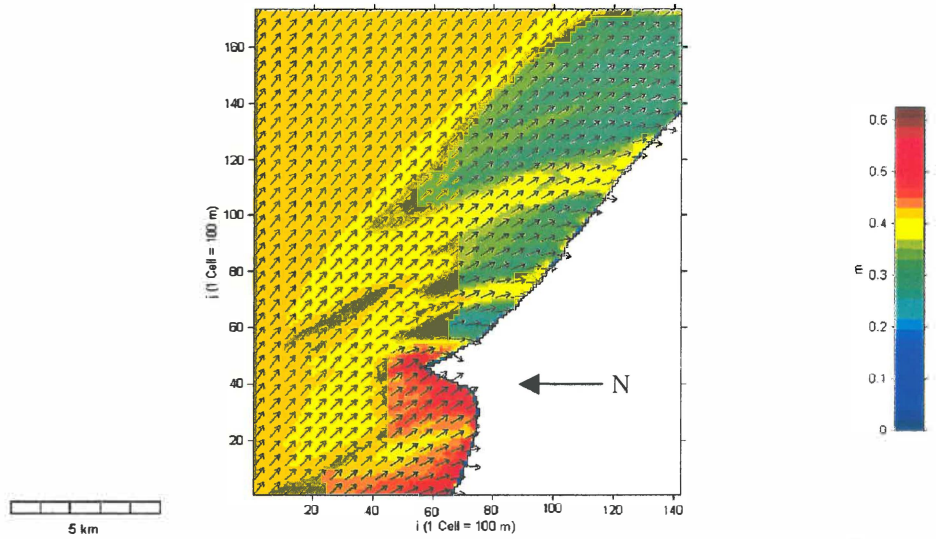

Figure 5.19 Scenario 12 (wave height 0.39 m, wave period 10.64 s, wave approach direction 56.73 °) illustrating how wave heights are reduced at the shoreline of Pukehina Beach, due to a sheltering effect created by Okurei Point when wave approach is from the northwest.

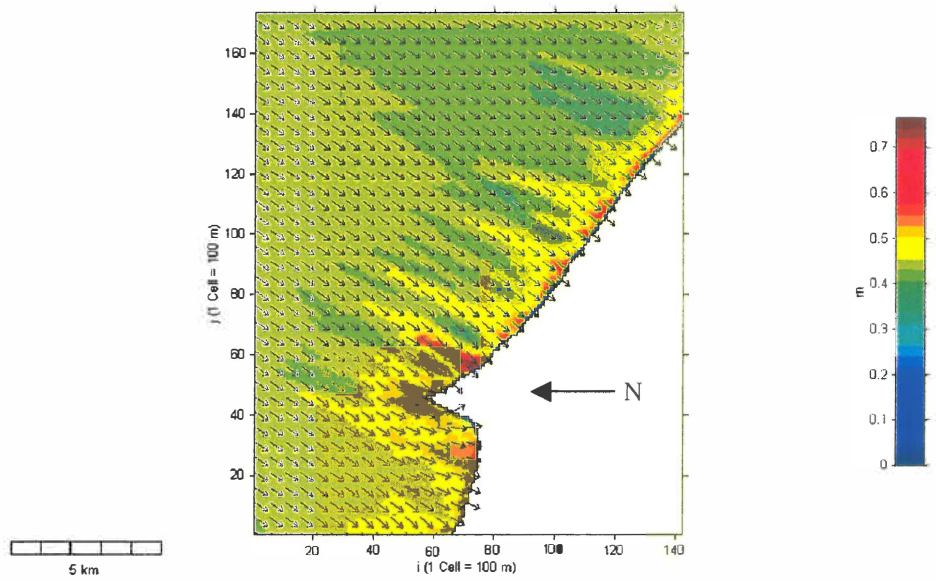

Figure 5.20 Scenario 4 (wave height 0.39 m, wave period 10.64 s, wave approach direction -34.73 °) illustrating how wave heights are increased at the shoreline of Pukehina Beach, when wave approach is from the northeast.

Wave focusing seems to concentrate in specific regions, and does not extend to other locations as wave angle is altered. This is possibly due to the shape of shoals and depressions. Wave energy focusing concentrates around sites benchmark 30, 29, 27, 26a and 26. The comparison of this data, with real world observations seems to be

justified, as historical aerial photograph results from chapter 4, indicate the distal end of Pukehina Spit is geomorphically unstable.

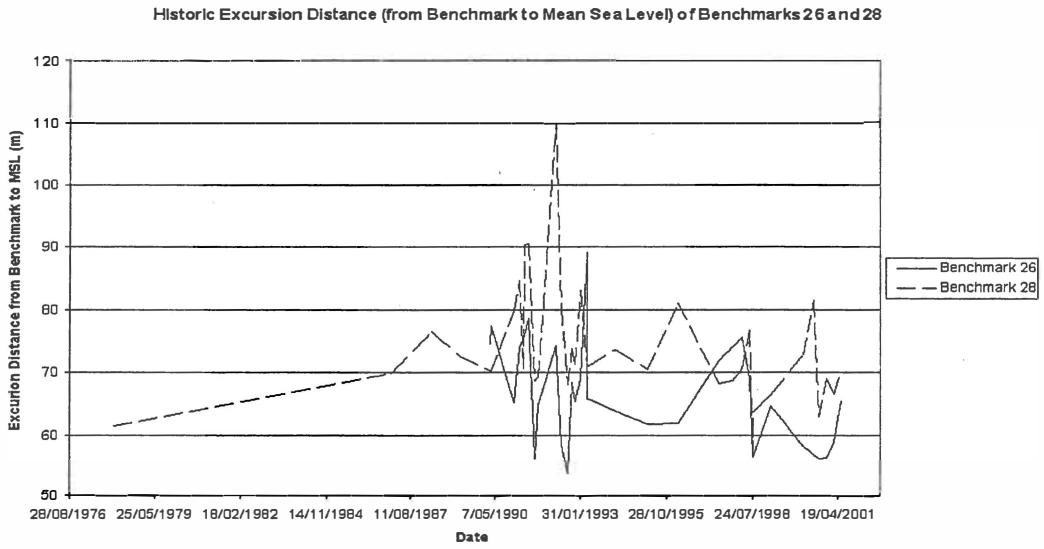

Figure 5.21 Historic excursion distance (distance from benchmark to MSL) for Benchmarks 26, which is a region of possible energy focusing, and benchmark 28, which is not influenced by wave energy focusing. Data collected by Environment Bay of Plenty.

Figure 5.21 illustrates historical excursion distances (distance between benchmark and MSL) at locations benchmark 26, a site predicted by WBEND where wave focusing may be occurring, and benchmark 28, a location where wave focusing is not as significant. Comparing these two plots, indicates that benchmark 26 had predominantly a smaller excursion distance than benchmark 28 over the last 10 years. Occasions when benchmark 26 has had larger excursion distances than benchmark 28 may be explained due to possible changes in wave climate. Changes in wave climate can occur due to ocean-atmosphere cyclic patterns (which will be investigated in chapter 6). Another possibility may be due to benchmark 26 being located in close proximity to cliffs situated at Pukehina Redoubt, which could source this region in sporadic occurrences.

Figure 5.22 illustrates a surface plot taken along the shoreline of the Pukehina coastal sector. Wave parameters used to generate figure 5.22 were average wave statistics (modal wave approach direction (355°), average mean significant wave height (0.39 m) and average mean significant wave period (10.64)) obtained by the directional current meter deployed offshore from Newdicks Beach.

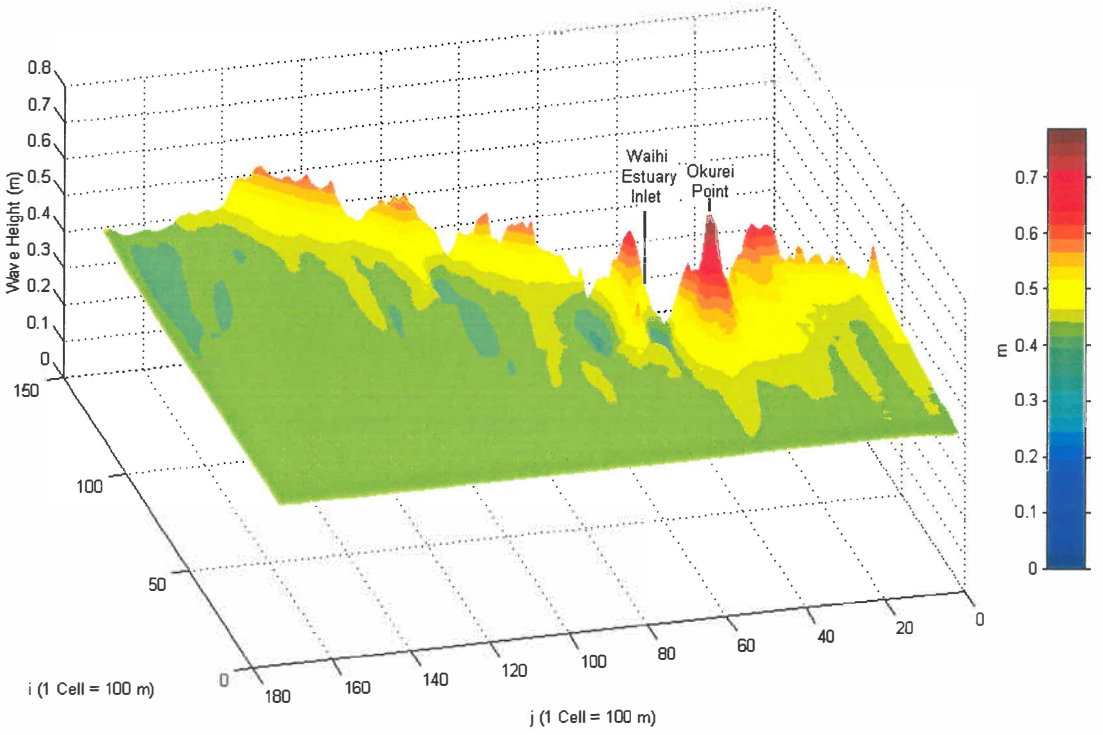

Figure 5.22 Surface plot of wave height along Pukehina coastal sector as obtained from the directional current meter deployed offshore from Newdicks Beach. Zones of wave focusing, may be illustrated by areas of increased wave height. Data used to generate plot were modal wave approach direction (355°), average mean significant wave height (0.39 m) and average mean significant wave period (10.64 s).

Figure 5.22 indicates greatest wave heights were present at Okurei Point. This is due to the ebb tidal delta present offshore from the Waihi Estuary inlet. The ebb tidal delta, is acting as a wave focusing lens, which is increasing wave heights approximately 0.2 m (under average recorded wave conditions (modal wave approach direction (355°), average mean significant wave height (0.39 m) and average mean significant wave period (10.64 s)), as figure 5.22 suggests. The ebb tidal delta causes wave focusing at differing locations, depending on the wave approach angle, as figures 5.19 and figure 5.20 suggest.

A region of reduced wave height may indicate areas of possible wave divergence or decrease of wave set-up and wave run-up. Three locations where decrease in wave energy can be made from the surface plot are at cells (71, 53), (86, 67), and (110, 98). These are approximate locations of benchmark 30a, benchmark 28 and benchmark 27. The significance of these three locations, in comparison to others, is nearshore depth.

The three locations are proximate to 'holes' or deeper areas of water, therefore, waves are able to diverge or have wave energy dissipated, leading to a reduction of wave energy at the shoreline.

5.6.3.1.2 Wave Height Simulations (scenarios 13-24)

Results obtained from model outcomes of increased wave height (1.63 m, maximum significant wave height recorded during both winter and summer deployments), caused regions of wave energy focusing (benchmarks 30, 29, 27, 26a and 26), to increase. Scenario 14 (wave height 1.63 m, wave period 10.64 s, wave approach direction -14.73 °) (figure 5.23) depicts a wave approach from the east-northeast direction. This scenario illustrates approximate 2 m wave heights upon the Pukehina coastal sector shoreline. Benchmarks 30a and 27 had wave heights greater than 2 m. Water depth in these areas is a lot shallower than other regions, therefore, waves should break further offshore and decrease the amount of wave energy impacting the shoreline in these locations.

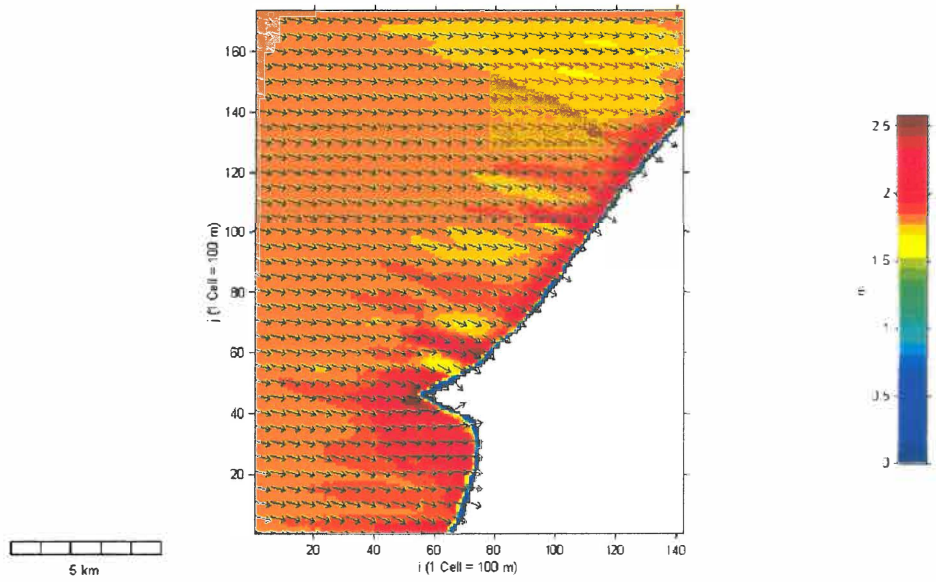

Figure 5.23 Wave height scenario 14 (wave height 1.63 m, wave period 10.64 s, wave approach direction -14.73 °), depicting a wave approach from the east-northeast direction. Wave heights, are increased more significantly (>2 m) at Benchmarks 30a and 27.

Comparing scenarios 13-24 (wave height simulations) with scenarios 1-12 (wave angle simulations), wave heights along Pukehina Beach shoreline are greater. Another observation is that the area of shoreline impacted by increased wave height along

Pukehina Beach shoreline is increased, as illustrated by scenarios 13 to 24. This is expected, as wave energy dissipation will not be as effective with greater wave heights, than with smaller wave heights.

Similar to wave angle scenarios, the ebb tidal delta offshore from Waihi Estuary inlet provides a focusing lens of increased wave height on the Newdicks Beach shoreline. Overall wave energy decreases along Pukehina Beach as wave direction tends west of north. This is due to a sheltering effect created by Okurei Point. In two locations, however, wave height is increased. This is most likely due to deeper water in the offshore region, thereby enabling wave height dissipation not to occur and allowing increased wave heights into nearshore zone. Figure 5.24 (Scenario 24: wave height 1.63 m, wave period 10.64 s, wave approach direction 56.73 °), illustrates that Okurei Point may act as an effective shelter from waves approaching from the northwest, and also illustrates the two locations of increased wave height at the Pukehina Beach shoreline, as discussed. Wave heights range from 2 m at the western side of Okurei Point to ~1 m along the Pukehina Beach shoreline. The possibility of a large wave event approaching from this direction, however, is limited due to the restricted fetch in this direction.

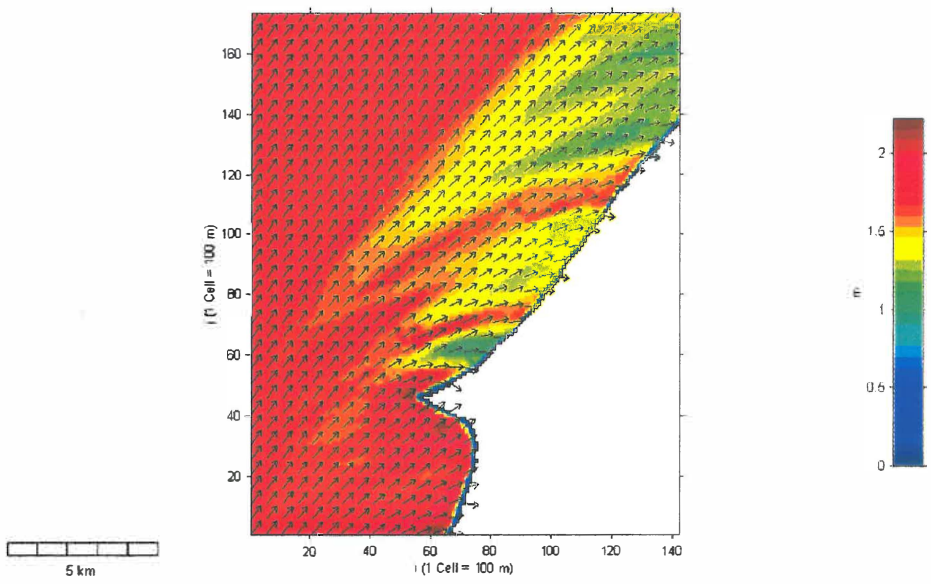

Figure 5.24 Scenario 24 (wave height 1.63 m, wave period 10.64 s, wave approach direction 56.73 °) illustrating how Okurei Point protects Pukehina Beach from increased wave heights. Wave heights however, are increased at benchmarks 28 and 26, possibly due to deeper water offshore, enabling wave height dissipation not to occur thereby allowing increased wave heights into nearshore zone.

5.6.3.1.3 Wave Period Simulations (scenarios 25-36)

By adjusting the wave period to measure long period swell waves (~15 s), the intensity of wave refraction would be expected to increase. Comparing scenarios 25 to 36, with scenarios 1 to 12, scenarios do illustrate a difference between one another (especially at the ebb tidal delta, offshore from Waihi Estuary inlet).

Wave heights at the shoreline using long swell period waves are focused more, thereby wave heights are subsequently increased. Figure 5.25 (Scenario 28: wave height 0.39 m, wave period 14.57 s, wave approach direction -34.73 °), illustrates a long period swell wave approaching from the east northeast. Comparing figure 5.25, to figure 5.20 (Scenario 4: wave height 0.39 m, wave period 10.64 s, wave approach direction -34.73 °, a wave with the same parameters, except a smaller wave period (10.64 s)), illustrates that an increased wave period results in greater wave heights at the shoreline. Specifically in figure 5.25, more intensive wave focusing can be seen occurring in the lee of the ebb tidal delta, offshore from the Waihi Estuary inlet (increase in wave height of an approximate difference of 0.2 m, between figure 5.25 and figure 5.20).

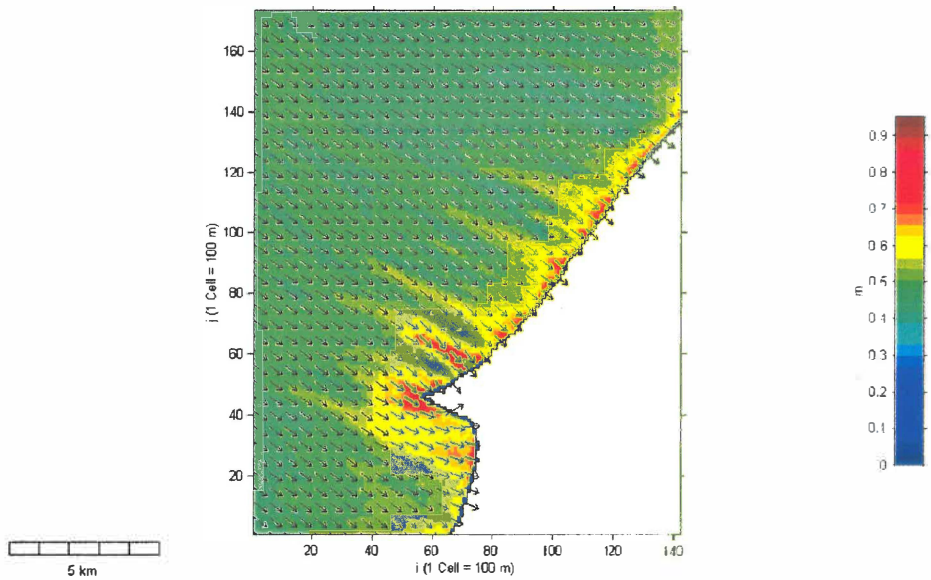

Figure 5.25 Increased wave period simulation (14.57 s) (Scenario 28: wave height 0.39 m, wave period 14.57 s, wave approach direction -34.73 °), illustrating that wave heights along the Pukehina shoreline increase as wave period increases, due to wave refraction being intensified. Specifically wave height is increased greatest in the lee of the ebb tidal delta offshore from Waihi Estuary inlet (increase in wave height of an approximate difference of 0.2 m, between this figure and figure 5.20).

Waves approaching from west of north also induce increased wave heights at the shoreline, when wave period is increased. Since wave refraction is intensified, waves are able to focus along the Pukehina shoreline, whereas in scenarios with smaller wave periods, this was not capable. Figure 5.26 illustrates a simulation from the north west, clearly showing that wave heights are increased. Comparing figure 5.26 (Scenario 36: wave height 0.39 m, wave period 14.57 s, wave approach direction 56.73 °) with figure 5.19 (Scenario 12: wave height 0.39 m, wave period 10.64 s, wave approach direction 56.73 °), the difference in wave height at the shoreline, due to the increased wave period, can be noted.

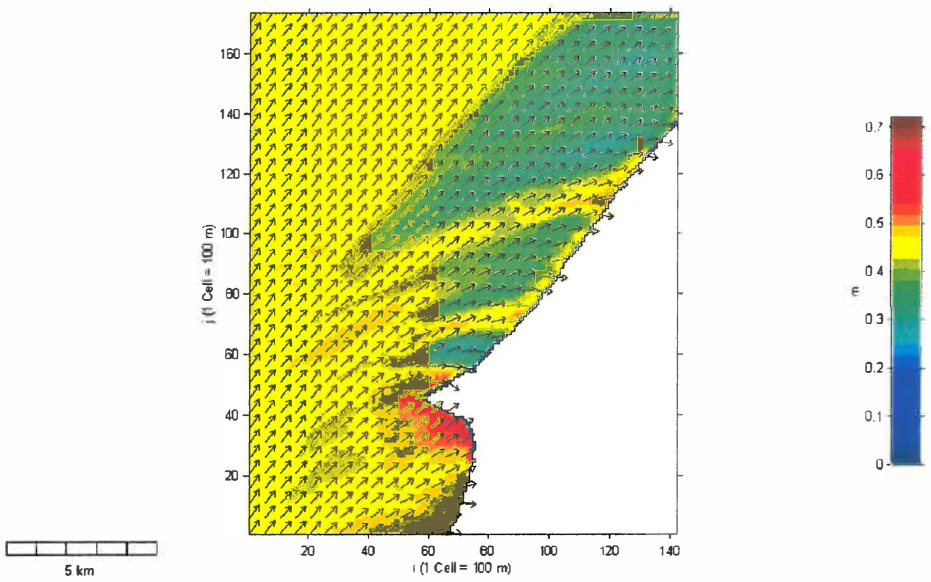

Figure 5.26 Scenario 36 (wave height 0.39 m, wave period 14.57 s, wave approach direction 56.73 °) illustrating that waves from west of north, have the potential of increasing wave height at the Pukehina Beach shoreline, when wave period is increased. Comparison with a smaller wave period, may be done using figure 5.19.

5.6.3.1.4 Storm Wave Simulations (scenarios 37-48)

Results obtained from the storm simulation illustrate generally similar trends with each scenario. However, wave focusing does not occur as such, in comparison to other scenarios. Figure 5.27 illustrates scenario 37 (wave height 9.9 m, wave period 9.5 s, wave approach direction -4.73 °), which shows a result similar to other storm simulations.

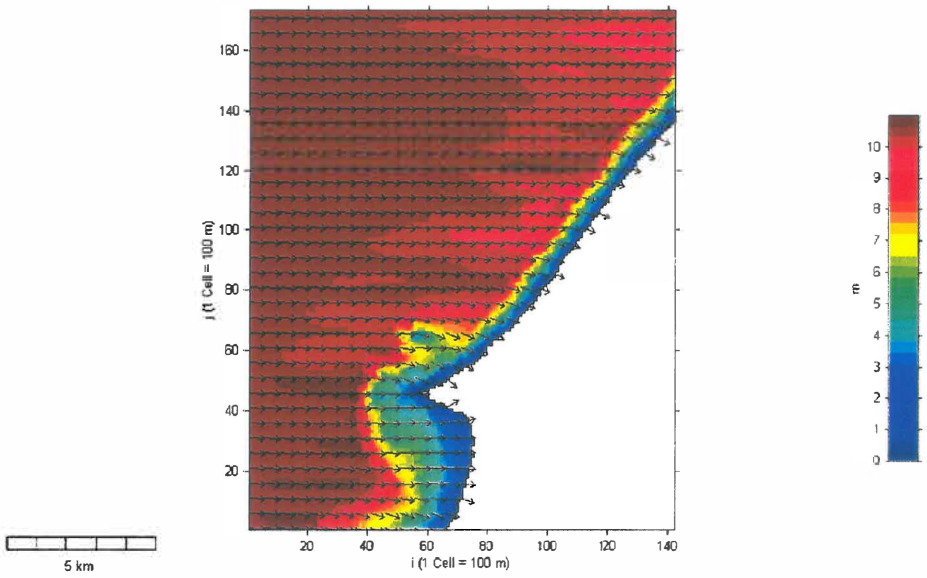

Figure 5.27 Scenario 37 (wave height 9.9 m, wave period 9.5 s, wave approach direction -4.73 °), illustrating results that are similar to all other storm simulations. Wave focusing does not occur as such, in comparison to other scenarios, which may be due to waves breaking offshore and energy being dissipated as the wave progresses towards the shoreline.

A possible reason as to why a lack of focusing is not occurring under the modelled parameters may be because of waves breaking offshore and wave energy becoming dissipated as the wave progresses towards the shoreline. However, the fact that the wave height at the Pukehina Beach shoreline is only approximately 1 m is questionable. With a wave height of 9.9 m, one might expect that wave height at the shoreline would be greater. Therefore, simulations of the storm event are uncertain.

It is worth noting from figure 5.27, that wave height is reduced at the ebb tidal delta, offshore from the Waihi Estuary inlet. This is likely due to wave breaking on the delta, thereby decreasing the wave energy.

5.7 Nearshore Littoral Drift and Sediment Transport by Waves

BLACK *et al.* (1998) and SAUNDERS (1999) have estimated littoral drift rates using the numerical model WBEND, at West End Ohope and Mangawhai-Pakiri respectively, based upon long-term wind and wave records.

A fundamental assumption is that the longshore transport rate (Q_l) depends on the longshore component of energy within the surf zone. Wave energy flux or power is evaluated at the breaker zone and is given by:

$$P_{ls} = (ECn)_b \sin\alpha_b \cos\alpha_b \qquad \text{Eqn. 5.16}$$

where n is the wave number, which is ½ in deep water and 1 in shallow water, α_b is the wave angle at breaking to the shoreline, and wave energy (E) is calculated at breaking depth, which can be written as:

$$E = \frac{1}{8}\rho g H_b^{\,2}. \qquad \text{Eqn. 5.17}$$

The wave celerity, can be approximated by

$$C = \frac{gT}{2\pi}\tanh\left(\frac{2\pi h}{L}\right) \qquad \text{Eqn. 5.18}$$

Following methods of SAUNDERS (1999), the root mean square of the wave height at breaking (H_b) was approximated using the ratio of water depth (h_b) and wave gamma (0.78)

The volume of sediment transported is given by:

$$Q_l = \frac{I_l}{(\rho_s - \rho)ga'} \qquad \text{Eqn. 5.19}$$

where I_l the immersed-weight transport rate is empirically related to the longshore component of wave power.

$$I_l = KP_l. \qquad \text{Eqn. 5.20}$$

K is a coefficient taken to be 0.77 following KOMAR AND INMAN (1970), and a' (sediment porosity) is given 0.6, as according to KOMAR (1998).

In order to examine littoral drift within the Pukehina coastal sector, the sector was divided into 8 sites as represented by the benchmarks, as illustrated in figure 3.3. This enables coverage of spatial variation in littoral drift rates. Data used to generate the

outcomes were the average mean significant wave height (0.39 m) and average mean significant wave period (10.64 s), during the summer deployment at Newdicks Beach (8/3/2001 - 7/4/2001). It must be noted that littoral drift directions and sediment transport rate outcomes generated by WBEND, are only relevant to data entered into the model.

To reduce the error of equation 5.16, each grid cell was divided into 2. Increasing the resolution of the grid cells enables a smoother shoreline contour, which subsequently is used to predict the beach orientation to the breaking wave. As a result 2 outcomes for each cell are generated.

5.7.1 Results of Nearshore Littoral Drift and Sediment Transport by Waves

Results of nearshore littoral drift direction and an estimate of possible direction and nearshore sediment transport rates (m^3/year) are summarised in the following and are listed in detail in appendix XI.

Outcomes obtained from the WBEND sediment transport model, indicate an easterly nearshore sediment transport direction along Pukehina Beach. Littoral drift direction at the apex of Okurei Point changes to a southeasterly direction, possibly due to the change in wave angle approach caused by change in bathymetry around Okurei Point. On the western side of Okurei Point, littoral drift rotates to a westerly direction, but then rotates back to an easterly littoral drift direction along Maketu Spit (grid cell 75, 23). Figure 5.28 illustrates longshore variation in nearshore transport rates (m^3/year), within the modelled region, illustrating that along Pukehina Beach, sediment transport is to the east.

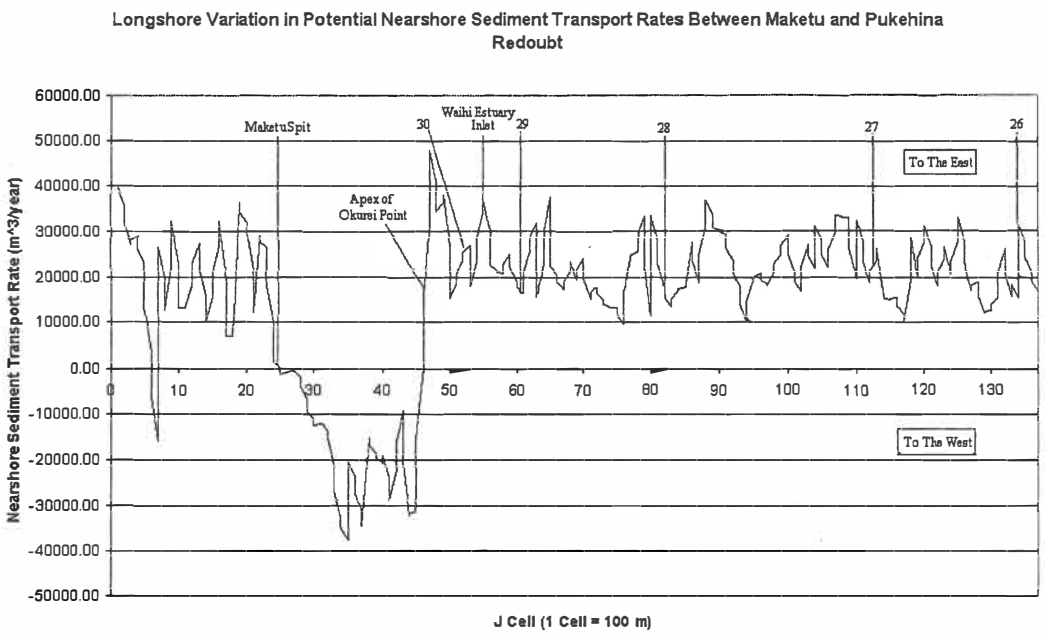

Figure 5.28 Longshore variation in nearshore transport rates (m^3/year) between Maketu and Pukehina Redoubt, illustrating that along Pukehina Beach, sediment transport is to the east.

Figure 5.29 illustrates nearshore littoral transport directions as determined by WBEND.

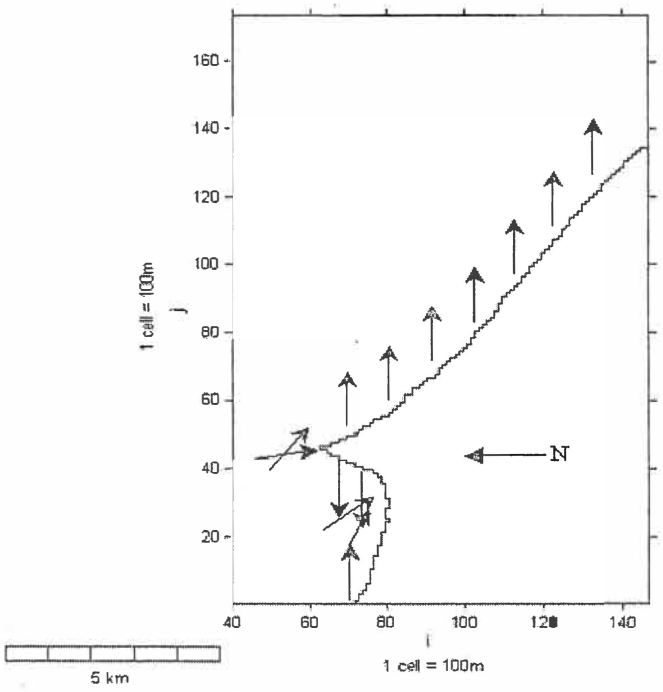

Figure 5.29 Nearshore littoral transport directions as determined by WBEND, using predominant wave direction (355°), average mean significant wave height (0.39 m) and average mean significant wave period (10.64 s), as collected from wave directional current meters during summer 2001, 8/3/2001 - 7/4/2001. Note arrows only illustrate littoral drift direction, they do not depict magnitude of littoral drift.

An easterly nearshore sediment transport direction along Pukehina Beach and the westerly nearshore sediment transport direction along the western side of Okurei Point resolved by WBEND, can be further justified by observing wave approach angles. When assessing wave approach directions along Pukehina Beach and the western side of Okurei Point, the angle of the wave in relation to the shoreline depicts a nearshore sediment transport direction in an easterly direction at Pukehina Beach, and a southerly nearshore sediment transport direction at the western side of Okurei Point. Figure 5.30a and 5.30b illustrates the wave approach under modal wave approach direction (355°), average significant wave height (0.39 m) and average significant wave period (10.64 s), as collected from the wave directional current meter situated offshore from Newdicks Beach.

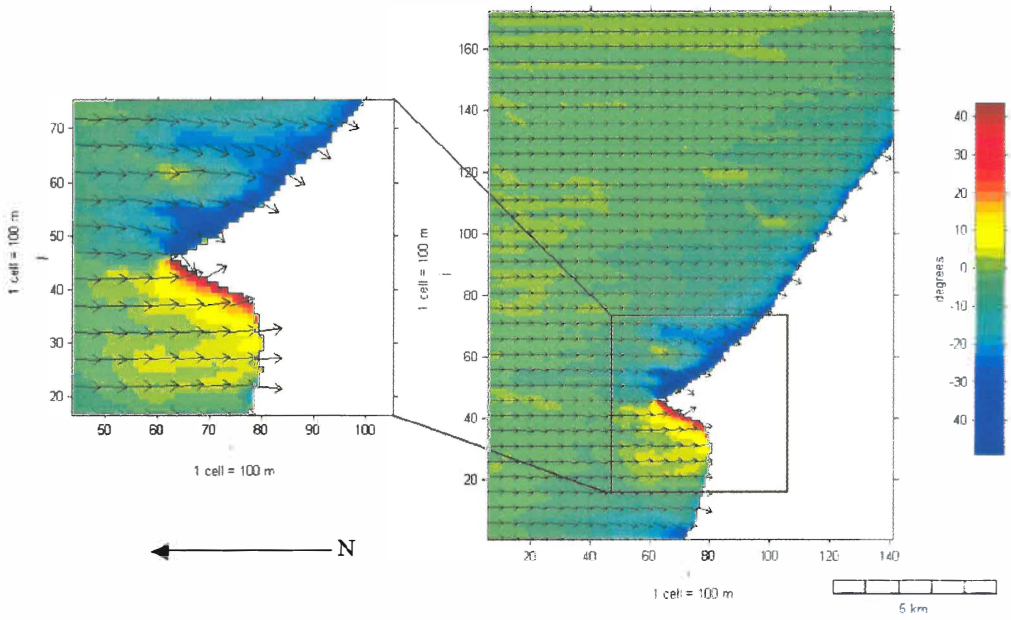

a)

Figure 5.30a Wave angle approach around Okurei Point, using predominant wave direction (355°), wave height (0.39 m) and average significant wave period (10.64 s), as collected from wave directional current meters during summer 2001, 8/3/2001 - 7/4/2001.

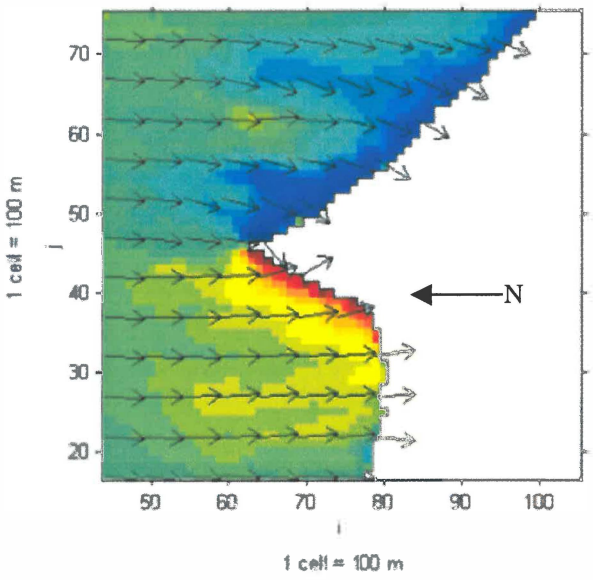

b)

Figure 5.30b Detailed illustration of wave angle approach around Okurei Point, using predominant wave direction (355°), wave height (0.39 m) and average significant wave period (10.64 s), as collected from wave directional current meters during summer 2001, 8/3/2001 - 7/4/2001.

If nearshore littoral drift is to the east, one must consider why does the Pukehina Spit oppose the nearshore littoral drift direction?

JENNINGS (1955) and DAVIES (1977) discuss zeta-formed embayments. A zeta-formed beach is named, due to the resemblance of the Greek letter zeta (ζ) (EPPS, 1987).

The formation of zeta-formed beaches has been suggested by DAVIES (1977, p. 136), to be due to 'the movement of sediment from one side of the bay to the other, under the influence of a predominant drift, but appear to be basically swash aligned features with their shape reflecting the wave crests of incoming swell waves, as they refract around each headland'

DAVIES (1977, p. 137) states that beaches along the New South Wales, Australia, coastline, have stream outlets orientated (similar to Pukehina Spit) towards the direction of littoral drift. DAVIES (1977) denotes this occurrence, to increased wave energy at the shoreline, where the stream would be presumed to be exiting. Increased wave energy at the shoreline, is suggested to correspond with an increased berm height and larger particle sizes (DAVIES, 1977).

Acknowledging DAVIES (1977) statements, observations of wave refraction simulations (Figure 5.18), and comparisons of historical beach profile data (Figure 5.31a and 5.31b), sediment textural characteristics (Appendix III) of benchmarks 30 and 28 were made. Observations and comparisons are similar to DAVIES (1977) statements. Therefore, the formation and orientation of Pukehina Spit, from data obtained during this investigation, suggests that the Pukehina coastline may be an imperative part of a zeta-formed coastline.

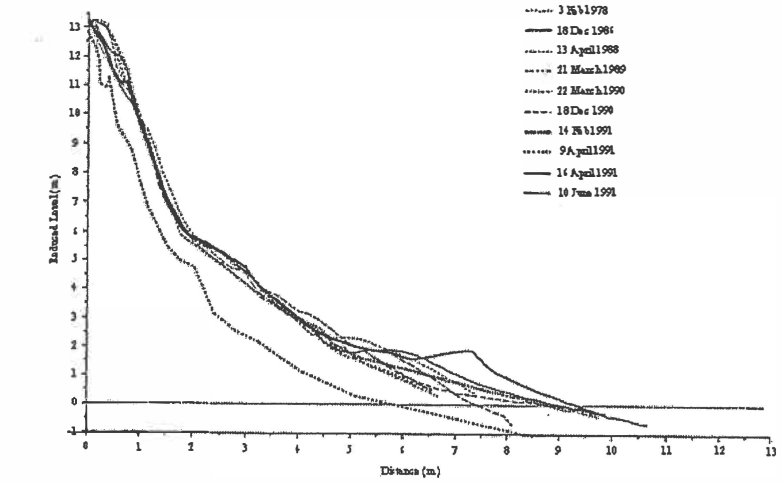

A)

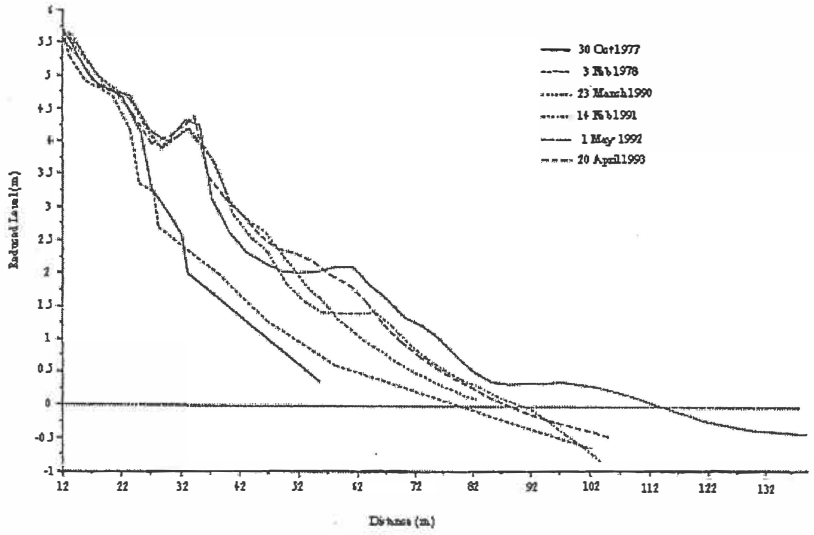

B)

Figure 5.31 Comparative plot of benchmarks a) 28 and b) 30, illustrating the difference in berm height. Historically berm elevation at benchmark 28 has been larger, and has had a smaller excursion distance. This is indicative that benchmark 28 has higher wave energy than at benchmark 30. This implies that a fluvial entrance would exit at benchmark 30 rather than benchmark 28, even though this will oppose the direction of littoral drift.

Nearshore sediment transport rates within the Pukehina coastal sector vary. The average net nearshore sediment transport rate within the entire grid examined was 22,289 m^3/year. This figure is consistent with values estimated by HEALY (1983) and PHIZACKLEA (1993).

Assessment of potential sediment transport, rates based upon the wave data applied in WBEND, between Okurei Point and Pukehina Redoubt, illustrate significant findings. The sediment transport potential from the data is illustrated in figure 5.32. The figure demonstrates the generally eastward moving littoral drift (except immediately west of Okurei Point). A regression analysis was carried out on the potential sediment transport for the two sectors (a) between Okurei Point and the Waihi Estuary inlet, and (b) between benchmarks 29 and 26 (figure 5.32).

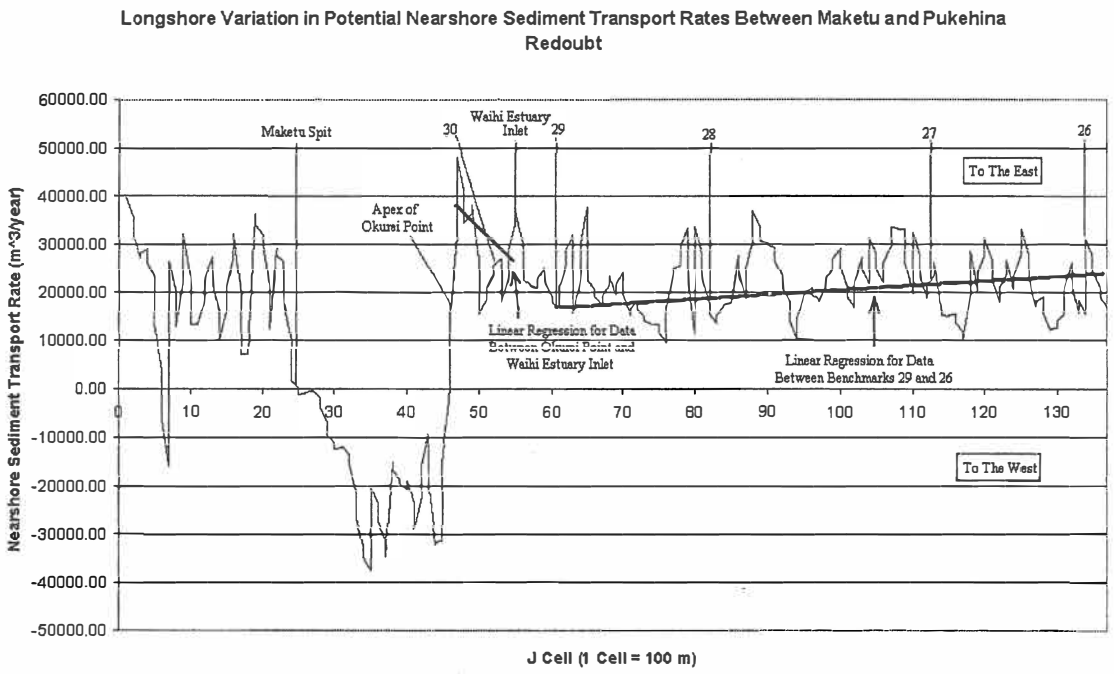

Figure 5.32. Nearshore sediment transport rates, as calculated by WBEND simulation. Regression analysis of data between Okurei Point and Waihi Estuary, illustrated a negative relationship, and thereby this region could be expected to have a tendency towards accretion. From benchmark 29 to 26, however, a positive relationship is observed, thereby one could expect sediment to be eroded from this region.

Outcomes of the regression analysis for sediment transport rate data between Okurei Point and Waihi Estuary inlet illustrates a greater potential for sediment transport at Okurei Point than at Waihi Estuary, thereby implying ~12,000 m^3/year sediment

would be expected to accumulate near the Waihi Estuary inlet. In effect the regression defines a littoral drift gradient.

From historical erosion/accretion trends (figure 5.33), calculated from beach (1912-1981) and dune (1943-1977) changes for Okurei Point to Waihi Estuary inlet, net accretion is observed towards the Waihi Estuary inlet. From observations along the Okurei Point-Waihi Estuary inlet sector, the likelihood of this region obtaining approximately 10 m^3/m is consistent with observations. A likely effect for the missing sediment is that some of it is being transported into the Waihi Estuary (chapter 6, identifies that ~1600 m^3/year is lost into the estuary).

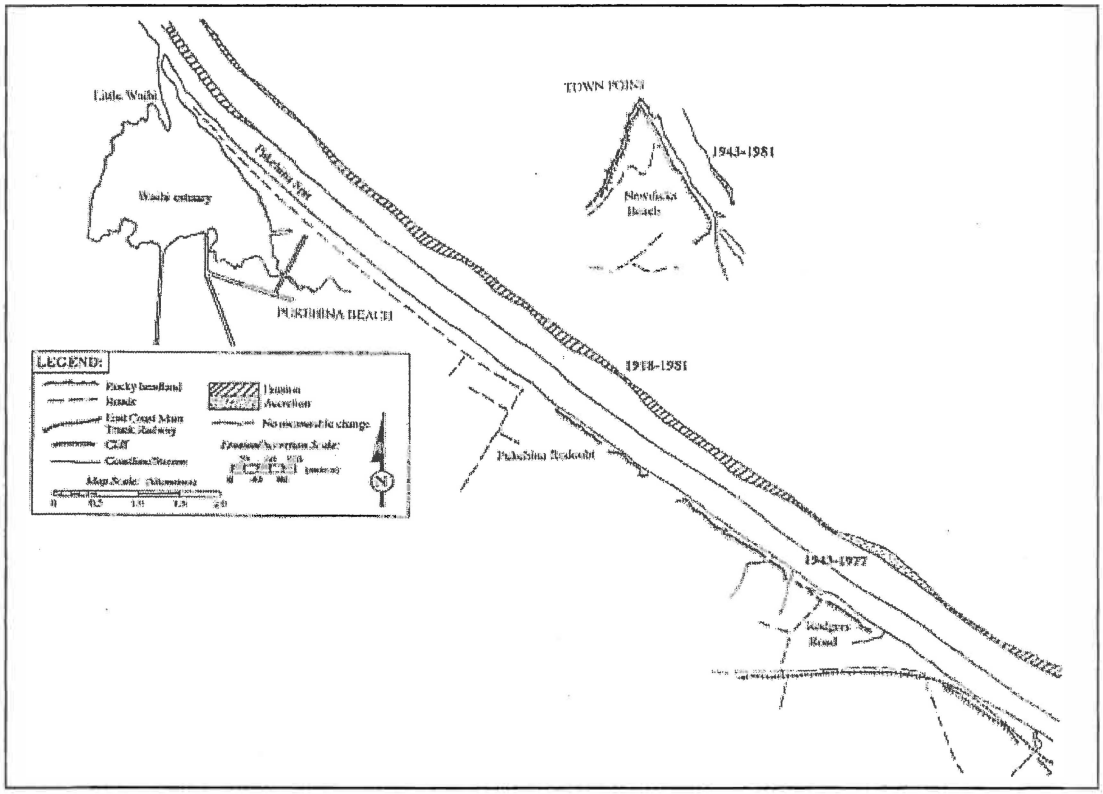

Figure 5.33 Historical erosion/accretion trends, calculated from beach (1912-1981) and dune (1943-1977) changes for Okurei Point to Otamarakau. Adopted from PHIZACKLEA (1993).

Between benchmark 29 and 26, the regression line for the potential sediment transport data has a positive littoral drift gradient, indicating a greater potential net eastward transport at benchmark 26 compared to benchmark 29. The implication of the littoral drift gradient is that there is ~7000 m^3/year of sediment 'sucked out' of the beach-

nearshore sediment budget from Pukehina Beach, i.e. ~12 m^3/m. This tendency implies a long-term sediment deficit for Pukehina Beach, and this effect, taken into conjunction with wave energy focusing along Pukehina Beach shoreline (section 5.6.3) seems to be the major component of the long-term 'erosion' problem at Pukehina Beach.

HODGES AND DEELY (1997, pp. 33-34) analysed historical beach profiles over an approximate 30 year period. They concluded stating 'Pukehina Beach and Spit has undergoing 10-30 m of retreat since 1912, with an net average shoreline retreat of approximately 10 m^3/m along all benchmark locations along Pukehina Beach. The two figures of 10 m^3/m loss of sediment is very consistent with the implied 12 m^3/m loss from the long-term gradient in potential littoral drift.

The nearshore sediment transport rate exiting the Pukehina coastal sector from the eastern boundary, was predicted from the WBEND simulation to be 24,620 m^3/year. At the apex of Okurei Point, the nearshore sediment transport rate was 14,591 m^3/year. PHIZACKLEA (1993) claimed that sediment transport is small (2,000 ± 2,000 m^3/year) at the apex of Okurei Point, due to the rocky nature of the coast around the apex of Okurei Point. This may be true, as different wave characteristics produce differing nearshore sediment transport rates, which was noted by Tonkin and Taylor (DE LANGE, *pers comm*), who analysed sediment transport rates within the Bay of Plenty and found that a slight modification in a wave parameter (specifically wave approach angle (± 2-3°) resulted in a significant change in nearshore sediment transport rates.

From nearshore sediment transport rate outcomes obtained from WBEND simulation, the effect the Okurei Point has on the nearshore sediment transport to the Pukehina coastal sector is minimal. From wave parameters applied to the WBEND model, nearshore sediment transport rates around the apex of Okurei Point are reduced, but in context to the sediment available at the western side of Okurei Point to the eastern side of Okurei Point the difference between the two are minimal (~1000 m^3/year). However, as previously stated PHIZACKLEA (1993) noted a marked reduction of

sediment transport a the apex of Okurei Point, therefore, the influence of Okurei Point inducing a sheltering effect of longshore sediment transport, may be dependent on the observed wave conditions.

Figure 5.30a and figure 5.30b illustrate that wave angle approach in relation to shoreline, on the western side of Okurei Point is more acute than elsewhere. Due to this, littoral drift direction alters and the quantity of sediment to this small region is restricted. The only sources of sediment to this region, under the examined conditions, are therefore the cliffs of Okurei Point, sediment ejected from the Maketu Estuary and reworked relict sediments on the sea floor. Erosion of Okurei Point cliffs has been estimated in chapter 2, to be retreating at a rate of 9.33 mm/year. Sediment load deposited at the western side of Okurei Point from the Maketu Estuary is dependent on how entrenched the inlet is and its orientation (DOMIJAN, 2000). With a restricted sediment input to this region, erosion is therefore, probable. Currently boulders are present in this region, thereby reducing erosion, but if boulders were to be removed it is highly likely significant erosion would occur.

Figure 5.34 Western side of Okurei Point. Sediment transport and littoral drift estimated are consistent with the beach geomorphology of a highly erosive area. Note boulders present, which may be currently preventing retreat, but indicate a lack of such. Photo: DOMIJAN, 2000.

5.8 Summary

Objectives of this chapter were to investigate the possibility of wave energy focusing upon the shoreline of the Pukehina coastal sector, predict the nearshore littoral drift direction within the Pukehina coastal sector and verify if Okurei Point may inhibit sediment transport by means of a sheltering effect.

Results indicate that focusing of wave energy is present within the sector, which may promote enhanced frontal dune erosion. Wave refraction simulations using the numerical model WBEND indicated, that varying wave parameters do influence wave height at the shoreline. Focusing of incoming waves was found to be largest in the lee of the ebb tidal delta, offshore from Waihi Estuary inlet. This promoted increased wave heights at the shoreline. The location of increased wave heights was found to be influenced by the wave approach direction, with northeasterly approaching wave concentrated around benchmark 30 and west northwest approaching wave concentrating around benchmark 29.

Particular areas of increased wave heights were concentrated at benchmarks 30, 29, 27, 26a and 26, thereby these location may be particularly prone to frontal dune erosion. Wave energy divergence is prominent at locations benchmark 30a, 28, and 27. Offshore depressions or 'holes' may possibly explain why wave energy diverges at these locations.

Based upon the limited measurements collected from the wave directional current meter situated offshore from Newdicks Beach during the summer deployment, nearshore littoral drift within the Pukehina coastal sector was indicated in an easterly direction. Net littoral drift for the Maketu-Otamarakau region was estimated as 22,289 m^3/year, this figure is consistent with values estimated by HEALY (1983) and PHIZACKLEA (1993).

On the western side of Okurei Point, the numerical simulation indicated a westerly sediment transport direction. This direction of littoral drift is only apparent in this area. Implications of this restricted littoral drift, may imply limited sediment accretion in this area, therefore this region could be in an erosive state.

Assessing nearshore sediment transport rates between Okurei Point and Pukehina Redoubt identified significant outcomes. A negative potential littoral drift gradient was identified in the region between Okurei Point and Waihi Estuary inlet. Outcomes suggest that there is a greater potential of sediment transport at Okurei Point compared to Waihi Estuary inlet. Implications of this indicate that an accumulation of sediments would be expected at Waihi Estuary inlet. Some of this sediment is evidently lost to the Waihi Estuary (as chapter 4 identified). Between benchmarks 29 and 26, a positive potential littoral drift gradient was identified. This implies that benchmark 26 has a greater potential of sediment transport, compared to benchmark 29. Outcomes suggested that approximately 7,000 m^3/year or 12 m^3/m is being 'sucked out' of the beach-nearshore sediment budget along Pukehina Beach. Implications of this, combined with wave energy focusing outcomes, demonstrate a potential long-term sediment deficit along Pukehina Beach.

Okurei Point has limited influence of sediment transport to the Pukehina coastal sector under investigated predominant wave climate. Due to the nearshore littoral drift direction, the likelihood of Okurei Point acting as a shelter to sediment transport is not significant. However, sediment transport at the apex of Okurei Point is notably smaller than elsewhere, possibly due to changes of the shoreline orientation, rocks present in this region and/or offshore bathymetry. PHIZACKLEA (1993) also noted similar findings, therefore, the influence of Okurei Point inducing a sheltering effect of longshore sediment transport, may be dependent on the observed wave conditions.

Chapter Six
Integrated Littoral Sediment Budget and Effects of Ocean-Atmosphere Cyclic Patterns on the Beach Budget

6.0 Introduction

Movement of sediment either by human intervention, parabathic/diabathic transport, or aeolian transport, is a constantly ongoing process. Since coastal erosion is apparent at Pukehina Beach, an assessment of existing and modelled data for sediment inputs, and outputs, are collated to form an integrated sediment budget. A sediment budget may be used to identify the extent of dune erosion occurring in the sector, and suggest possible reasons causing the enhanced frontal dune erosion.

This chapter also analyses the possible occurrence of cyclic ocean-atmosphere processes within the Bay of Plenty coastal region applicable to Pukehina Beach. Of particular interest, the El Niño Southern Oscillation (ENSO) and the Inter-decadal Pacific Oscillation (IPO) are assessed. These cycles could potentially influence the sediment supply to Pukehina Beach by altering wind and wave climates.

6.1 What is a Sediment Budget?

HEALY (1974) describes a beach sediment budget as 'being governed by its morphological response to short term, seasonal, and long term variations in the wave environment and littoral drift. Essentially, when additions to the beach-dune-nearshore system are greater than losses from it, accretion occurs. Similarly, if losses from the system are greater than the additions, then erosion results. Overall, the volume of sediment gained or lost from the beach-dune-nearshore system during the short term variations from the processes listed above is termed the sediment budget'.

The US ARMY CORPS OF ENGINEERS (1984, p. 4-113) state 'A sediment budget is a transport volume balance for a selected segment of the coast. It is based on quantification of sediment transportation, erosion, and deposition for a given control volume. Usually the sediment quantities are listed according to the sources, sinks, and processes causing the additions and subtractions'.

ROSATI *et al.* (1999) state (p. 806) that 'the difference between the sediment sources and the sinks in each cell, hence for the entire sediment budget, must equal the rate of sediment volume change occurring within that region. The sediment budget equation can be expressed as,

$$\sum Q_{source} - \sum Q_{sink} - \sum \Delta V + P - R = res. \qquad \text{Eqn. 6.1}$$

Where all terms are expressed as a volume or as a volumetric change rate, Q_{source} and Q_{sink} are the sources and sinks, respectively, ΔV is the net volume change within the cell, P and R are the amounts of material placed in and removed from the cell, respectively, and *res* represents the residual within the cell'.

One useful purpose of a sediment budget is that it can sometimes offer an explanation for the initiation of an erosion problem and may provide an avenue for remedial action (KOMAR, 1998).

A major problem when applying a sediment budget in the Bay of Plenty, is that the region consists of a series of 'leaky' littoral cells, where there is only partial sediment by-passing around major harbour entrances and rocky headlands (HEALY, 1980). This has implications in defining littoral cell boundaries. In theory, each cell should exist independently from one another, with little or no sediment transport occurring between cells (BEST AND GRIGGS, 1991). However, there can still be 'thin layer' sediment transport, i.e. a rolling carpet of grains over a stable morphological inner shelf-beach profile. DOLAN *et al.* (1987) suggest that the *closure depth* should be used to define the seaward boundary for the sediment budget analysis, as this is the depth at which, there are minimal sediment exchanges to the profile from year to year.

6.1.1 *Application of Sediment Budgets in the Bay of Plenty*

The application of sediment budgets within the Bay of Plenty littoral system to date, has been minimal, mainly due to the lack of data. Most sedimentary investigations have primarily involved identifying sedimentary processes and not evaluation of sediment volumes of sediment exchange within the study regions.

Sediment budget investigations by PHIZACKLEA (1993) in the Pukehina-Matata coastal sector, FOSTER *et al.* (1994) at Mount Maunganui, TONKIN AND TAYLOR (1999) at Otamarakau, and SAUNDERS (1999) at West End Ohope, are discussed in the following.

PHIZACKLEA (1993) compiled a sediment budget for the Pukehina-Matata coastal sector (figure 6.1) in order to assess the effects of sediment extraction at Otamarakau. PHIZACKLEA (1993) concluded that a deficit of 90,570 m^3, or approximately 3 m^3/m, was apparent in the Pukehina-Matata coastal sector between the years 1989 and 1993. In regard to the Pukehina coastal sector specifically, PHIZACKLEA's 1989-1993 sediment budget estimated a surplus of 6030 m^3 of sediment, or approximately 6 m^3/m. He also estimated a longer-term sediment budget between the years 1978 and 1993, which indicated a sediment surplus of 218,560 m^3, or approximately 7 m^3/m along the Pukehina-Matata coastline. PHIZACKLEA (1993, p. 307) further concluded that overall the volume changes in the Pukehina-Matata coastal sector are reasonably small, and variability of each sediment budget calculation (1989-1993 and 1978-1993) reflect both the dynamic nature, and the delicate state of equilibrium of the beach-dune-nearshore system.

FOSTER *et al.* (1994) utilised the diabathic transfer component of a sediment budget to assess volumetric changes of beach profiles at Mount Maunganui, Bay of Plenty, whilst beach renourishment was occurring in the region. They concluded that most of the total volume of 93,600 m^3 of sediment added to the nearshore profile between water depths of 4-7 m (relative to MSL) could be subsequently accounted for onshore.

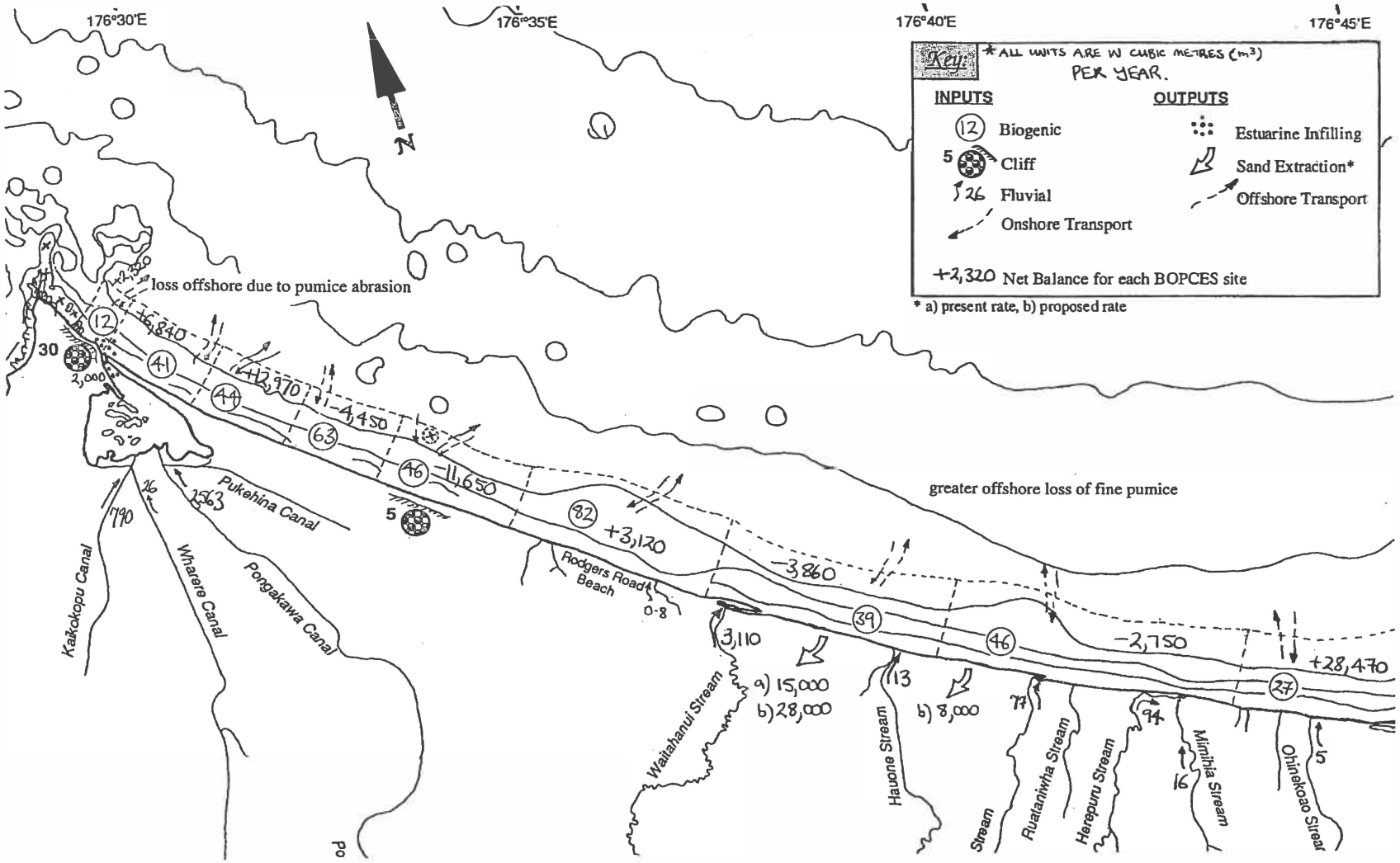

Figure 6.1 Littoral sediment budget for the Pukehina-Pikowai coastal sector, as calculated by PHIZACKLEA (1993)

In a technical appraisal of a resource consent application to continue mining of sediment aggregate at Otamarakau, submitted by SMITH *et al.* (1997), TONKIN AND TAYLOR (1999) reviewed data from SMITH *et al.* (1997), and created a sediment budget to assess the sustainability of continued sediment extraction at Otamarakau (figure 6.2). TONKIN AND TAYLOR (1999) concluded that the sustainability of sediment extraction at Otamarakau is questionable due to evidence (cut and fill volumes) and multiple uncertainties of coastal processes within the region, such as sediment supply and sediment transport direction. Their assessment suggested a long-term net loss of sand from Otamarakau in the order of 70,200 m^3/year, with inputs of 69,200 m^3/year. However, their model budget is questionable, relating to the diabathic transfers and the lack of littoral drift input.

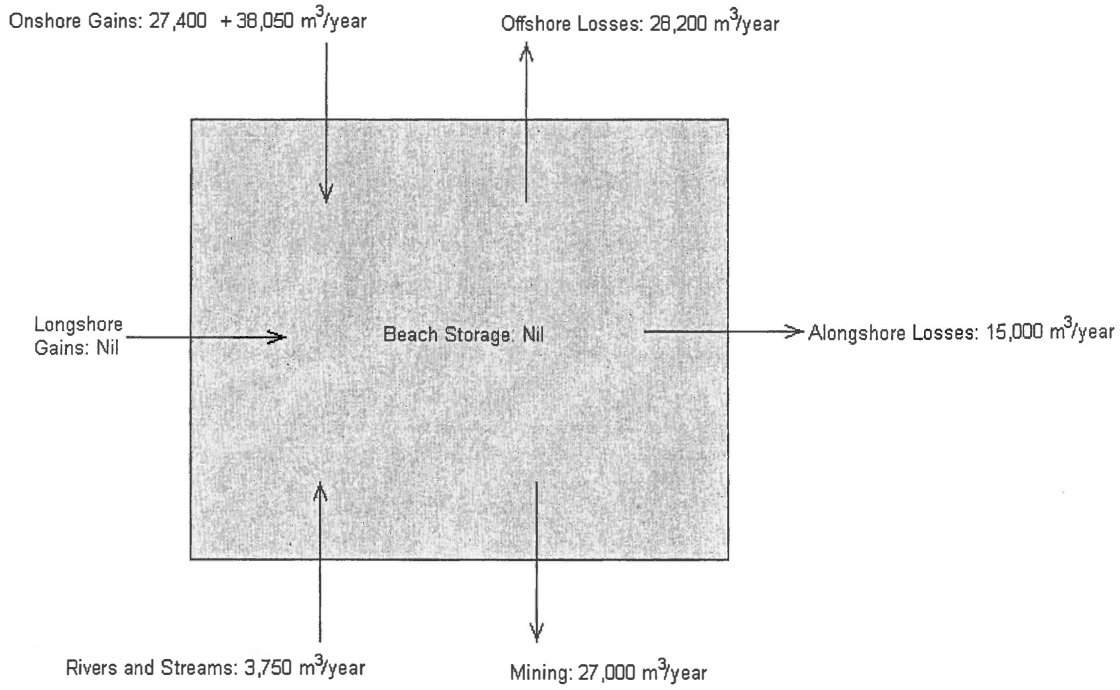

Figure 6.2 Littoral sediment budget for Otamarakau, as calculated by TONKIN AND TAYLOR (1999).

SAUNDERS (1999) applied an integrated sediment budget at West End Ohope in an attempt to explain the cause of shoreline erosion, and provide an avenue for remedial action (figure 6.3). SAUNDERS (1999) concluded that the sediment budget for West End Ohope (at the time of data collection) was imbalanced, with around 28,000 m^3/year of sand unaccounted for.

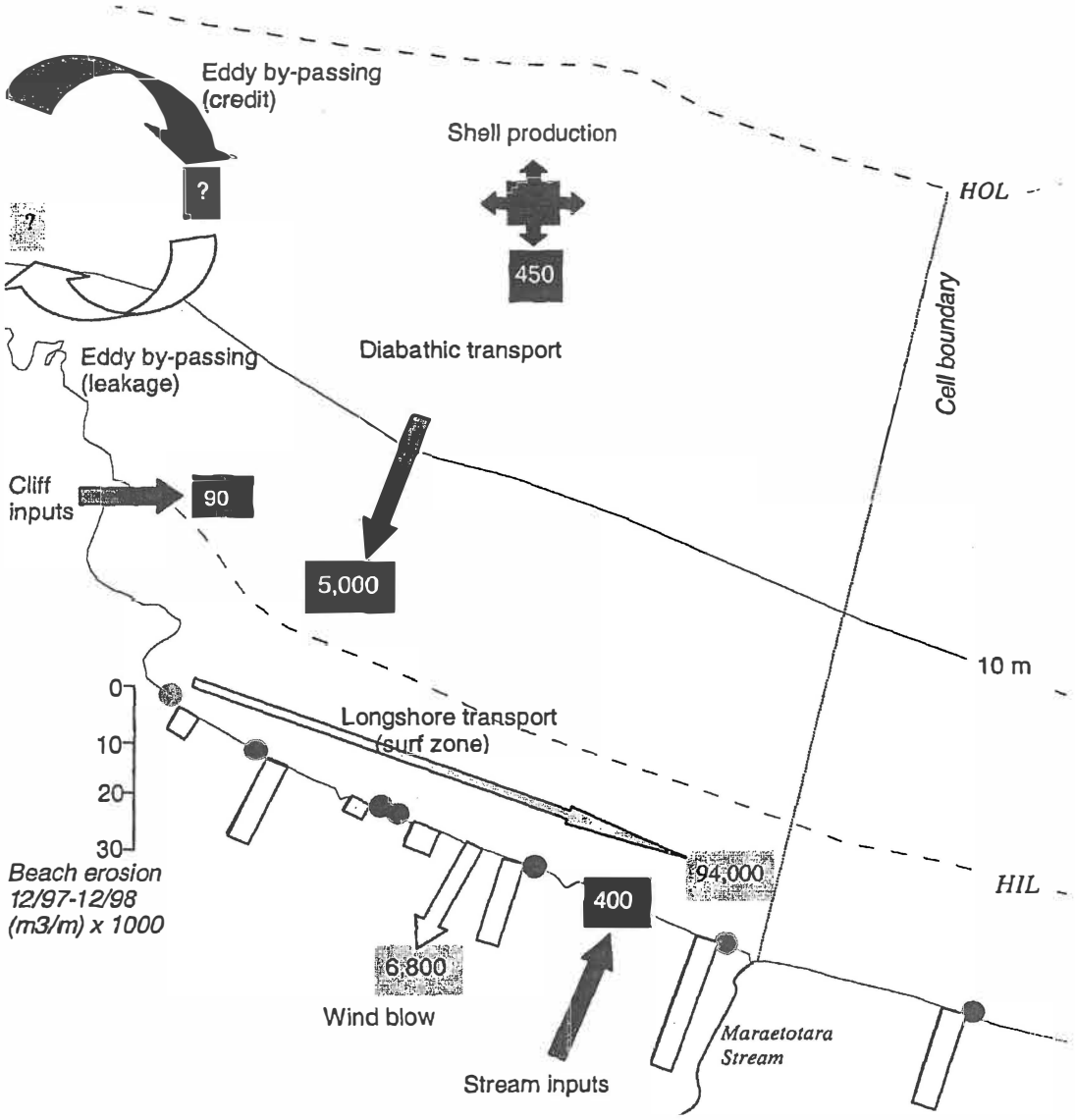

Figure 6.3 Littoral sediment budget for West End Ohope, as calculated by SAUNDERS (1999).

6.2 Pukehina Beach Sub-Littoral Cell

BEST AND GRIGGS (1991) claim that a littoral cell should be totally independent from a neighbouring cell. However, (from nearshore sediment transport calculations, chapter 5) within the Pukehina coastal sector (Pukehina-Otamarakau) no clearly defined cell exists. This was also noted by HEALY (1980). It is arguable that Okurei Point and Kohi Point, at Whakatane, create a significant barrier to the littoral drift and therefore, that between the

two headlands there is a littoral cell. However, within this cell there may be recognised sub-cells, which possess distinctive beach morphodynamic state and mineralogy. For the purpose of this investigation, the beach sector between Okurei Point and Pukehina Redoubt, is recognised as a littoral sub-cell.

DOLAN *et al.* (1987) suggest that closure depth should be used to define the seaward boundary of a littoral cell. The depth of closure at Pukehina was calculated using the HALLERMEIER (1981) limits. The Hallermeier limits define an inner limit, and an outer limit. The inner limit is associated with the seaward limit of the breaker zone, which is the effective boundary of active parabathic sediment transfer (BEST AND GRIGGS, 1991). The outer limit defines the seaward limit of diabathic sediment transport. PHIZACKLEA (1993) estimated that the Hallermeier outer limit (HOL) for Pukehina Beach was 11.78 m, and the Hallermeier inner limit (HIL) was 5.55 m, both depths relative to MSL. HOL and HIL limits calculated by PHIZACKLEA (1993), will also be utilised here.

Figure 6.4 illustrates a schematic of the Pukehina littoral sub-cell. Sediment inputs and outputs are indicated, which are to be evaluated and compared against changes in the sand storage on the beach.

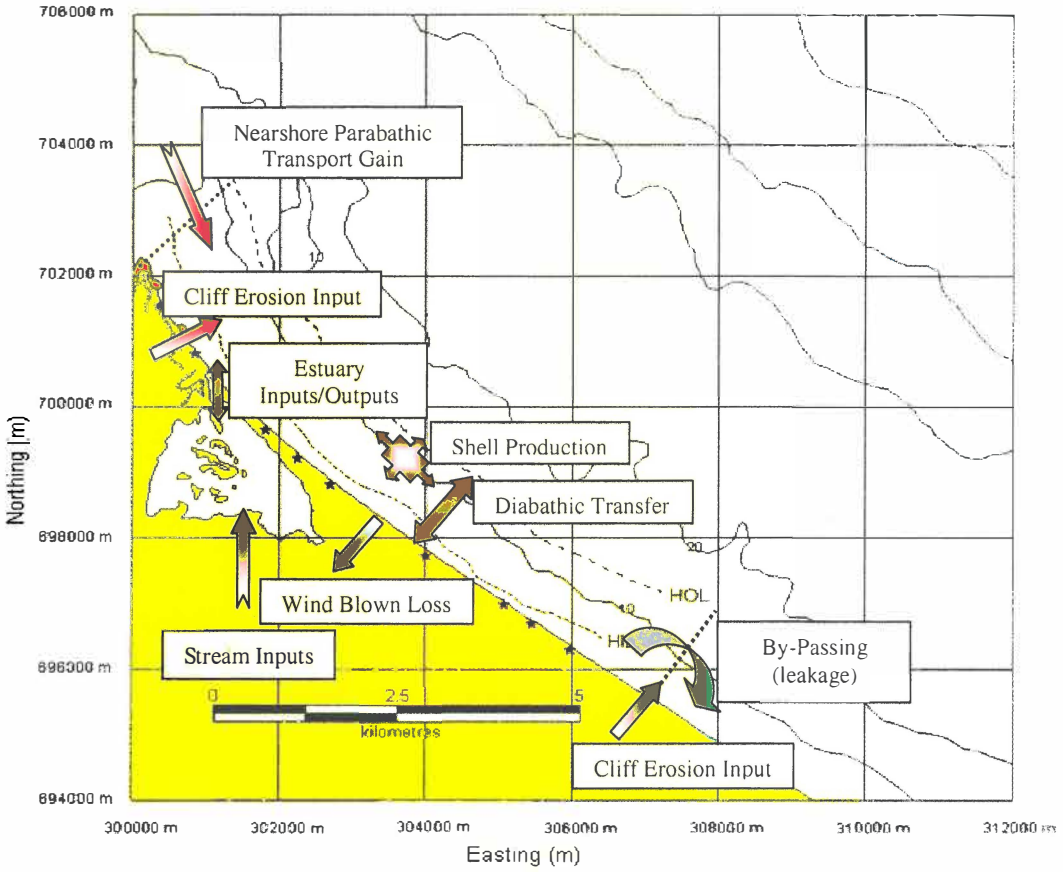

Figure 6.4 Schematic of Pukehina littoral sub-cell. Beach profile benchmarks used during this investigation are shown. Sediment transfers are indicated, which are to be evaluated and compared against changes in the sand storage on the beach. Bathymetry in metres.

6.3 Sediment Inputs into Pukehina Coastal Sector

As mentioned PHIZACKLEA (1993) compiled a sediment budget for the Pukehina-Matata coastal sector. Using 41 days of wave data collected from an S4 directional current meter, littoral drift estimates were made within the Pukehina coastal sector. Estimates were derived by using an empirical relationship between the longshore component of wave energy flux entering the surf zone and the immersed weight of sand moved, given by:

$$P_{ls} = 0.0884 \rho g^{3/2} H_{sb}^{5/2} \sin 2\alpha_o \qquad \text{Eqn. 6.3}$$

where P_{ls} is the longshore energy flux, ρ is the density of seawater (1025 kgm^{-3}), and g is gravitation acceleration (9.81 ms^{-1}). H_{sb} is the root mean square wave height for a

breaking wave and α_o is the angle of wave approach in deepwater, taken as the angle of onshore approaching wave from 90° to the shoreline.

From equation 6.3, PHIZACKLEA (1993) identified that annual net littoral drift in the Pukehina-Matata coastal sector was to the southeast. He estimated an annual littoral drift rate of 15,000 (± 10,000) m^3/year. However, PHIZACKLEA (1993) did comment that interpolation of annual net littoral drift from 41 days data is questionable, as it does not account for storm events that may occur outside of the sampled timeframe, and may not represent the long-term wave climate.

From littoral drift direction and sediment transport rates calculated in this study for the Pukehina coastal sector, by WBEND (chapter 5), littoral drift was predicted in an easterly direction along the Pukehina coastal sector (Pukehina-Otamarakau). The sediment transport rate entering the Pukehina coastal sector from the western cell boundary at Okurei Point was estimated as 14,591 (± 10,000) m^3/year. It must be stressed however, that estimates of littoral drift rates are only for the deployment period. An example of this is noted here, as PHIZACKLEA (1993) estimated that the sediment transport rate in the same location was 2,000 ± 2,000 m^3/year.

Streams within the Pukehina coastal sector (Pongakawa, Wharere, and Kaikokopu streams) have been estimated by PHIZACKLEA (1993) to provide approximately 3,000 (± 2,000) m^3 to the beach-dune-nearshore system. This sediment is likely deposited within the Waihi Estuary, but at times of flood sediment may be transported directly to the littoral beach zone.

From assessment of hydrodynamic investigations carried out within the Waihi Estuary (chapter 4), Waihi Estuary inlet was calculated as tending towards geomorphic and hydraulic instability, and therefore, an estimate of 1,000 (±1,000) m^3/year may be available to the beach-nearshore system. This value was estimated from figure 4.27 (tidal inlet stability), as approximately ¼ of the ebb tide is above the equilibrium shear stress, and therefore, scouring of the inlet occurs during this period of time and sediments are

provided to the adjacent coastline. Because Waihi Estuary was identified as unstable, the uncertainty of available sediment to the beach-nearshore system would be expected to fluctuate considerably as processes from the adjacent coast such as wave height and wave direction, vary. Therefore, a high value of uncertainty is appropriate.

Cliffs of Okurei Point and Pukehina Redoubt have been estimated to be retreating at a rate of 5.49 mm/year, or 35 m^3/year by PHIZACKLEA (1993). As previously mentioned in chapter 2, section 2.1.1, PHIZACKLEA's (1993) estimate was derived from investigations of the Waitemata Group sediments, within the Waitemata Harbour by GORDON (1993), which were presumed to be of similar structural lithology. However, MOON AND HEALY's (1994) investigation of the Waitemata formation indicated that the structural lithology is not comparable between the two formations, therefore PHIZACKLEA's (1993) estimate is subject to considerable uncertainty.

In this investigation, rates of cliff erosion were reassessed using the historical aerial photographs from 1943 and 1993 at scales of 1:10000. Using the methods as described in chapter 2 section 2.1.1, overlaying of historical aerial photographs was performed by utilising benchmarks and/or fixed points of known location (SMITH AND ZARILLO, 1990). Calculations of cliff retreat for Okurei Point and Pukehina Redoubt were obtained using the same aerial photographs as used to create figure 4.24. To obtain the most accurate predictions, aerial photographs were imported and geo-registered into MapInfo Professional Version 6.0 *. By measuring the distance of eroded cliff from 5 different representative profiles of Okurei Point, an average distance of cliff retreat can be obtained. This value is then subsequently divided by 50 years, to obtain a rate of coastal retreat (mm/year). As previously stated in chapter 2, the 1943 survey could not be overlayed using benchmarks, as these did not exist during this year, therefore, values of cliff erosion can only be treated as estimates.

* MapInfo Professional Version 6.0 by MapInfo Corporation, 1985

Profile No.	Distance of Horizontal Erosion (m)	Rate of Retreat (mm/year)
1	0.475	9.50
2	0.459	9.18
3	0.464	9.28
4	0.494	9.88
5	0.441	8.82

Table 6.1 Rates of coastal cliff retreat at Okurei Point. Profiles used to calculate rates of retreat are used as representative for the coastal cliff region.

Okurei Point cliffs are estimated to be retreating 9.33 mm/year or 59 m^3/year. By applying the same rate of retreat to cliffs in the vicinity of Pukehina Redoubt (9.33 mm/year), as geology is similar at each location (see figure 2.2), an estimate of 8 m^3/year is obtained.

The values of coastal cliff retreat at Okurei Point and Pukehina Redoubt are subject to significant uncertainty. The level of resolution of images imported into MapInfo is a function of the uncertainty of the rate of cliff retreat outcome. To enable accurate estimates of cliff erosion, aerial photographs were imported with resolutions of 1000 DPI (dots per square inch), therefore, the distance of 1 pixel in both vertical and horizontal dimensions were approximately 0.2 m. Preferably images would have been of a higher resolution, but a compensation had to be made between an outcome, or a result, if any (due to computer constraints), that may have taken a long duration to achieve. The level of uncertainty of the rate of cliff erosion is therefore, 9.33 (±4.00) mm/year or 59 (±25) m^3/year at Okurei Point, and 8 (±3.5) m^3/year at Pukehina Redoubt.

Biogenic inputs were estimated by PHIZACKLEA (1993) to supply approximately 299 m^3/year along the Pukehina-Otamarakau beach sector. This value was approximated from investigations from the Pakiri coast by HILTON (1990). PARK (1995) analysed species abundance and diversity, at exposed ocean sites and estuaries within the Bay of Plenty. In regard to Pukehina, Waihi Estuary was investigated, however, the closest exposed ocean sites to Pukehina were Papamoa and Otamarakau. PARK (1995, p. 26) noted that 'the variability in the particular species abundance within sites over time is possibly the result of both climatic association population recruitment/loss processes and the high fecundity R-strategist type ecology of most species encountered in these surveys. This results in

rapid population increases and fluctuations. However, the end result is that most of the species do not occur frequently enough in the surveys or at steady population levels to allow comparisons between years'.

Acknowledging this statement, biogenic production should have not altered since PHIZACKLEA's (1993) estimate, therefore the same estimate of 299 (±200) m^3/year will be used.

6.4 Sediment Loss from Pukehina Coastal Sector

From sediment transport rate calculations obtained in chapter 5, sediment loss due to net sediment being transported out of the Pukehina coastal sector (Pukehina Redoubt) using WBEND was estimated to be 24,620(± 10,000) m^3/year.

Chapter 4 analysed the hydrodynamics of Waihi Estuary, in which outcomes indicated the estuary is acting as a sediment sink. Based upon aerial photographs, PHIZACKLEA (1993) estimated that the estuary is infilling at a rate of 1,420 (±1,000) m^3/year. Since no previous tidal prism data for Waihi Estuary is available, it is difficult to identify whether the rate of infilling has increased or decreased. Thus the same value as used by PHIZACKLEA (1993), will be applied here. However, as previously stated, streams that enter the Waihi Estuary do not supply sediment to the open coast under normal flow conditions. Even if sediment were to be transported from the streams, sediment still may not reach the open coast due to the sediment transport pathways within the estuary (as identified in chapter 4). Therefore, the calculated estimate includes sediment volumes that may have been transported from the streams into the estuary during times of flood. Since sediment is dredged from the streams at unknown quantities, a volume of 100 m^3 (±100) m^3/year of sediment that may discharge from the streams during periods of flood is estimated. A new value of 1,320 (±1,100) m^3/year may be used as an estimate of sediment loss from the beach- nearshore system, for further analysis.

Further, PHIZACKLEA (1993) made an 'uncertain' estimate of a transfer of littoral sediment into the Waihi Estuary inlet of 2,000 (±2,000) m^3/year, which presumably is

deposited within the estuary. From tidal inlet analysis in the present study, outcomes (chapter 4) identified that the inlet was indeed unstable, tending towards deposition. It is felt that the 2,000 (±2,000) m^3/year is however, an overestimate from stability analysis, therefore, a value of 1,200 (±1,200) m^3/year should be utilised. This value accounts for both the deposition, as indicated by tidal stability analysis, and involves a high error value, which allows for variability of both sediment input and volume of water discharged, which subsequently alters the flushing capabilities of the inlet.

As a summary, sediment transfers (gains and losses) from the Waihi Estuary, as a whole, may be expressed as a net volume. Sediment transfer outcomes identified in the previous section, and from identified sediment outputs (section 6.3), denote a net loss of 1620 m^3/year.

PHIZACKLEA (1993) approximated a net loss of sand from aeolian processes as 2,000 (±1,000) m^3, in the Pukehina-Matata coastal sector. Erosion of frontal dune sediment, has been investigated by ARENS *et al.* (1995), who carried out a range of flow and sand transport experiments over various foredune types and under varying wind conditions. They found that the wind is topographically accelerated over foredunes, particularly up stoss slopes and over crests. However, vegetation cover and topography of foredunes leads to local decelerations and variations in roughness length. Accrediting ARENS *et al.*'s (1995) findings, PHIZACKLEA's (1993) value may have reduced over time due to vegetation growth, as figure 6.5 illustrates clearly over a 50 year period. Therefore, a value of 1,800 (±1,000) m^3 may be a more likely value for sediment loss to aeolian transport, at the present time in the Pukehina-Matata coastal sector. Adjusting this estimate of sediment loss so that it only includes the Pukehina coastal sector, a sediment loss of 600 (±400) m^3/year is obtained. This estimate is assessed from judgement of how much vegetation is present within the Pukehina coastal sector, compared to the entire Pukehina-Matata coastal sector.

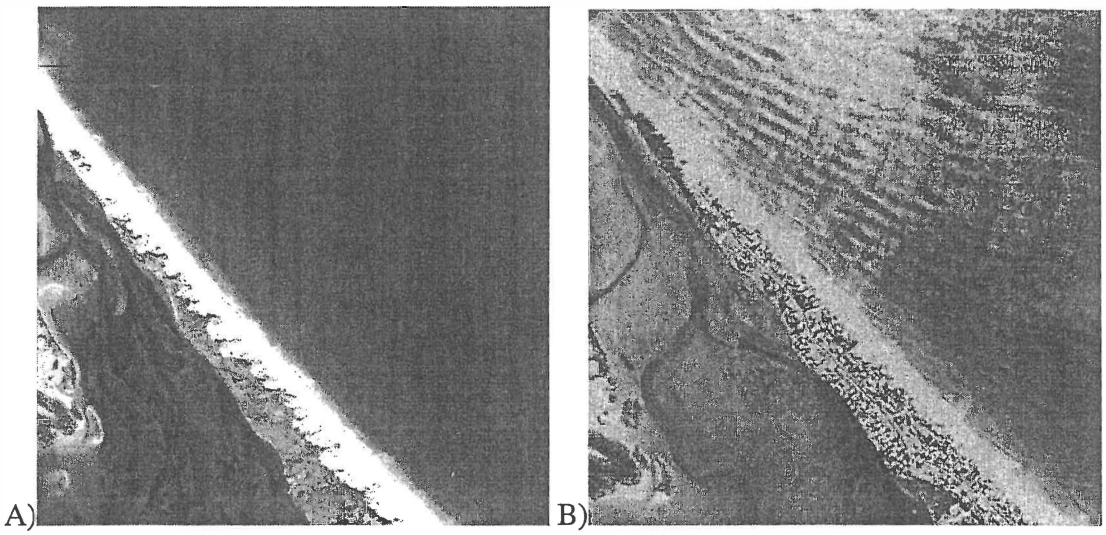

Figure 6.5 Comparison of the frontal dune at Pukehina Spit between the years a) 1943, and b) 1993, illustrating both the growth of dune vegetation at the distal end of Pukehina Spit, and also dune blowouts, which are clearly noticeable in the 1943 photograph.

6.5 Diabathic Transport in the Pukehina Coastal Sector

In earlier years, diabathic transport volumes were usually ignored, declared minimal, or used to 'balance' the system after all other sources/sinks were accounted for (REYNOLDS, 1987). However, the importance in exchange of sediments from the offshore bar for instance, has now become a 'normal' component of a sediment budget analysis (REYNOLDS, 1987).

Sediment may be transferred onshore or offshore depending on wave steepness and wind stress driving upwelling or downwelling circulation. High wave steepness combined with onshore winds favour offshore transport, while low wave steepness conditions combined with offshore winds favour onshore transport. Figures 6.6a and 6.6b illustrate how wave steepness and wind direction can modify diabathic transport transfer.

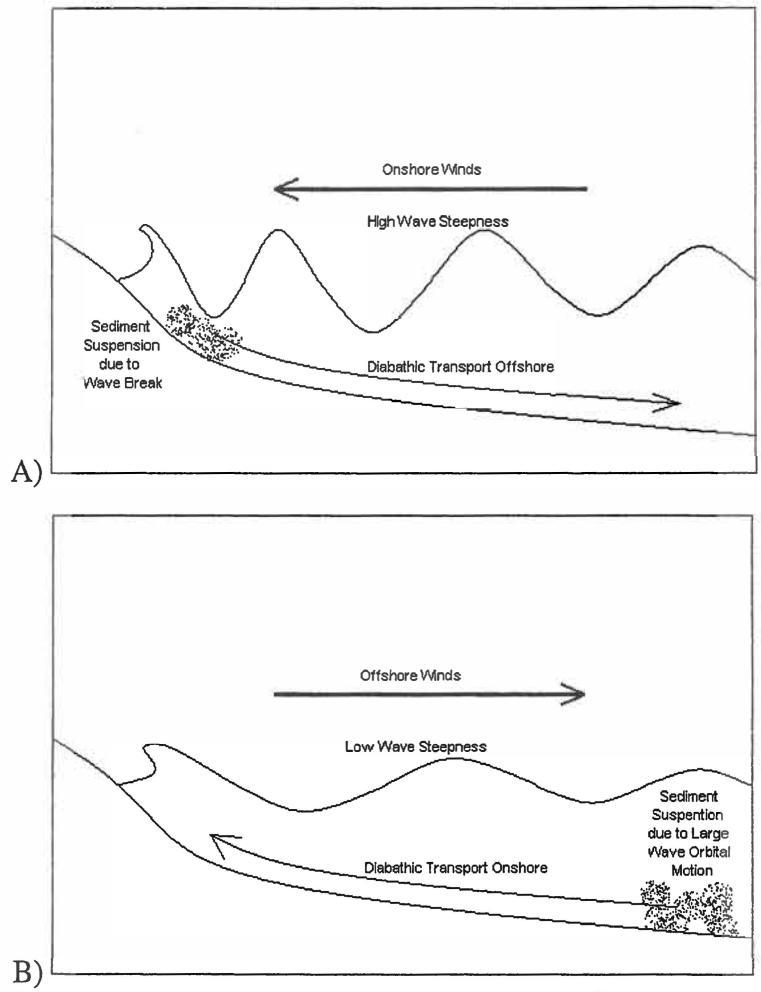

Figure 6.6 a) Diabathic transport offshore, induced by a high wave steepness and associated onshore winds. Water is pushed up on to the beach by wave and wind conditions, initiating a return flow or downwelling current, which subsequently entrains sediment and transports it offshore b) Diabathic transport onshore. Low wave steepness is associated with larger wave orbital motions, which can penetrate deeper into the water column. Subsequently sediment can be entrained and transported onshore by means of an upwelling current, which is initiated by offshore winds pushing surface water offshore.

Figure 6.6a illustrates diabathic transport offshore, which is induced by high wave steepness and associated onshore winds. Water is pushed up on to the beach by wave and wind conditions, which in turn initiates a downwelling current. The downwelling current may subsequently entrain beach sediment and transport it offshore. Diabathic transport onshore is illustrated in figure 6.6b. Low wave steepness is associated with larger wave orbital motions, which can penetrate deeper into the water column than waves with greater wave steepness and associated smaller wave orbital motion. Sediment can be

entrained by interaction of the orbital motion with the seabed. Consequently sediment may be transported onshore by means of an upwelling current, which is initiated by offshore winds pushing surface water offshore.

PHIZACKLEA (1993) estimated diabathic transport within the Pukehina-Matata coastal sector using the computer program *Mobile*, which calculates the potential predicted bedload and suspended load transport. PHIZACKLEA (1993, p. 292) stated from his measured conditions, "coarse sized sediment particles could only be entrained in storm wave conditions, as under 'normal' conditions, bottom currents were too small to induce entrainment of coarse sized sediments". This statement is subject to considerable uncertainty, as one would expect that swell waves would induce entrainment of coarse sized sediment particles, as long period waves have larger wave orbitals, which subsequently can penetrate deeper into the water column. PHIZACKLEA's (1993) estimate of bedload sediment transport over his deployment period was calculated using wave periods of 6-8.8 s, which are relatively short swell waves, and realised a net volume of 30,000-40,000 m^3/year of material onshore, which is available to the Pukehina-Matata beach sector.

By utilising the same bedload sediment transport value of 0.0253 m^3/m for fine and very fine sediments, calculated by PHIZACKLEA (1993) in his estimate, an approximate net estimate of 5,000 m^3/year, or 0.5 m^3/m of material would be available within the 9 km Pukehina coastal sector. This estimate however, would be expected to be larger with the inclusion of swell waves, and subsequent transport of coarse sized sediments, therefore, an 'uncertain' estimate of 7,500 (±2,500) m^3/year, or 0.8 m^3/m is used here as a diabathic transfer rate, for the Pukehina coastal sector.

6.6 Integrated Sediment Budget Outcome

Figure 6.7 represents an integrated sediment budget for the Pukehina Coastal sector.

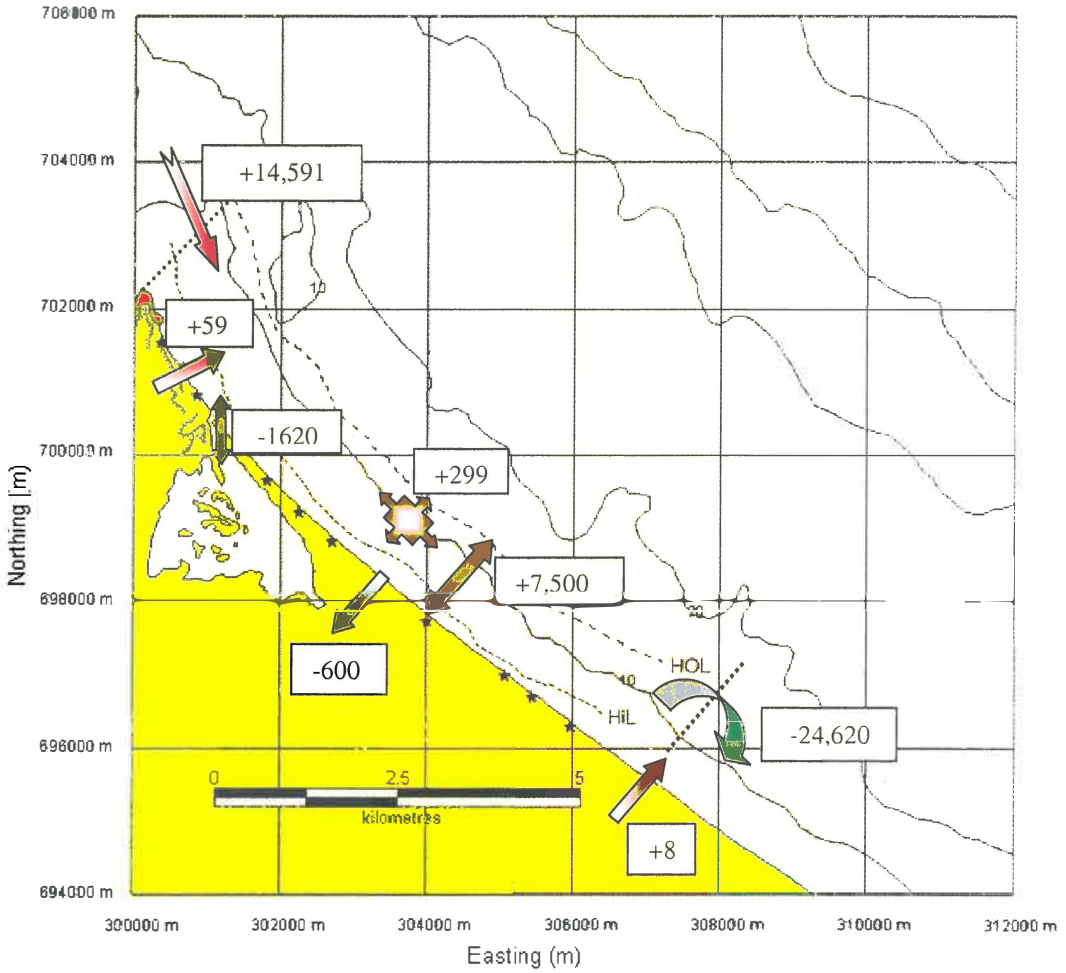

Figure 6.7 Net annual credits and debits to the sediment budget, along the Pukehina coastal sector. Units are in m^3/year.

Inputs –outputs = net erosion/accretion rate

14,591 + 59 + 299 + 7,500 + 8 - 1,620 - 600 - 24,620 = -4,383 m^3/year

Associated error of each estimation

±10,000 ±25 ±200 ±2,500 ±3.5 ±4,300 ±400 ±10,000 = ±27,428.5 m^3/year

6.6.1 *Discussion of Integrated Sediment Budget Outcome*

The net erosion/accretion rate obtained from the integrated sediment budget for the Pukehina coastal sector illustrates a negative value, indicating a net erosion rate. As previously stated, HODGES AND DEELY (1997, pp. 33-34) concluded that the Pukehina Beach and Spit has undergoing 10-30 m of retreat since 1912, with an net average shoreline retreat of approximately 10 m^3/m along all benchmark locations along Pukehina Beach'. The value -4,383 m^3/year or -0.5 m^3/m, therefore, is well below the expected erosion rate. One must therefore, consider why?

By examining the errors involved with estimations of sediment gains or debits, illustrates how such an outcome can occur. Summation of all errors from estimates made of sediment gains and losses, provides an overall error of up to ±27,428.5 m^3/year. The possibility of Pukehina Beach eroding even more than the calculated rate of retreat is, therefore, possible.

6.7 El Niño Southern Oscillation (ENSO) and Inter-Decadal Pacific Oscillation (IPO)

Erosion of the frontal dune in the Pukehina coastal sector by wave activity, normally occurs in episodic storms with enhanced storm surge activity and associated downwelling currents. Analysis of existing data sets (such as storm surge data sets) available within the Bay of Plenty region, may identify whether cyclic variations in climatic conditions affect storm surge frequency, thereby enhancing frontal dune erosion. Cyclic variations of particular interest are the El Niño Southern Oscillation (ENSO) and the Inter-Decadal Pacific Oscillation (IPO) (GORDON, 1985; DE LANGE, 2001).

ENSO represents an irregular, but coherent set of fluctuations in atmosphere and oceanic circulation patterns across the Pacific and Indian Oceans (DE LANGE, 2001). Fluctuations vary from 2 –10 years (DE LANGE AND GIBB, 2000). IPO is a combination of changes in ocean and atmospheric circulation over the North Pacific Ocean, and has been proposed

as the cause of climatic regime shifts at intervals of 25-35 years. The IPO is also suggested to produce similar climatic shifts in the Equatorial and South Pacific Ocean (DE LANGE, 2001).

The Southern Oscillation Index (SOI) is a measure of how severe an El Niño or La Niña event is. SOI values are obtained from the difference in atmospheric pressure measured in the east (Tahiti) and west Pacific (Darwin) (GORDON, 1985).

DE LANGE AND GIBB (2000) analysed storm surge data sets at two sites in Tauranga Harbour (at the slipway and Salisbury Wharf), for the period 1960 – 1998. In this analysis, storm surge was defined as 'Occasions when the residual level between the predicted high tide level and recorded water level exceeded 0.1 m'. Over the duration of the data set, 954 storm surge events were recorded. The magnitude and frequency of these storm surge events varied considerably between 1960 and 1997 (figure 6.8), ranging from a maximum of 48 events in 1960, to a minimum of 5 events in 1978. The magnitude of storm surges recorded, measured in terms of maximum water level reached during the storm surge are illustrated in figure 6.9.

Storm surge frequency in the Bay of Plenty, varies monthly (figure 6.10). However, DE LANGE AND GIBB (2000) could find no meaningful relationship between storm surge height and the Southern Oscillation Index (SOI), which suggests that the magnitude of storm surges in Tauranga Harbour may be unrelated to the state of the ENSO.

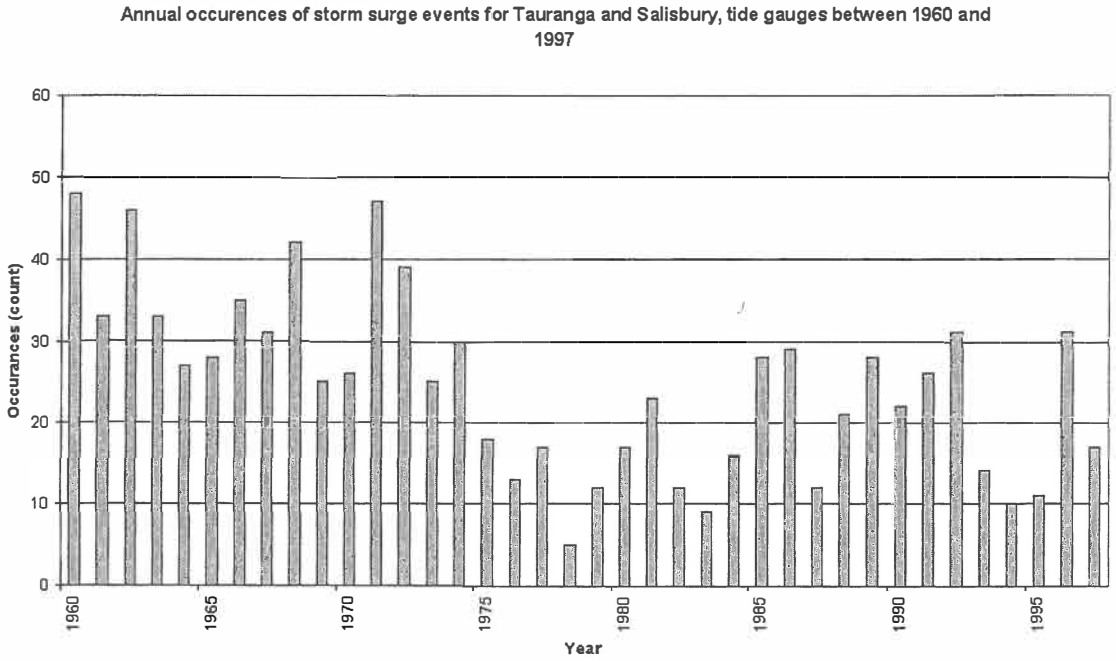

Figure 6.8 Annual occurrences of storm surge events for Tauranga and Salisbury tide gauges between 1960 and 1997. Source: DE LANGE AND GIBB, 2000.

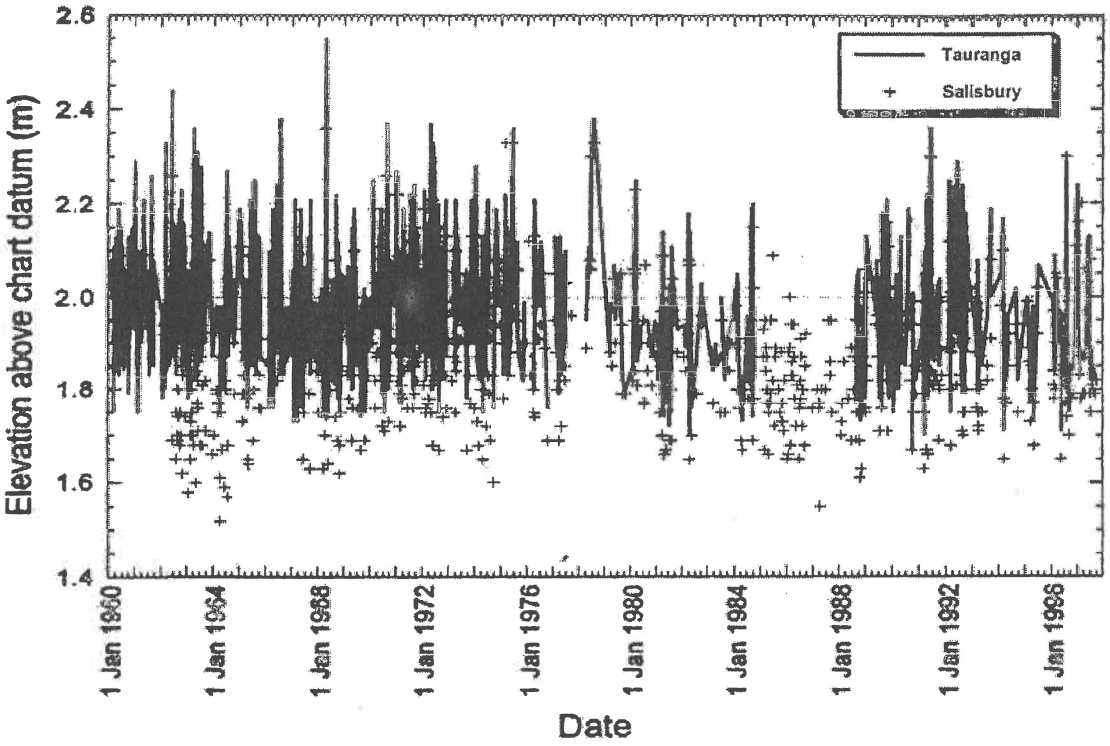

Figure 6.9 Maximum water level, including tides, relative to chart datum (-0.96 m Moturiki Datum) during storm surges at Tauranga and Salisbury tide gauges between 1960 and 1997. Source: DE LANGE AND GIBB (2000).

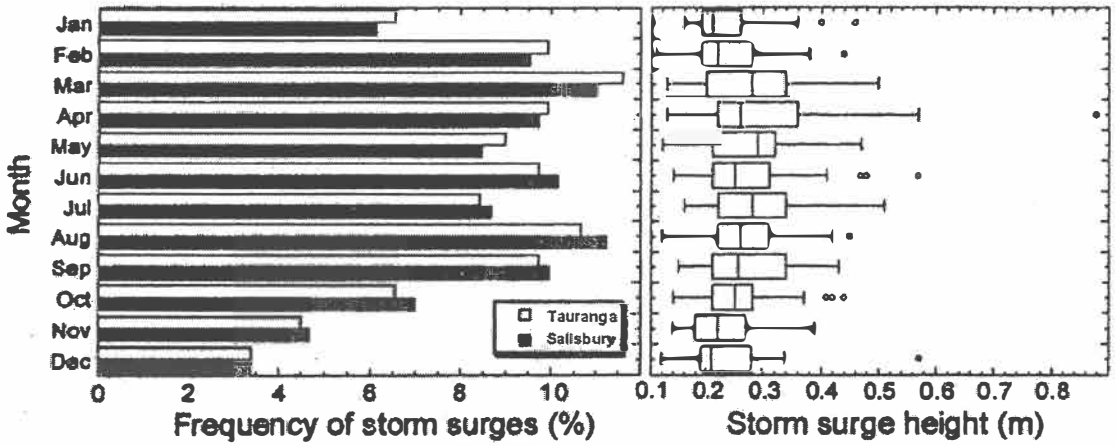

Figure 6.10 Monthly frequency of storm surges at the Tauranga and Salisbury tide gauges, and box plot of the monthly distribution of storm surge heights at Tauranga, between 1960 and 1997. For the box plot, each box encloses 50% of the data with the median value displayed as a line. Top and bottom of the box mark the limits of ±25% of the variable population. Lines extending from the top and bottom of each box mark the minimum and maximum values that fall within an acceptable range for the data obtained during the year. Any value outside of this range is displayed as an individual point. Source: DE LANGE AND GIBB (2000).

HAY (1991) and HAY *et al.* (1991) compiled a database of storm surges on the open-exposed coast of the Bay of Plenty since 1873, based upon historical newspaper reports. Accuracy of the records is questionable, but the results again found that the overall total storm frequency is not significantly correlated to the SOI. However, Tasman depressions appear to have a negative correlation, and tropical cyclones a positive correlation to the SOI.

On a larger scale QUINN AND NEAL (1987) compiled the occurrence of El Niño events since 1525AD and categorised them accordingly into strengths i.e. very strong, strong etc. During the investigated four and a half century period, 47 El Niño events were categorised as being very strong or strong. These events were categorised by multiple reports of the single event from differing sources. In regard to Pukehina Beach, a record database such as this may be used to identify what possible influences severe El Niño events cause, in terms of frontal dune erosion and alterations to 'normal' sediment transport mechanisms.

DE LANGE (2001) identified that the IPO modulates the frequency and intensity of ENSO extremes (figure 6.11). Since ~1976, the El Niño extreme has dominated, which has been associated with a suppression in eustatic sea level rise. Subsequently this has been associated with fewer and smaller storm surges and a tendency for coastline accretion (DE LANGE, 2001)

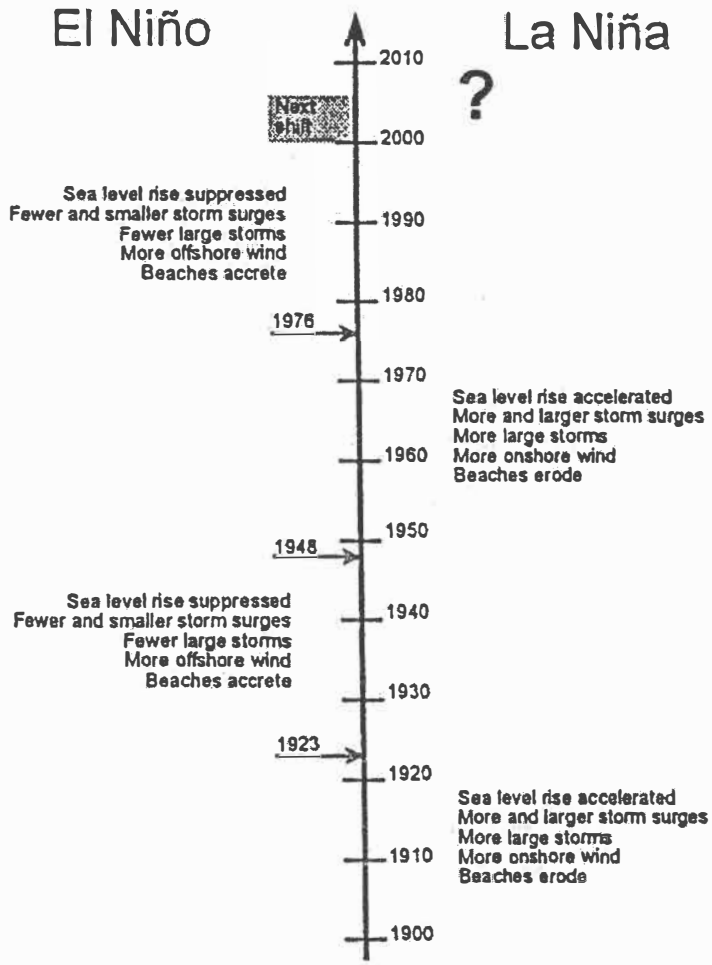

Figure 6.11 Summary of historical impacts of IPO induced climatic regime shifts between El Niño dominated and La Niña dominated, for beaches on the northeast coast of New Zealand (between North and East Capes) over the last century.

DE LANGE (2001, p. 659) states that for the northeast coast of New Zealand, during a La Niña dominated phase of the IPO, there is likely to be:

- an increased rate of sea level rise at the star of the phase; and

- a general tendency for sandy shorelines to retreat during this phase due to a higher incidence of erosion

During an El Niño dominated phase:

- secular sea level rise will be suppressed
- shoreline will tend to accrete due to fewer erosive events and the predominance of offshore winds.

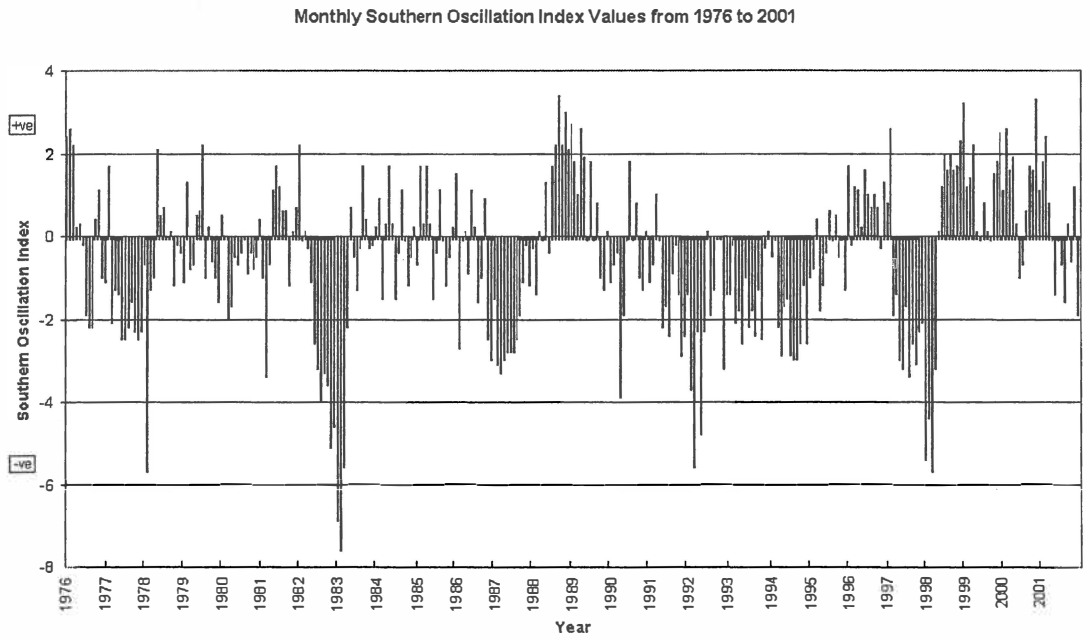

Figure 6.12 Monthly Southern Oscillation Index (SOI) values from 1976 to 2001. Source: NOAA-CIRES CLIMATE DIAGNOSTICS CENTRE, 2002.

Figure 6.12, illustrates recorded SOI values over the period 1976-2001.

From figure 6.12 and analysis of excursion distances obtained from historical beach profile surveys undertaken in the Pukehina coastal sector, investigation of whether climatic influences such as the ENSO and IPO are influencing erosion of frontal dunes, may be undertaken.

6.7.1 *Results of El Niño Southern Oscillation (ENSO) and Inter-Decadal Pacific Oscillation (IPO) Assessment*

Excursion distances, measured from benchmarks located in figure 3.3, to mean sea level are presented in figure 6.13a and figure 6.13b. By using a yearly time series of measured excursion distances, possible fluctuations may be compared with known dates of change in ENSO pattern (figure 6.12 and data available from QUINN AND NEAL (1987)). QUINN AND NEAL (1987) conclude that on a large scale, El Niño events in the past century have occurred in the following years:

- 1982-1983: Very strong event,
- 1972-1973: Strong event,
- 1957-1958: Strong event,
- 1940-1941: Strong event,
- 1932: Strong event,
- 1925-1926: Very strong event,
- 1917: Strong event,
- 1911-1912: Strong event.

These dates differ to DE LANGE (2001), as dates given by DE LANGE (2001) are specific to the Northeast coasts of New Zealand. However, the differences are not significant, and accordingly may also be used to estimate possible time intervals between locations of observation and the northeast coast of New Zealand.

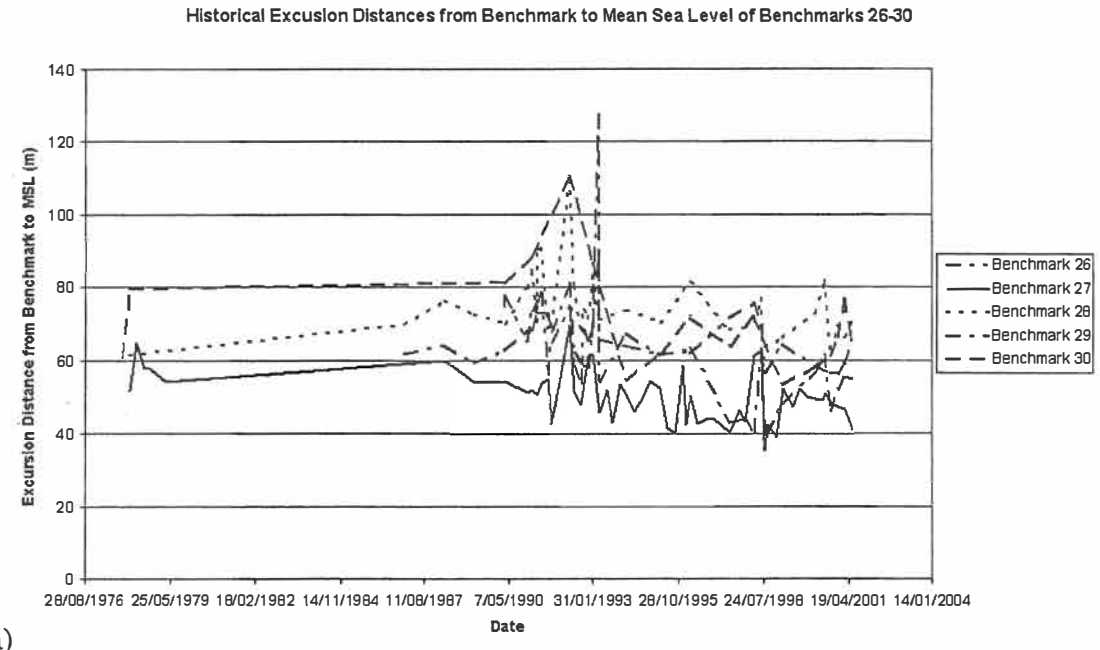

a)

Figure 6.13a Historic excursion distances (from benchmark to MSL) of benchmarks 26-30. Source: Environment Bay of Plenty.

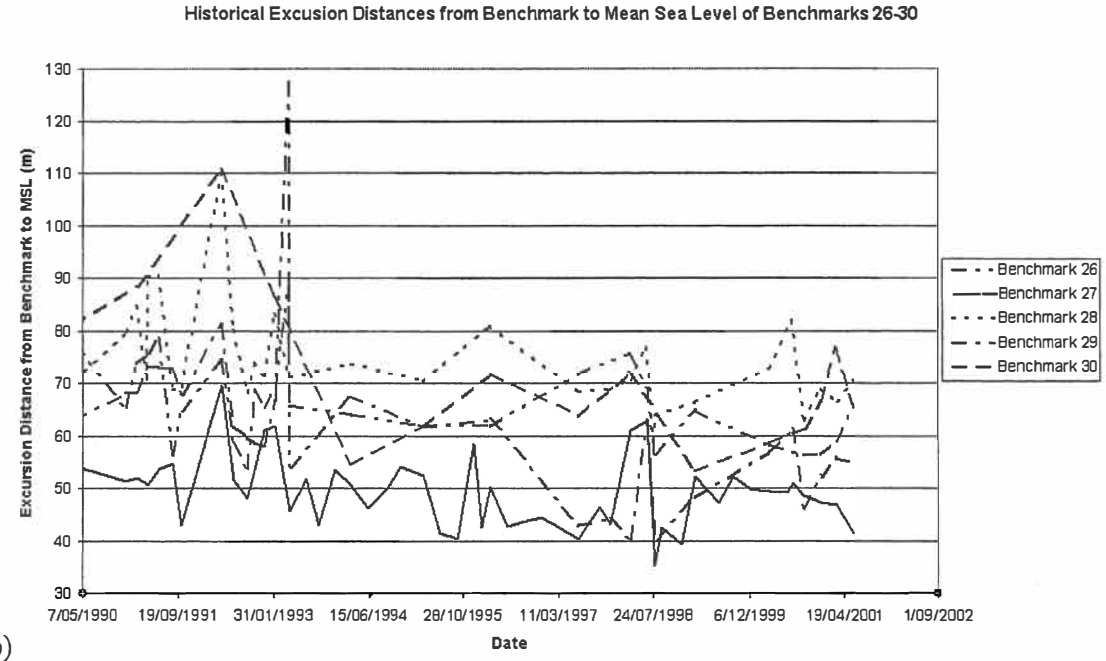

b)

Figure 6.13b Detailed plot of years of largest variation in historic excursion distances (from benchmark to MSL) of benchmarks 26-30. Source: Environment Bay of Plenty.

From comparing figures 6.13a and 6.13b with known dates of change in ENSO and IPO, no correlation can be made due to the lack of beach profile data. Also if a fluctuation did

coincide with a change in ENSO or IPO, a judgemental statement of whether or not ENSO or IPO affects sediment transport mechanisms can not be made with confidence, due to only one event occurring in the excursion distance data.

However, applying monthly averaged SOI values to known averaged beach volumes (m^3/m) in the same timeframe, an indication may be obtained in relation to whether ENSO or IPO affect sediment transport mechanisms in the Pukehina coastal sector. SMITH AND BENSON (2001) applied this technique within the Bay of Plenty, relating monthly averaged SOI values to known averaged beach volumes (m^3/m) at benchmark 21 (Matata). SMITH AND BENSON (2001) concluded that there was a negative relationship between SOI values and averaged beach volumes at benchmark 21, by obtaining an R-squared value of 0.45, which accounts for 45% of the data variance, using a linear regression analysis. A negative relationship indicates that during La Niña conditions, beach volume above the MSL datum is reduced. This result is expected, acknowledging DE LANGE's (2000) statements, as summarised in section 6.6.

For the present investigation, benchmarks 27 and 28 were taken as representing the Pukehina coastal sector, as other benchmarks were regarded as having increased sediment inputs influencing their profiles from proximate sediment sources (i.e. coastal cliff gains, Waihi Estuary sediment discharges).

Results of the average monthly beach volume (m^3/m) verse average monthly SOI values, are illustrated in figure 6.14.

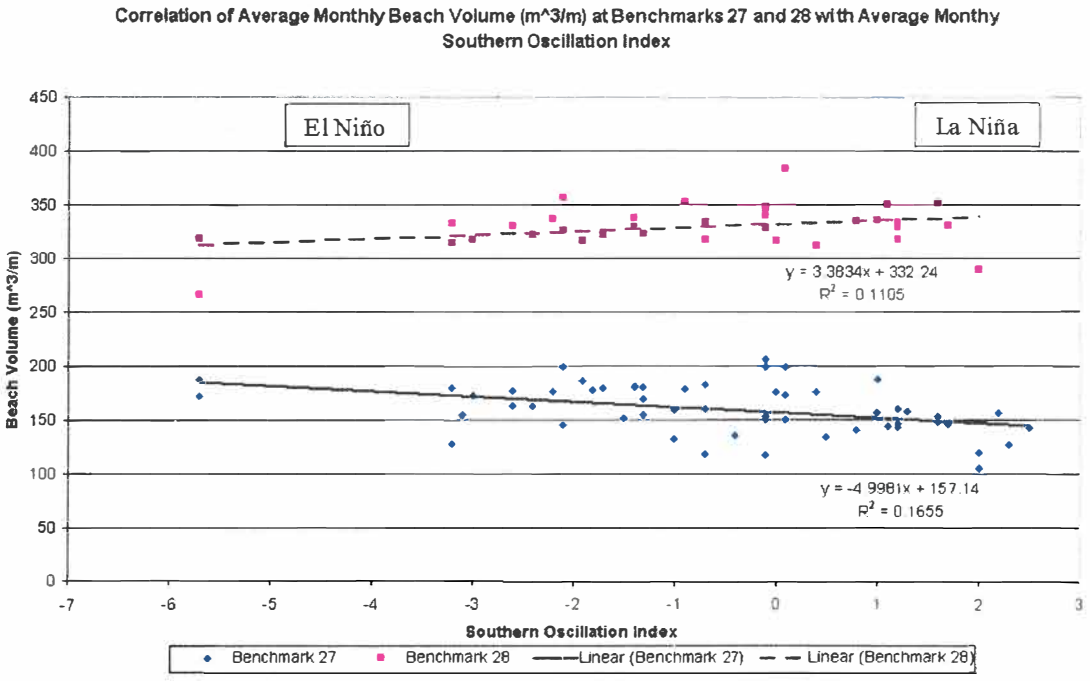

Figure 6.14 Correlation of average monthly beach volume (m^3/m) at Benchmarks 27 and 28 with average monthly Southern Oscillation Index. Southern Oscillation Index data supplied by NOAA-CIRES CLIMATE DIAGNOSTICS CENTRE, 2002. Beach volume data between the years 1978-2001, supplied by Environment Bay of Plenty, 2001.

From figure 6.14, only weak correlation is apparent at both benchmark locations. R-squared values obtained from linear regression analysis at benchmarks 27 and 28 were 0.17 or 17% and 0.11 or 11%, respectively. Therefore, the implications that ENSO and IPO events may influence beach volumetric state along the Pukehina coastal sector are not evidently supported by this data set.

6.8 Summary

Objectives of this chapter were to calculate an integrated sediment budget for the Pukehina coastal sector, in order to identify the major components, which are significant to the erosion of the frontal dune of Pukehina Beach. Further, an investigation of ocean-atmosphere interactions was assessed in order to identify whether such interactions could affect the state of the calculated integrated sediment budget.

From the sediment budget illustrated, the Pukehina coastal sector evidently receives a net erosion rate of approximately 4,500 m^3/year or -0.5 m^3/m per year. Compared to HODGES AND DEELY's (1997) estimate of 10 m^3/m per year, the estimate of net erosion is significantly smaller. However, from assessment of errors involved with individual component estimates, illustrates that erosion rate of retreat obtained could be larger.

Available sediment entering the Pukehina coastal sector from the eastern sub-littoral boundary is approximately 14,500 m^3/year, while approximately 24,600 m^3/year leaves the sector (western sub-littoral boundary). As discussed in chapter 5 a deficit of ~7,000 m^3/m is regarded as a major contributor to the long-term 'erosion' problem occurring at Pukehina Beach. Infilling of the Waihi Estuary was estimated causing a net loss of 1,620 m^3/year of sediment from the Pukehina coastal sector. Likewise a sediment loss of approximately 600 m^3/year to aeolian transport was identified. Ideas of potential remedial solutions to capture available sediment from processes, such as those identified will be further discussed in the following chapter.

The El Niño Southern Oscillation (ENSO) and the Inter-Decadal Pacific Oscillation (IPO) were assessed as possible cyclic ocean-atmosphere processes, which could implicate the calculated sediment budget of the Pukehina coastal sector. From outcomes however, no strong relationship could be identified.

Chapter Seven
Summaries, Conclusions and Potential Remedial Solutions for Pukehina Beach

7.0 Introduction

From results and observations undertaken in this study, possible causes and trends of the perceived erosion problem at Pukehina Beach, are summarised. From this assessment, potential remedial solutions to restrict or impede the rate of coastal retreat within Pukehina Beach are presented.

7.1 Summary of Key Findings

7.1.1 Environmental Processes Influencing Sediment Budget

Local geology, fluvial catchment geology, wind and wave climates, and storm and tropical cyclone activity were discussed to assess implications each induces to the sediment budget of the Pukehina coastal sector.

Geology of the region is dominated by quartzofelspatic sediments, which derive from mid Pleistocene and volcaniclastic silts, sands, gravels and conglomerates covered by Quarternary tephras and paleosoles (WEHRMANN, 2000). Outcrops of greywacke sediment are located inland from Otamarakau, and are also observed as sediment sources to Pukehina Beach (benchmark 26). Fluvial discharges from streams and rivers are sourced from the Taupo Volcanic Zone (TVZ), in particular the Okataina Volcanic centre. Sediments commonly comprise quartz, alkaline feldspar, pumice, volcanic glass and rock fragments. Of less abundance are plagioclase, hornblende, hypersthene, augite, cummingtonite, titanomagnetite and other opaque minerals. Suspended sediment load discharged from rivers are influenced significantly by afforestation/deforestation activity within their associated catchments, this was noted

in regard to the Tarawera and Kaituna catchments specifically, with an approximate 90-100% increase of suspended sediments discharged from each river during periods of human intervention.

Wind climate of the Bay of Plenty is influenced by surrounding topography. Wind direction at Tauranga is predominantly from the west to southwest, while at Whakatane northwesterly airstreams are dominant.

Wave parameters, such as wave height and wave direction within the Bay of Plenty region, are influenced by localised wind climate. Long-term wave power calculations were assessed in order to identify net littoral drift directions within the Bay of Plenty. Outcomes illustrated that for Tauranga Airport data, there was a slight tendency for a eastward net littoral drift direction, while for Whakatane data, net littoral drift direction was unidentified, due to the resultant wave power vector directed perpendicular to the coastline. Subsequently, in regard to Pukehina Beach, by applying the same resultant vector directions from Tauranga and Whakatane Airport, a net littoral drift direction to the east was also identified at Pukehina Beach.

7.1.2 Beach Morphodynamics and Sediment Characteristic of the Pukehina Coastal Sector

Offshore sediment textures were assessed to identify alterations of sediment distribution and sediment transportation patterns within the Pukehina coastal sector, since previously surveyed by PHIZACKLEA (1993). From comparative analysis utilising digital terrain models and side scan sonagraph outputs between the two surveys, both outcomes suggest a net gain of nearshore sediment toward the Okurei Point region. A reduction of previously exposed bedrock indicates mobility of sediment over the nearshore zone in this region. Possible reasons include an increase of river/stream discharge (most likely the Kaituna River to the west), littoral drift into the region, or diabathic transport.

Offshore sediment textures vary from fine sand sized sediments (2.64Ø) to very coarse sand sized sediments (0.06Ø), as calculated by PHIZACKLEA (1993). Nearshore sediment samples varied from medium sand, and became finer towards Okurei Point

(fine sand). Utilising both the SUNAMURA AND HORIKAWA (1972) and the MCLAREN (1981) sediment transport models, sediment transport was identified towards the west along Pukehina Beach. Increased concentration of heavy minerals (titanomagnetite) was observed during sample collection at benchmark 30a. The increased concentration of fine sized heavy mineral at this location caused both sediment transport models to predict bi-directional net littoral drift along Newdicks Beach. The likelihood of such an occurrence is, however, dubious.

The occurrence of onshore winds, were identified to increase suspended sediment concentrations significantly (approximately 500%), illustrating the fact that localised winds are a critical parameter of providing sediment to the Pukehina coastal sector. From sediment textural analysis, sediment of larger grain size was identified as being able to be suspended higher in the water column at Pukehina Redoubt, than at Newdicks Beach during all seasons. This is suggestive that a higher wave energy regime may be apparent at Pukehina Redoubt, that at Newdicks Beach.

7.1.3 Hydrodynamics of Waihi Estuary and Estuarine Sediments

Hydrodynamic and sediment transport outcomes both indicate strong reason to believe that Waihi Estuary is acting as a sediment sink. Tidal asymmetry was noticed within the estuary and was measured in terms of parameter D (equation 4.1). Outcomes identified that the asymmetry of the tidal signal within the estuary varied from 11 to 28%. Attenuation of the tidal signal within the estuary was also observed. Tidal amplitude decreased on average 0.3 m or 69%, between the inlet and the sub-tidal flat. These outcomes from each analysis, are indications that Waihi Estuary is infilling, most likely from sediment provided by the adjacent littoral system.

Sediments within the estuary vary from very coarse sand at the estuary inlet, to fine sand at the mid reaches of the estuary. On the sub-tidal flats sediments are of coarse sand texture.

The MCLAREN (1981) sediment transport model was utilised to identify sediment transport pathways within the estuary. Outcomes indicated that sediment transport within the estuary is flood dominated. This is in agreement with tidal data collected at

Waihi Estuary inlet, and visual evidence of the estuary, such as the formation of the flood tidal delta with a diminished ebb tidal delta, which denotes that sediment is being transported into the estuary.

Analysis of the tidal curve at the sub-tidal flats indicated fluctuations on the ebb tide, with water depth dropping 0.1 m over a 1-2 minute duration. A variety of hypotheses were suggested, including: instrument failure, alterations to hydraulic gradients at this location, internal seiching, which may be initiated by an external influence such as a coastal trapped wave or edge wave activity or channel and friction influences.

Geomorphic and hydraulic stability analyses were assessed in regard to the Waihi Estuary inlet. Both assessments illustrated that the inlet is tending towards instability. Assessment of geomorphic stability utilising aerial photography taken in 1943, 1981, and 1993, illustrated that the inlet has undergone significant change during this period. Possible processes driving this change include: the littoral drift processes and/or wave dynamics, primarily wave energy and wave direction. Hydraulic stability of the inlet was assessed by identifying the following parameters: tidal prism, inlet cross-sectional area, peak velocities, shear stresses, and discharges throughout the inlet gorge. Outcomes of a Ω/M_{total} ratio analysis and HUME AND HERDENDORF's (1986) area-prism relationship, both indicate that the inlet is tending towards deposition, while analysis of stability shear stress criteria indicated that the inlet is in a shoaling mode. Actual bottom shear stresses ranged from 2.92 Nm^{-2} to 1.88 Nm^{-2} during ebb and flood tides respectively, while the equilibrium shear stress for the inlet was calculated as 2.15 Nm^{-2}.

7.1.4 Wave Energy Focusing Upon Pukehina Beach and Nearshore Littoral Drift

Directional current meters were deployed offshore from Newdicks Beach and Pukehina Redoubt at 16 m water depth (relative to MSL). Results indicated that Pukehina Redoubt recorded larger wave heights than simultaneously collected data at Newdicks Beach (approximately 0.1 m larger). Differences were also noticed between wave approach directions. Data collected offshore from Newdicks Beach, tends to approach from a more westerly direction than offshore from Pukehina Redoubt. The difference may be explained by differing bathymetry surrounding each instrument

location, thereby causing wave refraction and altering the wave approach direction. The ebb tidal delta, nearby the Newdicks Beach directional current meter, and wave sheltering from Motiti Island, are suggested as possible reasons as to why Newdicks Beach has smaller wave heights than Pukehina Redoubt.

Utilising the numerical model WBEND, a wave refraction assessment within the Pukehina coastal sector was undertaken to identify regions of wave energy focusing. Simulated outcomes suggest that wave focussing is occurring along shoreline regions of the Pukehina coastal sector. Specific focussing was noted in the lee of the ebb tidal delta, offshore from Waihi Estuary inlet. From a variety of scenarios (differing wave angles, wave heights, and wave periods) along the Pukehina coastal sector, higher wave energy (observed as increased wave height) at the shoreline was commonly observed at benchmarks 30, 29, 27 and 26a.

Nearshore littoral drift within the Pukehina coastal sector, simulated by the numerical model WBEND, was identified to be heading in an easterly direction. Net sediment transport rates obtained, within the Pukehina coastal sector (Pukehina-Otamarakau), was estimated to be approximately 22,000 m^3/year.

Assessing nearshore sediment transport rates between Okurei Point and Pukehina Redoubt identified a negative potential littoral drift gradient between Okurei Point and Waihi Estuary inlet. Implications of this indicate that an accumulation of sediments would be expected at Waihi Estuary inlet, however, some of this sediment is evidently lost to the Waihi Estuary (as chapter 4 identified). Between benchmarks 29 and 26 a positive potential littoral drift gradient was identified. This implies that benchmark 26 has a greater potential of sediment transport compared to benchmark 29. Outcomes suggested that approximately 7,000 m^3/year or 12 m^3/m is being 'sucked out' of the beach-nearshore sediment budget along Pukehina Beach. Implications of this, combined with wave energy focusing outcomes, demonstrate a potential long-term sediment deficit along Pukehina Beach.

From nearshore littoral drift simulation, Okurei Point illustrated limited influence of restricting sediment transport by means of a sheltering effect, as 14,591 m^3/year was provided as a potential sediment transport rate at the apex of Okurei Point. However,

PHIZACKLEA (1993) did comment that sediment transport around Okurei Point was restricted during his survey, therefore differing wave approach directions used in simulations, may result in changes in sediment transport rates.

7.1.5 Integrated Sediment Budget and Ocean-Atmosphere Cyclic Patterns

An integrated sediment budget for the Pukehina coastal sector was calculated to identify major components, which are significant to the erosion of the frontal dune of Pukehina Beach. An assessment of ocean-atmosphere interactions was also undertaken, in order to ascertain whether they influence the sediment budget.

Outcomes of the integrated sediment budget illustrated that the Pukehina coastal sector had a net erosion rate of approximately 4,500 m^3/year or -0.5 m^3/m per year. This value is considerably smaller than estimates made by HODGES AND DEELY (1997), who estimated an annual rate of erosion of 10 m^3/m, however, the summation of involved errors illustrated that the rate of erosion obtained could be larger.

Components that were identified as significant loss of sediment to the Pukehina coastal sector were: nearshore littoral drift, infilling of Waihi Estuary, and aeolian transport. Nearshore sediment transport into the Pukehina coastal sector was estimated as approximately 14,500 m^3/year, while sediment transport out of the sector was estimated as approximately 24,600 m^3/year. In regard to Waihi Estuary, the net sediment transfer was estimated as -1620 m^3/year. Sediment loss due to aeolian transport of dune sediments was estimated as 600 m^3/year.

The El Niño Southern Oscillation (ENSO) and the Inter-Decadal Pacific Oscillation (IPO) were assessed to identify what influences each may cause to the volume of available beach sediment within Pukehina coastal sector. An assessment of historical beach profile excursion distances and years of known severe ENSO events was undertaken, but outcomes indicated no relationship between ENSO and erosion of the Pukehina coastal sector. Further, an assessment of the correlation between the Southern Oscillation Index (SOI) and beach profile volumes (m^3/m) for representable Pukehina Beach sites was undertaken. Likewise outcomes illustrated little to no correlation. Therefore, from available data within the Pukehina coastal sector, ocean-

atmosphere interactions are not suggestive to influence the volume of available sediment, thereby discrediting the calculated integrated sediment budget.

7.2 Coastal Management Options Available for Eroding Beaches

The US ARMY CORPS OF ENGINEERS (1984, p. 5-1) state that coastal engineering problems may be classified into four general categories: shoreline stabilisation, backshore protection (from waves and storm surges), inlet stabilisation, and harbour protection. A coastal problem may fall into multiple categories. Figure 7.1 illustrates the classification of coastal engineering problems, and possible structural, and/or management procedures, to remediate or reduce the coastal problem.

7.3 Public Perception

Whilst undertaking this study, many local inhabitants and holidaymakers have expressed their concerns about the frontal dune erosion at Pukehina Beach. Locals have differing opinions about what they perceive causes enhanced frontal dune erosion within the Pukehina coastal sector, and about what should be done to minimise or impede the rate of retreat. Some believe that the beach should be left to the forces of nature and no intervention should be undertaken. Others, however, believe that protection measures should be implemented to prevent further retreat.

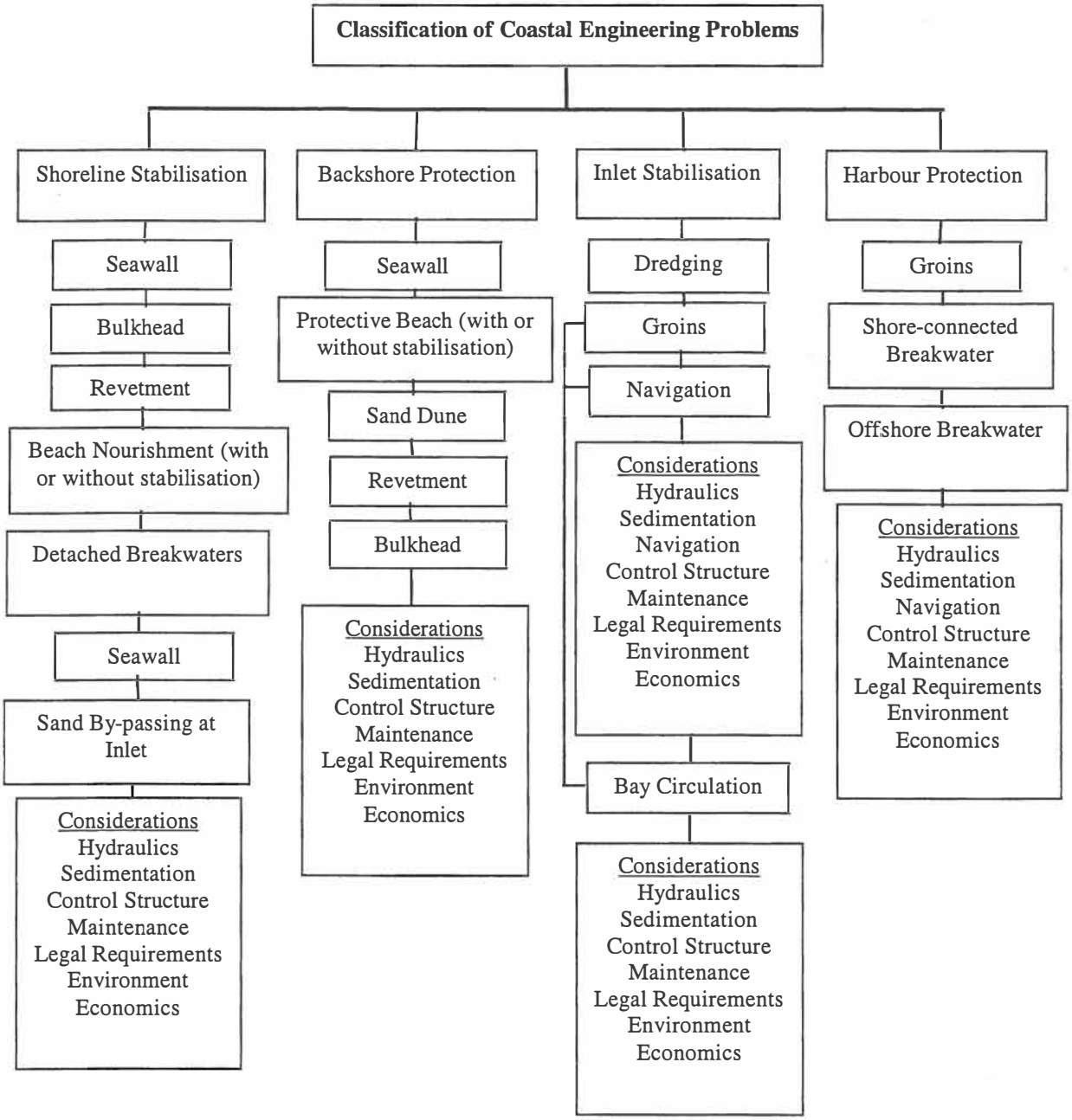

Figure 7.1 General classification of coastal engineering problems, and structural and/or management procedures, to remediate or reduce the coastal problem (Source: US ARMY CORPS OF ENGINEERS (1984)).

Protection of houses, land, and effort that has gone into properties, as well as substantial amounts of capital investment, are the primary reasons given to implement coastal protection measures.

A common perception from many local residents is that sand extraction, either the commercial operation at Otamarakau, or from the canals, which enter Waihi Estuary, are a significant cause of coastal erosion within the Pukehina sector. However, as already presented in chapters 3, 4, 5, and 6, other processes also implicate erosion eg. wave dynamics and energy concentrations, sediment transport patterns, and Waihi Estuary acting as a sediment sink.

7.3.1 Local Iwi

As stated by the RESOURCE MANAGEMENT ACT (1991), consultation of the local iwi must be carried out at each stage of developments.

The local iwi (Ngati Makino), regard the coast as a region with high important, as the oceans are said to provide for the iwi's life supporting capacity both physically and spiritually. It is therefore, Ngati Makino's best wishes that protection measures should be implemented within the Pukehina coastal sector (MS TAKIURA, *pers. comm.* (2002) (local citizen of Ngati Makino)). However, adversely the local iwi believe that remediation, may also influence an increase of holidaymakers to the Pukehina coastal sector, which could deplenish resources of the area, in particular the shellfish population (MS TAKIURA, *pers. comm.* (2002)).

In regard to Ngati Makino, shellfish present within the Waihi Estuary is of high importance, therefore conservation of this resource is a main concern when altering the coastal dynamics (MS TAKIURA, *pers. comm.* (2002).

A concern within the Ngati Makino is where materials for erosion protection structures might be sourced. An example is rocks used for the construction of a revetment. Ngati Makino believes that it is inappropriate to bring rocks sourced from the lands of another iwi into theirs without the consent of that iwi.

7.4 Initial Ideas on Possible Remedial Solutions

With any coastal measure suggested to restrict coastal erosion, numerical modelling of coastal processes is required. Direction and rates of current flows, wave generated sediment transport and other such processes in the region, must be first understood in order to test the sustainability of coastal measure. Since all coastal processes have not been identified at Pukehina Beach, the remedial solutions identified in the following are only to be considered as initial ideas, but are based from outcomes obtained during this study.

7.4.1 Stabilisation of the Distal End of Pukehina Spit

Chapter 4 analysed Waihi Estuary and the possible sediment dynamics within the estuary, and its implication towards the sediment budget of Pukehina coastal sector. Results strongly indicate that Waihi Estuary is acting as a sediment sink, furthermore the distal end of Pukehina Spit is illustrated by calculations and visual observations to be in a state of geomorphic and hydraulic instability. This may lead to possible sediment transport from the distal end of the spit into the estuary. Stabilisation of the distal end of Pukehina Spit may cause sediment that is possibly being lost, to remain deposited on the spit, therefore, increasing the volume of sediment at the distal end of Pukehina Spit. By installing a structure such as a fish tail groin on the Pukehina Spit, stabilisation of sediments could be achieved. On the western side of the inlet (Okurei Point side) a jetty could be constructed to trap sediment from the littoral drift system, thereby increasing the sediment volume along Newdicks Beach. The structures may also encourage scour of sediment in the Waihi Estuary inlet, due to the restriction of sediment being deposited into the inlet from the distal end of the spit and littoral drift system. This would benefit local boat users, as accessibility of using Waihi Estuary as an exit and entrance to the open ocean could be increased more than the current two-hours either side of high tide, which is current practice. The probability of sediment scour within the estuary inlet, reaching shellfish beds at Waihi Estuary is unlikely, due to location of these beds away from the main currents. The jetty towards the seaward end must be placed strategically. If the jetty were to be placed too far seaward, the distal end of Pukehina Spit may scour due to starvation of sediment, as inferred by the sediment transport direction (as discussed in chapter 5). However,

further to consideration of such a solution, the concept would need to be subject to further study including fine scale sediment transport and hydrodynamic modelling. Figure 7.2 illustrates, the implementation of both structures, in order to stabilise, and restrict sediment loss into the Waihi Estuary.

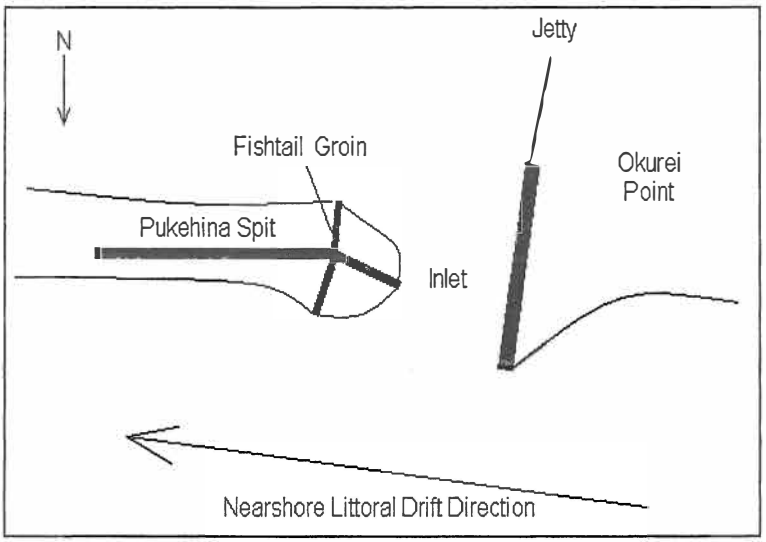

Figure 7.2 Illustration of a structure such as a fishtail groin and a jetty, which may be utilised to stabilise the distal end of Pukehina Spit.

7.4.2 Dune and Backshore Zone Protection Measures from Wave Action

Structures such as seawalls or revetments are often used to protect dunes and/or the backshore zone. Each protection management option has its positive and negative attributes. One positive quality of a seawall is they have been proven to succeed in protecting the land beyond the seawall, in differing coastal environments worldwide (PLANT AND GRIGGS, 1992; KRAUS AND MCDOUGAL, 1996; TWU AND LIAO, 1999). Negative qualities, however, are that like most structural protection measures, they do require ongoing maintenance. Seawalls also have been stated as being aesthetically unpleasing to the public, as suggested by T. HEALY, *pers comm.* (2002), in regard to the seawall presently at Waihi Beach, Bay of Plenty.

Seawalls have caused debate in past years. Vertical seawalls have been investigated as possible causes of sediment scour at the base of the structure, by means of wave reflection from the seawall (MILES *et al.* 2001) and also end scour (PLANT AND GRIGGS, 1992; KRAUS AND MCDOUGAL, 1996). TWU AND LIAO, (1999) suggest that

the utilisation of a sloping seawall may reduce scour at the front of the seawall, as wave energy can be dissipated and wave reflection reduced. However, a sloping seawall at Waihi Beach has not reduced scour at the front of that seawall (T. HEALY, *pers comm.*, 2002).

PLANT AND GRIGGS (1992) and KRAUS AND MCDOUGAL (1996) both discuss end scour as being due to water being held for a longer durations at the ends of seawalls than at the front, and thereby, water depth is increased as incoming waves meet the seawall. Water is then released as backwash in a large volume, which subsequently has potential to cause erosion of sediments.

From wave focussing analysis (chapter 5), wave heights (under modelled wave conditions) increased at locations along the shoreline of the Pukehina coastal sector. Specifically, wave heights were increased at benchmark locations 30, 29, 27, 26a and 26. Utilising this data, coastal protection measures, such as seawalls or revetments, could be constructed at these locations to minimise future enhanced frontal dune erosion.

7.4.3 Groin Fields

Groins are commonly implemented in regions with a high longshore sediment transport rate. Sediments that are transported by littoral drift are trapped by the structure, which extends seaward, perpendicular to the shoreline (approximately 40-60% of the average surf zone width), thereby moving the shoreline seaward (KOMAR, 1998). From nearshore sediment transport analysis (chapter 5), Pukehina Beach however, would not be categorised as having a high sediment transport rate, and therefore, if a groin field were to be considered, beach renourishment may also have to be part of the solution.

In general, a single groin is not enough, therefore, a groin field (a series of groins) is necessary (YÜKSEK *et al.*, 1995).

Laboratory studies have shown the optimal relationship between the groin length and the mutual distance (distance between two groins), is given as:

$$G/L \approx 1.75 \text{ to } 2.00 \qquad \text{Eqn 7.1}$$

where G is the groin length and G is the mutual distance between the two groins (YÜKSEK *et al.*, 1995).

The distance between the groins is, however, governed principally by the expected orientations of the fill in response to the changing wave directions (KOMAR, 1998).

YÜKSEK *et al.* (1995) also suggest that T or L shaped groins may be suitable, where the onshore-offshore sediment transport is dominant, rather that the longshore transport. Preventing the sediment to be transported to the offshore zones, these structures help sediment to keep deposited at the surf zone. This is a possible alternative for Pukehina Beach, if beach renourishment was not an option, as approximately net 7500 m^3/year was estimated to be transported onshore, via diabathic transport. In this case, the distance between the groins maybe larger, as wave orientation into the groin field is reduced ($G/L \approx 2.25$ to 2.5) (YÜKSEK *et al.*, 1995).

Depending on the magnitude of the protecting region, the sediment regime, and the nearshore beach slope, groin length may vary between 30-100 m (KOMAR, 1998).
Cost of a groin field is dependent on the option undertaken, and where source material is derived.

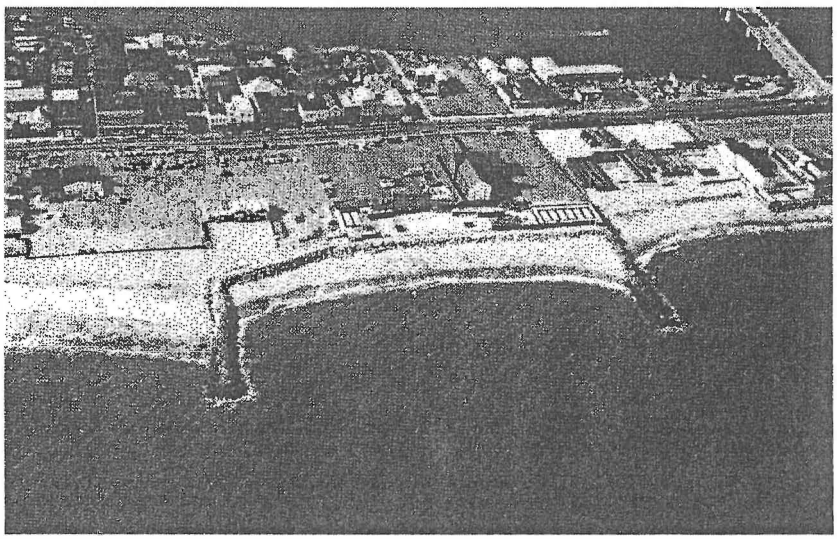

Figure 7.3 Groins at Seabright, New Jersey, which are designed to trap sand in order to build out a beach that provides protection to the coastal developments. Photo: KOMAR (1998).

7.4.4 Artificial Surfing Reefs

The implementation of an artificial surfing reef is both beneficial as a coastal erosion management option, and as a focus of increased recreational activity. RENNIE *et al* (1998, p. 9) identified both positive and negative social aspects of an artificial surfing reef to a community, proposed at Mount Maunganui, Bay of Plenty. Such aspects are listed below:

- Increased traffic movements.
- Increased pedestrian traffic over dune system, causing increased erosion.
- Increased litter.
- Increased cases of burglary and vandalism.
- Increased surfers profile.
- Increased scientific knowledge of the area and performance of the reef.
- International recognition as a world-class surfing facility.
- Increased fishing and diving recreational facility.
- Safer swimming in the lee of the reef.
- Economic impacts, such as additional expenditure generated from users of the reef.
- Relocation of boating activities.

In regard to Pukehina Beach, the most promising aspect of offshore reefs, is that they can decrease the rate of coastal retreat by reducing wave energy at the shoreline in the lee of the reef.

Materials required to construct an artificial reef can vary. The artificial surfing reef proposed for Mount Maunganui, envisaged using a variety of materials including: old tyres, which could be bound together to form the bottom layer of reef, high strength geo-textile material, would could be utilised as an alternative to tyres, and offshore sediment (beyond closure depth, ~14 m), which could be bagged to construct the shape of the reef (MEAD *et al.* 1998). Cost of construction of an artificial surfing reef is obviously dependent on the materials used, and the location of these source materials. However, as an estimate, approximately $3-5 million Australian is expected to be spent in the construction of the Narrowneck artificial surfing reef in Australia,

utilising geo-textile bags filled with sediment. Even though this expense is significant, an economic assessment indicated that the project would return more than 60 times the project cost (http://www.asrltd.co.nz/projectsgoldcoast.html).

Figure 7.4 Artificial surfing reef, offshore from Narrowneck Beach, Australia. Source: (http://www.asrltd.co.nz/projectsgoldcoast.html).

7.4.5 *Offshore Breakwaters*

An offshore breakwater functions to adjust the local littoral transport rate, modify local shoreline plan forms, limit erosion, provide protective recreational areas, and offer specific protection from wave attack (AHRENS AND COX, 1990). Breakwaters can be used in conjunction with other coastal structures to create a shore defence system. Aligned approximately parallel to the shoreline, breakwaters are designed to allow sediment transport between the structure and the shoreline, however, the beach in the lee of the structure is generally built out because of the structure's shadowing effect that reduces the wave energy and controls the pattern of wave refraction and diffraction (KOMAR, 1998).

Commonly breakwaters are designed as a series, in this formation they are often termed 'segmented breakwaters' or 'semi-detached breakwaters'. The gap distance between each breakwater is important in their design, together with the lengths of the breakwaters and the offshore distances. Breakwaters are typically 25-100 m long and are placed just offshore from the average width of the surf zone (KOMAR, 1998).

Breakwaters are commonly constructed from stone aggregate or concrete armoured units (VAN DER MEER AND HEYDRA, 1991). Some concern, however, has been focused

on the movement of the stone aggregate or concrete units, due to the waves breaking on the structure, and thereby, degrading the structure (AHRENS AND COX, 1990; VAN DER MEER AND HEYDRA, 1991). Stones must be tested for durability, as stones can vary from quarry to quarry, and also within a single quarry (AHRENS AND COX, 1990).

Generally there are three potential shoreline responses to a breakwater: a) the development of a tombolo with an attachment to the structure, b) the formation of a salient or cusp in the lee of the breakwater, but without attachment to the structure, or c) limited modification to the shoreline (KOMAR, 1998).

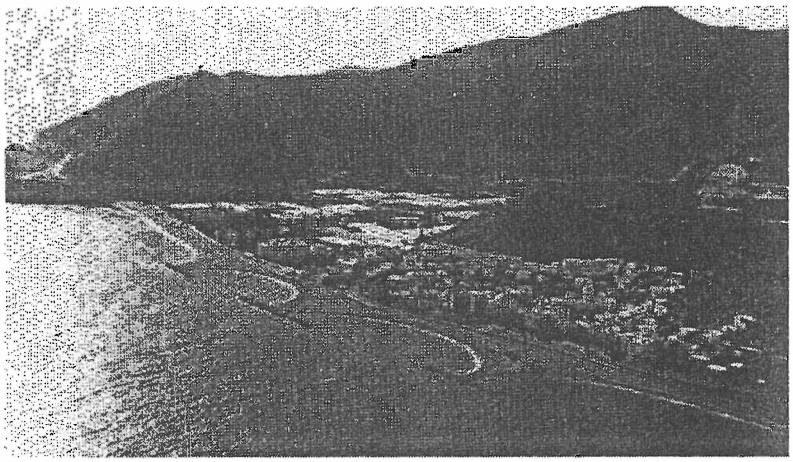

Figure 7.5 Detached breakwaters on the Mediterranean coast of Spain, the trapped sand having built out to the point where the beach is now attached to the breakwaters, forming tombolos. Photo: KOMAR (1998).

7.4.6 Beach Renourishment

KOMAR (1998, p. 500) states 'Beach renourishment involves the placement of large quantities of sand or gravel in the littoral zone to advance the shoreline seaward'. Sediment may also be placed directly onto the lower beach face, allowing wave action to distribute sediments accordingly, until an equilibrium beach profile is obtained.

Beach renourishment is a widely used method of coastal erosion management (VAN DE GRAAFF *et al.* 1991). Beach renourishment is also a favourable method of coastal erosion management among the local community, as it is the only form of shore protection that attempts to maintain a naturally appearing beach (KOMAR, 1998).

Sediment is commonly sourced from a different location than the eroding area, with 'sediment textural characteristics being coarser and more poorly sorted than the existing sediment of the eroded region' (SWART, 1991, p. 68).

At Omaha Beach, north of Auckland, sediments were dredged from the inner side of the adjacent tidal inlet gorge (HEALY *et al.* 1990). It was then pumped to the ocean, where it was emplaced by earth moving machinery. Similar methods could also be applied at Pukehina Beach. Waihi Estuary sediments were observed as having an overall larger sediment grainsize (chapter 4), than sediments from the adjacent coast (chapter 3), therefore, beach renourishment could be a realistic and viable option utilising these sediments. Sediments could either be pumped to the eroding shoreline, or by the utilisation of suction hopper dredge, which could transport the sediment to within the closure depth, allowing sediment to be transported onshore via wave processes.

If estuarine sediments could not be utilised, another alternative is to dredge existing sediment from outside of closure depth, and redeposit them inside the closure depth. This practice has been applied at Mount Maunganui Beach (FOSTER *et al.* 1994). A significant proportion of dredged sediments are sourced from the shipping channel to the Port of Tauranga, but also sediments are dredged offshore and transported to 5 m water depth, where sediments are subsequently transported onshore under natural wave processes (FOSTER *et al.* 1994).

Cost of beach renourishment varies depending on the differing options utilised. However, as an estimate using data from renourishment of Mount Maunganui Beach during 1993, dredging of sediment from outside the closure depth, and redepositing of sediments inside the closure depth cost approximately \$5 per m^3. Pumping of sediments onto the adjacent coast cost more, approximately \$10 per m^3 (T. HEALY *pers comm.,* 2002).

7.4.7 Dune Stabilisation

Currently the Pukehina coastal sector experiences dune blowouts (HEALY *et al.* 1977). By planting vegetation, such as existing *Spinifex* in areas where dune blowouts are or have occurred, may reduce the potential for future dune blowouts to occur. Plant roots hold sediment particles (peds) together, thereby minimising the chance for dune blowouts to occur. The ability for dune vegetation to also catch sediment that is being transported by aeolian processes, is also an advantage for increased dune dimensions. Currently dune vegetation has been implemented in the Pukehina coastal sector, but it must be maintained BERGIN (1999).

BERGIN (1999) states that maintenance of dune vegetation must be immediate as re-exposure of dune sediment may prompt erosion to restart and induce exposure of root systems of surrounding vegetation, thereby increasing the potential of further death of vegetation.

Planting density of *Spinifex* is dependent on the potential for erosion in that area. From wave energy focusing investigations, locations benchmarks 30, 29, 27 and 26a indicate a higher potential for erosion, therefore, these areas must have plants spaced closer than areas elsewhere. BERGIN (1999) states plants should be placed 50-60 cm apart in areas of high potential for erosion, whereas areas less erosion, 1 m spacing may be adequate.

7.4.8 Dune Fencing

Dune fencing may be used to promote dune dimension growth by 'catching' sediment that is being transported by aeolian processes. A dune fence is commonly made from cloth, therefore, due to salt spray, perishing from sun exposure, and sometimes severe wind conditions, maintenance of dune fences must be regular.

Currently dune fencing is used in areas within the Pukehina coastal sector, however, areas such as the distal end of Pukehina Spit, dune fencing could be implemented as this may restrict sediment being transported into the Waihi Estuary by aeolian processes.

Figure 7.6 Dune fencing and dune vegetation, currently present at benchmark 26a.

7.4.9 Informing Locals and Visitors for the Need of Beach Conservation

Simply by informing locals and visitors to Pukehina Beach of beach conservation measures, may assist to or restrict the rate of frontal dune retreat. The use of signs, pamphlets, and media, can be utilised to provide public awareness. In particular, the frontal dune must be conserved, as the frontal dune protects houses from events such as storm surge. By requesting the public to use only signposted access ways to the beach, this will prevent people walking over the frontal dune, thereby causing damage to dune vegetation. Stairs and wooden paths to prevent no person walking over the frontal dune at all, is an ideal solution.

Figure 7.7 Dune conservation sign currently in place at Pukehina Beach, more of this type of public information needs to be undertaken to minimise or restrict current ongoing coastal retreat.

Figure 7.8 Stairs build at beach access pathways, must be promoted to the public to minimise dune instability.

Speaking with local residents of Pukehina Beach (such as Ms Takiura), informing the public of the issues and reasons as to why coastal erosion is occurring in the sector, will encourage residents to take better care of Pukehina Beach. MS TAKIURA, *pers comm.* (2002), however did comment that 'getting the message across to holidaymakers will be of greater concern, as most local resident of Pukehina, do know that the coastal sector is in an erosive state, but holidaymakers do not. Therefore these people will have more potential of causing damage to coastal sector'.

7.5 Future Research at Pukehina Beach and Waihi Estuary

This investigation of the Pukehina coastal sector, focused primarily at identifying both sedimentary and physical processes, which influence coastal erosion within the sector. Several aspects of this investigation were assessed in a broad context. However, more detailed analysis of some processes, is required for improved understanding of coastal erosion within the Pukehina coastal sector. Further research is recommended in the following aspects:

- Assessment of processes within the Waihi Estuary, including specifically hydrological surveys to identify sediment scour or accumulation zones and rates. Cores (approximately 1 m) should be undertaken, from which biogenic material such as shells could be C^{14} dated, thereby allowing accurate estimates of long-term sediment accumulation rates. Also numerical modelling of current and sediment transport processes could be assessed to calculate rates of sediment infilling.
- Identification of the causes of the fluctuations observed during the ebb tide at the sub-tidal flats, could be assessed.
- Reassessment of wave refraction processes including the influence of Motiti Island. The grid used in this study excluded Motiti Island, but it is perceived to modify wave approach directions at western Pukehina Beach. Accordingly sediment transport rates will likely be modified.
- Evaluation of the volume of available sediment to Pukehina Beach, which is present offshore. This can be obtained by sub-bottom seismic profiling and/or stratigraphic cores. The outcome would assist identification of other potential remedial solutions, other than those mentioned previously.

References

AHRENS, J.P. AND COX, J. 1990. Design and performance of reef breakwaters. *Journal of Coastal Research, Special Issue, 7.* 61-76.

ALLAN, R., LINDESAY, J. AND PARKER, D. 1996. *El Niño Southern Oscillation & Climate Variability.* CSIRO Australia. 405p.

ARENS, S.M. AND VAN KAAM-PETERS, H. M. E. AND VAN BOXEL, J. H. 1995. Air flow over foredunes and implications for sand transport. *Earth Surface Processes and Landforms,* 20, 315-332.

BELL, R.G. AND GORING, D.G. 1996. Techniques for Analysing Sea level Records around New Zealand. *Marine Geodesy*, 19, 77-98.

BELL, R.G. AND GORING, D.G. 1998. Seasonal variability of sea level and sea-surface temperature on the northeast coast of New Zealand. *Estuarine, Coastal and Shelf Science*, 46, 307-318.

BERGIN, D. 1999. *Spinifex on coastal sand dunes: guidelines for seed collection, propagation and establishment.* New Zealand Forest Research Institute Limited, 28p.

BEST, T.C. AND GRIGGS, G.B. 1991. The Santa Cruz littoral cell: difficulties in defining a sediment budget. *Coastal Sediments '91,* A.S.C.E, 2262-2276.

BLACK, K.P. 1983. Sediment transport and tidal inlet hydraulics. Unpublished PhD thesis, Department of Earth Sciences, University of Waikato. 331p.

BLACK, K.P. 1994. Suspended sediment load during an asymmetric wave cycle over a plane bed. *Coastal Engineering*, 23, 95-114.

BLACK, K.P. AND HEALY, T.R. 1983. Northland forestry port Marsden Point, side scan survey. Unpublished report prepared for Northland Harbour Board. 88p.

BLACK, K.P. AND HEALY, T.R. 1988. Formation of rippled bands in a wave-convergence zone. *Journal of Sedimentary Petrology*, 58 (2), 195-207.

BLACK, K.P., OLDMAN, J.W. AND HUME, T.M. 1998. Mangawhai-Pakiri Sand Study. Module 5: Technical Report. Numerical Modelling. Prepared for the working party, ARC Environment, Auckland Regional Council. 66p.

BLACK, K.P. AND ROSENBERG, M.A. 1992. Semi-empirical treatment of wave transformation outside and inside the breaker line, *Coastal Engineering*, 16, 313-345.

BLACK, K.P. AND ROSENBERG, M.A. 1994. Suspended sand measurements in a turbulent environment : field comparison of optical and pump sampling techniques. *Coastal Engineering*, 24, 137-150.

BOPRC, 1991. Bay of Plenty Council Coastal Overview Report. BOPRC Technical Publication No.3. 98p.

BRADSHAW, B.E. 1991. Nearshore and inner shelf sedimentation on the East Coromandel Shelf, New Zealand. Unpublished PhD Thesis. Department of Earth Sciences, University of Waikato. 565p.

BRENSTRUM, E. 1994. Coastal Wind Patterns Revealed by Hourly Reports from a Ship at Sea. *Weather and Climate*, 14, 16-23.

BRUERE, A.C. 1994. Maketu and Waihi Estuaries classification. Bay of Plenty Regional Council, 23p.

BRUUN, P. 1978. *Stability of tidal inlets*. Elsevier Scientific Publishing Company. 506p.

BRUUN, P. AND GERRITSEN, F. 1960. *Stability of tidal inlets*. Amsterdam, North Holland Publishing Co., 123p.

BURTON, J.H. 1987. Tidal Inlet Hydraulics and Stability of Maketu Estuary. Unpublished MSC thesis, Department of Earth Sciences, University of Waikato. 233p.

BURTON, J.H AND HEALY, T.R. 1985. Tidal Inlet Hydraulics and Stability of the Maketu Inlet, Bay of Plenty. *Proceedings 7th Australasian Conference on Coastal and Ocean Engineering,* Christchurch, 139-150.

CARRANZA-EDWARDS, A. C. 2001. Grain size and sorting in modern beach sands. *Journal of Coastal Research* ,17 (1), 38-52.

DAVIES, J.L. 1977. *Geographical variation in coastal development.* Longman Group LTD. 204p.

DE LANGE, W.P. 1988. Wave climate and sediment transport within Tauranga Harbour, in the vicinity of Pilot Bay. Unpublished Ph.D. thesis. Department of Earth Sciences, University of Waikato. 225p.

DE LANGE, W.P. 1991. Wave climate for No 1. Reach, Port of Tauranga, Tauranga Harbour. Report to the Port of Tauranga Ltd. Marine Geosciences Group, University of Waikato, New Zealand. 18p.

DE LANGE, W.P. 1993. Extremal Significant Wave Analysis: Entrance to Tauranga Harbour. Report to the Port of Tauranga Ltd. Marine Geosciences Group, University of Waikato, New Zealand. 6p.

DE LANGE, W.P. 1996. Storm Surges on the New Zealand Coast. *Tephra*, 15 (1), 24-31.

DE LANGE, W.P. 2001. Inter-decadal Pacific Oscillation (IPO): a mechanism for forcing decadal scale coastal change? *Journal of Coastal Research Special Issue, 34.* 657-664.

DE LANGE, W., BLACK, K. AND HATTON, D. 1993. *Programs for the reduction and analysis of tidal data.* Victorian Institute of Marine Science, East Melbourne, Australia. 50p.

DE LANGE, W.P. AND GIBB, J.G. 2000. Seasonal, interannual, and decadal variability of storm surges at Tauranga, New Zealand. *New Zealand Journal of Marine and Freshwater Research,* 34, 419-134.

DE LISLE, J.F. AND KERR, I.S. 1963. The Climate and Weather of the Bay of Plenty Region. N.Z Met. S. Misc. Pub. 115 (1). 8p.

DINGMAN, S.L. 1994. *Physical Hydrology*, Prentice-Hall Inc. 575p.

DOLAN, T.J., CASTENS, P.G., SONU, C.J. AND EGENSE, A.K. 1987. Review of sediment budget morphology: Oceanside littoral cell, California. *Coastal Sediments '87.* A.S.C.E, 1289-1304.

DOMIJAN, N. 2000. The hydrodynamic and estuarine physics of Maketu Estuary. Unpublished PhD thesis, Department of Earth Sciences, University of Waikato. 408p.

DOMIJAN, N., BLACK, K.P. AND HEALY, T.R., 1997. Current measurements and an event of wind forcing at sub-tidal frequencies in the shallow Maketu Estuary. *Combined Australasian Coastal Engineering and Ports Conference*, Christchurch, 661-666.

DUNN, A.S. 2001. Coastal erosion at Wainui Beach, Gisborne. Unpublished MSc thesis, Department of Earth Sciences, University of Waikato. 244p.

DYER, K.R. 1973. *Estuaries: A physical introduction.* John Wiley & Sons Ltd. 140p.

EBERSOLE, B.A., CIALONE, M.A. AND PRATER, M.D. 1986. Regional coastal processes numerical modelling system, Report 1, A linear wave propagation model for engineering use. Technical report CERC-86-4, CERC, Department of the Army, WES, Corps of Engineers, Vicksburg, Mississippi.

EPPS, W.R. 1987. The influence of headland alignment on the plan shape of modelled zeta-formed beaches. *Australian Geographical Studies*, 25 (2), 47-53.

FLINT, S.B. 1998. Sediment trapping in the nearshore coastal environment. Unpublished MSc Thesis. Department of Earth Sciences, University of Waikato. 196p.

FOLK, R.L. 1968. *Petrology of sedimentary rocks.* Austin, Texas. Hemphills. 170p.

FOSTER, G.A. 1991. Beach nourishment from a nearshore dredge spoil dump at Mount Maunganui Beach. Unpublished MSc Thesis. Department of Earth Sciences, University of Waikato. 138p.

FOSTER, G.A., HEALY, T.R. AND DE LANGE, W.P. 1994. Sediment budget and equilibrium profiles applied to renourishment of an ebb tidal delta adjacent beach, Mt Maunganui, New Zealand. *Journal of Coastal Research*, 10 (3), 546-575.

FREDSØE, J. AND DEIGAARD, R. 1992. *Mechanics of coastal sediment transport.* World Scientific. 369p.

GOLDEN SOFTWARE INC. 1997. SURFER32 version 6.04 handbook. Golden Software Inc. 493p.

GORDON, D.A. 1993. A Holocene sediment budget for the Waitemata Harbour. Unpublished MSc thesis, Department of Earth Sciences, University of Waikato. 190p.

GORDON, N.D. 1985. The Southern Oscillation: a New Zealand perspective. *Journal of the Royal Society of New Zealand*, 15, 137-155.

HALL, A.R., TITCHMARSH, B.R., NGAPO, N.I., DONALD, L.A., PARK, S.G. AND MCINTOSH, J.I. 1993. Waihi Estuary Catchment Management Strategy. Bay of Plenty Regional Council, Operations Report Number 93/2.

HALLERMEIER, R.J. 1981. A profile zonation for seasonal sand beaches from wave climate. *Coastal Engineering* 4, 253-277.

HARMS, C. 1989. Dredge spoil disposal from an inner shelf dumpground. Unpublished MSc Thesis. Department of Earth Sciences, University of Waikato. 162p.

HARRIS, T.F.W. 1985. North Cape to East Cape, Aspects of Physical Oceanography. University of Auckland, Department of Physics and Marine Laboratory, Leigh, 178p.

HAY, D.N., 1991. Storm and oceanographic databases for the Western Bay of Plenty. Unpublished MSc thesis, Department of Earth Sciences, University of Waikato. 209p.

HAY, D.N., DE LANGE, W.P., AND HEALY, T.R. 1991. Storm and oceanographic databases for the Western Bay of Plenty. *Coastal Engineering – Climate for Change. Proceedings of the 10th Australasian Conference on Coastal and Ocean Engineering, Auckland.* 147-152.

HEALY, J. SCHOFIELD, J.C. AND THOMPSON, B.N. 1964. Sheet 5 Rotorua (1st ed). *Geological map of New Zealand*, 1:250,000. D.S.I.R., Wellington, New Zealand.

HEALY, T.R. 1974. The equilibrium beach: a model for real estate development and management of the coastal zone in the northeast of New Zealand. *Proceedings of the International Geographical Union Regional Conference and Eighth New Zealand Geography Conference.* 319-324.

HEALY, T.R. 1978a. Beach surveys 1977-78. Bay of Plenty Coastal Survey Report 78/2. 37p.

HEALY, T.R. 1978b. Nearshore hydrographic survey of beach bars. Bay of Plenty Coastal Survey Report 78/3. 38p.

HEALY, T.R. 1978c. Some Textural and Mineralogical Investigations of the Rangitaiki Plains Foreshore and River Sands. Bay of Plenty Coastal Erosion Survey Report 78/4. Bay of Plenty Catchment Commission. 74p.

HEALY, T.R. 1980. Erosion and sediment drift on the Bay of Plenty coast. *Soil and Water.* August 1980, 12-15.

HEALY, T.R. 1983. Assessment of the stability and natural hazard risk of the Whakatane Spit and inlet in relation to proposed marina development and environmental assessment of the sediment and hydrological aspects of the marina development. A report to the Whakatane District Council, 73p.

HEALY, T.R., 1987. The importance of wave focussing in the coastal erosion and sedimentation process. *Coastal Sediments '87.* A.S.C.E., 1472-1485.

HEALY, T.R., HARRAY, K.G., AND RICHMOND, B. 1977. *The Bay of Plenty Coastal Erosion Survey.* Occasional Report 3. Department of Earth Sciences, University of Waikato, 64p.

HEALY, T.R., KIRK, R.M., AND DE LANGE, W.P. 1990. Beach renourishment in New Zealand. *Journal of Coastal Research, Special Issue, 6*, 77-90.

HEALY, T.R. AND DEAN, R.G. 2000. Methodology for delineation of coastal hazard zones and development setback for open duned coasts. *In: Handbook of Coastal Engineering*, edited by HERBICH, J. B. McGraw-Hill.

HEEZEN, B.C. AND HOLLISTER, C.D. 1971. *The face of the deep.* Oxford University Press. 659p.

HICKS, D.M. AND HUME, T.M. 1993. Shelf morphology and processes near an ebb tidal delta, Katikati Inlet, New Zealand. *Proceedings of the 16th Australasian Conference on Coastal and Ocean Engineering*, 319-324.

HILTON, M.J. 1990. Processes of sedimentation in the shoreface and continental shelf, and the development of facies, Pakiri, New Zealand. Unpublished D.Phil. thesis, Geography Department, University of Auckland. 322p.

HODGES, S. AND DEELY, J., 1997. Coastal Monitoring Program Summary to 1992-1996. Environment BOP, Environmental Report 97/3. 53p.

HSU, T. AND WANG, H. 1997. Geometric characteristics of storm beach profiles. *Journal of Coastal Research,* 13 (4), 1102-1110.

HSU, T.W. AND WEN, C.C. 2001. A parabolic equation extended to account for rapidly varying topography. *Ocean Engineering* 28 (11), 1479-1498.

HUME, T.M., BLACK, K.P., OLDMAN, J.W., AND VENNELL, R. 1997. Signatures of wave and current forcing on the seabed about a large coastal headland. *Pacific Coasts and Ports, New Zealand Coastal Society Conference, Christchurch, New Zealand 7th - 11th*, 319-324.

HUME, T.M. AND HERDENDORF, C.E. 1986. Tidal inlet stability: proceedings of a workshop. *Water and Soil Miscellaneous Publication 108,* National Water and Soil Conservation Authority, Wellington. 80p.

HUTT, 1997. Bathymetry and wave parameters defining the surfing quality of 5 adjacent reefs. Unpublished MSc thesis, Department of Earth Sciences, University of Waikato. 170p.

INTEROCEAN SYSTEMS, INC. 1990. S4 Current Meter, Users Manual. Copyright InterOcean Systems, Inc., 90p.

JENNINGS, J.N. 1955. The influence of wave action on coastal outline in plan. *The Australian Geographer*, 6 (4), 36-44.

KANA, T. W. 1978. Surf zone measurements of suspended sediment. *Proceedings of the 16th Coastal Engineering Conference*, 1725-1743.

KING, C.A.M. 1972. *Beaches and Coasts.* Edward Arnold Publishers LTD. 570p.

KIRBY, J.T. AND DALRYMPLE, R.A. 1991. Users Manual, combined refraction/diffraction model, Ref/Dif-1, Version 2.3. Centre for Applied Coastal Research, Department of Civil Engineering, University of Delaware, Newark.

KOMAR, P.D. 1976. *Beach Processes and Sedimentation.* 1st Edition. Prentice-Hall. 429p

KOMAR, P.D. 1998. *Beach Processes and Sedimentation.* 2nd Edition. Prentice-Hall. 544p.

KOMAR, P.D. AND INMAN, D.L. 1970. Longshore sand transport on beaches. *Journal of Geophysical Research* 75(30), 5914-5927.

KRAUS, N.C. AND MCDOUGAL, W.G. 1996. The effects of seawalls on the beach: Part I, an updated literature review. *Journal of Coastal Research*, 12 (3), 691-701.

LARSON, R., MORANG, A., AND GORMAN, L. 1997. Monitoring the Coastal Environment; Part II: Sediment sampling and geotechnical methods. *Journal of Coastal Research,* 13 (2), 311-327.

LOOMB, C.A.M. 2001. Muddy sedimentation in a sheltered estuarine marina, Westpark Marina, Auckland. Unpublished MSC thesis, Department of Earth Sciences, University of Waikato. 228p.

MAA, J.P.-Y., HSU, T,-W, TSAI, C.H. AND JUANG, W.J. 2000. Comparison of wave refraction and diffraction models. *Journal of Coastal Research*, 16 (4), 1073-1082.

MAA, J.P.-Y, AND HWUNG, H.-H. 1997. A transformation model for harbour planning. *Proceedings, 3rd International Symposium on Ocean Wave Measurement and Analysis.* WAVES 97. 256-270.

MAA, J.P.-Y., HWUNG, H.-H. and HSU, T.-W. 1998. A simple wave transformation model, PBCG, for harbour planning. *Proceedings of the 3rd International Conference on Hydrodynamics.* Seoul, Korea: UIAM Publishers, 1, 407-412.

MADSEN, P.A. AND LARSEN, J. 1987. An efficient finite-difference approach to the mild-slope equation. *Coastal Engineering,* 11, 329-351.

MATHEW, J. 1997. Morphologic changes of tidal deltas and an inner shelf dump ground. Unpublished PhD thesis, Department of Earth Sciences, University of Waikato. 351p.

MCLAREN, P. 1981. An interpretation of trends in grain size measures. *Journal of Sedimentary Petrology,* 51 (2), 611-624.

MCLAREN, P. AND BOWLES, D. 1985. The effects of sediment transport on grainsize distributions. *Journal of Sedimentary Petrology,* 55 (4), 457-470.

MEAD, S.T., BLACK, K.P. AND HUTT, J.A. 1998. Application for resource consent for a coastal structure at Tay Street-Mount Maunganui Beach. Report 1, Reef design and physical and biological processes. The Artificial Reefs Program, Department of Earth Science, University of Waikato and National Institute of Water and Atmospheric Research LTD, 106p.

MILES, J.R., RUSSELL, P.E. AND HUNTLEY, D.A. 2001. Field measurements of sediment dynamics in front of a seawall. *Journal of Coastal Research*, 17 (1), 195-206.

MONSERRAT, D.G.S. AND TINTORE, J. 1993. Pressure-forced seiches of large amplitude in inlets of the Balearic Islands. *Journal of Geophysical Research*, vol 98 (C8), 14. 14,437-14,445.

MOON, V.G. AND HEALY, T.R. 1994. Mechanisms of coastal cliff retreat and hazard zone delineation in soft flysch deposits. *Journal of Coastal Research*, 10 (3), 663-680.

MURRAY, K.N. 1978. Ecology and geomorphology of Maketu Estuary, Bay of Plenty. Unpublished MSc thesis, Department of Earth Sciences, University of Waikato. 146p.

NAIRN, I.A. 1975. Land Use Capability Assessment of the Kaituna River Catchment. Water and Soil Division. Ministry of Works and Development for The National Water and Soil Conservation Organisation, 32p.

NIEDORODA, A.W., SWIFT, D.J., HOPKINS, T.S. AND MA, C. 1984. Shoreface Morphodynamics on wave-dominated coasts. *Marine Geology*, 60, 331-354.

NIELSON, P. 1986. Suspended sediment concentrations under waves. *Coastal Engineering*, 10, 23-31.

PANG, L. 1993. Tarawera River Flow Analysis. Environmental Report 93-2. Environment Bay of Plenty, 102p.

PAPPS, D.A. AND PRIESTLEY, S.J. (1997) Engineering applications of the 'McLaren' sediment trend analysis. *Proceedings of the 13th Australasian Coastal and Ocean Engineering Conference and the 6th Australasian Port and Harbour Conference, Christchurch. Centre for Advanced Engineering, University of Canterbury*, 137–142.

PARK, S. 1995. Natural environment regional monitoring network coastal and estuarine ecology programme 1994/1995. Environment BOP, Environmental report 95/20, 155p.

PHIZACKLEA, D.J.D. 1993. Littoral sediment budget and beach morphodynamics, Pukehina Beach to Matata, Bay of Plenty. Unpublished MSc thesis, Department of Earth Sciences, University of Waikato. 322p.

PHIZACKLEA, D.J.D. 1999. Evidence of David Johnathon Dominac Phizacklea. Otamarakau Sand Extraction Appeal - Evidence to the Environmental Court 17 July 2000. *Unpublished Report*. 36p.

PICKETT V, HEALY T.R., AND DE LANGE W.P. 1997. Equilibrium Status of Beach Profiles on Bay of Plenty Beaches: Application of the Dean Profile for Coastal Hazard Identification. *Pacific Coasts and Ports, New Zealand Coastal Society Conference, Christchurch, New Zealand 7th – 11th*, 353-358.

PLANT, N.G. AND GRIGGS, G.B. 1992. Interactions between nearshore processes and beach morphology near a seawall. *Journal of Coastal Research*, 8 (1), 183-200.

POWELL, A.W.B. 1979. *New Zealand Mollusca.* William Collins Publishes Ltd, 500p.

QUAYLE, A.M. 1984. The Climate and Weather of the Bay of Plenty Region. N.Z Met. S. Misc. Pub. 115 (1) 2nd Edition.

QUINN, W.H. AND NEAL, V.T. 1987. El Niño occurrences over the past four and a half centuries. *Journal of Geophysical Research,* 92, 14449-14461.

RENNIE, H.G., MAKGILL, D. AND MAKGILL, C.A. 1998. An artificial offshore reef at Tay Street, Mount Maunganui. ANNEX III D: Consultation and social impact report. The Artificial Reefs Program, Department of Earth Science, University of Waikato and National Institute of Water and Atmospheric Research LTD, 19p.

RESOURCE MANAGEMENT ACT. 1991. *Resource Management Act.* Government of New Zealand. 382p.

REYNOLDS, W.J. 1987. Sediment budget analysis and interpretation. *Coastal Sediments '87.* A.S.C.E., 113-124.

RIDDLE, B.B. 2000. Side scan sonar mapping of surficial seafloor sediments in the outer Hauraki Gulf, New Zealand. Unpublished MSc thesis, Department of Earth Sciences, University of Waikato. 201p.

ROSATI, J.D., GRAVENS, M.B. AND SMITH, W.G. 1999. Regional sediment budget for Fire Island to Montauk Point, New York, USA. *Coastal Sediments '99.* A.S.C.E., 802-817.

SAUNDERS, H.A., 1999. Coastal processes influencing beach erosion at West End Ohope. Unpublished MSc thesis, Department of Earth Sciences, University of Waikato. 229p.

SMITH, G.L. AND ZARILLO, G.A. 1990. Calculating long-term shoreline recession rates using aerial photographic and beach profiling techniques. *Journal of Coastal Research*, 6 (1), 111-120.

SMITH, R.K. 1986. Sand resources of the beaches between Otamarakau and Matata and potential sites for sand mining. *Unpublished Report.* Water Quality Centre Consultancy Report, Ministry of Works and Development, Hamilton. 50p.

SMITH, R.K., 1999. Supplementary information regarding the application to mine beach sand at Otamarakau, Bay of Plenty. NIWA client report: PAT 80202/2. 21p.

SMITH, R.K., TURNER S.J., HALLIDAY N.J., AND OVERDEN R., 1997. Environment impact assessment of a proposed sand extraction program at Otamarakau. NIWA client report: PAT 80201/3. 57p.

SMITH, R.K. AND BENSON, A.P. 2001. Beach profiling monitoring: how frequent is sufficient? *Journal of Coastal Research Special Issue, 34,* 573-579.

SPERANSKI AND CALLIARI, 2001. Bathymetric lenses and localised coastal erosion in Southern Brazil. *Journal of Coastal Research Special Issue, 34,* 209-215.

STEPHENS, S.A. 1996. The Formation of Accurate Duneline Embayments at Waihi Beach, New Zealand. Unpublished MSc thesis, Department of Earth Sciences, University of Waikato. 91p.

STEPHENS, S.A. 2001. Wind, shelf-current and density-driven circulation in Poverty Bay, New Zealand. Unpublished PhD thesis, Department of Earth Sciences, University of Waikato. 320p.

STEPHENS, S.A., HEALY, T.R., BLACK, K.P. AND DE LANGE, W.P. 1999. Arcuate duneline embayments, infragravity signals, rip currents and wave refraction at Waihi Beach, New Zealand. *Journal of Coastal Research.* 15 (3), 823-829.

STURMAN, A.P. AND TAPPER, N.J. 1996, The Weather and Climate of Australia and New Zealand. Oxford University Press, 476p.

SUNAMURA, T. AND HORIKAWA, K. 1971. A study on the prevailing direction of littoral drift along the Kashiwazaki coast, Japan. Annual Report of the Engineering Research Institute. Faculty of Engineering, University of Tokyo. 30, 21-28.

SUNAMURA, T. AND HORIKAWA, K. 1972. An improved method for inferring the direction of littoral drift from grain size properties of beach sands. Annual Report of the Engineering Research Institute. Faculty of Engineering, University of Tokyo. 31, 61-68.

SWART, D.H. 1991. Beach renourishment and particle size. *Journal of Coastal Engineering,* 16 (1), 61-82.

THOMPSON, S. 1981. Fish of the marine reserve: A guide to the identification and biology of common fish of the north-eastern New Zealand. Leigh Laboratory, University of Auckland, 364p.

TITCHMARSH, B.R. 1992. Whakatane River Scheme, Middle Reaches Investigation. Bay of Plenty Regional Council. Technical Report Number 36, 24p.

TONKIN AND TAYLOR LIMITED. 1999. Technical appraisal of resource consent application: J.W. Paterson & Sons application to mine sand from Otamarakau Beach. Tonkin and Taylor, reference number: 50251. 33p.

TRENHAILE, A.S. 1997. *Coastal dynamics and landforms.* Clarendon Press, Oxford. 366p.

TRITON ELICS INTERNATIONAL, INC. 1988. Isis User's Manual. Triton Technology, Inc, California, USA, 310p.

TWU, S-W., AND LIAO, W-M. 1999. Effects of seawall slopes on scour depth. *Journal of Coastal Research,* 15 (4), 985-990.

US ARMY CORPS OF ENGINEERS, 1984. *Shore Protection Manual.* 4th edition. Department of Army Corps of Engineers, Virginia. U.S. Coastal Engineering Research Centre.

VAN DE GRAAFF, J., NIEMEYER, H.D., AND VAN OVEREEM, J. 1991. Beach renourishment, philosophy, and coastal protection policy. *Journal of Coastal Engineering,* 16 (1), 3-22.

VAN DE KREEKE, J. 1990. Can multiple tidal inlets be stable? *Estuarine, Coastal and Shelf Science,* 30, 261-273.

VAN DER MEER, J.W., AND HEYDRA, G. 1991. Rocking armor units: Number, location and impact velocity. *Journal of Coastal Engineering,* 15 (1-2), 21-40.

WEHRMANN, H. 2000, Lahar deposits and Tephrostratigraphy, Okurei Point, Bay of Plenty, New Zealand. Unpublished MSc thesis, Department of Earth Sciences, University of Waikato. 111p.

WILLIAMS, B.L. (1985), Ocean Outfall Handbook: A manual for the planning, investigation, design and monitoring of ocean outfalls to comply with water quality management objectives. *Water and Soil Miscellaneous Publication No. 76*. 218p.

YÜKSEK, Ö., ÖNSOY, H. BIRBEN, A.R. AND ÖZÖKER, I.H. 1995. Coastal erosion in Eastern Black Sea Region, Turkey. *Journal of Coastal Engineering*, 26 (2-3), 225-240.

World Wide Web Addresses

ASR LTD. 2002. http://www.asrltd.co.nz/projectsgoldcoast.html.

NOAA-CIRES CLIMATE DIAGNOSTICS CENTRE. 2002. http://www.cdc.noaa.gov/ENSO/enso.current.html

Appendix I

All GPS co-ordinates are in Bay of Plenty Circuit.

1.0 Benchmark GPS Co-ordinates

Benchmark	Easting	Northing
26	305975.46	696297.63
26a	305447.40	696697.10
27	305070.85	696983.48
27a	304001.18	697738.13
28	302691.73	698821.15
28a	302236.05	699222.04
29	301808.62	699663.63
30	300835.93	700811.23
30a	300351.72	701532.72

1.1 Video GPS Co-ordinates

Video Location	Easting	Northing	Water Depth (m)	Video Location	Easting	Northing	Water Depth (m)
1	303200	705500	28	7	309200	700900	30
2	300700	702200	6	8	308100	695900	10
3	305000	704100	28	9	312100	698700	29
4	304500	703100	22	10	312300	697600	27
5	305900	700700	20	11	310800	694100	10
6	304400	698900	10	12	315500	694800	24

1.2 Sediment Trap GPS Co-ordinates

Sediment Trap Site	Easting	Northing
Newdicks Beach	301290.77	701435.63
Pukehina Redoubt	309190.01	694769.38

1.3 Estuarine Depth-Current Meter GPS Co-ordinates

Estuarine Depth-Current Meter Site	Easting	Northing
Waihi Estuary Inlet	301293.71	700090.45
Waihi Estuary Sub-Tidal Flats	302257.16	698538.76

1.4 Estuary Core GPS Co-ordinates

Core Number	Northing	Easting	Core Number	Northing	Easting
1	700484.060	301026.220	9	698810.822	301703.565
2	700430.024	301052.335	10	698621.360	301411.643
3	700413.925	301075.978	11	698420.651	302302.186
4	700105.986	301161.970	12	698390.491	301652.788
5	699608.372	301441.471	13	698235.243	301934.041
6	699365.960	300790.288	14	698338.327	301210.423
7	699302.653	301636.472	15	699530.746	301091.170
8	698656.254	300684.662			

1.5 Wave Direction-Current GPS Co-ordinates

Wave Depth-Direction-Current Site	Easting	Northing
Newdicks Beach	302611.91	702004.16
Pukehina Redoubt	309586.34	695591.00

Appendix II

The following appendix can be obtained in the Appendix CD. Beach profiles are presented as Microsoft Excel files. Numerical data is presented as a spreadsheet defining each elevation and distance from the associated benchmark. A graphical illustration of the data is provided as a line graph, which can be viewed by pressing the chart tab in the lower left corner.

Appendix III

The following appendix can be obtained in the Appendix CD. Sieve analyses and sediment statistics for each sediment sample location, are presented as Microsoft Excel files. Numerical data is presented as a spreadsheet defining the weight of sediment, and cumulative weight at differing phi from the associated benchmark. Statistical information regarding the sediment sample is provided. Statistics are based from FOLK (1968). A graphical illustration of weight and cumulative percentages are provided as line graphs, which can be viewed by pressing the chart tab in the lower left corner.

Appendix IV

Sediment trend matrices for the SUNAMURA AND HORIKAWA (1972) model and the MCLAREN (1981) model, are illustrated. For the SUNAMURA AND HORIKAWA (1972) model, each matched pair of sediment sample consists of two values: mean grain size and sorting, relating the deposited sediment (at right) to the possible sediment source (top)

For the MCLAREN (1981) model, each matched pair of sediment sample consists of three values: mean grain size, sorting and skewness, relating the deposited sediment (at right) to the possible sediment source (top).

		Sediment Source									
		1	2	3	4	5	6	7	8	9	GSC
Sediment Deposit	1		Finer Better	Finer Better	Finer Better	Finer Better	Finer Better	Finer Better	Finer Better	Finer Better	M (Φ) SD (Φ)
	2	Courser Poorer		Courser Poorer	Finer Better	Finer Better	Finer Better	Finer Better	Finer Better	Finer Better	M (Φ) SD (Φ)
	3	Courser Poorer	Finer Better		Finer Poorer	Finer Poorer	Finer Poorer	Finer Poorer	Finer Poorer	Finer Poorer	M (Φ) SD (Φ)
	4	Courser Poorer	Courser Poorer	Courser Better		Finer Poorer	Finer Poorer	Finer Poorer	Finer Poorer	Finer Poorer	M (Φ) SD (Φ)
	5	Courser Poorer	Courser Poorer	Courser Better	Courser Better		Finer Poorer	Finer Better	Finer Poorer	Finer Poorer	M (Φ) SD (Φ)
	6	Courser Poorer	Courser Poorer	Courser Better	Courser Better	Courser Better		Courser Better	Finer Better	Finer Better	M (Φ) SD (Φ)
	7	Courser Poorer	Courser Poorer	Courser Better	Courser Better	Courser Poorer	Finer Poorer		Finer Poorer	Finer Poorer	M (Φ) SD (Φ)
	8	Courser Poorer	Courser Poorer	Courser Better	Courser Better	Courser Better	Courser Poorer	Courser Better		Finer Better	M (Φ) SD (Φ)
	9	Courser Poorer	Courser Poorer	Courser Better	Courser Better	Courser Better	Courser Poorer	Courser Better	Courser Poorer		M (Φ) SD (Φ)

Sediment trend matrix for the SUNAMURA AND HORIKAWA (1972) model.

		Sediment Source									
		1	2	3	4	5	6	7	8	9	GSC
Sediment Deposit	1		Finer Better +	Finer Better +	Finer Better +	Finer Better +	Finer Better +	Finer Better +	Finer Better +	Finer Better +	M (Φ) SD (Φ) Sk (Φ)
	2	Courser Poorer -		Courser Poorer -	Finer Better -	Finer Better -	Finer Better -	Finer Better -	Finer Better -	Finer Better +	M (Φ) SD (Φ) Sk (Φ)
	3	Courser Poorer -	Finer Better +		Finer Poorer -	Finer Poorer -	Finer Poorer -	Finer Poorer -	Finer Poorer -	Finer Poorer +	M (Φ) SD (Φ) Sk (Φ)
	4	Courser Poorer -	Courser Poorer +	Courser Better +		Finer Poorer -	Finer Poorer +	Finer Poorer -	Finer Poorer +	Finer Poorer +	M (Φ) SD (Φ) Sk (Φ)
	5	Courser Poorer -	Courser Poorer +	Courser Better +	Courser Better +		Finer Poorer +	Finer Better +	Finer Poorer +	Finer Poorer +	M (Φ) SD (Φ) Sk (Φ)
	6	Courser Poorer -	Courser Poorer +	Courser Better +	Courser Better -	Courser Better -		Courser Better -	Finer Better Same	Finer Better +	M (Φ) SD (Φ) Sk (Φ)
	7	Courser Poorer -	Courser Poorer +	Courser Better +	Courser Better +	Courser Poorer -	Finer Poorer +		Finer Poorer +	Finer Poorer +	M (Φ) SD (Φ) Sk (Φ)
	8	Courser Poorer -	Courser Poorer +	Courser Better +	Courser Better -	Courser Better -	Courser Poorer Same	Courser Better -		Finer Better +	M (Φ) SD (Φ) Sk (Φ)
	9	Courser Poorer -	Courser Poorer -	Courser Better -	Courser Better -	Courser Better -	Courser Poorer -	Courser Better -	Courser Poorer -		M (Φ) SD (Φ) Sk (Φ)

Sediment trend matrix for the McLaren (1981) model.

Appendix V

RSA analyses of sediment textural characteristics and settling velocity are presented in the following.

PARTICLE SIZE ANALYSIS

Earth Sciences - University of Waikato

Sample: Newdicks Beach 0.35m Deploy 1

Size distribution histogram

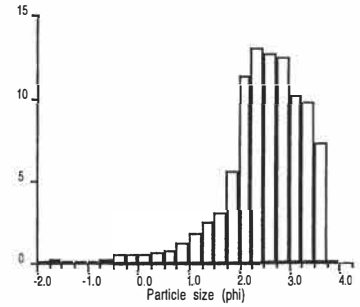

Cumulative frequency

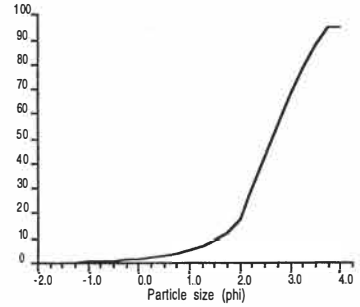

Cumulative frequency

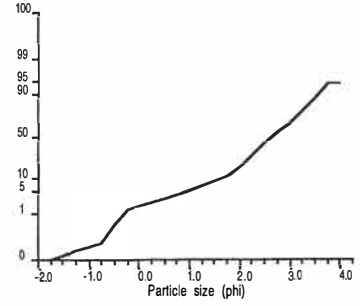

Results summary

Textural size classes

Gravel= 0.30% Sand= 94.45% Silt= 0.00% Clay= 0.00%

Gravel bearing detrital sediment

Slightly Gravelly Sand

Moment method parameters (phi)

Mean= 2.37 Sorting= 0.82Skewness= -0.86 Kurtosis= 5.21

Graphical method parameters (phi)

Mean= 2.66

Median= 2.65 C= -0.36 D35= 2.36 D65= 2.95

Textural description:

Raw data summary

Size (phi)	Size (mm)	Cumulative weight (g)	Interval frequency (%)	Cumulative frequency (%)
-1.75	3.3636	0.00	0.00	0.00
-1.50	2.8284	0.02	0.15	0.15
-1.25	2.3784	0.03	0.07	0.22
-1.00	2.0000	0.04	0.07	0.30
-0.75	1.6818	0.05	0.07	0.37
-0.50	1.4142	0.09	0.30	0.67
-0.25	1.1892	0.17	0.60	1.27
0.00	1.0000	0.24	0.52	1.80
0.25	0.8409	0.32	0.60	2.40
0.50	0.7071	0.42	0.75	3.15
0.75	0.5946	0.53	0.82	3.97
1.00	0.5000	0.69	1.20	5.17
1.25	0.4204	0.92	1.72	6.90
1.50	0.3536	1.25	2.47	9.37
1.75	0.2973	1.65	3.00	12.37
2.00	0.2500	2.39	5.55	17.92
2.25	0.2102	3.90	11.32	29.24
2.50	0.1768	5.64	13.04	42.28
2.75	0.1487	7.34	12.74	55.02
3.00	0.1250	9.00	12.44	67.47
3.25	0.1051	10.37	10.27	77.74
3.50	0.0884	11.67	9.75	87.48
3.75	0.0743	12.64	7.27	94.75
4.00	0.0625	12.64	0.00	94.75

Total weight = 13.34 g

PARTICLE SIZE ANALYSIS

Earth Sciences - University of Waikato

Sample: Newdicks Beach 0.5m Deploy 1

Size distribution histogram

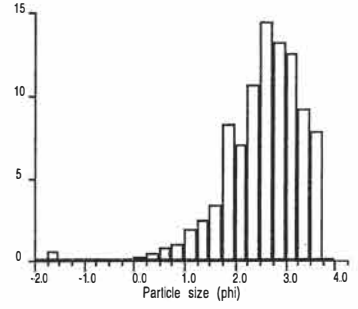

Cumulative frequency

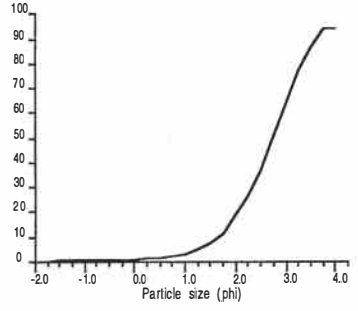

Cumulative frequency

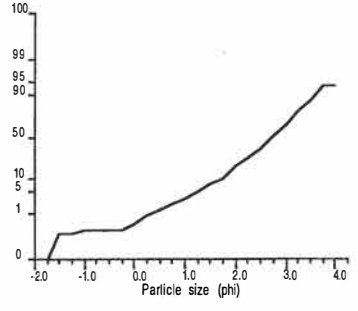

Results summary

Textural size classes

Gravel= 0.59% Sand= 93.57% Silt= 0.00% Clay= 0.00%

Gravel bearing detrital sediment

Slightly Gravelly Sand

Moment method parameters (phi)

Mean= 2.42 Sorting= 0.77Skewness= -0.83 Kurtosis= 6.44

Graphical method parameters (phi)

Mean= 2.69

Median= 2.73 C= 0.27 D35= 2.46 D65= 3.01

Textural description:

Raw data summary

Size (phi)	Size (mm)	Cumulative weight (g)	Interval frequency (%)	Cumulative frequency (%)
-1.75	3.3636	0.00	0.00	0.00
-1.50	2.8284	0.07	0.52	0.52
-1.25	2.3784	0.07	0.00	0.52
-1.00	2.0000	0.08	0.07	0.59
-0.75	1.6818	0.08	0.00	0.59
-0.50	1.4142	0.08	0.00	0.59
-0.25	1.1892	0.08	0.00	0.59
0.00	1.0000	0.09	0.07	0.67
0.25	0.8409	0.13	0.30	0.96
0.50	0.7071	0.19	0.44	1.40
0.75	0.5946	0.30	0.81	2.22
1.00	0.5000	0.43	0.96	3.18
1.25	0.4204	0.69	1.92	5.10
1.50	0.3536	1.02	2.44	7.54
1.75	0.2973	1.48	3.40	10.94
2.00	0.2500	2.60	8.28	19.22
2.25	0.2102	3.55	7.02	26.24
2.50	0.1768	4.99	10.64	36.88
2.75	0.1487	6.95	14.49	51.37
3.00	0.1250	8.74	13.23	64.60
3.25	0.1051	10.44	12.56	77.16
3.50	0.0884	11.68	9.16	86.33
3.75	0.0743	12.74	7.83	94.16
4.00	0.0625	12.74	0.00	94.16

Total weight = 13.53 g

PARTICLE SIZE ANALYSIS

Earth Sciences - University of Waikato

Sample: Newdicks Beach 0.8m Deploy 1

Size distribution histogram

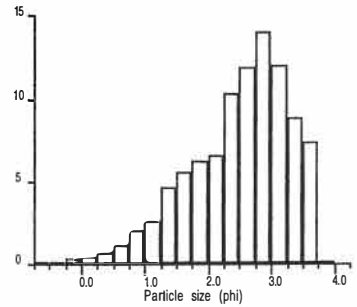

Cumulative frequency

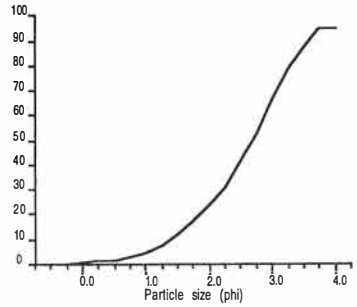

Cumulative frequency

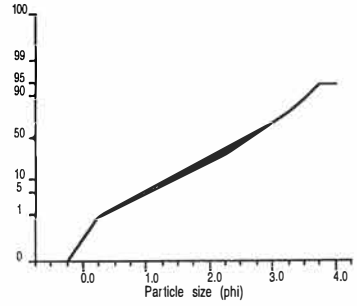

Results summary

Textural size classes

Gravel= 0.00% Sand= 94.84% Silt= 0.00% Clay= 0.00%

Gravel free detrital sediment

Sand

Moment method parameters (phi)

Mean= 2.37 Sorting= 0.78 Skewness= -0.26 Kurtosis= 2.83

Graphical method parameters (phi)

Mean= 2.59

Median= 2.69 C= 0.29 D35= 2.36 D65= 2.97

Textural description:

Raw data summary

Size (phi)	Size (mm)	Cumulative weight (g)	Interval frequency (%)	Cumulative frequency (%)
-0.50	1.4142	0.00	0.00	0.00
-0.25	1.1892	0.01	0.07	0.07
0.00	1.0000	0.06	0.37	0.44
0.25	0.8409	0.12	0.44	0.88
0.50	0.7071	0.22	0.74	1.62
0.75	0.5946	0.38	1.18	2.80
1.00	0.5000	0.65	1.99	4.79
1.25	0.4204	1.01	2.65	7.44
1.50	0.3536	1.64	4.64	12.09
1.75	0.2973	2.40	5.60	17.69
2.00	0.2500	3.25	6.26	23.95
2.25	0.2102	4.15	6.63	30.58
2.50	0.1768	5.55	10.32	40.90
2.75	0.1487	7.15	11.79	52.69
3.00	0.1250	9.05	14.00	66.69
3.25	0.1051	10.68	12.01	78.70
3.50	0.0884	11.88	8.84	87.55
3.75	0.0743	12.87	7.30	94.84
4.00	0.0625	12.87	0.00	94.84

Total weight = 13.57 g

PARTICLE SIZE ANALYSIS

Earth Sciences - University of Waikato

Sample: Newdicks Beach 1.2m Deploy 1

Size distribution histogram

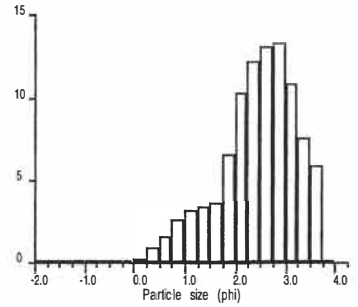

Cumulative frequency

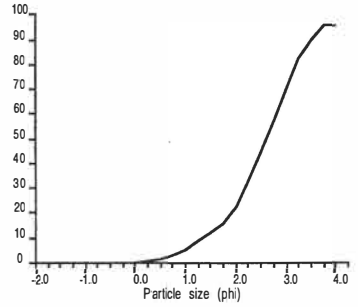

Cumulative frequency

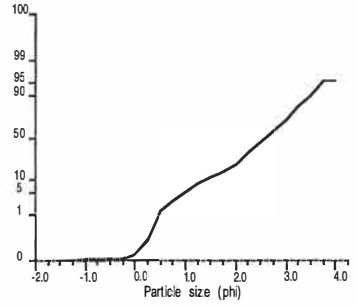

Results summary

Textural size classes

Gravel= 0.08% Sand= 95.52% Silt= 0.00% Clay= 0.00%

Gravel bearing detrital sediment

Slightly Gravelly Sand

Moment method parameters (phi)

Mean= 2.35 Sorting= 0.76 Skewness= -0.32 Kurtosis= 3.09

Graphical method parameters (phi)

Mean= 2.56 Sorting= 0.81 Skewness= -0.14 Kurtosis= 1.11

Median= 2.60 C= 0.42 D35= 2.30 D65= 2.88

Textural description:

Moderately sorted, Coarse skewed, Leptokurtic

Raw data summary

Size (phi)	Size (mm)	Cumulative weight (g)	Interval frequency (%)	Cumulative frequency (%)
-1.75	3.3636	0.00	0.00	0.00
-1.50	2.8284	0.00	0.00	0.00
-1.25	2.3784	0.00	0.00	0.00
-1.00	2.0000	0.01	0.08	0.08
-0.75	1.6818	0.01	0.00	0.08
-0.50	1.4142	0.01	0.00	0.08
-0.25	1.1892	0.01	0.00	0.08
0.00	1.0000	0.02	0.08	0.17
0.25	0.8409	0.05	0.25	0.42
0.50	0.7071	0.15	0.85	1.27
0.75	0.5946	0.34	1.61	2.87
1.00	0.5000	0.65	2.62	5.49
1.25	0.4204	1.03	3.21	8.71
1.50	0.3536	1.43	3.38	12.09
1.75	0.2973	1.86	3.63	15.72
2.00	0.2500	2.63	6.51	22.23
2.25	0.2102	3.85	10.31	32.54
2.50	0.1768	5.29	12.17	44.72
2.75	0.1487	6.85	13.19	57.90
3.00	0.1250	8.43	13.36	71.26
3.25	0.1051	9.71	10.82	82.08
3.50	0.0884	10.61	7.61	89.69
3.75	0.0743	11.31	5.92	95.60
4.00	0.0625	11.31	0.00	95.60

Total weight = 11.83 g

PARTICLE SIZE ANALYSIS

Earth Sciences - University of Waikato

Sample: Pukehina Redoubt 0.35m Deploy 1

Size distribution histogram

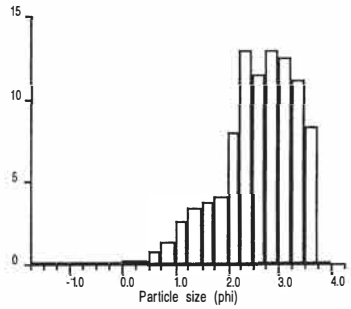

Cumulative frequency

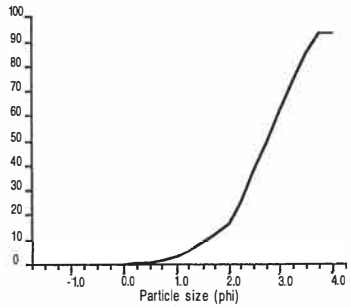

Cumulative frequency

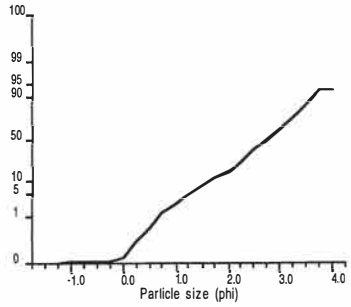

Results summary

Textural size classes

Gravel= 0.09% Sand= 93.22% Silt= 0.00% Clay= 0.00%

Gravel bearing detrital sediment

Slightly Gravelly Sand

Moment method parameters (phi)

Mean= 2.43 Sorting= 0.73 Skewness= -0.12 Kurtosis= 3.14

Graphical method parameters (phi)

Mean= 2.74

Median= 2.77 C= 0.59 D35= 2.45 D65= 3.07

Textural description:

Raw data summary

Size (phi)	Size (mm)	Cumulative weight (g)	Interval frequency (%)	Cumulative frequency (%)
-1.50	2.8284	0.00	0.00	0.00
-1.25	2.3784	0.00	0.00	0.00
-1.00	2.0000	0.01	0.09	0.09
-0.75	1.6818	0.01	0.00	0.09
-0.50	1.4142	0.01	0.00	0.09
-0.25	1.1892	0.01	0.00	0.09
0.00	1.0000	0.02	0.09	0.18
0.25	0.8409	0.05	0.26	0.44
0.50	0.7071	0.08	0.26	0.70
0.75	0.5946	0.17	0.79	1.50
1.00	0.5000	0.32	1.32	2.82
1.25	0.4204	0.61	2.56	5.37
1.50	0.3536	1.00	3.44	8.81
1.75	0.2973	1.42	3.70	12.51
2.00	0.2500	1.88	4.05	16.56
2.25	0.2102	2.78	7.93	24.49
2.50	0.1768	4.24	12.86	37.36
2.75	0.1487	5.53	11.37	48.72
3.00	0.1250	6.99	12.86	61.59
3.25	0.1051	8.40	12.42	74.01
3.50	0.0884	9.66	11.10	85.11
3.75	0.0743	10.59	8.19	93.30
4.00	0.0625	10.59	0.00	93.30

Total weight = 11.35 g

PARTICLE SIZE ANALYSIS

Earth Sciences - University of Waikato

Sample: Pukehina Redoubt 0.5m Deploy 1

Size distribution histogram

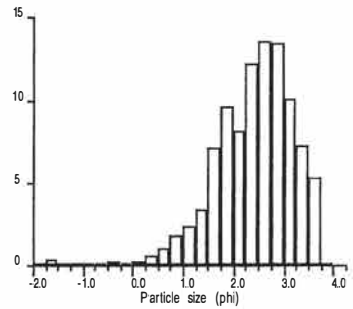

Cumulative frequency

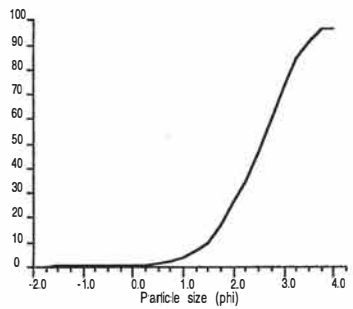

Cumulative frequency

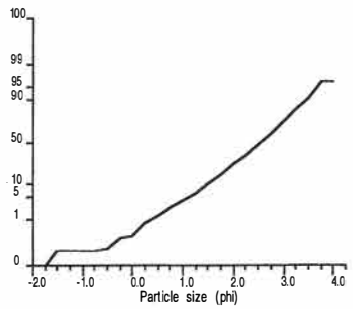

Results summary

Textural size classes

Gravel= 0.32% Sand= 96.39% Silt= 0.00% Clay= 0.00%

Gravel bearing detrital sediment

Slightly Gravelly Sand

Moment method parameters (phi)

Mean= 2.34 Sorting= 0.76 Skewness= -0.65 Kurtosis= 4.95

Graphical method parameters (phi)

Mean= 2.50 Sorting= 0.78 Skewness= -0.12 Kurtosis= 0.99

Median= 2.55 C= 0.31 D35= 2.25 D65= 2.83

Textural description:

Moderately sorted, Coarse skewed, Mesokurtic

Raw data summary

Size (phi)	Size (mm)	Cumulative weight (g)	Interval frequency (%)	Cumulative frequency (%)
-1.75	3.3636	0.00	0.00	0.00
-1.50	2.8284	0.06	0.32	0.32
-1.25	2.3784	0.06	0.00	0.32
-1.00	2.0000	0.06	0.00	0.32
-0.75	1.6818	0.06	0.00	0.32
-0.50	1.4142	0.07	0.05	0.38
-0.25	1.1892	0.10	0.16	0.54
0.00	1.0000	0.11	0.05	0.59
0.25	0.8409	0.16	0.27	0.86
0.50	0.7071	0.26	0.54	1.40
0.75	0.5946	0.45	1.02	2.42
1.00	0.5000	0.78	1.78	4.20
1.25	0.4204	1.23	2.42	6.62
1.50	0.3536	1.86	3.39	10.02
1.75	0.2973	3.19	7.16	17.18
2.00	0.2500	4.98	9.64	26.82
2.25	0.2102	6.48	8.08	34.89
2.50	0.1768	8.74	12.17	47.07
2.75	0.1487	11.26	13.57	60.64
3.00	0.1250	13.77	13.52	74.15
3.25	0.1051	15.63	10.02	84.17
3.50	0.0884	16.97	7.22	91.38
3.75	0.0743	17.96	5.33	96.72
4.00	0.0625	17.96	0.00	96.72

Total weight = 18.57 g

PARTICLE SIZE ANALYSIS

Earth Sciences - University of Waikato

Sample: Pukehina Redoubt 1.2m Deploy 1

Size distribution histogram

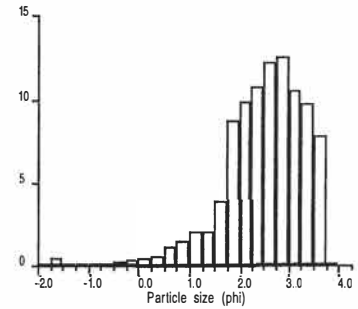

Results summary

Textural size classes

Gravel= 0.47% Sand= 93.98% Silt= 0.00% Clay= 0.00%

Gravel bearing detrital sediment

Slightly Gravelly Sand

Moment method parameters (phi)

Mean= 2.37 Sorting= 0.80 Skewness= -0.68 Kurtosis= 5.29

Graphical method parameters (phi)

Mean= 2.65

Median= 2.67 C= 0.04 D35= 2.34 D65= 2.97

Textural description:

Cumulative frequency

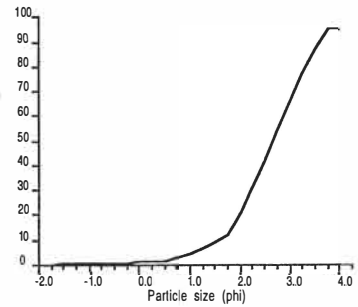

Cumulative frequency

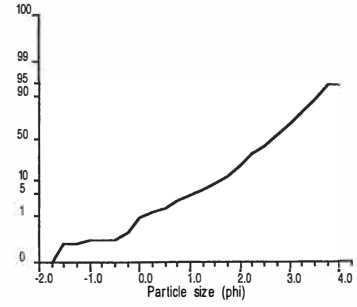

Raw data summary

Size (phi)	Size (mm)	Cumulative weight (g)	Interval frequency (%)	Cumulative frequency (%)
-1.75	3.3636	0.00	0.00	0.00
-1.50	2.8284	0.06	0.40	0.40
-1.25	2.3784	0.06	0.00	0.40
-1.00	2.0000	0.07	0.07	0.47
-0.75	1.6818	0.07	0.00	0.47
-0.50	1.4142	0.07	0.00	0.47
-0.25	1.1892	0.09	0.13	0.60
0.00	1.0000	0.14	0.33	0.94
0.25	0.8409	0.20	0.40	1.34
0.50	0.7071	0.28	0.53	1.87
0.75	0.5946	0.45	1.14	3.01
1.00	0.5000	0.68	1.54	4.55
1.25	0.4204	0.98	2.01	6.55
1.50	0.3536	1.29	2.07	8.62
1.75	0.2973	1.87	3.88	12.50
2.00	0.2500	3.18	8.76	21.26
2.25	0.2102	4.64	9.76	31.02
2.50	0.1768	6.25	10.76	41.78
2.75	0.1487	8.08	12.23	54.01
3.00	0.1250	9.95	12.50	66.51
3.25	0.1051	11.52	10.49	77.01
3.50	0.0884	12.97	9.69	86.70
3.75	0.0743	14.13	7.75	94.45
4.00	0.0625	14.13	0.00	94.45

Total weight = 14.96 g

PARTICLE SIZE ANALYSIS

Earth Sciences - University of Waikato

Sample: Pukehina Redoubt 0.8m Deploy 1

Size distribution histogram

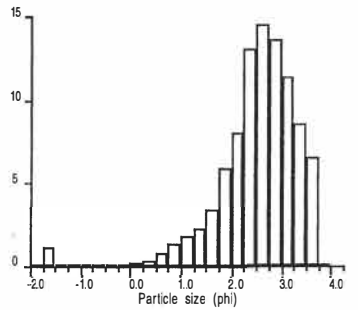

Results summary

Textural size classes

Gravel= 1.21% Sand= 92.25% Silt= 0.00% Clay= 0.00%

Gravel bearing detrital sediment

Slightly Gravelly Sand

Moment method parameters (phi)

Mean= 2.36 Sorting= 0.82 Skewness= -1.29 Kurtosis= 8.25

Graphical method parameters (phi)

Mean= 2.68

Median= 2.69 C= -1.53 D35= 2.43 D65= 2.97

Textural description:

Cumulative frequency

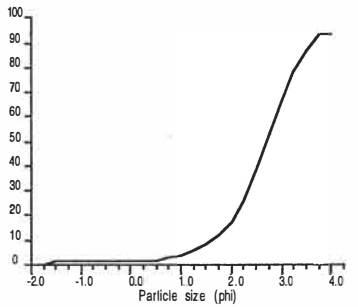

Cumulative frequency

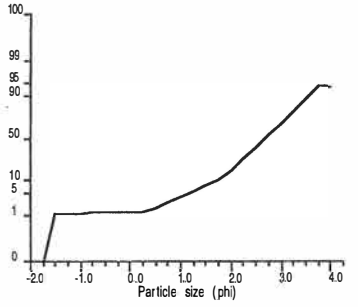

Raw data summary

Size (phi)	Size (mm)	Cumulative weight (g)	Interval frequency (%)	Cumulative frequency (%)
-1.75	3.3636	0.00	0.00	0.00
-1.50	2.8284	0.14	1.13	1.13
-1.25	2.3784	0.15	0.08	1.21
-1.00	2.0000	0.15	0.00	1.21
-0.75	1.6818	0.16	0.08	1.29
-0.50	1.4142	0.16	0.00	1.29
-0.25	1.1892	0.17	0.08	1.37
0.00	1.0000	0.17	0.00	1.37
0.25	0.8409	0.19	0.16	1.53
0.50	0.7071	0.23	0.32	1.86
0.75	0.5946	0.33	0.81	2.67
1.00	0.5000	0.50	1.37	4.04
1.25	0.4204	0.73	1.86	5.90
1.50	0.3536	1.01	2.26	8.16
1.75	0.2973	1.43	3.39	11.55
2.00	0.2500	2.16	5.90	17.45
2.25	0.2102	3.15	8.00	25.44
2.50	0.1768	4.78	13.17	38.61
2.75	0.1487	6.59	14.62	53.23
3.00	0.1250	8.28	13.65	66.88
3.25	0.1051	9.69	11.39	78.27
3.50	0.0884	10.75	8.56	86.83
3.75	0.0743	11.57	6.62	93.46
4.00	0.0625	11.57	0.00	93.46

Total weight = 12.38 g

PARTICLE SIZE ANALYSIS

Earth Sciences - University of Waikato

Sample: Newdicks Beach 0.5m Deploy 2

Size distribution histogram

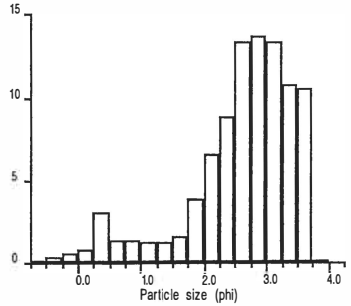

Cumulative frequency

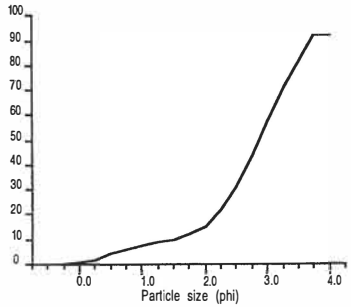

Cumulative frequency

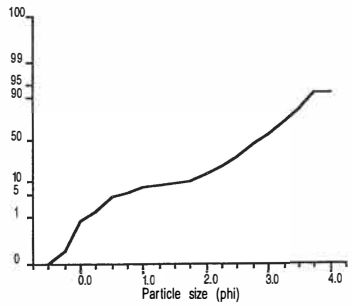

Results summary

Textural size classes

Gravel= 0.00% Sand= 92.25% Silt= 0.00% Clay= 0.00%

Gravel free detrital sediment

Sand

Moment method parameters (phi)

Mean= 2.41 Sorting= 0.85 Skewness= -0.55 Kurtosis= 3.41

Graphical method parameters (phi)

Mean= 2.81

Median= 2.86 C= 0.06 D35= 2.58 D65= 3.14

Textural description:

Raw data summary

Size (phi)	Size (mm)	Cumulative weight (g)	Interval frequency (%)	Cumulative frequency (%)
-0.50	1.4142	-0.01	-0.06	-0.06
-0.25	1.1892	0.05	0.35	0.29
0.00	1.0000	0.14	0.52	0.82
0.25	0.8409	0.27	0.76	1.57
0.50	0.7071	0.80	3.09	4.66
0.75	0.5946	1.04	1.40	6.06
1.00	0.5000	1.27	1.34	7.40
1.25	0.4204	1.48	1.22	8.62
1.50	0.3536	1.69	1.22	9.85
1.75	0.2973	1.97	1.63	11.48
2.00	0.2500	2.62	3.79	15.27
2.25	0.2102	3.76	6.64	21.91
2.50	0.1768	5.28	8.86	30.77
2.75	0.1487	7.56	13.29	44.06
3.00	0.1250	9.90	13.64	57.69
3.25	0.1051	12.19	13.34	71.04
3.50	0.0884	14.03	10.72	81.76
3.75	0.0743	15.83	10.49	92.25
4.00	0.0625	15.83	0.00	92.25

Total weight = 17.16 g

PARTICLE SIZE ANALYSIS

Earth Sciences - University of Waikato

Sample: Newdicks Beach 0.35m Deploy 2

Size distribution histogram

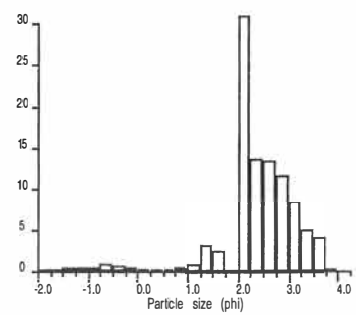

Cumulative frequency

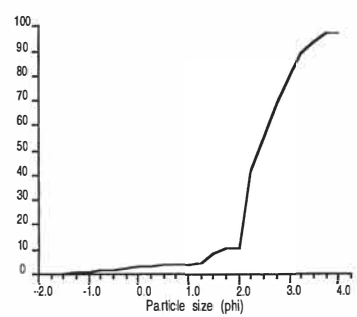

Cumulative frequency

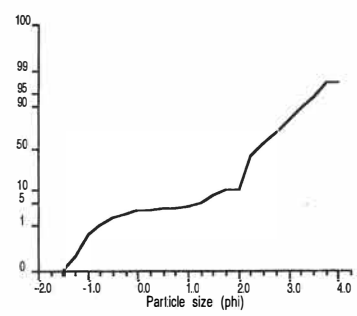

Results summary

Textural size classes

Gravel= 0.71% Sand= 97.03% Silt= 0.00% Clay= 0.00%

Gravel bearing detrital sediment

Slightly Gravelly Sand

Moment method parameters (phi)

Mean= 2.33 Sorting= 0.77 Skewness= -1.63 Kurtosis= 8.63

Graphical method parameters (phi)

Mean= 2.52 Sorting= 0.62 Skewness= 0.17 Kurtosis= 1.24

Median= 2.40 C= -0.80 D35= 2.20 D65= 2.68

Textural description:

Moderately well sorted, Fine skewed, Leptokurtic

Raw data summary

Size (phi)	Size (mm)	Cumulative weight (g)	Interval frequency (%)	Cumulative frequency (%)
-1.75	3.3636	0.00	0.00	0.00
-1.50	2.8284	0.01	0.04	0.04
-1.25	2.3784	0.08	0.28	0.32
-1.00	2.0000	0.18	0.40	0.71
-0.75	1.6818	0.27	0.36	1.07
-0.50	1.4142	0.48	0.83	1.90
-0.25	1.1892	0.64	0.63	2.53
0.00	1.0000	0.76	0.47	3.01
0.25	0.8409	0.80	0.16	3.17
0.50	0.7071	0.83	0.12	3.28
0.75	0.5946	0.88	0.20	3.48
1.00	0.5000	1.02	0.55	4.04
1.25	0.4204	1.26	0.95	4.99
1.50	0.3536	2.07	3.21	8.19
1.75	0.2973	2.69	2.45	10.65
2.00	0.2500	2.69	0.00	10.65
2.25	0.2102	10.52	30.99	41.63
2.50	0.1768	13.97	13.65	55.28
2.75	0.1487	17.36	13.42	68.70
3.00	0.1250	20.29	11.59	80.29
3.25	0.1051	22.41	8.39	88.68
3.50	0.0884	23.67	4.99	93.67
3.75	0.0743	24.70	4.08	97.74
4.00	0.0625	24.70	0.00	97.74

Total weight = 25.27 g

PARTICLE SIZE ANALYSIS

Earth Sciences - University of Waikato

Sample: Newdicks Beach 0.8m Deploy 2

Size distribution histogram

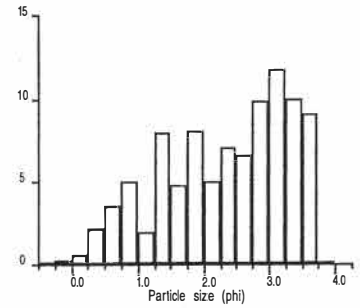

Cumulative frequency

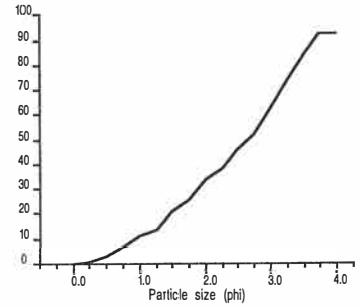

Cumulative frequency

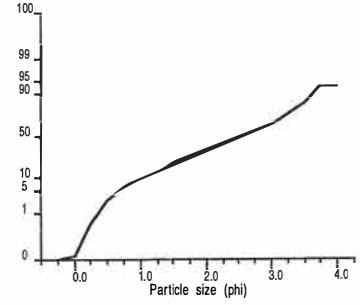

Results summary

Textural size classes

Gravel= 0.00% Sand= 93.05% Silt= 0.00% Clay= 0.00%

Gravel free detrital sediment

Sand

Moment method parameters (phi)

Mean= 2.19 Sorting= 0.93 Skewness= 0.06 Kurtosis= 2.00

Graphical method parameters (phi)

Mean= 2.50

Median= 2.65 C= 0.28 D35= 2.05 D65= 3.06

Textural description:

Raw data summary

Size (phi)	Size (mm)	Cumulative weight (g)	Interval frequency (%)	Cumulative frequency (%)
-0.25	1.1892	-0.01	-0.07	-0.07
0.00	1.0000	0.02	0.21	0.14
0.25	0.8409	0.10	0.57	0.71
0.50	0.7071	0.41	2.20	2.91
0.75	0.5946	0.91	3.54	6.45
1.00	0.5000	1.61	4.96	11.41
1.25	0.4204	1.88	1.91	13.32
1.50	0.3536	3.00	7.94	21.26
1.75	0.2973	3.67	4.75	26.01
2.00	0.2500	4.80	8.01	34.02
2.25	0.2102	5.50	4.96	38.98
2.50	0.1768	6.48	6.95	45.92
2.75	0.1487	7.41	6.59	52.52
3.00	0.1250	8.80	9.85	62.37
3.25	0.1051	10.45	11.69	74.06
3.50	0.0884	11.86	9.99	84.05
3.75	0.0743	13.13	9.00	93.05
4.00	0.0625	13.13	0.00	93.05

Total weight = 14.11 g

PARTICLE SIZE ANALYSIS

Earth Sciences - University of Waikato

Sample: Newdicks Beach 1.2m Deploy 2

Size distribution histogram

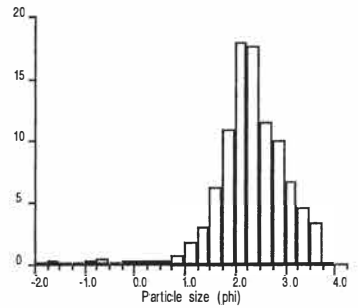

Cumulative frequency

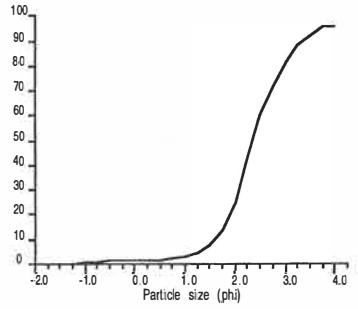

Cumulative frequency

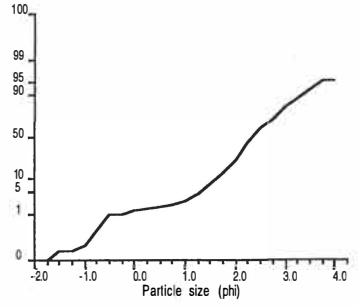

Results summary

Textural size classes

Gravel= 0.31% Sand= 95.62% Silt= 0.00% Clay= 0.00%

Gravel bearing detrital sediment

Slightly Gravelly Sand

Moment method parameters (phi)

Mean= 2.23 Sorting= 0.70 Skewness= -0.81 Kurtosis= 7.22

Graphical method parameters (phi)

Mean= 2.42 Sorting= 0.69 Skewness= 0.12 Kurtosis= 1.18

Median= 2.36 C= -0.50 D35= 2.15 D65= 2.61

Textural description:

Moderately well sorted, Fine skewed, Leptokurtic

Raw data summary

Size (phi)	Size (mm)	Cumulative weight (g)	Interval frequency (%)	Cumulative frequency (%)
-1.75	3.3636	0.00	0.00	0.00
-1.50	2.8284	0.04	0.25	0.25
-1.25	2.3784	0.04	0.00	0.25
-1.00	2.0000	0.05	0.06	0.31
-0.75	1.6818	0.09	0.25	0.56
-0.50	1.4142	0.16	0.44	1.00
-0.25	1.1892	0.17	0.06	1.06
0.00	1.0000	0.21	0.25	1.31
0.25	0.8409	0.25	0.25	1.57
0.50	0.7071	0.28	0.19	1.75
0.75	0.5946	0.34	0.38	2.13
1.00	0.5000	0.46	0.75	2.88
1.25	0.4204	0.74	1.75	4.63
1.50	0.3536	1.22	3.01	7.64
1.75	0.2973	2.20	6.14	13.78
2.00	0.2500	3.92	10.77	24.55
2.25	0.2102	6.78	17.91	42.45
2.50	0.1768	9.60	17.66	60.11
2.75	0.1487	11.43	11.46	71.57
3.00	0.1250	13.00	9.83	81.40
3.25	0.1051	14.06	6.64	88.04
3.50	0.0884	14.79	4.57	92.61
3.75	0.0743	15.32	3.32	95.93
4.00	0.0625	15.32	0.00	95.93

Total weight = 15.97 g

PARTICLE SIZE ANALYSIS

Earth Sciences - University of Waikato

Sample: Pukehina Redoubt 0.35m Deploy 2

Size distribution histogram

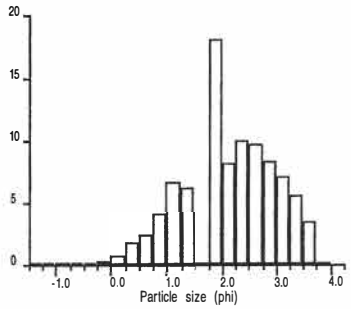

Cumulative frequency

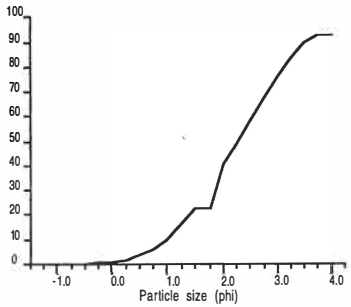

Cumulative frequency

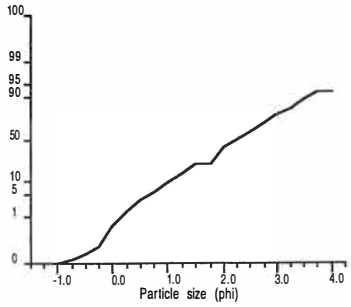

Results summary

Textural size classes

Gravel= 0.06% Sand= 92.62% Silt= 0.00% Clay= 0.00%

Gravel bearing detrital sediment

Slightly Gravelly Sand

Moment method parameters (phi)

Mean= 1.99 Sorting= 0.84 Skewness= 0.16 Kurtosis= 2.65

Graphical method parameters (phi)

Mean= 2.26

Median= 2.28 C= 0.08 D35= 1.92 D65= 2.67

Textural description:

Raw data summary

Size (phi)	Size (mm)	Cumulative weight (g)	Interval frequency (%)	Cumulative frequency (%)
-1.25	2.3784	-0.01	-0.06	-0.06
-1.00	2.0000	0.01	0.11	0.06
-0.75	1.6818	0.02	0.06	0.11
-0.50	1.4142	0.04	0.11	0.22
-0.25	1.1892	0.06	0.11	0.34
0.00	1.0000	0.13	0.39	0.73
0.25	0.8409	0.28	0.84	1.57
0.50	0.7071	0.59	1.73	3.30
0.75	0.5946	1.04	2.52	5.82
1.00	0.5000	1.75	3.97	9.79
1.25	0.4204	2.92	6.54	16.33
1.50	0.3536	4.01	6.10	22.43
1.75	0.2973	4.01	0.00	22.43
2.00	0.2500	7.24	18.06	40.49
2.25	0.2102	8.70	8.17	48.66
2.50	0.1768	10.46	9.84	58.50
2.75	0.1487	12.19	9.68	68.18
3.00	0.1250	13.69	8.39	76.57
3.25	0.1051	14.95	7.05	83.61
3.50	0.0884	15.94	5.54	89.15
3.75	0.0743	16.57	3.52	92.67
4.00	0.0625	16.57	0.00	92.67

Total weight = 17.88 g

PARTICLE SIZE ANALYSIS

Earth Sciences - University of Waikato

Sample: Pukehina Redoubt 0.5m Deploy 2

Size distribution histogram

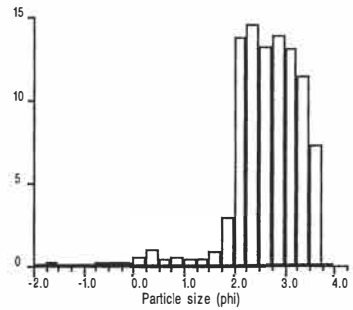

Cumulative frequency

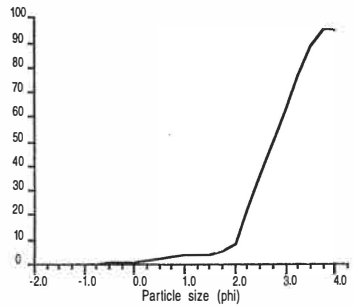

Cumulative frequency

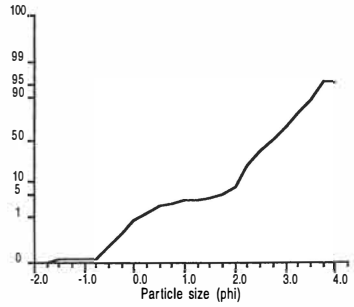

Results summary

Textural size classes

Gravel= 0.13% Sand= 95.24% Silt= 0.00% Clay= 0.00%

Gravel bearing detrital sediment

Slightly Gravelly Sand

Moment method parameters (phi)

Mean= 2.53 Sorting= 0.70 Skewness= -1.05 Kurtosis= 7.00

Graphical method parameters (phi)

Mean= 2.77 Sorting= 0.62 Skewness= 0.00 Kurtosis= 0.90

Median= 2.76 C= 0.05 D35= 2.48 D65= 3.03

Textural description:

Moderately well sorted, Near symmetrical, Mesokurtic

Raw data summary

Size (phi)	Size (mm)	Cumulative weight (g)	Interval frequency (%)	Cumulative frequency (%)
-1.75	3.3636	0.00	0.00	0.00
-1.50	2.8284	0.02	0.13	0.13
-1.25	2.3784	0.02	0.00	0.13
-1.00	2.0000	0.02	0.00	0.13
-0.75	1.6818	0.02	0.00	0.13
-0.50	1.4142	0.05	0.20	0.33
-0.25	1.1892	0.09	0.27	0.60
0.00	1.0000	0.13	0.27	0.87
0.25	0.8409	0.22	0.60	1.47
0.50	0.7071	0.36	0.94	2.41
0.75	0.5946	0.42	0.40	2.81
1.00	0.5000	0.50	0.54	3.35
1.25	0.4204	0.56	0.40	3.75
1.50	0.3536	0.63	0.47	4.22
1.75	0.2973	0.76	0.87	5.09
2.00	0.2500	1.20	2.95	8.04
2.25	0.2102	3.27	13.86	21.90
2.50	0.1768	5.44	14.53	36.44
2.75	0.1487	7.41	13.19	49.63
3.00	0.1250	9.49	13.93	63.56
3.25	0.1051	11.45	13.13	76.69
3.50	0.0884	13.16	11.45	88.14
3.75	0.0743	14.24	7.23	95.38
4.00	0.0625	14.24	0.00	95.38

Total weight = 14.93 g

PARTICLE SIZE ANALYSIS

Earth Sciences - University of Waikato

Sample: Pukehina Redoubt 0.8m Deploy 2

Size distribution histogram

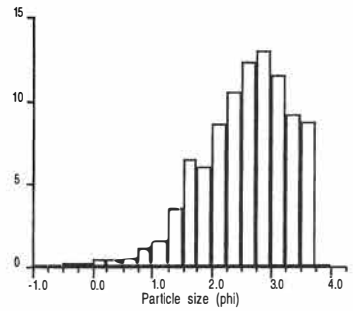

Cumulative frequency

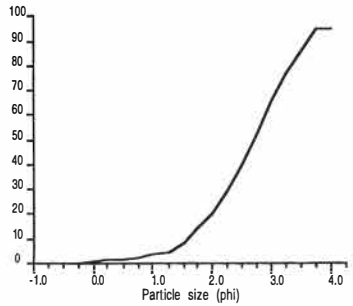

Cumulative frequency

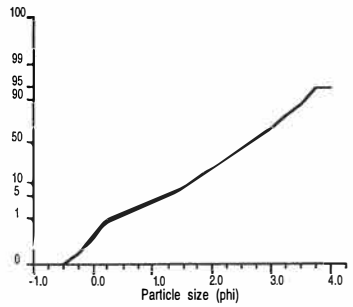

Results summary

Textural size classes

Gravel= 0.00% Sand= 94.83% Silt= 0.00% Clay= 0.00%

Gravel free detrital sediment

Sand

Moment method parameters (phi)

Mean= 2.42 Sorting= 0.75 Skewness= -0.25 Kurtosis= 3.24

Graphical method parameters (phi)

Mean= 2.65

Median= 2.70 C= 0.25 D35= 2.38 D65= 2.99

Textural description:

Raw data summary

Size (phi)	Size (mm)	Cumulative weight (g)	Interval frequency (%)	Cumulative frequency (%)
-0.75	1.6818	-0.01	-0.05	-0.05
-0.50	1.4142	0.01	0.10	0.05
-0.25	1.1892	0.05	0.21	0.26
0.00	1.0000	0.10	0.26	0.52
0.25	0.8409	0.19	0.47	0.99
0.50	0.7071	0.28	0.47	1.46
0.75	0.5946	0.40	0.63	2.09
1.00	0.5000	0.62	1.15	3.24
1.25	0.4204	0.93	1.62	4.86
1.50	0.3536	1.61	3.55	8.41
1.75	0.2973	2.84	6.43	14.84
2.00	0.2500	3.99	6.01	20.85
2.25	0.2102	5.63	8.57	29.41
2.50	0.1768	7.64	10.50	39.92
2.75	0.1487	10.01	12.38	52.30
3.00	0.1250	12.51	13.06	65.36
3.25	0.1051	14.72	11.55	76.91
3.50	0.0884	16.47	9.14	86.05
3.75	0.0743	18.15	8.78	94.83
4.00	0.0625	18.15	0.00	94.83

Total weight = 19.14 g

PARTICLE SIZE ANALYSIS

Earth Sciences - University of Waikato

Sample: Pukehina Redoubt 1.2m Deploy 2

Size distribution histogram

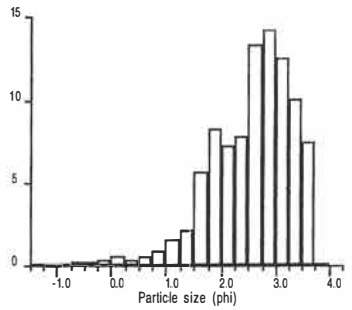

Cumulative frequency

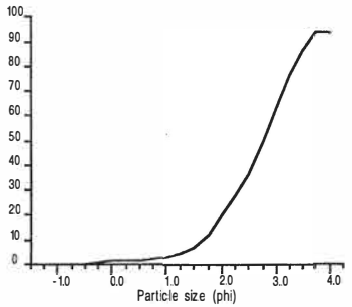

Cumulative frequency

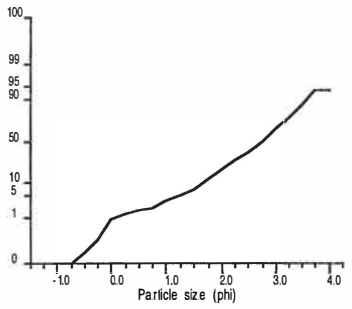

Results summary

Textural size classes

Gravel= 0.00% Sand= 93.66% Silt= 0.00% Clay= 0.00%

Gravel free detrital sediment

Sand

Moment method parameters (phi)

Mean= 2.41 Sorting= 0.76 Skewness= -0.38 Kurtosis= 3.84

Graphical method parameters (phi)

Mean= 2.69

Median= 2.76 C= 0.05 D35= 2.47 D65= 3.03

Textural description:

Raw data summary

Size (phi)	Size (mm)	Cumulative weight (g)	Interval frequency (%)	Cumulative frequency (%)
-1.25	2.3784	0.00	0.00	0.00
-1.00	2.0000	0.00	0.00	0.00
-0.75	1.6818	0.01	0.06	0.06
-0.50	1.4142	0.05	0.22	0.28
-0.25	1.1892	0.09	0.22	0.50
0.00	1.0000	0.16	0.39	0.89
0.25	0.8409	0.26	0.56	1.45
0.50	0.7071	0.33	0.39	1.84
0.75	0.5946	0.42	0.50	2.34
1.00	0.5000	0.58	0.89	3.23
1.25	0.4204	0.87	1.61	4.84
1.50	0.3536	1.25	2.11	6.96
1.75	0.2973	2.27	5.68	12.63
2.00	0.2500	3.75	8.24	20.87
2.25	0.2102	5.05	7.23	28.10
2.50	0.1768	6.46	7.85	35.95
2.75	0.1487	8.85	13.30	49.25
3.00	0.1250	11.42	14.30	63.55
3.25	0.1051	13.67	12.52	76.07
3.50	0.0884	15.48	10.07	86.14
3.75	0.0743	16.83	7.51	93.66
4.00	0.0625	16.83	0.00	93.66

Total weight = 17.97 g

PARTICLE SIZE ANALYSIS

Earth Sciences - University of Waikato

Sample: NEWDICKS 0.35M D1 SUMMER

Size distribution histogram

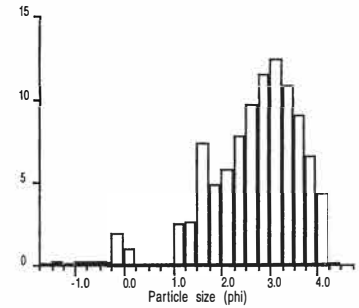

Cumulative frequency

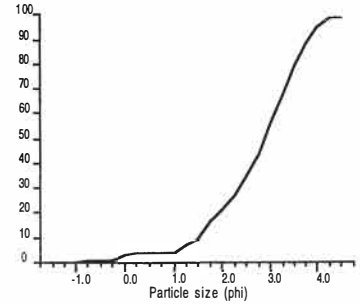

Cumulative frequency

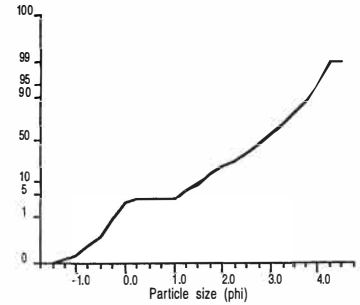

Results summary

Textural size classes

Gravel= 0.20% Sand= 94.51% Silt= 5.28% Clay= 0.00%

Gravel bearing detrital sediment

Slightly Gravelly Sand

Moment method parameters (phi)

Mean= 2.67 Sorting= 0.95 Skewness= -0.97 Kurtosis= 4.37

Graphical method parameters (phi)

Mean= 2.75 Sorting= 0.91 Skewness= -0.20 Kurtosis= 0.96

Median= 2.87 C= -0.23 D35= 2.51 D65= 3.18

Textural description:

Moderately sorted, Coarse skewed, Mesokurtic

Raw data summary

Size (phi)	Size (mm)	Cumulative weight (g)	Interval frequency (%)	Cumulative frequency (%)
-1.50	2.8284	0.00	0.00	0.00
-1.25	2.3784	0.04	0.14	0.14
-1.00	2.0000	0.06	0.07	0.20
-0.75	1.6818	0.10	0.14	0.34
-0.50	1.4142	0.15	0.17	0.51
-0.25	1.1892	0.24	0.31	0.82
0.00	1.0000	0.82	1.98	2.79
0.25	0.8409	1.14	1.09	3.89
0.50	0.7071	1.14	0.00	3.89
0.75	0.5946	1.14	0.00	3.89
1.00	0.5000	1.14	0.00	3.89
1.25	0.4204	1.86	2.45	6.34
1.50	0.3536	2.60	2.52	8.86
1.75	0.2973	4.76	7.36	16.22
2.00	0.2500	6.18	4.84	21.06
2.25	0.2102	7.89	5.83	26.89
2.50	0.1768	10.17	7.77	34.66
2.75	0.1487	13.01	9.68	44.34
3.00	0.1250	16.40	11.55	55.90
3.25	0.1051	20.04	12.41	68.30
3.50	0.0884	23.22	10.84	79.14
3.75	0.0743	25.86	9.00	88.14
4.00	0.0625	27.79	6.58	94.72
4.25	0.0526	29.06	4.33	99.05
4.50	0.0442	29.06	0.00	99.05

Total weight = 29.34 g

PARTICLE SIZE ANALYSIS

Earth Sciences - University of Waikato

Sample: NEWDICKS 0.5M D1 SUMMER

Size distribution histogram

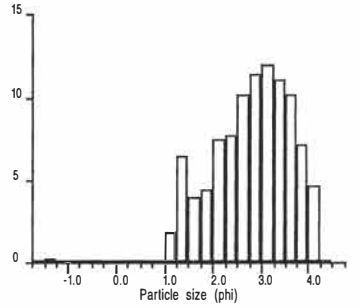

Cumulative frequency

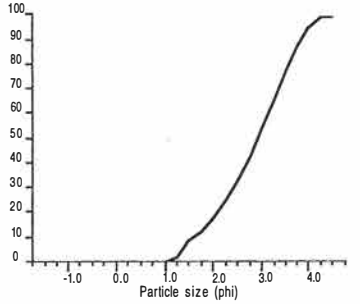

Cumulative frequency

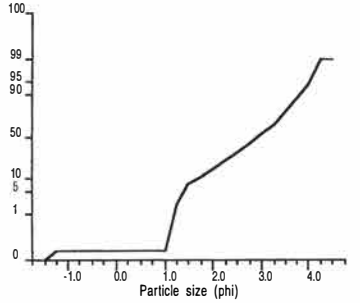

Results summary

Textural size classes

Gravel= 0.25% Sand= 94.01% Silt= 5.74% Clay= 0.00%

Gravel bearing detrital sediment

Slightly Gravelly Sand

Moment method parameters (phi)

Mean= 2.78 Sorting= 0.81 Skewness= -0.50 Kurtosis= 3.66

Graphical method parameters (phi)

Mean= 2.85 Sorting= 0.84 Skewness= -0.14 Kurtosis= 0.92

Median= 2.92 C= 1.11 D35= 2.57 D65= 3.23

Textural description:

Moderately sorted, Coarse skewed, Mesokurtic

Raw data summary

Size (phi)	Size (mm)	Cumulative weight (g)	Interval frequency (%)	Cumulative frequency (%)
-1.50	2.8284	0.00	0.00	0.00
-1.25	2.3784	0.07	0.25	0.25
-1.00	2.0000	0.07	0.00	0.25
-0.75	1.6818	0.07	0.00	0.25
-0.50	1.4142	0.07	0.00	0.25
-0.25	1.1892	0.07	0.00	0.25
0.00	1.0000	0.07	0.00	0.25
0.25	0.8409	0.07	0.00	0.25
0.50	0.7071	0.07	0.00	0.25
0.75	0.5946	0.07	0.00	0.25
1.00	0.5000	0.07	0.00	0.25
1.25	0.4204	0.58	1.79	2.03
1.50	0.3536	2.41	6.42	8.45
1.75	0.2973	3.54	3.96	12.42
2.00	0.2500	4.81	4.46	16.87
2.25	0.2102	6.96	7.54	24.42
2.50	0.1768	9.15	7.68	32.10
2.75	0.1487	12.05	10.17	42.27
3.00	0.1250	15.31	11.44	53.71
3.25	0.1051	18.74	12.03	65.74
3.50	0.0884	21.91	11.12	76.86
3.75	0.0743	24.84	10.28	87.14
4.00	0.0625	26.87	7.12	94.26
4.25	0.0526	28.19	4.63	98.89
4.50	0.0442	28.19	0.00	98.89

Total weight = 28.51 g

PARTICLE SIZE ANALYSIS

Earth Sciences - University of Waikato

Sample: NEWDICKS 0.8M D1 SUMMER

Size distribution histogram

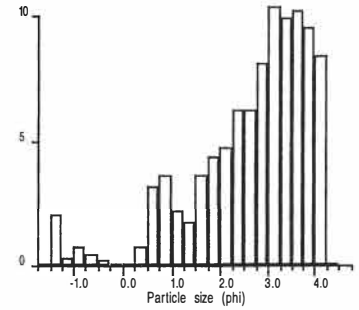

Cumulative frequency

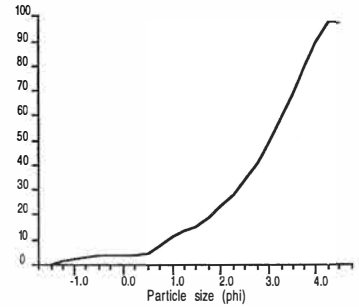

Cumulative frequency

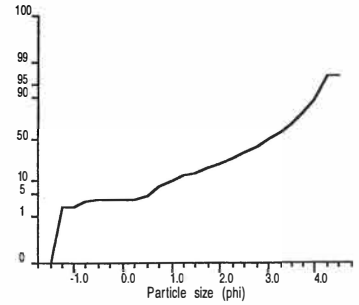

Results summary

Textural size classes

Gravel= 2.31% Sand= 86.59% Silt= 11.10% Clay= 0.00%

Gravel bearing detrital sediment

Slightly Gravelly Muddy Sand

Moment method parameters (phi)

Mean= 2.60 Sorting= 1.22 Skewness= -1.09 Kurtosis= 4.28

Graphical method parameters (phi)

Mean= 2.82 Sorting= 1.13 Skewness= -0.32 Kurtosis= 0.96

Median= 3.03 C= -1.38 D35= 2.53 D65= 3.40

Textural description:

Poorly sorted, Strongly Coarse skewed, Mesokurtic

Raw data summary

Size (phi)	Size (mm)	Cumulative weight (g)	Interval frequency (%)	Cumulative frequency (%)
-1.50	2.8284	0.00	0.00	0.00
-1.25	2.3784	0.38	2.04	2.04
-1.00	2.0000	0.43	0.27	2.31
-0.75	1.6818	0.57	0.75	3.06
-0.50	1.4142	0.66	0.48	3.55
-0.25	1.1892	0.70	0.22	3.76
0.00	1.0000	0.71	0.05	3.82
0.25	0.8409	0.71	0.00	3.82
0.50	0.7071	0.85	0.75	4.57
0.75	0.5946	1.44	3.17	7.74
1.00	0.5000	2.11	3.60	11.34
1.25	0.4204	2.51	2.15	13.49
1.50	0.3536	2.83	1.72	15.21
1.75	0.2973	3.51	3.66	18.87
2.00	0.2500	4.33	4.41	23.27
2.25	0.2102	5.22	4.78	28.06
2.50	0.1768	6.38	6.24	34.29
2.75	0.1487	7.55	6.29	40.58
3.00	0.1250	9.06	8.12	48.70
3.25	0.1051	11.00	10.43	59.13
3.50	0.0884	12.85	9.94	69.07
3.75	0.0743	14.76	10.27	79.34
4.00	0.0625	16.54	9.57	88.90
4.25	0.0526	18.11	8.44	97.34
4.50	0.0442	18.11	0.00	97.34

Total weight = 18.60 g

PARTICLE SIZE ANALYSIS

Earth Sciences - University of Waikato

Sample: NEWDICKS 1.2M D1 SUMMER

Size distribution histogram

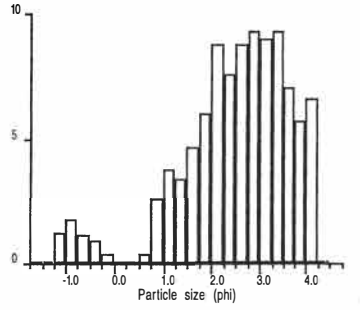

Cumulative frequency

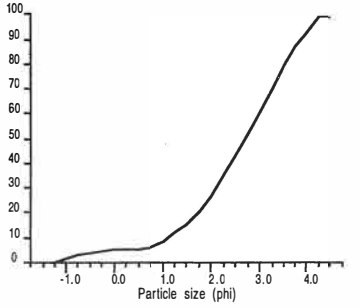

Cumulative frequency

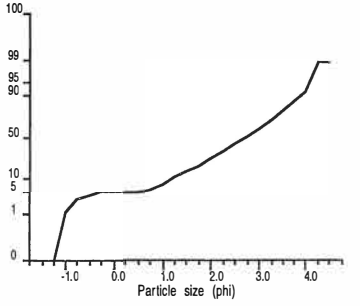

Results summary

Textural size classes

Gravel= 1.23% Sand= 90.91% Silt= 7.86% Clay= 0.00%

Gravel bearing detrital sediment

Slightly Gravelly Sand

Moment method parameters (phi)

Mean= 2.49 Sorting= 1.16 Skewness= -0.99 Kurtosis= 4.19

Graphical method parameters (phi)

Mean= 2.63 Sorting= 1.19 Skewness= -0.23 Kurtosis= 1.24

Median= 2.71 C= -1.05 D35= 2.25 D65= 3.12

Textural description:

Poorly sorted, Coarse skewed, Leptokurtic

Raw data summary

Size (phi)	Size (mm)	Cumulative weight (g)	Interval frequency (%)	Cumulative frequency (%)
-1.50	2.8284	0.00	0.00	0.00
-1.25	2.3784	0.01	0.04	0.04
-1.00	2.0000	0.28	1.18	1.23
-0.75	1.6818	0.67	1.71	2.93
-0.50	1.4142	0.93	1.14	4.07
-0.25	1.1892	1.13	0.88	4.95
0.00	1.0000	1.23	0.44	5.39
0.25	0.8409	1.23	0.00	5.39
0.50	0.7071	1.23	0.00	5.39
0.75	0.5946	1.31	0.35	5.74
1.00	0.5000	1.90	2.58	8.32
1.25	0.4204	2.76	3.77	12.09
1.50	0.3536	3.54	3.42	15.50
1.75	0.2973	4.61	4.69	20.19
2.00	0.2500	5.98	6.00	26.19
2.25	0.2102	8.00	8.85	35.03
2.50	0.1768	9.75	7.66	42.70
2.75	0.1487	11.76	8.80	51.50
3.00	0.1250	13.89	9.33	60.83
3.25	0.1051	15.96	9.06	69.89
3.50	0.0884	18.10	9.37	79.26
3.75	0.0743	19.73	7.14	86.40
4.00	0.0625	21.04	5.74	92.14
4.25	0.0526	22.56	6.66	98.79
4.50	0.0442	22.56	0.00	98.79

Total weight = 22.84 g

PARTICLE SIZE ANALYSIS

Earth Sciences - University of Waikato

Sample: NEWDICKS 0.35M D2 SUMMER

Size distribution histogram

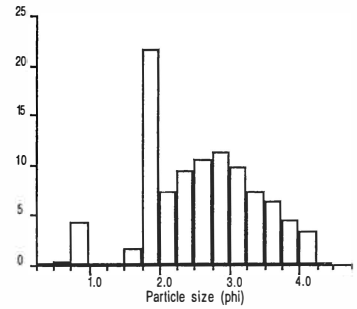

Cumulative frequency

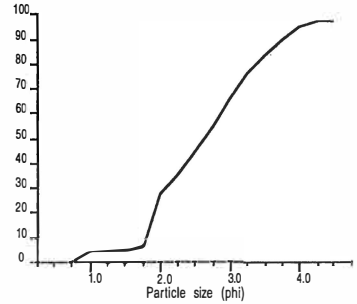

Cumulative frequency

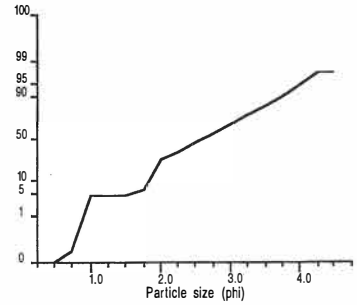

Results summary

Textural size classes

Gravel= 0.00% Sand= 94.48% Silt= 5.52% Clay= 0.00%

Gravel free detrital sediment

Sand

Moment method parameters (phi)

Mean= 2.55 Sorting= 0.77 Skewness= 0.16 Kurtosis= 2.61

Graphical method parameters (phi)

Mean= 2.67 Sorting= 0.79 Skewness= 0.11 Kurtosis= 0.81

Median= 2.63 C= 0.79 D35= 2.25 D65= 2.97

Textural description:

Moderately sorted, Fine skewed, Platykurtic

Raw data summary

Size (phi)	Size (mm)	Cumulative weight (g)	Interval frequency (%)	Cumulative frequency (%)
0.50	0.7071	-0.01	-0.03	-0.03
0.75	0.5946	0.09	0.29	0.26
1.00	0.5000	1.56	4.25	4.51
1.25	0.4204	1.58	0.06	4.56
1.50	0.3536	1.58	0.00	4.56
1.75	0.2973	2.12	1.56	6.12
2.00	0.2500	9.62	21.66	27.79
2.25	0.2102	12.15	7.31	35.09
2.50	0.1768	15.42	9.44	44.54
2.75	0.1487	19.08	10.57	55.11
3.00	0.1250	22.99	11.29	66.40
3.25	0.1051	26.40	9.85	76.25
3.50	0.0884	28.97	7.42	83.67
3.75	0.0743	31.14	6.27	89.94
4.00	0.0625	32.71	4.53	94.48
4.25	0.0526	33.86	3.32	97.80
4.50	0.0442	33.86	0.00	97.80

Total weight = 34.62 g

PARTICLE SIZE ANALYSIS

Earth Sciences - University of Waikato

Sample: NEWDICKS 0.5M D2 SUMMER

Size distribution histogram

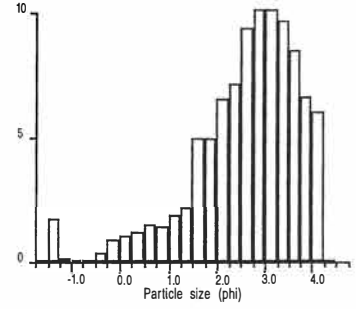

Cumulative frequency

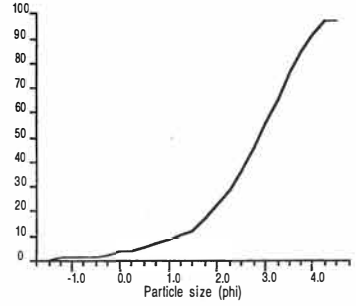

Cumulative frequency

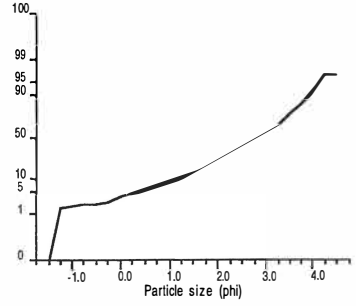

Results summary

Textural size classes

Gravel= 1.91% Sand= 88.98% Silt= 9.11% Clay= 0.00%

Gravel bearing detrital sediment

Slightly Gravelly Sand

Moment method parameters (phi)

Mean= 2.53 Sorting= 1.11 Skewness= -1.02 Kurtosis= 4.60

Graphical method parameters (phi)

Mean= 2.76 Sorting= 1.09 Skewness= -0.23 Kurtosis= 1.12

Median= 2.86 C= -1.35 D35= 2.46 D65= 3.23

Textural description:

Poorly sorted, Coarse skewed, Leptokurtic

Raw data summary

Size (phi)	Size (mm)	Cumulative weight (g)	Interval frequency (%)	Cumulative frequency (%)
-1.50	2.8284	0.00	0.00	0.00
-1.25	2.3784	0.43	1.71	1.71
-1.00	2.0000	0.48	0.20	1.91
-0.75	1.6818	0.50	0.08	1.99
-0.50	1.4142	0.50	0.00	1.99
-0.25	1.1892	0.61	0.44	2.43
0.00	1.0000	0.83	0.88	3.31
0.25	0.8409	1.10	1.08	4.38
0.50	0.7071	1.39	1.16	5.54
0.75	0.5946	1.77	1.51	7.05
1.00	0.5000	2.14	1.47	8.52
1.25	0.4204	2.61	1.87	10.40
1.50	0.3536	3.15	2.15	12.55
1.75	0.2973	4.40	4.98	17.53
2.00	0.2500	5.65	4.98	22.50
2.25	0.2102	7.29	6.53	29.04
2.50	0.1768	9.09	7.17	36.21
2.75	0.1487	11.46	9.44	45.65
3.00	0.1250	14.01	10.16	55.80
3.25	0.1051	16.57	10.20	66.00
3.50	0.0884	19.01	9.72	75.72
3.75	0.0743	21.15	8.52	84.24
4.00	0.0625	22.82	6.65	90.89
4.25	0.0526	24.33	6.01	96.91
4.50	0.0442	24.33	0.00	96.91

Total weight = 25.11 g

PARTICLE SIZE ANALYSIS

Earth Sciences - University of Waikato

Sample: NEWDICKS 0.8M D2 SUMMER

Size distribution histogram

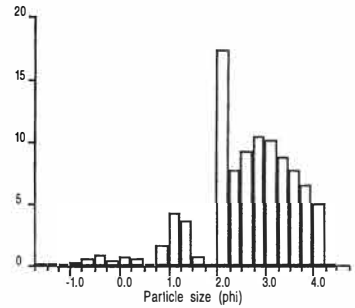

Results summary

Textural size classes

Gravel= 0.29% Sand= 91.62% Silt= 8.09% Clay= 0.00%

Gravel bearing detrital sediment

Slightly Gravelly Sand

Moment method parameters (phi)

Mean= 2.55 Sorting= 0.99 Skewness= -0.75 Kurtosis= 4.16

Graphical method parameters (phi)

Mean= 2.84 Sorting= 0.91 Skewness= -0.03 Kurtosis= 1.05

Median= 2.79 C= -0.54 D35= 2.37 D65= 3.15

Textural description:

Moderately sorted, Near symmetrical, Mesokurtic

Cumulative frequency

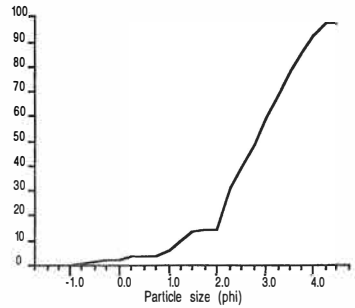

Cumulative frequency

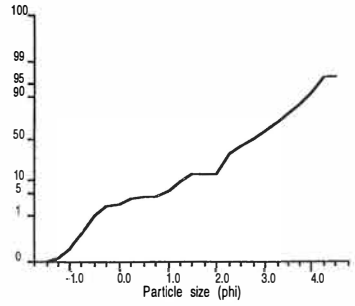

Raw data summary

Size (phi)	Size (mm)	Cumulative weight (g)	Interval frequency (%)	Cumulative frequency (%)
-1.50	2.8284	0.00	0.00	0.00
-1.25	2.3784	0.04	0.14	0.14
-1.00	2.0000	0.08	0.14	0.29
-0.75	1.6818	0.15	0.25	0.54
-0.50	1.4142	0.30	0.54	1.09
-0.25	1.1892	0.57	0.98	2.06
0.00	1.0000	0.70	0.47	2.53
0.25	0.8409	0.92	0.80	3.33
0.50	0.7071	1.08	0.58	3.91
0.75	0.5946	1.10	0.07	3.98
1.00	0.5000	1.55	1.63	5.61
1.25	0.4204	2.72	4.24	9.85
1.50	0.3536	3.72	3.62	13.47
1.75	0.2973	3.92	0.72	14.19
2.00	0.2500	3.92	0.00	14.19
2.25	0.2102	8.68	17.24	31.43
2.50	0.1768	10.82	7.75	39.18
2.75	0.1487	13.37	9.23	48.41
3.00	0.1250	16.23	10.36	58.77
3.25	0.1051	19.01	10.07	68.84
3.50	0.0884	21.43	8.76	77.60
3.75	0.0743	23.59	7.82	85.42
4.00	0.0625	25.38	6.48	91.91
4.25	0.0526	26.75	4.96	96.87
4.50	0.0442	26.75	0.00	96.87

Total weight = 27.62 g

PARTICLE SIZE ANALYSIS

Earth Sciences - University of Waikato

Sample: NEWDICK 1.2M D2 SUMMER

Size distribution histogram

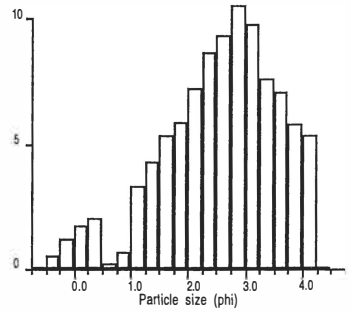

Results summary

Textural size classes

Gravel= 0.00% Sand= 91.43% Silt= 8.57% Clay= 0.00%

Gravel free detrital sediment

Sand

Moment method parameters (phi)

Mean= 2.49 Sorting= 0.99 Skewness= -0.40 Kurtosis= 2.95

Graphical method parameters (phi)

Mean= 2.67 Sorting= 1.09 Skewness= -0.16 Kurtosis= 1.09

Median= 2.74 C= -0.14 D35= 2.32 D65= 3.10

Textural description:

Poorly sorted, Coarse skewed, Mesokurtic

Cumulative frequency

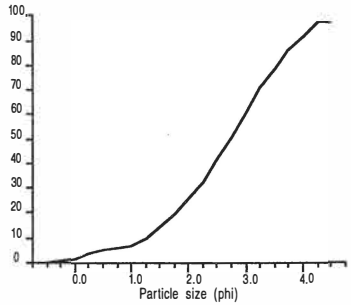

Cumulative frequency

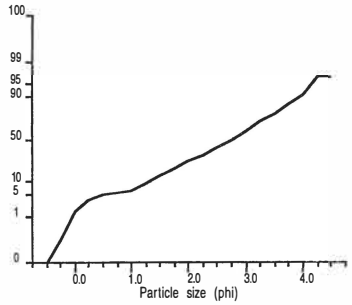

Raw data summary

Size (phi)	Size (mm)	Cumulative weight (g)	Interval frequency (%)	Cumulative frequency (%)
-0.50	1.4142	-0.02	-0.09	-0.09
-0.25	1.1892	0.10	0.55	0.46
0.00	1.0000	0.36	1.20	1.66
0.25	0.8409	0.74	1.76	3.42
0.50	0.7071	1.19	2.08	5.50
0.75	0.5946	1.24	0.23	5.73
1.00	0.5000	1.38	0.65	6.38
1.25	0.4204	2.10	3.33	9.71
1.50	0.3536	3.03	4.30	14.01
1.75	0.2973	4.19	5.36	19.37
2.00	0.2500	5.46	5.87	25.24
2.25	0.2102	7.03	7.26	32.49
2.50	0.1768	8.90	8.64	41.14
2.75	0.1487	10.92	9.34	50.48
3.00	0.1250	13.21	10.59	61.06
3.25	0.1051	15.33	9.80	70.86
3.50	0.0884	16.98	7.63	78.49
3.75	0.0743	18.52	7.12	85.61
4.00	0.0625	19.78	5.82	91.43
4.25	0.0526	20.94	5.36	96.79
4.50	0.0442	20.94	0.00	96.79

Total weight = 21.63 g

PARTICLE SIZE ANALYSIS

Earth Sciences - University of Waikato

Sample: PUKEHINA REDOUBT 0.35M SUMMER

Size distribution histogram

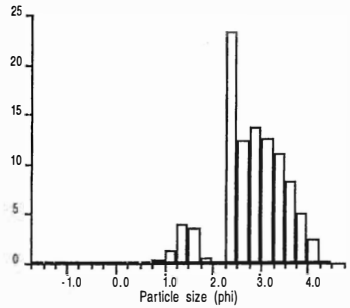

Results summary

Textural size classes

Gravel= 0.15% Sand= 96.43% Silt= 3.42% Clay= 0.00%

Gravel bearing detrital sediment

Slightly Gravelly Sand

Moment method parameters (phi)

Mean= 2.78 Sorting= 0.70Skewness= -0.63 Kurtosis= 4.86

Graphical method parameters (phi)

Mean= 2.89 Sorting= 0.68Skewness= 0.02 Kurtosis= 1.13

Median= 2.83 C= 1.04 D35= 2.53 D65= 3.11

Textural description:

Moderately well sorted, Near symmetrical, Leptokurtic

Cumulative frequency

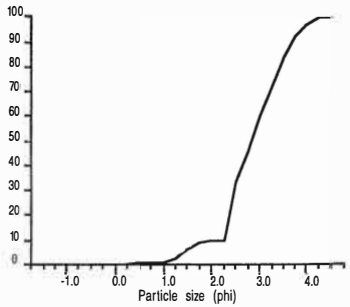

Cumulative frequency

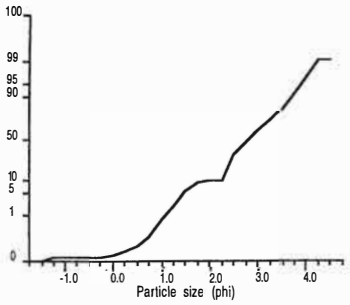

Raw data summary

Size (phi)	Size (mm)	Cumulative weight (g)	Interval frequency (%)	Cumulative frequency (%)
-1.50	2.8284	0.00	0.00	0.00
-1.25	2.3784	0.05	0.15	0.15
-1.00	2.0000	0.05	0.00	0.15
-0.75	1.6818	0.05	0.00	0.15
-0.50	1.4142	0.05	0.00	0.15
-0.25	1.1892	0.05	0.00	0.15
0.00	1.0000	0.06	0.03	0.18
0.25	0.8409	0.08	0.06	0.24
0.50	0.7071	0.11	0.09	0.32
0.75	0.5946	0.17	0.18	0.50
1.00	0.5000	0.27	0.29	0.80
1.25	0.4204	0.71	1.30	2.09
1.50	0.3536	2.06	3.98	6.07
1.75	0.2973	3.25	3.51	9.58
2.00	0.2500	3.43	0.53	10.12
2.25	0.2102	3.43	0.00	10.12
2.50	0.1768	11.36	23.39	33.50
2.75	0.1487	15.55	12.36	45.86
3.00	0.1250	20.17	13.62	59.48
3.25	0.1051	24.48	12.71	72.19
3.50	0.0884	28.25	11.12	83.31
3.75	0.0743	31.06	8.29	91.60
4.00	0.0625	32.75	4.98	96.58
4.25	0.0526	33.62	2.57	99.15
4.50	0.0442	33.62	0.00	99.15

Total weight = 33.91 g

PARTICLE SIZE ANALYSIS

Earth Sciences - University of Waikato

Sample: PUKEHINA REDOUBT 0.5M SUMMER

Size distribution histogram

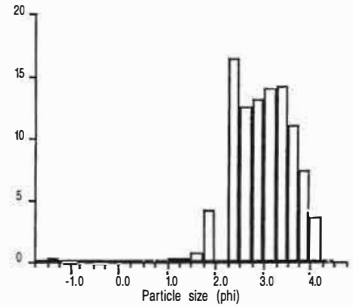

Results summary

Textural size classes

Gravel= 0.24% Sand= 94.57% Silt= 5.19% Clay= 0.00%

Gravel bearing detrital sediment

Slightly Gravelly Sand

Moment method parameters (phi)

Mean= 2.96 Sorting= 0.63Skewness= -0.82 Kurtosis= 7.76

Graphical method parameters (phi)

Mean= 3.04 Sorting= 0.63Skewness= -0.02 Kurtosis= 0.92

Median= 3.03 C= 1.44 D35= 2.75 D65= 3.30

Textural description:

Moderately well sorted, Near symmetrical, Mesokurtic

Cumulative frequency

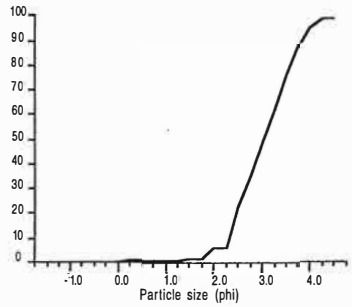

Cumulative frequency

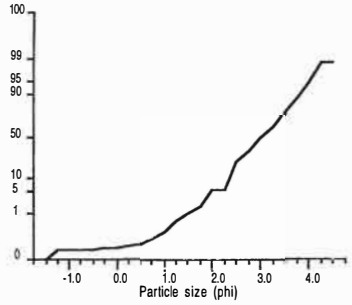

Raw data summary

Size (phi)	Size (mm)	Cumulative weight (g)	Interval frequency (%)	Cumulative frequency (%)
-1.50	2.8284	0.00	0.00	0.00
-1.25	2.3784	0.08	0.24	0.24
-1.00	2.0000	0.08	0.00	0.24
-0.75	1.6818	0.08	0.00	0.24
-0.50	1.4142	0.08	0.00	0.24
-0.25	1.1892	0.09	0.03	0.27
0.00	1.0000	0.09	0.00	0.27
0.25	0.8409	0.10	0.03	0.30
0.50	0.7071	0.11	0.03	0.33
0.75	0.5946	0.14	0.09	0.42
1.00	0.5000	0.18	0.12	0.54
1.25	0.4204	0.25	0.21	0.75
1.50	0.3536	0.36	0.33	1.08
1.75	0.2973	0.59	0.69	1.77
2.00	0.2500	2.00	4.24	6.02
2.25	0.2102	2.00	0.00	6.02
2.50	0.1768	7.46	16.42	22.44
2.75	0.1487	11.64	12.57	35.01
3.00	0.1250	16.01	13.14	48.16
3.25	0.1051	20.68	14.05	62.21
3.50	0.0884	25.42	14.26	76.46
3.75	0.0743	29.07	10.98	87.44
4.00	0.0625	31.52	7.37	94.81
4.25	0.0526	32.79	3.82	98.63
4.50	0.0442	32.79	0.00	98.63

Total weight = 33.24 g

PARTICLE SIZE ANALYSIS

Earth Sciences - University of Waikato

Sample: PUKEHINA REDOUBT 1.2M SUMMER

Size distribution histogram

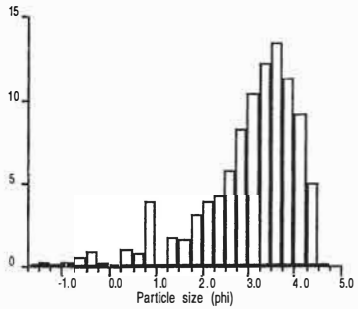

Cumulative frequency

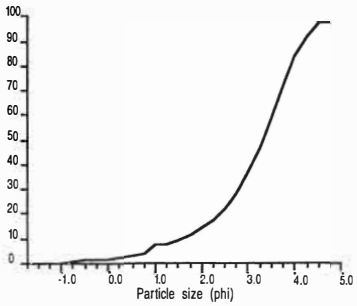

Cumulative frequency

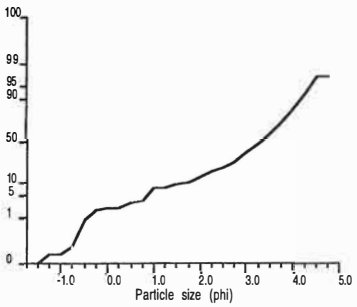

Results summary

Textural size classes

Gravel= 0.24% Sand= 83.10% Silt= 16.67% Clay= 0.00%

Gravel bearing detrital sediment

Slightly Gravelly Muddy Sand

Moment method parameters (phi)

Mean= 2.96 Sorting= 1.04 Skewness= -1.14 Kurtosis= 4.60

Graphical method parameters (phi)

Mean= 3.16 Sorting= 1.01 Skewness= -0.34 Kurtosis= 1.23

Median= 3.32 C= -0.47 D35= 2.97 D65= 3.62

Textural description:

Poorly sorted, Strongly Coarse skewed, Leptokurtic

Raw data summary

Size (phi)	Size (mm)	Cumulative weight (g)	Interval frequency (%)	Cumulative frequency (%)
-1.50	2.8284	0.00	0.00	0.00
-1.25	2.3784	0.05	0.24	0.24
-1.00	2.0000	0.05	0.00	0.24
-0.75	1.6818	0.08	0.14	0.38
-0.50	1.4142	0.19	0.52	0.89
-0.25	1.1892	0.38	0.89	1.79
0.00	1.0000	0.42	0.19	1.98
0.25	0.8409	0.44	0.09	2.07
0.50	0.7071	0.64	0.94	3.01
0.75	0.5946	0.81	0.80	3.81
1.00	0.5000	1.64	3.91	7.72
1.25	0.4204	1.64	0.00	7.72
1.50	0.3536	1.99	1.65	9.37
1.75	0.2973	2.32	1.55	10.92
2.00	0.2500	2.97	3.06	13.98
2.25	0.2102	3.77	3.77	17.75
2.50	0.1768	4.67	4.24	21.99
2.75	0.1487	5.89	5.74	27.73
3.00	0.1250	7.64	8.24	35.97
3.25	0.1051	9.85	10.40	46.38
3.50	0.0884	12.44	12.19	58.57
3.75	0.0743	15.30	13.47	72.03
4.00	0.0625	17.70	11.30	83.33
4.25	0.0526	19.64	9.13	92.47
4.50	0.0442	20.69	4.94	97.41
4.75	0.0372	20.69	0.00	97.41

Total weight = 21.24 g

PARTICLE SIZE ANALYSIS

Earth Sciences - University of Waikato

Sample: PUKEHINA REDOUBT 0.8M SUMMER

Size distribution histogram

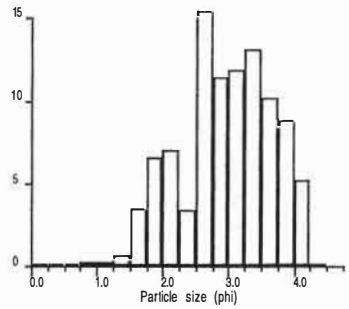

Cumulative frequency

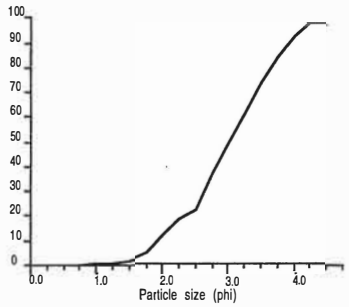

Cumulative frequency

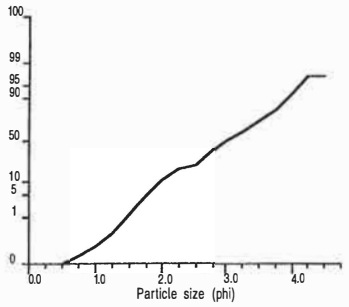

Results summary

Textural size classes

Gravel= 0.00% Sand= 92.18% Silt= 7.82% Clay= 0.00%

Gravel free detrital sediment

Sand

Moment method parameters (phi)

Mean= 2.89 Sorting= 0.69 Skewness= -0.01 Kurtosis= 2.45

Graphical method parameters (phi)

Mean= 2.99 Sorting= 0.76 Skewness= -0.08 Kurtosis= 0.98

Median= 3.04 C= 1.42 D35= 2.72 D65= 3.34

Textural description:

Moderately sorted, Near symmetrical, Mesokurtic

Raw data summary

Size (phi)	Size (mm)	Cumulative weight (g)	Interval frequency (%)	Cumulative frequency (%)
0.25	0.8409	-0.01	-0.04	-0.04
0.50	0.7071	0.02	0.11	0.07
0.75	0.5946	0.05	0.11	0.18
1.00	0.5000	0.09	0.15	0.33
1.25	0.4204	0.16	0.26	0.59
1.50	0.3536	0.32	0.59	1.18
1.75	0.2973	1.23	3.36	4.54
2.00	0.2500	2.99	6.50	11.05
2.25	0.2102	4.91	7.09	18.14
2.50	0.1768	5.82	3.36	21.50
2.75	0.1487	9.97	15.33	36.83
3.00	0.1250	13.05	11.38	48.21
3.25	0.1051	16.27	11.90	60.11
3.50	0.0884	19.82	13.12	73.23
3.75	0.0743	22.58	10.20	83.42
4.00	0.0625	24.95	8.76	92.18
4.25	0.0526	26.35	5.17	97.35
4.50	0.0442	26.35	0.00	97.35

Total weight = 27.07 g

SETTLING VELOCITY ANALYSIS

Earth Sciences - University of Waikato

Sample: Newdicks Beach 0.5m Deploy 1

Size distribution histogram

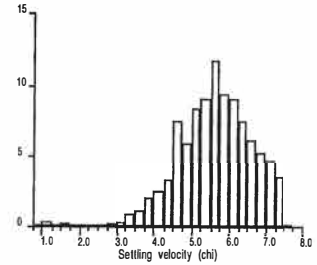

Results summary

Moment method parameters (chi)

Mean= 5.57 Sorting= 0.99Skewness= -0.44 Kurtosis= 4.10

Cumulative frequency

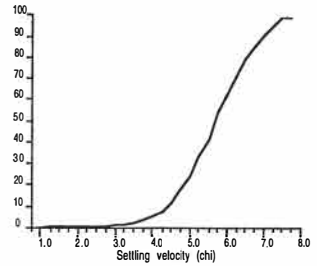

Cumulative frequency

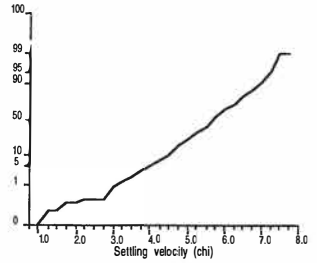

Raw data summary

Velocity (chi)	Velocity (m/s)	Cumulative weight (g)	Interval frequency (%)	Cumulative frequency (%)
1.00	0.5000	0.00	0.00	0.00
1.25	0.4204	0.05	0.37	0.37
1.50	0.3536	0.05	0.00	0.37
1.75	0.2973	0.07	0.15	0.52
2.00	0.2500	0.07	0.00	0.52
2.25	0.2102	0.08	0.07	0.59
2.50	0.1768	0.08	0.00	0.59
2.75	0.1487	0.08	0.00	0.59
3.00	0.1250	0.12	0.30	0.89
3.25	0.1051	0.17	0.37	1.26
3.50	0.0884	0.29	0.89	2.14
3.75	0.0743	0.44	1.11	3.25
4.00	0.0625	0.71	2.00	5.25
4.25	0.0526	1.05	2.51	7.76
4.50	0.0442	1.49	3.25	11.01
4.75	0.0372	2.49	7.39	18.40
5.00	0.0312	3.29	5.91	24.32
5.25	0.0263	4.43	8.43	32.74
5.50	0.0221	5.65	9.02	41.76
5.75	0.0186	7.24	11.75	53.51
6.00	0.0156	8.52	9.46	62.97
6.25	0.0131	9.74	9.02	71.99
6.50	0.0110	10.76	7.54	79.53
6.75	0.0093	11.58	6.06	85.59
7.00	0.0078	12.29	5.25	90.84
7.25	0.0066	12.91	4.58	95.42
7.50	0.0055	13.39	3.55	98.97
7.75	0.0046	13.39	0.00	98.97

Total weight = 13.53 g

University of Waikato
Rapid Sediment Analyser
Operating System Version 7.1

SETTLING VELOCITY ANALYSIS

Earth Sciences - University of Waikato

Sample: Newdicks Beach 0.35m Deploy 1

Size distribution histogram

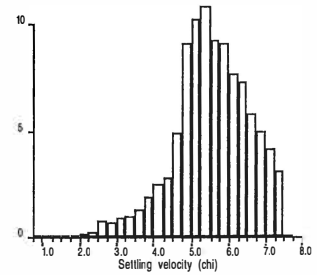

Results summary

Moment method parameters (chi)

Mean= 5.49 Sorting= 1.02Skewness= -0.39 Kurtosis= 3.52

Cumulative frequency

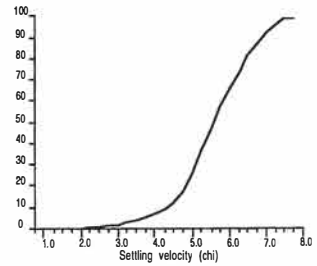

Cumulative frequency

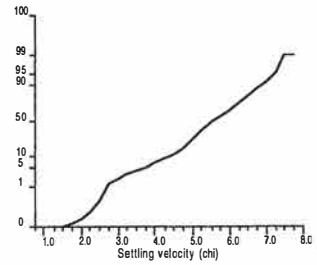

Raw data summary

Velocity (chi)	Velocity (m/s)	Cumulative weight (g)	Interval frequency (%)	Cumulative frequency (%)
1.00	0.5000	0.00	0.00	0.00
1.25	0.4204	0.01	0.07	0.07
1.50	0.3536	0.01	0.00	0.07
1.75	0.2973	0.02	0.07	0.15
2.00	0.2500	0.03	0.07	0.22
2.25	0.2102	0.05	0.15	0.37
2.50	0.1768	0.08	0.22	0.60
2.75	0.1487	0.18	0.75	1.35
3.00	0.1250	0.27	0.67	2.02
3.25	0.1051	0.39	0.90	2.92
3.50	0.0884	0.52	0.97	3.90
3.75	0.0743	0.69	1.27	5.17
4.00	0.0625	0.94	1.87	7.05
4.25	0.0526	1.27	2.47	9.52
4.50	0.0442	1.65	2.85	12.37
4.75	0.0372	2.30	4.87	17.24
5.00	0.0312	3.52	9.15	26.39
5.25	0.0263	4.89	10.27	36.66
5.50	0.0221	6.34	10.87	47.53
5.75	0.0186	7.58	9.30	56.82
6.00	0.0156	8.80	9.15	65.97
6.25	0.0131	9.83	7.72	73.69
6.50	0.0110	10.80	7.27	80.96
6.75	0.0093	11.58	5.85	86.81
7.00	0.0078	12.24	4.95	91.75
7.25	0.0066	12.80	4.20	95.95
7.50	0.0055	13.21	3.07	99.03
7.75	0.0046	13.21	0.00	99.03

Total weight = 13.34 g

University of Waikato
Rapid Sediment Analyser
Operating System Version 7.1

SETTLING VELOCITY ANALYSIS

Earth Sciences - University of Waikato

Sample: Newdicks Beach 0.8m Deploy 1

Size distribution histogram

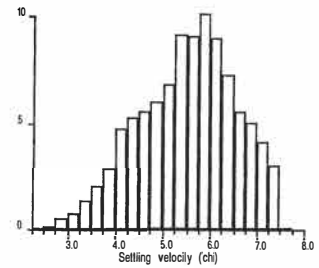

Results summary

Moment method parameters (chi)

Mean= 5.48 Sorting= 1.01 Skewness= -0.13 Kurtosis= 2.46

Cumulative frequency

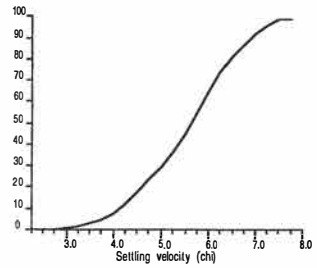

Cumulative frequency

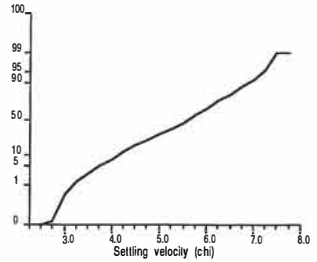

Raw data summary

Velocity (chi)	Velocity (m/s)	Cumulative weight (g)	Interval frequency (%)	Cumulative frequency (%)
2.50	0.1768	0.00	0.00	0.00
2.75	0.1487	0.02	0.15	0.15
3.00	0.1250	0.09	0.52	0.66
3.25	0.1051	0.19	0.74	1.40
3.50	0.0884	0.37	1.33	2.73
3.75	0.0743	0.65	2.06	4.79
4.00	0.0625	1.04	2.87	7.66
4.25	0.0526	1.69	4.79	12.45
4.50	0.0442	2.41	5.31	17.76
4.75	0.0372	3.17	5.60	23.36
5.00	0.0312	3.99	6.04	29.40
5.25	0.0263	4.92	6.85	36.26
5.50	0.0221	6.17	9.21	45.47
5.75	0.0186	7.41	9.14	54.61
6.00	0.0156	8.79	10.17	64.78
6.25	0.0131	10.02	9.06	73.84
6.50	0.0110	11.02	7.37	81.21
6.75	0.0093	11.78	5.60	86.81
7.00	0.0078	12.47	5.08	91.89
7.25	0.0066	13.03	4.13	96.02
7.50	0.0055	13.44	3.02	99.04
7.75	0.0046	13.44	0.00	99.04

Total weight = 13.57 g

University of Waikato
Rapid Sediment Analyser
Operating System Version 7.1

SETTLING VELOCITY ANALYSIS

Earth Sciences - University of Waikato

Sample: Newdicks Beach 1.2m Deploy 1

Size distribution histogram

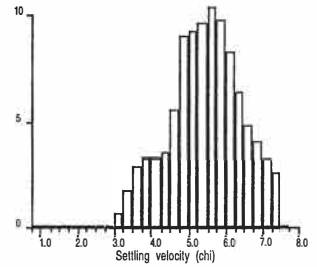

Results summary

Moment method parameters (chi)

Mean= 5.40 Sorting= 0.97 Skewness= -0.04 Kurtosis= 2.64

Cumulative frequency

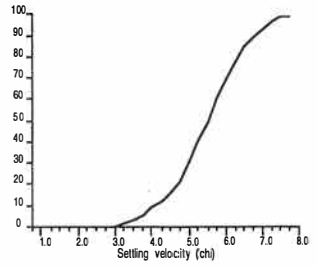

Cumulative frequency

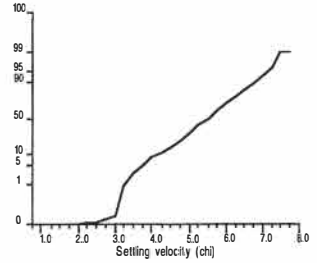

Raw data summary

Velocity (chi)	Velocity (m/s)	Cumulative weight (g)	Interval frequency (%)	Cumulative frequency (%)
1.00	0.5000	0.00	0.00	0.00
1.25	0.4204	0.00	0.00	0.00
1.50	0.3536	0.00	0.00	0.00
1.75	0.2973	0.00	0.00	0.00
2.00	0.2500	0.00	0.00	0.00
2.25	0.2102	0.01	0.08	0.08
2.50	0.1768	0.01	0.00	0.08
2.75	0.1487	0.02	0.08	0.17
3.00	0.1250	0.03	0.08	0.25
3.25	0.1051	0.11	0.68	0.93
3.50	0.0884	0.32	1.78	2.70
3.75	0.0743	0.66	2.87	5.58
4.00	0.0625	1.06	3.38	8.96
4.25	0.0526	1.45	3.30	12.26
4.50	0.0442	1.87	3.55	15.81
4.75	0.0372	2.53	5.58	21.39
5.00	0.0312	3.60	9.04	30.43
5.25	0.0263	4.70	9.30	39.73
5.50	0.0221	5.84	9.64	49.37
5.75	0.0186	7.07	10.40	59.76
6.00	0.0156	8.23	9.81	69.57
6.25	0.0131	9.21	8.28	77.85
6.50	0.0110	9.97	6.42	84.28
6.75	0.0093	10.54	4.82	89.10
7.00	0.0078	11.02	4.06	93.15
7.25	0.0066	11.40	3.21	96.37
7.50	0.0055	11.70	2.54	98.90
7.75	0.0046	11.70	0.00	98.90

Total weight = 11.83 g

University of Waikato
Rapid Sediment Analyser
Operating System Version 7.1

SETTLING VELOCITY ANALYSIS

Earth Sciences - University of Waikato

Sample: Pukehina Redoubt 0.35m Deploy 1

Size distribution histogram

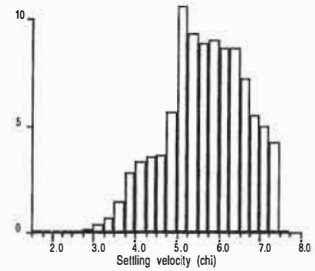

Results summary

Moment method parameters (chi)

Mean= 5.63 Sorting= 0.97 Skewness= -0.14 Kurtosis= 2.56

Cumulative frequency

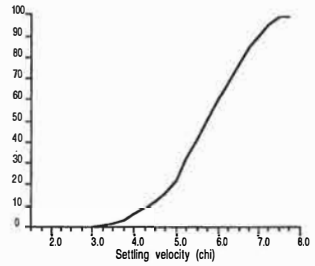

Cumulative frequency

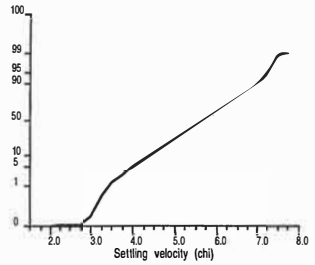

Raw data summary

Velocity (chi)	Velocity (m/s)	Cumulative weight (g)	Interval frequency (%)	Cumulative frequency (%)
1.75	0.2973	-0.01	-0.09	-0.09
2.00	0.2500	0.00	0.09	0.00
2.25	0.2102	0.01	0.09	0.09
2.50	0.1768	0.01	0.00	0.09
2.75	0.1487	0.01	0.00	0.09
3.00	0.1250	0.03	0.18	0.26
3.25	0.1051	0.08	0.44	0.70
3.50	0.0884	0.16	0.70	1.41
3.75	0.0743	0.32	1.41	2.82
4.00	0.0625	0.64	2.82	5.64
4.25	0.0526	1.02	3.35	8.99
4.50	0.0442	1.42	3.52	12.51
4.75	0.0372	1.83	3.61	16.12
5.00	0.0312	2.47	5.64	21.76
5.25	0.0263	3.68	10.66	32.42
5.50	0.0221	4.74	9.34	41.76
5.75	0.0186	5.75	8.90	50.66
6.00	0.0156	6.78	9.07	59.74
6.25	0.0131	7.77	8.72	68.46
6.50	0.0110	8.75	8.63	77.09
6.75	0.0093	9.57	7.22	84.32
7.00	0.0078	10.19	5.46	89.78
7.25	0.0066	10.76	5.02	94.80
7.50	0.0055	11.24	4.23	99.03
7.75	0.0046	11.24	0.00	99.03

Total weight = 11.35 g

University of Waikato
Rapid Sediment Analyser
Operating System Version 7.1

SETTLING VELOCITY ANALYSIS

Earth Sciences - University of Waikato

Sample: Pukehina Redoubt 0.5m Deploy 1

Size distribution histogram

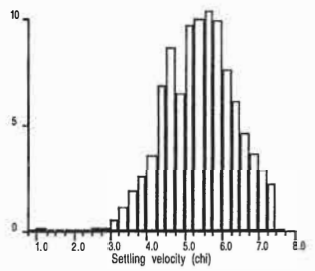

Results summary

Moment method parameters (chi)

Mean= 5.38 Sorting= 0.96 Skewness= -0.21 Kurtosis= 3.35

Cumulative frequency

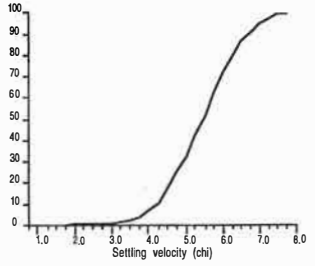

Cumulative frequency

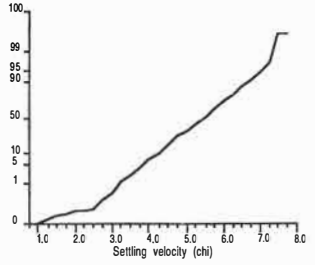

Raw data summary

Velocity (chi)	Velocity (m/s)	Cumulative weight (g)	Interval frequency (%)	Cumulative frequency (%)
1.00	0.5000	0.00	0.00	0.00
1.25	0.4204	0.03	0.16	0.16
1.50	0.3536	0.04	0.05	0.22
1.75	0.2973	0.05	0.05	0.27
2.00	0.2500	0.06	0.05	0.32
2.25	0.2102	0.06	0.00	0.32
2.50	0.1768	0.07	0.05	0.38
2.75	0.1487	0.10	0.16	0.54
3.00	0.1250	0.13	0.16	0.70
3.25	0.1051	0.23	0.54	1.24
3.50	0.0884	0.44	1.13	2.37
3.75	0.0743	0.79	1.88	4.25
4.00	0.0625	1.27	2.58	6.84
4.25	0.0526	1.93	3.55	10.39
4.50	0.0442	3.21	6.89	17.29
4.75	0.0372	4.83	8.72	26.01
5.00	0.0312	6.03	6.46	32.47
5.25	0.0263	7.83	9.69	42.16
5.50	0.0221	9.69	10.02	52.18
5.75	0.0186	11.62	10.39	62.57
6.00	0.0156	13.47	9.96	72.54
6.25	0.0131	14.88	7.59	80.13
6.50	0.0110	16.02	6.14	86.27
6.75	0.0093	16.87	4.58	90.85
7.00	0.0078	17.54	3.61	94.45
7.25	0.0066	18.08	2.91	97.36
7.50	0.0055	18.48	2.15	99.52
7.75	0.0046	18.48	0.00	99.52

Total weight = 18.57 g

University of Waikato
Rapid Sediment Analyser
Operating System Version 7.1

SETTLING VELOCITY ANALYSIS

Earth Sciences - University of Waikato

Sample: Pukehina Redoubt 0.8m Deploy 1

Size distribution histogram

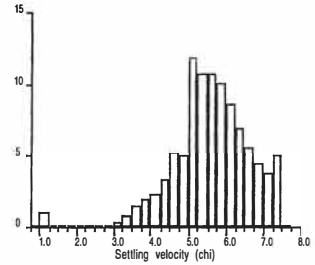

Results summary

Moment method parameters (chi)

Mean= 5.56 Sorting= 1.04 Skewness= -0.82 Kurtosis= 5.46

Cumulative frequency

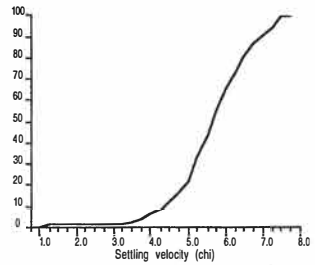

Cumulative frequency

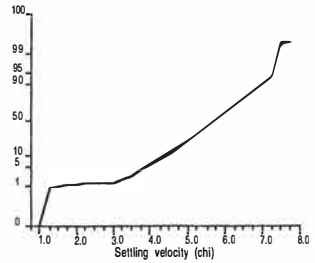

Raw data summary

Velocity (chi)	Velocity (m/s)	Cumulative weight (g)	Interval frequency (%)	Cumulative frequency (%)
1.00	0.5000	0.00	0.00	0.00
1.25	0.4204	0.12	0.97	0.97
1.50	0.3536	0.13	0.08	1.05
1.75	0.2973	0.14	0.08	1.13
2.00	0.2500	0.15	0.08	1.21
2.25	0.2102	0.16	0.08	1.29
2.50	0.1768	0.16	0.00	1.29
2.75	0.1487	0.17	0.08	1.37
3.00	0.1250	0.18	0.08	1.45
3.25	0.1051	0.22	0.32	1.78
3.50	0.0884	0.32	0.81	2.58
3.75	0.0743	0.51	1.53	4.12
4.00	0.0625	0.75	1.94	6.06
4.25	0.0526	1.03	2.26	8.32
4.50	0.0442	1.43	3.23	11.55
4.75	0.0372	2.07	5.17	16.72
5.00	0.0312	2.69	5.01	21.73
5.25	0.0263	4.16	11.87	33.60
5.50	0.0221	5.49	10.74	44.35
5.75	0.0186	6.82	10.74	55.09
6.00	0.0156	8.07	10.10	65.19
6.25	0.0131	9.13	8.56	73.75
6.50	0.0110	9.98	6.87	80.61
6.75	0.0093	10.67	5.57	86.19
7.00	0.0078	11.22	4.44	90.63
7.25	0.0066	11.68	3.72	94.35
7.50	0.0055	12.30	5.01	99.35
7.75	0.0046	12.30	0.00	99.35

Total weight = 12.38 g

University of Waikato
Rapid Sediment Analyser
Operating System Version 7.1

SETTLING VELOCITY ANALYSIS

Earth Sciences - University of Waikato

Sample: Pukehina Redoubt 1.2m Deploy 1

Size distribution histogram

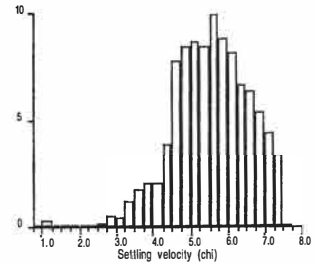

Results summary

Moment method parameters (chi)

Mean= 5.49 Sorting= 1.02 Skewness= -0.29 Kurtosis= 3.53

Cumulative frequency

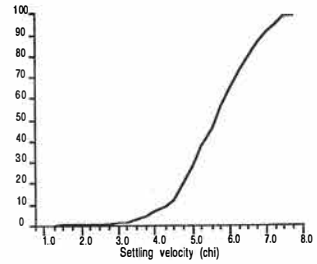

Cumulative frequency

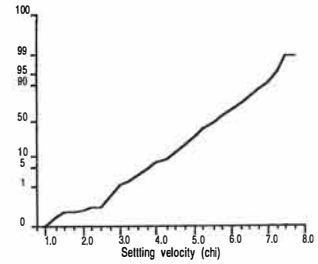

Raw data summary

Velocity (chi)	Velocity (m/s)	Cumulative weight (g)	Interval frequency (%)	Cumulative frequency (%)
1.00	0.5000	0.00	0.00	0.00
1.25	0.4204	0.04	0.27	0.27
1.50	0.3536	0.05	0.07	0.33
1.75	0.2973	0.05	0.00	0.33
2.00	0.2500	0.06	0.07	0.40
2.25	0.2102	0.07	0.07	0.47
2.50	0.1768	0.07	0.00	0.47
2.75	0.1487	0.10	0.20	0.67
3.00	0.1250	0.18	0.53	1.20
3.25	0.1051	0.25	0.47	1.67
3.50	0.0884	0.43	1.20	2.87
3.75	0.0743	0.69	1.74	4.61
4.00	0.0625	1.00	2.07	6.68
4.25	0.0526	1.31	2.07	8.76
4.50	0.0442	1.88	3.81	12.57
4.75	0.0372	3.04	7.75	20.32
5.00	0.0312	4.31	8.49	28.81
5.25	0.0263	5.61	8.69	37.50
5.50	0.0221	6.87	8.42	45.92
5.75	0.0186	8.36	9.96	55.88
6.00	0.0156	9.68	8.82	64.71
6.25	0.0131	10.90	8.16	72.86
6.50	0.0110	11.89	6.62	79.48
6.75	0.0093	12.84	6.35	85.83
7.00	0.0078	13.64	5.35	91.18
7.25	0.0066	14.29	4.34	95.52
7.50	0.0055	14.78	3.28	98.80
7.75	0.0046	14.78	0.00	98.80

Total weight = 14.96 g

University of Waikato
Rapid Sediment Analyser
Operating System Version 7.1

SETTLING VELOCITY ANALYSIS

Earth Sciences - University of Waikato

Sample: Newdicks Beach 0.35m Deploy 2

Size distribution histogram

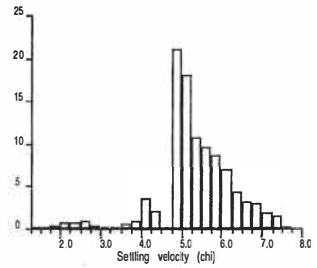

Results summary

Moment method parameters (chi)

Mean= 5.32 Sorting= 0.90 Skewness= -0.63 Kurtosis= 5.20

Cumulative frequency

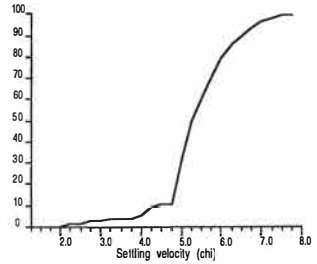

Cumulative frequency

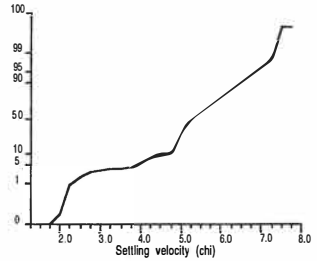

Raw data summary

Velocity (chi)	Velocity (m/s)	Cumulative weight (g)	Interval frequency (%)	Cumulative frequency (%)
1.50	0.3536	0.00	0.00	0.00
1.75	0.2973	0.01	0.04	0.04
2.00	0.2500	0.07	0.24	0.28
2.25	0.2102	0.24	0.67	0.95
2.50	0.1768	0.44	0.79	1.74
2.75	0.1487	0.69	0.99	2.73
3.00	0.1250	0.78	0.36	3.09
3.25	0.1051	0.83	0.20	3.28
3.50	0.0884	0.87	0.16	3.44
3.75	0.0743	1.03	0.63	4.08
4.00	0.0625	1.28	0.99	5.07
4.25	0.0526	2.17	3.52	8.59
4.50	0.0442	2.69	2.06	10.65
4.75	0.0372	2.69	0.00	10.65
5.00	0.0312	8.04	21.17	31.82
5.25	0.0263	12.60	18.05	49.86
5.50	0.0221	15.32	10.76	60.63
5.75	0.0186	17.76	9.66	70.28
6.00	0.0156	19.96	8.71	78.99
6.25	0.0131	21.70	6.89	85.87
6.50	0.0110	22.76	4.19	90.07
6.75	0.0093	23.59	3.28	93.35
7.00	0.0078	24.32	2.89	96.24
7.25	0.0066	24.81	1.94	98.18
7.50	0.0055	25.18	1.46	99.64
7.75	0.0046	25.18	0.00	99.64

Total weight = 25.27 g

University of Waikato
Rapid Sediment Analyser
Operating System Version 7.1

SETTLING VELOCITY ANALYSIS

Earth Sciences - University of Waikato

Sample: Newdicks Beach 0.5m Deploy 2

Size distribution histogram

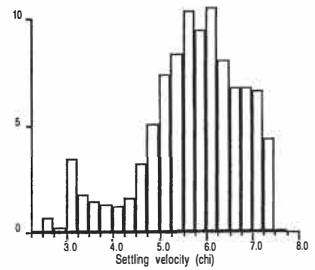

Results summary

Moment method parameters (chi)

Mean= 5.65 Sorting= 1.07 Skewness= -0.52 Kurtosis= 3.06

Cumulative frequency

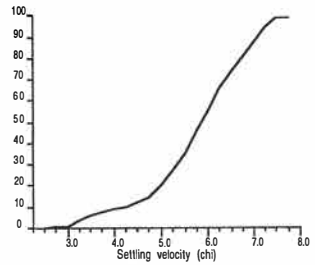

Cumulative frequency

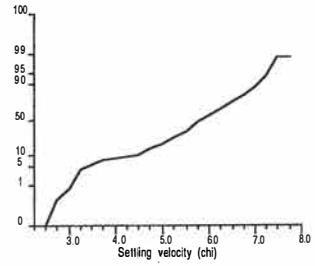

Raw data summary

Velocity (chi)	Velocity (m/s)	Cumulative weight (g)	Interval frequency (%)	Cumulative frequency (%)
2.50	0.1768	-0.01	-0.06	-0.06
2.75	0.1487	0.10	0.64	0.58
3.00	0.1250	0.14	0.23	0.82
3.25	0.1051	0.73	3.44	4.25
3.50	0.0884	1.02	1.69	5.94
3.75	0.0743	1.27	1.46	7.40
4.00	0.0625	1.49	1.28	8.68
4.25	0.0526	1.70	1.22	9.91
4.50	0.0442	1.97	1.57	11.48
4.75	0.0372	2.52	3.21	14.69
5.00	0.0312	3.39	5.07	19.76
5.25	0.0263	4.66	7.40	27.16
5.50	0.0221	6.09	8.33	35.49
5.75	0.0186	7.88	10.43	45.92
6.00	0.0156	9.52	9.56	55.48
6.25	0.0131	11.33	10.55	66.03
6.50	0.0110	12.71	8.04	74.07
6.75	0.0093	13.87	6.76	80.83
7.00	0.0078	15.03	6.76	87.59
7.25	0.0066	16.17	6.64	94.23
7.50	0.0055	16.93	4.43	98.66
7.75	0.0046	16.93	0.00	98.66

Total weight = 17.16 g

University of Waikato
Rapid Sediment Analyser
Operating System Version 7.1

SETTLING VELOCITY ANALYSIS

Earth Sciences - University of Waikato

Sample: Newdicks Beach 0.8m Deploy 2

Size distribution histogram

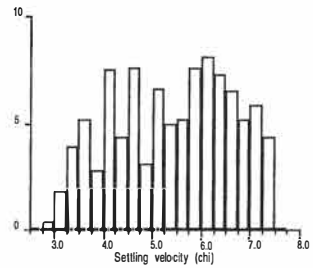

Results summary

Moment method parameters (chi)

Mean= 5.36 Sorting= 1.20 Skewness= -0.01 Kurtosis= 1.90

Cumulative frequency

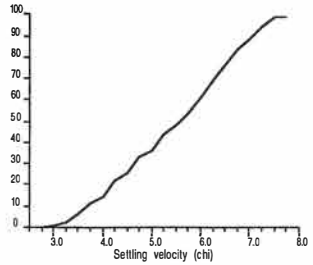

Cumulative frequency

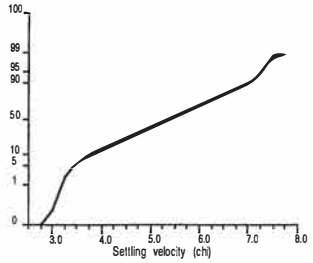

Raw data summary

Velocity (chi)	Velocity (m/s)	Cumulative weight (g)	Interval frequency (%)	Cumulative frequency (%)
2.75	0.1487	-0.01	-0.07	-0.07
3.00	0.1250	0.05	0.43	0.35
3.25	0.1051	0.31	1.84	2.20
3.50	0.0884	0.87	3.97	6.17
3.75	0.0743	1.61	5.24	11.41
4.00	0.0625	2.00	2.76	14.17
4.25	0.0526	3.06	7.51	21.69
4.50	0.0442	3.68	4.39	26.08
4.75	0.0372	4.75	7.58	33.66
5.00	0.0312	5.18	3.05	36.71
5.25	0.0263	6.12	6.66	43.37
5.50	0.0221	6.82	4.96	48.33
5.75	0.0186	7.55	5.17	53.51
6.00	0.0156	8.63	7.65	61.16
6.25	0.0131	9.78	8.15	69.31
6.50	0.0110	10.82	7.37	76.68
6.75	0.0093	11.75	6.59	83.27
7.00	0.0078	12.49	5.24	88.52
7.25	0.0066	13.32	5.88	94.40
7.50	0.0055	13.94	4.39	98.80
7.75	0.0046	13.94	0.00	98.80

Total weight = 14.11 g

University of Waikato
Rapid Sediment Analyser
Operating System Version 7.1

SETTLING VELOCITY ANALYSIS

Earth Sciences - University of Waikato

Sample: Newdicks Beach 1.2m Deploy 2

Size distribution histogram

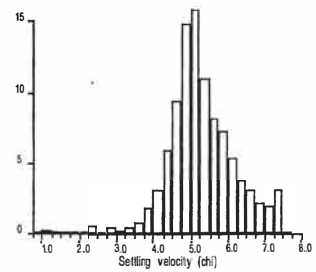

Results summary

Moment method parameters (chi)

Mean= 5.26 Sorting= 0.90 Skewness= 0.03 Kurtosis= 4.43

Cumulative frequency

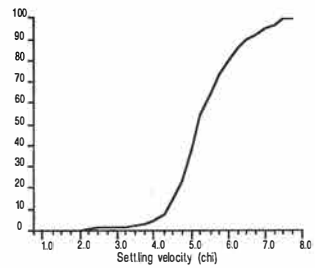

Cumulative frequency

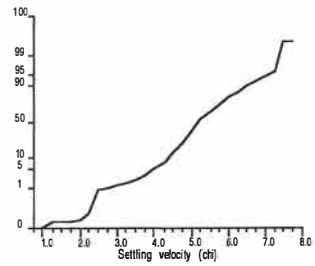

Raw data summary

Velocity (chi)	Velocity (m/s)	Cumulative weight (g)	Interval frequency (%)	Cumulative frequency (%)
1.00	0.5000	0.00	0.00	0.00
1.25	0.4204	0.03	0.19	0.19
1.50	0.3536	0.03	0.00	0.19
1.75	0.2973	0.03	0.00	0.19
2.00	0.2500	0.04	0.06	0.25
2.25	0.2102	0.06	0.13	0.38
2.50	0.1768	0.15	0.56	0.94
2.75	0.1487	0.17	0.13	1.06
3.00	0.1250	0.24	0.44	1.50
3.25	0.1051	0.27	0.19	1.69
3.50	0.0884	0.34	0.44	2.13
3.75	0.0743	0.47	0.81	2.94
4.00	0.0625	0.76	1.82	4.76
4.25	0.0526	1.26	3.13	7.89
4.50	0.0442	2.21	5.95	13.84
4.75	0.0372	3.72	9.46	23.29
5.00	0.0312	6.09	14.84	38.13
5.25	0.0263	8.62	15.84	53.98
5.50	0.0221	10.37	10.96	64.93
5.75	0.0186	11.66	8.08	73.01
6.00	0.0156	12.82	7.26	80.28
6.25	0.0131	13.67	5.32	85.60
6.50	0.0110	14.26	3.69	89.29
6.75	0.0093	14.74	3.01	92.30
7.00	0.0078	15.08	2.13	94.43
7.25	0.0066	15.39	1.94	96.37
7.50	0.0055	15.88	3.07	99.44
7.75	0.0046	15.88	0.00	99.44

Total weight = 15.97 g

University of Waikato
Rapid Sediment Analyser
Operating System Version 7.1

SETTLING VELOCITY ANALYSIS

Earth Sciences - University of Waikato

Sample: Pukehina Redoubt 0.35m Deploy 2

Size distribution histogram

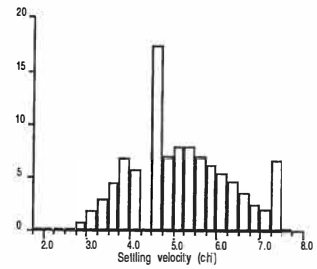

Results summary

Moment method parameters (chi)

Mean= 5.18 Sorting= 1.12 Skewness= 0.23 Kurtosis= 2.42

Cumulative frequency

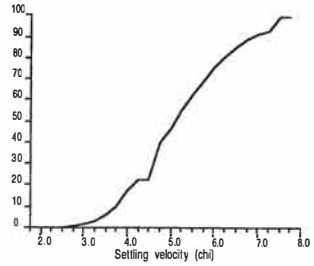

Cumulative frequency

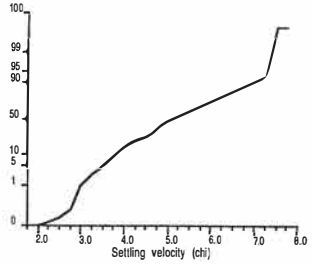

Raw data summary

Velocity (chi)	Velocity (m/s)	Cumulative weight (g)	Interval frequency (%)	Cumulative frequency (%)
2.00	0.2500	-0.01	-0.06	-0.06
2.25	0.2102	0.02	0.17	0.11
2.50	0.1768	0.04	0.11	0.22
2.75	0.1487	0.07	0.17	0.39
3.00	0.1250	0.19	0.67	1.06
3.25	0.1051	0.50	1.73	2.80
3.50	0.0884	1.00	2.80	5.59
3.75	0.0743	1.77	4.31	9.90
4.00	0.0625	3.00	6.88	16.78
4.25	0.0526	4.01	5.65	22.43
4.50	0.0442	4.01	0.00	22.43
4.75	0.0372	7.12	17.39	39.82
5.00	0.0312	8.36	6.94	46.76
5.25	0.0263	9.76	7.83	54.59
5.50	0.0221	11.16	7.83	62.42
5.75	0.0186	12.41	6.99	69.41
6.00	0.0156	13.49	6.04	75.45
6.25	0.0131	14.43	5.26	80.70
6.50	0.0110	15.24	4.53	85.23
6.75	0.0093	15.87	3.52	88.76
7.00	0.0078	16.31	2.46	91.22
7.25	0.0066	16.66	1.96	93.18
7.50	0.0055	17.82	6.49	99.66
7.75	0.0046	17.82	0.00	99.66

Total weight = 17.88 g

University of Waikato
Rapid Sediment Analyser
Operating System Version 7.1

SETTLING VELOCITY ANALYSIS

Earth Sciences - University of Waikato

Sample: Pukehina Redoubt 0.5m Deploy 2

Size distribution histogram

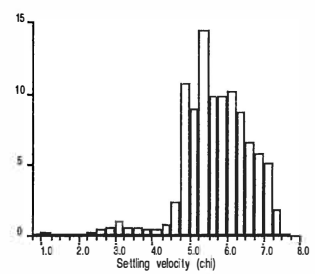

Results summary

Moment method parameters (chi)

Mean= 5.67 Sorting= 0.89 Skewness= -0.59 Kurtosis= 4.62

Cumulative frequency

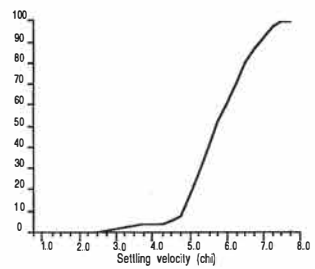

Cumulative frequency

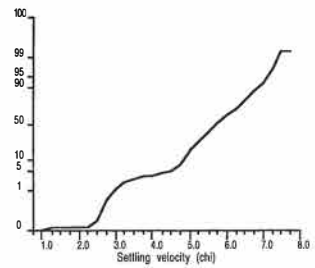

Raw data summary

Velocity (chi)	Velocity (m/s)	Cumulative weight (g)	Interval frequency (%)	Cumulative frequency (%)
1.00	0.5000	0.00	0.00	0.00
1.25	0.4204	0.02	0.13	0.13
1.50	0.3536	0.02	0.00	0.13
1.75	0.2973	0.02	0.00	0.13
2.00	0.2500	0.02	0.00	0.13
2.25	0.2102	0.02	0.00	0.13
2.50	0.1768	0.04	0.13	0.27
2.75	0.1487	0.10	0.40	0.67
3.00	0.1250	0.18	0.54	1.21
3.25	0.1051	0.33	1.00	2.21
3.50	0.0884	0.41	0.54	2.75
3.75	0.0743	0.50	0.60	3.35
4.00	0.0625	0.57	0.47	3.82
4.25	0.0526	0.64	0.47	4.29
4.50	0.0442	0.76	0.80	5.09
4.75	0.0372	1.12	2.41	7.50
5.00	0.0312	2.73	10.78	18.29
5.25	0.0263	4.06	8.91	27.19
5.50	0.0221	6.22	14.47	41.66
5.75	0.0186	7.69	9.85	51.51
6.00	0.0156	9.16	9.85	61.35
6.25	0.0131	10.67	10.11	71.47
6.50	0.0110	11.97	8.71	80.17
6.75	0.0093	12.94	6.50	86.67
7.00	0.0078	13.79	5.69	92.36
7.25	0.0066	14.56	5.16	97.52
7.50	0.0055	14.82	1.74	99.26
7.75	0.0046	14.82	0.00	99.26

Total weight = 14.93 g

University of Waikato
Rapid Sediment Analyser
Operating System Version 7.1

SETTLING VELOCITY ANALYSIS

Earth Sciences - University of Waikato

Sample: Pukehina Redoubt 0.8m Deploy 2

Size distribution histogram

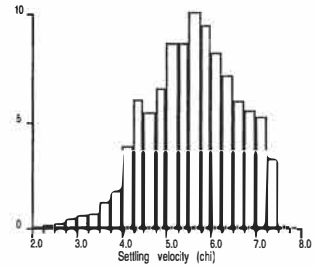

Results summary

Moment method parameters (chi)

Mean= 5.55 Sorting= 0.98 Skewness= -0.12 Kurtosis= 2.60

Cumulative frequency

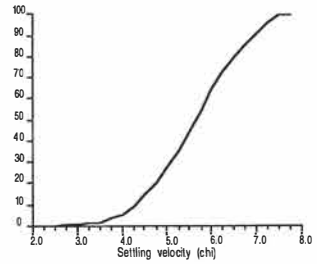

Cumulative frequency

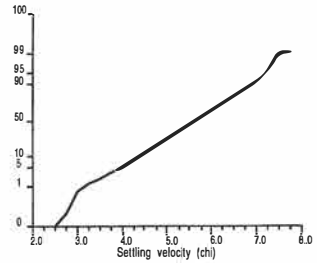

Raw data summary

Velocity (chi)	Velocity (m/s)	Cumulative weight (g)	Interval frequency (%)	Cumulative frequency (%)
2.25	0.2102	-0.01	-0.05	-0.05
2.50	0.1768	0.01	0.10	0.05
2.75	0.1487	0.06	0.26	0.31
3.00	0.1250	0.15	0.47	0.78
3.25	0.1051	0.26	0.57	1.36
3.50	0.0884	0.39	0.68	2.04
3.75	0.0743	0.63	1.25	3.29
4.00	0.0625	0.96	1.72	5.02
4.25	0.0526	1.69	3.81	8.83
4.50	0.0442	2.85	6.06	14.89
4.75	0.0372	3.89	5.43	20.32
5.00	0.0312	5.15	6.58	26.91
5.25	0.0263	6.80	8.62	35.53
5.50	0.0221	8.47	8.73	44.25
5.75	0.0186	10.41	10.14	54.39
6.00	0.0156	12.22	9.46	63.85
6.25	0.0131	13.80	8.25	72.10
6.50	0.0110	15.17	7.16	79.26
6.75	0.0093	16.31	5.96	85.21
7.00	0.0078	17.36	5.49	90.70
7.25	0.0066	18.36	5.22	95.92
7.50	0.0055	18.98	3.24	99.16
7.75	0.0046	18.98	0.00	99.16

Total weight = 19.14 g

SETTLING VELOCITY ANALYSIS

Earth Sciences - University of Waikato

Sample: Pukehina Redoubt 1.2m Deploy 2

Size distribution histogram

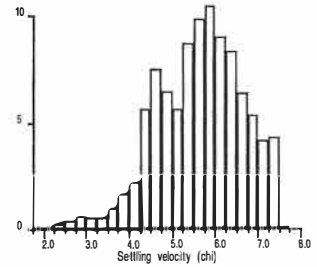

Results summary

Moment method parameters (chi)

Mean= 5.59 Sorting= 0.99 Skewness= -0.23 Kurtosis= 2.86

Cumulative frequency

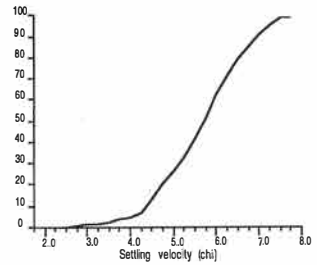

Cumulative frequency

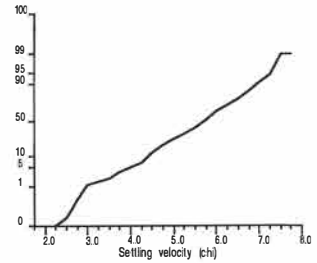

Raw data summary

Velocity (chi)	Velocity (m/s)	Cumulative weight (g)	Interval frequency (%)	Cumulative frequency (%)
2.00	0.2500	0.00	0.00	0.00
2.25	0.2102	0.00	0.00	0.00
2.50	0.1768	0.04	0.22	0.22
2.75	0.1487	0.11	0.39	0.61
3.00	0.1250	0.22	0.61	1.22
3.25	0.1051	0.31	0.50	1.73
3.50	0.0884	0.41	0.56	2.28
3.75	0.0743	0.59	1.00	3.28
4.00	0.0625	0.89	1.67	4.95
4.25	0.0526	1.28	2.17	7.12
4.50	0.0442	2.29	5.62	12.74
4.75	0.0372	3.64	7.51	20.26
5.00	0.0312	4.80	6.46	26.71
5.25	0.0263	5.82	5.68	32.39
5.50	0.0221	7.39	8.74	41.12
5.75	0.0186	9.17	9.91	51.03
6.00	0.0156	11.05	10.46	61.49
6.25	0.0131	12.68	9.07	70.56
6.50	0.0110	14.18	8.35	78.91
6.75	0.0093	15.33	6.40	85.31
7.00	0.0078	16.29	5.34	90.65
7.25	0.0066	17.03	4.12	94.77
7.50	0.0055	17.80	4.28	99.05
7.75	0.0046	17.80	0.00	99.05

Total weight = 17.97 g

SETTLING VELOCITY ANALYSIS

Earth Sciences - University of Waikato

Sample: NEWDICKS 0.35M D1 SUMMER

Size distribution histogram

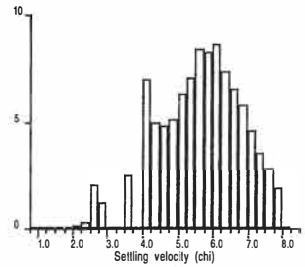

Results summary

Moment method parameters (chi)

Mean= 5.63 Sorting= 1.20 Skewness= -0.43 Kurtosis= 3.01

Cumulative frequency

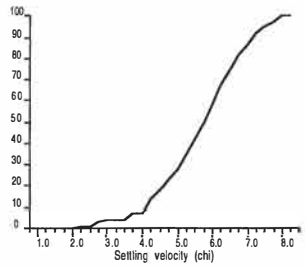

Cumulative frequency

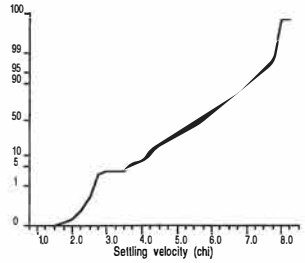

Raw data summary

Velocity (chi)	Velocity (m/s)	Cumulative weight (g)	Interval frequency (%)	Cumulative frequency (%)
1.00	0.5000	0.00	0.00	0.00
1.25	0.4204	0.02	0.07	0.07
1.50	0.3536	0.02	0.00	0.07
1.75	0.2973	0.04	0.07	0.14
2.00	0.2500	0.06	0.07	0.20
2.25	0.2102	0.11	0.17	0.37
2.50	0.1768	0.19	0.27	0.65
2.75	0.1487	0.79	2.04	2.69
3.00	0.1250	1.14	1.19	3.89
3.25	0.1051	1.14	0.00	3.89
3.50	0.0884	1.14	0.00	3.89
3.75	0.0743	1.86	2.45	6.34
4.00	0.0625	1.86	0.00	6.34
4.25	0.0526	3.92	7.02	13.36
4.50	0.0442	5.37	4.94	18.30
4.75	0.0372	6.78	4.81	23.11
5.00	0.0312	8.28	5.11	28.22
5.25	0.0263	10.15	6.37	34.59
5.50	0.0221	12.22	7.06	41.65
5.75	0.0186	14.71	8.49	50.14
6.00	0.0156	17.15	8.32	58.45
6.25	0.0131	19.71	8.73	67.18
6.50	0.0110	21.88	7.40	74.57
6.75	0.0093	23.81	6.58	81.15
7.00	0.0078	25.52	5.83	86.98
7.25	0.0066	26.87	4.60	91.58
7.50	0.0055	27.91	3.54	95.13
7.75	0.0046	28.72	2.76	97.89
8.00	0.0039	29.28	1.91	99.80
8.25	0.0033	29.28	0.00	99.80

University of Waikato
Rapid Sediment Analyser
Operating System Version 7.1

SETTLING VELOCITY ANALYSIS

Earth Sciences - University of Waikato

Sample: NEWDICKS 0.5M D1 SUMMER

Size distribution histogram

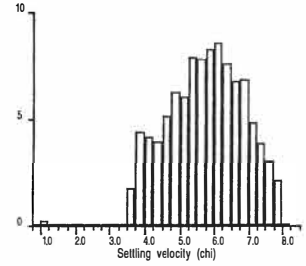

Results summary

Moment method parameters (chi)

Mean= 5.75 Sorting= 1.09 Skewness= -0.19 Kurtosis= 2.79

Cumulative frequency

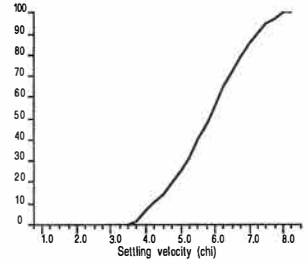

Cumulative frequency

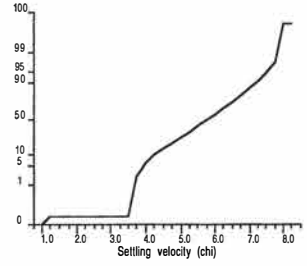

Raw data summary

Velocity (chi)	Velocity (m/s)	Cumulative weight (g)	Interval frequency (%)	Cumulative frequency (%)
1.00	0.5000	0.00	0.00	0.00
1.25	0.4204	0.07	0.25	0.25
1.50	0.3536	0.07	0.00	0.25
1.75	0.2973	0.07	0.00	0.25
2.00	0.2500	0.07	0.00	0.25
2.25	0.2102	0.07	0.00	0.25
2.50	0.1768	0.07	0.00	0.25
2.75	0.1487	0.07	0.00	0.25
3.00	0.1250	0.07	0.00	0.25
3.25	0.1051	0.07	0.00	0.25
3.50	0.0884	0.07	0.00	0.25
3.75	0.0743	0.58	1.79	2.03
4.00	0.0625	1.84	4.42	6.45
4.25	0.0526	3.03	4.17	10.63
4.50	0.0442	4.15	3.93	14.56
4.75	0.0372	5.61	5.12	19.68
5.00	0.0312	7.41	6.31	25.99
5.25	0.0263	9.13	6.03	32.03
5.50	0.0221	11.40	7.96	39.99
5.75	0.0186	13.63	7.82	47.81
6.00	0.0156	16.00	8.31	56.13
6.25	0.0131	18.44	8.56	64.69
6.50	0.0110	20.60	7.58	72.26
6.75	0.0093	22.55	6.84	79.10
7.00	0.0078	24.51	6.88	85.98
7.25	0.0066	25.88	4.81	90.79
7.50	0.0055	26.97	3.82	94.61
7.75	0.0046	27.83	3.02	97.63
8.00	0.0039	28.43	2.10	99.73
8.25	0.0033	28.43	0.00	99.73

University of Waikato
Rapid Sediment Analyser
Operating System Version 7.1

SETTLING VELOCITY ANALYSIS

Earth Sciences - University of Waikato

Sample: NEWDICKS 0.8M D1 SUMMER

Size distribution histogram

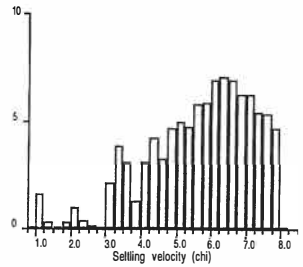

Results summary

Moment method parameters (chi)

Mean= 5.68 Sorting= 1.51 Skewness= -0.73 Kurtosis= 3.21

Cumulative frequency

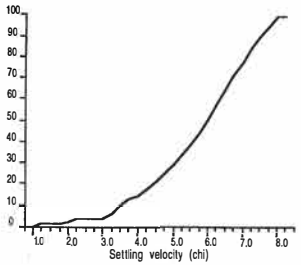

Cumulative frequency

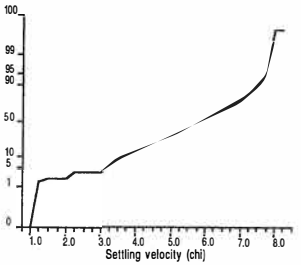

Raw data summary

Velocity (chi)	Velocity (m/s)	Cumulative weight (g)	Interval frequency (%)	Cumulative frequency (%)
1.00	0.5000	0.00	0.00	0.00
1.25	0.4204	0.30	1.61	1.61
1.50	0.3536	0.36	0.32	1.94
1.75	0.2973	0.37	0.05	1.99
2.00	0.2500	0.42	0.27	2.26
2.25	0.2102	0.61	1.02	3.28
2.50	0.1768	0.69	0.43	3.71
2.75	0.1487	0.71	0.11	3.82
3.00	0.1250	0.71	0.00	3.82
3.25	0.1051	1.10	2.10	5.91
3.50	0.0884	1.81	3.82	9.73
3.75	0.0743	2.38	3.06	12.79
4.00	0.0625	2.62	1.29	14.08
4.25	0.0526	3.19	3.06	17.15
4.50	0.0442	3.98	4.25	21.39
4.75	0.0372	4.58	3.23	24.62
5.00	0.0312	5.44	4.62	29.24
5.25	0.0263	6.37	5.00	34.24
5.50	0.0221	7.26	4.78	39.02
5.75	0.0186	8.34	5.81	44.83
6.00	0.0156	9.43	5.86	50.69
6.25	0.0131	10.72	6.93	57.62
6.50	0.0110	12.03	7.04	64.66
6.75	0.0093	13.32	6.93	71.60
7.00	0.0078	14.48	6.24	77.83
7.25	0.0066	15.65	6.29	84.12
7.50	0.0055	16.66	5.43	89.55
7.75	0.0046	17.66	5.38	94.92
8.00	0.0039	18.54	4.73	99.65
8.25	0.0033	18.54	0.00	99.65

University of Waikato
Rapid Sediment Analyser
Operating System Version 7.1

SETTLING VELOCITY ANALYSIS

Earth Sciences - University of Waikato

Sample: NEWDICKS 1.2M D1 SUMMER

Size distribution histogram

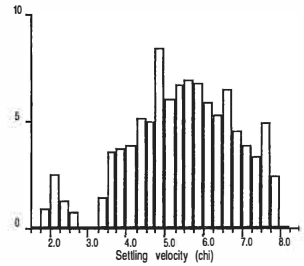

Results summary

Moment method parameters (chi)

Mean= 5.45 Sorting= 1.38 Skewness= -0.38 Kurtosis= 2.82

Cumulative frequency

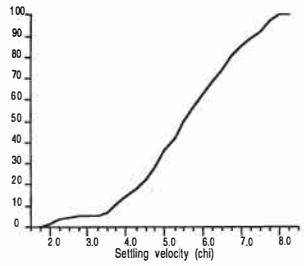

Cumulative frequency

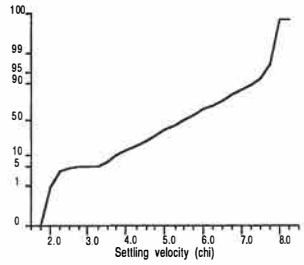

Raw data summary

Velocity (chi)	Velocity (m/s)	Cumulative weight (g)	Interval frequency (%)	Cumulative frequency (%)
1.75	0.2973	-0.01	-0.04	-0.04
2.00	0.2500	0.21	0.96	0.92
2.25	0.2102	0.77	2.45	3.37
2.50	0.1768	1.06	1.27	4.64
2.75	0.1487	1.23	0.74	5.39
3.00	0.1250	1.23	0.00	5.39
3.25	0.1051	1.23	0.00	5.39
3.50	0.0884	1.57	1.49	6.88
3.75	0.0743	2.37	3.50	10.38
4.00	0.0625	3.22	3.72	14.10
4.25	0.0526	4.11	3.90	18.00
4.50	0.0442	5.28	5.12	23.12
4.75	0.0372	6.42	4.99	28.11
5.00	0.0312	8.35	8.45	36.57
5.25	0.0263	9.73	6.04	42.61
5.50	0.0221	11.26	6.70	49.31
5.75	0.0186	12.85	6.96	56.27
6.00	0.0156	14.40	6.79	63.06
6.25	0.0131	15.75	5.91	68.97
6.50	0.0110	16.96	5.30	74.27
6.75	0.0093	18.44	6.48	80.75
7.00	0.0078	19.47	4.51	85.26
7.25	0.0066	20.35	3.85	89.11
7.50	0.0055	21.12	3.37	92.49
7.75	0.0046	22.24	4.90	97.39
8.00	0.0039	22.79	2.41	99.80
8.25	0.0033	22.79	0.00	99.80

University of Waikato
Rapid Sediment Analyser
Operating System Version 7.1

Total weight = 22.84 g

SETTLING VELOCITY ANALYSIS

Earth Sciences - University of Waikato

Sample: NEWDICKS 0.35M D2 SUMMER

Size distribution histogram

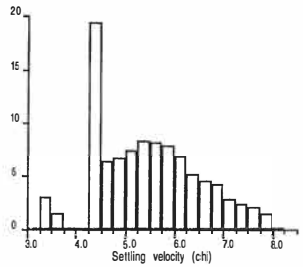

Results summary

Moment method parameters (chi)

Mean= 5.37 Sorting= 1.04 Skewness= 0.53 Kurtosis= 2.57

Cumulative frequency

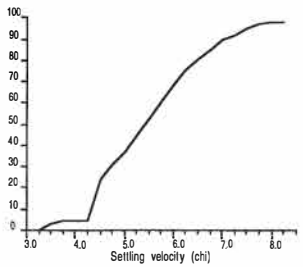

Cumulative frequency

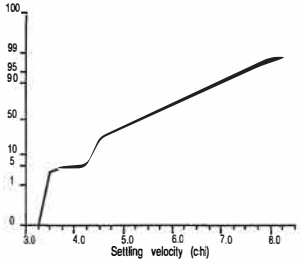

Raw data summary

Velocity (chi)	Velocity (m/s)	Cumulative weight (g)	Interval frequency (%)	Cumulative frequency (%)
3.25	0.1051	-0.01	-0.03	-0.03
3.50	0.0884	1.05	3.06	3.03
3.75	0.0743	1.58	1.53	4.56
4.00	0.0625	1.58	0.00	4.56
4.25	0.0526	1.58	0.00	4.56
4.50	0.0442	8.31	19.44	24.00
4.75	0.0372	10.49	6.30	30.30
5.00	0.0312	12.82	6.73	37.03
5.25	0.0263	15.39	7.42	44.45
5.50	0.0221	18.24	8.23	52.68
5.75	0.0186	21.06	8.15	60.83
6.00	0.0156	23.78	7.86	68.68
6.25	0.0131	26.14	6.82	75.50
6.50	0.0110	27.91	5.11	80.61
6.75	0.0093	29.46	4.48	85.09
7.00	0.0078	30.91	4.19	89.28
7.25	0.0066	31.93	2.95	92.22
7.50	0.0055	32.80	2.51	94.74
7.75	0.0046	33.53	2.11	96.85
8.00	0.0039	34.06	1.53	98.38
8.25	0.0033	34.06	0.00	98.38

Total weight = 34.62 g

University of Waikato
Rapid Sediment Analyser
Operating System Version 7.1

SETTLING VELOCITY ANALYSIS

Earth Sciences - University of Waikato

Sample: NEWDICKS 0.5M D2 SUMMER

Size distribution histogram

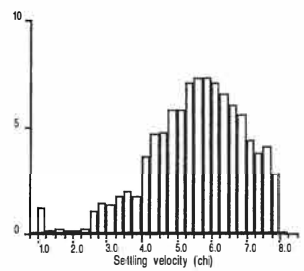

Results summary

Moment method parameters (chi)

Mean= 5.47 Sorting= 1.37 Skewness= -0.44 Kurtosis= 3.34

Cumulative frequency

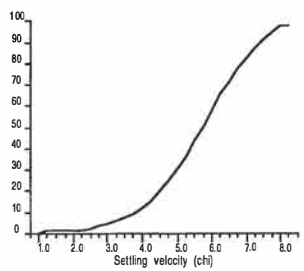

Cumulative frequency

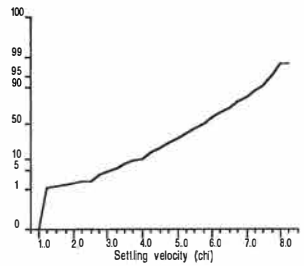

Raw data summary

Velocity (chi)	Velocity (m/s)	Cumulative weight (g)	Interval frequency (%)	Cumulative frequency (%)
1.00	0.5000	0.00	0.00	0.00
1.25	0.4204	0.31	1.23	1.23
1.50	0.3536	0.36	0.20	1.43
1.75	0.2973	0.42	0.24	1.67
2.00	0.2500	0.47	0.20	1.87
2.25	0.2102	0.50	0.12	1.99
2.50	0.1768	0.56	0.24	2.23
2.75	0.1487	0.82	1.04	3.27
3.00	0.1250	1.17	1.39	4.66
3.25	0.1051	1.51	1.35	6.01
3.50	0.0884	1.95	1.75	7.77
3.75	0.0743	2.43	1.91	9.68
4.00	0.0625	2.88	1.79	11.47
4.25	0.0526	3.78	3.58	15.06
4.50	0.0442	4.96	4.70	19.76
4.75	0.0372	6.16	4.78	24.54
5.00	0.0312	7.62	5.82	30.35
5.25	0.0263	9.08	5.82	36.17
5.50	0.0221	10.87	7.13	43.30
5.75	0.0186	12.71	7.33	50.62
6.00	0.0156	14.56	7.37	57.99
6.25	0.0131	16.33	7.05	65.04
6.50	0.0110	17.97	6.53	71.57
6.75	0.0093	19.48	6.01	77.59
7.00	0.0078	20.88	5.58	83.17
7.25	0.0066	21.98	4.38	87.55
7.50	0.0055	22.92	3.74	91.29
7.75	0.0046	23.94	4.06	95.35
8.00	0.0039	24.64	2.79	98.14
8.25	0.0033	24.64	0.00	98.14

University of Waikato
Rapid Sediment Analyser
Operating System Version 7.1

SETTLING VELOCITY ANALYSIS

Earth Sciences - University of Waikato

Sample: NEWDICKS 0.8M D2 SUMMER

Size distribution histogram

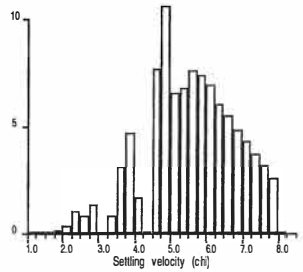

Results summary

Moment method parameters (chi)

Mean= 5.47 Sorting= 1.24 Skewness= -0.08 Kurtosis= 2.82

Cumulative frequency

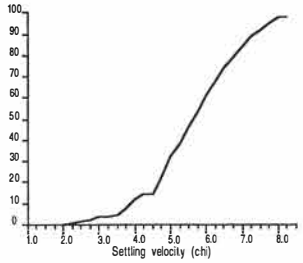

Cumulative frequency

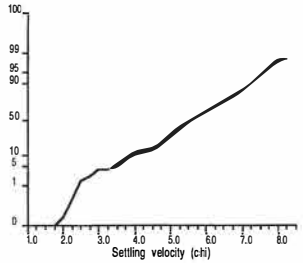

Raw data summary

Velocity (chi)	Velocity (m/s)	Cumulative weight (g)	Interval frequency (%)	Cumulative frequency (%)
1.25	0.4204	0.00	0.00	0.00
1.50	0.3536	0.00	0.00	0.00
1.75	0.2973	0.02	0.07	0.07
2.00	0.2500	0.07	0.18	0.25
2.25	0.2102	0.17	0.36	0.62
2.50	0.1768	0.47	1.09	1.70
2.75	0.1487	0.70	0.83	2.53
3.00	0.1250	1.08	1.38	3.91
3.25	0.1051	1.08	0.00	3.91
3.50	0.0884	1.30	0.80	4.71
3.75	0.0743	2.15	3.08	7.79
4.00	0.0625	3.45	4.71	12.49
4.25	0.0526	3.91	1.67	14.16
4.50	0.0442	3.92	0.04	14.19
4.75	0.0372	6.05	7.71	21.91
5.00	0.0312	8.99	10.65	32.55
5.25	0.0263	10.80	6.55	39.11
5.50	0.0221	12.67	6.77	45.88
5.75	0.0186	14.77	7.60	53.48
6.00	0.0156	16.82	7.42	60.91
6.25	0.0131	18.74	6.95	67.86
6.50	0.0110	20.42	6.08	73.94
6.75	0.0093	21.94	5.50	79.45
7.00	0.0078	23.27	4.82	84.26
7.25	0.0066	24.46	4.31	88.57
7.50	0.0055	25.49	3.73	92.30
7.75	0.0046	26.37	3.19	95.49
8.00	0.0039	27.09	2.61	98.10
8.25	0.0033	27.09	0.00	98.10

Total weight = 27.62 g

University of Waikato
Rapid Sediment Analyser
Operating System Version 7.1

SETTLING VELOCITY ANALYSIS

Earth Sciences - University of Waikato

Sample: NEWDICK 1.2M D2 SUMMER

Size distribution histogram

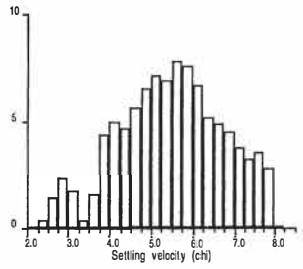

Results summary

Moment method parameters (chi)

Mean= 5.40 Sorting= 1.26 Skewness= 0.09 Kurtosis= 2.46

Cumulative frequency

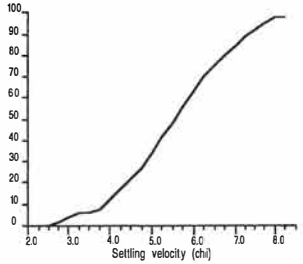

Cumulative frequency

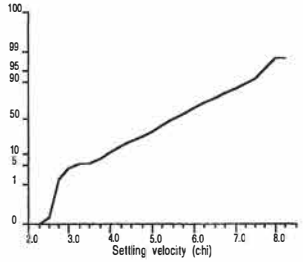

Raw data summary

Velocity (chi)	Velocity (m/s)	Cumulative weight (g)	Interval frequency (%)	Cumulative frequency (%)
2.25	0.2102	-0.05	-0.23	-0.23
2.50	0.1768	0.04	0.42	0.18
2.75	0.1487	0.35	1.43	1.62
3.00	0.1250	0.86	2.36	3.98
3.25	0.1051	1.23	1.71	5.69
3.50	0.0884	1.31	0.37	6.06
3.75	0.0743	1.65	1.57	7.63
4.00	0.0625	2.60	4.39	12.02
4.25	0.0526	3.68	4.99	17.01
4.50	0.0442	4.69	4.67	21.68
4.75	0.0372	5.91	5.64	27.32
5.00	0.0312	7.33	6.56	33.88
5.25	0.0263	8.88	7.16	41.05
5.50	0.0221	10.38	6.93	47.98
5.75	0.0186	12.07	7.81	55.79
6.00	0.0156	13.73	7.67	63.46
6.25	0.0131	15.18	6.70	70.17
6.50	0.0110	16.31	5.22	75.39
6.75	0.0093	17.37	4.90	80.29
7.00	0.0078	18.35	4.53	84.82
7.25	0.0066	19.17	3.79	88.61
7.50	0.0055	19.87	3.24	91.85
7.75	0.0046	20.63	3.51	95.36
8.00	0.0039	21.24	2.82	98.18
8.25	0.0033	21.24	0.00	98.18

Total weight = 21.63 g

University of Waikato
Rapid Sediment Analyser
Operating System Version 7.1

SETTLING VELOCITY ANALYSIS

Earth Sciences - University of Waikato

Sample: PUKEHINA REDOUBT 0.35M SUMMER

Size distribution histogram

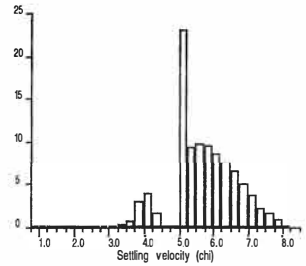

Results summary

Moment method parameters (chi)

Mean= 5.70 Sorting= 0.92Skewness= -0.13 Kurtosis= 3.60

Cumulative frequency

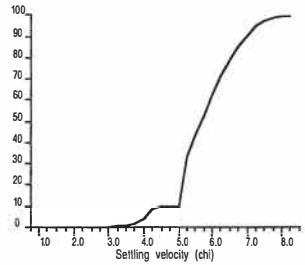

Cumulative frequency

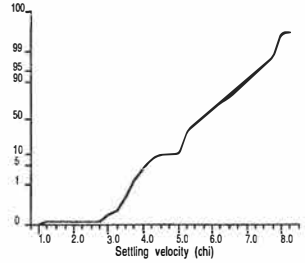

Raw data summary

Velocity (chi)	Velocity (m/s)	Cumulative weight (g)	Interval frequency (%)	Cumulative frequency (%)
1.00	0.5000	0.00	0.00	0.00
1.25	0.4204	0.04	0.12	0.12
1.50	0.3536	0.05	0.03	0.15
1.75	0.2973	0.05	0.00	0.15
2.00	0.2500	0.05	0.00	0.15
2.25	0.2102	0.05	0.00	0.15
2.50	0.1768	0.05	0.00	0.15
2.75	0.1487	0.05	0.00	0.15
3.00	0.1250	0.09	0.12	0.27
3.25	0.1051	0.12	0.09	0.35
3.50	0.0884	0.21	0.27	0.62
3.75	0.0743	0.46	0.74	1.36
4.00	0.0625	1.45	2.92	4.28
4.25	0.0526	2.82	4.04	8.32
4.50	0.0442	3.43	1.80	10.12
4.75	0.0372	3.43	0.00	10.12
5.00	0.0312	3.43	0.00	10.12
5.25	0.0263	11.33	23.30	33.41
5.50	0.0221	14.54	9.47	42.88
5.75	0.0186	17.87	9.82	52.70
6.00	0.0156	21.13	9.61	62.31
6.25	0.0131	24.08	8.70	71.01
6.50	0.0110	26.71	7.76	78.77
6.75	0.0093	28.97	6.66	85.43
7.00	0.0078	30.73	5.19	90.62
7.25	0.0066	32.02	3.80	94.43
7.50	0.0055	32.83	2.39	96.82
7.75	0.0046	33.42	1.74	98.56
8.00	0.0039	33.75	0.97	99.53
8.25	0.0033	33.75	0.00	99.53

University of Waikato
Rapid Sediment Analyser
Operating System Version 7.1

SETTLING VELOCITY ANALYSIS

Earth Sciences - University of Waikato

Sample: PUKEHINA REDOUBT 0.5M SUMMER

Size distribution histogram

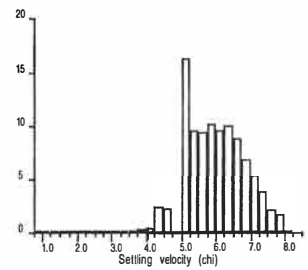

Results summary

Moment method parameters (chi)

Mean= 5.93 Sorting= 0.87Skewness= -0.13 Kurtosis= 4.36

Cumulative frequency

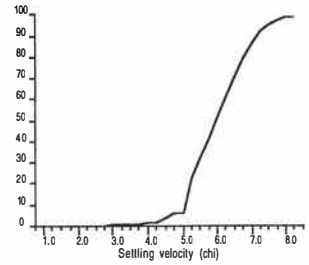

Cumulative frequency

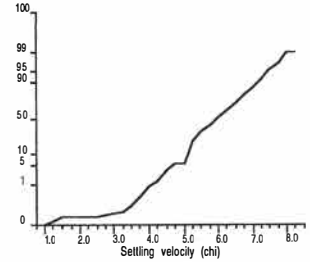

Raw data summary

Velocity (chi)	Velocity (m/s)	Cumulative weight (g)	Interval frequency (%)	Cumulative frequency (%)
1.00	0.5000	0.00	0.00	0.00
1.25	0.4204	0.04	0.12	0.12
1.50	0.3536	0.07	0.09	0.21
1.75	0.2973	0.07	0.00	0.21
2.00	0.2500	0.08	0.03	0.24
2.25	0.2102	0.08	0.00	0.24
2.50	0.1768	0.08	0.00	0.24
2.75	0.1487	0.09	0.03	0.27
3.00	0.1250	0.10	0.03	0.30
3.25	0.1051	0.11	0.03	0.33
3.50	0.0884	0.16	0.15	0.48
3.75	0.0743	0.21	0.15	0.63
4.00	0.0625	0.30	0.27	0.90
4.25	0.0526	0.46	0.48	1.38
4.50	0.0442	1.25	2.38	3.76
4.75	0.0372	2.00	2.26	6.02
5.00	0.0312	2.00	0.00	6.02
5.25	0.0263	7.38	16.18	22.20
5.50	0.0221	10.55	9.54	31.73
5.75	0.0186	13.64	9.29	41.03
6.00	0.0156	17.01	10.14	51.17
6.25	0.0131	20.18	9.54	60.70
6.50	0.0110	23.49	9.96	70.66
6.75	0.0093	26.38	8.69	79.35
7.00	0.0078	28.66	6.86	86.21
7.25	0.0066	30.43	5.32	91.53
7.50	0.0055	31.70	3.82	95.35
7.75	0.0046	32.42	2.17	97.52
8.00	0.0039	32.95	1.59	99.11
8.25	0.0033	32.95	0.00	99.11

University of Waikato
Rapid Sediment Analyser
Operating System Version 7.1

SETTLING VELOCITY ANALYSIS

Earth Sciences - University of Waikato

Sample: PUKEHINA REDOUBT 0.8M SUMMER

Size distribution histogram

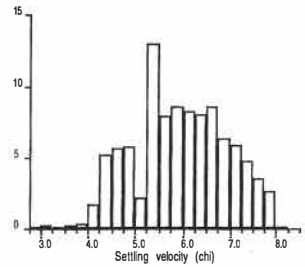

Results summary

Moment method parameters (chi)

Mean= 5.89 Sorting= 0.97Skewness= 0.20 Kurtosis= 2.28

Cumulative frequency

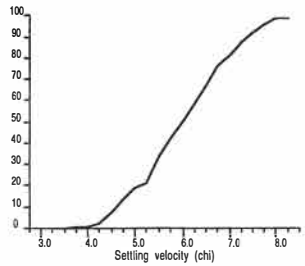

Cumulative frequency

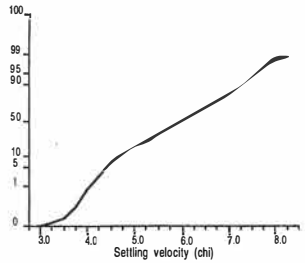

Raw data summary

Velocity (chi)	Velocity (m/s)	Cumulative weight (g)	Interval frequency (%)	Cumulative frequency (%)
3.00	0.1250	-0.01	-0.04	-0.04
3.25	0.1051	0.03	0.15	0.11
3.50	0.0884	0.06	0.11	0.22
3.75	0.0743	0.12	0.22	0.44
4.00	0.0625	0.22	0.37	0.81
4.25	0.0526	0.68	1.70	2.51
4.50	0.0442	2.08	5.17	7.68
4.75	0.0372	3.61	5.65	13.34
5.00	0.0312	5.17	5.76	19.10
5.25	0.0263	5.74	2.11	21.21
5.50	0.0221	9.28	13.08	34.29
5.75	0.0186	11.43	7.94	42.23
6.00	0.0156	13.76	8.61	50.84
6.25	0.0131	15.97	8.16	59.00
6.50	0.0110	18.15	8.05	67.06
6.75	0.0093	20.46	8.53	75.59
7.00	0.0078	22.18	6.35	81.95
7.25	0.0066	23.78	5.91	87.86
7.50	0.0055	25.06	4.73	92.59
7.75	0.0046	26.02	3.55	96.13
8.00	0.0039	26.72	2.59	98.72
8.25	0.0033	26.72	0.00	98.72

Total weight = 27.07 g

University of Waikato
Rapid Sediment Analyser
Operating System Version 7.1

SETTLING VELOCITY ANALYSIS

Earth Sciences - University of Waikato

Sample: PUKEHINA REDOUBT 1.2M SUMMER

Size distribution histogram

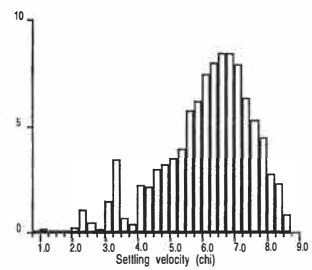

Results summary

Moment method parameters (chi)

Mean= 6.18 Sorting= 1.38Skewness= -0.77 Kurtosis= 3.34

Cumulative frequency

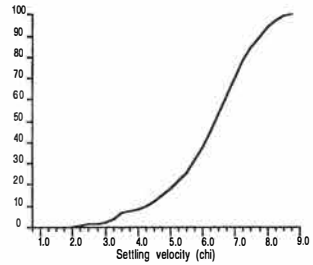

Cumulative frequency

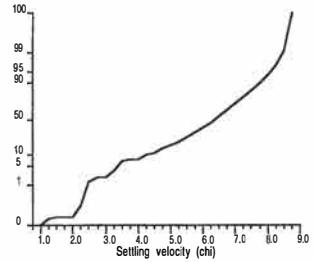

Raw data summary

Velocity (chi)	Velocity (m/s)	Cumulative weight (g)	Interval frequency (%)	Cumulative frequency (%)
1.00	0.5000	0.00	0.00	0.00
1.25	0.4204	0.04	0.19	0.19
1.50	0.3536	0.05	0.05	0.24
1.75	0.2973	0.05	0.00	0.24
2.00	0.2500	0.05	0.00	0.24
2.25	0.2102	0.10	0.24	0.47
2.50	0.1768	0.32	1.04	1.51
2.75	0.1487	0.42	0.47	1.98
3.00	0.1250	0.45	0.14	2.12
3.25	0.1051	0.76	1.46	3.58
3.50	0.0884	1.49	3.44	7.02
3.75	0.0743	1.64	0.71	7.72
4.00	0.0625	1.71	0.33	8.05
4.25	0.0526	2.17	2.17	10.22
4.50	0.0442	2.62	2.12	12.34
4.75	0.0372	3.25	2.97	15.30
5.00	0.0312	3.92	3.15	18.46
5.25	0.0263	4.66	3.48	21.94
5.50	0.0221	5.50	3.95	25.89
5.75	0.0186	6.71	5.70	31.59
6.00	0.0156	8.02	6.17	37.76
6.25	0.0131	9.61	7.49	45.25
6.50	0.0110	11.31	8.00	53.25
6.75	0.0093	13.10	8.43	61.68
7.00	0.0078	14.89	8.43	70.10
7.25	0.0066	16.56	7.86	77.97
7.50	0.0055	17.91	6.36	84.32
7.75	0.0046	19.04	5.32	89.64
8.00	0.0039	19.99	4.47	94.12
8.25	0.0033	20.57	2.73	96.85
8.50	0.0028	21.06	2.31	99.15

University of Waikato
Rapid Sediment Analyser
Operating System Version 7.1

Appendix VI

THANAL analysis results identifying tidal components extracted from collected data obtained at Newdicks Beach (16 m water depth) and Waihi Estuary (inlet and sub-tidal flats).

1.1 Newdicks Beach

```
Station statistics:
  Station name = Newdicks beach (summer Cycle)
  Station id =
  Latitude =-37 44.96S  Longitude = 176 29.54E
  Number of days of data =   30
  Recording interval =   60 min
  Total number of records =    720
  Data file type = 0- 2   mnm = 549.000
  Time zone = NZST
  First record at 10: 9 on  9  3 2001
  Last record at  24: 0 on  7  4 2001
```

Component	Period	Frequency	Amplitude	Phase
Z0	0.0000	0.0000	12.2044	0.00
MSF	354.3671	0.0028	0.0162	208.48
2Q1	28.0062	0.0357	0.0028	306.48
Q1	26.8684	0.0372	0.0022	211.47
O1	25.8193	0.0387	0.0154	281.17
NO1	24.8332	0.0403	0.0046	292.95
K1	23.9345	0.0418	0.0438	326.79
J1	23.0985	0.0433	0.0010	353.45
OO1	22.3061	0.0448	0.0057	17.20
UPS1	21.5782	0.0463	0.0021	22.19
N2	12.6583	0.0790	0.1549	106.15
M2	12.4206	0.0805	0.7254	142.67
S2	12.0000	0.0833	0.1245	211.21
ETA2	11.7545	0.0851	0.0004	114.81
MO3	8.3863	0.1192	0.0021	183.81
M3	8.2804	0.1208	0.0052	282.93
MK3	8.1771	0.1223	0.0015	44.12
SK3	7.9927	0.1251	0.0027	302.51
MN4	6.2692	0.1595	0.0022	131.58
M4	6.2103	0.1610	0.0037	154.11
MS4	6.1033	0.1638	0.0018	347.87
S4	6.0000	0.1667	0.0021	65.27
2MK5	4.9309	0.2028	0.0003	297.13
2SK5	4.7974	0.2084	0.0017	237.99
2MN6	4.1663	0.2400	0.0005	122.09
M6	4.1402	0.2415	0.0014	195.59
2MS6	4.0924	0.2444	0.0024	357.08
2SM6	4.0457	0.2472	0.0010	66.61
3MK7	3.5296	0.2833	0.0007	300.90
M8	3.1052	0.3220	0.0003	82.62

1.2 Waihi Estuary Inlet Winter Cycle Deployment One

```
Station statistics:
  Station name = Waihi Estuary inlet deployment One (winter cycle)
  Station id =
  Latitude =-37 45.56S  Longitude = 176 28.67E
  Number of days of data =    4
  Recording interval =    5 min
  Total number of records =     93
  Data file type = 0- 2   mnm = 760.000
  Time zone = NZST
  First record at  2: 0 on 16  5 2000
  Last record at  22: 0 on 20  5 2000
```

Component	Period	Frequency	Amplitude	Phase
Z0	0.0000	0.0000	1.5796	0.00
K1	23.9345	0.0418	0.0020	306.21
M2	12.4206	0.0805	0.0485	206.88
M3	8.2804	0.1208	0.0054	140.31
M4	6.2103	0.1610	0.3535	297.56
2MK5	4.9309	0.2028	0.0090	95.25
M6	4.1402	0.2415	0.0068	280.22
3MK7	3.5296	0.2833	0.0030	328.98
M8	3.1052	0.3220	0.0446	105.35

1.3 Waihi Estuary Inlet Winter Cycle Deployment Two

```
Station statistics:
  Station name = Waihi Estuary inlet Deployment Two (winter cycle)
  Station id =
  Latitude =-37 45.56S  Longitude = 176 28.67E
  Number of days of data =   10
  Recording interval =   10 min
  Total number of records =    237
  Data file type = 0- 2   mnm = 579.000
  Time zone = NZST
  First record at  2: 0 on 26  5 2000
  Last record at  22: 0 on  4  6 2000
```

Component	Period	Frequency	Amplitude	Phase
Z0	0.0000	0.0000	1.5511	0.00
K1	23.9345	0.0418	0.0402	202.36
M2	12.4206	0.0805	0.3215	217.17
M3	8.2804	0.1208	0.0067	348.17
M4	6.2103	0.1610	0.0358	321.44
2MK5	4.9309	0.2028	0.0068	311.82
2SK5	4.7974	0.2084	0.0018	338.23
M6	4.1402	0.2415	0.0175	345.05
3MK7	3.5296	0.2833	0.0023	51.25
M8	3.1052	0.3220	0.0062	98.80

1.4 Waihi Estuary Sub-Tidal Flats Winter Cycle Deployment One

```
Station statistics:
  Station name = Waihi Estuary Sub-tidal deployment 1 (Winter Cycle)
  Station id =
  Latitude =-37 46.53S  Longitude = 176 29.33E
  Number of days of data =    8
  Recording interval =   30 min
  Total number of records =    190
  Data file type = 0- 2   mnm = 947.000
  Time zone = NZST
  First record at  2: 0 on 16  5 2000
  Last record at  23: 0 on 23  5 2000
```

Component	Period	Frequency	Amplitude	Phase
Z0	0.0000	0.0000	0.3790	0.00
K1	23.9345	0.0418	0.0167	134.04
M2	12.4206	0.0805	0.2003	259.40
M3	8.2804	0.1208	0.0099	261.54
M4	6.2103	0.1610	0.0501	79.36
2MK5	4.9309	0.2028	0.0025	144.10
2SK5	4.7974	0.2084	0.0036	226.04
M6	4.1402	0.2415	0.0075	221.21
3MK7	3.5296	0.2833	0.0033	164.19
M8	3.1052	0.3220	0.0044	336.67

1.5 Waihi Estuary Sub-Tidal Flats Winter Cycle Deployment Two

```
Station statistics:
  Station name = Waihi Estuary Sub-tidal deployment 2 (Winter Cycle)
  Station id =
  Latitude =-37 46.53S  Longitude = 176 29.33E
  Number of days of data =   13
  Recording interval =   30 min
  Total number of records =    310
  Data file type = 0- 2   mnm = 510.000
  Time zone = NZST
  First record at  2: 0 on 26  5 2000
  Last record at  23: 0 on  7  6 2000
```

Component	Period	Frequency	Amplitude	Phase
Z0	0.0000	0.0000	0.5492	0.00
K1	23.9345	0.0418	0.0311	205.26
M2	12.4206	0.0805	0.2189	251.66
M3	8.2804	0.1208	0.0152	80.06
M4	6.2103	0.1610	0.0508	72.35
2MK5	4.9309	0.2028	0.0042	96.31
2SK5	4.7974	0.2084	0.0025	199.19
M6	4.1402	0.2415	0.0026	225.79
3MK7	3.5296	0.2833	0.0031	192.79
M8	3.1052	0.3220	0.0055	235.43

1.6 Waihi Estuary Inlet Summer Cycle

```
Station statistics:
  Station name = Waihi Estuary inlet (Summer cycle)
  Station id =
  Latitude =-37 45.56S  Longitude = 176 28.67E
  Number of days of data =  12
  Recording interval =   30 min
  Total number of records =    286
  Data file type = 0- 2   mnm =1140.000
  Time zone = NZST
  First record at  2: 0 on  9  3 2001
  Last record at  23: 0 on 20  3 2001
```

Component	Period	Frequency	Amplitude	Phase
Z0	0.0000	0.0000	1.3304	0.00
K1	23.9345	0.0418	0.0276	193.75
M2	12.4206	0.0805	0.3870	247.15
M3	8.2804	0.1208	0.0016	261.07
M4	6.2103	0.1610	0.0468	15.09
2MK5	4.9309	0.2028	0.0013	134.81
2SK5	4.7974	0.2084	0.0025	252.81
M6	4.1402	0.2415	0.0249	89.42
3MK7	3.5296	0.2833	0.0017	233.85
M8	3.1052	0.3220	0.0070	236.81

1.7 Waihi Estuary Sub-Tidal Flats Summer Cycle

```
Station statistics:
  Station name = Waihi Estuary Sub-tidal (Summer Cycle)
  Station id =
  Latitude =-37 46.53S  Longitude = 176 29.33E
  Number of days of data =   10
  Recording interval =    1 min
  Total number of records =    237
  Data file type = 0- 2   mnm =1140.000
  Time zone = NZST
  First record at  2: 0 on  9  3 2001
  Last record at  22: 0 on 18  3 2001
```

Component	Period	Frequency	Amplitude	Phase
Z0	0.0000	0.0000	0.6047	0.00
K1	23.9345	0.0418	0.0195	277.07
M2	12.4206	0.0805	0.2773	283.87
M3	8.2804	0.1208	0.0135	245.33
M4	6.2103	0.1610	0.0647	130.66
2MK5	4.9309	0.2028	0.0031	304.50
2SK5	4.7974	0.2084	0.0016	181.56
M6	4.1402	0.2415	0.0078	293.43
3MK7	3.5296	0.2833	0.0020	354.66
M8	3.1052	0.3220	0.0085	76.01

Appendix VII

RSA analyses of sediment textural characteristics are presented in the following.

PARTICLE SIZE ANALYSIS

Earth Sciences - University of Waikato

Sample: core 1

Size distribution histogram

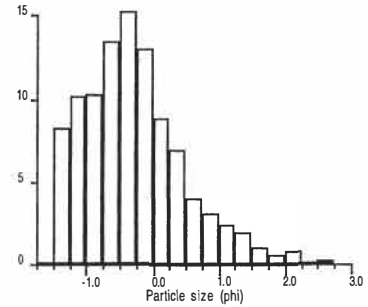

Results summary

Textural size classes

Gravel= 18.43% Sand= 81.57% Silt= 0.00% Clay= 0.00%

Gravel bearing detrital sediment

Gravelly Sand

Moment method parameters (phi)

Mean= -0.28 Sorting= 0.76Skewness= 0.83 Kurtosis= 3.67

Graphical method parameters (phi)

Mean= -0.34 Sorting= 0.76Skewness= 0.15 Kurtosis= 1.08

Median= -0.37 C= -1.47 D35= -0.63 D65= -0.10

Textural description:

Moderately sorted, Fine skewed, Mesokurtic

Cumulative frequency

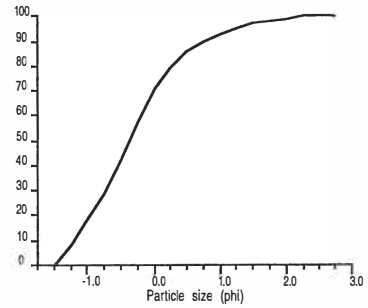

Cumulative frequency

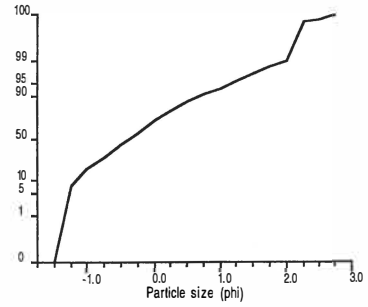

Raw data summary

Size (phi)	Size (mm)	Cumulative weight (g)	Interval frequency (%)	Cumulative frequency (%)
-1.50	2.8284	0.00	0.00	0.00
-1.25	2.3784	3.59	8.17	8.17
-1.00	2.0000	8.10	10.26	18.43
-0.75	1.6818	12.63	10.31	28.74
-0.50	1.4142	18.56	13.50	42.24
-0.25	1.1892	25.25	15.23	57.47
0.00	1.0000	30.95	12.97	70.44
0.25	0.8409	34.84	8.85	79.29
0.50	0.7071	37.85	6.85	86.14
0.75	0.5946	39.60	3.98	90.12
1.00	0.5000	40.90	2.96	93.08
1.25	0.4204	41.95	2.39	95.47
1.50	0.3536	42.81	1.96	97.43
1.75	0.2973	43.25	1.00	98.43
2.00	0.2500	43.51	0.59	99.02
2.25	0.2102	43.87	0.82	99.84
2.50	0.1768	43.88	0.02	99.87
2.75	0.1487	43.97	0.20	100.07

Total weight = 43.94 g

PARTICLE SIZE ANALYSIS

Earth Sciences - University of Waikato

Sample: core 2

Size distribution histogram

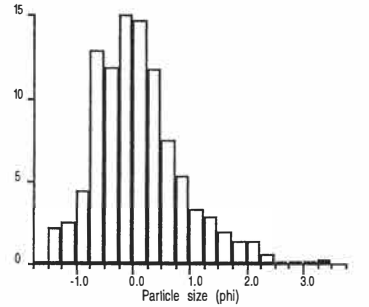

Results summary

Textural size classes

Gravel= 4.62% Sand= 95.38% Silt= 0.00% Clay= 0.00%

Gravel bearing detrital sediment

Slightly Gravelly Sand

Moment method parameters (phi)

Mean= 0.11 Sorting= 0.77Skewness= 0.83 Kurtosis= 4.13

Graphical method parameters (phi)

Mean= 0.07 Sorting= 0.75Skewness= 0.17 Kurtosis= 1.14

Median= 0.02 C= -1.38 D35= -0.23 D65= 0.28

Textural description:

Moderately sorted, Fine skewed, Leptokurtic

Cumulative frequency

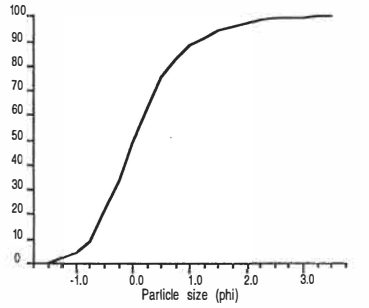

Cumulative frequency

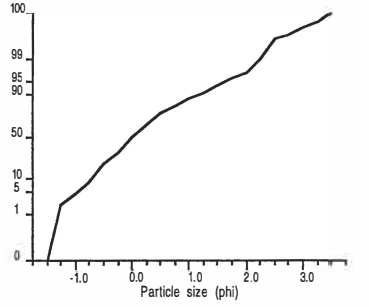

Raw data summary

Size (phi)	Size (mm)	Cumulative weight (g)	Interval frequency (%)	Cumulative frequency (%)
-1.50	2.8284	0.00	0.00	0.00
-1.25	2.3784	0.80	2.11	2.11
-1.00	2.0000	1.75	2.51	4.62
-0.75	1.6818	3.42	4.41	9.03
-0.50	1.4142	8.30	12.89	21.92
-0.25	1.1892	12.81	11.91	33.83
0.00	1.0000	18.49	15.00	48.82
0.25	0.8409	24.06	14.71	63.53
0.50	0.7071	28.50	11.72	75.26
0.75	0.5946	31.35	7.53	82.78
1.00	0.5000	33.37	5.33	88.12
1.25	0.4204	34.60	3.25	91.36
1.50	0.3536	35.67	2.83	94.19
1.75	0.2973	36.42	1.98	96.17
2.00	0.2500	36.91	1.29	97.46
2.25	0.2102	37.45	1.43	98.89
2.50	0.1768	37.67	0.58	99.47
2.75	0.1487	37.70	0.08	99.55
3.00	0.1250	37.75	0.13	99.68
3.25	0.1051	37.79	0.11	99.79
3.50	0.0884	37.88	0.24	100.03

Total weight = 37.87 g

PARTICLE SIZE ANALYSIS

Earth Sciences - University of Waikato

Sample: core 3

Size distribution histogram

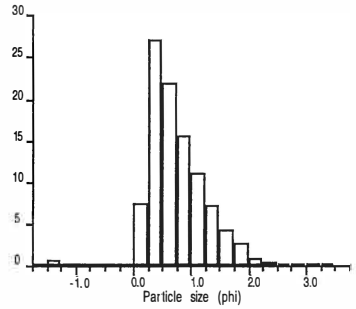

Results summary

Textural size classes

Gravel= 0.66% Sand= 99.34% Silt= 0.00% Clay= 0.00%

Gravel bearing detrital sediment

Slightly Gravelly Sand

Moment method parameters (phi)

Mean= 0.77 Sorting= 0.52Skewness= 0.59 Kurtosis= 5.92

Graphical method parameters (phi)

Mean= 0.75 Sorting= 0.47Skewness= 0.30 Kurtosis= 1.00

Median= 0.67 C= 0.01 D35= 0.50 D65= 0.88

Textural description:

Well sorted, Fine skewed, Mesokurtic

Cumulative frequency

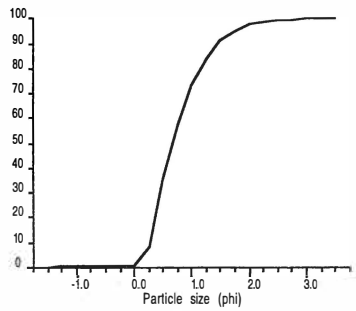

Cumulative frequency

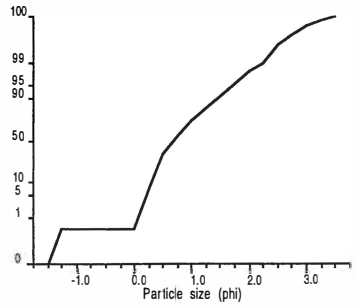

Raw data summary

Size (phi)	Size (mm)	Cumulative weight (g)	Interval frequency (%)	Cumulative frequency (%)
-1.50	2.8284	0.00	0.00	0.00
-1.25	2.3784	0.24	0.66	0.66
-1.00	2.0000	0.24	0.00	0.66
-0.75	1.6818	0.24	0.00	0.66
-0.50	1.4142	0.24	0.00	0.66
-0.25	1.1892	0.24	0.00	0.66
0.00	1.0000	0.24	0.00	0.66
0.25	0.8409	2.90	7.33	7.99
0.50	0.7071	12.76	27.16	35.14
0.75	0.5946	20.70	21.87	57.01
1.00	0.5000	26.38	15.64	72.65
1.25	0.4204	30.43	11.15	83.81
1.50	0.3536	33.06	7.24	91.05
1.75	0.2973	34.66	4.41	95.46
2.00	0.2500	35.67	2.78	98.24
2.25	0.2102	35.98	0.85	99.09
2.50	0.1768	36.11	0.36	99.45
2.75	0.1487	36.18	0.19	99.64
3.00	0.1250	36.23	0.14	99.78
3.25	0.1051	36.27	0.11	99.89
3.50	0.0884	36.31	0.11	100.00

Total weight = 36.31 g

PARTICLE SIZE ANALYSIS

Earth Sciences - University of Waikato

Sample: core 4 layer a

Size distribution histogram

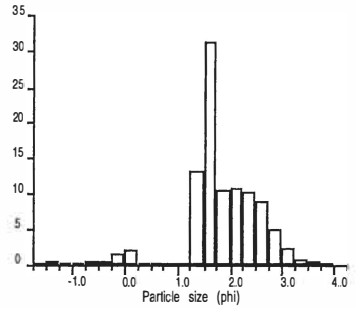

Results summary

Textural size classes

Gravel= 0.63% Sand= 99.28% Silt= 0.00% Clay= 0.00%

Gravel bearing detrital sediment

Slightly Gravelly Sand

Moment method parameters (phi)

Mean= 1.85 Sorting= 0.73Skewness= -1.14 Kurtosis= 6.41

Graphical method parameters (phi)

Mean= 1.91 Sorting= 0.69Skewness= 0.15 Kurtosis= 1.46

Median= 1.75 C= -0.71 D35= 1.63 D65= 2.09

Textural description:

Moderately well sorted, Fine skewed, Leptokurtic

Cumulative frequency

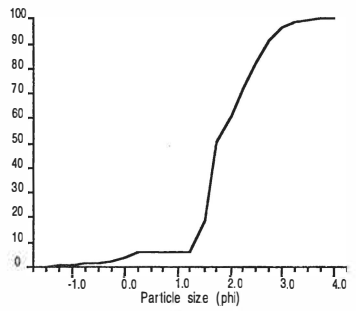

Cumulative frequency

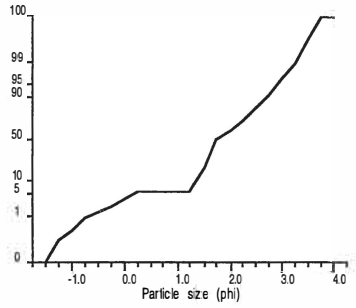

Raw data summary

Size (phi)	Size (mm)	Cumulative weight (g)	Interval frequency (%)	Cumulative frequency (%)
-1.50	2.8284	0.00	0.00	0.00
-1.25	2.3784	0.11	0.46	0.46
-1.00	2.0000	0.15	0.17	0.63
-0.75	1.6818	0.22	0.29	0.93
-0.50	1.4142	0.33	0.46	1.39
-0.25	1.1892	0.49	0.67	2.06
0.00	1.0000	0.87	1.60	3.66
0.25	0.8409	1.35	2.02	5.69
0.50	0.7071	1.40	0.21	5.90
0.75	0.5946	1.40	0.00	5.90
1.00	0.5000	1.40	0.00	5.90
1.25	0.4204	1.40	0.00	5.90
1.50	0.3536	4.51	13.10	19.00
1.75	0.2973	12.01	31.59	50.59
2.00	0.2500	14.49	10.45	61.04
2.25	0.2102	17.10	10.99	72.03
2.50	0.1768	19.54	10.28	82.31
2.75	0.1487	21.69	9.06	91.36
3.00	0.1250	22.92	5.18	96.55
3.25	0.1051	23.45	2.23	98.78
3.50	0.0884	23.63	0.76	99.54
3.75	0.0743	23.72	0.38	99.92
4.00	0.0625	23.72	0.00	99.92

Total weight = 23.74 g

PARTICLE SIZE ANALYSIS

Earth Sciences - University of Waikato

Sample: core 4 layer b

Size distribution histogram

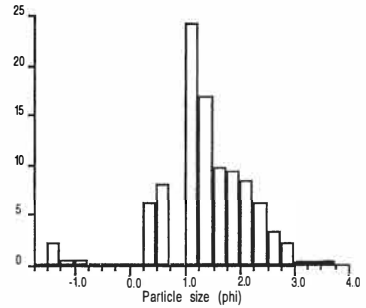

Results summary

Textural size classes

Gravel= 2.96% Sand= 97.04% Silt= 0.00% Clay= 0.00%

Gravel bearing detrital sediment

Slightly Gravelly Sand

Moment method parameters (phi)

Mean= 1.39 Sorting= 0.81 Skewness= -0.84 Kurtosis= 5.39

Graphical method parameters (phi)

Mean= 1.40 Sorting= 0.71 Skewness= 0.08 Kurtosis= 1.14

Median= 1.36 C= -1.39 D35= 1.17 D65= 1.64

Textural description:

Moderately sorted, Near symmetrical, Leptokurtic

Cumulative frequency

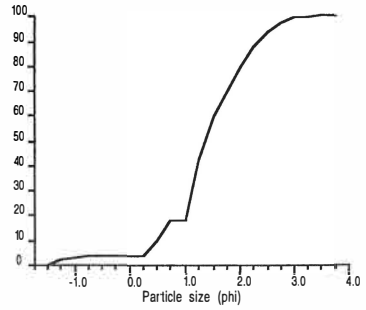

Cumulative frequency

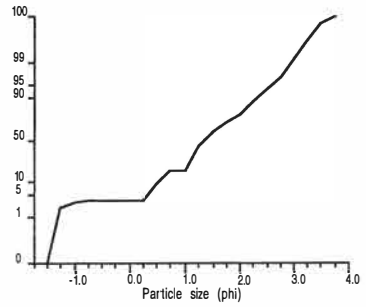

Raw data summary

Size (phi)	Size (mm)	Cumulative weight (g)	Interval frequency (%)	Cumulative frequency (%)
-1.50	2.8284	0.00	0.00	0.00
-1.25	2.3784	0.36	2.37	2.37
-1.00	2.0000	0.45	0.59	2.96
-0.75	1.6818	0.53	0.53	3.48
-0.50	1.4142	0.56	0.20	3.68
-0.25	1.1892	0.56	0.00	3.68
0.00	1.0000	0.56	0.00	3.68
0.25	0.8409	0.56	0.00	3.68
0.50	0.7071	1.51	6.25	9.93
0.75	0.5946	2.75	8.15	18.08
1.00	0.5000	2.77	0.13	18.21
1.25	0.4204	6.48	24.39	42.60
1.50	0.3536	9.08	17.09	59.70
1.75	0.2973	10.57	9.80	69.49
2.00	0.2500	12.00	9.40	78.89
2.25	0.2102	13.29	8.48	87.37
2.50	0.1768	14.24	6.25	93.62
2.75	0.1487	14.76	3.42	97.04
3.00	0.1250	15.09	2.17	99.21
3.25	0.1051	15.14	0.33	99.54
3.50	0.0884	15.18	0.26	99.80
3.75	0.0743	15.25	0.46	100.26

Total weight = 15.21 g

PARTICLE SIZE ANALYSIS

Earth Sciences - University of Waikato

Sample: core 4 layer c

Size distribution histogram

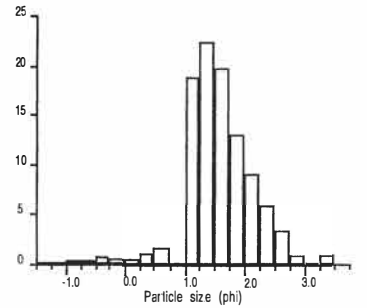

Results summary

Textural size classes

Gravel= 0.07% Sand= 99.93% Silt= 0.00% Clay= 0.00%

Gravel bearing detrital sediment

Slightly Gravelly Sand

Moment method parameters (phi)

Mean= 1.58 Sorting= 0.59 Skewness= -0.44 Kurtosis= 5.68

Graphical method parameters (phi)

Mean= 1.60 Sorting= 0.53 Skewness= 0.12 Kurtosis= 1.17

Median= 1.54 C= -0.43 D35= 1.37 D65= 1.73

Textural description:

Moderately well sorted, Fine skewed, Leptokurtic

Cumulative frequency

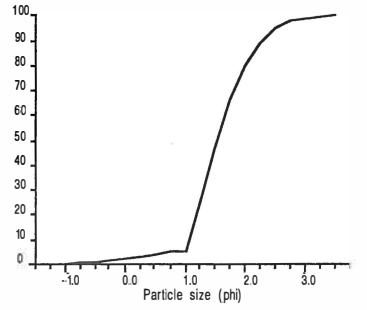

Cumulative frequency

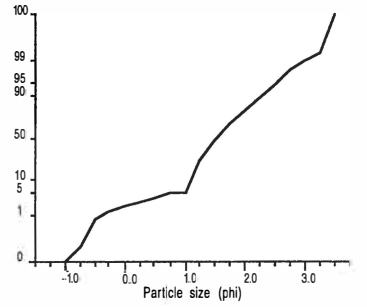

Raw data summary

Size (phi)	Size (mm)	Cumulative weight (g)	Interval frequency (%)	Cumulative frequency (%)
-1.25	2.3784	0.00	0.00	0.00
-1.00	2.0000	0.03	0.07	0.07
-0.75	1.6818	0.13	0.24	0.31
-0.50	1.4142	0.34	0.50	0.82
-0.25	1.1892	0.63	0.70	1.51
0.00	1.0000	0.87	0.58	2.09
0.25	0.8409	1.14	0.65	2.73
0.50	0.7071	1.62	1.15	3.88
0.75	0.5946	2.31	1.65	5.54
1.00	0.5000	2.32	0.02	5.56
1.25	0.4204	10.15	18.77	24.33
1.50	0.3536	19.48	22.37	46.70
1.75	0.2973	27.79	19.92	66.62
2.00	0.2500	33.27	13.14	79.76
2.25	0.2102	37.04	9.04	88.79
2.50	0.1768	39.48	5.85	94.64
2.75	0.1487	40.88	3.36	98.00
3.00	0.1250	41.32	1.05	99.05
3.25	0.1051	41.41	0.22	99.27
3.50	0.0884	41.80	0.93	100.20

Total weight = 41.72 g

PARTICLE SIZE ANALYSIS

Earth Sciences - University of Waikato

Sample: core 5 layer a

Size distribution histogram

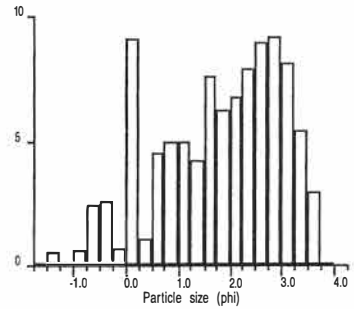

Results summary

Textural size classes

Gravel= 0.52% Sand= 98.29% Silt= 0.00% Clay= 0.00%

Gravel bearing detrital sediment

Slightly Gravelly Sand

Moment method parameters (phi)

Mean= 1.78 Sorting= 1.17 Skewness= -0.42 Kurtosis= 2.25

Graphical method parameters (phi)

Mean= 1.79 Sorting= 1.27 Skewness= -0.25 Kurtosis= 0.84

Median= 2.02 C= -0.79 D35= 1.47 D65= 2.52

Textural description:

Poorly sorted, Coarse skewed, Platykurtic

Cumulative frequency

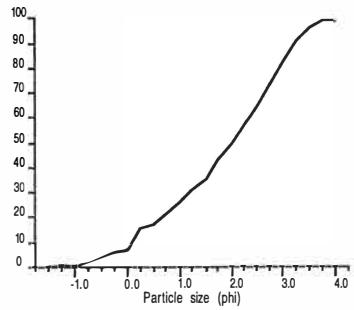

Cumulative frequency

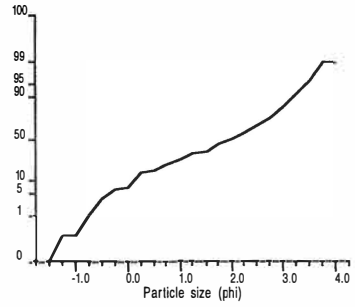

Raw data summary

Size (phi)	Size (mm)	Cumulative weight (g)	Interval frequency (%)	Cumulative frequency (%)
-1.50	2.8284	0.00	0.00	0.00
-1.25	2.3784	0.10	0.52	0.52
-1.00	2.0000	0.10	0.00	0.52
-0.75	1.6818	0.21	0.57	1.09
-0.50	1.4142	0.68	2.44	3.52
-0.25	1.1892	1.18	2.59	6.11
0.00	1.0000	1.30	0.62	6.74
0.25	0.8409	3.06	9.12	15.86
0.50	0.7071	3.26	1.04	16.89
0.75	0.5946	4.13	4.51	21.40
1.00	0.5000	5.08	4.92	26.32
1.25	0.4204	6.04	4.97	31.30
1.50	0.3536	6.86	4.25	35.55
1.75	0.2973	8.34	7.67	43.21
2.00	0.2500	9.55	6.27	49.48
2.25	0.2102	10.86	6.79	56.27
2.50	0.1768	12.38	7.88	64.15
2.75	0.1487	14.10	8.91	73.06
3.00	0.1250	15.87	9.17	82.23
3.25	0.1051	17.45	8.19	90.42
3.50	0.0884	18.50	5.44	95.86
3.75	0.0743	19.07	2.95	98.81
4.00	0.0625	19.07	0.00	98.81

Total weight = 19.30 g

PARTICLE SIZE ANALYSIS

Earth Sciences - University of Waikato

Sample: core 5 layer b

Size distribution histogram

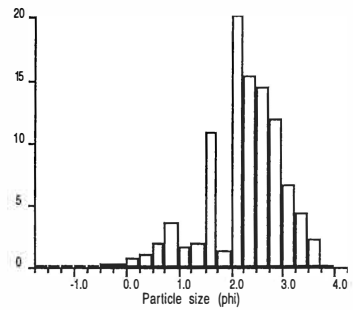

Results summary

Textural size classes

Gravel= 0.22% Sand= 99.31% Silt= 0.00% Clay= 0.00%

Gravel bearing detrital sediment

Slightly Gravelly Sand

Moment method parameters (phi)

Mean= 2.24 Sorting= 0.76 Skewness= -0.97 Kurtosis= 4.68

Graphical method parameters (phi)

Mean= 2.29 Sorting= 0.74 Skewness= -0.16 Kurtosis= 1.42

Median= 2.34 C= -0.02 D35= 2.13 D65= 2.59

Textural description:

Moderately sorted, Coarse skewed, Leptokurtic

Cumulative frequency

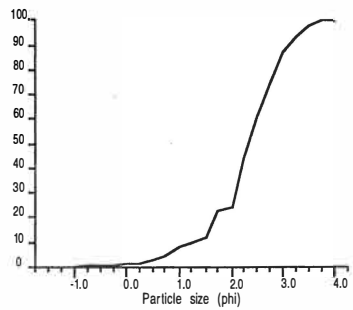

Cumulative frequency

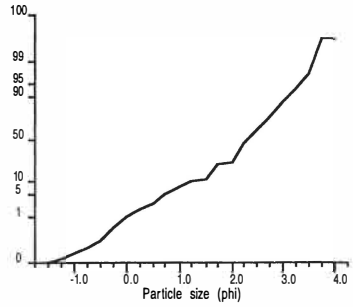

Raw data summary

Size (phi)	Size (mm)	Cumulative weight (g)	Interval frequency (%)	Cumulative frequency (%)
-1.50	2.8284	0.00	0.00	0.00
-1.25	2.3784	0.04	0.15	0.15
-1.00	2.0000	0.06	0.07	0.22
-0.75	1.6818	0.09	0.11	0.33
-0.50	1.4142	0.12	0.11	0.44
-0.25	1.1892	0.18	0.22	0.66
0.00	1.0000	0.28	0.37	1.03
0.25	0.8409	0.48	0.74	1.77
0.50	0.7071	0.78	1.11	2.88
0.75	0.5946	1.32	1.99	4.87
1.00	0.5000	2.30	3.61	8.48
1.25	0.4204	2.76	1.70	10.18
1.50	0.3536	3.29	1.95	12.13
1.75	0.2973	6.21	10.77	22.90
2.00	0.2500	6.55	1.25	24.15
2.25	0.2102	12.04	20.25	44.40
2.50	0.1768	16.23	15.45	59.85
2.75	0.1487	20.15	14.46	74.31
3.00	0.1250	23.38	11.91	86.22
3.25	0.1051	25.21	6.75	92.97
3.50	0.0884	26.39	4.35	97.32
3.75	0.0743	26.99	2.21	99.53
4.00	0.0625	26.99	0.00	99.53

Total weight = 27.12 g

PARTICLE SIZE ANALYSIS

Earth Sciences - University of Waikato

Sample: core 5 layer c

Size distribution histogram

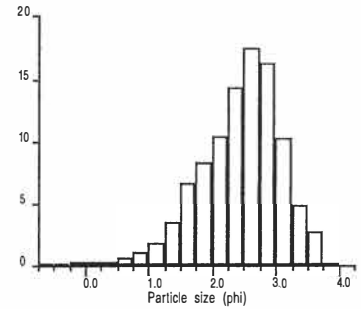

Results summary

Textural size classes

Gravel= 0.00% Sand= 99.41% Silt= 0.00% Clay= 0.00%

Gravel free detrital sediment

Sand

Moment method parameters (phi)

Mean= 2.42 Sorting= 0.65 Skewness= -0.73 Kurtosis= 4.03

Graphical method parameters (phi)

Mean= 2.46 Sorting= 0.64 Skewness= -0.17 Kurtosis= 1.03

Median= 2.53 C= 0.45 D35= 2.28 D65= 2.75

Textural description:

Moderately well sorted, Coarse skewed, Mesokurtic

Cumulative frequency

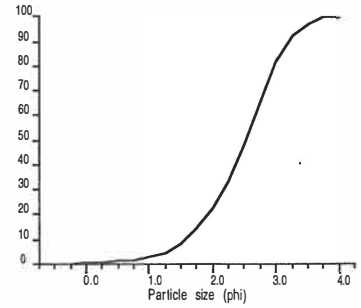

Cumulative frequency

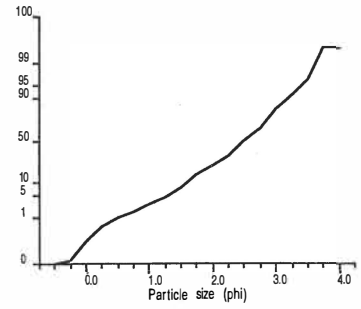

Raw data summary

Size (phi)	Size (mm)	Cumulative weight (g)	Interval frequency (%)	Cumulative frequency (%)
-0.50	1.4142	0.00	0.00	0.00
-0.25	1.1892	0.03	0.12	0.12
0.00	1.0000	0.11	0.32	0.44
0.25	0.8409	0.18	0.28	0.72
0.50	0.7071	0.27	0.36	1.08
0.75	0.5946	0.42	0.60	1.68
1.00	0.5000	0.69	1.08	2.75
1.25	0.4204	1.14	1.80	4.55
1.50	0.3536	2.03	3.55	8.10
1.75	0.2973	3.68	6.58	14.69
2.00	0.2500	5.77	8.34	23.03
2.25	0.2102	8.35	10.30	33.32
2.50	0.1768	11.96	14.41	47.73
2.75	0.1487	16.35	17.52	65.25
3.00	0.1250	20.45	16.36	81.61
3.25	0.1051	23.01	10.22	91.82
3.50	0.0884	24.23	4.87	96.69
3.75	0.0743	24.91	2.71	99.41
4.00	0.0625	24.91	0.00	99.41

Total weight = 25.06 g

PARTICLE SIZE ANALYSIS

Earth Sciences - University of Waikato

Sample: core 6 layer a

Size distribution histogram

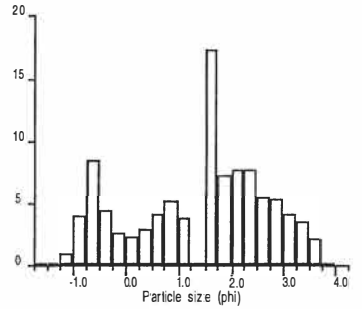

Results summary

Textural size classes

Gravel= 1.05% Sand= 97.64% Silt= 0.00% Clay= 0.00%

Gravel bearing detrital sediment

Slightly Gravelly Sand

Moment method parameters (phi)

Mean= 1.39 Sorting= 1.27 Skewness= -0.31 Kurtosis= 2.08

Graphical method parameters (phi)

Mean= 1.36 Sorting= 1.40 Skewness= -0.23 Kurtosis= 0.88

Median= 1.67 C= -1.01 D35= 1.04 D65= 2.07

Textural description:

Poorly sorted, Coarse skewed, Platykurtic

Cumulative frequency

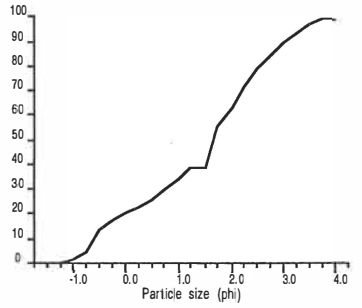

Cumulative frequency

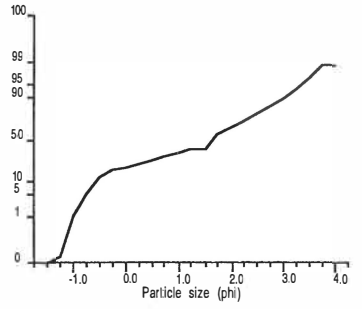

Raw data summary

Size (phi)	Size (mm)	Cumulative weight (g)	Interval frequency (%)	Cumulative frequency (%)
-1.50	2.8284	0.00	0.00	0.00
-1.25	2.3784	0.03	0.16	0.16
-1.00	2.0000	0.20	0.90	1.05
-0.75	1.6818	0.93	3.84	4.90
-0.50	1.4142	2.53	8.43	13.32
-0.25	1.1892	3.36	4.37	17.70
0.00	1.0000	3.85	2.58	20.28
0.25	0.8409	4.27	2.21	22.49
0.50	0.7071	4.81	2.84	25.33
0.75	0.5946	5.58	4.06	29.39
1.00	0.5000	6.53	5.00	34.39
1.25	0.4204	7.25	3.79	38.18
1.50	0.3536	7.25	0.00	38.18
1.75	0.2973	10.54	17.33	55.51
2.00	0.2500	11.93	7.32	62.83
2.25	0.2102	13.40	7.74	70.57
2.50	0.1768	14.86	7.69	78.26
2.75	0.1487	15.88	5.37	83.64
3.00	0.1250	16.89	5.32	88.95
3.25	0.1051	17.68	4.16	93.12
3.50	0.0884	18.34	3.48	96.59
3.75	0.0743	18.74	2.11	98.70
4.00	0.0625	18.74	0.00	98.70

Total weight = 18.99 g

PARTICLE SIZE ANALYSIS

Earth Sciences - University of Waikato

Sample: core 6 layer b

Size distribution histogram

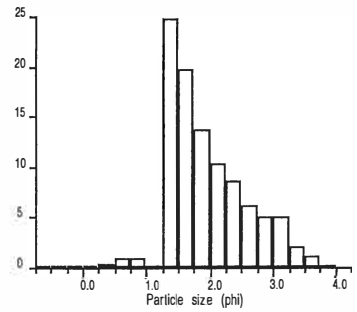

Cumulative frequency

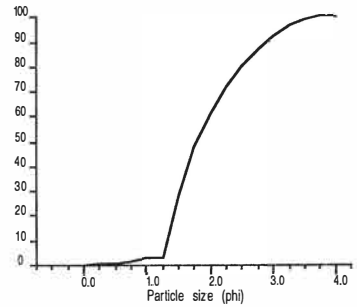

Cumulative frequency

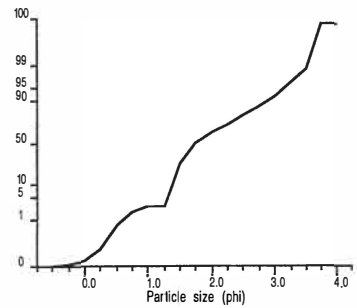

Results summary

Textural size classes

Gravel= 0.00% Sand= 99.85% Silt= 0.00% Clay= 0.00%

Gravel free detrital sediment

Sand

Moment method parameters (phi)

Mean= 1.94 Sorting= 0.63 Skewness= 0.54 Kurtosis= 3.17

Graphical method parameters (phi)

Mean= 1.94 Sorting= 0.61 Skewness= 0.40 Kurtosis= 0.89

Median= 1.80 C= 0.55 D35= 1.59 D65= 2.09

Textural description:

Moderately well sorted, Strongly fine skewed, Platykurtic

Raw data summary

Size (phi)	Size (mm)	Cumulative weight (g)	Interval frequency (%)	Cumulative frequency (%)
-0.50	1.4142	0.00	0.00	0.00
-0.25	1.1892	0.03	0.10	0.10
0.00	1.0000	0.05	0.07	0.17
0.25	0.8409	0.10	0.17	0.34
0.50	0.7071	0.23	0.44	0.77
0.75	0.5946	0.55	1.08	1.85
1.00	0.5000	0.83	0.94	2.80
1.25	0.4204	0.83	0.00	2.80
1.50	0.3536	8.21	24.86	27.66
1.75	0.2973	14.09	19.81	47.47
2.00	0.2500	18.15	13.68	61.14
2.25	0.2102	21.24	10.41	71.55
2.50	0.1768	23.80	8.62	80.18
2.75	0.1487	25.64	6.20	86.37
3.00	0.1250	27.18	5.19	91.56
3.25	0.1051	28.69	5.09	96.65
3.50	0.0884	29.28	1.99	98.64
3.75	0.0743	29.64	1.21	99.85
4.00	0.0625	29.64	0.00	99.85

Total weight = 29.68 g

PARTICLE SIZE ANALYSIS

Earth Sciences - University of Waikato

Sample: core 6 layer c

Size distribution histogram

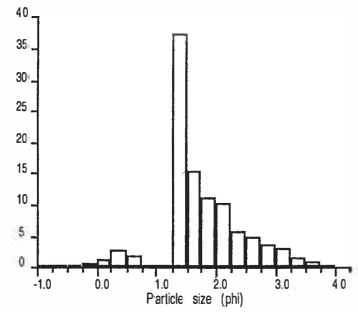

Cumulative frequency

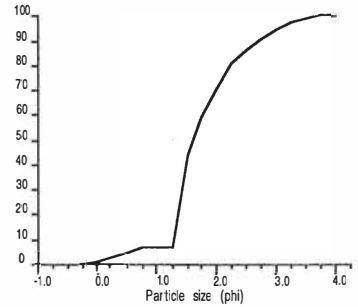

Cumulative frequency

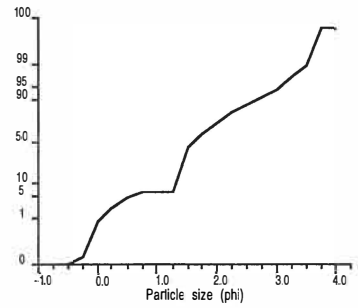

Results summary

Textural size classes

Gravel= 0.00% Sand= 99.76% Silt= 0.00% Clay= 0.00%

Gravel free detrital sediment

Sand

Moment method parameters (phi)

Mean= 1.75 Sorting= 0.66 Skewness= 0.29 Kurtosis= 3.88

Graphical method parameters (phi)

Mean= 1.78 Sorting= 0.65 Skewness= 0.32 Kurtosis= 1.38

Median= 1.60 C= 0.04 D35= 1.44 D65= 1.88

Textural description:

Moderately well sorted, Strongly fine skewed, Leptokurtic

Raw data summary

Size (phi)	Size (mm)	Cumulative weight (g)	Interval frequency (%)	Cumulative frequency (%)
-0.75	1.6818	-0.01	-0.04	-0.04
-0.50	1.4142	0.00	0.04	0.00
-0.25	1.1892	0.05	0.20	0.20
0.00	1.0000	0.20	0.60	0.81
0.25	0.8409	0.52	1.29	2.09
0.50	0.7071	1.14	2.50	4.59
0.75	0.5946	1.60	1.85	6.44
1.00	0.5000	1.60	0.00	6.44
1.25	0.4204	1.60	0.00	6.44
1.50	0.3536	10.87	37.32	43.76
1.75	0.2973	14.66	15.26	59.02
2.00	0.2500	17.41	11.07	70.09
2.25	0.2102	19.95	10.23	80.32
2.50	0.1768	21.33	5.56	85.87
2.75	0.1487	22.52	4.79	90.67
3.00	0.1250	23.42	3.62	94.29
3.25	0.1051	24.19	3.10	97.39
3.50	0.0884	24.55	1.45	98.84
3.75	0.0743	24.78	0.93	99.76
4.00	0.0625	24.78	0.00	99.76

Total weight = 24.84 g

PARTICLE SIZE ANALYSIS

Earth Sciences - University of Waikato

Sample: core 7 layer a

Size distribution histogram

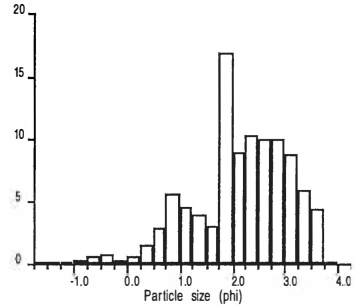

Cumulative frequency

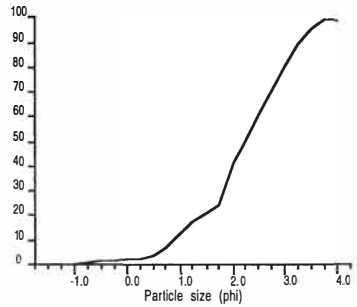

Cumulative frequency

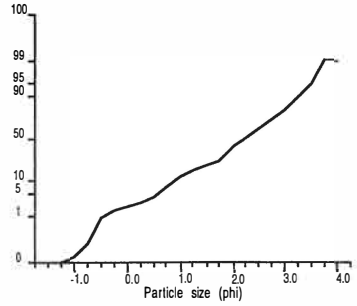

Results summary

Textural size classes

Gravel= 0.16% Sand= 98.90% Silt= 0.00% Clay= 0.00%

Gravel bearing detrital sediment

Slightly Gravelly Sand

Moment method parameters (phi)

Mean= 2.14 Sorting= 0.91 Skewness= -0.60 Kurtosis= 3.28

Graphical method parameters (phi)

Mean= 2.18 Sorting= 0.93 Skewness= -0.13 Kurtosis= 1.09

Median= 2.25 C= -0.50 D35= 1.91 D65= 2.62

Textural description:

Moderately sorted, Coarse skewed, Mesokurtic

Raw data summary

Size (phi)	Size (mm)	Cumulative weight (g)	Interval frequency (%)	Cumulative frequency (%)
-1.50	2.8284	0.00	0.00	0.00
-1.25	2.3784	0.01	0.05	0.05
-1.00	2.0000	0.03	0.11	0.16
-0.75	1.6818	0.07	0.22	0.38
-0.50	1.4142	0.18	0.60	0.99
-0.25	1.1892	0.31	0.71	1.70
0.00	1.0000	0.38	0.38	2.09
0.25	0.8409	0.48	0.55	2.64
0.50	0.7071	0.76	1.54	4.18
0.75	0.5946	1.30	2.97	7.14
1.00	0.5000	2.32	5.60	12.75
1.25	0.4204	3.13	4.45	17.20
1.50	0.3536	3.84	3.90	21.10
1.75	0.2973	4.40	3.08	24.18
2.00	0.2500	7.46	16.81	40.99
2.25	0.2102	9.08	8.90	49.89
2.50	0.1768	10.94	10.22	60.11
2.75	0.1487	12.75	9.95	70.06
3.00	0.1250	14.58	10.06	80.11
3.25	0.1051	16.16	8.68	88.79
3.50	0.0884	17.24	5.93	94.73
3.75	0.0743	18.03	4.34	99.07
4.00	0.0625	18.03	0.00	99.07

Total weight = 18.20 g

PARTICLE SIZE ANALYSIS

Earth Sciences - University of Waikato

Sample: core 7 layer b

Size distribution histogram

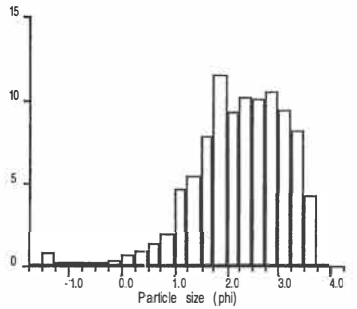

Cumulative frequency

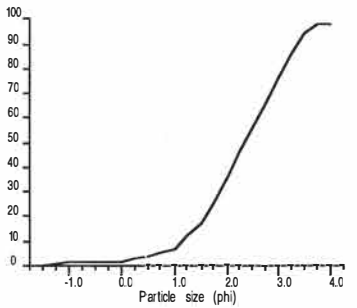

Cumulative frequency

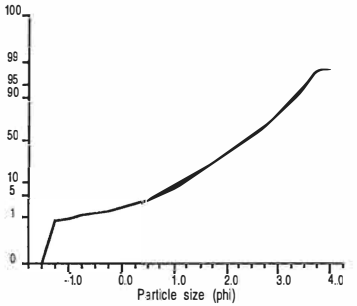

Results summary

Textural size classes

Gravel= 0.99% Sand= 97.23% Silt= 0.00% Clay= 0.00%

Gravel bearing detrital sediment

Slightly Gravelly Sand

Moment method parameters (phi)

Mean= 2.21 Sorting= 0.89 Skewness= -0.85 Kurtosis= 4.68

Graphical method parameters (phi)

Mean= 2.34 Sorting= 0.86 Skewness= -0.09 Kurtosis= 0.95

Median= 2.36 C= -0.99 D35= 1.97 D65= 2.73

Textural description:

Moderately sorted, Near symmetrical, Mesokurtic

Raw data summary

Size (phi)	Size (mm)	Cumulative weight (g)	Interval frequency (%)	Cumulative frequency (%)
-1.50	2.8284	0.00	0.00	0.00
-1.25	2.3784	0.15	0.83	0.83
-1.00	2.0000	0.18	0.17	0.99
-0.75	1.6818	0.21	0.17	1.16
-0.50	1.4142	0.25	0.22	1.38
-0.25	1.1892	0.30	0.28	1.65
0.00	1.0000	0.36	0.33	1.99
0.25	0.8409	0.49	0.72	2.70
0.50	0.7071	0.65	0.88	3.58
0.75	0.5946	0.91	1.43	5.02
1.00	0.5000	1.26	1.93	6.95
1.25	0.4204	2.10	4.63	11.58
1.50	0.3536	3.09	5.46	17.04
1.75	0.2973	4.50	7.78	24.82
2.00	0.2500	6.60	11.58	36.40
2.25	0.2102	8.28	9.27	45.66
2.50	0.1768	10.13	10.20	55.87
2.75	0.1487	11.96	10.09	65.96
3.00	0.1250	13.87	10.53	76.49
3.25	0.1051	15.58	9.43	85.92
3.50	0.0884	17.05	8.11	94.03
3.75	0.0743	17.81	4.19	98.22
4.00	0.0625	17.81	0.00	98.22

Total weight = 18.13 g

PARTICLE SIZE ANALYSIS

Earth Sciences - University of Waikato

Sample: core 7 layer c

Size distribution histogram

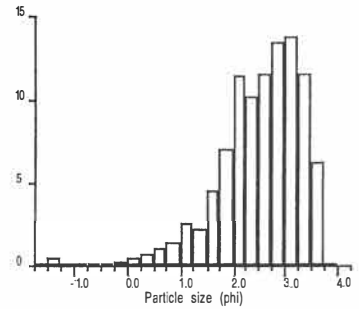

Cumulative frequency

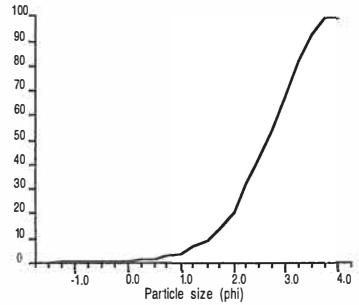

Cumulative frequency

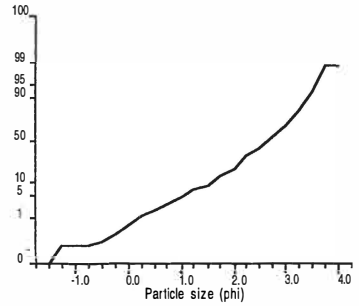

Results summary

Textural size classes

Gravel= 0.40% Sand= 98.25% Silt= 0.00% Clay= 0.00%

Gravel bearing detrital sediment

Slightly Gravelly Sand

Moment method parameters (phi)

Mean= 2.50 Sorting= 0.78 Skewness= -1.04 Kurtosis= 5.25

Graphical method parameters (phi)

Mean= 2.61 Sorting= 0.75 Skewness= -0.20 Kurtosis= 0.99

Median= 2.67 C= 0.16 D35= 2.32 D65= 2.96

Textural description:

Moderately sorted, Coarse skewed, Mesokurtic

Raw data summary

Size (phi)	Size (mm)	Cumulative weight (g)	Interval frequency (%)	Cumulative frequency (%)
-1.50	2.8284	0.00	0.00	0.00
-1.25	2.3784	0.07	0.40	0.40
-1.00	2.0000	0.07	0.00	0.40
-0.75	1.6818	0.07	0.00	0.40
-0.50	1.4142	0.08	0.06	0.46
-0.25	1.1892	0.10	0.11	0.57
0.00	1.0000	0.13	0.17	0.74
0.25	0.8409	0.20	0.40	1.14
0.50	0.7071	0.32	0.69	1.83
0.75	0.5946	0.50	1.03	2.85
1.00	0.5000	0.75	1.43	4.28
1.25	0.4204	1.19	2.51	6.79
1.50	0.3536	1.58	2.23	9.02
1.75	0.2973	2.37	4.51	13.53
2.00	0.2500	3.60	7.02	20.55
2.25	0.2102	5.60	11.42	31.97
2.50	0.1768	7.37	10.10	42.07
2.75	0.1487	9.40	11.59	53.66
3.00	0.1250	11.76	13.47	67.14
3.25	0.1051	14.17	13.76	80.89
3.50	0.0884	16.20	11.59	92.48
3.75	0.0743	17.28	6.17	98.65
4.00	0.0625	17.28	0.00	98.65

Total weight = 17.52 g

PARTICLE SIZE ANALYSIS

Earth Sciences - University of Waikato

Sample: core 7 layer d

Size distribution histogram

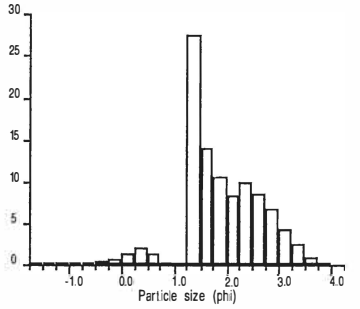

Cumulative frequency

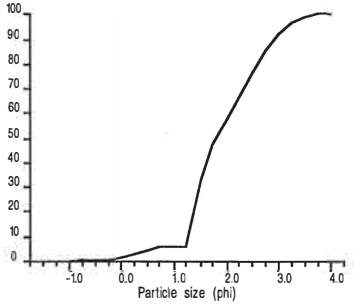

Cumulative frequency

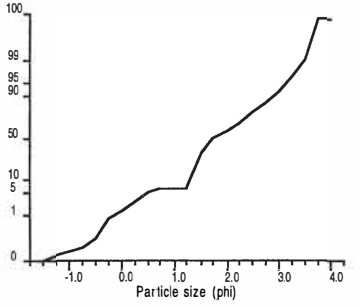

Results summary

Textural size classes

Gravel= 0.21% Sand= 99.65% Silt= 0.00% Clay= 0.00%

Gravel bearing detrital sediment

Slightly Gravelly Sand

Moment method parameters (phi)

Mean= 1.91 Sorting= 0.75 Skewness= -0.31 Kurtosis= 3.89

Graphical method parameters (phi)

Mean= 1.96 Sorting= 0.74 Skewness= 0.18 Kurtosis= 1.03

Median= 1.81 C= -0.19 D35= 1.52 D65= 2.20

Textural description:

Moderately sorted, Fine skewed, Mesokurtic

Raw data summary

Size (phi)	Size (mm)	Cumulative weight (g)	Interval frequency (%)	Cumulative frequency (%)
-1.50	2.8284	0.00	0.00	0.00
-1.25	2.3784	0.06	0.18	0.18
-1.00	2.0000	0.07	0.03	0.21
-0.75	1.6818	0.10	0.09	0.30
-0.50	1.4142	0.16	0.18	0.48
-0.25	1.1892	0.28	0.36	0.84
0.00	1.0000	0.51	0.69	1.52
0.25	0.8409	0.96	1.34	2.86
0.50	0.7071	1.59	1.88	4.74
0.75	0.5946	2.06	1.40	6.14
1.00	0.5000	2.06	0.00	6.14
1.25	0.4204	2.06	0.00	6.14
1.50	0.3536	11.27	27.47	33.61
1.75	0.2973	15.95	13.96	47.57
2.00	0.2500	19.49	10.56	58.13
2.25	0.2102	22.31	8.41	66.54
2.50	0.1768	25.61	9.84	76.39
2.75	0.1487	28.52	8.68	85.06
3.00	0.1250	30.85	6.95	92.01
3.25	0.1051	32.35	4.47	96.49
3.50	0.0884	33.19	2.51	98.99
3.75	0.0743	33.48	0.86	99.86
4.00	0.0625	33.48	0.00	99.86

Total weight = 33.53 g

PARTICLE SIZE ANALYSIS

Earth Sciences - University of Waikato

Sample: core 8 layer a

Size distribution histogram

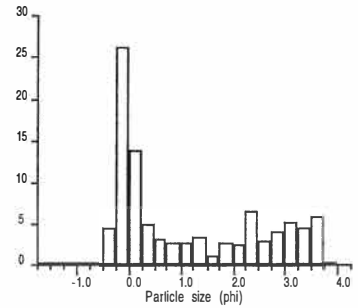

Cumulative frequency

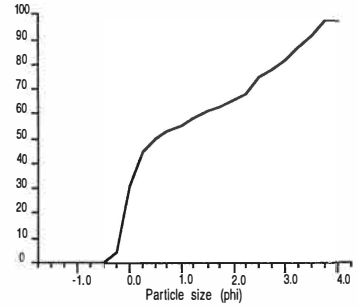

Cumulative frequency

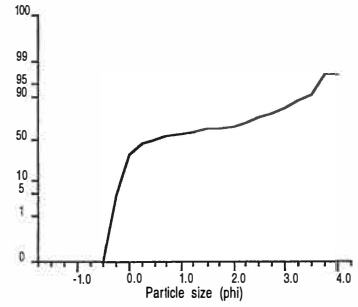

Results summary

Textural size classes

Gravel= 0.00% Sand= 97.22% Silt= 0.00% Clay= 0.00%

Gravel free detrital sediment

Sand

Moment method parameters (phi)

Mean= 1.11 Sorting= 1.35Skewness= 0.64 Kurtosis= 1.83

Graphical method parameters (phi)

Mean= 1.17 Sorting= 1.40Skewness= 0.60 Kurtosis= 0.62

Median= 0.53 C= -0.45 D35= 0.07 D65= 1.95

Textural description:

Poorly sorted, Strongly fine skewed, Very platykurtic

Raw data summary

Size (phi)	Size (mm)	Cumulative weight (g)	Interval frequency (%)	Cumulative frequency (%)
-1.50	2.8284	0.00	0.00	0.00
-1.25	2.3784	0.00	0.00	0.00
-1.00	2.0000	0.00	0.00	0.00
-0.75	1.6818	0.00	0.00	0.00
-0.50	1.4142	0.00	0.00	0.00
-0.25	1.1892	0.76	4.58	4.58
0.00	1.0000	5.13	26.32	30.90
0.25	0.8409	7.41	13.73	44.64
0.50	0.7071	8.24	5.00	49.64
0.75	0.5946	8.78	3.25	52.89
1.00	0.5000	9.22	2.65	55.54
1.25	0.4204	9.65	2.59	58.13
1.50	0.3536	10.20	3.31	61.44
1.75	0.2973	10.40	1.20	62.65
2.00	0.2500	10.88	2.89	65.54
2.25	0.2102	11.30	2.53	68.07
2.50	0.1768	12.39	6.57	74.63
2.75	0.1487	12.90	3.07	77.71
3.00	0.1250	13.57	4.04	81.74
3.25	0.1051	14.41	5.06	86.80
3.50	0.0884	15.17	4.58	91.38
3.75	0.0743	16.14	5.84	97.22
4.00	0.0625	16.14	0.00	97.22

Total weight = 16.60 g

PARTICLE SIZE ANALYSIS

Earth Sciences - University of Waikato

Sample: core 8 layer b

Size distribution histogram

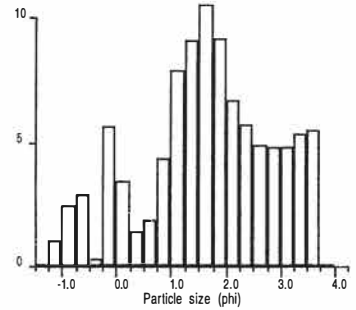

Cumulative frequency

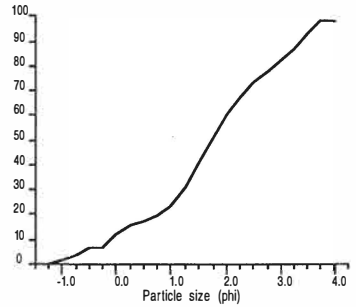

Cumulative frequency

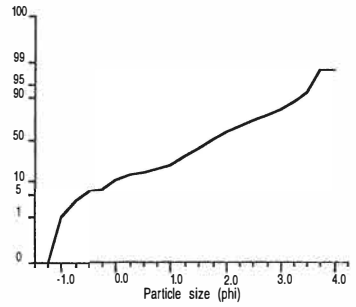

Results summary

Textural size classes

Gravel= 1.04% Sand= 97.21% Silt= 0.00% Clay= 0.00%

Gravel bearing detrital sediment

Slightly Gravelly Sand

Moment method parameters (phi)

Mean= 1.64 Sorting= 1.19Skewness= -0.26 Kurtosis= 2.51

Graphical method parameters (phi)

Mean= 1.69 Sorting= 1.34Skewness= -0.07 Kurtosis= 1.11

Median= 1.72 C= -1.01 D35= 1.35 D65= 2.17

Textural description:

Poorly sorted, Near symmetrical, Mesokurtic

Raw data summary

Size (phi)	Size (mm)	Cumulative weight (g)	Interval frequency (%)	Cumulative frequency (%)
-1.25	2.3784	0.00	0.00	0.00
-1.00	2.0000	0.11	1.04	1.04
-0.75	1.6818	0.37	2.45	3.49
-0.50	1.4142	0.68	2.92	6.41
-0.25	1.1892	0.71	0.28	6.69
0.00	1.0000	1.31	5.65	12.34
0.25	0.8409	1.68	3.49	15.83
0.50	0.7071	1.83	1.41	17.24
0.75	0.5946	2.03	1.88	19.12
1.00	0.5000	2.50	4.43	23.55
1.25	0.4204	3.34	7.91	31.46
1.50	0.3536	4.31	9.14	40.60
1.75	0.2973	5.43	10.55	51.15
2.00	0.2500	6.41	9.23	60.38
2.25	0.2102	7.12	6.69	67.07
2.50	0.1768	7.73	5.75	72.82
2.75	0.1487	8.25	4.90	77.71
3.00	0.1250	8.76	4.80	82.52
3.25	0.1051	9.27	4.80	87.32
3.50	0.0884	9.84	5.37	92.69
3.75	0.0743	10.43	5.56	98.25
4.00	0.0625	10.43	0.00	98.25

Total weight = 10.62 g

PARTICLE SIZE ANALYSIS

Earth Sciences - University of Waikato

Sample: core 9 layer a

Size distribution histogram

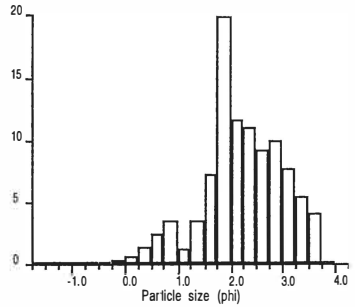

Cumulative frequency

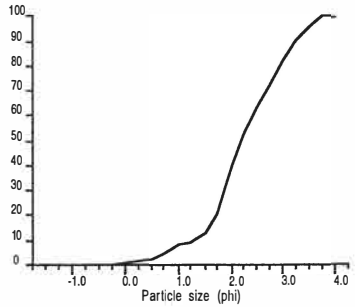

Cumulative frequency

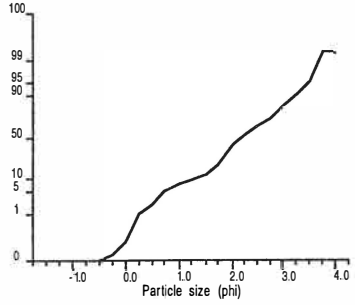

Results summary

Textural size classes

Gravel= 0.03% Sand= 99.24% Silt= 0.00% Clay= 0.00%

Gravel bearing detrital sediment

Slightly Gravelly Sand

Moment method parameters (phi)

Mean= 2.22 Sorting= 0.77 Skewness= -0.35 Kurtosis= 3.19

Graphical method parameters (phi)

Mean= 2.29 Sorting= 0.78 Skewness= 0.05 Kurtosis= 1.10

Median= 2.21 C= 0.24 D35= 1.94 D65= 2.56

Textural description:

Moderately sorted, Near symmetrical, Mesokurtic

Raw data summary

Size (phi)	Size (mm)	Cumulative weight (g)	Interval frequency (%)	Cumulative frequency (%)
-1.50	2.8284	0.00	0.00	0.00
-1.25	2.3784	0.01	0.03	0.03
-1.00	2.0000	0.01	0.00	0.03
-0.75	1.6818	0.01	0.00	0.03
-0.50	1.4142	0.02	0.03	0.07
-0.25	1.1892	0.05	0.10	0.17
0.00	1.0000	0.12	0.23	0.40
0.25	0.8409	0.31	0.64	1.04
0.50	0.7071	0.70	1.30	2.34
0.75	0.5946	1.42	2.41	4.75
1.00	0.5000	2.46	3.48	8.23
1.25	0.4204	2.82	1.20	9.43
1.50	0.3536	3.88	3.55	12.98
1.75	0.2973	6.02	7.16	20.14
2.00	0.2500	11.97	19.90	40.04
2.25	0.2102	15.46	11.67	51.71
2.50	0.1768	18.76	11.04	62.75
2.75	0.1487	21.52	9.23	71.98
3.00	0.1250	24.52	10.03	82.02
3.25	0.1051	26.84	7.76	89.78
3.50	0.0884	28.45	5.39	95.16
3.75	0.0743	29.68	4.11	99.28
4.00	0.0625	29.68	0.00	99.28

Total weight = 29.90 g

PARTICLE SIZE ANALYSIS

Earth Sciences - University of Waikato

Sample: core 9 layer b

Size distribution histogram

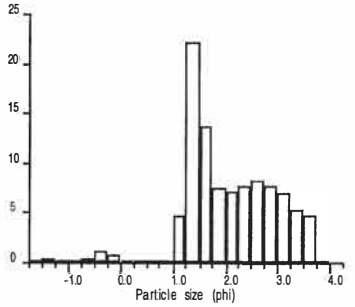

Cumulative frequency

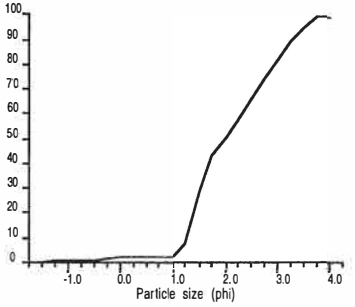

Cumulative frequency

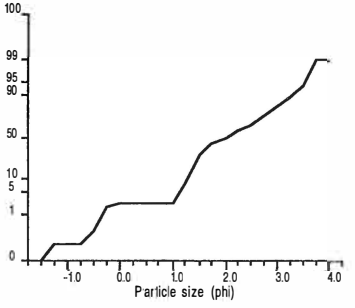

Results summary

Textural size classes

Gravel= 0.35% Sand= 98.56% Silt= 0.00% Clay= 0.00%

Gravel bearing detrital sediment

Slightly Gravelly Sand

Moment method parameters (phi)

Mean= 2.06 Sorting= 0.85 Skewness= -0.20 Kurtosis= 3.67

Graphical method parameters (phi)

Mean= 2.13 Sorting= 0.80 Skewness= 0.28 Kurtosis= 0.74

Median= 1.98 C= -0.41 D35= 1.60 D65= 2.48

Textural description:

Moderately sorted, Fine skewed, Platykurtic

Raw data summary

Size (phi)	Size (mm)	Cumulative weight (g)	Interval frequency (%)	Cumulative frequency (%)
-1.50	2.8284	0.00	0.00	0.00
-1.25	2.3784	0.09	0.35	0.35
-1.00	2.0000	0.09	0.00	0.35
-0.75	1.6818	0.09	0.00	0.35
-0.50	1.4142	0.15	0.24	0.59
-0.25	1.1892	0.45	1.18	1.76
0.00	1.0000	0.64	0.74	2.51
0.25	0.8409	0.67	0.12	2.63
0.50	0.7071	0.67	0.00	2.63
0.75	0.5946	0.67	0.00	2.63
1.00	0.5000	0.67	0.00	2.63
1.25	0.4204	1.88	4.74	7.37
1.50	0.3536	7.55	22.22	29.59
1.75	0.2973	11.03	13.64	43.22
2.00	0.2500	12.94	7.48	50.71
2.25	0.2102	14.78	7.21	57.92
2.50	0.1768	16.78	7.84	65.76
2.75	0.1487	18.91	8.35	74.10
3.00	0.1250	20.89	7.76	81.86
3.25	0.1051	22.67	6.98	88.84
3.50	0.0884	24.03	5.33	94.17
3.75	0.0743	25.24	4.74	98.91
4.00	0.0625	25.24	0.00	98.91

Total weight = 25.52 g

PARTICLE SIZE ANALYSIS

Earth Sciences - University of Waikato

Sample: core 9 layer c

Size distribution histogram

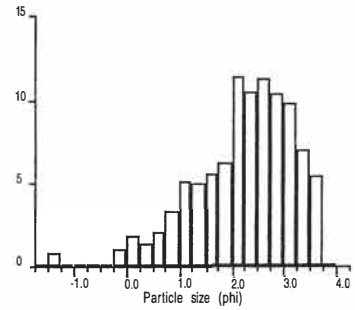

Cumulative frequency

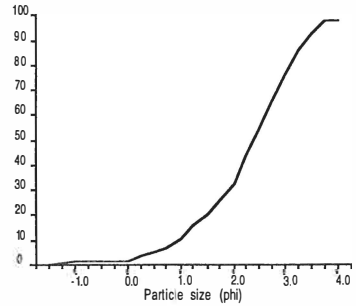

Cumulative frequency

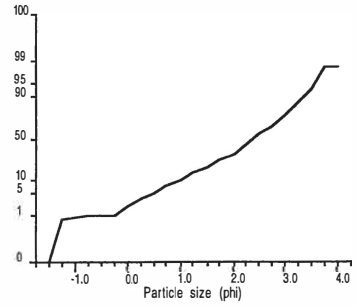

Results summary

Textural size classes

Gravel= 0.89% Sand= 97.42% Silt= 0.00% Clay= 0.00%

Gravel bearing detrital sediment

Slightly Gravelly Sand

Moment method parameters (phi)

Mean= 2.20 Sorting= 0.94 Skewness= -0.80 Kurtosis= 3.88

Graphical method parameters (phi)

Mean= 2.29 Sorting= 0.96 Skewness= -0.20 Kurtosis= 1.01

Median= 2.40 C= -0.50 D35= 2.06 D65= 2.74

Textural description:

Moderately sorted, Coarse skewed, Mesokurtic

Raw data summary

Size (phi)	Size (mm)	Cumulative weight (g)	Interval frequency (%)	Cumulative frequency (%)
-1.50	2.8284	0.00	0.00	0.00
-1.25	2.3784	0.15	0.79	0.79
-1.00	2.0000	0.17	0.11	0.89
-0.75	1.6818	0.19	0.11	1.00
-0.50	1.4142	0.19	0.00	1.00
-0.25	1.1892	0.20	0.05	1.05
0.00	1.0000	0.39	1.00	2.05
0.25	0.8409	0.74	1.84	3.89
0.50	0.7071	1.00	1.37	5.26
0.75	0.5946	1.38	2.00	7.26
1.00	0.5000	2.00	3.26	10.52
1.25	0.4204	2.97	5.10	15.62
1.50	0.3536	3.91	4.94	20.56
1.75	0.2973	4.96	5.52	26.08
2.00	0.2500	6.15	6.26	32.33
2.25	0.2102	8.34	11.51	43.85
2.50	0.1768	10.34	10.52	54.36
2.75	0.1487	12.48	11.25	65.62
3.00	0.1250	14.46	10.41	76.03
3.25	0.1051	16.34	9.88	85.91
3.50	0.0884	17.67	6.99	92.90
3.75	0.0743	18.70	5.42	98.32
4.00	0.0625	18.70	0.00	98.32

Total weight = 19.02 g

PARTICLE SIZE ANALYSIS

Earth Sciences - University of Waikato

Sample: core 10 layer a

Size distribution histogram

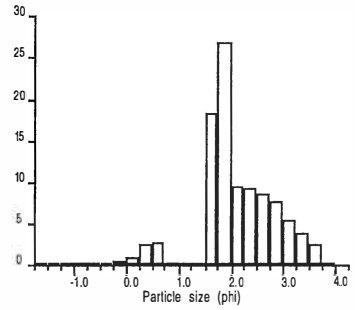

Cumulative frequency

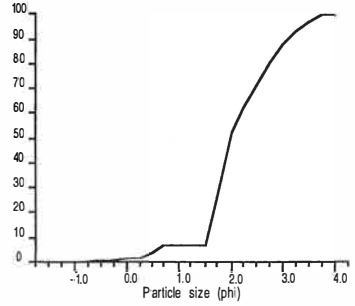

Cumulative frequency

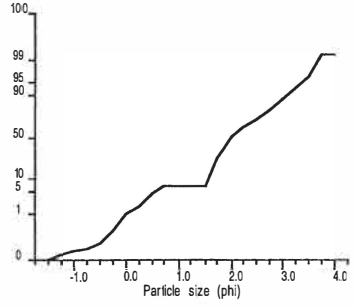

Results summary

Textural size classes

Gravel= 0.22% Sand= 99.02% Silt= 0.00% Clay= 0.00%

Gravel bearing detrital sediment

Slightly Gravelly Sand

Moment method parameters (phi)

Mean= 2.09 Sorting= 0.74 Skewness= -0.50 Kurtosis= 4.61

Graphical method parameters (phi)

Mean= 2.16 Sorting= 0.75 Skewness= 0.22 Kurtosis= 1.33

Median= 1.98 C= -0.04 D35= 1.84 D65= 2.34

Textural description:

Moderately sorted, Fine skewed, Leptokurtic

Raw data summary

Size (phi)	Size (mm)	Cumulative weight (g)	Interval frequency (%)	Cumulative frequency (%)
-1.50	2.8284	0.00	0.00	0.00
-1.25	2.3784	0.04	0.17	0.17
-1.00	2.0000	0.05	0.04	0.22
-0.75	1.6818	0.06	0.04	0.26
-0.50	1.4142	0.08	0.09	0.35
-0.25	1.1892	0.13	0.22	0.56
0.00	1.0000	0.25	0.52	1.08
0.25	0.8409	0.44	0.82	1.90
0.50	0.7071	1.00	2.42	4.32
0.75	0.5946	1.63	2.72	7.04
1.00	0.5000	1.63	0.00	7.04
1.25	0.4204	1.63	0.00	7.04
1.50	0.3536	1.63	0.00	7.04
1.75	0.2973	5.89	18.40	25.45
2.00	0.2500	12.08	26.74	52.19
2.25	0.2102	14.30	9.59	61.78
2.50	0.1768	16.46	9.33	71.11
2.75	0.1487	18.46	8.64	79.75
3.00	0.1250	20.23	7.65	87.40
3.25	0.1051	21.48	5.40	92.80
3.50	0.0884	22.38	3.89	96.69
3.75	0.0743	22.97	2.55	99.24
4.00	0.0625	22.97	0.00	99.24

Total weight = 23.15 g

PARTICLE SIZE ANALYSIS

Earth Sciences - University of Waikato

Sample: core 10 layer b

Size distribution histogram

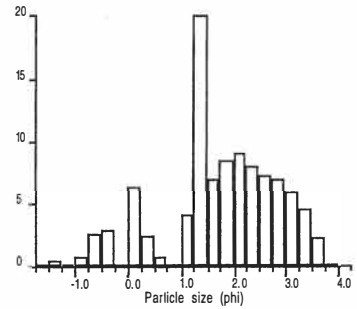

Cumulative frequency

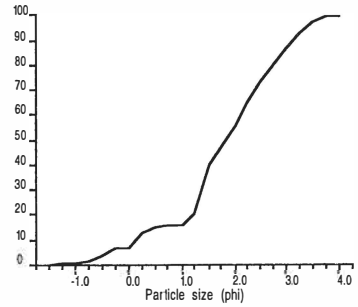

Cumulative frequency

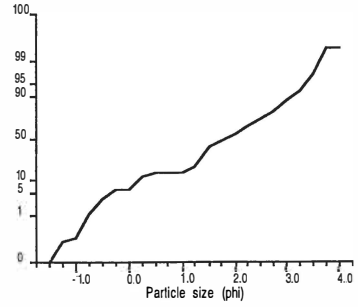

Results summary

Textural size classes

Gravel= 0.50% Sand= 98.86% Silt= 0.00% Clay= 0.00%

Gravel bearing detrital sediment

Slightly Gravelly Sand

Moment method parameters (phi)

Mean= 1.76 Sorting= 1.06 Skewness= -0.52 Kurtosis= 2.91

Graphical method parameters (phi)

Mean= 1.82 Sorting= 1.11 Skewness= -0.10 Kurtosis= 1.22

Median= 1.83 C= -0.81 D35= 1.44 D65= 2.26

Textural description:

Poorly sorted, Near symmetrical, Leptokurtic

Raw data summary

Size (phi)	Size (mm)	Cumulative weight (g)	Interval frequency (%)	Cumulative frequency (%)
-1.50	2.8284	0.00	0.00	0.00
-1.25	2.3784	0.13	0.43	0.43
-1.00	2.0000	0.15	0.07	0.50
-0.75	1.6818	0.35	0.66	1.16
-0.50	1.4142	1.12	2.54	3.70
-0.25	1.1892	1.99	2.87	6.58
0.00	1.0000	1.99	0.00	6.58
0.25	0.8409	3.91	6.34	12.92
0.50	0.7071	4.64	2.41	15.33
0.75	0.5946	4.85	0.69	16.03
1.00	0.5000	4.85	0.00	16.03
1.25	0.4204	6.09	4.10	20.12
1.50	0.3536	12.15	20.02	40.15
1.75	0.2973	14.26	6.97	47.12
2.00	0.2500	16.84	8.52	55.64
2.25	0.2102	19.58	9.05	64.70
2.50	0.1768	22.01	8.03	72.73
2.75	0.1487	24.17	7.14	79.86
3.00	0.1250	26.27	6.94	86.80
3.25	0.1051	28.05	5.88	92.68
3.50	0.0884	29.40	4.46	97.14
3.75	0.0743	30.07	2.21	99.36
4.00	0.0625	30.07	0.00	99.36

Total weight = 30.26 g

PARTICLE SIZE ANALYSIS

Earth Sciences - University of Waikato

Sample: core 10 layer c

Size distribution histogram

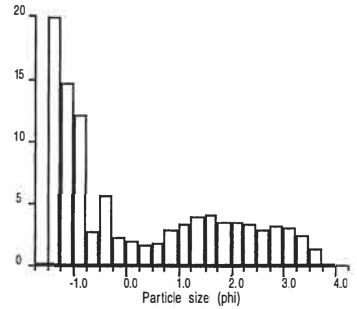

Cumulative frequency

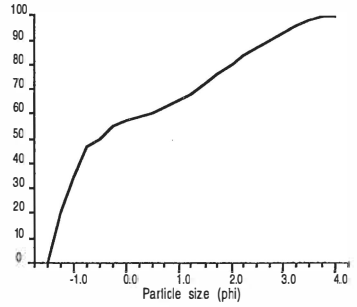

Cumulative frequency

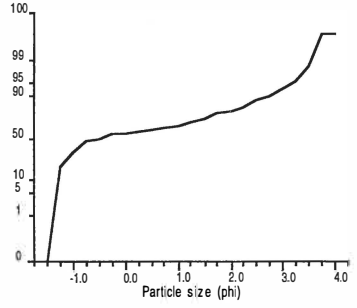

Results summary

Textural size classes

Gravel= 34.56% Sand= 65.02% Silt= 0.00% Clay= 0.00%

Gravel bearing detrital sediment

Sandy Gravel

Moment method parameters (phi)

Mean= 0.23 Sorting= 1.60 Skewness= 0.63 Kurtosis= 1.91

Graphical method parameters (phi)

Mean= 0.18 Sorting= 1.60 Skewness= 0.56 Kurtosis= 0.67

Median= -0.47 C= -1.49 D35= -0.99 D65= 0.99

Textural description:

Poorly sorted, Strongly fine skewed, Very platykurtic

Raw data summary

Size (phi)	Size (mm)	Cumulative weight (g)	Interval frequency (%)	Cumulative frequency (%)
-1.50	2.8284	0.00	0.00	0.00
-1.25	2.3784	5.29	19.89	19.89
-1.00	2.0000	9.19	14.67	34.56
-0.75	1.6818	12.38	12.00	46.56
-0.50	1.4142	13.09	2.67	49.23
-0.25	1.1892	14.56	5.53	54.76
0.00	1.0000	15.16	2.26	57.01
0.25	0.8409	15.68	1.96	58.97
0.50	0.7071	16.11	1.62	60.59
0.75	0.5946	16.57	1.73	62.32
1.00	0.5000	17.31	2.78	65.10
1.25	0.4204	18.19	3.31	68.41
1.50	0.3536	19.22	3.87	72.28
1.75	0.2973	20.32	4.14	76.42
2.00	0.2500	21.24	3.46	79.88
2.25	0.2102	22.17	3.50	83.38
2.50	0.1768	23.05	3.31	86.69
2.75	0.1487	23.83	2.93	89.62
3.00	0.1250	24.69	3.23	92.85
3.25	0.1051	25.49	3.01	95.86
3.50	0.0884	26.14	2.44	98.31
3.75	0.0743	26.48	1.28	99.59
4.00	0.0625	26.48	0.00	99.59

Total weight = 26.59 g

PARTICLE SIZE ANALYSIS

Earth Sciences - University of Waikato

Sample: core 11 layer a

Size distribution histogram

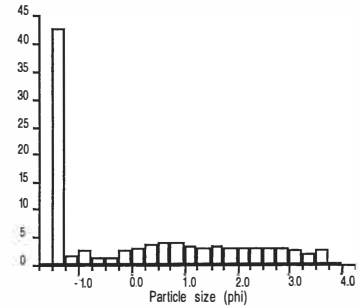

Cumulative frequency

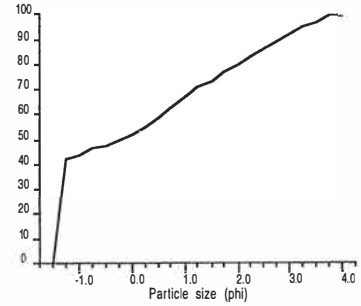

Cumulative frequency

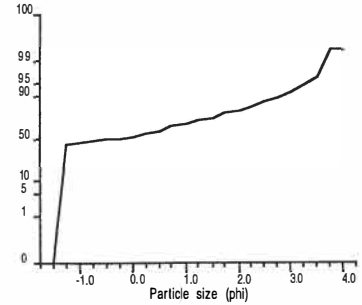

Results summary

Textural size classes

Gravel= 44.14% Sand= 55.19% Silt= 0.00% Clay= 0.00%

Gravel bearing detrital sediment

Sandy Gravel

Moment method parameters (phi)

Mean= 0.18 Sorting= 1.67 Skewness= 0.58 Kurtosis= 1.92

Graphical method parameters (phi)

Mean= 0.25 Sorting= 1.66 Skewness= 0.41 Kurtosis= 0.66

Median= -0.19 C= -1.49 D35= -1.29 D65= 0.87

Textural description:

Poorly sorted, Strongly fine skewed, Very platykurtic

Raw data summary

Size (phi)	Size (mm)	Cumulative weight (g)	Interval frequency (%)	Cumulative frequency (%)
-1.50	2.8284	0.00	0.00	0.00
-1.25	2.3784	11.32	42.56	42.56
-1.00	2.0000	11.74	1.58	44.14
-0.75	1.6818	12.43	2.59	46.73
-0.50	1.4142	12.75	1.20	47.93
-0.25	1.1892	13.13	1.43	49.36
0.00	1.0000	13.83	2.63	52.00
0.25	0.8409	14.64	3.05	55.04
0.50	0.7071	15.63	3.72	58.76
0.75	0.5946	16.76	4.25	63.01
1.00	0.5000	17.83	4.02	67.03
1.25	0.4204	18.75	3.46	70.49
1.50	0.3536	19.52	2.89	73.39
1.75	0.2973	20.43	3.42	76.81
2.00	0.2500	21.27	3.16	79.97
2.25	0.2102	22.04	2.89	82.86
2.50	0.1768	22.90	3.23	86.09
2.75	0.1487	23.70	3.01	89.10
3.00	0.1250	24.47	2.89	92.00
3.25	0.1051	25.15	2.56	94.55
3.50	0.0884	25.69	2.03	96.58
3.75	0.0743	26.42	2.74	99.33
4.00	0.0625	26.42	0.00	99.33

Total weight = 26.60 g

PARTICLE SIZE ANALYSIS

Earth Sciences - University of Waikato

Sample: core 11 layer b

Size distribution histogram

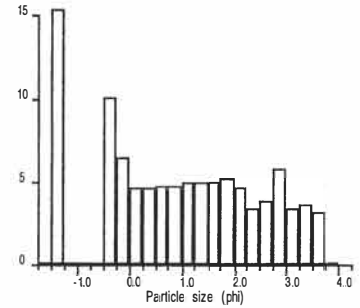

Cumulative frequency

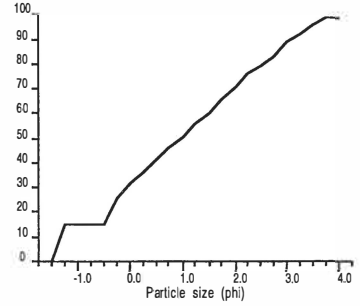

Cumulative frequency

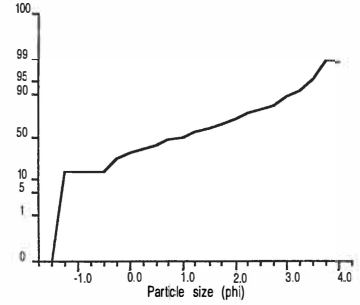

Results summary

Textural size classes

Gravel= 15.46% Sand= 83.41% Silt= 0.00% Clay= 0.00%

Gravel bearing detrital sediment

Gravelly Sand

Moment method parameters (phi)

Mean= 0.93 Sorting= 1.51 Skewness= 0.04 Kurtosis= 1.93

Graphical method parameters (phi)

Mean= 1.09 Sorting= 1.56 Skewness= 0.07 Kurtosis= 0.81

Median= 0.96 C= -1.48 D35= 0.16 D65= 1.71

Textural description:

Poorly sorted, Near symmetrical, Platykurtic

Raw data summary

Size (phi)	Size (mm)	Cumulative weight (g)	Interval frequency (%)	Cumulative frequency (%)
-1.50	2.8284	0.00	0.00	0.00
-1.25	2.3784	4.82	15.46	15.46
-1.00	2.0000	4.82	0.00	15.46
-0.75	1.6818	4.82	0.00	15.46
-0.50	1.4142	4.82	0.00	15.46
-0.25	1.1892	7.96	10.07	25.54
0.00	1.0000	9.97	6.45	31.99
0.25	0.8409	11.44	4.72	36.70
0.50	0.7071	12.87	4.59	41.29
0.75	0.5946	14.36	4.78	46.07
1.00	0.5000	15.85	4.78	50.85
1.25	0.4204	17.40	4.97	55.82
1.50	0.3536	18.97	5.04	60.86
1.75	0.2973	20.50	4.91	65.77
2.00	0.2500	22.13	5.23	71.00
2.25	0.2102	23.59	4.68	75.68
2.50	0.1768	24.66	3.43	79.11
2.75	0.1487	25.84	3.79	82.90
3.00	0.1250	27.62	5.71	88.61
3.25	0.1051	28.69	3.43	92.04
3.50	0.0884	29.82	3.63	95.67
3.75	0.0743	30.82	3.21	98.88
4.00	0.0625	30.82	0.00	98.88

Total weight = 31.17 g

PARTICLE SIZE ANALYSIS

Earth Sciences - University of Waikato

Sample: core 11 layer c

Size distribution histogram

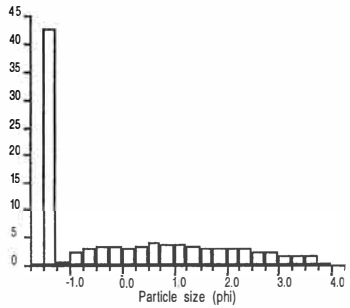

Cumulative frequency

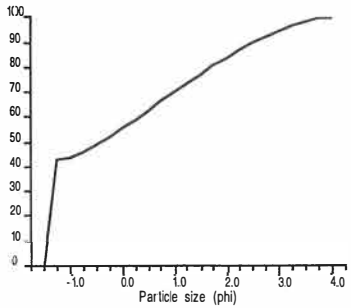

Cumulative frequency

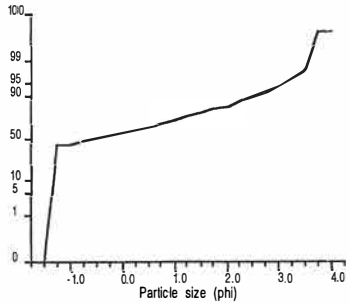

Results summary

Textural size classes

Gravel= 43.34% Sand= 56.31% Silt= 0.00% Clay= 0.00%

Gravel bearing detrital sediment

Sandy Gravel

Moment method parameters (phi)

Mean= 0.07 Sorting= 1.57 Skewness= 0.67 Kurtosis= 2.10

Graphical method parameters (phi)

Mean= 0.08 Sorting= 1.55 Skewness= 0.48 Kurtosis= 0.69

Median= -0.40 C= -1.49 D35= -1.30 D65= 0.67

Textural description:

Poorly sorted, Strongly fine skewed, Platykurtic

Raw data summary

Size (phi)	Size (mm)	Cumulative weight (g)	Interval frequency (%)	Cumulative frequency (%)
-1.50	2.8284	0.00	0.00	0.00
-1.25	2.3784	12.09	42.73	42.73
-1.00	2.0000	12.26	0.60	43.34
-0.75	1.6818	12.94	2.40	45.74
-0.50	1.4142	13.77	2.93	48.67
-0.25	1.1892	14.75	3.46	52.14
0.00	1.0000	15.73	3.46	55.60
0.25	0.8409	16.64	3.22	58.82
0.50	0.7071	17.62	3.46	62.28
0.75	0.5946	18.77	4.06	66.35
1.00	0.5000	19.82	3.71	70.06
1.25	0.4204	20.86	3.68	73.73
1.50	0.3536	21.86	3.53	77.27
1.75	0.2973	22.74	3.11	80.38
2.00	0.2500	23.63	3.15	83.53
2.25	0.2102	24.42	2.79	86.32
2.50	0.1768	25.31	3.15	89.46
2.75	0.1487	26.02	2.51	91.97
3.00	0.1250	26.68	2.33	94.31
3.25	0.1051	27.23	1.94	96.25
3.50	0.0884	27.71	1.70	97.95
3.75	0.0743	28.19	1.70	99.64
4.00	0.0625	28.19	0.00	99.64

Total weight = 28.29 g

PARTICLE SIZE ANALYSIS

Earth Sciences - University of Waikato

Sample: core 11 layer d

Size distribution histogram

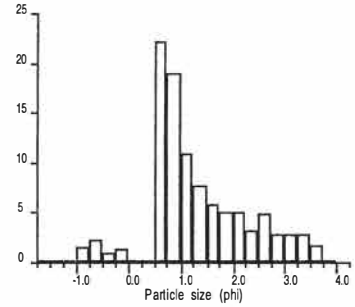

Cumulative frequency

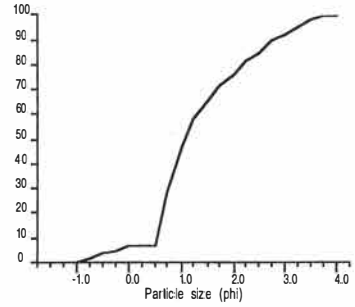

Cumulative frequency

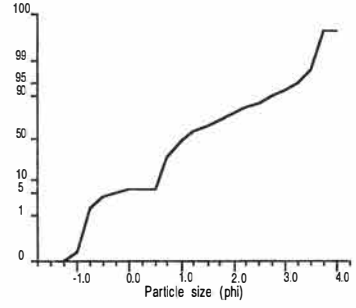

Results summary

Textural size classes

Gravel= 0.25% Sand= 99.41% Silt= 0.00% Clay= 0.00%

Gravel bearing detrital sediment

Slightly Gravelly Sand

Moment method parameters (phi)

Mean= 1.31 Sorting= 0.95 Skewness= 0.42 Kurtosis= 3.12

Graphical method parameters (phi)

Mean= 1.37 Sorting= 0.98 Skewness= 0.38 Kurtosis= 1.17

Median= 1.06 C= -0.88 D35= 0.84 D65= 1.48

Textural description:

Moderately sorted, Strongly fine skewed, Leptokurtic

Raw data summary

Size (phi)	Size (mm)	Cumulative weight (g)	Interval frequency (%)	Cumulative frequency (%)
-1.50	2.8284	0.00	0.00	0.00
-1.25	2.3784	0.01	0.04	0.04
-1.00	2.0000	0.07	0.21	0.25
-0.75	1.6818	0.50	1.52	1.76
-0.50	1.4142	1.17	2.36	4.12
-0.25	1.1892	1.41	0.85	4.97
0.00	1.0000	1.77	1.27	6.24
0.25	0.8409	1.77	0.00	6.24
0.50	0.7071	1.77	0.00	6.24
0.75	0.5946	8.05	22.14	28.38
1.00	0.5000	13.42	18.93	47.31
1.25	0.4204	16.49	10.82	58.13
1.50	0.3536	18.65	7.61	65.74
1.75	0.2973	20.30	5.82	71.56
2.00	0.2500	21.70	4.94	76.49
2.25	0.2102	23.14	5.08	81.57
2.50	0.1768	24.05	3.21	84.78
2.75	0.1487	25.43	4.86	89.64
3.00	0.1250	26.24	2.86	92.50
3.25	0.1051	27.02	2.75	95.25
3.50	0.0884	27.82	2.82	98.07
3.75	0.0743	28.27	1.59	99.65
4.00	0.0625	28.27	0.00	99.65

Total weight = 28.37 g

PARTICLE SIZE ANALYSIS

Earth Sciences - University of Waikato

Sample: core 12 layer a

Size distribution histogram

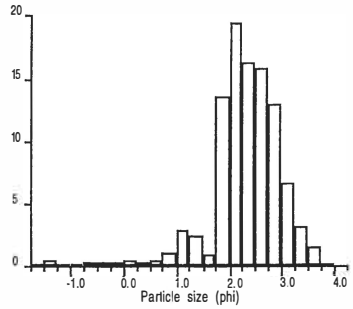

Results summary

Textural size classes

Gravel= 0.49% Sand= 98.99% Silt= 0.00% Clay= 0.00%

Gravel bearing detrital sediment

Slightly Gravelly Sand

Moment method parameters (phi)

Mean= 2.30 Sorting= 0.68 Skewness= -1.50 Kurtosis= 8.44

Graphical method parameters (phi)

Mean= 2.38 Sorting= 0.59 Skewness= -0.04 Kurtosis= 1.21

Median= 2.36 C= -0.23 D35= 2.15 D65= 2.59

Textural description:

Moderately well sorted, Near symmetrical, Leptokurtic

Cumulative frequency

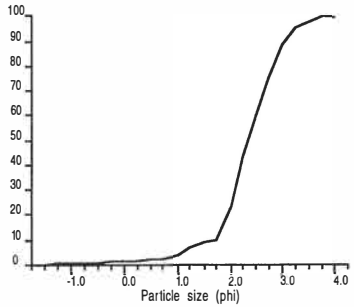

Cumulative frequency

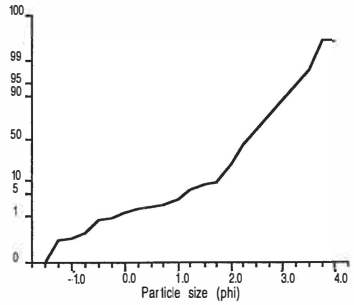

Raw data summary

Size (phi)	Size (mm)	Cumulative weight (g)	Interval frequency (%)	Cumulative frequency (%)
-1.50	2.8284	0.00	0.00	0.00
-1.25	2.3784	0.12	0.45	0.45
-1.00	2.0000	0.13	0.04	0.49
-0.75	1.6818	0.16	0.11	0.60
-0.50	1.4142	0.21	0.19	0.79
-0.25	1.1892	0.26	0.19	0.97
0.00	1.0000	0.34	0.30	1.27
0.25	0.8409	0.47	0.49	1.76
0.50	0.7071	0.57	0.37	2.14
0.75	0.5946	0.69	0.45	2.59
1.00	0.5000	0.96	1.01	3.60
1.25	0.4204	1.73	2.89	6.48
1.50	0.3536	2.40	2.51	8.99
1.75	0.2973	2.64	0.90	9.89
2.00	0.2500	6.29	13.68	23.57
2.25	0.2102	11.49	19.48	43.05
2.50	0.1768	15.87	16.41	59.46
2.75	0.1487	20.07	15.74	75.20
3.00	0.1250	23.51	12.89	88.09
3.25	0.1051	25.29	6.67	94.76
3.50	0.0884	26.13	3.15	97.90
3.75	0.0743	26.55	1.57	99.48
4.00	0.0625	26.55	0.00	99.48

Total weight = 26.69 g

PARTICLE SIZE ANALYSIS

Earth Sciences - University of Waikato

Sample: core 12 layer b

Size distribution histogram

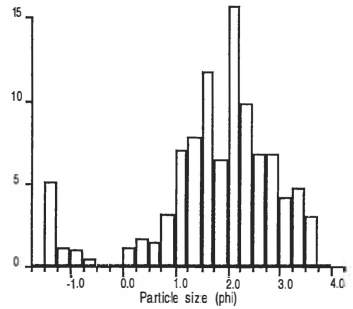

Results summary

Textural size classes

Gravel= 6.22% Sand= 92.74% Silt= 0.00% Clay= 0.00%

Gravel bearing detrital sediment

Slightly Gravelly Sand

Moment method parameters (phi)

Mean= 1.79 Sorting= 1.15 Skewness= -1.08 Kurtosis= 4.31

Graphical method parameters (phi)

Mean= 1.98 Sorting= 1.18 Skewness= -0.24 Kurtosis= 1.59

Median= 2.03 C= -1.45 D35= 1.61 D65= 2.28

Textural description:

Poorly sorted, Coarse skewed, Very leptokurtic

Cumulative frequency

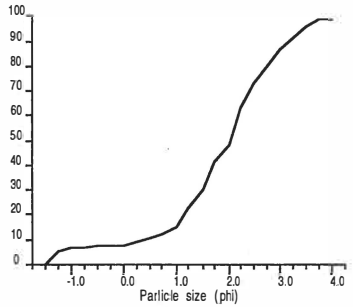

Cumulative frequency

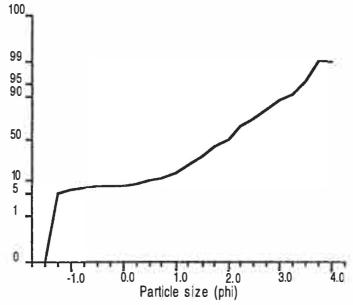

Raw data summary

Size (phi)	Size (mm)	Cumulative weight (g)	Interval frequency (%)	Cumulative frequency (%)
-1.50	2.8284	0.00	0.00	0.00
-1.25	2.3784	0.82	5.10	5.10
-1.00	2.0000	1.00	1.12	6.22
-0.75	1.6818	1.15	0.93	7.15
-0.50	1.4142	1.22	0.44	7.59
-0.25	1.1892	1.23	0.06	7.65
0.00	1.0000	1.23	0.00	7.65
0.25	0.8409	1.41	1.12	8.77
0.50	0.7071	1.68	1.68	10.45
0.75	0.5946	1.92	1.49	11.94
1.00	0.5000	2.43	3.17	15.12
1.25	0.4204	3.55	6.97	22.08
1.50	0.3536	4.80	7.78	29.86
1.75	0.2973	6.69	11.76	41.61
2.00	0.2500	7.72	6.41	48.02
2.25	0.2102	10.24	15.67	63.69
2.50	0.1768	11.81	9.77	73.46
2.75	0.1487	12.90	6.78	80.24
3.00	0.1250	13.99	6.78	87.02
3.25	0.1051	14.66	4.17	91.19
3.50	0.0884	15.43	4.79	95.98
3.75	0.0743	15.91	2.99	98.96
4.00	0.0625	15.91	0.00	98.96

Total weight = 16.08 g

PARTICLE SIZE ANALYSIS

Earth Sciences - University of Waikato

Sample: core 12 layer c

Size distribution histogram

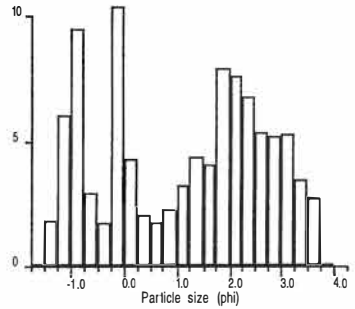

Cumulative frequency

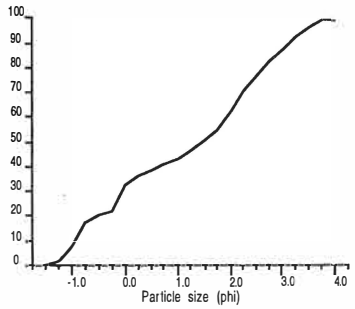

Cumulative frequency

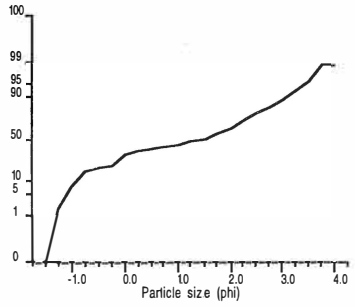

Results summary

Textural size classes

Gravel= 7.81% Sand= 90.93% Silt= 0.00% Clay= 0.00%

Gravel bearing detrital sediment

Slightly Gravelly Sand

Moment method parameters (phi)

Mean= 1.14 Sorting= 1.49 Skewness= -0.10 Kurtosis= 1.67

Graphical method parameters (phi)

Mean= 1.18 Sorting= 1.59 Skewness= -0.20 Kurtosis= 0.71

Median= 1.48 C= -1.36 D35= 0.16 D65= 2.09

Textural description:

Poorly sorted, Coarse skewed, Platykurtic

Raw data summary

Size (phi)	Size (mm)	Cumulative weight (g)	Interval frequency (%)	Cumulative frequency (%)
-1.50	2.8284	0.00	0.00	0.00
-1.25	2.3784	0.32	1.81	1.81
-1.00	2.0000	1.38	6.00	7.81
-0.75	1.6818	3.05	9.45	17.26
-0.50	1.4142	3.57	2.94	20.20
-0.25	1.1892	3.87	1.70	21.90
0.00	1.0000	5.71	10.41	32.31
0.25	0.8409	6.47	4.30	36.61
0.50	0.7071	6.83	2.04	38.65
0.75	0.5946	7.14	1.75	40.40
1.00	0.5000	7.55	2.32	42.72
1.25	0.4204	8.12	3.23	45.94
1.50	0.3536	8.89	4.36	50.30
1.75	0.2973	9.61	4.07	54.38
2.00	0.2500	11.01	7.92	62.30
2.25	0.2102	12.36	7.64	69.94
2.50	0.1768	13.56	6.79	76.73
2.75	0.1487	14.51	5.38	82.10
3.00	0.1250	15.42	5.15	87.25
3.25	0.1051	16.36	5.32	92.57
3.50	0.0884	16.97	3.45	96.02
3.75	0.0743	17.45	2.72	98.74
4.00	0.0625	17.45	0.00	98.74

Total weight = 17.67 g

PARTICLE SIZE ANALYSIS

Earth Sciences - University of Waikato

Sample: core 13 layer a

Size distribution histogram

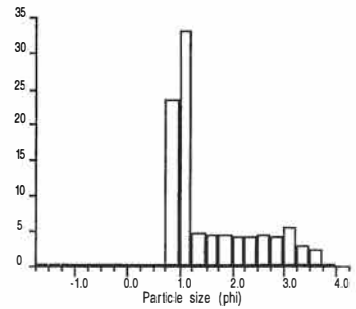

Cumulative frequency

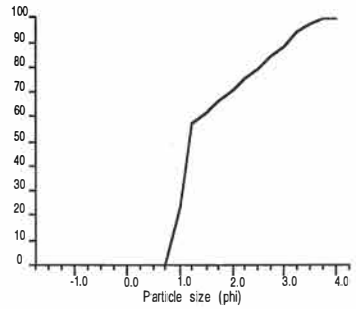

Cumulative frequency

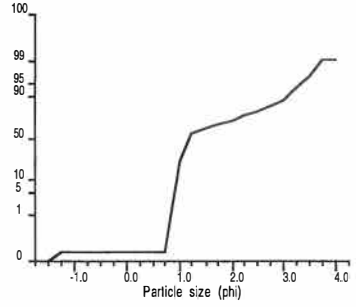

Results summary

Textural size classes

Gravel= 0.24% Sand= 98.90% Silt= 0.00% Clay= 0.00%

Gravel bearing detrital sediment

Slightly Gravelly Sand

Moment method parameters (phi)

Mean= 1.59 Sorting= 0.83 Skewness= 0.93 Kurtosis= 2.98

Graphical method parameters (phi)

Mean= 1.62 Sorting= 0.84 Skewness= 0.69 Kurtosis= 0.85

Median= 1.20 C= 0.76 D35= 1.08 D65= 1.68

Textural description:

Moderately sorted, Strongly fine skewed, Platykurtic

Raw data summary

Size (phi)	Size (mm)	Cumulative weight (g)	Interval frequency (%)	Cumulative frequency (%)
-1.50	2.8284	0.00	0.00	0.00
-1.25	2.3784	0.04	0.24	0.24
-1.00	2.0000	0.04	0.00	0.24
-0.75	1.6818	0.04	0.00	0.24
-0.50	1.4142	0.04	0.00	0.24
-0.25	1.1892	0.04	0.00	0.24
0.00	1.0000	0.04	0.00	0.24
0.25	0.8409	0.04	0.00	0.24
0.50	0.7071	0.04	0.00	0.24
0.75	0.5946	0.04	0.00	0.24
1.00	0.5000	3.95	23.44	23.68
1.25	0.4204	9.52	33.39	57.06
1.50	0.3536	10.32	4.80	61.86
1.75	0.2973	11.06	4.44	66.29
2.00	0.2500	11.83	4.62	70.91
2.25	0.2102	12.56	4.38	75.28
2.50	0.1768	13.28	4.32	79.60
2.75	0.1487	14.04	4.56	84.16
3.00	0.1250	14.75	4.26	88.41
3.25	0.1051	15.68	5.57	93.99
3.50	0.0884	16.15	2.82	96.80
3.75	0.0743	16.54	2.34	99.14
4.00	0.0625	16.54	0.00	99.14

Total weight = 16.68 g

PARTICLE SIZE ANALYSIS

Earth Sciences - University of Waikato

Sample: core 13 layer b

Size distribution histogram

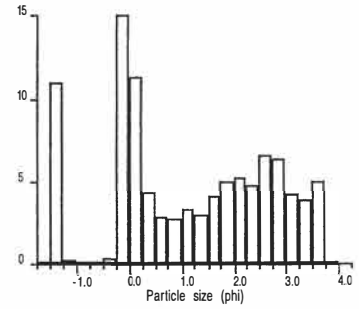

Cumulative frequency

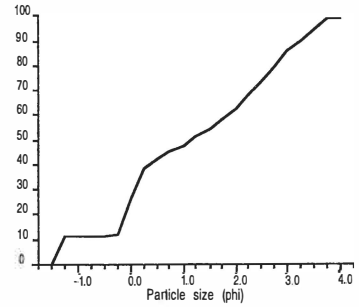

Cumulative frequency

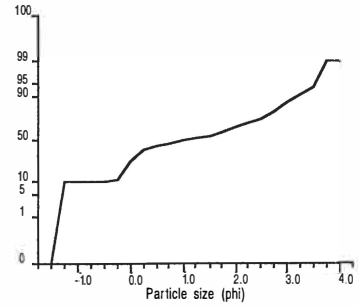

Results summary

Textural size classes

Gravel= 11.30% Sand= 87.69% Silt= 0.00% Clay= 0.00%

Gravel bearing detrital sediment

Slightly Gravelly Sand

Moment method parameters (phi)

Mean= 1.16 Sorting= 1.51 Skewness= -0.03 Kurtosis= 1.86

Graphical method parameters (phi)

Mean= 1.31 Sorting= 1.52 Skewness= 0.05 Kurtosis= 0.78

Median= 1.16 C= -1.48 D35= 0.18 D65= 2.10

Textural description:

Poorly sorted, Near symmetrical, Platykurtic

Raw data summary

Size (phi)	Size (mm)	Cumulative weight (g)	Interval frequency (%)	Cumulative frequency (%)
-1.50	2.8284	0.00	0.00	0.00
-1.25	2.3784	2.23	11.05	11.05
-1.00	2.0000	2.28	0.25	11.30
-0.75	1.6818	2.28	0.00	11.30
-0.50	1.4142	2.28	0.00	11.30
-0.25	1.1892	2.35	0.35	11.65
0.00	1.0000	5.39	15.07	26.72
0.25	0.8409	7.66	11.25	37.97
0.50	0.7071	8.53	4.31	42.28
0.75	0.5946	9.10	2.83	45.11
1.00	0.5000	9.66	2.78	47.89
1.25	0.4204	10.31	3.22	51.11
1.50	0.3536	10.89	2.88	53.98
1.75	0.2973	11.70	4.02	58.00
2.00	0.2500	12.69	4.91	62.91
2.25	0.2102	13.74	5.20	68.11
2.50	0.1768	14.70	4.76	72.87
2.75	0.1487	16.02	6.54	79.41
3.00	0.1250	17.31	6.39	85.81
3.25	0.1051	18.17	4.26	90.07
3.50	0.0884	18.96	3.92	93.99
3.75	0.0743	19.97	5.01	98.99
4.00	0.0625	19.97	0.00	98.99

Total weight = 20.17 g

PARTICLE SIZE ANALYSIS

Earth Sciences - University of Waikato

Sample: core 13 layer c

Size distribution histogram

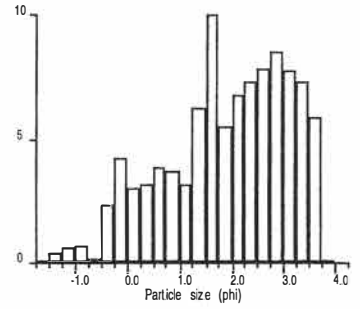

Cumulative frequency

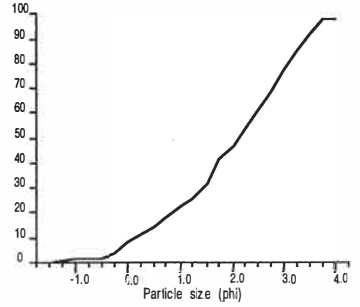

Cumulative frequency

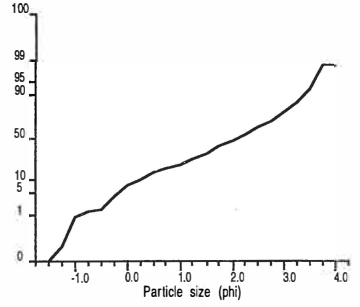

Results summary

Textural size classes

Gravel= 0.90% Sand= 97.63% Silt= 0.00% Clay= 0.00%

Gravel bearing detrital sediment

Slightly Gravelly Sand

Moment method parameters (phi)

Mean= 1.90 Sorting= 1.16 Skewness= -0.45 Kurtosis= 2.42

Graphical method parameters (phi)

Mean= 1.97 Sorting= 1.23 Skewness= -0.19 Kurtosis= 0.92

Median= 2.11 C= -0.96 D35= 1.59 D65= 2.62

Textural description:

Poorly sorted, Coarse skewed, Mesokurtic

Raw data summary

Size (phi)	Size (mm)	Cumulative weight (g)	Interval frequency (%)	Cumulative frequency (%)
-1.50	2.8284	0.00	0.00	0.00
-1.25	2.3784	0.04	0.33	0.33
-1.00	2.0000	0.11	0.57	0.90
-0.75	1.6818	0.19	0.65	1.55
-0.50	1.4142	0.21	0.16	1.72
-0.25	1.1892	0.50	2.37	4.09
0.00	1.0000	1.02	4.25	8.34
0.25	0.8409	1.39	3.03	11.37
0.50	0.7071	1.78	3.19	14.55
0.75	0.5946	2.25	3.84	18.40
1.00	0.5000	2.70	3.68	22.08
1.25	0.4204	3.09	3.19	25.26
1.50	0.3536	3.85	6.21	31.48
1.75	0.2973	5.08	10.06	41.54
2.00	0.2500	5.75	5.48	47.01
2.25	0.2102	6.58	6.79	53.80
2.50	0.1768	7.48	7.36	61.16
2.75	0.1487	8.44	7.85	69.01
3.00	0.1250	9.48	8.50	77.51
3.25	0.1051	10.43	7.77	85.28
3.50	0.0884	11.33	7.36	92.64
3.75	0.0743	12.05	5.89	98.52
4.00	0.0625	12.05	0.00	98.52

Total weight = 12.23 g

PARTICLE SIZE ANALYSIS

Earth Sciences - University of Waikato

Sample: core 14 layer a

Size distribution histogram

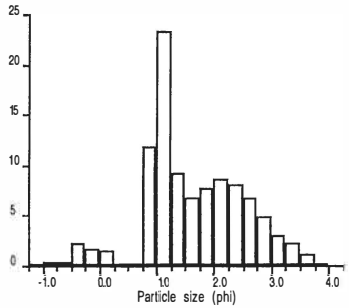

Cumulative frequency

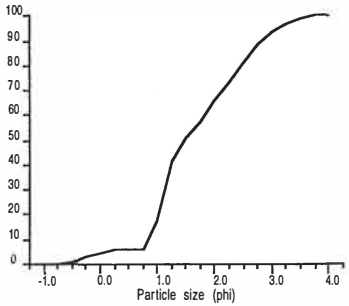

Cumulative frequency

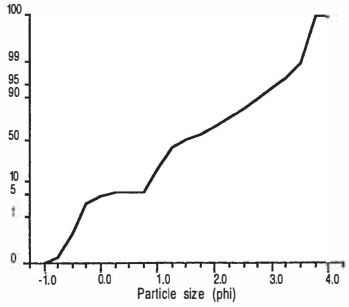

Results summary

Textural size classes

Gravel= 0.00% Sand= 100.00% Silt= 0.00% Clay= 0.00%

Gravel free detrital sediment

Sand

Moment method parameters (phi)

Mean= 1.65 Sorting= 0.86 Skewness= 0.02 Kurtosis= 2.89

Graphical method parameters (phi)

Mean= 1.68 Sorting= 0.87 Skewness= 0.22 Kurtosis= 1.03

Median= 1.49 C= -0.45 D35= 1.18 D65= 2.00

Textural description:

Moderately sorted, Fine skewed, Mesokurtic

Raw data summary

Size (phi)	Size (mm)	Cumulative weight (g)	Interval frequency (%)	Cumulative frequency (%)
-1.00	2.0000	-0.03	-0.10	-0.10
-0.75	1.6818	0.05	0.27	0.17
-0.50	1.4142	0.18	0.44	0.60
-0.25	1.1892	0.83	2.18	2.78
0.00	1.0000	1.34	1.71	4.49
0.25	0.8409	1.77	1.44	5.93
0.50	0.7071	1.77	0.00	5.93
0.75	0.5946	1.77	0.00	5.93
1.00	0.5000	5.34	11.95	17.88
1.25	0.4204	12.32	23.37	41.24
1.50	0.3536	15.10	9.31	50.55
1.75	0.2973	17.14	6.83	57.38
2.00	0.2500	19.42	7.63	65.01
2.25	0.2102	22.01	8.67	73.69
2.50	0.1768	24.44	8.14	81.82
2.75	0.1487	26.44	6.70	88.52
3.00	0.1250	27.90	4.89	93.40
3.25	0.1051	28.83	3.11	96.52
3.50	0.0884	29.50	2.24	98.76
3.75	0.0743	29.84	1.14	99.90
4.00	0.0625	29.84	0.00	99.90

Total weight = 29.87 g

PARTICLE SIZE ANALYSIS

Earth Sciences - University of Waikato

Sample: core 14 layer b

Size distribution histogram

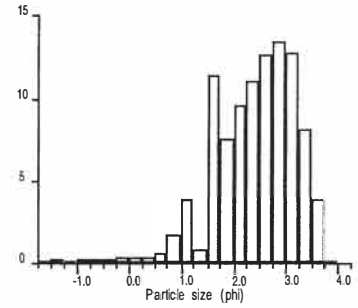

Cumulative frequency

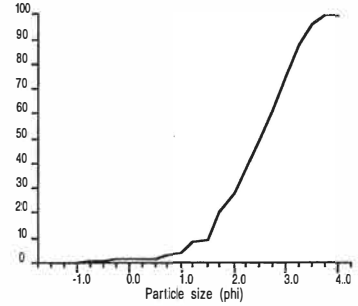

Cumulative frequency

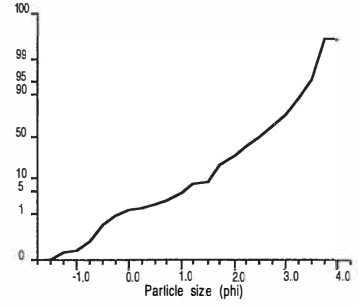

Results summary

Textural size classes

Gravel= 0.24% Sand= 99.25% Silt= 0.00% Clay= 0.00%

Gravel bearing detrital sediment

Slightly Gravelly Sand

Moment method parameters (phi)

Mean= 2.39 Sorting= 0.78 Skewness= -0.96 Kurtosis= 4.80

Graphical method parameters (phi)

Mean= 2.45 Sorting= 0.75 Skewness= -0.18 Kurtosis= 0.90

Median= 2.53 C= -0.19 D35= 2.18 D65= 2.82

Textural description:

Moderately sorted, Coarse skewed, Mesokurtic

Raw data summary

Size (phi)	Size (mm)	Cumulative weight (g)	Interval frequency (%)	Cumulative frequency (%)
-1.50	2.8284	0.00	0.00	0.00
-1.25	2.3784	0.04	0.19	0.19
-1.00	2.0000	0.05	0.05	0.24
-0.75	1.6818	0.08	0.14	0.39
-0.50	1.4142	0.14	0.29	0.67
-0.25	1.1892	0.19	0.24	0.91
0.00	1.0000	0.26	0.34	1.25
0.25	0.8409	0.34	0.39	1.64
0.50	0.7071	0.42	0.39	2.02
0.75	0.5946	0.55	0.63	2.65
1.00	0.5000	0.89	1.64	4.28
1.25	0.4204	1.70	3.90	8.18
1.50	0.3536	1.86	0.77	8.95
1.75	0.2973	4.24	11.46	20.41
2.00	0.2500	5.81	7.56	27.96
2.25	0.2102	7.80	9.58	37.54
2.50	0.1768	10.11	11.12	48.66
2.75	0.1487	12.75	12.71	61.37
3.00	0.1250	15.53	13.38	74.75
3.25	0.1051	18.18	12.75	87.50
3.50	0.0884	19.87	8.13	95.64
3.75	0.0743	20.67	3.85	99.49
4.00	0.0625	20.67	0.00	99.49

Total weight = 20.78 g

PARTICLE SIZE ANALYSIS

Earth Sciences - University of Waikato

Sample: core 14 layer c

Size distribution histogram

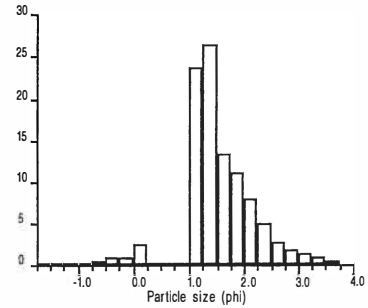

Cumulative frequency

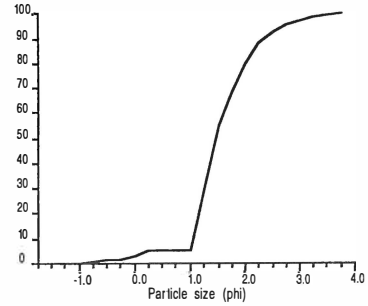

Cumulative frequency

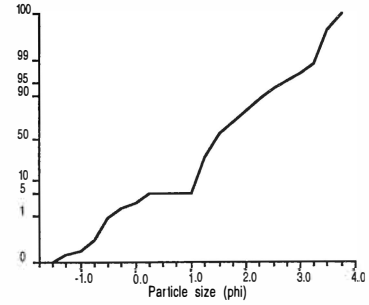

Results summary

Textural size classes

Gravel= 0.28% Sand= 99.72% Silt= 0.00% Clay= 0.00%

Gravel bearing detrital sediment

Slightly Gravelly Sand

Moment method parameters (phi)

Mean= 1.54 Sorting= 0.66 Skewness= -0.23 Kurtosis= 5.59

Graphical method parameters (phi)

Mean= 1.56 Sorting= 0.62 Skewness= 0.17 Kurtosis= 1.49

Median= 1.45 C= -0.48 D35= 1.31 D65= 1.68

Textural description:

Moderately well sorted, Fine skewed, Leptokurtic

Raw data summary

Size (phi)	Size (mm)	Cumulative weight (g)	Interval frequency (%)	Cumulative frequency (%)
-1.50	2.8284	0.00	0.00	0.00
-1.25	2.3784	0.05	0.20	0.20
-1.00	2.0000	0.07	0.08	0.28
-0.75	1.6818	0.11	0.16	0.43
-0.50	1.4142	0.23	0.47	0.91
-0.25	1.1892	0.47	0.95	1.85
0.00	1.0000	0.71	0.95	2.80
0.25	0.8409	1.32	2.40	5.20
0.50	0.7071	1.32	0.00	5.20
0.75	0.5946	1.32	0.00	5.20
1.00	0.5000	1.32	0.00	5.20
1.25	0.4204	7.37	23.85	29.05
1.50	0.3536	14.08	26.45	55.50
1.75	0.2973	17.49	13.44	68.94
2.00	0.2500	20.33	11.19	80.13
2.25	0.2102	22.35	7.96	88.10
2.50	0.1768	23.60	4.93	93.02
2.75	0.1487	24.26	2.60	95.62
3.00	0.1250	24.70	1.73	97.36
3.25	0.1051	25.05	1.38	98.74
3.50	0.0884	25.28	0.91	99.65
3.75	0.0743	25.38	0.39	100.04

Total weight = 25.37 g

PARTICLE SIZE ANALYSIS

Earth Sciences - University of Waikato

Sample: core 14 layer d

Size distribution histogram

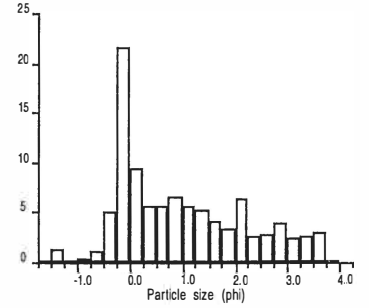

Cumulative frequency

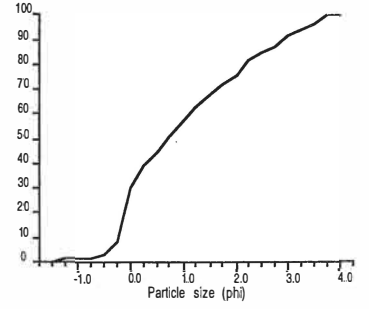

Cumulative frequency

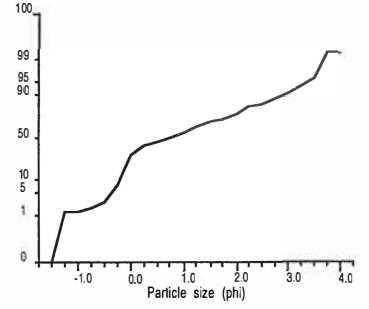

Results summary

Textural size classes

Gravel= 1.34% Sand= 97.91% Silt= 0.00% Clay= 0.00%

Gravel bearing detrital sediment

Slightly Gravelly Sand

Moment method parameters (phi)

Mean= 0.98 Sorting= 1.21 Skewness= 0.59 Kurtosis= 2.32

Graphical method parameters (phi)

Mean= 1.02 Sorting= 1.23 Skewness= 0.36 Kurtosis= 0.76

Median= 0.73 C= -1.31 D35= 0.14 D65= 1.36

Textural description:

Poorly sorted, Strongly fine skewed, Platykurtic

Raw data summary

Size (phi)	Size (mm)	Cumulative weight (g)	Interval frequency (%)	Cumulative frequency (%)
-1.50	2.8284	0.00	0.00	0.00
-1.25	2.3784	0.12	1.34	1.34
-1.00	2.0000	0.12	0.00	1.34
-0.75	1.6818	0.16	0.45	1.78
-0.50	1.4142	0.26	1.11	2.90
-0.25	1.1892	0.72	5.12	8.02
0.00	1.0000	2.67	21.72	29.74
0.25	0.8409	3.52	9.47	39.21
0.50	0.7071	4.02	5.57	44.78
0.75	0.5946	4.52	5.57	50.35
1.00	0.5000	5.11	6.57	56.92
1.25	0.4204	5.62	5.68	62.60
1.50	0.3536	6.09	5.24	67.84
1.75	0.2973	6.46	4.12	71.96
2.00	0.2500	6.76	3.34	75.30
2.25	0.2102	7.33	6.35	81.65
2.50	0.1768	7.57	2.67	84.32
2.75	0.1487	7.82	2.78	87.11
3.00	0.1250	8.17	3.90	91.01
3.25	0.1051	8.39	2.45	93.46
3.50	0.0884	8.63	2.67	96.13
3.75	0.0743	8.91	3.12	99.25
4.00	0.0625	8.91	0.00	99.25

Total weight = 8.98 g

PARTICLE SIZE ANALYSIS

Earth Sciences - University of Waikato

Sample: core 14 layer e

Size distribution histogram

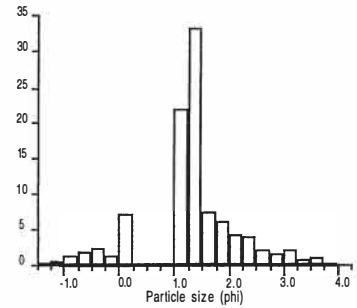

Cumulative frequency

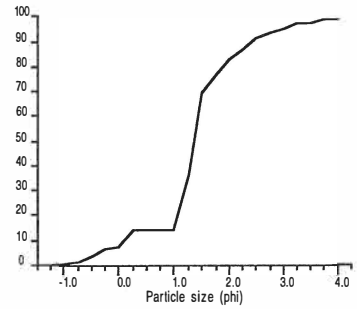

Cumulative frequency

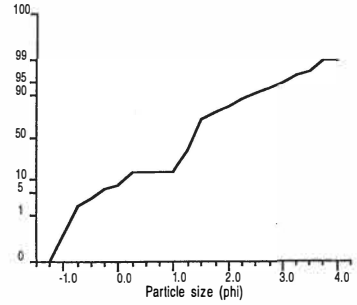

Results summary

Textural size classes

Gravel= 0.52% Sand= 98.43% Silt= 0.00% Clay= 0.00%

Gravel bearing detrital sediment

Slightly Gravelly Sand

Moment method parameters (phi)

Mean= 1.32 Sorting= 0.84 Skewness= -0.21 Kurtosis= 4.17

Graphical method parameters (phi)

Mean= 1.47 Sorting= 0.77 Skewness= 0.16 Kurtosis= 2.46

Median= 1.35 C= -0.92 D35= 1.23 D65= 1.47

Textural description:

Moderately sorted, Fine skewed, Very leptokurtic

Raw data summary

Size (phi)	Size (mm)	Cumulative weight (g)	Interval frequency (%)	Cumulative frequency (%)
-1.25	2.3784	-0.01	-0.07	-0.07
-1.00	2.0000	0.07	0.60	0.52
-0.75	1.6818	0.26	1.41	1.94
-0.50	1.4142	0.52	1.94	3.87
-0.25	1.1892	0.83	2.31	6.18
0.00	1.0000	0.99	1.19	7.37
0.25	0.8409	1.94	7.07	14.44
0.50	0.7071	1.94	0.00	14.44
0.75	0.5946	1.94	0.00	14.44
1.00	0.5000	1.94	0.00	14.44
1.25	0.4204	4.88	21.89	36.33
1.50	0.3536	9.34	33.21	69.54
1.75	0.2973	10.33	7.37	76.91
2.00	0.2500	11.17	6.25	83.17
2.25	0.2102	11.73	4.17	87.34
2.50	0.1768	12.26	3.95	91.28
2.75	0.1487	12.53	2.01	93.29
3.00	0.1250	12.75	1.64	94.93
3.25	0.1051	13.03	2.08	97.02
3.50	0.0884	13.14	0.82	97.84
3.75	0.0743	13.29	1.12	98.95
4.00	0.0625	13.29	0.00	98.95

Total weight = 13.43 g

PARTICLE SIZE ANALYSIS

Earth Sciences - University of Waikato

Sample: core 14 layer f

Size distribution histogram

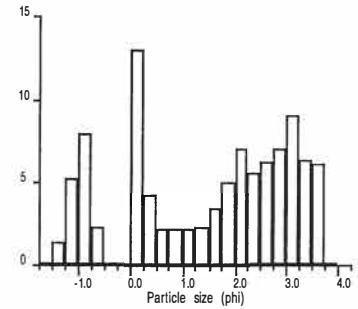

Cumulative frequency

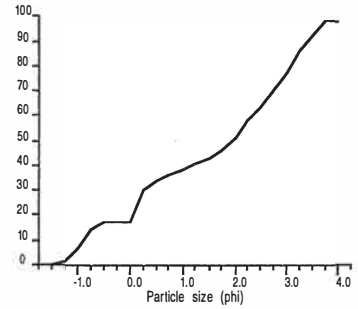

Cumulative frequency

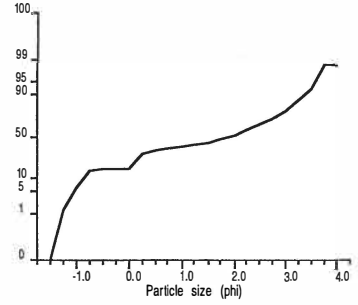

Results summary

Textural size classes

Gravel= 6.57% Sand= 91.71% Silt= 0.00% Clay= 0.00%

Gravel bearing detrital sediment

Slightly Gravelly Sand

Moment method parameters (phi)

Mean= 1.47 Sorting= 1.54 Skewness= -0.28 Kurtosis= 1.75

Graphical method parameters (phi)

Mean= 1.52 Sorting= 1.66 Skewness= -0.31 Kurtosis= 0.69

Median= 1.95 C= -1.32 D35= 0.62 D65= 2.56

Textural description:

Poorly sorted, Strongly Coarse skewed, Platykurtic

Raw data summary

Size (phi)	Size (mm)	Cumulative weight (g)	Interval frequency (%)	Cumulative frequency (%)
-1.50	2.8284	0.00	0.00	0.00
-1.25	2.3784	0.13	1.36	1.36
-1.00	2.0000	0.63	5.22	6.57
-0.75	1.6818	1.39	7.93	14.50
-0.50	1.4142	1.61	2.30	16.80
-0.25	1.1892	1.61	0.00	16.80
0.00	1.0000	1.61	0.00	16.80
0.25	0.8409	2.86	13.04	29.84
0.50	0.7071	3.26	4.17	34.01
0.75	0.5946	3.46	2.09	36.10
1.00	0.5000	3.67	2.19	38.29
1.25	0.4204	3.87	2.09	40.38
1.50	0.3536	4.09	2.30	42.67
1.75	0.2973	4.41	3.34	46.01
2.00	0.2500	4.89	5.01	51.02
2.25	0.2102	5.56	6.99	58.01
2.50	0.1768	6.09	5.53	63.54
2.75	0.1487	6.69	6.26	69.80
3.00	0.1250	7.36	6.99	76.79
3.25	0.1051	8.23	9.08	85.87
3.50	0.0884	8.84	6.36	92.24
3.75	0.0743	9.42	6.05	98.29
4.00	0.0625	9.42	0.00	98.29

Total weight = 9.58 g

PARTICLE SIZE ANALYSIS

Earth Sciences - University of Waikato

Sample: core 15 layer a

Size distribution histogram

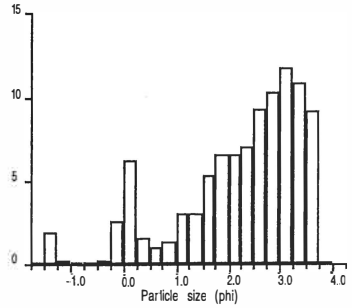

Cumulative frequency

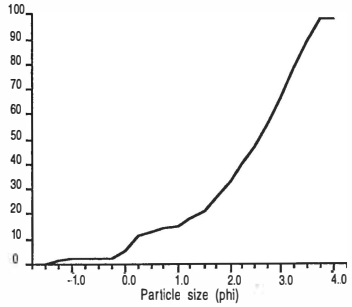

Cumulative frequency

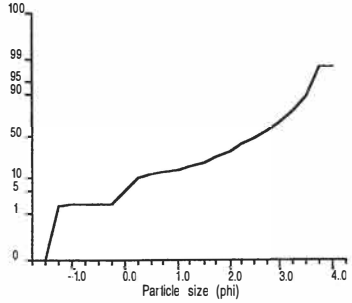

Results summary

Textural size classes

Gravel= 2.08% Sand= 96.03% Silt= 0.00% Clay= 0.00%

Gravel bearing detrital sediment

Slightly Gravelly Sand

Moment method parameters (phi)

Mean= 2.19 Sorting= 1.18 Skewness= -0.94 Kurtosis= 3.35

Graphical method parameters (phi)

Mean= 2.34 Sorting= 1.14 Skewness= -0.36 Kurtosis= 0.99

Median= 2.58 C= -1.37 D35= 2.06 D65= 2.97

Textural description:

Poorly sorted, Strongly Coarse skewed, Mesokurtic

Raw data summary

Size (phi)	Size (mm)	Cumulative weight (g)	Interval frequency (%)	Cumulative frequency (%)
-1.50	2.8284	0.00	0.00	0.00
-1.25	2.3784	0.32	1.90	1.90
-1.00	2.0000	0.35	0.18	2.08
-0.75	1.6818	0.36	0.06	2.14
-0.50	1.4142	0.36	0.00	2.14
-0.25	1.1892	0.40	0.24	2.38
0.00	1.0000	0.85	2.68	5.06
0.25	0.8409	1.91	6.31	11.36
0.50	0.7071	2.18	1.61	12.97
0.75	0.5946	2.35	1.01	13.98
1.00	0.5000	2.59	1.43	15.41
1.25	0.4204	3.09	2.97	18.39
1.50	0.3536	3.60	3.03	21.42
1.75	0.2973	4.49	5.30	26.72
2.00	0.2500	5.60	6.60	33.32
2.25	0.2102	6.70	6.54	39.86
2.50	0.1768	7.88	7.02	46.89
2.75	0.1487	9.43	9.22	56.11
3.00	0.1250	11.16	10.29	66.40
3.25	0.1051	13.13	11.72	78.12
3.50	0.0884	14.95	10.83	88.95
3.75	0.0743	16.49	9.16	98.12
4.00	0.0625	16.49	0.00	98.12

Total weight = 16.81 g

PARTICLE SIZE ANALYSIS

Earth Sciences - University of Waikato

Sample: core 15 layer b

Size distribution histogram

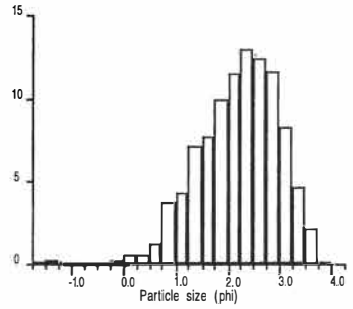

Cumulative frequency

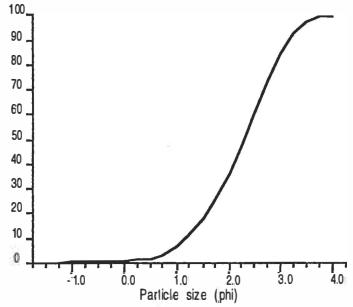

Cumulative frequency

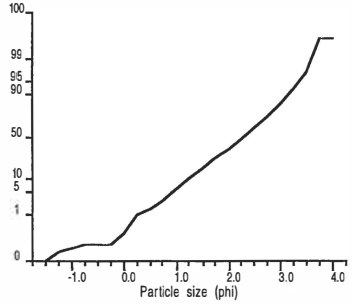

Results summary

Textural size classes

Gravel= 0.31% Sand= 99.21% Silt= 0.00% Clay= 0.00%

Gravel bearing detrital sediment

Slightly Gravelly Sand

Moment method parameters (phi)

Mean= 2.21 Sorting= 0.76 Skewness= -0.60 Kurtosis= 3.84

Graphical method parameters (phi)

Mean= 2.24 Sorting= 0.77 Skewness= -0.13 Kurtosis= 0.95

Median= 2.30 C= 0.20 D35= 1.98 D65= 2.59

Textural description:

Moderately sorted, Coarse skewed, Mesokurtic

Raw data summary

Size (phi)	Size (mm)	Cumulative weight (g)	Interval frequency (%)	Cumulative frequency (%)
-1.50	2.8284	0.00	0.00	0.00
-1.25	2.3784	0.04	0.24	0.24
-1.00	2.0000	0.05	0.06	0.31
-0.75	1.6818	0.06	0.06	0.37
-0.50	1.4142	0.06	0.00	0.37
-0.25	1.1892	0.06	0.00	0.37
0.00	1.0000	0.09	0.18	0.55
0.25	0.8409	0.18	0.55	1.10
0.50	0.7071	0.27	0.55	1.65
0.75	0.5946	0.47	1.22	2.87
1.00	0.5000	1.07	3.67	6.54
1.25	0.4204	1.78	4.34	10.89
1.50	0.3536	2.95	7.16	18.04
1.75	0.2973	4.20	7.65	25.69
2.00	0.2500	5.83	9.97	35.66
2.25	0.2102	7.72	11.56	47.22
2.50	0.1768	9.86	13.09	60.31
2.75	0.1487	11.89	12.42	72.72
3.00	0.1250	13.80	11.68	84.41
3.25	0.1051	15.15	8.26	92.66
3.50	0.0884	15.91	4.65	97.31
3.75	0.0743	16.27	2.20	99.51
4.00	0.0625	16.27	0.00	99.51

Total weight = 16.35 g

PARTICLE SIZE ANALYSIS

Earth Sciences - University of Waikato

Sample: core 15 layer c

Size distribution histogram

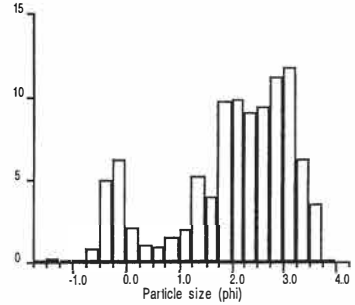

Cumulative frequency

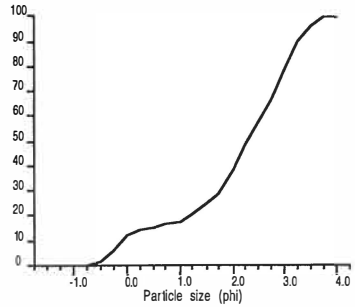

Cumulative frequency

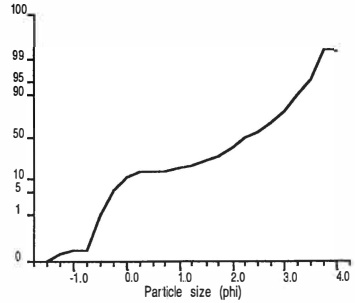

Results summary

Textural size classes

Gravel= 0.26% Sand= 99.05% Silt= 0.00% Clay= 0.00%

Gravel bearing detrital sediment

Slightly Gravelly Sand

Moment method parameters (phi)

Mean= 2.02 Sorting= 1.15 Skewness= -0.83 Kurtosis= 2.76

Graphical method parameters (phi)

Mean= 2.03 Sorting= 1.19 Skewness= -0.35 Kurtosis= 1.08

Median= 2.29 C= -0.51 D35= 1.91 D65= 2.70

Textural description:

Poorly sorted, Strongly Coarse skewed, Mesokurtic

Raw data summary

Size (phi)	Size (mm)	Cumulative weight (g)	Interval frequency (%)	Cumulative frequency (%)
-1.50	2.8284	0.00	0.00	0.00
-1.25	2.3784	0.03	0.19	0.19
-1.00	2.0000	0.04	0.06	0.26
-0.75	1.6818	0.04	0.00	0.26
-0.50	1.4142	0.16	0.78	1.03
-0.25	1.1892	0.94	5.04	6.08
0.00	1.0000	1.90	6.21	12.28
0.25	0.8409	2.22	2.07	14.35
0.50	0.7071	2.39	1.10	15.45
0.75	0.5946	2.52	0.84	16.29
1.00	0.5000	2.75	1.49	17.78
1.25	0.4204	3.05	1.94	19.72
1.50	0.3536	3.85	5.17	24.89
1.75	0.2973	4.46	3.94	28.84
2.00	0.2500	5.96	9.70	38.53
2.25	0.2102	7.49	9.89	48.43
2.50	0.1768	8.88	8.99	57.41
2.75	0.1487	10.32	9.31	66.72
3.00	0.1250	12.06	11.25	77.97
3.25	0.1051	13.87	11.70	89.68
3.50	0.0884	14.82	6.14	95.82
3.75	0.0743	15.36	3.49	99.31
4.00	0.0625	15.36	0.00	99.31

Total weight = 15.47 g

Appendix VIII

The following appendix can be obtained in the Appendix CD. The appendix can be opened by Microsoft Word. Photographs of each core and layers within are provided, also, minerals and shell species identified in each layer are included.

Appendix IX

Sediment trend matrix for the McLAREN(1981) model. Each matched pair of sediment samples consists of three values; mean grain size, sorting and skewness, relating the deposited sediment (at right) to the possible sediment source (top).

Sediment Deposit		Sediment Source															
		1	2	3	4	5	6	7	8	9	10	11	12	13	14	15	GSC
	1		Courser Better Same	Courser Poorer +	Courser Poorer +	Courser Better +	Courser Better +	Courser Better +	Courser Better +	Courser Better +	Courser Poorer +	Courser Better +	Courser Poorer +	Courser Better -	Courser Better +	Courser Better +	M (Φ) SD (Φ) Sk (Φ)
	2	Finer Poorer Same		Courser Poorer +	Courser Poorer +	Courser Better +	Courser Better +	Courser Better +	Courser Better +	Courser Same +	Courser Poorer +	Courser Better +	Courser Poorer +	Courser Better -	Courser Better +	Courser Better +	M (Φ) SD (Φ) Sk (Φ)
	3	Finer Better -	Finer Better -		Courser Better +	Courser Better +	Courser Better +	Courser Better +	Courser Better -	Courser Better +	Courser Better +	Finer Better +	Courser Better +	Courser Better -	Courser Better +	Courser Better +	M (Φ) SD (Φ) Sk (Φ)
	4	Finer Better -	Finer Better -	Finer Poorer -		Finer Better -	Finer Better -	Courser Better -	Finer Better -	Courser Better -	Courser Better -	Finer Better -	Courser Poorer +	Finer Better -	Finer Better -	Courser Better -	M (Φ) SD (Φ) Sk (Φ)
	5	Finer Poorer -	Finer Poorer -	Finer Poorer -	Courser Poorer +		Finer Better -	Courser Poorer +	Finer Better -	Courser Poorer -	Courser Poorer +	Finer Better -	Courser Poorer +	Finer Poorer -	Finer Poorer -	Courser Better +	M (Φ) SD (Φ) Sk (Φ)
	6	Finer Poorer -	Finer Poorer -	Finer Poorer -	Courser Poorer +	Courser Poorer +		Courser Poorer +	Finer Better -	Courser Poorer +	Courser Poorer +	Finer Better -	Courser Poorer +	Courser Poorer -	Finer Poorer -	Courser Poorer +	M (Φ) SD (Φ) Sk (Φ)
	7	Finer Poorer -	Finer Poorer -	Finer Poorer -	Finer Poorer +	Finer Better -	Finer Better -		Finer Better -	Courser Poorer -	Finer Poorer -	Finer Better -	Courser Poorer +	Finer Poorer -	Finer Poorer -	Courser Better +	M (Φ) SD (Φ) Sk (Φ)
	8	Finer Poorer -	Finer Poorer -	Finer Poorer +	Courser Poorer +	Courser Poorer +	Courser Poorer +	Courser Poorer +		Courser Poorer +	Courser Poorer +	Finer Better +	Courser Poorer +	Courser Poorer -	Courser Poorer +	Courser Poorer +	M (Φ) SD (Φ) Sk (Φ)
	9	Finer Poorer -	Finer Same -	Finer Poorer -	Finer Poorer +	Finer Better +	Finer Better -	Finer Better +	Finer Better -		Finer Poorer +	Finer Better -	Courser Poorer +	Finer Better -	Finer Better -	Finer Better +	M (Φ) SD (Φ) Sk (Φ)
	10	Finer Better -	Finer Better -	Finer Poorer +	Finer Poorer +	Finer Better -	Finer Better -	Courser Better +	Finer Better -	Courser Better -		Finer Better -	Courser Poorer +	Finer Better -	Finer Better -	Courser Better +	M (Φ) SD (Φ) Sk (Φ)
	11	Finer Poorer -	Finer Poorer -	Courser Poorer +	Courser Poorer +	Courser Poorer +	Courser Poorer +	Courser Poorer +	Courser Poorer -	Courser Poorer +	Courser Poorer +		Courser Poorer +	Courser Poorer -	Courser Poorer +	Courser Poorer +	M (Φ) SD (Φ) Sk (Φ)
	12	Finer Better -	Finer Better -	Finer Poorer -	Finer Better -	Finer Better -	Finer Better -	Finer Better -	Finer Better -	Finer Better -	Finer Better -	Finer Better -		Finer Better -	Finer Better -	Finer Better -	M (Φ) SD (Φ) Sk (Φ)
	13	Finer Poorer +	Finer Poorer +	Finer Poorer +	Courser Poorer +	Courser Better +	Finer Better +	Courser Better +	Finer Better +	Courser Poorer +	Courser Poorer +	Finer Better +	Courser Poorer +		Courser Better +	Courser Better +	M (Φ) SD (Φ) Sk (Φ)
	14	Finer Poorer -	Finer Poorer -	Finer Poorer +	Courser Poorer +	Courser Better +	Courser Better +	Courser Better -	Finer Better +	Courser Poorer +	Courser Poorer +	Finer Better -	Courser Poorer +	Finer Poorer -		Courser Better +	M (Φ) SD (Φ) Sk (Φ)
	15	Finer Poorer -	Finer Poorer -	Finer Poorer +	Finer Poorer +	Finer Poorer -	Finer Better -	Finer Poorer -	Finer Better -	Courser Poorer -	Finer Poorer -	Finer Better -	Courser Poorer +	Finer Poorer -	Finer Poorer -		M (Φ) SD (Φ) Sk (Φ)

Appendix X

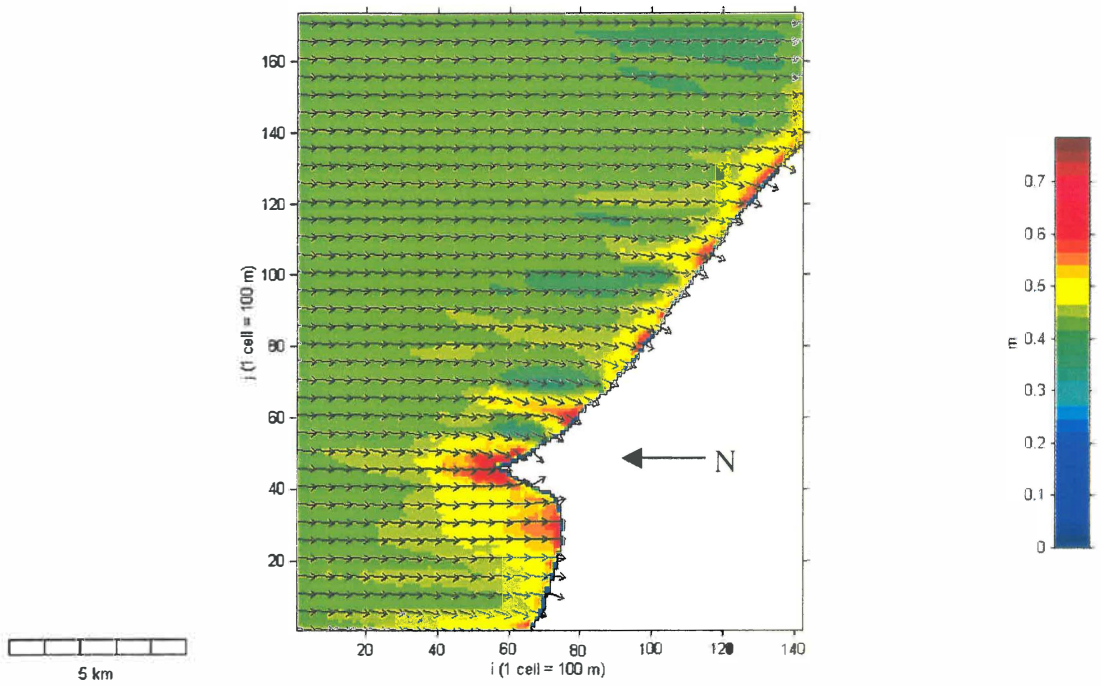

Scenario 1 0.39 m, 10.64 s, -4.73º.

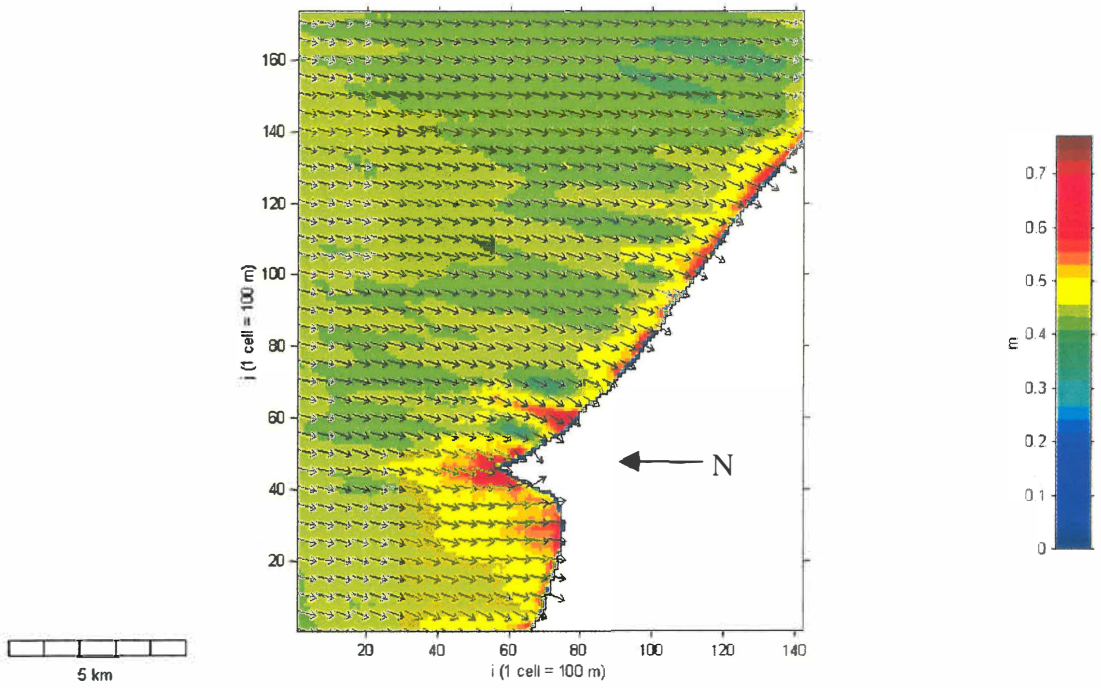

Scenario 2 0.39 m, 10.64 s, -14.73 º.

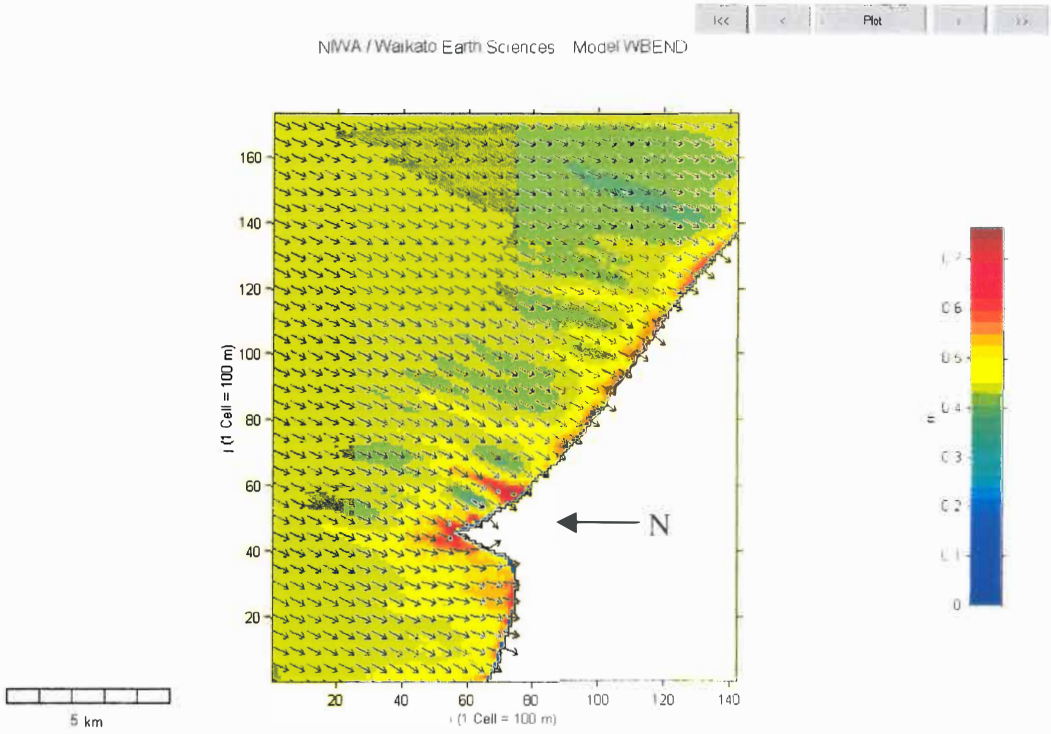

Scenario 3 0.39 m, 10.64 s, -24.73 °.

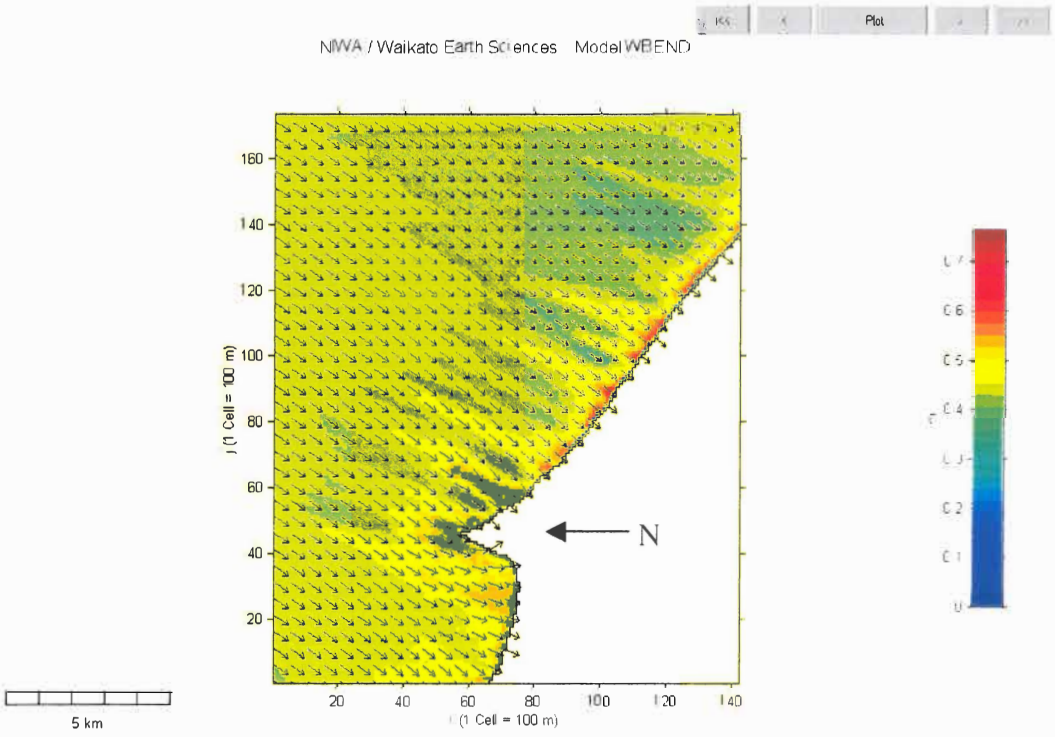

Scenario 4 0.39 m, 10.64 s, -34.73 °.

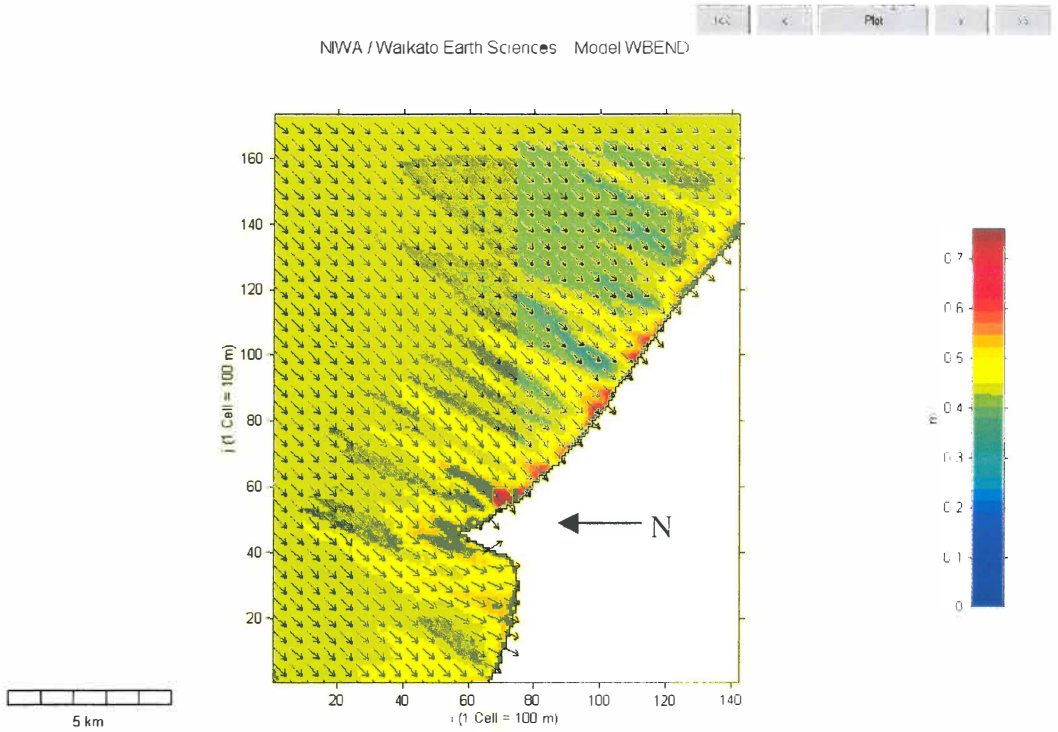

Scenario 5 0.39 m, 10.64 s, -44.73 º.

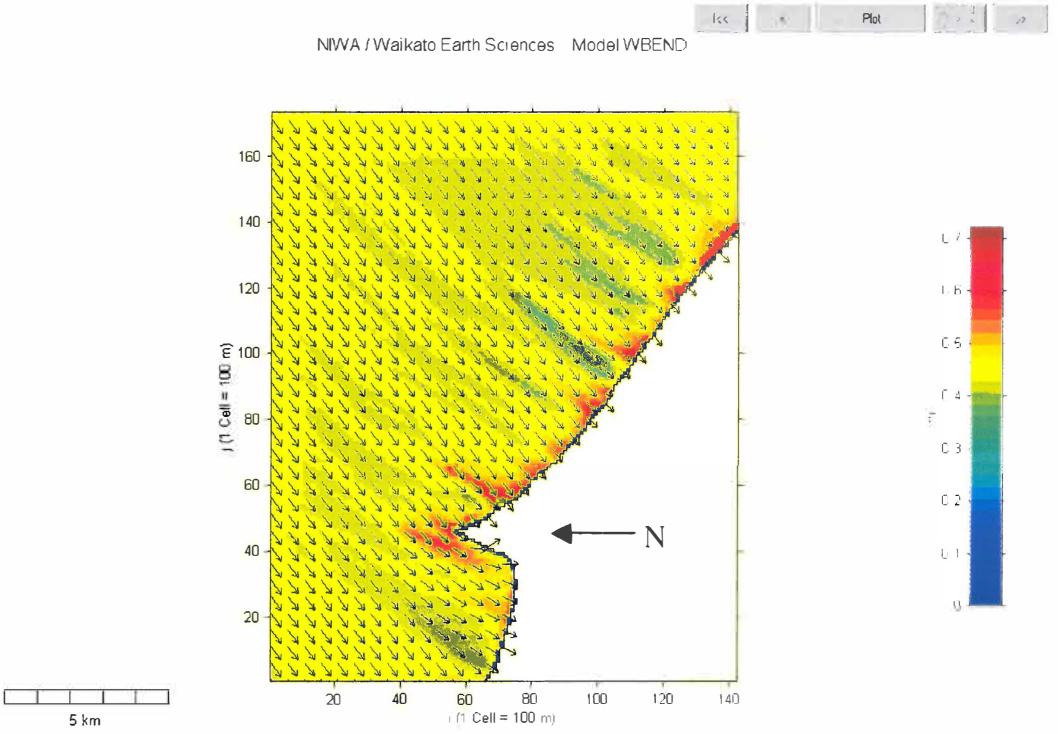

Scenario 6 0.39 m, 10.64 s, -54.73 º.

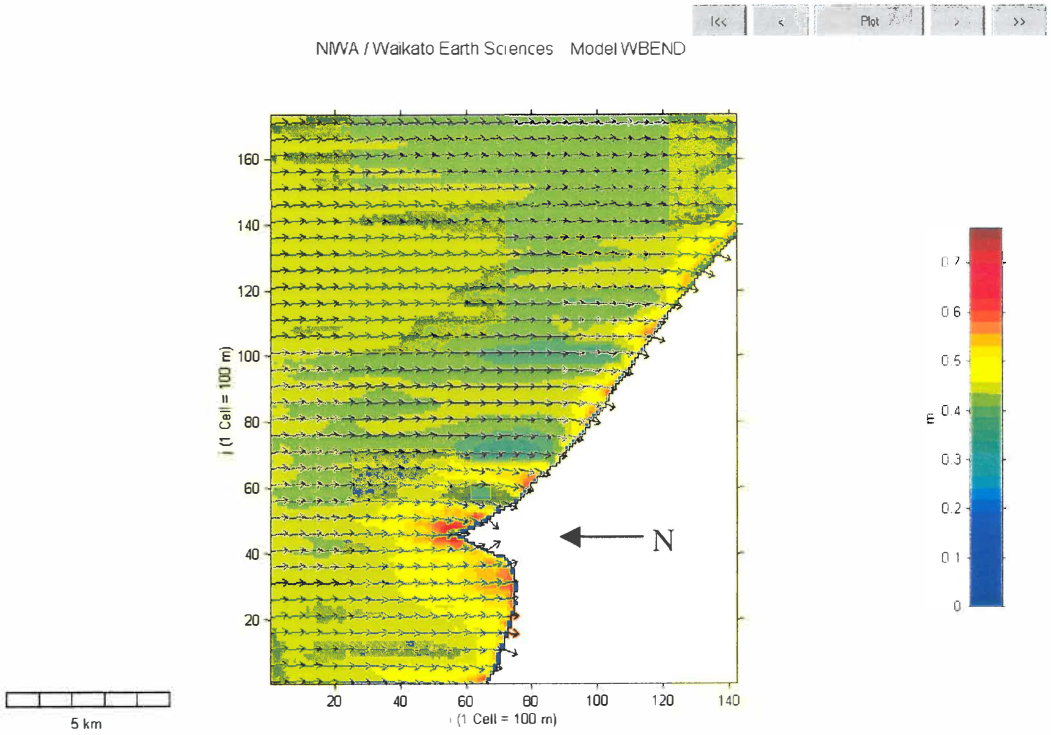

Scenario 7 0.39 m, 10.64 s, 6.73 º.

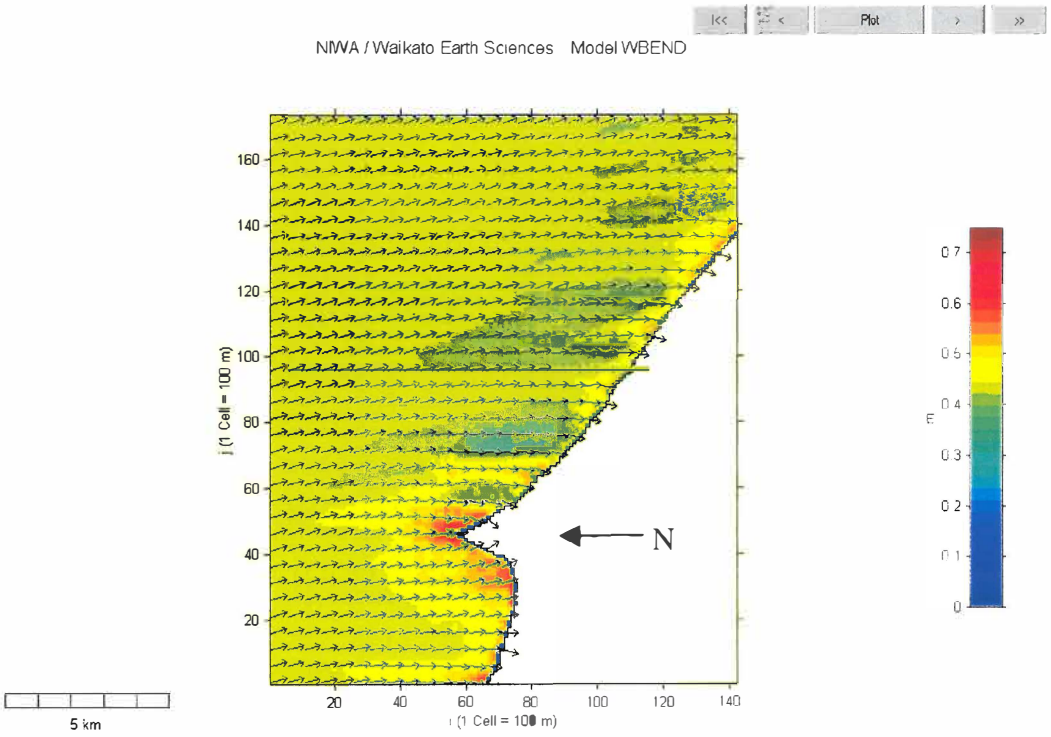

Scenario 8 0.39 m, 10.64 s, 16.73 º.

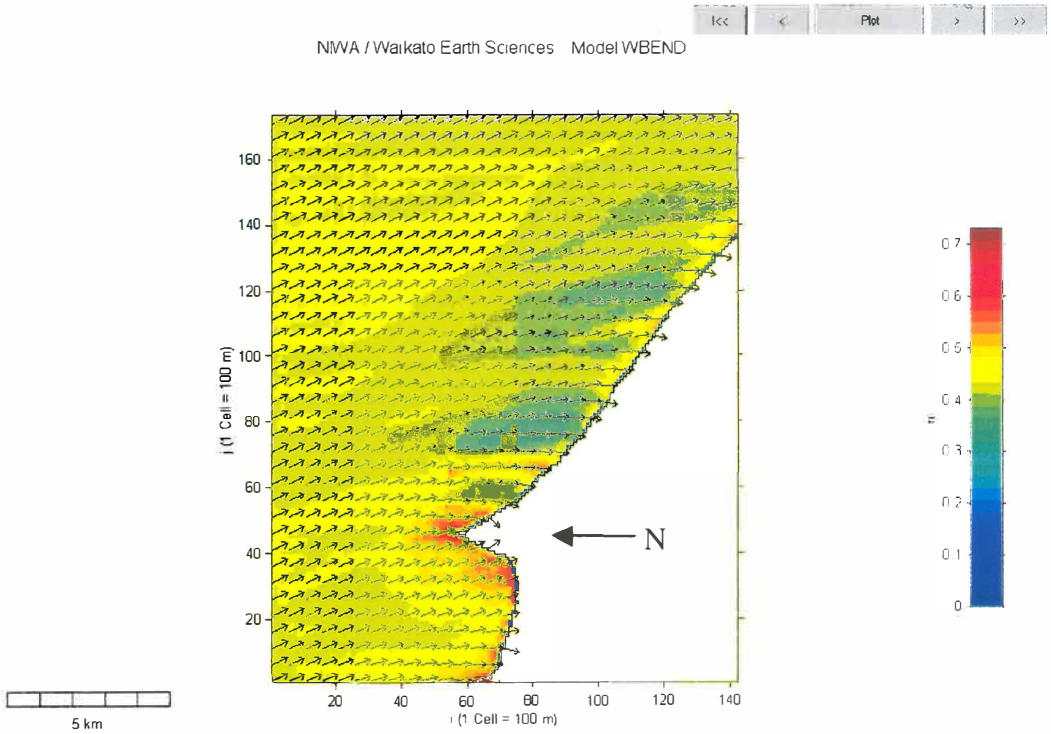

Scenario 9 0.39 m, 10.64 s, 26.73 °.

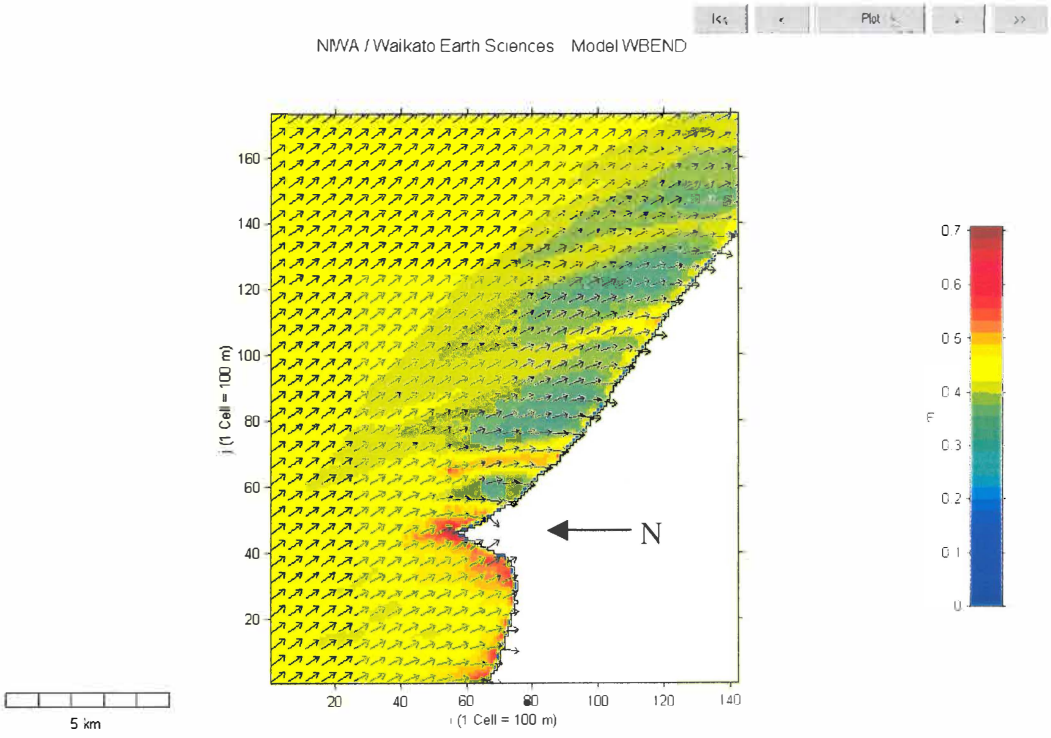

Scenario 10 0.39 m, 10.64 s, 36.73 °.

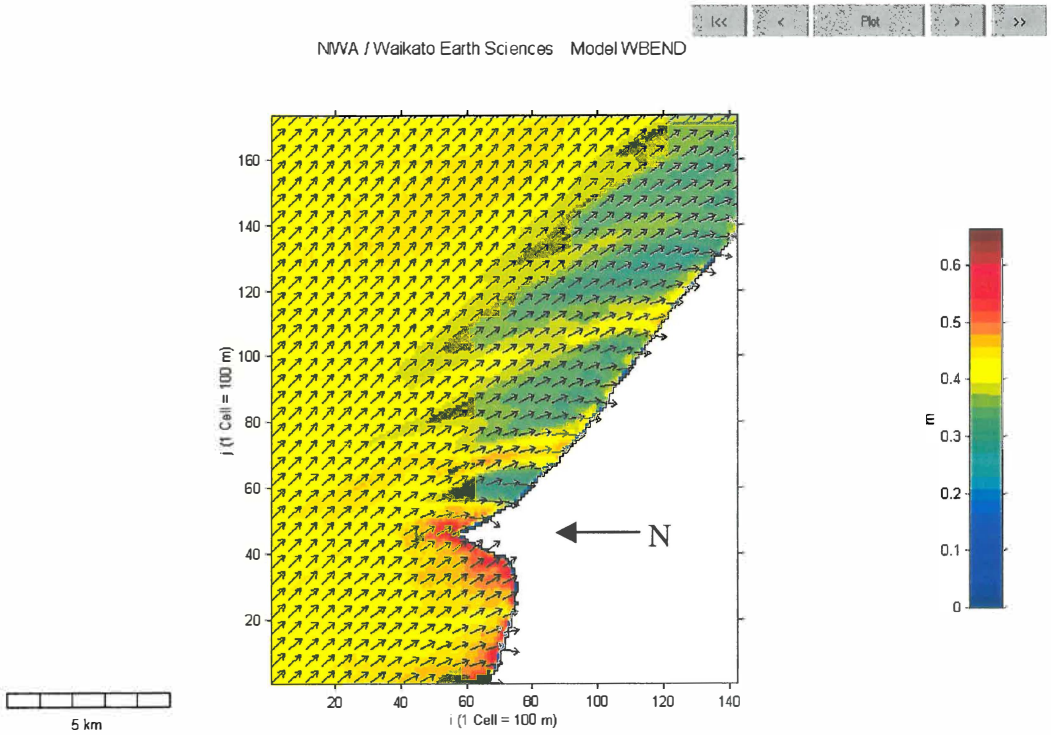

Scenario 11 0.39 m, 10.64 s, 46.73 º.

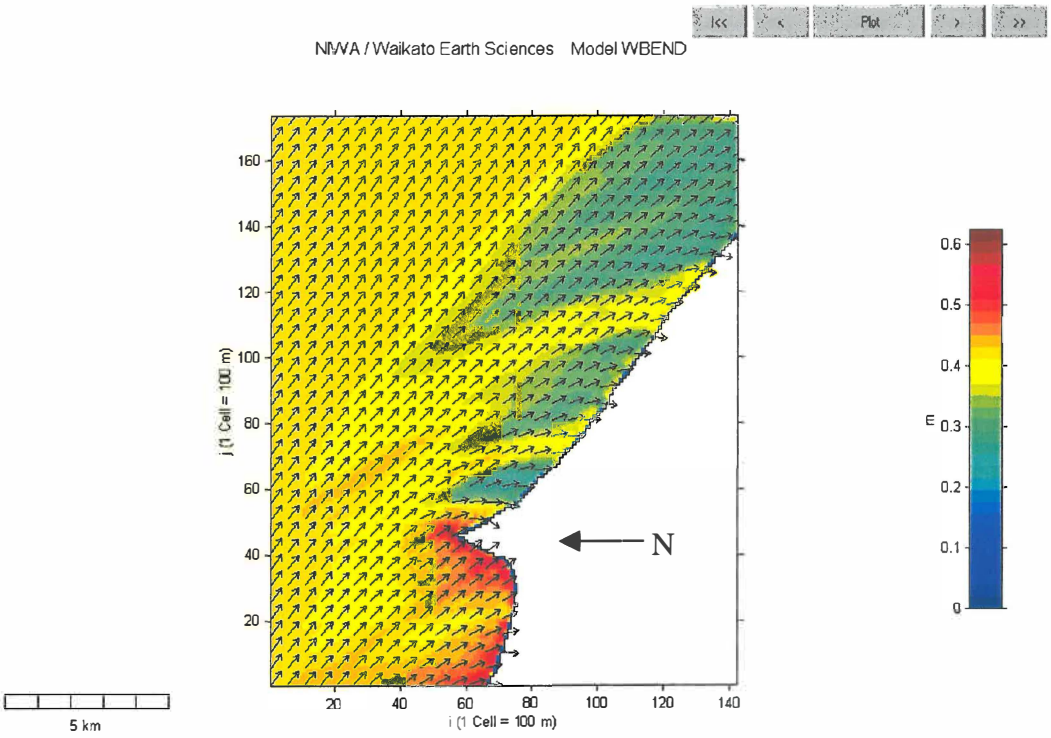

Scenario 12 0.39 m, 10.64 s, 56.73 º.

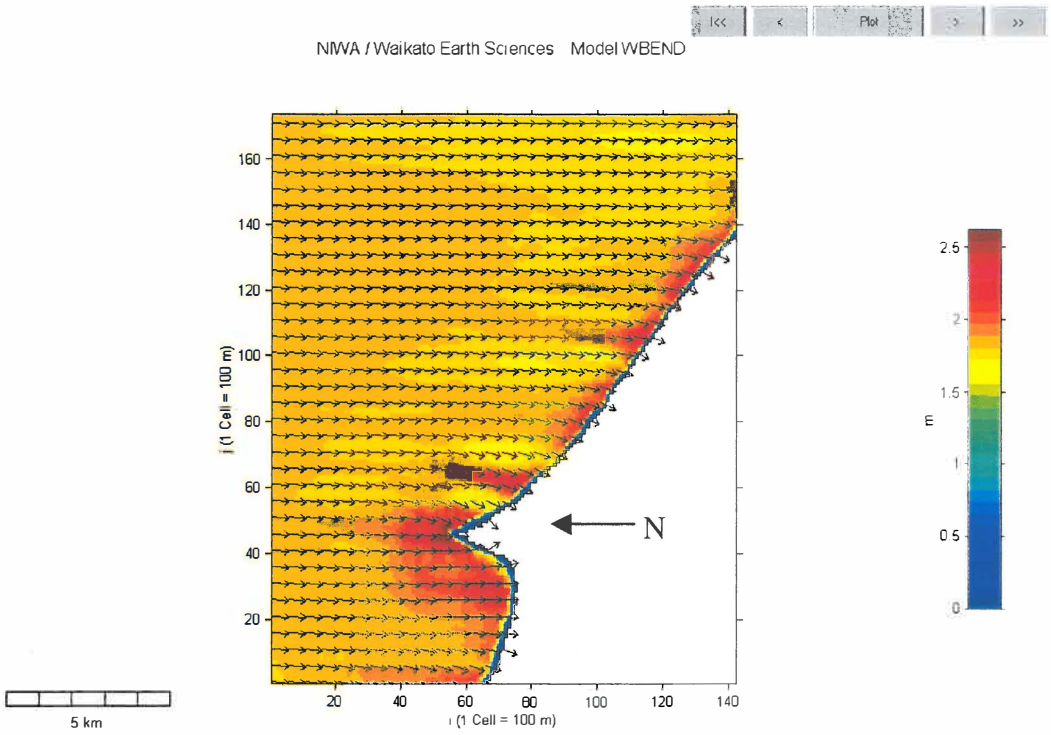

Scenario 13 1.63 m, 10.64 s, -4.73 º.

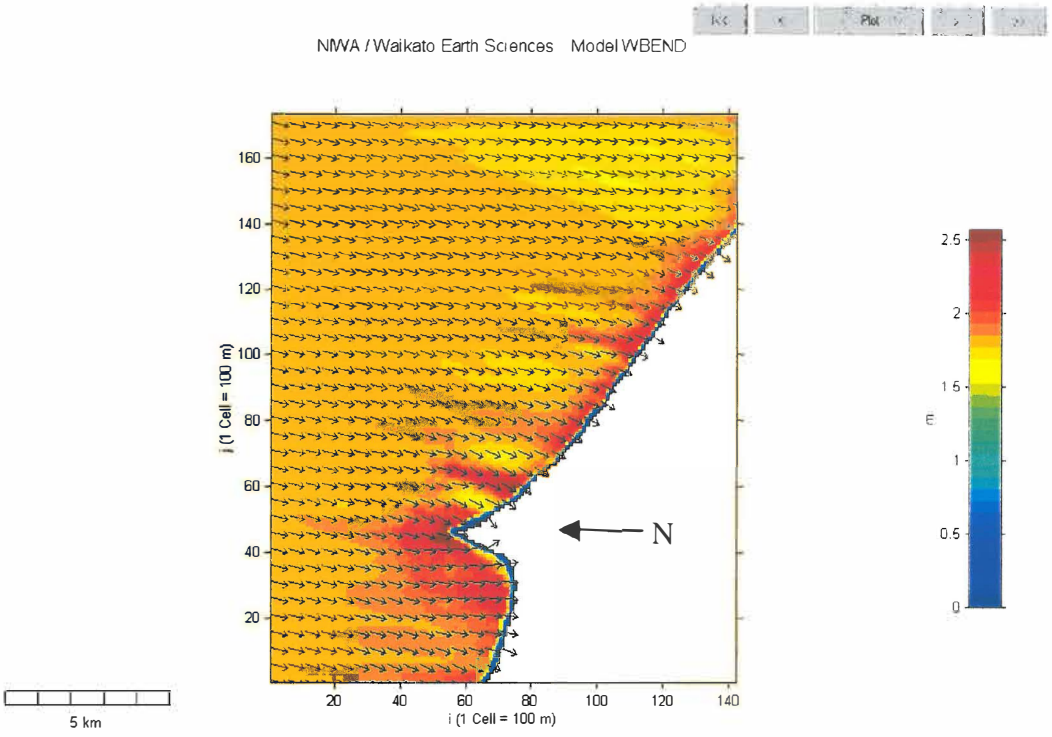

Scenario 14 1.63 m, 10.64 s, -14.73 º.

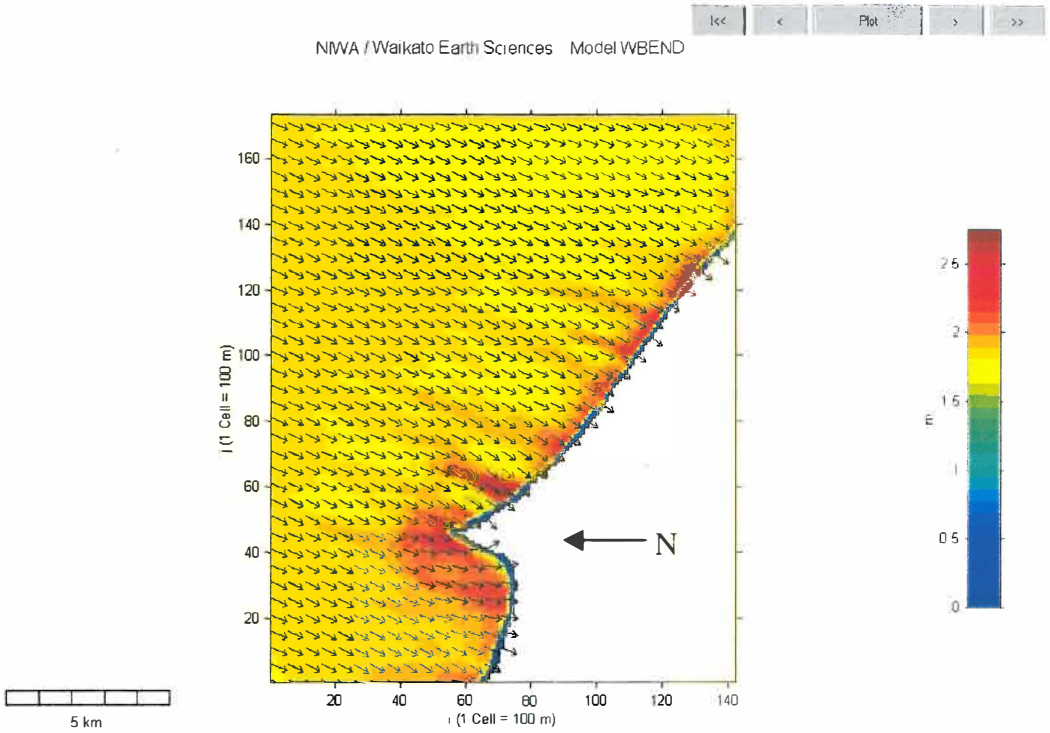

Scenario 15 1.63 m, 10.64 s, -24.73 º.

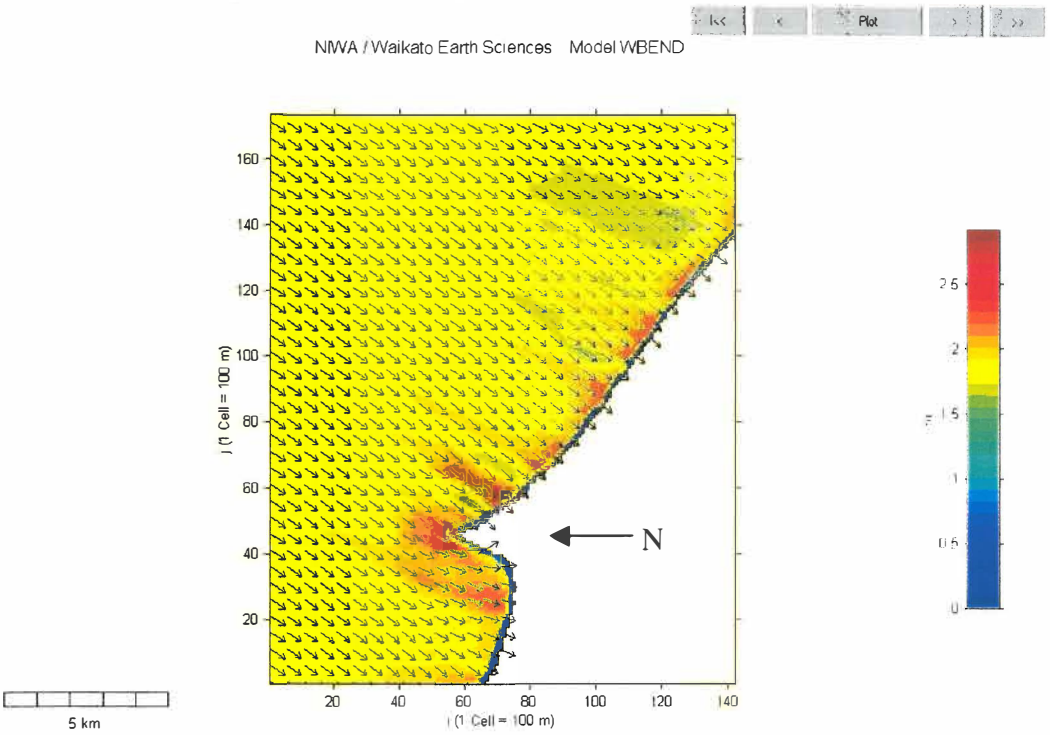

Scenario 16 1.63 m, 10.64 s, -34.73 º.

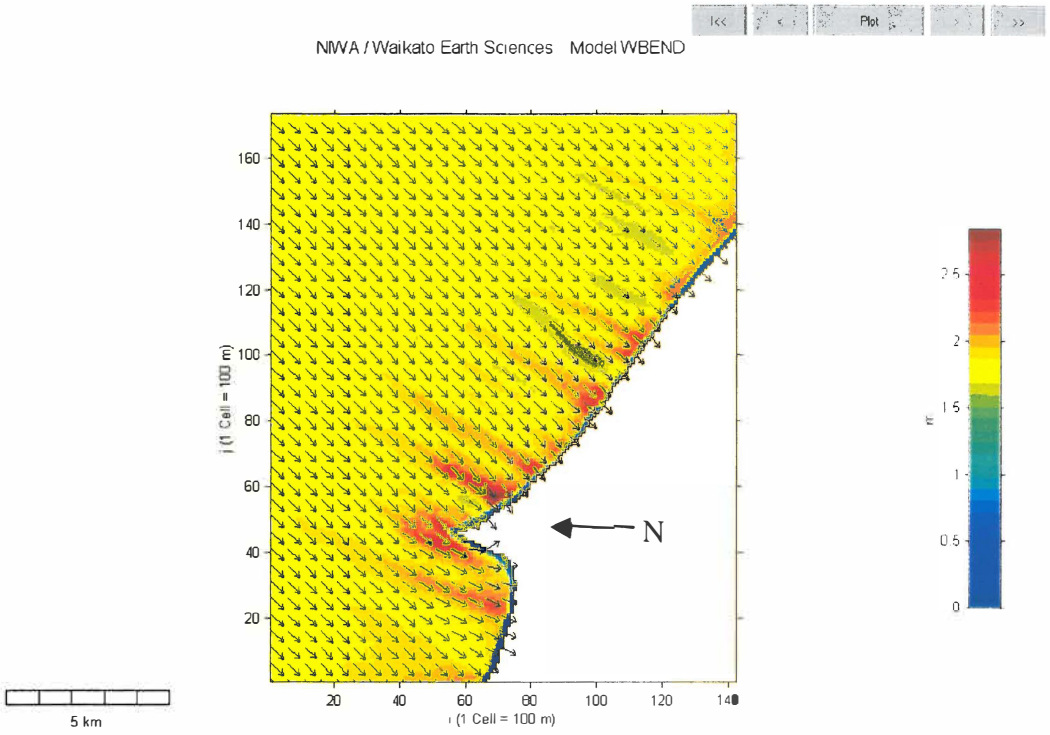

Scenario 17 1.63 m, 10.64 s, -44.73 º.

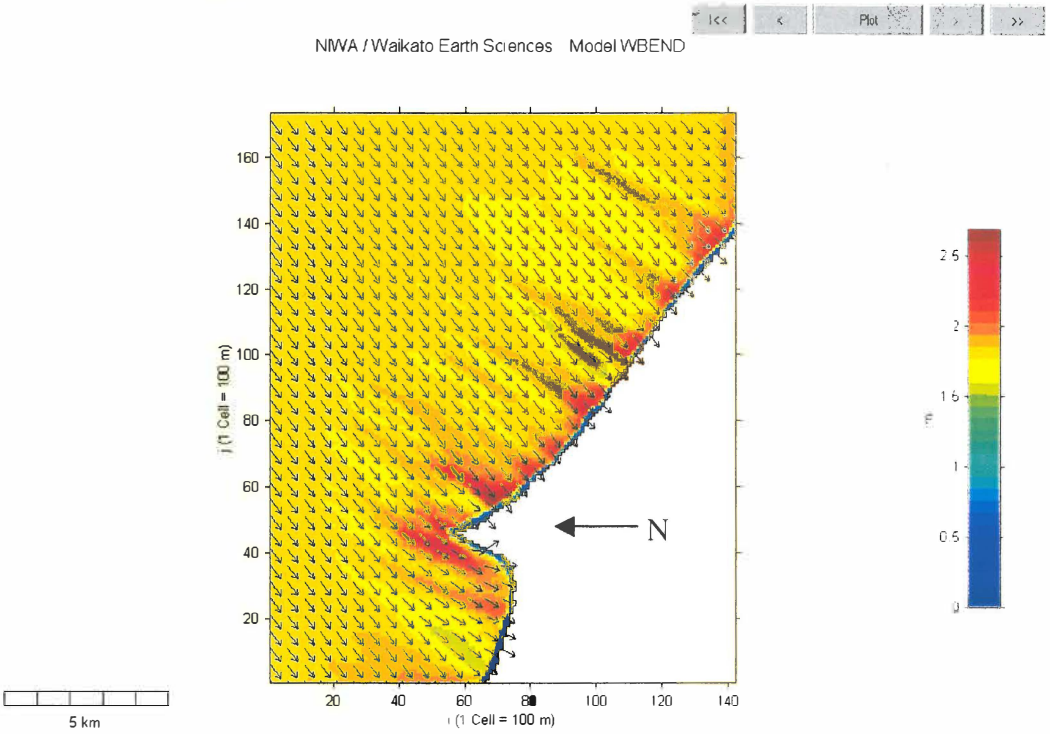

Scenario 18 1.63 m, 10.64 s, -54.73 º.

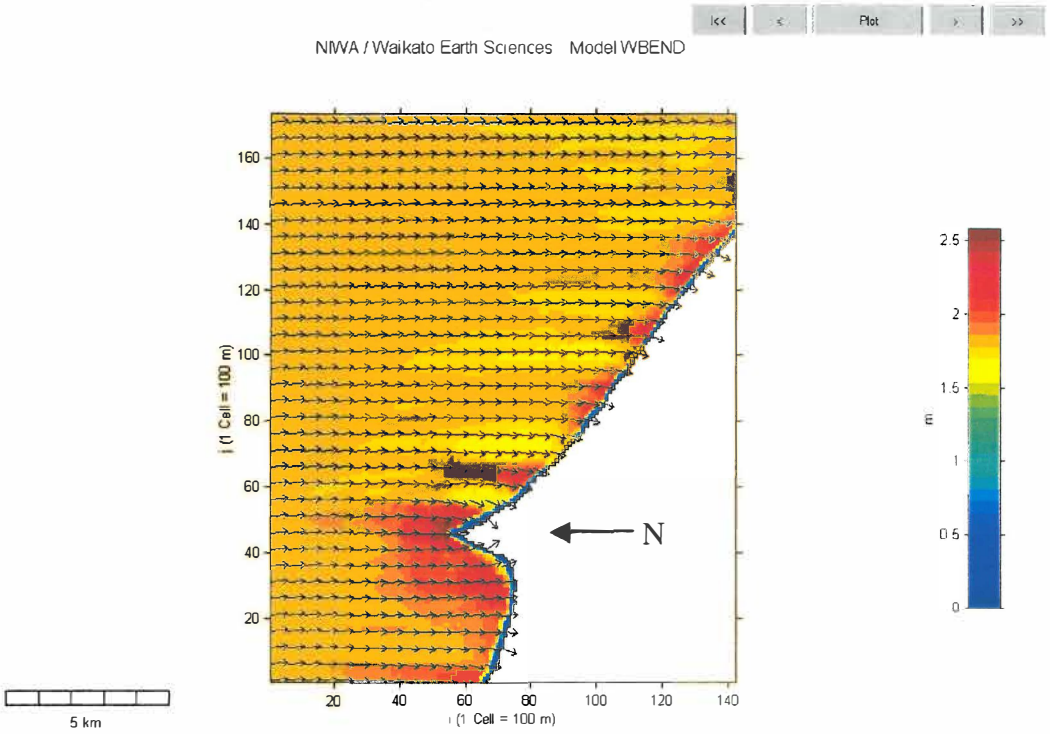

Scenario 19 1.63 m, 10.64 s, 6.73 °.

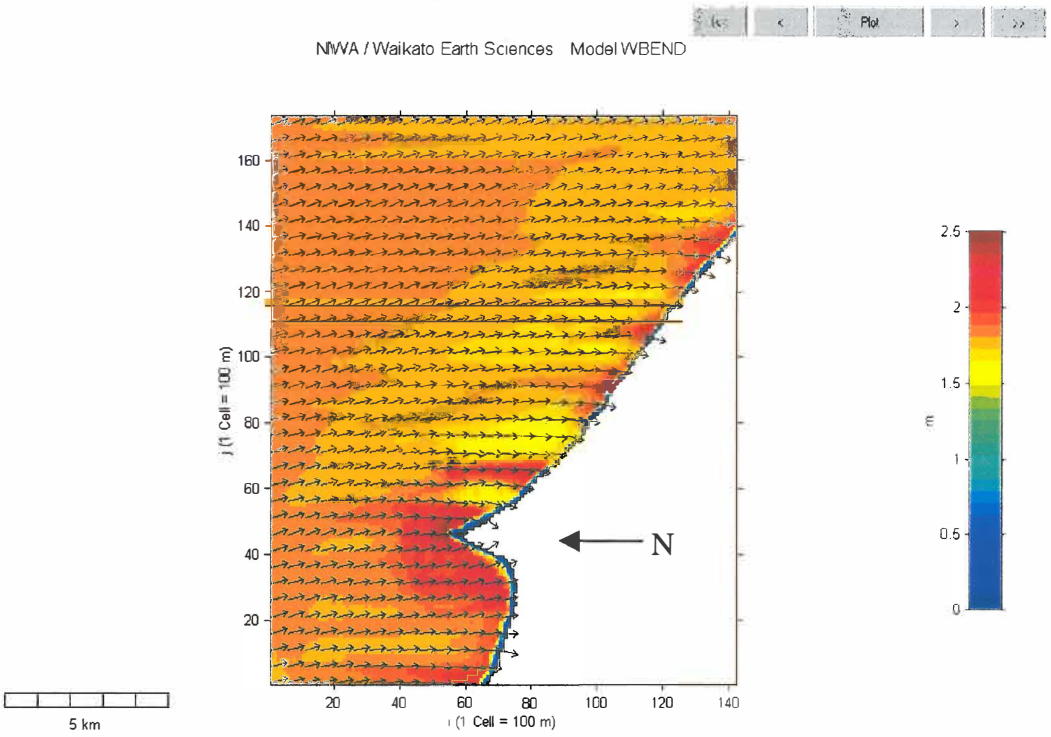

Scenario 20 1.63 m, 10.64 s, 16.73 °.

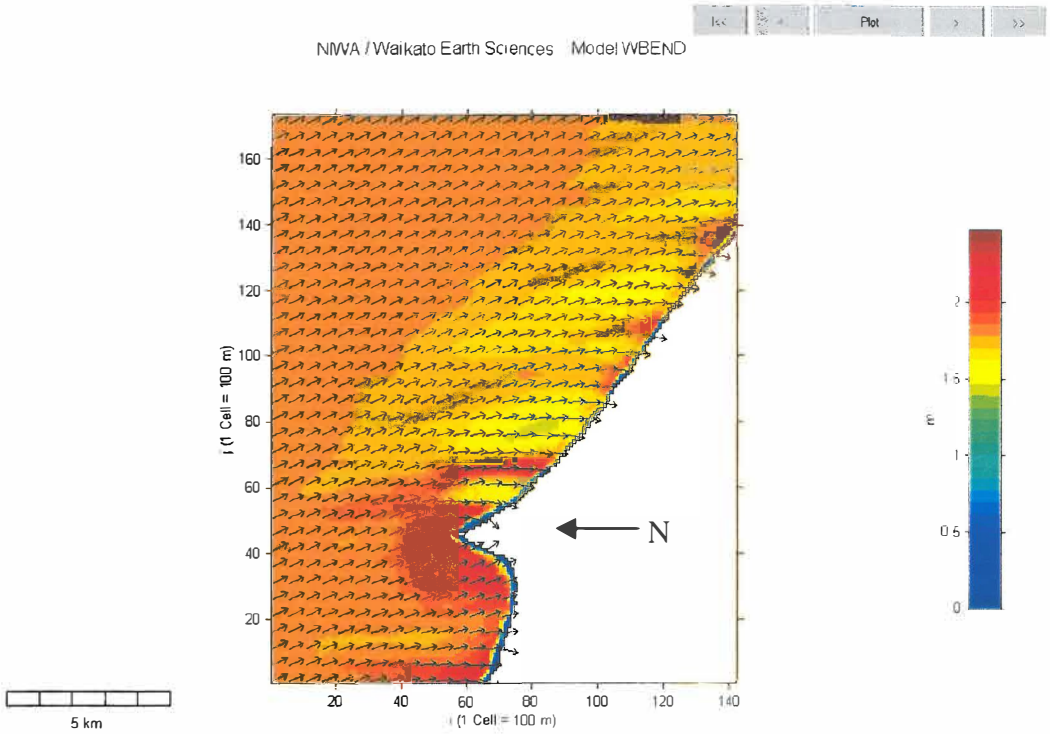

Scenario 21 1.63 m, 10.64 s, 26.73 °.

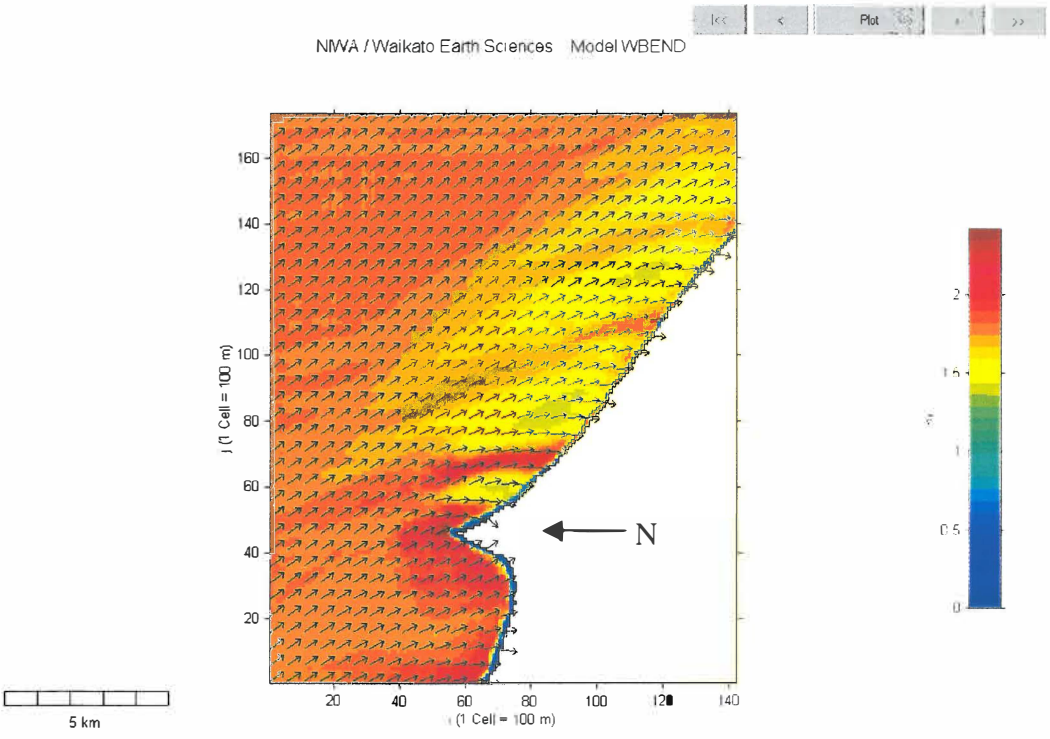

Scenario 22 1.63 m, 10.64 s, 36.73 °.

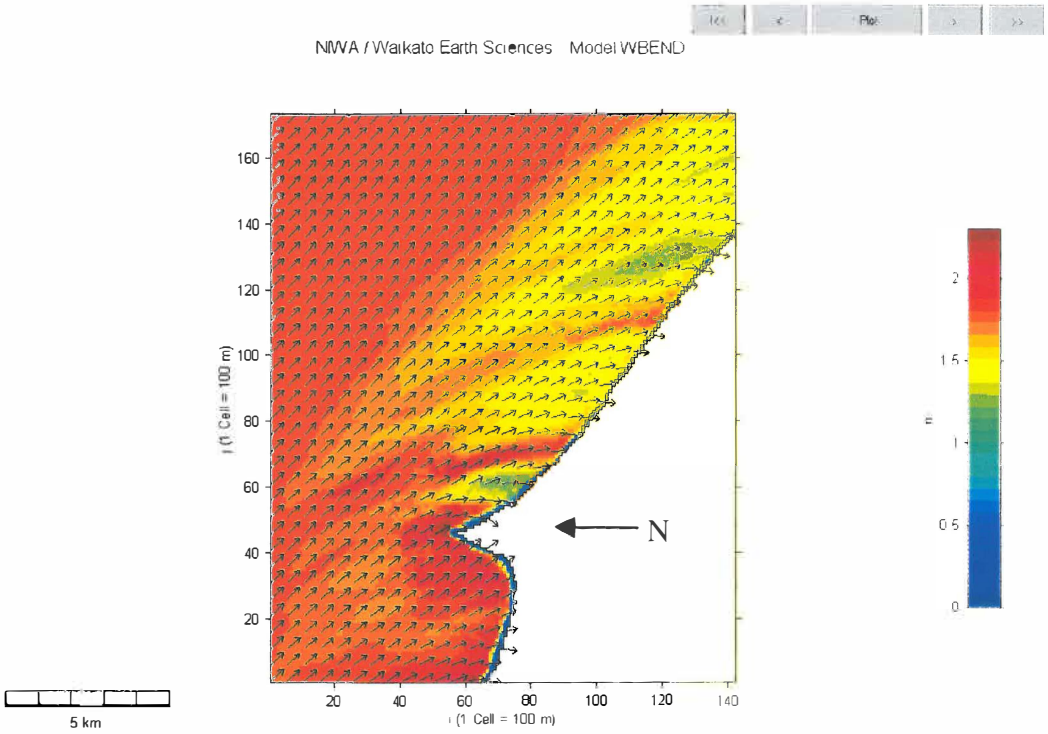

Scenario 23 1.63 m, 10.64 s, 46.73 °.

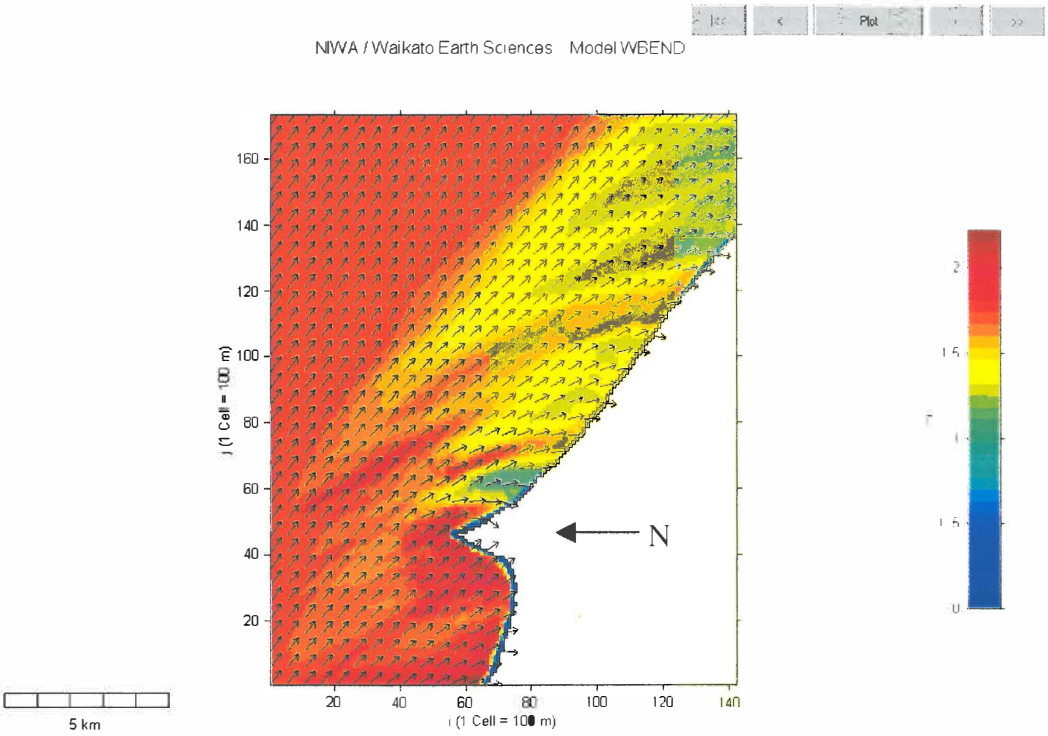

Scenario 24 1.63 m, 10.64 s, 56.73 °.

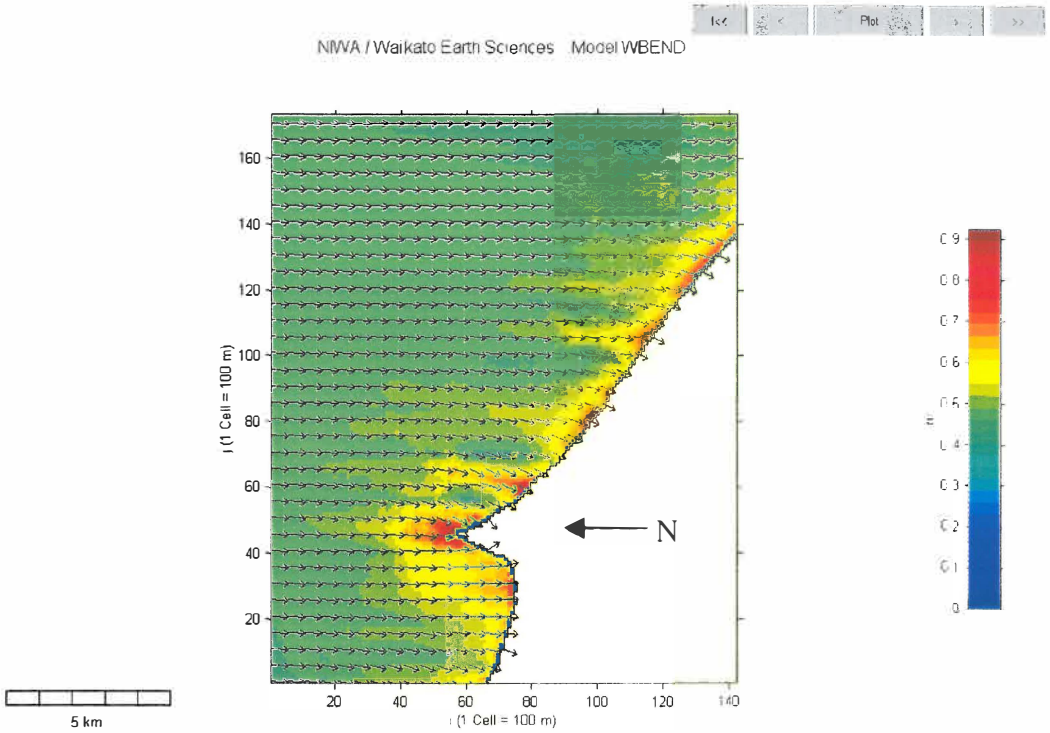

Scenario 25 0.39 m, 14.57 s, -4.73 º.

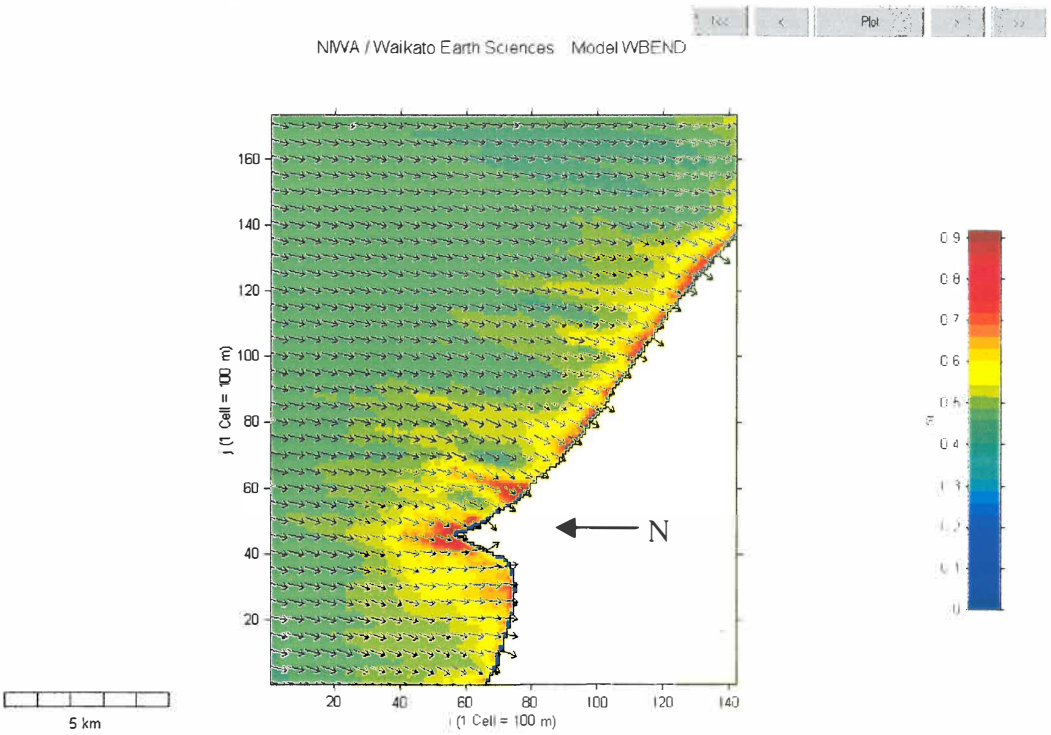

Scenario 26 0.39 m, 14.57 s, -14.73 º.

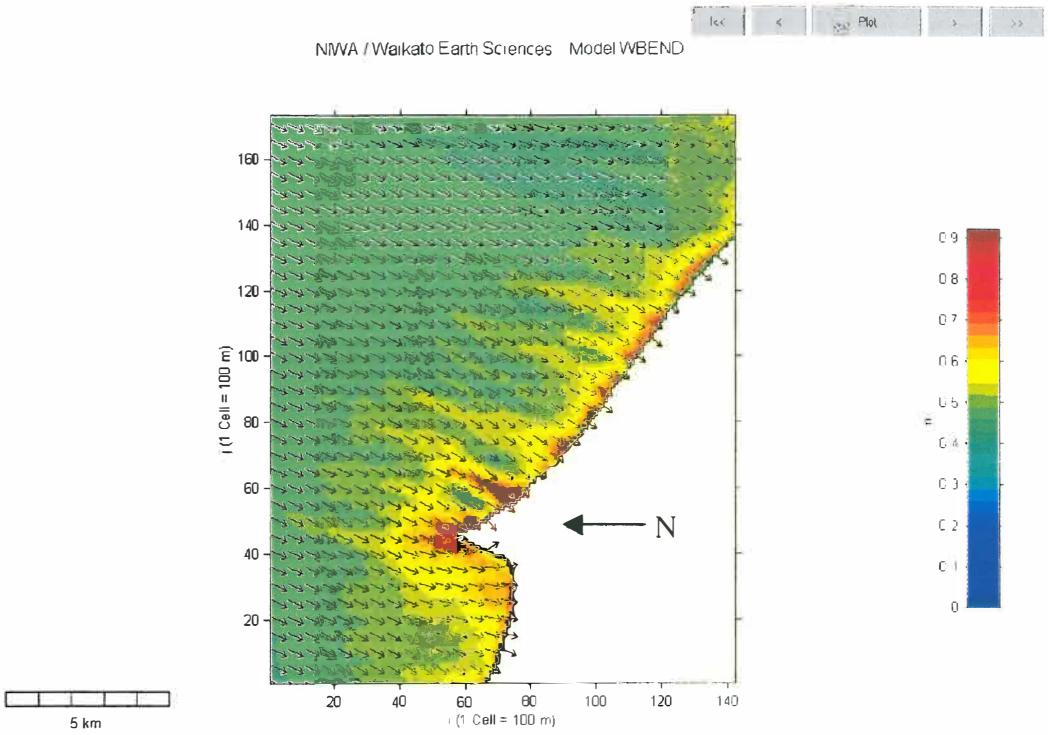

Scenario 27 0.39 m, 14.57 s, -24.73 º.

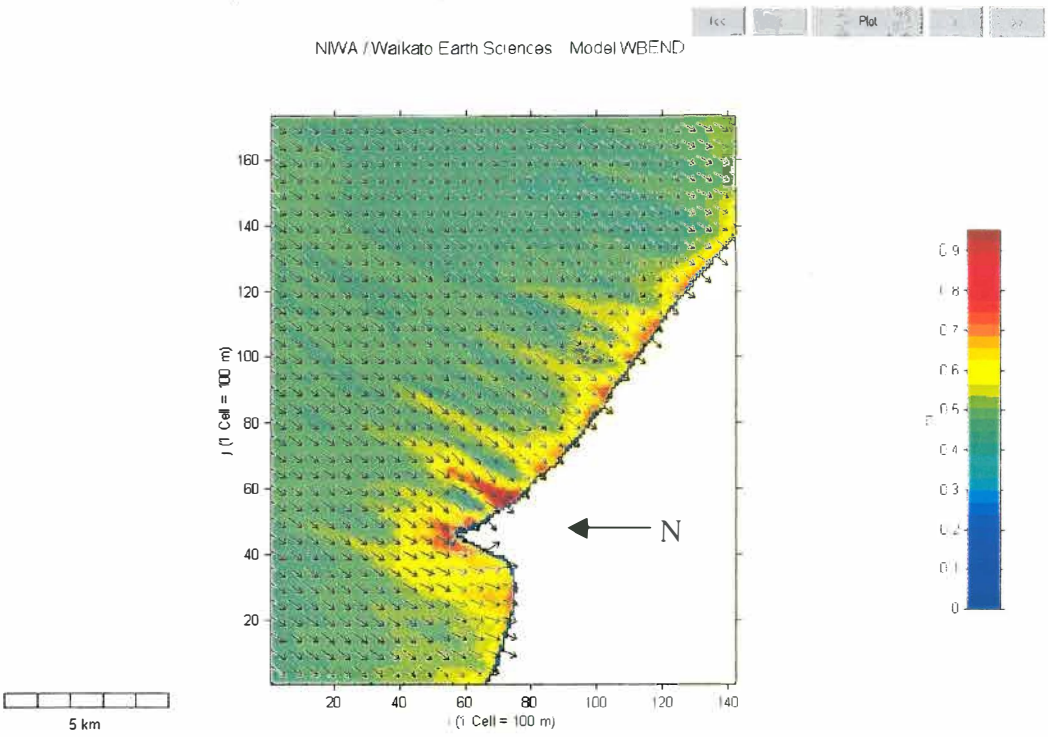

Scenario 28 0.39 m, 14.57 s, -34.73 º.

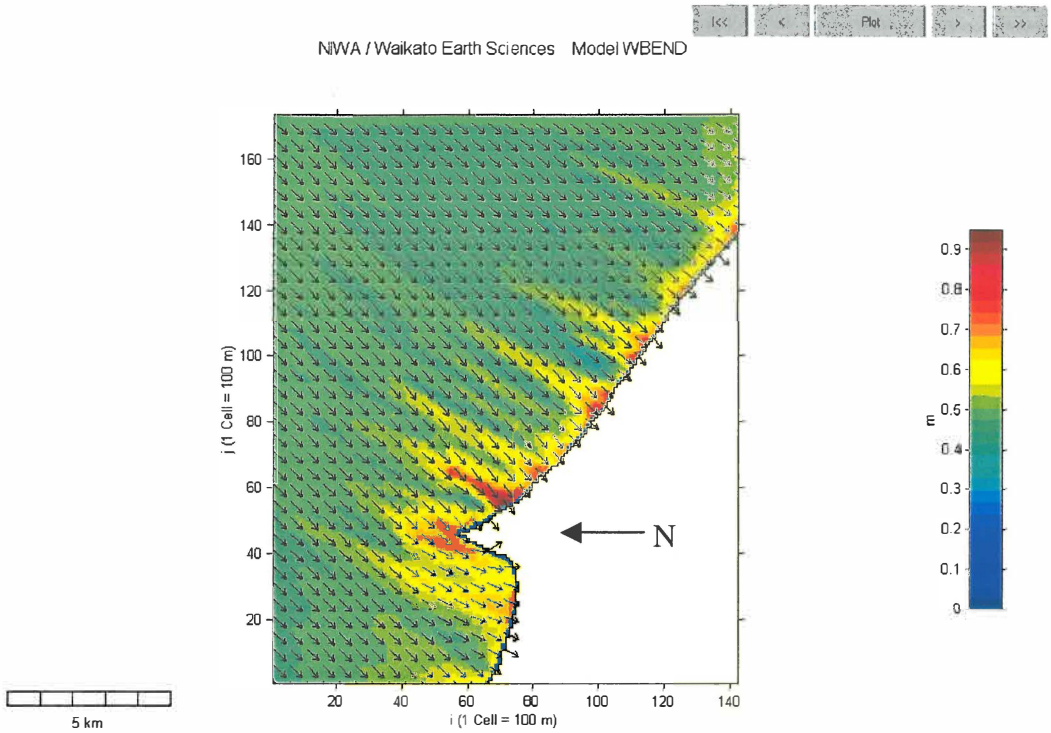

Scenario 29 0.39 m, 14.57 s, -44.73 º.

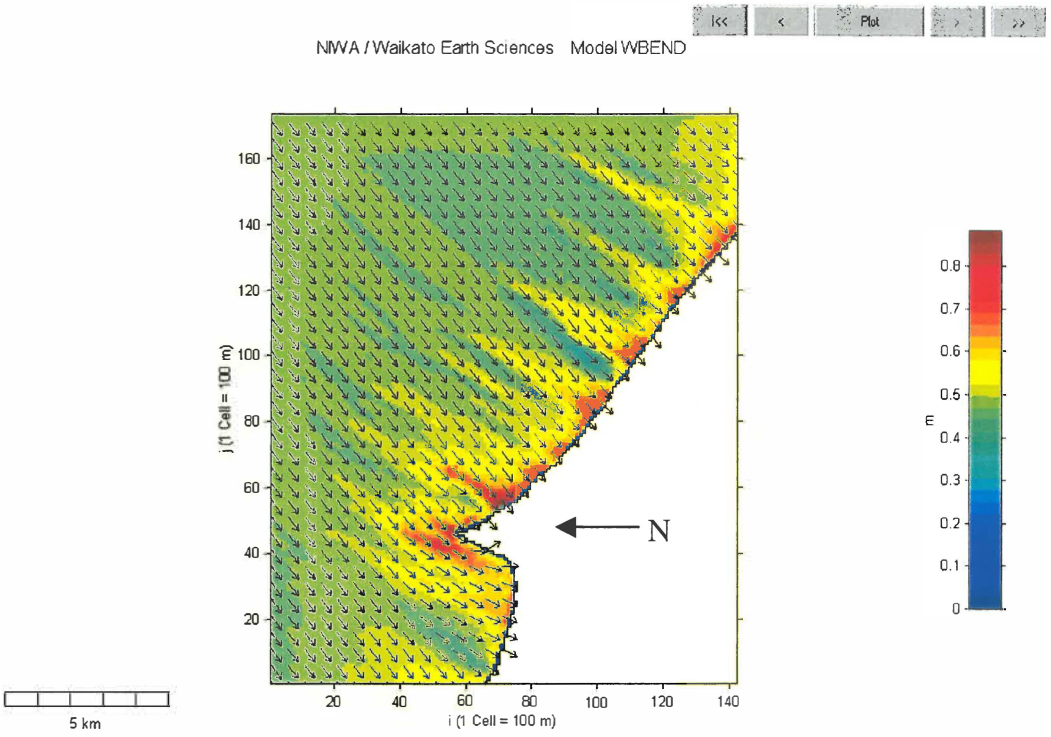

Scenario 30 0.39 m, 14.57 s, -54.73 º.

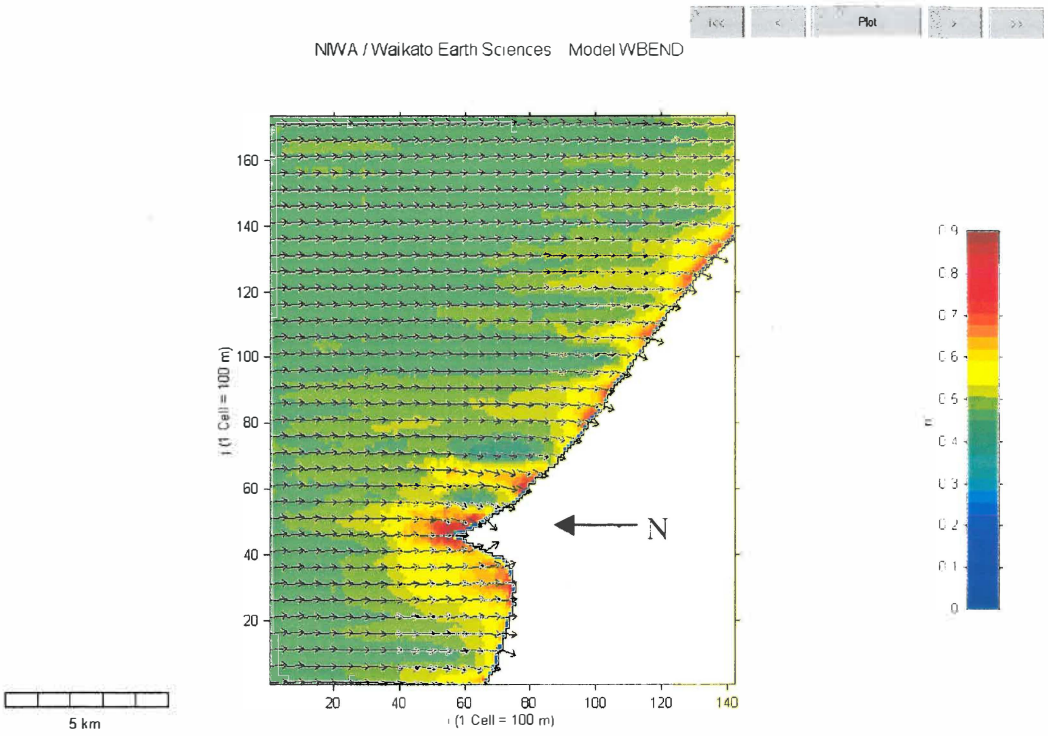

Scenario 31 0.39 m, 14.57 s, 6.73 °.

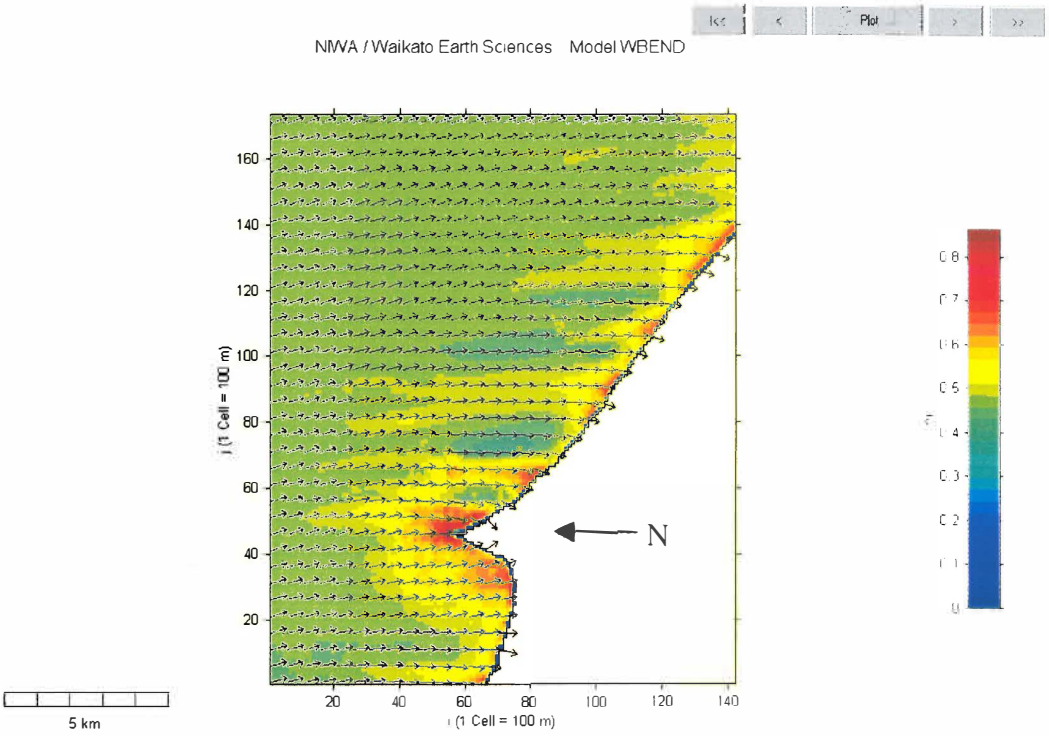

Scenario 32 0.39 m, 14.57 s, 16.73 °.

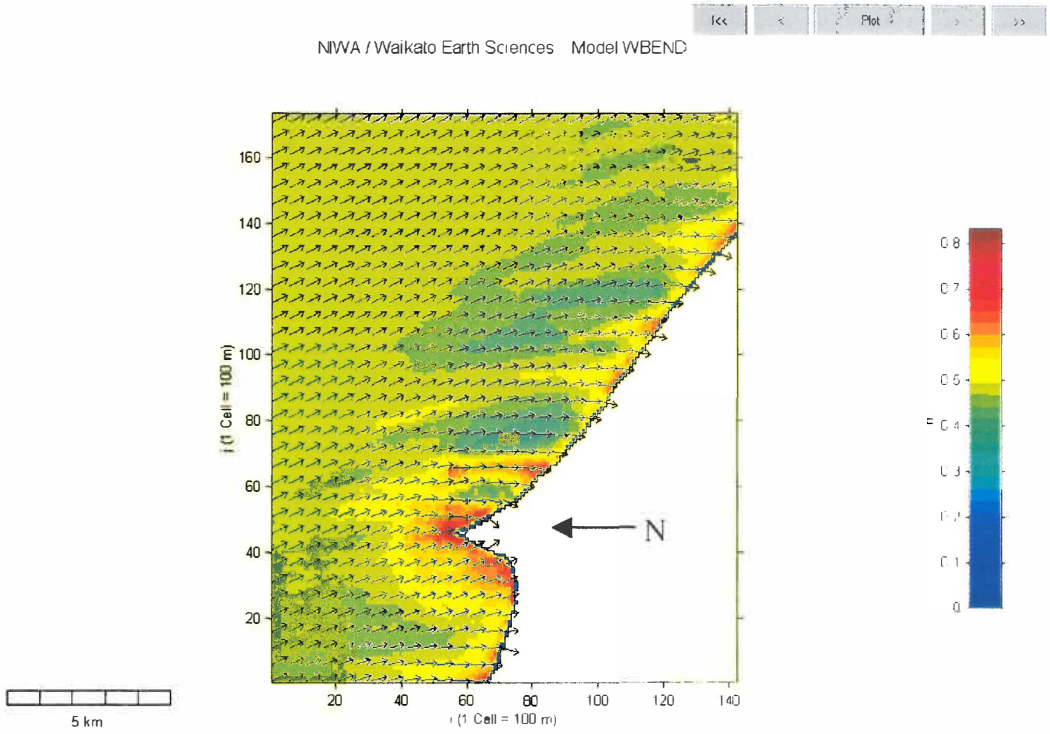

Scenario 33 0.39 m, 14.57 s, 26.73 °.

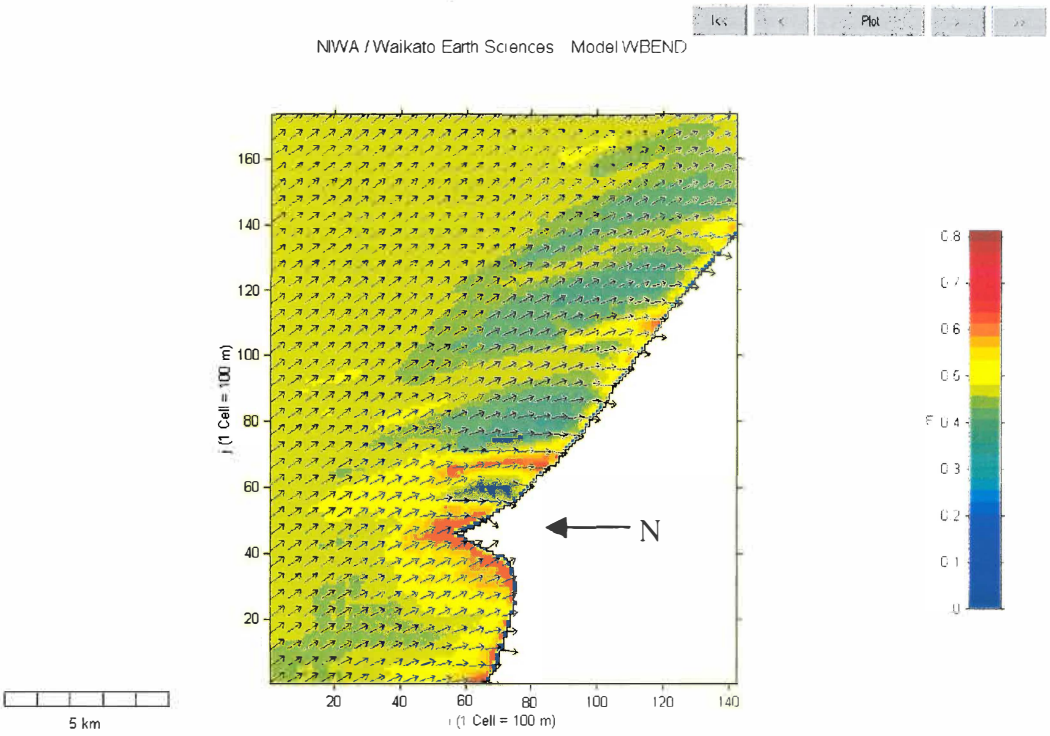

Scenario 34 0.39 m, 14.57 s, 36.73 °.

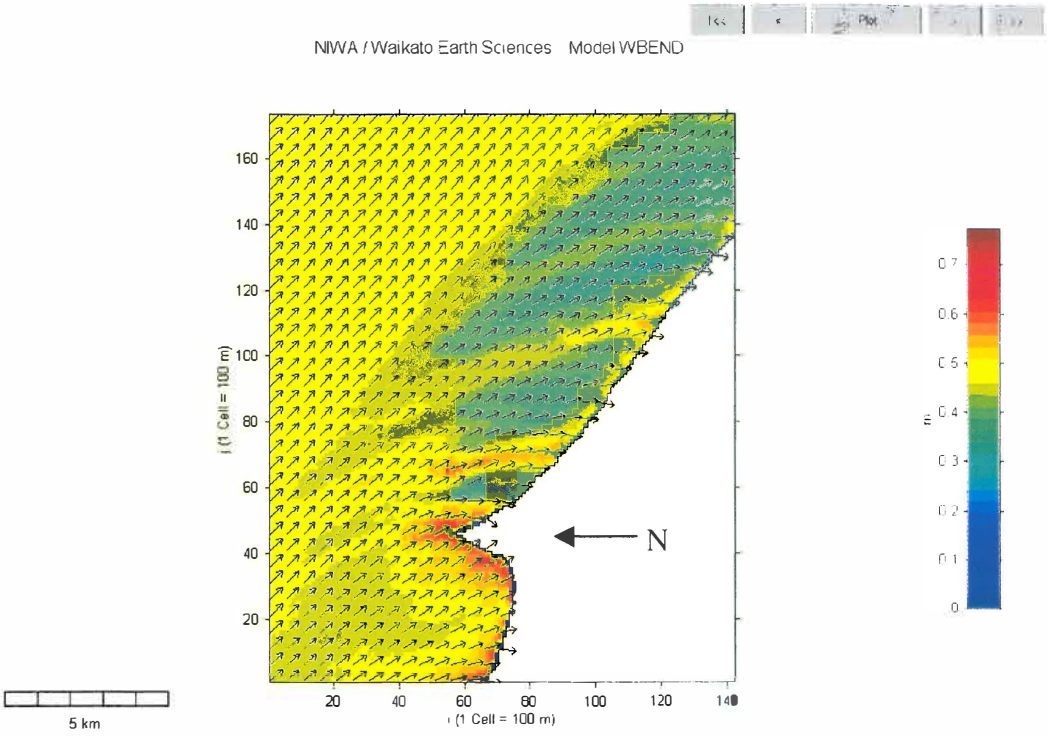

Scenario 35 0.39 m, 14.57 s, 46.73 °.

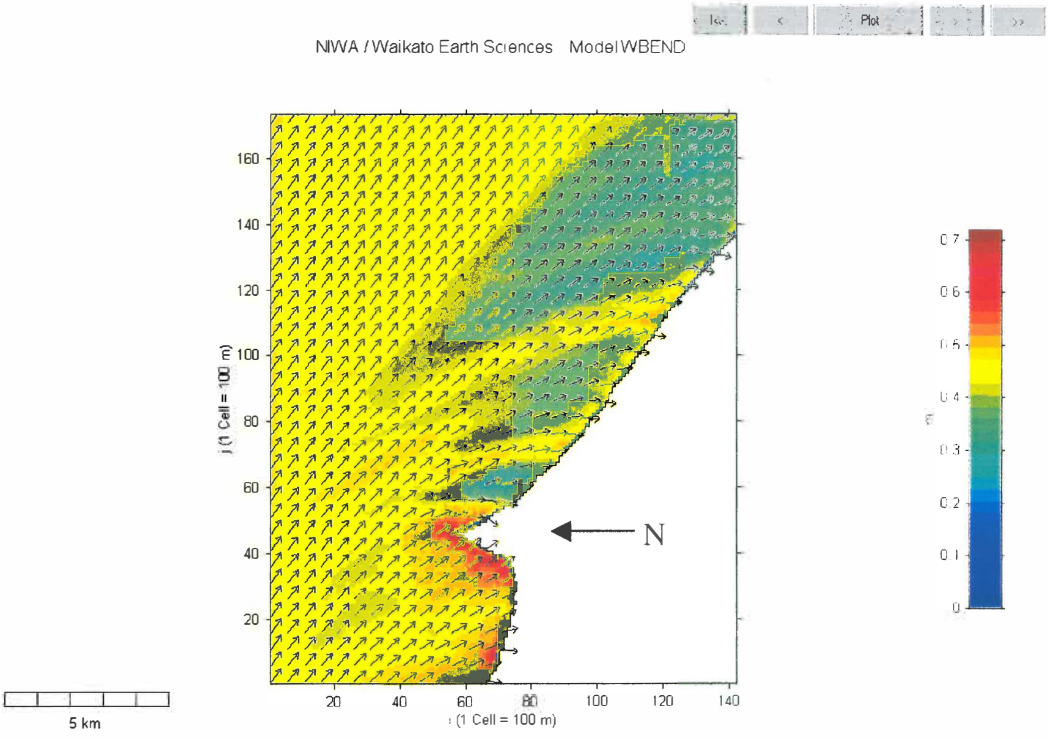

Scenario 36 0.39 m, 14.57 s, 56.73 °.

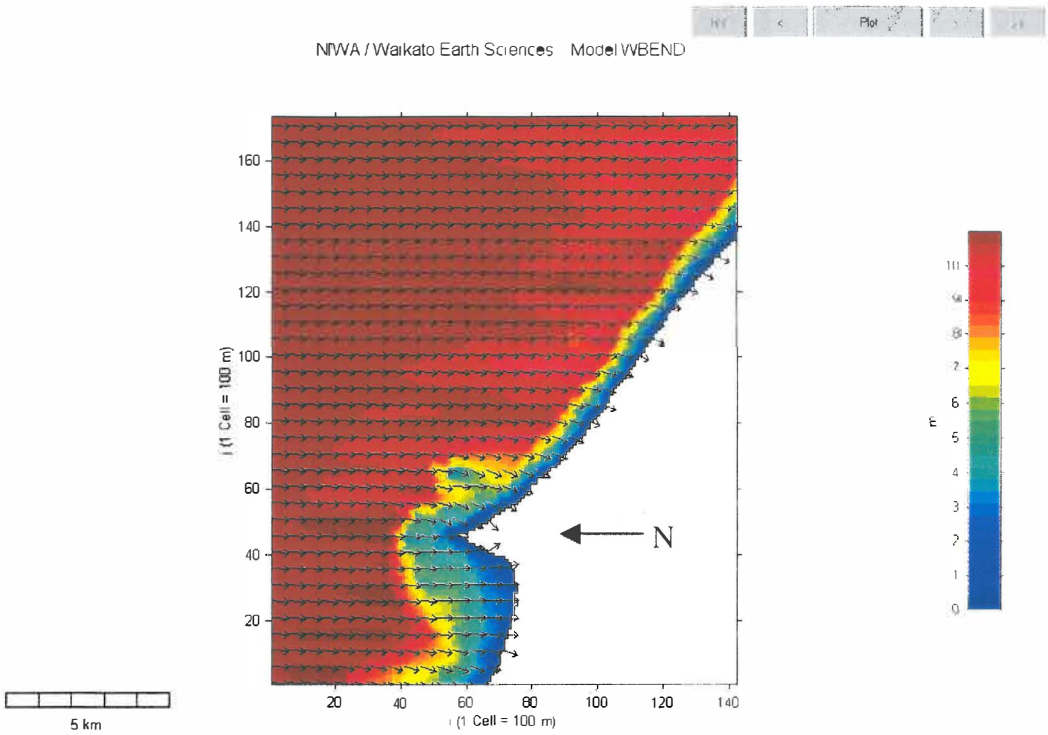

Scenario 37 9.9 m, 9.5 s, -4.73 º.

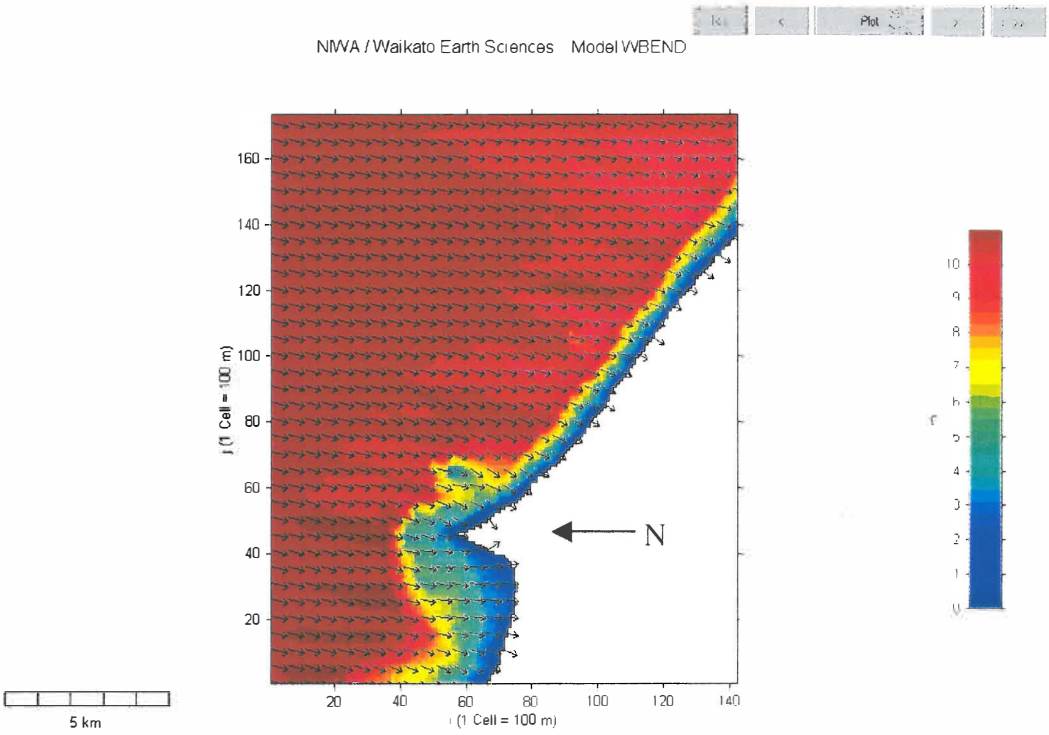

Scenario 38 9.9 m, 9.5 s, -14.73 º.

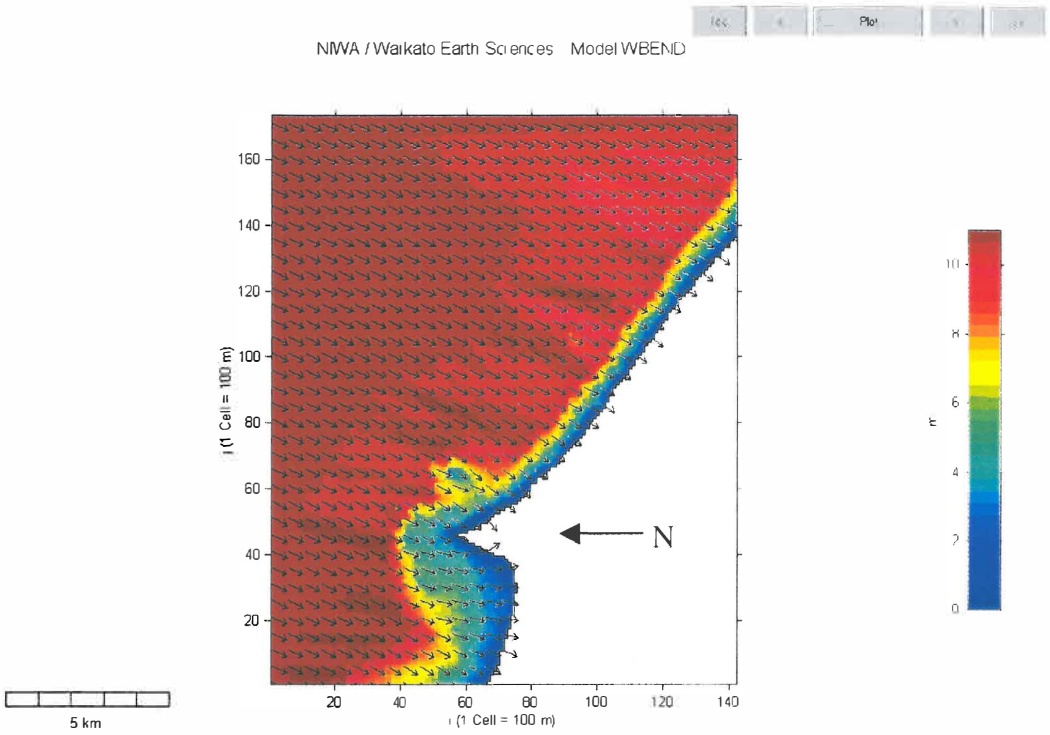

Scenario 39 9.9 m, 9.5 s, -24.73 º.

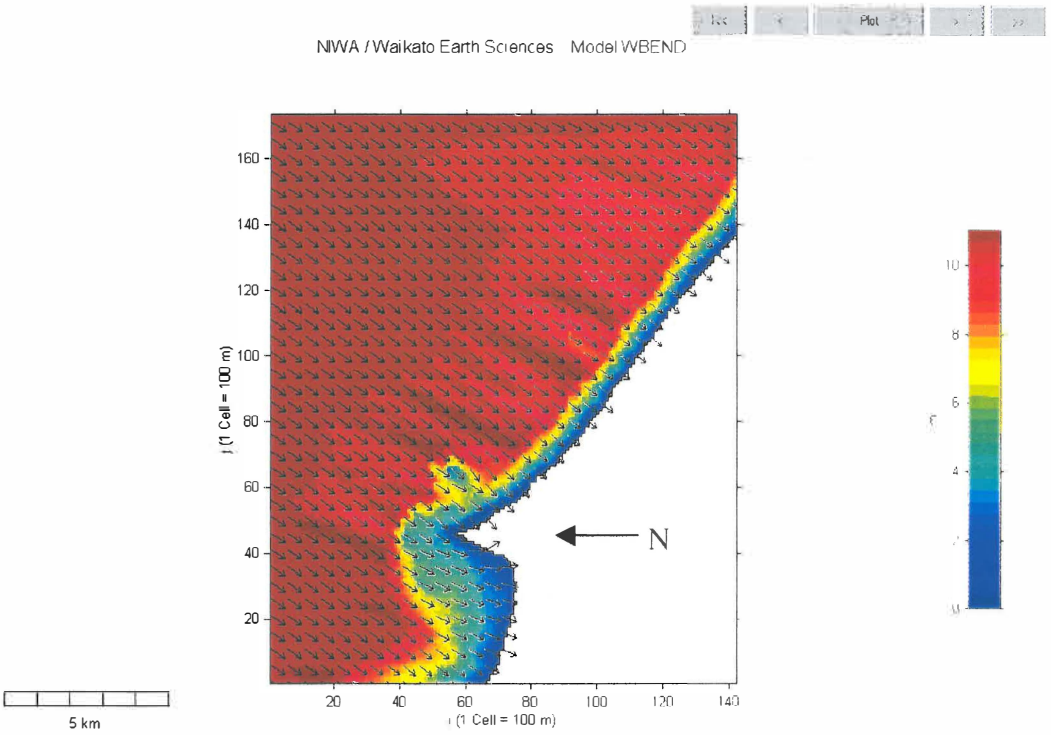

Scenario 40 9.9 m, 9.5 s, -34.73 º.

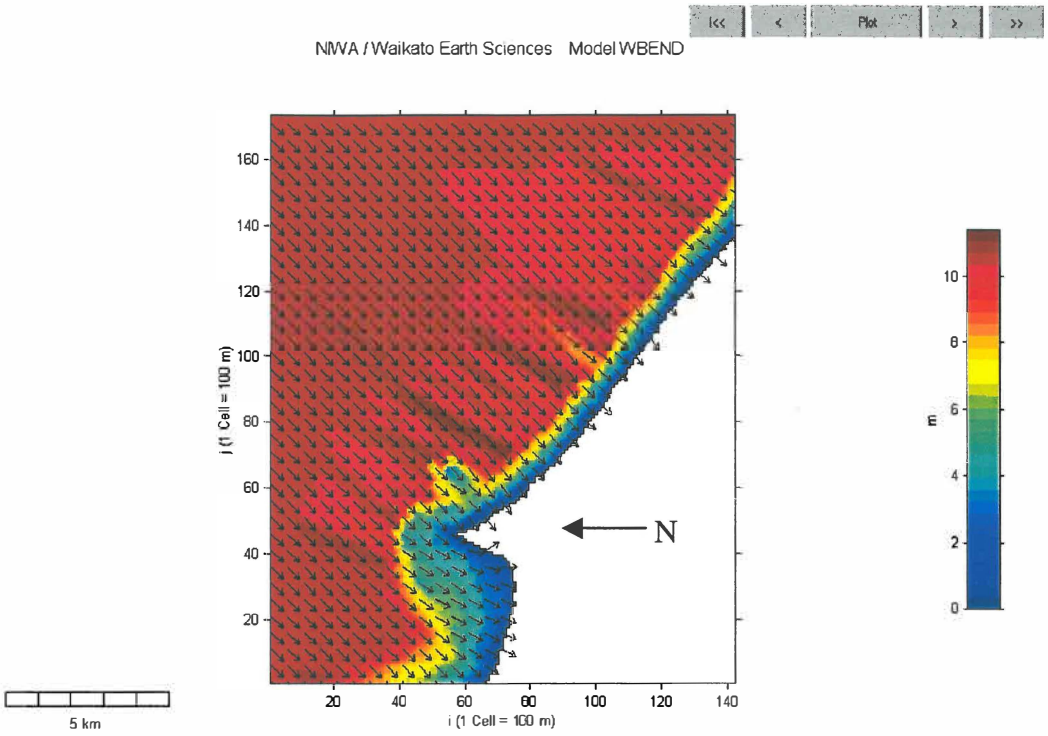

Scenario 41 9.9 m, 9.5 s, -44.73 º.

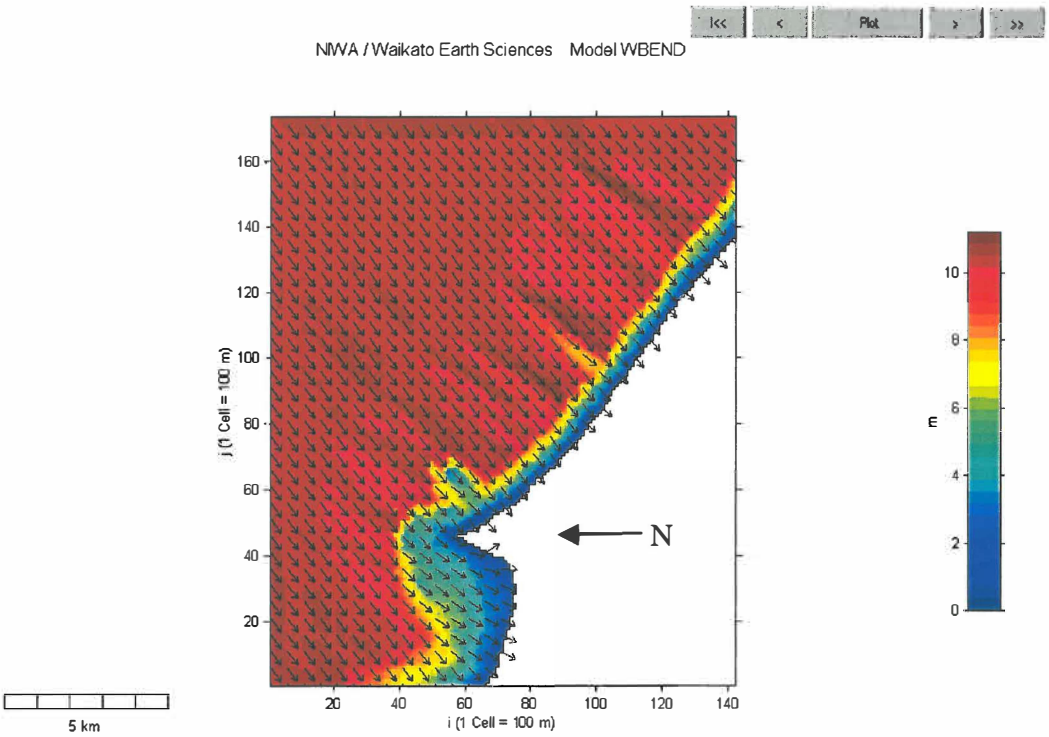

Scenario 42 9.9 m, 9.5 s, -54.73 º.

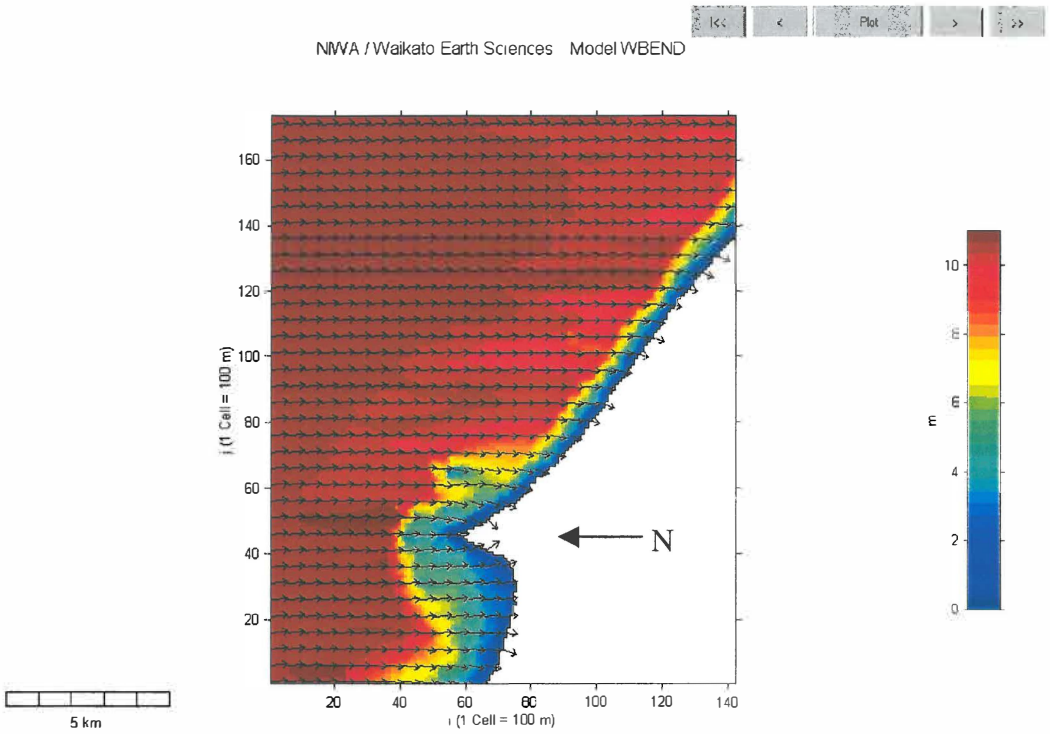

Scenario 43 9.9 m, 9.5 s, 6.73 °.

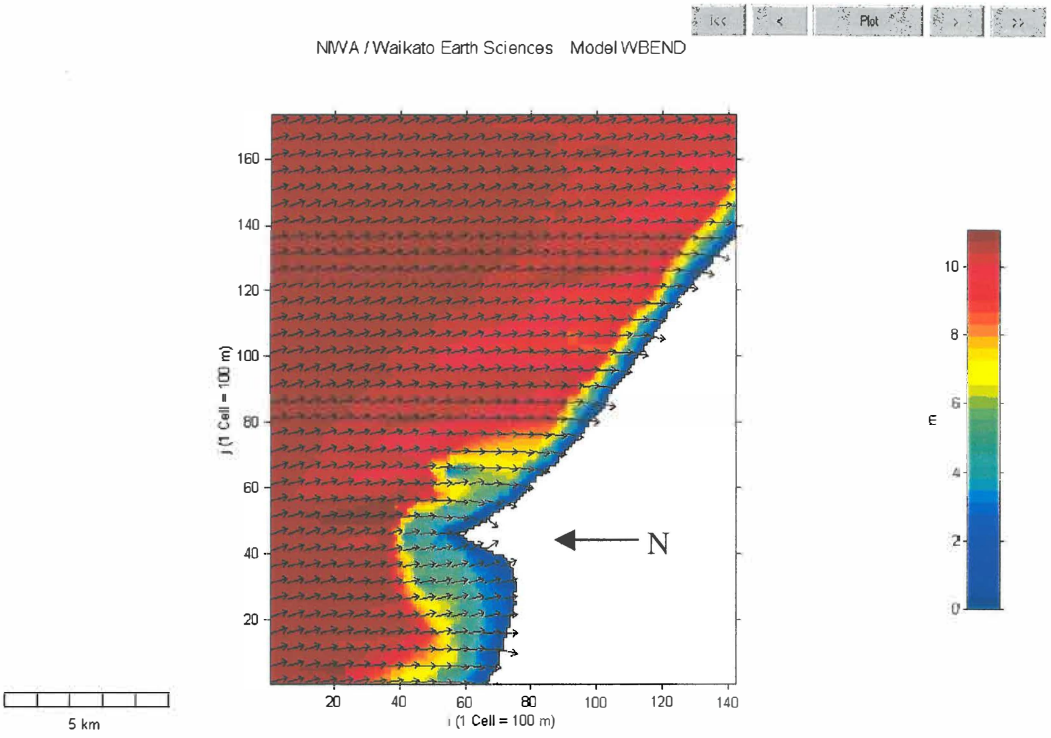

Scenario 44 9.9 m, 9.5 s, 16.73 °.

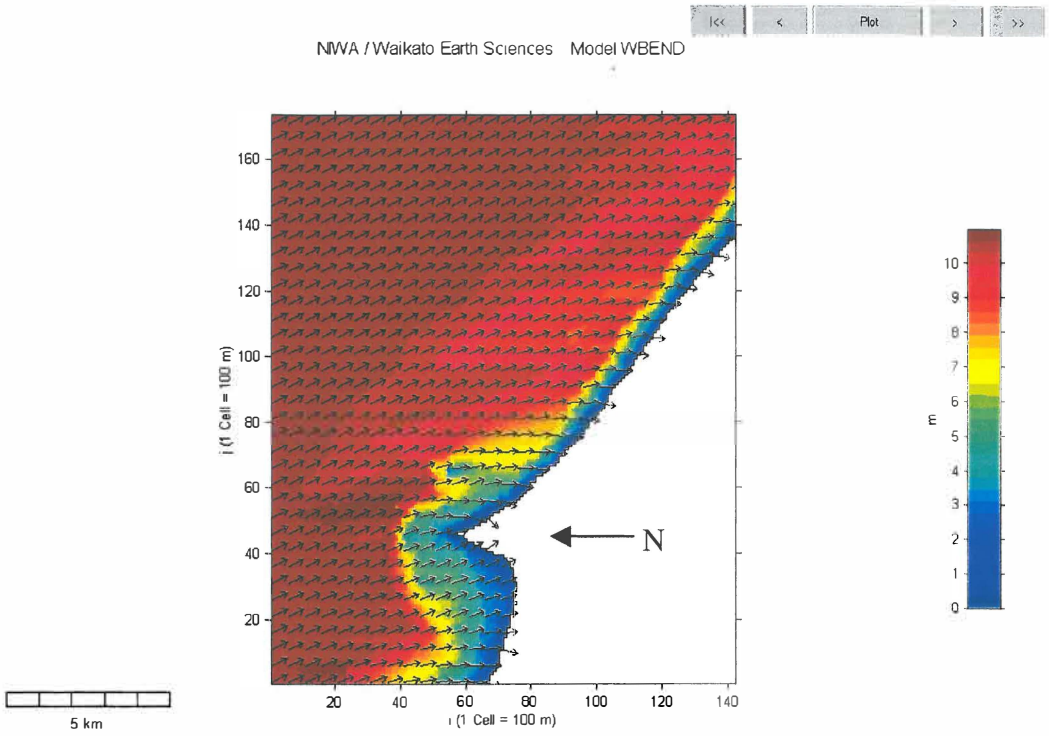

Scenario 45 9.9 m, 9.5 s, 26.73 º.

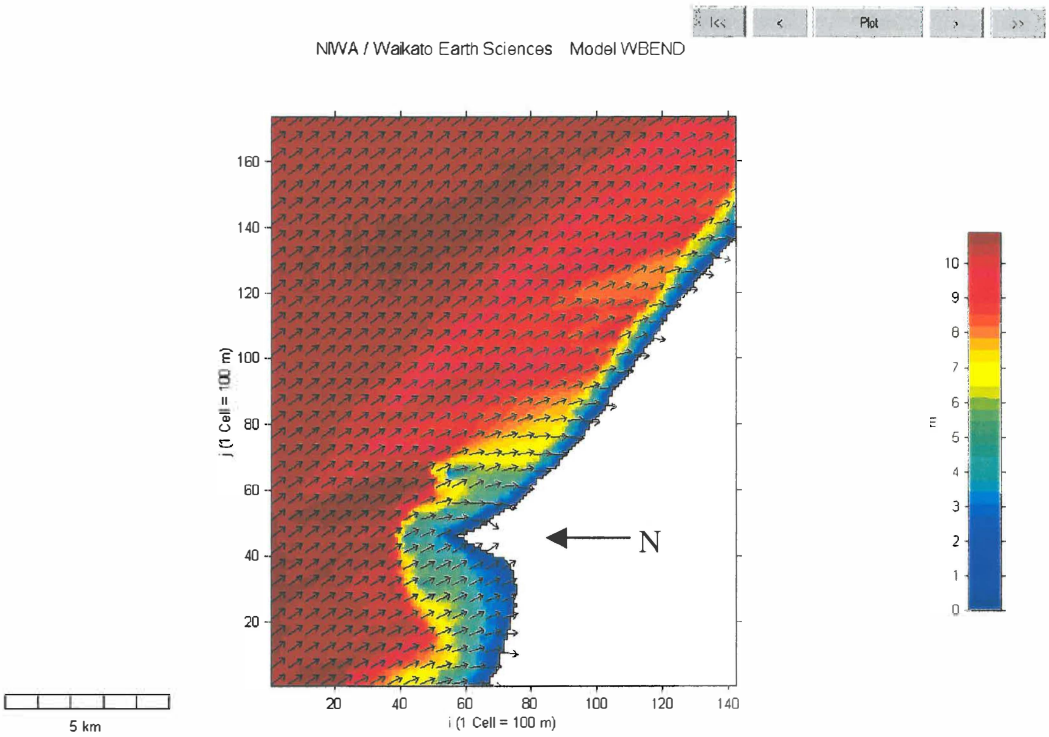

Scenario 46 9.9 m, 9.5 s, 36.73 º.

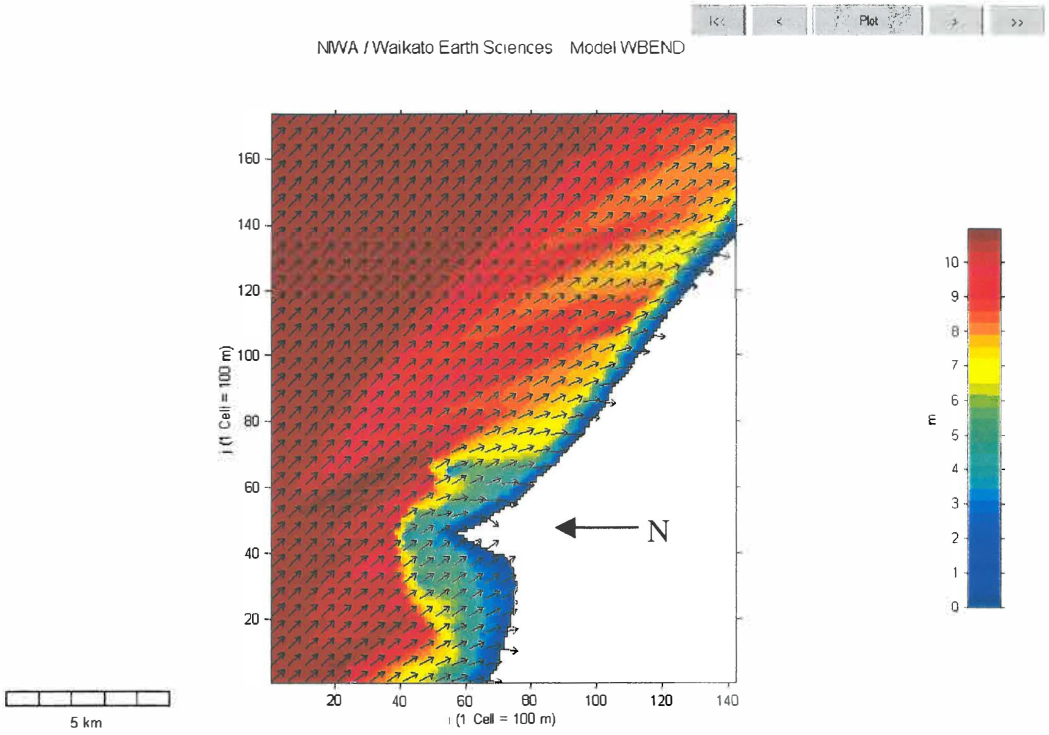

Scenario 47 9.9 m, 9.5 s, 46.73 º.

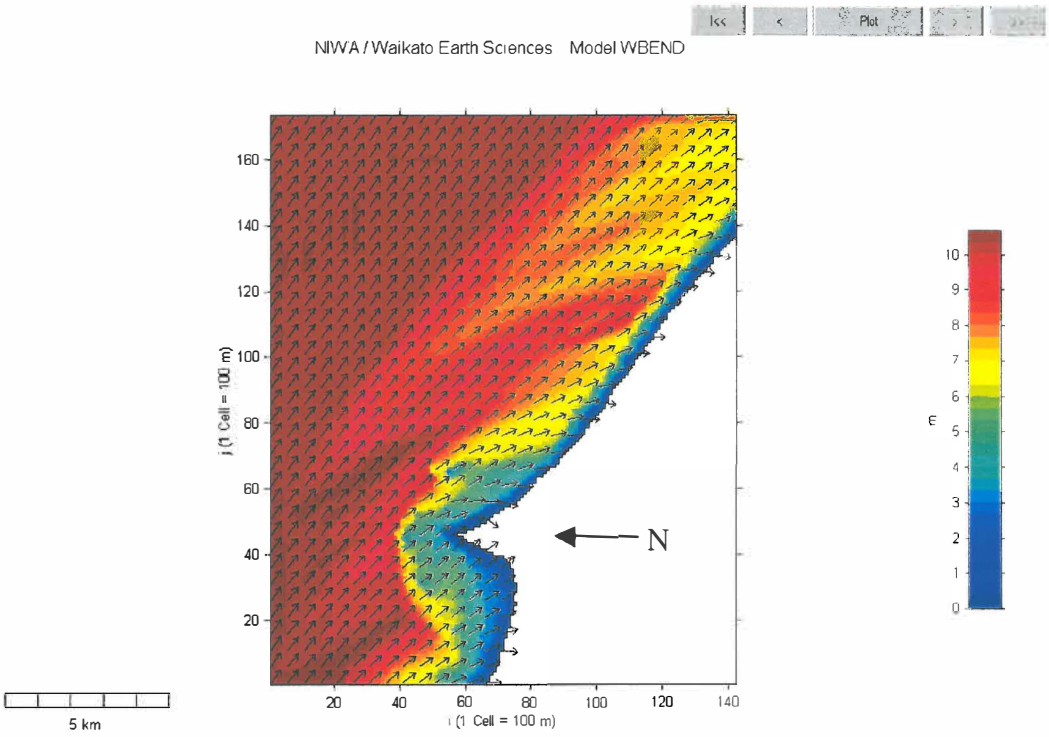

Scenario 48 9.9 m, 9.5 s, 56.73 º.

Appendix XI

The following appendix can be obtained in the Appendix CD. Nearshore sediment transport rates are presented as a Microsoft Excel file. Numerical data is presented with the following column labels: i CELL, j CELL, SOUTH, and NORTH.

i CELL and j CELL define the grid co-ordinate of the sediment transport rate value, while SOUTH, and NORTH define the sediment transport rate in the associated labeled direction.